Shrinkage Characterisation, Behavioural Properties and Durability of Cement-Stabilised Pavement Materials

by

Alex Ndiku Mbaraga

Dissertation presented for the degree of Doctor of Philosophy in Pavement Engineering in the Faculty of Engineering, at Stellenbosch University

Promoter

Professor Kim J Jenkins Ph.D. Pr.Eng.
SANRAL Chair in Pavement Engineering
Department of Civil Engineering
University of Stellenbosch

March 2015

Declaration

By submitting this thesis electronically, I declare that the entirety of the work contained therein is my own, original work, that I am the authorship owner thereof (unless to the extent explicitly otherwise stated) and that I have not previously in its entirety or in part submitted it for obtaining any qualification.

Signature:……

Date: ……

Abstract

With the depletion of high quality conventional materials for road pavements, the consideration of cement stabilisation for sub-base and base layer materials often provide a feasible solution to the road industry. Like all pavement material types, the design inputs should be determined using reliable test methods, which provide a good indication of the property of materials. Any evaluation should provide a better understanding of the engineering and behavioural properties of the materials. This should form the basis for ascertaining their suitability for use in the pavement structure. However, the road industry is dependent on strength testing of cement-stabilised materials as a means to ascertain material suitability for use. Strength alone does not offer reliable insight regarding the performance and durability of the stabilised layer. This is because a cement-stabilised layer may be very stiff but not strong enough to withstand the loading and endure adverse environmental conditions. Similarly, the stabilised layer may be prone to cracking emanating from shrinkage, which leads to performance and durability related distresses.

A stabilised sub-base and base of the pavement structure experiences tensile stresses and strains under traffic loading. At laboratory level, the flexural beam test simulates to an acceptable degree the mode of stress to strain to which the pavement layer experiences. However, the test lacks a standard test protocol. This leads to inconsistencies while evaluating the same material type. Due to this fact, the formulation of a standard laboratory test procedure is necessary.

Shrinkage cracking is one of the major causes of pavement failure. The manifestation of wide cracks leads to performance related distresses. Cracks provide zones for the infiltration of water into the underlying layers, an aspect that results in further deterioration of the pavement structure. However, the evaluation of shrinkage at laboratory level is not usually undertaken. Disregarding shrinkage evaluation stems from the fact that a number of guidelines consider it as a natural material characteristic. The road industry frequently depends on the use of low cement contents among other techniques as a means to mitigate shrinkage cracking in cement-stabilised layers. The selection of a mitigation measure usually lacks reliable data concerning the material's shrinkage potential. Because of this, the requirement to evaluate shrinkage at laboratory level as part of a material property measure provides a good indication regarding the quality of material.

Nanotechnology products such as the Nanotterra Soil® a polymer cement additive are purported to mitigate shrinkage cracking in cement-stabilised layers. However, their suitability for use remains unspecified and dependent on the stakeholders. With the development of a shrinkage method, the evaluation of shrinkage reducing products can be undertaken.

This research proposes a flexural beam test protocol for cement-stabilised materials, comprising of a span-depth ratio of nine or greater as fitting to provide a reliable measure of the material's flexural strength and elastic modulus. The developed shrinkage test method provides a good repeatability and is user friendly. The test provides a good indication of the shrinkage criteria of ferricrete and hornfels with and without the polymer. The efficacy of the polymer is dependent on the cement content in the mix and the type and quality of the material. The research provides insight pertaining to the characterisation of shrinkage, behavioural properties, and durability of cement-stabilised materials. Analysis of the shrinkage crack pattern reveals that use of the polymer lessens the development of tensile stress in a cement-stabilised layer. Equally, the application of the low cement contents for stabilisation may not result in cracking of the stabilised layer. This research contributes to a better understanding of cement-stabilised materials.

Opsomming

Namate hoë kwaliteit konvensionele materiale uitgeput raak, word sementstabilisasie van stutlaag en kroonlaag materiale al hoe meer oorweeg en is dit 'n geskikte oplossing vir die padbou-nywerheid. Soos vir alle padboumateriale moet die ontwerpeienskappe bepaal word deur middel van betroubare toetsmetodes wat 'n goeie aanduiding van die materiaal se eienskappe sal gee. Enige evaluering moet 'n beter insae in die materiaal se ingenieurseienskappe en gedrag oplewer. Dit moet dan die basis vorm om die materiaal se gebruik in 'n padstruktuur te evalueer. Die padbou-nywerheidmaak grootliks staat op die toetsing van skuifsterkte van sementgestabiliseerde materiaal om die geskiktheid daarvan vir gebruik te bepaal. Sterkte op sigself lewer egter nie 'n betroubare maatstaf van die materiaal se gedrag en duursaamheid nie. Dit is aangesien 'n sementgestabiliseerde laag baie solied mag wees maar nogtans nie sterk genoeg om belasting te weerstaan en bestand teen omgewingstoestande te wees nie. Net so mag 'n gestabiliseerde laag vatbaar vir kraakvorming as gevolg van krimping wees en dit kan lei tot duursaamheid-verwante en werkverwante skade.

'n Gestabiliseerde stutlaag en kroonlaag in die plaveiselstruktuur is onderhewig aan trekspannings en vervormings as gevolg van verkeerslaste. Op laboratoriumvlak boots die balkbuigtoets die spanning en vervorming wat 'n plaveisellaag ondervind tot 'n aanvaarbaar hoë mate na. Die toets beskik nie oor 'n standaard-toetsprosedure nie. Dit lei tot afwykings terwyl dieselfde materiaal evalueer word. Om hierdie rede is die ontwikkeling van 'n standaard-laboratoriumprosedure nodig.

Krimpkraking is een van die grootste oorsake van plaveiselswigting. Die onwikkeling van wye krake lei tot werksverwante skade. Krake veroorsaak areas vir die infiltrasie van water in die onderliggende plaveisellae wat verdere agteruitgang van die plaveiselstruktuur veroorsaak. Desnieteenstaande word 'n evaluering van kraking op laboratoriumvlak selde gedoen. Dit spruit uit die feit dat 'n aantal ontwerp-riglyne kraking as 'n natuurlike materiaaleienskap beskou. Die padbounywerheid moet dikwels staatmaak, op onder andere, 'n lae sementinhoud om krimpkraking te minimeer. Hierdie tipe benadering gaan dikwels mank aan betroubare inligting oor die materiaal se krimpingspotensiaal. Om hierdie rede is die ondersoek van krimping op laboratoriumvlak nodig as deel van die ondersoek van die materiaaleienskappe om die kwaliteit van materiale te bepaal.

Minimeringstegnieke verander deurlopend. Die toepassing van nanotegnologieprodukte, soos Nanotterra Soil®, 'n polimeersement bymiddel, wat na bewering krimpkraking in sementgestabiliseerde lae kan minimeer, kom voortdurend op die mark. Nogtans bly hulle geskiktheid ongespesifiseerd en afhanklik van die leweransiers. Indien 'n krimptoetsmetode ontwikkel word, sal die effektiwiteit van krimpverminderingsmiddels getoets kan word.

Hierdie navorsing stel die ontwikkeling van 'n toetsprosedure vir 'n balkbuigtoets voor met 'n spanlengte tot diepteverhouding van minstens nege as betroubare maatstaf van 'n materiaal se buigsterkte en modulus van elastisiteit. Die ontwikkelde krimptoetsmetode lewer 'n goeie herhaalbaarheid en is gebruikersvriendelik. Die toets verskaf 'n goeie aanduiding van krimpingskriteria van ferrikreet en horingfels met en sonder polimeer. Die effektiwiteit van die polimeer hang af van die sementinhoud in die mengsel asook die tipe en kwaliteit van die materiaal. Die navorsing verskaf insig aangaande die karakterisering van krimping, gedragseienskappe en duursaamheid van sementgestabiliseerde materiale. Die navorsing help mee om sementgestabiliseerde materiale beter te verstaan.

Acknowledgements

I greatly acknowledge the following persons:

- Professor Kim Jenkins for his valuable, dedication and selfless contribution of time, support and assistance including his insightful and inspirational guidance
- The Raubex Group Limited for their sponsorship. Special thanks go to Mr Koos Raubenheimer and his technical and management team
- Ir. L.J.M. Houben of Delft University of Technology in the Netherlands for availing the analysis software, including his keen and insightful guidance
- Professors Martin van de Ven and Andre Molenaar of Delft University of Technology in the Netherlands for their most treasured insightful contributions
- Dr Phil Paige-Green, Dr Harold Bofinger and Dr Marius de Wet for their valuable and insightful guidance
- Ms. Christa de Wet, Ms. Hellen Venter and Catherine Hurley for their keen and dedicated commitment in proof reading this dissertation
- My fellow researchers at the institute of integrated technology [IIT] and other research institutes with whom we have shared the most insightful discussions over the years
- Laboratory assistants and workshop managers for their availability, commitment and dedication; special thanks go to Mr Colin Isaacs and Mr Gavin Williams
- My dear friends both near and afar, who not only encouraged me during the difficult times, but also dedicated time to counsel and support me.
- My entire family especially my late father, Dr. John C. Ndiku and mother, Ms. Harriet O. Ndiku for laying the foundation for me, my late wife, Ms. Crystal Rwivanga-Mbaraga for her treasured love and support she showed
- To the Almighty God for the Strength and Health given; Isaiah 49:16 "*Behold, I have inscribed you on the palms of My hands; Your walls are continually before Me.*"

Dedications

I dedicate this research work to the following:
My late father, Dr. John Chrysostom Ndiku [1947 – 2013]
My late wife, Ms. Crystal Ingabire Rwivanga-Mbaraga [1984 – 2012]
My late uncle, Prof. Enoch Nshakira Kwizera [1950 – 2013]

You all remain the most cherished people that I will continually reminisce to have shared a good life with,
Rest in Eternal Peace.

USED ABBREVIATIONS

C&Ci	Cement and Concrete Institute
C-S-H	Calcium-Silicate-Hydrates
CT	Computerised Tomography
CTE	Coefficient of Thermal Expansion
EG	Equivalent Granular
FLAC^{+}	Fluid-Loss Control Agents
ITS	Indirect Tensile Strength
MDD	Maximum Dry Density
NTS®	Nanoterra Soil®
OMC	Optimum Moisture Content
OPC	Ordinary Portland Cement
PCA	Portland Cement Association
RSD	Rotational Shear Device
SRA	Shrinkage-Reducing Additives
UCS	Unconfined Compressive Strength
XRD	X-Ray Diffraction

Table of Contents

Chapter 1: Introduction

1.1 Background

The key objective of pavement design is to provide a cost effective pavement structure that offers a satisfactory level of service. In order to achieve this design objective, materials used to construct the pavement layers must possess viable engineering properties and characteristics. This suggests that the designer must have knowledge regarding materials selected and information relating to traffic and the environment. Information relating to the performance of materials as well as the anticipated traffic and environment is essential. Bearing in mind the variables and interactions that influence the design of pavements, consideration of a systematic method remains indispensable. Pavement design is dependent on the obtained data and knowledge concerning material performance and their durability.

The philosophy pertaining treatment of materials presumes that use of stabilisers such as cement enhances the original engineering properties of materials. By adding cement to material, the engineering properties of soils and gravels such as plasticity, strength and permeability are usually improved. Modification is the application of low quantities of cement or stabiliser to materials. However, certain materials exhibit moderate property enhancement with low quantities of cement. Cementation involves the use of high cement contents and normally results in significant improvement of engineering properties, [TRH13, 1986].

Cement-stabilised layers provide an excellent support for the pavement structure. This is because stabilised materials are more resilient, uniform and water resistant than equivalent un-stabilised types. The use of stabilised layers in the construction of the pavement structure lessens the incidence of stress-related distress. However, cement-stabilised layers [either as base or sub-base] are a source of cracking [drying shrinkage] and pavement failure. Shrinkage cracking is a natural material characteristic caused by drying of the stabilised layer [Bofinger *et al.* 1978]. Despite the occurrence of shrinkage, the consideration of cement stabilisation remains widely carried out as an alternative to constructing pavements. Detrimental effects emanating from shrinkage cracks are a significant challenge to the road industry. The cracking of a stabilised layer normally leads to poor load transfer, particularly in the region of the crack where the resultant crack width is wide. Several factors contribute to the consideration of stabilised layer and these include [Bofinger *et al.* 1978; Epps *et al.* 1979, TRH13, 1986; Paige-Green, 2008]:

a) scarcity of high-quality materials
b) long-hauling distances
c) high-energy costs
d) the need to reduce aggregate usage for environmental and conservational reasons

1.2 Cement Stabilisation

Stabilisation of pavement layers dates back to over 2000 years ago when the Romans used lime to improve the quality of the base and sub-base layers. Epps *et al.* [1979] state that material modification became prominent in the road and airfield constructions after the Second World War; this was predominantly due to scarcity of conventional aggregates. Currently increases in axle loads contribute towards the use of cement-stabilised layers in both road and airfield pavement constructions.

For stabilising materials, Ordinary Portland cement [OPC] is preferred. The cement type consists of calcium oxide, calcium silicates and aluminates. In the presence of moisture, the cement hydrates forming hydrated compounds, which eventually harden over time producing a cemented matrix. The cemented matrix binds the material particles together and is responsible for an increase in strength. Strength of stabilised materials originates from the

hydrated cement matrix, [Epps *et al.* 1979; Lay, 1986; TRH13, 1986]. Stabilisation using cement has proven successful with most materials except with soils or gravels that contain high organic content. High organic matter retards the hydration process causing less cementation effect, [Bofinger *et al.* 1978; Epps *et al.* 1979, TRH13, 1986 and Paige-Green, 2008]. Chapter 2 notes on cement hydration, related theoretical principles, as well as the resultant material strength.

There are different types of stabilisation and each has its benefits and disadvantages besides providing different material quality and characteristics. Primarily, the quantity of cement in the mix plays a significant role in the resultant quality and material performance. The quality of the material along with the added cement content influences the resultant engineering properties and characteristics after stabilisation. Apart from cement stabilisation, other common stabilisation types include:

a) mechanical stabilisation
b) lime stabilisation
c) bitumen or tar stabilisation
d) other stabilisation types that incorporate the use of blast furnace slag, pozzolana and non-pozzolanic chemical stabilisers

Material stabilisation can be categorised as chemical or non-chemical categories. Lime, bitumen and cement stabilisation are categorised as chemical. Mechanical stabilisation is categorised as non-chemical because it does not involve any use of chemical additives. Mechanical stabilisation involves adding other material type with a purpose of improving their quality, [Epps *et al.* 1979].

Lime stabilisation is only effective with materials that contain quantities of clay; it is material specific. Attempts to use lime as a binder in the same manner as with cement, has proved mostly futile, [Watson, 1994]. Figure 1-1 shows lime and cement limitations based on the compressive strength tests. Cement and lime stabilised materials are usually approved based on strength tests.

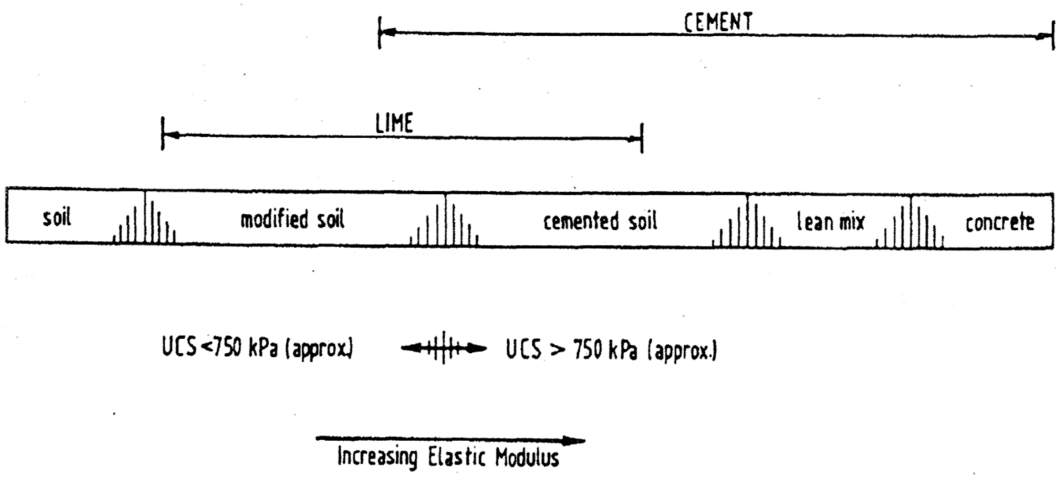

Figure 1-1 Modification and cementation using lime and cement [Dunlop, 1978]

Bitumen stabilisation provides additional benefits related to the visco-elastic nature of bitumen. Other forms of stabilisation types such as blast-furnace slag do not offer substantial engineering properties. Practice seldom considers these forms of stabilisation in combination with cement. The addition of cement improves the cementation properties, [O'Flaherty,

1988]. Preference of cement stabilisation stems from significant enhancement of the material properties besides its availability and extensive experience with practice.

1.2.1 Cement-Stabilised Material Types

The binding properties of cement are greater than that of lime of an equal quantity, [Dumbleton, 1962; Sherwood, 1993]. The amount of cement in the mix influences the particle bond-strength and thus, the overall material strength. There are three categories of cement-stabilised materials, [Lay 1986; Croney *et al.* 1998]:

a) soil-cement materials
b) cement bound granular materials
c) lean concrete

1.2.2 Problems Associated with Cement-Stabilised Layers

Cement-stabilised layers exhibit specific problems related to material characteristics, construction procedure, as well as overall stabilisation. Even though the application of cement results in improved engineering properties, the manifestation of shrinkage cracks could cause detrimental effects to the pavement structure. With careful material selection allied with evaluation and quality control measures, several of these demerits associated with cement stabilisation can be minimised. The problems associated with the use of cement-stabilised materials are categorised under construction and durability as follows:

a) construction related problems include;
    i. material evaluation and thereafter, interpretation of test data
    ii. cement content and appropriate mixing criteria of the constituent components
    iii. compaction technique relative to achievable density
    iv. curing procedure
b) durability related problems include;
    i. carbonation
    ii. sulphate and salt damage
    iii. shrinkage cracking [dry shrinkage]
    iv. material disintegration [layer break-up and deterioration]

Problems associated with cement-stabilised materials not only suggest that the correct cement content is required but the selected material and overall mixture should be effectively carried out. Preparation of cement-stabilised materials includes rationing, mixing, compaction, as well as curing. The curing technique adopted must provide suitable conditions to retain moisture in order to allow for substantial strength-gain but minimal shrinkage. By applying appropriate curing procedures along with ensuring that the mix possesses the correct cement content minimises the effects of carbonation, [Paige-Green *et al.* 1990]. With reference to the layer and material disintegration, De Beer and Visser, [1997] establish that contact stress patterns of a tyre are concentrated at the tyre edges. If a stabilised layer is directly underneath a thin surfacing layer or bituminous seal, crushing of the stabilised layer will occur because of the prevailing low abrasion resistance. Chapter 2 notes on the principles pertaining shrinkage, layer cracking, behavioural properties and durability.

1.3 Shrinkage Cracking in Stabilised Layers

A freshly compacted stabilised layer contains some amount of moisture. The hydration process, partly consumes a percentage of the layer moisture and the rest is lost through evaporation. The exposure of the layer to temperature and air [thermal effects] results in the evaporation of moisture. The rate of moisture loss [evaporation] is dependent on the prevailing temperature and humidity. As the stabilised layer dries out, it tends to reduce in

size [shrink] due to the loss of moisture. However, the layer is restrained to a certain degree, which contributes to the development of tensile stresses. Shrinkage is due to the self-desiccation [drying-out] of material. Several factors, including restraints, thermal effects and material characteristics influence the rate and magnitude of shrinkage and the resultant cracking, [George, 1973; Bofinger *et al*, 1978]. Chapter 2 provides the theoretical principles on shrinkage crack patterns along with its causal factors.

1.3.1 Methods for Mitigating Shrinkage Cracks

Shrinkage is a natural characteristic of cement-stabilised materials, [TRH13, 1986]. The stabilised layer develops tensile stresses as differences in temperature and moisture arise; the induced stresses are only relieved by cracking. However, several methods are applied as a means to mitigate shrinkage cracks in a stabilised layer. The methods used to mitigate shrinkage cracks in a cement-stabilised layer include:

a) reducing cement content
b) pre-cutting the stabilised layer
c) pre-cracking the freshly compacted stabilised layer
d) use of shrinkage reducing additives and admixtures

The amount of cement in the mix plays a significant role because of its direct influence on moisture consumption and strength gain. The pre-cutting technique involves introducing cuts [grooves] at close intervals within a stabilised layer; the aim is to control the resultant crack pattern. Similarly, pre-cracking a freshly compacted stabilised layer induces numerous fine cracks at closer spacing, which also controls the resultant crack pattern. A number of shrinkage reducing additives and admixtures normally apply physical and/or chemical mechanisms to lessen the rate of moisture loss and/or increase early initial strength gain. However, a lack of experience and confidence regarding suitability of shrinkage-reducing products has led to their limited use. Chapter 2 notes on the mitigation of shrinkage relative to the inherent theoretical principles.

1.3.2 Shrinkage Cracking and Technological Innovations

Research into shrinkage of cement-stabilised materials and layer cracking offers different concepts. Nakayama and Handy [1965] performed research on soil-cement mixtures and reported that there is no relationship between cement content and shrinkage despite conclusions from other researchers. Bofinger *et al.* [1978] researched on fined-grained soil-cement mixtures and reported that an increase in cement content results in a decrease in shrinkage. George [1973] and Scullion *et al.* [2000] assert that total shrinkage is minimal at optimal cement content. Generally, different materials possess dissimilar characteristics and properties, thus diverse shrinkage criteria. Shrinkage is dependent on several factors, including restraints, material characteristics [cement and moisture contents] as well as temperature and humidity. Chapter 2 of this dissertation reviews the various studies along with the hypothesis, findings and deductions made.

Autogenous and drying shrinkage are the two categories of shrinkage. Drying shrinkage causes the majority of shrinkage cracking in cement-stabilised layers, [George, 1973; Scullion *et al.* 2000]. Research into dry shrinkage cracking continues to gain interest, particularly with the intensified scientific innovations that aim at its alleviation.

Nanotechnology has gained interest in several research fields, including engineering, medicine and material science; it involves material alterations. The focus on the mitigation of shrinkage cracking in cementitious materials is of interest in this research. The use of nano-particles in materials leads to the alteration of their functionalities and properties. Use of nano-particles in cementitious materials reported different characteristics and performance criteria. Research into nanotechnology and cementitious mixtures reveal the following:

a) The efficacy of nano-particles is dependent on their interaction with the calcium-silicate-hydrates [C-S-H] in cement and material particles, [Tao, 2005].
b) Tao, [2005] notes that in concrete the nano-SiO_2 particles react with calcium hydroxide ($Ca(OH)_2$) crystals producing C-S-H gel.
c) Luciano *et al.* [2009] assert that nano-SiO_2 can fill spaces between particles of C-S-H gel [acting as nano-filler].
d) Tao, [2005] states that the addition of nano-SiO_2 particles to concrete reduces the voids content and thus, improves the microstructure.
e) Qing *et al.* [2007] note that nano-SiO_2 particles reduce the calcium-leaching rate of cementitious materials an aspect that improves durability.

Reaction of nano-SiO_2 particles with calcium hydroxide crystals leads to a reduction in size and amount of crystals. As a result, the interfacial transition zone of aggregates and cement besides the general microstructure are changed. A reduction of the material porosity not only influences the permeability properties but the loss of moisture; this alters the resultant total shrinkage.

1.4 Material Behavioural Properties and Durability

Material behavioural properties take into account mechanical and deformation properties along with the resultant response due to loading and non-loading effects. The mechanics of deformation and fracturing behaviour of stabilised layers are characterised by their deformation and response criteria. Fracture mechanics pertaining to cement-stabilised materials are dependent on several factors that include:

a) the loading mode relative to specimen geometric characteristics
b) particle bond-strength
c) existence of cracks and cracking behaviour
d) heterogeneity of the materials

In order to ensure that the quality of stabilised materials is adequate strength tests are carried out, [Lay 1986]. Several design guidelines specify a 7-day cured strength test or its equivalent. However, evaluation of materials in terms of strength alone neither provides a good reliability of the engineering properties nor ascertains the long-term performance criterion.

Long-term performance of cement-stabilised materials encompasses the assessment of their durability. Durability is a time-reliant factor influenced by the present state of the material in relation to the level of weathering. In evaluating the durability of stabilised materials the abrasion-resistance tests while following specific conditioning criteria are carried out. The wet-dry and freeze-thaw test are commonly used tests, [TRH13 1986]. The durability of a cement-stabilised layer is primarily concerned with the effect of chemical reversal associated with moisture intrusion and movement, [Paige-Green *et al.* 1990]. In order to ensure that the cement-stabilised layer is capable of providing a long-term service, implementation of control measures during design and construction are emphasised. Chapter 2 notes on the concepts and principles pertaining to control measures in relation to material durability.

1.5 Contextualisation of Pavement Design and Materials

Pavement materials are a function of their engineering properties which include strength, elastic moduli or stiffness, [Austroads, 1992; TRH14, 1996]. Austroads, [1992] notes that to design a feasible pavement structure sufficient knowledge and information should include:

a) durability [influential factors and mechanism of deterioration]
b) load-response and behavioural characteristics [stress and strain parameters necessary for quantifying the rate and degree of distress relative to its damaging effects]
c) material limitations in proportion to traffic loading and environmental conditions

The philosophy and aim of stabilising materials is to extend the normal pavement service life. Usually the performance of a stabilised material is anticipated to be at least equal to, if not better than that of good quality natural materials. The key objective of cement stabilisation is to improve the performance of materials by enhancing their engineering properties. Any pavement design ought to reflect the relative cost of construction and rehabilitation as well as typify the viability of materials used. This proposes that pavement layer materials must possess feasible engineering properties capable of withstanding traffic loads and enduring the adverse environmental conditions. Material engineering properties and characteristics such as strength and elastic modulus are essential to the design of pavements.

Before stabilising materials, a laboratory test programme is carried out. The aim of the laboratory tests is to determine the necessary moisture and cement contents; this phase of evaluation is part of the mix design criteria. The objective of mix design is to select an appropriate combination of materials with viable strength and acceptable permanency. Structural design ensures that the selected materials provide feasible support to the anticipated traffic loads. Durability is a diverse measure of the present state of materials. Material evaluation is an essential phase for both mix and pavement designs; it provides insights concerning the suitability of materials.

1.6 Problem Statement

Breaking or fracturing typifies a failure criterion of any civil engineering structure; this occurs when the applied load exceeds the maximum load carrying capacity of the structure. In pavement engineering, the applied load on the structure is usually lower than material strength. In general, one traffic load does not fail the pavement structure; this could cause some infinitesimal damage. Damage to the pavement structure gradually increases until it results in an unacceptable level of service. Deterioration of the pavement structure is primarily dependent on the quality and type of the layer materials along with its unison in withstanding load and environment.

In Southern Africa, a maximum design-life of 20 years for flexible pavements is usually considered as acceptable. However, a number of pavements can neither sustain traffic loads nor endure the adverse environmental conditions for the specified design-life. Several factors, including heavy traffic loads and a shortage of viable natural material types contribute to early pavement distresses. One of the major factors for considering a stabilised layer in the pavement structure is because of its excellent load-support. However, stabilised layers crack due to drying shrinkage; this contributes to early pavement distresses and increased damage emanating from the environment and traffic loads.

The evaluation of material shrinkage at laboratory level is rarely considered. A lack of adequate evaluation of materials not only leads to a poor comprehension of their suitability but also results in early pavement failure [before the end of the design-life]. If the resultant shrinkage cracks become wider, degradation of the pavement structure normally occurs. Poor riding quality along with the delamination of the layers [localised failure at the region of crack] signify pavement degradation. The objective of pavement design is to avoid excessive stressing of the layer, which ultimately causes failure. Occurrence of wide shrinkage cracks within the pavement structure results in a poor load - transfer. Equally, the wider the crack width the more water infiltration and subsequent pumping of fines from the under-layer. An increase in the load induced stresses [especially at the crack edges] results in secondary cracks.

Following this background, a disregard to evaluate shrinkage presents various knowledge-gaps concerning material suitability and layer cracking; this could also lead to an erroneous consideration of a different mitigation technique. Alleviation of shrinkage helps to control the tendency of a stabilised layer to crack. Without any substantial information regarding

material shrinkage, the appropriate mitigation technique may not provide the 'desirable' crack pattern. Several factors besides the cement content in the mix contribute to layer cracking. Current measures to mitigate shrinkage using low cement dosages do not embrace all materials. Some studies have shown that material quality and related intrinsic properties play a more significant role in layer cracking than cement content.

Evaluation of materials should include test methods that reliably provide an actual measure of the properties; this offers dependable insights regarding their suitability for use. Assessment of material shrinkage should follow suit; the test method should provide a reasonable measure. The current measure of stabilised material and approval of their suitability encompasses strength tests. In ascertaining the suitability of stabilised materials, consideration of strength as a benchmark predominates any other property measure. However, consideration of strength alone does not validate material suitability. A reliable measure of the stress-strain behaviour [elastic moduli] of the stabilised materials is essential. This is because a stabilised material might exhibit significant strength but poor load-response. Therefore, a measure of the material elastic modulus in addition to its strength is necessary.

In the measure of material strength, the commonly used methods do not typify the forces subjected to the stabilised layer. Commonly used strength tests include the Unconfined Compressive Strength [UCS] and Indirect Tensile Strength [ITS]. A stabilised layer experiences tensile stresses and strains emanating from the traffic loads. This proposes that evaluation of stabilised material tensile strength is essential. Strength is a property required in the mechanistic pavement design. The consideration of strength as a construction control measure is often undertaken.

For the tensile strength measure, the flexural beam test is preferred. The beam test simulates to an acceptable degree the mode of stress, which the stabilised layer experiences under a wheel loading; the test is seldom used to evaluate stabilised materials. As an alternative, the UCS test data is used to estimate the material strength and elastic moduli. The UCS test only characterises the degree of cement treatment by subjecting all specimen fibres to compression forces; the test does not simulate field criteria. In order to establish a reliable measure of the stress-strain behaviour of the stabilised layer a test should simulate field behavioural criteria.

Selecting an applicable elastic moduli parameter of stabilised materials is further complicated because of the lack of standardising the flexural beam test. For the same materials, different flexural strength and elastic modulus values result due to the dissimilarities within the test protocols. The extent of the deviation of the flexural strength and elastic moduli from the actual material measure depends on several factors, which include:

a) the beam geometric characteristics [span/depth ratio]
b) degree of fixity at the support ends
c) loading application points
d) maximum aggregate particle size and overall particle distribution relative to specimen geometric characteristics

The need to standardise the flexural beam test for the evaluation of cement-stabilised materials, is essential. By not standardising the flexural strength beam test not only results in divergent measure of material but also obscures the designing of pavements. Development of a shrinkage test method is necessary for the evaluation of material shrinkage. With the increased quest for and consideration of alternative materials, the need to ascertain their suitability for use in the pavement structure is even more critical than before. The present economic recession, environmental stewardship and scarcity of good quality materials intensify the consideration of stabilisation, reliable evaluation and overall control measures as well as adhere to sustainable practices.

1.7 Key Objectives and Significance of the Research

The key research objectives and significance include:

a) *To develop a shrinkage test method to evaluate stabilised materials:* The method and overall procedure must provide better reliability and repeatability both with the test setup and in the measure of material shrinkage. Additionally, it is important that the test method be feasible, simple and quick to conduct without intensive training. Resultant shrinkage test data should provide a good understanding of material suitability for use in the pavement structure.
b) *To predict a shrinkage crack pattern [crack width and crack spacing]*: A translation of the test data to field shrinkage criteria is an objective of this research. This requires modelling of the test data. Analysis of the layer crack pattern [crack width and spacing] provides the opportunity of assessing the long-term performance and to an acceptable degree, the durability.
c) *To evaluate the influence of cement contents on material shrinkage criteria*: Different materials portray varying shrinkage criteria. The hypothesis that shrinkage is fundamentally dependent on cement content presents a simplistic approach. In this research study, the influence of cement content with respect to material type is considered. This assessment offers insights into shrinkage criteria relative to cement content and material. These insights help examine the fundamental factors concerning shrinkage and material characteristics.
d) *To evaluate the suitability of nanotechnology products in mitigating material shrinkage*: This evaluation is limited to the polymer as a representative nanotechnology product that is purported to reduce shrinkage. The polymer is a cement additive. The evaluation also encompasses the determination of the polymer application rate, its effect on cement and stabilised materials.
e) *To evaluate on the material moisture susceptibility as a durability measure and influence of the polymer*: The measure of the material's durability and the influence of the polymer are required. This experimentation assesses the effect of the polymer on the engineering properties of stabilised materials.
f) *To propose a standard flexural beam test protocol, including beam geometric characteristics* with acceptable reliability for the effective measure of material mechanical and flexibility properties.

1.8 Scope and Limitations of the Research

The research focuses on the evaluation of cement-stabilised materials in terms of shrinkage, behavioural properties and durability. A gravel-crushed aggregate [hornfels] and natural soil material [ferricrete is also referred to as laterite] with significantly different classifications are considered. The research also includes the evaluation of a polymer with the aim of establishing scientific criteria under which new products are studied.

Due to contractual related matters from the stakeholder, no chemical analysis of the polymer is carried out. The research is limited to, establishing the optimum application rate of polymer to cement and assess its effect on stabilised materials at laboratory level. Chapter 3 lays out the research methodology. The research covers a laboratory evaluation of the engineering properties of hornfels and ferricrete. Tests conducted include standard strength tests on top of the flexural beam and shrinkage tests. Based on a concrete flexural beam testing, an approach to developing the flexural beam and related configurations followed. This included varying the span/depth ratio with respect to beam geometric characteristics and maximum aggregate particle size. This experimentation phase investigated the influence of beam shear stresses on the mechanical behavioural response [beam deflection]. Mechanical properties typify the mix quality [particle bond strength], which is fundamental in the computation of flexural strength and elastic moduli parameters.

1.9 Research Contributions

This research contributes literature regarding shrinkage cracking, behavioural properties and durability of cement-stabilised materials. Development of a shrinkage test method provides an approach for material evaluation, especially following the consideration of alternative types. Insights gathered from the shrinkage test data and related analysis offer additional understanding regarding material suitability for use in the pavement structure.

As the concept of reliability gains significance in material science and engineering the prerequisite to evaluate materials in line with field criteria is key. Laboratory evaluation should provide feasible insights regarding the suitability of material for use in the pavement structure. This infers that laboratory test interpretations are the backbone of the decision-making process regarding the consideration of a field evaluation and related implementation. This research proposes a standard test method for flexural beam testing including the analysis. In view of technological innovation [polymer], this research contributes to the understanding of nanotechnology products and their applicability in cement-stabilised materials [road industry as a whole]. Current knowledge-gaps concerning nanotechnology and its product efficacy in altering material functionalities and performance require a research based approach and analysis.

1.10 Organisation of the Dissertation

The following chapters provide the theoretical principles, test protocols adopted along with acquired test results and related analysis. The last chapter of this dissertation provides research conclusions as well as recommendations. This dissertation includes literature, research methodology and material engineering properties [results and analysis].

Chapter 2 Literature Review: This section provides theoretical principles and knowledge-based data from previous studies. In this chapter, shrinkage cracking mechanisms and its influence on performance and durability are stated. Factors that influence shrinkage cracking and its occurrence are also stated, together with the control measures so far in place. The relationship between shrinkage cracking and pavement durability is noted. The discussion of the concepts regarding 'desirable' crack pattern [fine crack width at short spacing] is noted. This chapter sets the knowledge base for this research by laying out the fundamental theoretical principles, concepts and practical implications with cognisance of material viability and cement content.

Chapter 3 Research Methodology: The chapter lays out the research approach adopted, including the materials, test procedures and variables within the research. Test parameters and criteria along with the test method and inherent concepts are stated. The chapter also notes on the mix design criteria with reference to the Southern African practice and related technical specifications.

Chapter 4 Material Characterisation, Strength and Durability Results: This chapter discusses the characterisation of materials, standard strength and durability results. Material characterisation includes index test results such as Atterberg limits and material gradation. In addition, mix design results based on the compressive and indirect tensile strengths are stated. This chapter includes analysis and discussion of results based on standard tests as usually adopted by the practice.

Chapter 5 Flexural Strength Results: In this chapter, the flexural strength results following selected test configurations relative to beam geometric characteristics are stated. Resultant beam shear stresses based on both laboratory test data and Finite Element Modelling [FEM] are also noted. Material parameters including flexural strength, elastic moduli, fracture energy and strain-at-break are noted. The chapter provides results regarding flexural beam testing of cement-stabilised materials.

Chapter 6 Shrinkage Measurement: Shrinkage test data along with partial analysis is noted. The chapter includes cylindrical [axial and circumferential shrinkage] and beam [linear shrinkage] shrinkage results for stabilised materials. The characterisation of material shrinkage based on the test trend is laid out. Additionally conceptualisation and assessment of material drying shrinkage at laboratory level under specified test conditions are stated.

Chapter 7 Analysis of Crack Pattern in Cement-Stabilised Layers: This chapter provides an in-depth analysis of the obtained laboratory results by making specific reference to the probable material field criteria. In this chapter, prediction of the shrinkage crack pattern based on material properties and influential factors to layer cracking including environment and restraints is carried out. The analysis also provides insights related to polymer application and its effectiveness. Fundamental discussions along with the relevant findings to the field material performance are stated. The chapter provides an in-depth assessment of the material properties in relation to field criteria.

Chapter 8 Conclusions and Recommendations: This chapter contains the significant conclusions of the research along with recommendations for further research. In this chapter a summary of the research findings, insight and further investigations are stated.

1.11 References

Austroads (1992) *Pavement Design: A Guide to the Structural Design of Road Pavements*. Australian Road Research Board, ARRB.

Bofinger, H.E., Hassan, H.O. and Williams, R.I.T., (1978) *The Shrinkage of Fine-Grained Soil-Cement*. TRRL Supplementary Report 398, Transport and Road Research Laboratory (TRRL).

Croney, D. and Croney, P., (1998) *The Design and Performance of Road Pavements* 3rd Edition Published by McGraw-Hill

De Beer, M., Fisher, C. and Jooste, F.J., (1997) *Determination of Tyre/Pavement Interface Contact Stresses Under Moving Loads and Some Effects on Pavements with Thin Asphalt Surfacing*, Technical Report No. TR-96/050, CSIR.

Dunlop, R.J., (1978) *Some aspects of pavement design and performance incorporating lime and cement stabilised layers in New Zealand*, Ministry of Works and Development.

Dumbleton, M.J., (1962) *Investigations to Assess the Potentials of Lime for Soil Stabilisation in the UK*, Road Research Technical Research Paper No. 64, HMSO, London, UK

Epps, J.A., Terrel, R.L., Barenberg, E.J., Mitchell, J.K. and Thompson, M.R., (1979), *Soil Stabilisation in Pavement Structures; A User's Manual Volume 1 Pavement Design and Construction Considerations*, Federal Highway Administration Department of Transportation, Washington DC 20590.

George, K.P., (1973) *Mechanism of Shrinkage Cracking of Soil-Cement Bases*, Highway Research Record 442, HRB, National Research Council, Washington DC pp. 1-10.

Lay, M.G., (1986) *Handbook of Road Technology* Includes Chapter 10: Stabilisation (Re-drafted 1988) Published by Gordon & Breach.

Luciano, S., Labrincha, J.A., Ferreira, V.M., Dachamir, H. and Wellington, R.L., (2009) *Effect of Nano-Silica on Rheology and Fresh Properties of Cement Pastes and Mortars*, Construction and Building Materials 23 (2009) Pp. 2487-2491.

Nakayama, H. and Handy, R.L., (1965) *Factors Influencing Shrinkage of Soil-Cement*, Highway Research Record 86 HRB National Research Council, Washington DC pp.15-27.

O'Flaherty, C.A., (1988) *Highway Engineering* 3rd Edition Volume 2 Published by Edward Arnold.

Paige-Green. P., Netterberg, F. and Sampson, L.R., (1990) *The Carbonation of Chemically Stabilised Road Construction Materials: Guide to Its Avoidance*, CSIR Report No. PR 89/146/1.

Paige-Green, P., (2008) *A Reassessment of Some Road Material Stabilization Problems*, 7-11 July 2008, Proceedings of the 27th Southern Africa Transport Conference (SATC, 2008) ISBN Number 978-1-920017-34-7, Pretoria South Africa.

Qing, Y., Zenan, Z., Deyu, K. and Rongshen, C., (2009) *Influence of Nano-SiO_2 Addition on the Properties of Hardened Cement Paste as Compared with Silica Fume,* Construction and Building Materials 21 pp. 539 – 545.

Sherwood, P.T., (1993) *Soil Stabilisation with Cement and Lime*, Transport Research Laboratory State of the Art Review, Published by HMSO.

Scullion. T., Sebesta S.J., Harris, P. and Syed, I., (2000) *A Balanced Approach to Selecting the Optimal Cement Content for Soil-Cement Bases* Report 404611-1.

Tao, J., (2005) *Preliminary Study on the Water Permeability and Microstructure of Concrete Incorporating Nano-SiO_2* , Cement and Concrete Research 35 pp. 1943-1947.

TRH13., (1986), *Cementituos Stabilisers in Road Construction,* Technical Recommendations for Highways, TRH 1986, ISBN 07988 3674, Pretoria South Africa

TRH14., (1996) *Structural Design of Flexible Pavements for Interurban and Rural Roads*, ISBN 1-86844-218-7, Pretoria South Africa

Watson, J., (1994) *Highway Construction and Maintenance*, 2nd Edition. Published by Longman Group.

Chapter 2: Literature Review

2.1 Background

This chapter provides key research principles related to the mechanism of material shrinkage, cracking criteria as well as behavioural properties and durability. In order to establish a good understanding, fundamental principles and aspects related to material types and their structural capacity are studied. Current requirements regarding approval of materials for use in the pavement structure include:

a) strength and/or stiffness parameters required to quantify the load bearing properties
b) variations of engineering property parameters due to changes in moisture, ageing and cumulative distress during pavement service-life
c) a material load - response which provides indications regarding the rate of distress
d) material permanence which includes the rate of deterioration as related to durability
e) performance criteria which suggest defining the limiting values of stresses and strains for a given degree of distress

Strength and elastic modulus [stress-strain behaviour] of stabilised materials are the parameters required for the design of pavements. The ratio of stress to strain typifies the stiffness properties. The elastic modulus parameter characterises the behavioural properties and load-response in a stress-strain criterion under load, [Papagiannakis and Masad, 2007].

For cement-stabilised materials, selection of an appropriate elastic modulus value for design purposes is usually complex because of the difficulty in testing. Different test methods provide dissimilar property values for the same material. The elastic modulus value obtained using the tension mode of testing is usually lower than that acquired using the compression approach, [Bofinger, 1970; Chou, 1977; Raad, 1976]. Cement-stabilised materials [like most cementitious material types] are stronger in compression than in tension. However, the relationship between flexural strength and modulus of elasticity comes highly recommended in lieu of testing; the flexural beam test is normally considered. At laboratory level, the value of any material property depends on the test method particularly its test configurations relative to specimen geometric characteristics. At field level, a stabilised layer experiences tensile stresses and strains. This suggests that some form of tensile strength and stress-strain criterion is necessary in evaluating suitability of the stabilised materials.

The tendency of a cement-stabilised layer to crack emanates from restrained thermal and shrinkage movements, [Bofinger *et al.* 1978]. Stabilised layers are major structural elements in the pavement structure because of their contribution in the reduction of deflection [reduced stress]. Occurrence of cracks in the pavement structure may lead to poor load-transfer, particularly in the region of the crack, which is dependent on the resultant shrinkage crack width. However, by applying specific mitigation techniques such as pre-cutting and pre-cracking of the stabilised layer detrimental effects due to cracking are minimised. Pre-cutting and pre-cracking of the stabilised layer lessens the occurrence of wide cracks, [George, 2001].

In this chapter, concepts and philosophies related to concrete and cement paste are considered in order to clarify the underlying principles regarding the behavioural properties, shrinkage characteristics and durability criteria of cement-stabilised materials. However, effects due to higher cement usage in concrete and cement paste compared to cement-stabilised materials must be taken into account. For instance, the resultant tensile strength and stiffness properties of concrete are higher compared to those exhibited by cement-stabilised materials.

2.2 Behavioural Properties of Cement-Stabilised Layers

In order to understand the behavioural properties of cement-stabilised layers consideration of the parameters influencing stabilised material properties is essential. This is because stabilised material properties primarily influence the behavioural states of the stabilised layer and overall pavement structure since the pavement works in unison. Freeme [1984] provides background to behavioural trends of pavement structures relative to layer materials. Engineering properties of stabilised materials contribute to the performance and structural integrity of the pavement structure. Pavement layers should offer sufficient strength capable of sustaining the load and reducing the stresses directed to the subgrade layer, [Papagiannakis and Masad, 2007]. The process for the design of pavements makes assumptions regarding cement-stabilised materials, which includes:

a) cement-stabilised materials are isotopic
b) elastic response of cement-stabilised material is linear
c) a uniform modulus in tension and compression are assumed equal
d) Poisson ratio has little influence

A stabilised layer [base or sub-base] exhibits several characteristics that contribute to their performance. The cement-stabilised layer usually exhibits excellent load-dispersion properties and is minimally affected by moisture, [NAASRA, 1986; TRH13, 1986; Netterberg, 1987]. The layer preserves the integrity of the pavement structure by cushioning subgrade movements. Strength, elastic modulus and material density influence the characteristics and properties exhibited by the stabilised layer; these factors also dictate behavioural response and ultimately pavement performance.

2.2.1 Behavioural Properties

By considering the layer elastic modulus, the behavioural properties are illustrated. The assessment of the layer elastic modulus must take traffic and the environment into account, [De Beer, 1985; Freeme 1984]. Freeme [1984] evaluated the changes in elastic modulus of a stabilised material class C2 [South African material classification system]; Figure 2-1 illustrates the assessment made.

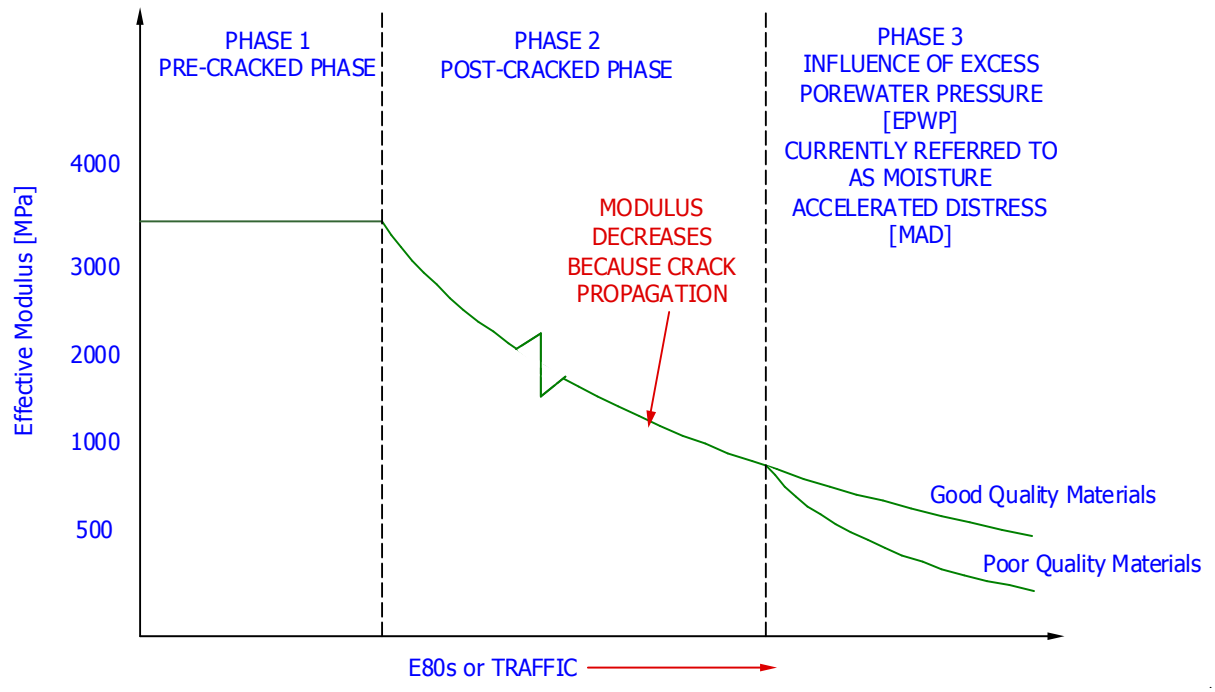

Figure 2-1: Change in Elastic Modulus of a Cement Stabilised Layer [Freeme, 1984]

The phases, pre-cracked, post cracked and influence of moisture-accelerated distress [MAD] exemplifies the trends a stabilised layer undergoes. In the pre-cracked phase, the effective modulus is relatively high and the stabilised layer is intact; it behaves like a concrete slab, [De Beer, 1985; Freeme, 1984]. The occurrence of shrinkage cracks along with repeated loading reduces layer modulus. Although an intact stabilised layer preserves the pavement structural integrity due to its excellent load-dispersion properties, occurrence of cracks reduces the service-life of the pavement; water infiltration and poor load-transfer across the cracks occur, [George, 2001]. Depending on the characteristics of the crack pattern [width of the crack and spacing], localised damage, particularly in the region of a crack may take place due to trafficking; this leads to secondary cracking.

De Beer [1985] establishes that a reduction in modulus will occur even though the individually formed blocks still possess the initial effective modulus; this refers to the load-transfer mechanism around the region of a crack. A reduction in effective modulus is a gradual trend. The final behaviour of the cracked stabilised layer is that of the equivalent granular material. This is dependent on the quality of the original stabilised material type. Other factors influencing the resultant crack pattern include mixing efficiency, material characteristics and restraints imposed on the stabilised layer. Most of the structural and functional life of the stabilised layer takes place in the post-cracked phase.

In Phase 3, due to the spaces between the cracks, water infiltrates into the underlying pavement layers. Cracking attributed to drying shrinkage results in secondary cracking due to localised damage [traffic induced cracking] that leads to discrete blocks. Spaces between blocks offer further passage to the infiltration of water. Water infiltration into the pavement structure leads to a reduction in the layer modulus and strength. The continued water ingress develops in excess pore-water pressure as well as layer instability, [De Beer, 1985; Freeme, 1984]. Development of excess pore-water pressure leads to increased layer deformation due to material shearing and erodibility. In order to characterise the state of a stabilised pavement layer during Phase 3, an assessment of its resilient deflections provides insights regarding its state. Typically, a low deflection suggests a high modulus and thus typifies that the layer is stable. A high deflection denotes that the layer possess a low modulus and suggests instability within the pavement structure. In conducting resilient deflections on a stabilised layer, ascertaining its moisture content is essential; this is because the test is sensitive to moisture.

Figure 2-2 shows the relative behaviour of cement stabilised layers of different material strengths. The equivalent granular [EG] is dependent on the quality of stabilised material; essentially a high-quality cement-stabilised layer ends up as a high equivalent granular type.

The changes in the stabilised layer as typified by the three degrading phases in Figure 2-1 suggest specific recommendations regarding their design. De Beer, [1985] recommends a three-phase approach during the design of cement stabilised layers:

a) mitigation of excessive shrinkage cracking
b) control of the effects emanating from repeated loading and crack propagation
c) control of shear deformation of the layer during its final phase [equivalent granular]

The overall strength of a stabilised layer is dependent on the particle bond-strength [TRH13, 1986]. Factors including material type, cement content and density have an influence on particle bond-strength. Compaction moisture and curing conditions are other factors that influence material strength and elastic modulus. Additionally, the rate of strength-gain increases with rise of curing temperature. For this fact, the development of accelerated test methods makes use of the effect of temperature on material strength.

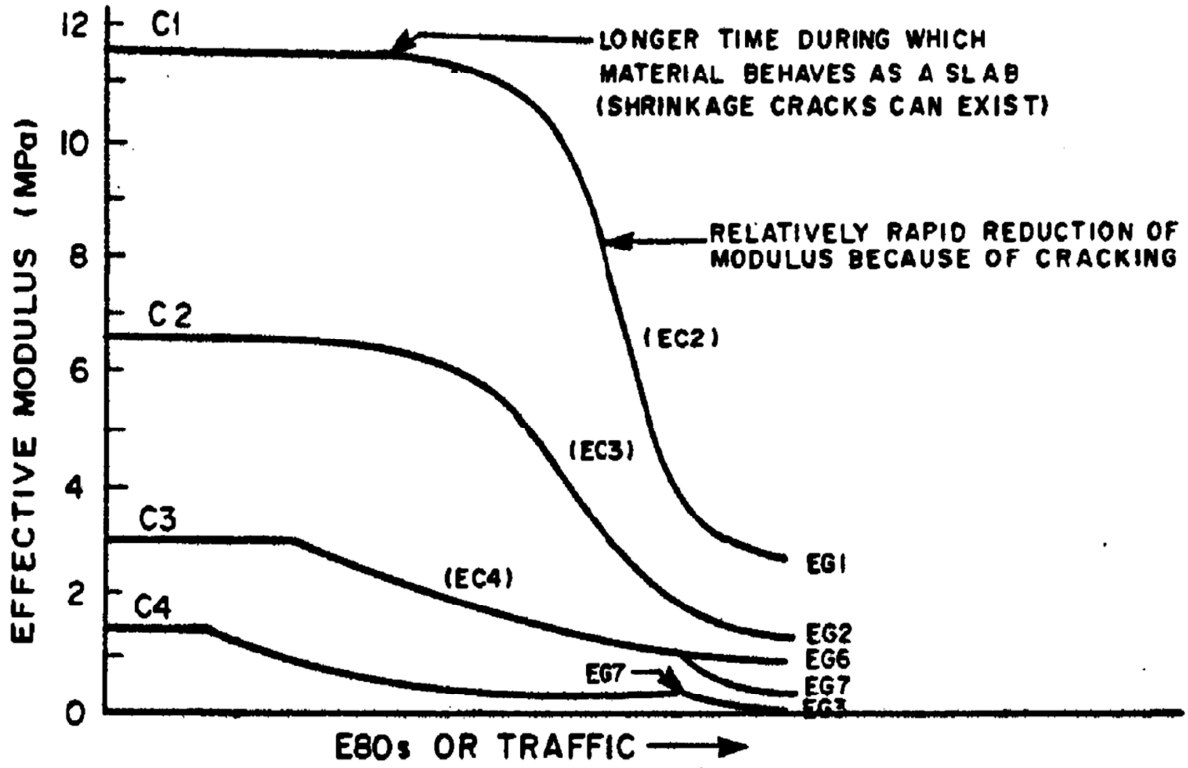

Figure 2-2: Relative Behaviour of Cement Stabilised Materials of Different Quality [Freeme, 1984]

Fatigue resistance of cement-stabilised materials decreases with increasing strength at a given strain level; this typifies the material's response to repeated loading [NAASRA, 1986]. Characteristically, stiffer mixes tolerate fewer load repetitions than weaker mix types. Fatigue properties of stabilised materials exhibit a semi-brittle behaviour, [Larsen and Nussbaum, 1967]. Brittleness of the stabilised layer increases with the addition of cement to the mix. This is dependent on the material characteristics and achieved density among other factors. The strains generated within a cement-stabilised layer with high elastic modulus are usually low, [Papagiannakis and Masad, 2007].

Moisture content and density of cement-stabilised layers are interrelated; a variation of moisture content results in a corresponding decrease in density at a given compactive effort. Mixing efficiency is influential to the resultant strength and elastic modulus. An inefficient mixing results in pockets of material particles without sufficient cement to effect strength; this creates zones of weakness, [Terrel *et al.* 1979; NAASRA, 1986; TRH13, 1986]. When stress concentrations occur around such zones of weakness, failure results.

Cement content relative to material characteristics and attained density influence the behavioural properties of stabilised layers. Even though the sole aim of stabilisation is to achieve the required engineering properties, material quality must meet certain durability criteria. However, the amount of cement required to satisfy the performance criteria usually results in a rigid layer whereby upon shrinkage, cracks develop. Layer cracking results in a reduction in the service-life as illustrated in Figure 2-1. Shrinkage cracking of cement-stabilised layers reduces the effective working modulus of the cement-stabilised layer. Depending on the resultant crack width and spacing, [crack pattern] a compromise of the pavement structural capacity will emanate. Fine shrinkage cracks usually retain sufficient interlock and exhibit a satisfactory structural capacity. However, fine shrinkage cracks might offer entry to water. Infiltration of water leads to localised softening and/or pumping of fines as well as erosion of the stabilised layer. However, with appropriate curing procedures along

with a number of mitigation techniques the detrimental effects due to layer cracking are minimised, [George, 2000; 2001].

2.2.2 Role of a Stabilised Base

A base layer plays a significant role in the short and long-term performance of the pavement structure. The base layer provides a stable construction platform, uniform support and prevents pumping [Terrel *et al.* 1979; NAASRA 1986; TRH13, 1986; Netterberg, 1987; George, 2001]. In a rigid pavement system, high-strength bases are neither required nor recommended because the top concrete slab carries most of the applied load. However, a reasonable uniform support over a high-strength stabilised base layer is usually preferred. A well-designed and constructed base layer underneath the concrete slab provides a reliable foundation support. Under such circumstances, the base layer helps reduce stress and deflections as well as improving the load transfer across concrete slab joints, which minimises the cracking, and faulting that would have resulted.

In airport pavements, Arellano and Marshall [1998] establish that a stabilised base layer underneath a concrete slab is important for structural capacity. The impacted high stress levels from the gross aircraft loads require a rigid layer underneath a concrete slab. Use of a stabilised layer underneath a concrete slab increases the modulus and thus, reduces the total stresses within the pavement system.

In the flexible pavement structure, the use of a stabilised base layer is not usually considered. This is due to the incidence of reflective cracking. Shrinkage cracks in a stabilised base layer propagate to the surface layer, causing reflective cracks, [George, 2001]. Shrinkage cracking in the stabilised base layer is the causal factor for reflective cracks in the surface layer. For reflective cracks to appear three conditions should prevail, [Wayne and Luhr, 2004]:

a) cracks in the stabilised base must be wide enough to generate stress concentrations to the surface layer
b) the generated stresses from the stabilised base are not relieved apart from cracking the surface layer
c) the surface layer should be brittle enough to crack owing to the upward propagation of the generated stresses

NAASRA [1987] recommends a granular cover of about 125-mm to 150-mm thickness between the stabilised base and surface layer. The granular layer retards shrinkage cracks from reflecting to the surface.

2.2.3 Role of a Stabilised Sub-base

The sub-base pavement layer plays a significant role in both flexible and rigid pavement types. The significance of the sub-base layer is that it [TRL, 1993]:

a) helps spread the wheel loads so that the subgrade is not overstressed and thus acts as the structural layer within the pavement structure
b) separates the base and subgrade layers as well as providing a good working platform on which the transportation, laying and compaction of other paving materials is carried out
c) often times it acts as a drainage layer for the pavement structure, but this involves specialised construction

The selection of materials and design of the sub-base layer depends on the intended function and expected in-situ moisture conditions. In a flexible pavement system, when the sub-base is stabilised then an unbound granular base is preferred as a means to mitigate reflective cracking to the surfacing layer, [Netterberg, 1987]. Lay [1986] refers to this

pavement system as 'upside-down' pavement. A typical mode of deterioration of the 'upside-down' pavement is a slight rutting attributed to the unbound granular layer and eventually fine transverse cracking attributed to repeated-trafficking. The significance of a stabilised sub-base layer in a flexible pavement system usually relates to structural purposes. When the sub-base is stabilised it is stiffer; this offers greater load-spreading ability and thus, a reduction in stresses. Owing to its structural rigidity, use of a stabilised sub-base layer results in a reduction in rutting.

In a rigid pavement system, a stabilised sub-base layer is below the concrete slab. A concrete slab withstands most of the traffic-induced stresses due to its high elastic modulus. The induced traffic-stresses transform into bending stresses and as a result, some sort of support is required. A stabilised sub-base layer ensures uniform support to the concrete slab by counteracting the effect of the unsatisfactory subgrade support, [TRRL, 1978; O'Flaherty 1988]. If the subgrade is sufficient in providing support to the concrete slab, then the stabilised sub-base layer might not be necessary. It is only if the subgrade exhibits sufficient support that placement of the concrete slab directly onto the prepared in-situ soil [subgrade] is acceptable. However, the subgrade material must exhibit good quality and natural uniformity. Uniformity of the subgrade is a crucial factor to consider. Weak or expansive materials will result in pavement failure due to the non-uniform support. The alternative approach to substitute weak or expansive materials with suitable material types provides little [if any] support to the concrete slab, [TRRL, 1978].

2.3 Chemistry of Cement and Constituents of Stabilised Materials

Cement-stabilised materials are a mixture of mainly cement and aggregates. Terzaghi *et al.* [1948] defines aggregate as natural soils and crushed mineral rock particles. Properties of stabilised material constituents influence both physical and chemical properties, [Dixon and Weed, 1989]. A mineralogical testing to identify and quantify individual mineral constituents is necessary. Use of x-ray diffraction [XRD] for the qualitative identification of minerals provides insights related to the chemistry as well as chemical influence on performance and durability. Equally, imaging microscopy offers insights about the morphological structure, including shape, size, angularity and agglomeration. Physical and chemical characteristics are important factors for consideration while assessing the engineering properties of materials.

2.3.1 Cement Properties

Standards SAN50197 or EN197-1 specifies common cement types used in South Africa. Table 2-1 provides an overview of the chemical composition of Portland cement along with the nomenclature. Southern Africa has a number of cement types that exhibit different characteristics. Paige-Green and Netterberg [2004] provide a background, evaluation and discussion of the specific cement types used in Southern Africa.

Following the addition of water to cement, an exothermic chemical reaction takes place. Wainwright, [2005] states that the hydration reaction includes the following:

a) being exothermic, heat is released and an increase in temperature results
b) all four main compounds react with water; the dicalciumsilicate and tricalciumsilicate reactions are similar but differ from the tricalciumaluminate and tetracalciumaluminoferrite
c) the reactions take place at different rates
d) the reactions occur at the surface of the individual particles of the cement
e) the hydration products are stable in water [hydraulic reaction]
f) the resultant compounds do not exist in a pure state

Table 2-1: Chemical composition of Portland cement [Wainwright, 2005]

Name	Chemical Compound	Nomenclature
Calcium oxide	CaO	C
Silicon dioxide	SiO_2	S
Aluminium oxide	Al_2O_3	A
iron oxide	Fe_2O_3	F
magnesium oxide	MgO	M
Alkali [Sodium, Potassium]	Na_2O_2, K_2O	-
Sulphur Trioxide	SO_3	-
The Four Main Compounds in Cement		
Compound Name		Symbol Used
Tricalciumsilicate		C_3S
Dicalciumsilicate		C_2S
Tricalciumaluminate		C_3A
Tetracalciumaluminoferrite		C_4AF

Tricalciumaluminate reactions

The reaction between tricalciumaluminate and water is violent. The addition of gypsum helps to control the reaction.

$C_3A + 26\ CSH_2 = C_3A\ 3CSH_{32}$ Equation 2-1

Where: H – Water
CSH – calcium sulphate [gypsum]
$C_3A\ 3CSH_{32}$ – calcium sulphate aluminate hydrate

The reaction between tricalciumaluminate and water results in the following, [Wainwright, 2005]:

a) formation of ettringite a hydrous calcium aluminium sulphate compound of formula $Ca_6Al_2(SO_4)_3(OH)_{12}{\cdot}26H_2O$
b) formation of a monosulphate with ettringite as a catalyst

Formation of the ettringite slows the hydration of tricalciumaluminate by creating a barrier around the cement particles, [Cohen, 1983; Wainwright, 2005]. The ettringite becomes unstable after a certain consumption of sulphate; thereafter a second reaction occurs.

$C_3A + 10H + CSH_2 = C_3A\ CSH_{12}$ Equation 2-2

The paste begins to stiffen when the second reaction [Equation 2-2] occurs.

Tricalciumsilicate and dicalciumsilicate reactions

When tricalciumsilicate and dicalciumsilicate react with water, it leads to the formation of calcium-silicate-hydrates [C-S-H]. The C-S-H is responsible for the majority of strength and low permeability. The hydration reaction of tricalciumsilicate and dicalciumsilicate are similar and only differ in the rate of occurrence and quantity of calcium hydroxide formed. Tricalciumsilicate and dicalciumsilicate react with water to form [Cohen, 1983]:

$2C_3S + 6H = C_3S_2\ H_3 + 3CH$ [early strength] Equation 2-3

Where: $2C_3S$ – alite [impure tricalcium silicate]
$C_3S_2\ H_3$ – calcium silicate hydrate
3CH – calcium hydroxide

$2C_2S + 4H = C_3S_2H_3 + CH$ [early strength] Equation 2-4

Where: $2C_2S$ – blite

Several theories and models attempt to explain the mechanism of ettringite formation as well as the expansion. Crystal growth and swelling theories are the most acceptable. Crystal growth theory states that growth in the ettringite causes the expansion. The growth of these crystals is responsible for the crystallisation pressure and thence expansion, [Cohen, 1983]. The swelling theory stipulates that ettringite particles exhibit a colloidal size [gel]. The gel has a specific surface area similar to the C-S-H gel. When the gel takes up water, it produces an overall expansion by swelling. During the hydration reaction, both tricalciumsilicate and dicalciumsilicate react with water forming calciumsilicate hydrate gel [$C_3S_2H_3$]. Calciumsilicate hydrate gel crystallises slowly and forms needle-like crystals, which interlock with one another. Figure 2-3 shows the reactivity of the cement compounds as listed in Table 2-1.

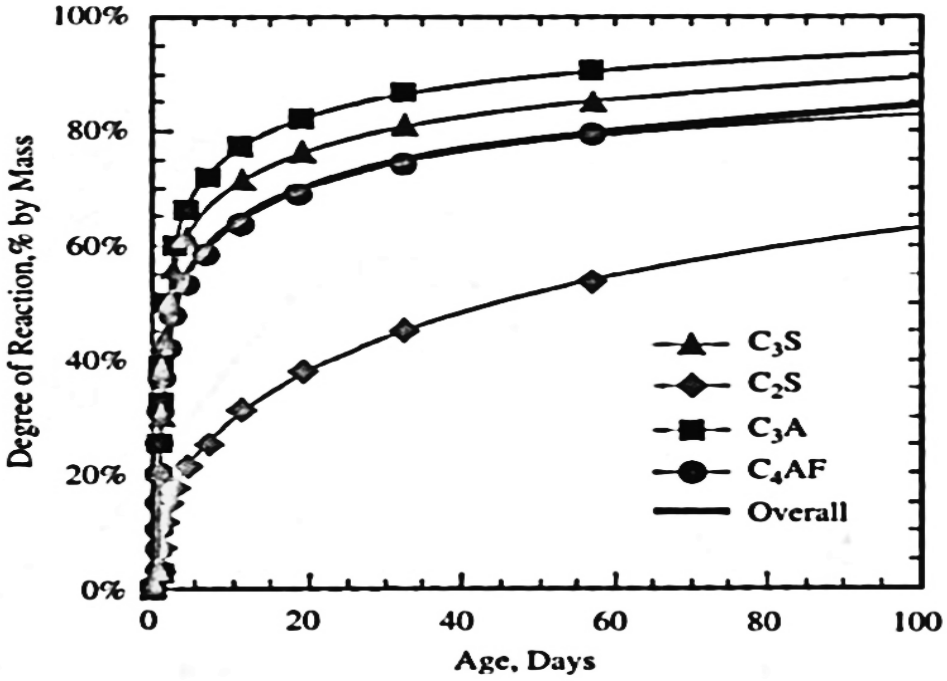

Figure 2-3: Degree of Reaction of Cement Compounds [Tennis et al. 2000]

Figure 2-4 illustrates the five stages of the hydration process that include mixing, dormancy, hardening, cooling and densification.

a) During the mixing stage, a sharp rise in heat generation results; this is due to the reaction between tricalciumaluminate and water, Equation 2-1. The reaction produces tetracalciumaluminoferrite, which forms a gel.
b) During the dormancy stage, the material is plastic. At this stage, completion of the compaction process ought to be finalised before the material begins to harden.
c) The hardening stage involves the silicate reactions, Equations 2-3 and 2-4, which form calcium-silicate-hydrate chains [C-S-H]. Tricalciumsilicate is responsible for the early strength-gain while dicalciumsilicate contributes to long-term strength-gain and low permeability.
d) During the cooling stage, the material shrinks. As the material shrinks, a build-up of internal tensile stresses within the material occurs.
e) The densification stage is dependent on the available moisture; hydration continues as long as moisture is available within the material matrix.

Several factors influence the hydration of Portland cement and these include the following:

a) chemical composition
b) water/cement ratio
c) presence of mineral additives and fineness
d) temperature variations

Stutzman [1999] and Copeland *at el.* [1960] provide a detailed account regarding the factors that influence the cement hydration process. A variation of the curing temperatures not only affects the stability of the hydration products but also influences porosity, bound water and ionic pore solution within the material matrix. High curing temperatures lead to early compressive strength-gain but have an adverse effect on the material mechanical properties. At elevated curing temperatures, there is a high initial rate of hydration, which results in a non-uniform distribution of hydration products across the material microstructure, [Elkhadiri *et al.* 2009]. Non-uniformity of hydration products influences the mechanical properties of stabilised materials; this affects the particle bond-strength.

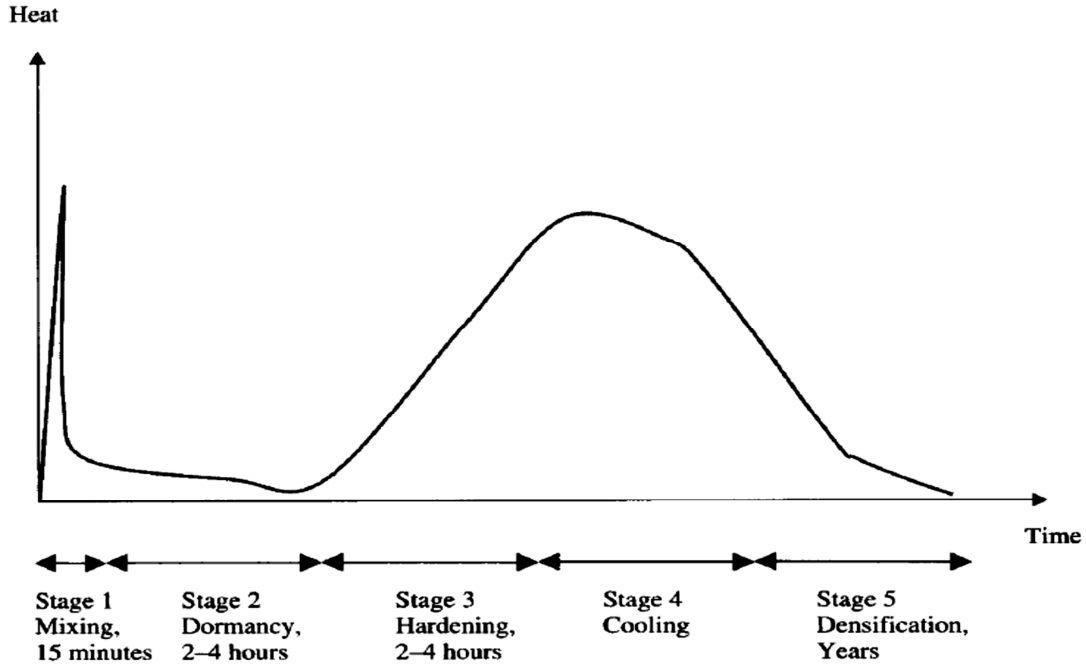

Figure 2-4: Different Stages of Hydration [Taylor *et al.* 2004]

Stutzman [1999] and Elkhadiri et al. [2009] state that curing at elevated temperatures result in the formation of dense clusters on the grains; this retard subsequent hydration and increases porosity. An increase in porosity suggests that the material is more prone to moisture ingress and chemical attack. Elkhadiri *et al.* [2008] show that curing at 85ºC increases porosity both meso and macro-porosity. With an increased porosity, curing of cement paste at 85ºC exhibits lower strength than mix types cured at ambient temperature.

Curing temperature has a visible effect on the C-S-H gel structure, [Copeland *et al.* 1960; Elkhadiri *et al.* 2009]. Elevating the curing temperature leads to an increase in C-S-H gel polymerisation. Stutzman [1999] elaborates that curing temperature influences the inner and the outer C-S-H gel structure. Elkhadiri *et al.* [2008] state that curing at 85ºC results in a cement paste that is more fibrous and typifies a morphology reminiscent of pastes hydrated with calcium chloride accelerators.

With reference to cement stabilisation, the amount of cement content in the stabilised materials is lower than that in cement paste. Cement hardens and gives strength to the material-cement mix, [Terrel *et al.* 1979; TRH13, 1986 and Paige-Green *et al.* 2004]. The

liberated lime during the hydration process reacts with material particles and results in a reduction in plasticity and swell. Addition of cement to materials results in an increase in strength and bearing capacity. Due to the rapid reactions that take place, effective mixing and compaction are crucial tasks for a successful stabilisation process. This is because a loss in strength and density is normally a result of excessive time between mixing of cement with material and compaction. TRH13 [1986] specifies a 24-hour accelerated curing at temperatures ranging between 70ºC to 75ºC for stabilised compressive strength evaluation as equivalent 7-day compressive strength cured at 22ºC.

2.3.2 Effect of Cement Fillers, Additives and Admixtures

The main use of cement filler, additive and admixture is to change and improve the physical and mechanical properties of materials, [Zelic *et al.* 2000; Lawrence *et al.* 2008; Jayapalan *et al.* 2010]. The Cement and Concrete Institute [C&Ci] of South Africa define cementituos materials as fine mineral powders, which have a significant influence on the dimensional stability of hardened cement, concrete and any other cement treated materials. Standards SANS 1491 [Parts 1, 2 and 3] specifies Portland cement extenders. Cement extenders influence the rate of early ageing and strength-gain; these are responsible for the 'fine-filler' effect.

Globally, silica fumes, limestone filler and fly ash are the most common cement extenders. The main purpose of fillers such as fly ash is to reduce the amount of voids in the mix, [Terrel *et al.* 1979]. Silica fume and ultra-fine fly ash react with calcium hydroxide in the presence of water to form cementing compounds consisting of calcium silicate hydrate. Calcium silicate hydrate is the main product of the hydration of Portland cement, which forms about 60% of the cement paste volume.

Chemistry of cement continues to gain interest because of the prevailing quest for alternative materials with improved functionalities. Analysis of cement samples at nanoscale level has provided new insights and fundamental observations concerning the nature of hydrated cement phases and their interaction with additives, fillers and admixtures. Knowledge concerning the interactions of cement phases has provided researchers with the possibility of modifying cement reactions. This has led to the creation of new interfaces and surface chemistries and analytical approaches such as nano-science in addition to developing new products, [Bouasker *et al.* 2008; Jayapalan *et al.* 2010; Raki *et al.* 2010]. Cement fillers, additives and admixtures improve the quality and properties of cement and cement treated materials. Addition of fillers, additives and admixtures alter the performance and durability of materials. Portland Cement Association [PCA] groups admixtures according to their functions as follows:

a) water-reducing admixtures reduce the water content in the mix
b) retarding admixtures slow down the setting rate of the mix
c) accelerating admixtures increase the rate of early strength development and reduce the time required for prolonged curing
d) super-plasticizers [or plasticisers] are high range water reducers and are applied to improve the mix workability

Michaux *et al.* [1986] group cement additives under eight major categories:

a) accelerators reduce the setting time of cement but speed up strength development
b) retarders extend the setting time and allow sufficient time for mix placement and compaction
c) extenders reduce the cement density and usage
d) weighting agents increase cement density
e) dispersants reduce cement viscosity and ensure mud removal during placement

f) fluid-loss control agents [FLAC^{+}] control water-loss from the mix and includes some of the shrinkage-reducing additives [SRA]
g) lost-circulation control agents reduce the loss of cement slurry
h) special additives such as antifoam agents and fibres are property specific additives

Several fine fillers alter the quality and properties of the material, including strength and shrinkage by influencing the hydration process. The following publications provide insights regarding the application of fine fillers and their resultant effects:

a) acceleration of cement hydration has been observed when fine fillers are added to cement, [Gutteridge and Dalziel, 1990; Kadri and Duval, 2002]
b) fine powders of limestone, quartz, silica fume and pulverized fly ash when added to cement resulted in an increase in the rate of cement hydration, [Lothenbach *et al.* 2008; Lawrence *et al.* 2008; Zelic *et al.* 2000]
c) addition of fine fillers influences the mix dimensional stability by increasing shrinkage, [Jayapalan *et al.* 2010]
d) an increase in chemical shrinkage results when fillers are added to cement paste, [Bouasker *et al.* 2008]

Adding fine non-reactive fillers to cement alters the hydration reaction; this is primarily due to the dilution or modification of the particle-size distribution and heterogeneous nucleation, [Bouasker *et al.* 2008]. Increasing the dosage rates of inert filler, results in a decrease in the total cement content in the mix. Addition of inert fillers changes the mix porosity thereby altering the particle-size distribution, [Jayapalan *et al.* 2010]; this has an influence on the material density, mechanical strength and total shrinkage. The surface of the fine filler provides additional sites for nucleation [for the calcium-silicate-hydrate]; such fine filler crystallises, [Lawrence *et al.* 2008]. The efficacy of catalysis depends on the fineness and dosage of filler. However, other relevant phenomenological factors that influence catalysis include:

a) water absorption or adsorption by the nanoparticles
b) interaction of the nanoparticle surface modification and treatment
c) reaction of materials

Fine fillers react chemically during the hydration process; however, there is limited literature to account for their reactivity. Limestone reacts with the aluminate phase in the Portland cement forming monocarboaluminate, [Lothenbach *et al.* 2008]. Increased interest emanating from successes allied to nanotechnology has led to the need to investigate and understand the effect of nano-filler on cementitious materials.

2.3.3 Calcium Silicate Hydrate [C-S-H]

In order to understand the purposes of enhancing the mechanical properties of materials study of the structure and behaviour of C-S-H gel is important. C-S-H is the principal binding phase in cement paste and is responsible for not only strength and durability but also shrinkage, [Thomas and Jennings, 2004]. During the past 60 years, research into the establishment of C-S-H structure is registered. C-S-H exhibits a layered structure similar to tobermorite [$Ca_5Si_6O_{16}$ (OH) $\cdot 7H_2O$] [5] and jennite [$Ca_9Si_6O_{18}$ (OH) $_6 \cdot 8H_2O$][6]. However, Taylor [1986], Dolando *et al.* [2010] and Skinner *et al.* [2010] state that the atomic structure of C-S-H remains undefined. Knowledge concerning the atomic structure of C-S-H is essential for the optimisation of C-S-H based concrete and other cement treated materials. The difficultly to ascertain the atomic structure of C-S-H is related to the failure in separating C-S-H from other phases and its broad diffraction signal.

The state of water in a C-S-H structure is also undefined. Jennings [2004], Dolando *et al.* [2010] and Skinner *et al.* [2010] hypothesise that water might be present in the C-S-H

interlayer structure and that the water molecules could be physically absorbed on the surface of the solid phases. Dolando *et al.* [2010] state that at the molecular level C-S-H gel comprises of silicate chains held together by calcium oxide layers.

C-S-H gel possesses a crystalline ordering at specific distances with irregular assemblages of layers with absorbed water as well as interlayer water molecules, [Jennings, 2004; Feldman and Sereda, 1970]. The removal of water from the interlayer spaces occurs upon drying shrinkage. Excess water in the interlayer spaces leads to swelling. C-S-H forms with an intrinsic pore system [gel pores] which constitute some water molecules. Water is an important part of the microstructure, its removal during the drying phase causes shrinkage [constriction of the matrix].

Thomas and Jennings [2004] stress that so far there is no defined quantitative analysis of cement microstructure in place. Microstructure of cement has a significant influence on the characterisation of material shrinkage. Models and hypotheses proposed for explaining the microstructure of cement relative to shrinkage are many to include within this research scope. Several of these models state that drying leads to differential shrinkage because the surface dries out first [shrinks first] and because of the restraints, cracking occurs. PCA suggests that the restraints to shrinkage are the causal factor to cracking. The colloidal structure models including that suggested by Jennings [2004] reveal the following:

a) drying shrinkage is a gradual change
b) the degree of polymerisation of silicate in early-aged paste increases significantly after drying and rewetting; this suggests that drying causes ageing of the cement paste
c) inclusion of aggregate into the cement paste matrix adds a restraining phase
d) cement, concrete or cement treated materials shrink because the C-S-H gel shrinks within the framework of restraining phases
e) chemical solubility of C-S-H and its degree of polymerisation depends on the chemical characteristics of individual components
f) packing density and volume of C-S-H are significant aspects of the microstructure stability
g) drying leading to shrinkage forms low density C-S-H which is different from a well-hydrated C-S-H
h) the volume of C-S-H always shrinks upon drying; this is dependent on material age and curing conditions
i) if the C-S-H shrinks on drying in a constrained pore-space, the bonds will undergo tensile stress, [Neubauer and Jennings, 2000; Thomas and Jennings, 2003]
j) shrinkage and creep are a function of ageing of the C-S-H and are dependent on three main factors that include time, temperature or rate of drying and relative humidity

Ageing is the process of polymerisation of the silicates in the C-S-H, [Neubauer and Jennings, 2000; Thomas and Jennings, 2003; Jennings, 2004]. As C-S-H ages, the globules become more tightly packed [constrict and move closer]. Elevating the curing temperature increases the rate of drying and thereby accelerates the ageing process. The mechanism of deformation depends on several factors, including the age of the C-S-H. C-S-H contains a more disorderly arrangement of its nanograins, [Neubauer and Jennings, 2000]. With a continued understanding of the C-S-H structure, an improvement of the engineering properties shall result. The C-S-H structure allows for the alteration of material properties and functionalities including drying shrinkage.

2.3.3.1 C-S-H Gel and Pore Structure

Cement pastes that exhibit low tensile strength properties have a high tendency to crack due to drying shrinkage; such mix types also exemplify reduced durability, [Selvan *et al.* 2011]. Increasing the tensile strength of materials could potentially minimise the effects of drying

shrinkage particularly the consequents of cracking. For a material to crack the developed tensile stresses should exceed its strength. Tensile stresses develop due to differences in temperature and moisture; cracking relieves the stresses. Formation of C-S-H gel controls the strength and cohesion properties of materials. In order to mitigate cracking due to drying shrinkage a distinct study of the C-S-H gel structure is necessary. Cement has multiple elements [Ca, Si, O and H], which contribute to the formation of C-S-H gel; this further complicates the definition and study of the C-S-H gel structure.

Several studies, including Thomas and Jennings, [2003] and Jennings, [2004] reveal that C-S-H gel influences the engineering properties of materials. The influence of C-S-H gel on material is due to its continuous layer, which contributes to the cohesive properties of the mix. C-S-H gel grows outwards of the cement grains and develops miniature pores [gel pores]. The gel pores are considerably smaller than the capillary pores. Water in the gel pores is physically isolated and assumed not to undergo any chemical reaction with cement minerals, [Selvan *et al.* 2011]; this partly clarifies ranges of water content in the gel. C-S-H gel occupies more volume than tricalciumsilicate and dicalciumsilicate minerals. Expansion of C-S-H gel is a continuous phase. Cement paste does not significantly change in volume after mixing with water. However, an increase in volume of the solid phases causes a corresponding decrease in the capillary pores; this is dependent on the water/cement [w/c] ratio. A decrease in the capillary reduces the material's permeability.

Asamoto S *et al.* [2012] studied the effect of moisture loss and drying shrinkage based on pore structure of mix types with and without admixtures. The experimentation considered mineral admixtures such as blast-furnace slag and fly ash with 40% fine aggregate in all specimens. The study revealed that:

a) Curing at high temperature accelerated the hydration reaction. However, the differences in pore structure resulted in dissimilar moisture losses under specific curing conditions. Mix types with admixture [exhibiting a dense pore structure] showed reduced moisture loss compared to their equivalent mix types without the admixture. This shows that inclusion of fine particles reduces void content [alters the pore structure] and ultimately influences the moisture loss.
b) Assuming that shrinkage is due to only capillary tension showed different tends from the experimental outcomes amongst the mix proportions. This suggested that other factors other than capillary tension influence drying shrinkage.

2.3.3.2 C-S-H Gel and Nano-Particles [Nano-Silica]

For over 20 years, the use of amorphous silica in cement and other cement treated materials has shown different property changes. Taylor [1997] notes that silica induces a pozzolanic reaction that decreases the amount of calcium hydroxide in the cement paste. However, the degree of purity and nature of impurities contained in the silica fume has an influence on its efficacy. Equally, the particle size of the silica contributes to its efficacy. Silica particles usually measure a mean diameter of 100 nm [Gaitero *et al.* 2010]. Dispersion of both mean particle size values and purity of silica is much smaller; unlike silica fumes, nano-silica particles are not industrial by-products.

Nano-silica particles have a defined diameter range of about 10 nm to 50 nm and 100% purity, [Gaitero *et al.* 2010]. Achievement of reduced particle size involves the use of stabilisers in the dispersions, which aid to adjust the pH values. The pH value of the reaction system influences the efficacy of nano-silica particles, [Singh *et al.* 2011]. Supply of the nano-silica particles is either in the form of dry powders or as colloidal dispersions. The surface area of nano-silica is larger than that of silica fumes. This proposes that the nano-silica particles are more reactive than the silica fumes despite a similar chemical and

structural composition, [Qing *et al.* 2007]. This proposes that the reaction kinetics and hydration products obtained by adding nano-silica and silica fume to cement will vary.

A number of researchers, including Qing *et al.* [2007] and Thomas [2009] studying the effects of adding nano-silica to OPC cement type revealed that:

a) Adding nano-silica particles to cement at a w/c ratio of 0.4 showed an initial acceleration in the reaction rate; this acceleration in the reaction rate corresponded with an increase in nano-silica to cement.
b) In a comparison of mix types with and without nano-silica, mix types with nano-silica exhibited less exothermic than their reference mix types. Thomas [2009] expounds that this is because nano-silica particles act as nucleation sites for growth of cement hydrates. The nucleation effect and its resultant growth of hydrates lead to a reduction in porosity of cement paste and moisture loss.
c) Great reactivity and the pozzolanic effect of the nano-silica increase the reaction rate by reducing the amount of calcium ions in the hydration of water. However, particle size and dispersions of nano-silica particles influence the processes. Pozzolanic reaction with calcium hydroxide results in an increase in C-S-H amount, which leads to high material densification; this improves the strength and durability [permeability] of materials.
d) In the presence of nano-silica are silicon ions. Silicon ions facilitate the incorporation of aluminium atoms into the C-S-H gel. As a result, longer silicate chains of the C-S-H gel in the cement paste result. Nano-silica promotes the merging effect of the silicate chains. The C-S-H gel chain effect of the silicates plays a significant role in the mechanical properties of cement and cement treated materials.
e) An appropriate percentage of nano-silica is required. Application rates ranging from as small as less than 1.0% up to 5.0% by dry mass of cement are registered. Owing to the agglomeration caused by the difficulties to disperse nano-particles, best benefits occur at specific application rates to cement and materials. Adding nano-particles decrease the amount of lubricating water available in the mix; this shows the effect of particle fineness [increased surface area] relative to water consumption.
f) The yield stress increases with further addition of nano-particles, which affects the mix rheological properties [workability].

Neville [1997] reveals that incorporation of ultra-fine particles into Portland cement paste results in different characteristics and to an extent, functionalities. The performance of the cement-based materials depends on the nano-sized solid particles, C-S-H gel chains and pore spaces at the interfacial transition zone between cement and aggregate particles. Properties affected by the nano-sized particles include strength, durability and shrinkage. The nano-silica particles fill the spaces between particles of the C-S-H gel [act as a nano-filler]. Qing *et al.* [2007] state that nano-particles in the mix change material properties in both fresh and hardened states.

The drying shrinkage of cement paste is categorised into two; reversible and irreversible categories, [Thomas and Jennings, 2003; Jennings, 2004]. Irreversible shrinkage is the final length change after the cement paste specimen undergoes drying and is re-saturated. In the case of irreversible shrinkage, strains due to physical and/or chemical changes of the paste result. These changes lead to the re-arrangement of C-S-H gel particles during the drying out phase. Under irreversible shrinkage, resultant changes following drying out are permanent and influence the packing density. The primary driving factors of drying shrinkage include:

a) relative humidity levels from 100% down to about 50% where capillary tension occurs in the pores
b) disjoining pressure between the particles of cement

As the cement paste ages, the total amount of drying shrinkage reduces, [Neubauer and Jennings, 2000; Thomas and Jennings, 2003; Jennings, 2004]. Aged cement pastes at elevated temperatures and humidity shrink less. Parrot [2000] analysed cement paste cured at 60ºC [short curing period] and revealed that not only was the resultant drying shrinkage irreversible but also minimal. Mindess and Young [1981] mention that heat treatment of about 65ºC reduces irreversible shrinkage by two-thirds. Various inferences of heat treatment [curing temperature] on drying shrinkage at a given relative humidity suggest the following:

a) the polymerisation process involves cement ageing and this increases the stiffness [modulus] of the gel
b) shrinkage strain is low after ageing
c) due to ageing the pore size distribution is transformed

Bentur [1980] studied pore volumes of cement paste hydrated at different temperatures; the study revealed that paste hydrated at 65ºC had more capillary porosity but less meso-porosity than their equivalent types hydrated at 25ºC. The study indicates that an increase in the rate of hydration [using elevated temperature] results in the alteration of the mix pore structure.

Parrot [2000] illustrates that an increase in weight loss of cement paste resulted following drying from 100% to 85% relative humidity. This observation suggests that reducing relative humidity results in increased evaporation. Variations in temperature and relative humidity influence the resultant shrinkage. For any given relative humidity and temperature, drying leads to emptying of the large pores followed by the small pore-sizes, [Kelvin equation]. Resultant shrinkage stresses are dependent on the size of the smallest pores emptied as well as the volume of available pores.

C-S-H gels shrink due to drying and high-localised stresses that emanate because of the moisture gradients as well as presence of the restraining phases. However, Thomas and Jennings, [2003] and Jennings [2004] suggest that by reducing meso-porosity, which is responsible for drying stresses at moderate relative humidity levels, the ageing effect is minimised. This suggests that C-S-H gel becomes less prone to collapse and/or a rearrangement as the cement paste ages. Jennings [2004] surmises that stresses that cause the gel to collapse during drying are sufficient to cause local fracture within the material; this refers to the relationship of the tensile stresses and strength.

2.4 Aggregates

Cement paste mixes are restricted to specific engineering tasks due to their limited properties. Cement paste mixes suffer from two main drawbacks which include high dimensional changes [low stiffness, but high shrinkage] and cost, [Frigioine and Marra, 1976; Knudsen, 1984]. The inclusion of aggregates in the cement paste to produce either concrete or stabilised pavement materials minimises these drawbacks. Even though aggregate in the cement paste may be inert, it still influences the physical properties of hardened concrete.

The mineralogical, physical and chemical characteristics of rocks are determined from their geological history. However, the crushing or excavation method employed to obtain the aggregate influences their physical characteristics predominately the particle-size and shape. Classification of aggregates is according to their rock type, surface texture and particle shape. TRH14 [1985] provides the various road construction materials, including their classification. According to the particle size, aggregate is termed as fine, medium or coarse, [Austroads, 2003]. Mechanical properties of aggregates influence the quality of stabilised materials. The most important mechanical properties include:

a) strength – aggregate crushing value [ACV], 10% fine test [10% FACT]
b) impact strength – aggregate impact test
c) abrasion – aggregate abrasion test

The taxonomies of aggregates for road construction use involve the assessment of several factors, including the particle-size distribution. The properties of the aggregate in both un-compacted and compacted states are vital for consideration. The source of the aggregate dictates its quality and ultimately contributes to its performance and durability, [Weinert, 1980]. The primary concern in selecting an aggregate type for use is that any deviations from the specified performance and durability requirements affect the design-life of the pavement.

Terrel *et al.* [1979] and Weinert [1980] assert that the relationship between the specified material requirements and the actual field performance criteria is essential. Several road authorities use performance criteria based on performance index tests on compacted laboratory specimens to verify material suitability for use. However, this approach is limited to traditional [standard] material types with known field performance. For new and/or alternative material types, challenges in accruing information for establishing material suitability arise, [Terrel *et al.* 1979; Austroads, 2003].

2.4.1 Cement and Aggregate Interaction

The chemical reaction of Portland cement is too complex and extensive to cover within the scope of this research. Frigioine and Marra, [1976], Knudsen [1984], Osbaeck and Johansen [1989] and Wakasugi *et al.* [1998] note on the relationship of cement particle size and the hydration process. A reduction in the median cement particle size results in an increased hydration rate, an aspect that improves early strength properties. The fineness of the cement plays a key role in the material strength - gain. However, Mehta [1997] cautions on durability related issues attributed to using finer cement types. Current research recommendations mention using coarser cement types with relatively low water/cement [w/c] ratios; Osbaeck and Johansen [1989] state that an equivalent long-term performance of that with finer cements is normally realised. The addition of cement to material usually results in an increase in optimal moisture content [OMC] but a decrease in the maximum dry density [MDD]. The increase in moisture content is due to the flocculation effect and water demand by the cement fines.

Cement is effective in stabilising medium to low plasticity aggregates, [TRH13, 1986]; different aggregates can be stabilised using cement. An increase in cement content normally results in an increase in material strength, [Austroads, 2014]. The degree of strength increase [bond strength] depends on the fineness of aggregates as well as on general material characteristics, [Terrel *et al.* 1979]. Fine-graded and clayey material types are difficult to stabilise using only cement. Such fine and clayey material types require high cement contents along with lime to completely modify the material and effectively mix.

Knudsen [1984] mentions a reduction in density or absolute volumes of all compounds after every hydration reaction. This is associated with the effect of shrinkage. Autogenous and drying shrinkage are noted. Autogenous shrinkage refers to an occurrence in which the cementitious materials shrink at a constant temperature without a change in weight; the term 'autogenous volume change' is sometimes used, [Davis, 1940]. Drying shrinkage is a time-dependent material deformation due to a loss of water or moisture, [Hansen, 1987]. The appearance of shrinkage cracks reduces the bond-strength between the particles. In the cement-stabilised materials, a disruption and weakening of the bond-strength between the aggregate and cement leads to poor load transfer.

Cement-stabilised materials like concrete are significantly dependent on temperature and relative humidity [thermal effects], [Davis, 1940; Terrel *et al.* 1979; Wakasugi *et al.* 1998]. The hydration process begins after adding water to the cement-material mixture. The quality and quantity of the mixture components, including available water in the mix as well as temperature and humidity control the rate of hydration, [Hansen, 1987]. Cement and moisture content besides aggregate characteristics influence the properties of cement-stabilised materials; aggregates make up the bulk of cement-stabilised materials, [Terrel *et al.* 1979].

Depending on the material constituents, high temperatures cause varying changes to cementitious materials, [Hansen, 1987; Thomas and Jennings, 2003; Jennings, 2004]. Coefficient of thermal expansion [CTE] defines a unit change in length per degree of temperature change, [Naik *et al.* 2011]. Aggregate restrains the thermal movement of the cement paste; typical values of cement paste CTE vary between 11.0 x 10^{-6} and 20.0 x 10^{-6} per degree centigrade, [Neville, 1997; 2000]. Since aggregates undergo a pre-heating process during geological formation, the CTE of lightweight aggregates is lower than that of gravel; gravel exhibits a CTE range between 7.4 x 10^{-6} and about 12.0 x 10^{-6} per degree centigrade. Thermal expansions of concrete and cementitious materials vary depending on the aggregate type used, [Neville, 2000].

Cementitious materials expand as temperature rises and contracts as the temperature falls; the variations in temperature are primarily due to environmental conditions. Evidently, most materials expand and contract depending on the level of temperature regimes. Curing regimes influence the development of microstructural attributes, [Naik *et al.* 2011]. Cementitious materials exhibit two phases of materials [the paste and aggregate], which have dissimilar CTE values, [Neville, 2000]. The CTE of cement treated materials is dependent on the constituent factors, which include cement paste, aggregates, moisture regimes, age and environmental factors such as variations in temperature and humidity, [Mindess and Young, 1981]. Variation of CTE due to changes in cement contents is not as significant as changing the aggregate type, [Mindess and Young, 1981; Naik *et al.* 2011]. Aggregates are a major factor of influence to material expansion and contraction as well as shrinkage.

Aggregates occupy more than 90% of stabilised material volume. The aggregate matrix contains dispersions of cement particles; this makes up stabilised materials of particular quality. The compaction of cement-stabilised materials takes place at the optimum moisture content [OMC]. Van der Waals forces effect adhesion between the hydration products and aggregates [Wainwright, 2005]. Presence of voids in the mix weakens the forces of attraction [Van der Waals]. With continued ageing strength between aggregates and cement increases. However, the occurrence of micro cracking within the stabilised matrix influences the resultant bond strength. As a result, any further movements resulting from either traffic-loads and drying shrinkage will emanate in additional cracks. Due to the presence of micro cracks, the stabilised layer fails at low stress levels than either aggregate or cement.

Suitable materials are those that derive their shear strength partly from friction and cohesion, [Papagiannakis and Masad, 2007]. Cement-stabilised materials should exhibit strength levels capable of sustaining the traffic-loads while maintaining a satisfactory stability, [Austroads, 2006; 2014].

Reduction in aggregate particle-size results in a corresponding increase of its surface-area and thus, high water requirements. The surface area water requirements rule influences the maximum achievable density for a given compactive effort. The level of material fineness or aggregate particle-size in the mix influences the cement requirements. Application of high cement contents for stabilisation purposes results in rigid pavement layers as well as cracking due to drying shrinkage. Use of fine-grained materials for stabilisation necessitates

application of high cement contents an aspect that increases the possibility of drying shrinkage and layer cracking, [Lay, 1988]. Netterberg [1987] cautions that unless proven through material evaluation, any material should not be over-improved [increased cement contents]. Stabilising well-graded materials requires less cement than stabilising fine-grained materials. For base layer stabilisation, natural materials suitable for use in the sub-base layer are recommended. The main objective of applying such approaches to stabilisation practice is to limit material ranges [consideration of specific material quality].

For most materials, an increase in cement content results in a corresponding increase in material strength, [Austroads, 2006; 2014]. Lay [1986; 1988] shows that a strength increase of approximately 500 kPa to 1000 kPa [based on UCS strength] for every 1% of cement added to well-graded granular materials was registered. Figure 2-5 illustrates the relationship of binder content to compressive strength [UCS test]. Low cement contents correspond to reduced compressive strength properties. However, the addition of high cement contents does not necessarily translate to satisfactory material performance and/or durability, [Netterberg, 1987]. Several factors, including material characteristics and curing regimes influence the engineering properties of stabilised materials, [Austroads, 2014]. In order to achieve a feasible strength, plant mixing is preferred, [Croney *et al.* 1998; DETR, 1998]. For the purposes of effective bonding, the even distribution of cement particles is necessary, [Ingles and Metcalf, 1972]. Guthrie *et al.* [2002] details the various measures undertaken to select optimum cement content for various material types.

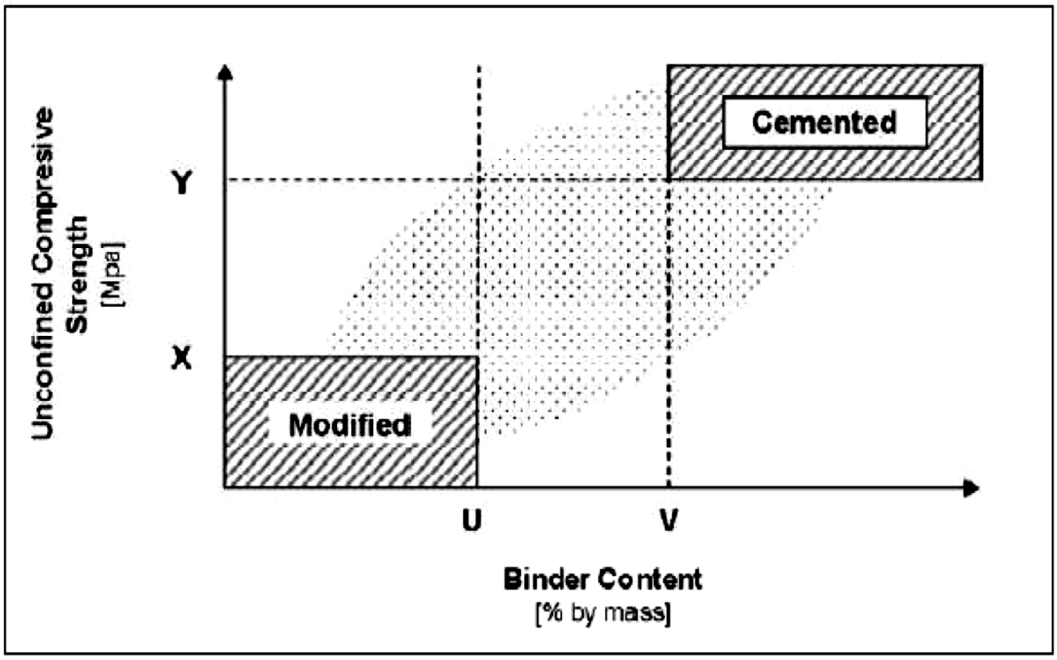

Figure 2-5: Characterisation of Modified (Unbound) and Cemented (Bound) Materials [Gray *et al.* 2011]

2.5 Shrinkage Cracking

Section 1.3 introduces the shrinkage-cracking phenomenon of a cement-stabilised pavement layer. Subsequent to mixing cement and aggregates with water during stabilisation, compaction of the mix follows; these tasks are part of constructing a stabilised layer. Available water within the stabilised layer eventually evaporates; this leads to drying shrinkage and subsequently cracking of the layer. Exposure of the layer surface to varying thermal effects results in different shrinkage rates, which contribute to the development of tensile stresses [George, 1973; Bofinger *et al.* 1978]. External and internal restraints also contribute to the development of tensile stresses within the stabilised layer. Restraints

prevent the layer from relieving the generated tensile stresses [undergo stress relaxation]. In order to relieve the induced tensile stresses the stabilised layer cracks. Characteristics of the crack pattern depends on several factors, including generated tensile stresses relative to strength [age] and imposed restraints. Cracks result when the generated tensile stresses exceed the layer tensile strength. This typifies that cracking due to drying shrinkage occurs in tension or contraction.

The tensile strength of stabilised materials increases with time. However, drying shrinkage decreases as the tensile strength between the aggregate particles increases; this is dependent on several factors including material characteristics and curing conditions. Drying shrinkage is the reduction in layer length following a loss of moisture from the capillary pores. It is a time dependent deformation that involves moisture loss at a given temperature and relative humidity, [Hansen, 1987]. The degree of shrinkage is dependent on several factors including the rate of moisture loss. Pore structure and available moisture in the mix influence the rate of shrinkage and cracking criteria. The factors influential to drying shrinkage include:

a) cement and available moisture content
b) curing conditions relative to age of the mix
c) material characteristics, including fineness and gradation

Shrinkage occurs over a considerable period and its rate decreases with time as the material gains high tensile strength. Volumetric changes alone do not result in tensile stresses. The restraints imposed on the stabilised layer and dimensional changes are responsible for the development of tensile stress [George, 1973]. Stress can result due to a variation in temperature, which influences the rate of moisture loss. Frictional forces at the interlayer between the stabilised and underlying layer restrict the stabilised layer from constricting owing to drying shrinkage [moisture loss]; this influences the resultant crack pattern.

Several factors, including temperature and tensile strength, influence the resultant crack pattern. At an early age of the stabilised layer, the generated stresses occur over a long and intact layer length [George, 1973; Bofinger *et al.* 1978]; the developed tensile strength is usually lower during the initial stages [days after the construction]. The spacing, direction and width of the cracks characterise the crack pattern. The common factors influencing the crack pattern include:

a) susceptibility of material to shrinkage due to moisture loss as well as internal moisture redistribution [pore structure] as the cement hydrates
b) dimensional changes relative to temperature and thermal effects
c) internal and external restraints imposed on the stabilised layer
d) resultant tensile properties of a hardened stabilised layer, i.e. strength, stress, modulus of elasticity and ability to relieve critical conditions

Bofinger *et al.* [1978] states that the ability of a crack in a stabilised layer to reflect to the surface depends on:

a) type and thickness of the surface layer
b) effect of climate and age on the viscosity of binder
c) volume and magnitude of the traffic-loads

When the stabilised layer shrinks, its volume reduces due to the withdrawal of water from pore spaces; this results in layer movements as a form of material response [material relaxation]. Friction prevailing at the interlayer restrains the stabilised layer from completely relaxing, [George, 1973; Bofinger *et al.* 1978; Houben, 2008]. As a result, tensile stresses build up and cracks emanate when the induced tensile stresses exceed the material tensile strength.

Detrimental effects due to cracking of the stabilised layer relate to the characteristics of the crack pattern. Shrinkage mitigation techniques aim at realising a 'desirable' crack pattern. A 'desirable' crack pattern typifies a minimal crack width at shorter spacings; this link with the concept behind pre-cracking a freshly constructed stabilised layer. Curing conditions allow the stabilised layer to achieve a maximum increase in tensile strength and thus minimise the prospect of layer cracking; this does not necessarily result in a 'desirable' crack pattern. Bofinger *et al.* [1978] and Bisschop [2002] show that ideal curing conditions only minimise cracking due to differential drying shrinkage by enclosing moisture within the layer material matrix. However, autogenous shrinkage under any curing conditions still takes place. Bofinger *et al.* [1978] declares that to achieve ideal curing conditions is difficult in practice but suggests that adopted curing conditions should be as close as possible to the conditions of autogenous shrinkage. Without any curing procedures in place, the resultant drying shrinkage reduces the potential tensile strength of the stabilised layer.

Bofinger *et al.* [1978], Bisschop [2002] and George [1973] reveal that moisture loss due to self-desiccation and evaporation cause shrinkage. Cement-stabilised pavement layers shrink due to drying either from loss of moisture or moisture depletion; shrinkage is rather due to drying shrinkage than to autogenous shrinkage. Studies by George [1973] and Bofinger *et al.* [1978] reveal that drying shrinkage causes the majority of cracking. However, other factors also contribute to layer cracking.

Kuhlman [1994] and El-Rahim and George [2001] analysed the mechanism of drying shrinkage and concluded that its reduction is through:

a) the control of the amount of clay particles and mineralogical elements influencing shrinkage
b) applying admixtures such as fly ash and organic compounds
c) construction quality control measures
d) using various techniques purposed for inducing required crack-pattern

Other studies such as Sobhan *et al.* [1999] report on the inclusion of fibre into the cement-stabilised materials. Fibres in stabilised materials increase the tensile strength of the material; this reduces the potential of induced tensile stresses exceeding material tensile strength. The addition of fibre to cement-stabilised materials also increases the compressive strength and energy absorption capacity, [Maher and Ho, 1993].

In studies on early age cracking in concrete, the role of regulating mix proportions as a mitigation to shrinkage cracking has proven beneficial, [Krauss *et al.* 1995; Bentur, 2002]. This has encouraged the development of many methods to reduce shrinkage cracking. In concrete mixtures, methods to reduce shrinkage cracking include:

a) use of higher aggregate volumes, [Shilstone, 1990]
b) use of expansive additives, [ACI 223.98 1998]
c) use of modified cement binders

Lately, the use of chemical additives including shrinkage-reducing admixtures [SRA] is slowly gaining interest in the concrete and cement industry. SRA reduces shrinkage cracking by altering the surface tension of the concrete pore fluid, [Weiss and Berke, 2002; Rajabipour *et al.* 2008]. The use of water-saturated porous additives including Light Weight Aggregate [LWA] is another method. These additives supply additional water during the hydration process and this water is used for internal curing purposes, [Bentz *et al.* 2007; Mack, 2006]. Both methods show great potential, however, to gain anticipated benefits from such methods their applicability and suitability must be determined based on field related investigations; this remains beyond the scope of this research.

Dissimilar to concrete mixtures, cement-stabilised materials use low cement contents and thus exhibit reduced strength and different behavioural properties compared to concrete. In the road industry, wide cracks greater than 6.0 mm in width cause poor load-transfer besides increasing stress within the pavement system, [Wayne and Luhr, 2004]. In order to apply suitable mitigation procedures the mechanism of drying shrinkage is essential.

2.5.1 Mechanisms of Autogenous and Drying Shrinkage

In this section, influential factors concerning shrinkage and cracking due to drying are stated. Mechanisms of drying shrinkage along with the factors pertaining to cracking are noted. Type and degree of restraint determine the characteristics of the resultant crack pattern. Drying shrinkage is due to the loss of moisture for a given temperature and humidity conditions. Shrinkage in a stabilised layer is categorised as autogenous or drying shrinkage. Autogenous shrinkage does not usually involve significant moisture loss because of the hydration of cement, [Tazawa and Miyazawa, 1992; George, 1973]. Hydration of cement involves the movement of water. As some quantity of water is consumed, more is required to replace the consumed quantity; this results in movement of water from high to low saturation zones. Several factors, including internal chemical and structural reactions cause autogenous shrinkage. Detrimental effects emanating from autogenous shrinkage are insignificant compared to those from drying shrinkage, [Sebasta, 2005].

Hydration of cementitious materials leads to shrinkage because the volume of hydrated products is smaller than the sum of the un-hydrated [original] cement and water [Tazawa and Miyazawa, 1992]. Autogenous shrinkage is a concern in high strength cement-treated materials. During autogenous shrinkage, water is lost due to internal reactions attributed to hydration. Similar to drying shrinkage, tensile stresses develop during autogenous shrinkage, [Bisschop 2002; Hansen 1987; Bofinger *et al.* 1978; George, 1973]. The generated tensile stresses pull the material particles closer [material constriction] registering some dimensional changes; this occurs in the early stages when the material has not gained sufficient strength or hardened. Tensile stresses in the early stages of the freshly constructed stabilised layer can result in dimensional changes, which may be not as detrimental to the layer as if it were hardened.

The process of additional drying or autogenous shrinkage will slow down as the material gains strength; this relates to the material tensile strength-gain with time but a reduction in moisture and stresses. Variation in temperature, airflow and relative humidity influence autogenous shrinkage. Autogenous shrinkage is a macroscopic dimensional change. As the hydration of cement progresses, the consumption of capillary pore water occurs [Tazawa and Miyazawa, 1992]. Due to reduced water, an increase in negative pressure takes place. The capillary tension theory elaborates on this mechanism further.

Experimenting on the cement paste Tazawa and Miyazawa, [1992] reveals that self-desiccation cause autogenous shrinkage. Self-desiccation is a result of the formation of fine pores within the microstructure and water consumption by the hydration reaction. The cement minerals produce various hydrates whereby the total volume of solid and liquid phases reduces; this results in the formation of voids within the microstructure. Formation of the ettringite creates a large volume in fine voids in the hardened material. The amount of free water in the hardened cement decreases due to the hydration reaction; this leads to self-desiccation. A comparison of drying to autogenous shrinkage suggests that:

a) drying shrinkage is due to the loss of water [or moisture] through evaporation to the outside environment [diffusion of water]
b) autogenous shrinkage is the consumption of water by the hydration reaction
c) influential factors to both shrinkage categories include humidity and temperature

d) the mechanism of drying shrinkage, such as the capillary tension theory also applies to autogenous shrinkage
e) alleviation of autogenous shrinkage encompasses the reduction of the micro-pore structure
f) mitigation of drying shrinkage includes water retention [preventing diffusion] or supply of water [maintaining a constant level]
g) mineral composition in the cement influence autogenous and drying shrinkage

In order to comprehend the shrinkage criteria of various materials the analysis of the shrinkage mechanism is essential, [Bisschop, 2002]. Presently no unified theory exists that explains the drying shrinkage behaviour over an entire range of relative humidity. Hansen [1987] proposes the following drying shrinkage mechanisms and related theories:

a) surface free energy [i.e. Gibbs-Bangham shrinkage]
b) capillary tension
c) movement of interlayer water
d) disjoining pressure

Hansen, [1987] and Bisschop [2002] assert that drying shrinkage involves more than one mechanism. Hansen [1987] who studied the drying shrinkage mechanism of OPC cement mortar at w/c ratios of 0.4 and 0.6 using different mechanisms reveals that:

a) moisture gradients and duration of shrinkage do not affect total shrinkage [dynamic shrinkage-weight loss curves]
b) the surface free energy mechanism is active over a wide range of relative humidity compared to the other mechanisms

Hansen [1987] and Bisschop [2002] state that there are various mechanisms and factors, which control drying shrinkage in cementitious materials and which operate within the microstructure at different scales. Aspects include the rate of hydration and resultant products such as C-S-H gel and interface characteristics, among other factors influencing drying shrinkage. Particle size distribution of cement and aggregates, cement content, aggregate type and quality, have a significant influence on drying shrinkage.

The magnitude of drying shrinkage cracking is dependent on the degree of restraint against shrinkage and other influential factors related to material, [Bisschop 2002; Hansen 1987; TRH13 1986; Bofinger *et al.* 1978; George, 1973]. The mechanism of drying shrinkage is dependent on the type of restraint that causes and influences shrinkage cracking; this restraint might be external or internal, [Hansen, 1987]. Cracking due to internal restraint is due to self-restraining and the presence of stiff constituents. Self-restraining induces tensile stresses in the region of drying and compressive stresses deeper in the layer [extreme point from the region of drying]. The induced tensile stresses are parallel to the drying surface and therefore cracks emanate perpendicular to the drying surface, [Hwang and Young, 1984]. The extent of cracking and the crack pattern resulting from self-restraining is dependent on the stabilised layer's characteristics and rate of drying, [Hansen, 1987; Bisschop, 2002]. Material and layer heterogeneity play a significant role in the resultant crack pattern.

Conditional to the rate of drying and layer characteristics, different cracks will result; first, second, third and other subsequent cracks occur, [Bisschop, 2002]. The presence of stiff aggregates influences the orientation of the cracks and crack-pattern within the stabilised layer. When the induced tensile stresses reach the material tensile strength, microcracking emanates and orientation of resultant cracks is usually perpendicular to the aggregate perimeter, [Goltermann, 1995]. The formation of bond cracks is due to shearing along the aggregate surface. Due to the induced compressive stresses, the bond cracks close, [Hwang and Young, 1984]. Owing to self-restraining and presence of stiff aggregate, the crack pattern in any cementituos matrix is undefined. Any cement treated material, which dries out

and is externally restrained or in a restrained shrinkage test will show cracks because of the superimposed stresses from both the external and internal restraints.

2.5.2 Volumetric Change and Drying Shrinkage

Volumetric changes of materials are a significant factor of influence to their durability and serviceability, [Bofinger *et al.* 1978; George, 1973; TRH13 1986; Hansen, 1987; Goltermann, 1995; Bisschop, 2002]. Change in volume because of moisture movement attributed to variations in temperature and relative humidity, influence material stability. Time-scale deformations, hydration of cement, internal and external restraint with respect to temperature and relative humidity simultaneously influence the extent of volumetric change of a material, [Hansen, 1987]. Time-scale deformation characteristics attributed to drying shrinkage and/or moisture loss, contribute to the damaging of the stabilised layer, [George, 1973].

Tazawa and Miyazawa, [1992] declares that the identification and description of volumetric reduction in cementituos materials, is complex. Volumetric changes in cementituos materials include material expansion due to hydration as well as contraction owing to drying out and/or loss of moisture. Subjecting a material to a given temperature and relative humidity results in the evaporation of water/moisture from its microstructure; this leads to the desiccation, [Hansen, 1987; Goltermann, 1995; Bisschop, 2002]. Withdrawal of moisture from the microstructure leads to a reduction in volume. Heat from cement hydration induces thermal strain while variations in temperature and relative humidity lead to loss of moisture, [Hansen, 1987].

2.5.3 Drying Shrinkage and Cracking in Stabilised Layers

Drying shrinkage comprises loss of water from the material's capillary pores. This leads to a reduction in the disjoining pressures resulting in shrinkage of hydrated cement compounds during exposure to drying conditions, [Hansen, 1987; Goltermann, 1995; Bisschop, 2002]. In the previous section, the effects of drying shrinkage as the primary cause of cracking and deformation are stated. George [1999] states that the mineralogy of the material influences shrinkage cracking. Caltabiano and Rawlings [1992] notes that several factors influence the degree of shrinkage cracking including:

a) amount of cement
b) moisture content
c) aggregate properties
d) adequacy of the curing procedures
e) weathering conditions
f) degree of restraint [interlayer bonding/friction]
g) type and time of placement of final surface

The degree of cracking is proportional to the amount of moisture lost upon drying, [TRH13 1986; Bofinger *et al.* 1978; George, 1973]. Wet materials exhibit a high degree of cracking attributed to high moisture loss and increased shrinking. Application of high cement contents for stabilisation increases moisture consumption and ultimately shrinkage, [Little *et al.* 1995]. Field related studies have reported that excessive cracking with wide shrinkage cracks is a result of high cement contents. Several technical guidelines caution judiciously regarding selecting appropriate cement content as, to abate drying shrinkage and associated layer cracking.

Factors such as type of restraint at the interlayer influence the degree of cracking [crack pattern]. Bisschop *et al.* [2002] states that even with small-scale laboratory specimens [without restraint imposed], microcracking occurs because of superimposed stresses caused by internal restraints. Hwang and Young [1984] elaborate that in drying out specimens a

moisture gradient develops across the drying specimen, which contributes to non-uniform shrinkage [self-restraint]. The self-restraint due to internal specimen parts shrinking much slower than the outer cause the microcracking; this establishes that different shrinkage rates cause cracking. In cement paste, self-restraint leads to propagation of cracks perpendicular to the dried surface at varying depth. In the cement-stabilised materials, stresses resulting from the restraining effect of aggregate particles contribute to drying shrinkage and microcracking. The restraining effect emanating from the aggregate particles leads to radial and circumferential microcracking around the aggregate particles [Goltermann 1995].

Hwang and Young [1984], Goltermann [1995], Bisschop *et al.* [2002] and Houben [2009] state that:

a) in a hardened cement paste specimen, microcracking due to drying shrinkage is solely due to the stresses created by self-restraint [non-uniform shrinkage]
b) in the cement-stabilised materials, inclusion of aggregates in cement matrix results in additional stresses emanating from the aggregate restraint
c) in concrete, cement-stabilised materials and cement paste , the rate of drying influences the resulting effect and rate of stress development [with respect to the rate of stress-relaxation]
d) an increased drying rate results in more extensive microcracking
e) cracking due to aggregate restraint is influenced by the rate of drying
f) additional factors such as cement type, w/c ratio, aggregate bond strength and drying conditions also contribute to drying shrinkage and resultant cracking

Self-desiccation of materials and friction at the interlayer are significant factors influential to shrinkage cracking particularly the resultant crack pattern. Other factors, including material stress relaxation, thermal effects, moisture content and overall material properties influence layer crack pattern [Hwang and Young, 1984; Goltermann, 1995; Houben 2009; Houben 2011]. Stress relaxation describes the tendency of material to relieve developed tensile stresses under a constant strain, [Meyers *et al.* 1999; Junisbekov, 2003]. Stress relaxation behaviour varies for different materials and to an extent, mix types. In material science, particularly concrete research, use of the creep test to evaluate the stress relaxation behaviour is common. A plot of the stress versus time represents the test data while the slope of the curve at any point defines the stress relaxation rate. Principal factors affecting the stress relaxation factor and thermal coefficient include:

a) age
b) moisture content
c) proportion of the mix
d) frictional forces and/or magnitude of restraint
e) curing conditions

With reference to concrete Houben [2011] asserts that a build-up of tensile stresses usually results. However, as the concrete mix, ages the tensile stresses reduce because of the effect of stress relaxation. Regarding cement-stabilised materials, cognisance of the low cement applications must be included in accounting for the stress relaxation. Stress relaxation factors of stabilised materials and concrete differ owing to the dissimilarities in material characteristics and properties. Figure 2-6 schematically illustrates the shrinkage cracking phenomena, [TRH13, 1986].

Cracks appear when the tensile stresses exceed the material tensile strength. In the early stages before the material hardens [gains strength] the resultant cracks are narrower compared to the situation if the material has hardened. Wide cracks emanate when the tensile stresses exceed the layer strength; this crack pattern depending on the resultant

crack width might be detrimental to the pavement structure. As a general overview, George [1970], Little *et al.* [1995] and Bisschop *et al.* [2002] state that:

a) a cement stabilised layer shrinks due to drying shrinkage
b) friction at the interlayer restrains the stabilised layer from constricting and this induces tensile stresses
c) this influences the resultant crack pattern
d) internal tensile stresses develop within the stabilised layer and upon exceeding the material tensile strength cracks manifest
e) not all cracks are due to drying shrinkage cracks; reflecting load-induced fatigue cracks because of heavy truck traffic, fatigue cracks induced at the bottom of the surface layer, thermal cracks and cracks due to asphalt surface ageing [emanate from the surface] also develop

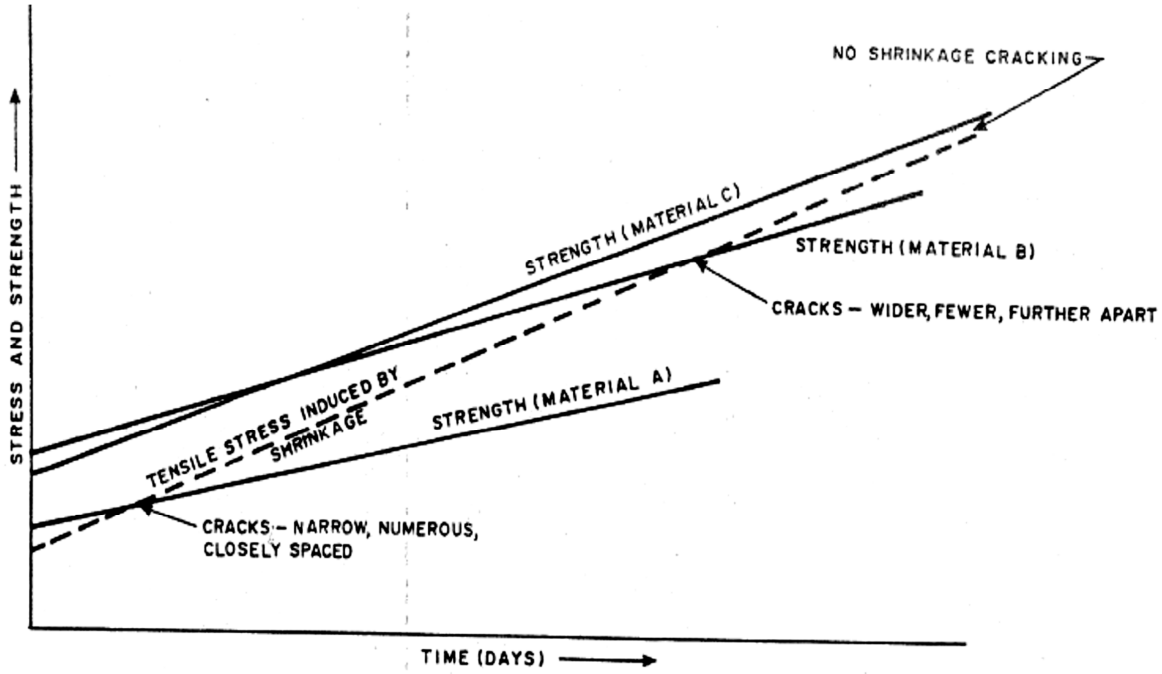

Figure 2-6: Shrinkage Cracking Mechanism Interrelationship between Shrinkage Stress, Strength and Time [TRH13 1986]

Several methods aimed at lessening shrinkage and resultant cracking in stabilised layers in order to bring about a 'desirable' crack-pattern, are in place. The terminology 'desirable' crack-pattern refers to cracks, which do not result in significant structural deficiency, [George, 1970; 1971; 1998]. The width of cracks and sequential appearance [crack width and spacing] has significant influence on long-term pavement performance and durability. Wide cracks have the tendency to reflect through the overlying layer, [George, 2001].

2.5.4 Methods for Mitigating Shrinkage Cracks

Practice continues to apply a number of procedures or techniques to mitigate shrinkage cracks in cement-stabilised pavement layers. George [1971], Caltabiano and Rawlings [1992], George [1999] and Shalid and Thom [1996], provide a comprehensive description of techniques and procedures used to alleviate shrinkage and even reflective cracking. Research studies by William [1986] and George [1999] highlight the trends and efforts put across to alleviate shrinkage cracking in stabilised layers. The research work by Caltabiano and Rawlings [1992] places emphasis on material selection and mix design criteria. Several technical guidelines, including the South African specifications consider material selection and mix design procedures as a means to control shrinkage and resultant cracking. Procedures and/or techniques adopted include:

a) control maximum shrinkage and consequent cracking by proportioning materials that is make checks entailing limits on linear bar shrinkage of fines, maximum amount passing No. 200 sieve or 0.075 mm
b) minimum content consistent with long-term durability which include specifying limits to fines and cement contents as well as ensuring practical minimum moisture content during compaction
c) introduction of blended cements such as expansive cement, fly ash cement or secondary additives and numerous organic compounds including nanotechnology products
d) quality control during construction that includes achieving density close to the maximum dry density and curing procedures
e) controlling shrinkage cracking in the stabilised layer as a means to minimise reflective cracking in the surfacing layer

Most common techniques used to alleviate shrinkage cracking include [George 2000]:

a) control and limit of material consideration on the basis of material quality and type
b) pre-cracking of the stabilised layer by either delaying placement of the surface layer or mechanically by immediately opening it to traffic or using the vibratory roller
c) pre-cutting the stabilised layer
d) use of inter-layers as surface treatment or stress relieving layers which inhibits the propagation of cracks from the stabilised layer to the surfacing layer
e) use of thick surfacing and stabilised layers with reduced cement content

Experience and field-testing have revealed that excessive shrinkage leads to wide cracks and corresponds with a high dosage of cement and material characteristics. Little *et al.* [1995] examined heavily stabilised pavement layers and deduced that:

a) Although the use of high cement contents results in high strength the resultant crack pattern, reduces the pavement service-life.
b) Cracks allow water to infiltrate the lower layers resulting in the de-bonding of the layers but also offer passage to pumping of the underlying fine materials.

George [2000] and Sebesta [2005] studied the cracking phenomena in the stabilised layer and deduce that a number of factors contribute to layer cracking. The layer tensile strength, creep characteristics, restraint by friction at the interlayer, temperature and thermal effects, the amount and type of clay in the stabilised materials, pre-treatment and moulding moisture influence the degree of drying shrinkage and cracking characteristics. Even though assumed that cement predominately influences shrinkage and the resultant crack pattern other researchers have concluded otherwise. As a result, efforts to mitigate shrinkage cracking provide a feasible alternative.

A number of mitigation techniques focus on controlling desiccation through moist curing. Other mitigation techniques utilise stress relief layers such as chip seals and Geosynthetics to reduce or retard reflective cracking. Researchers, including George [2000] and Sebesta [2005] detail at length the viability of these techniques in abating shrinkage cracks in stabilised layers.

Pre-cutting stabilised layer

The original principle of pre-cutting a stabilised layer was to introduce grooves or cuts at close intervals to control of the crack width, [Colombier and Marchand, 1993]. Presently the consideration of pre-cutting the stabilised layer is to prevent an occurrence of occasional but relatively wide and damaging natural cracks. The driving factor for pre-cutting is to minimise wide cracks from propagating through the stabilised layer to the surface layer. Shalid *et al.* [1996] reported that pre-cutting induced frequent cracks of less than 0.5-mm width in a

stabilised base layer. The width of natural cracking was more than 10 mm [Shalid *et al.* 1996]. Pre-cutting the layer resulted in a reduction in crack width.

Several field-related studies, including George [2001] show that there is no specified pre-cutting period since this is dependent on various factors such as material characteristics and thermal effects. Time for pre-cutting a stabilised layer varies from hours to a few days after construction; this depends on the layer strength at the time of grooving. The recommended groove depth or cut-depth to pre-cut a stabilised layer varies from one-third to one-half of the thickness of the stabilised layer. The recommended pre-cut width at the top of the groove is about 10 mm to 15 mm. Pre-cut spacing reported in the various field studies ranges from 3.0 m to about 18.0 m. Colombier and Marchand, [1993] illustrate the benefits of pre-cutting the stabilised layer and its ability to alleviate reflection cracking. Lefort [1996] details the benefits of pre-cutting which includes the mitigation of wide shrinkage crack width at specified spacing.

Pre-cracking less aged/ "young" stabilised layer

Pre-cracking aims at reducing wide shrinkage cracking through inducing micro-cracks in the stabilised layer. Microcracking is the creation of a network of fine cracks, which makes use of heavy traffic or vibratory rollers. By microcracking the stabilised layer, the proliferation of wide shrinkage cracks is minimised, [George, 2001]. Pre-cracking is undertaken one to three days after placement of the stabilised layer, [Litzka and Haslehner, 1995]. The key objective of pre-cracking is to lessen the detrimental effects emanating from wide shrinkage cracks. The first successful pre-cracking experiment was in Japan; this provided encouraging results, [Yamanonchi and Ihido, 1982]. Brandl [1999] reported that of all the available options for minimising shrinkage cracking, the micro-cracking technique is the most suitable. The construction test sites in Texas, where an investigation of micro cracking took place revealed that without microcracking severe cracking occurred, [Sebesta 2005].

Fly ash in cement-stabilised materials

Davidson [1958] reports that the addition of fly ash to the soil-cement mixtures increases strength. Sastry [1998] states that, fly ash decreases drying shrinkage without compromising the long-term strength of the materials. The setting rate [or hardening rate] of the cement and fly ash mixture is curtailed with a consequent reduction in cracking, [George, 2001]. El-Rahim and George, [2001] among other researchers, report that by replacing a part of the cement with fly ash, resultant shrinkage cracks were narrower compared to their reference mix types [without fly ash].

Ground granulated blast-furnace slag

The use of ground granulated blast furnace slag (GGBF) has been in place for over 60 years ago. The efficacy of GGBF depends on its ores, fluxing stone and impurities in the coke charged into the blast furnace, [George, 2001]. The blending of GGBF in cement [by replacing 50% of the cement with GGBF in concrete mixtures] results in the alteration of physical properties, which are characteristic of the dominant material. As the percentage of slag increases, a slower rate of strength-gain is obtained, particularly at early ages which influences drying shrinkage and resultant cracking criteria, [ASTM Standards 1987; Okamoto 1990; Geogauge, 2000; Gress, 2001].

2.5.5 Technological Innovations to Alleviate Shrinkage Cracking

The significance of narrower cracks compared to wider cracks cannot be over-emphasised. Cement admixtures and additives have varying effects on the properties and characteristics of materials [El-Rahim and George, 2001]. Consideration of shrinkage reducing additives [SRA] is gaining prominence when using cement and concrete. SRA is suitable for specific

cement types and/or quality; efficacy of SRA varies with cement types and content, [Gress, 2001]. SRA reduces both autogenous and drying shrinkage, [Engstrand 1997; Bentz 2001; Nmai *et al.* 1998].

By analysing water-SRA interactions, observations made so far infer that SRA reduce shrinkage by means of reducing the surface tension, [Engstrand 1997; Bentz 2001; Nmai *et al.* 1998]. Mix types with SRA showed a reduction in crack width [reduced shrinkage and alteration of the material's pore structure] besides increasing the material strength. SRA is mainly organic chemicals [surfactants] and when mixed with water, reduce the surface tension of the liquid, [Bentz, 2001]. By reducing the material's pore fluid, SRA minimise the magnitude of capillary stresses, thereby decreasing shrinkage strains that emanate due to a loss of moisture, [Goto *et al.* 1985; Berke *et al.* 1996].

Internal curing is another alternative method used to abate shrinkage and the resultant cracking. Internal curing comprises pre-wetting of the lightweight aggregate in order to avail water to the mix, [Kovler and Jensen, 2007]. Experiments conducted at a laboratory scale showed that internal curing significantly reduces the self-desiccation of materials.

Concrete mixes contain particles ranging from 300 nm to about 37 mm, [Fuller and Thompson, 1907; Reinhardt, 1998; Neville, 2000]. In concrete, particle size influences the flow properties and workability [in its fresh state] as well as strength and durability [in its hardened state], [Husken and Brouwers, 2008]. In order to improve material packing, an increase in solid size range is necessary; this suggests considering particle sizes below 300 nm. Materials capable of ensuring a dense packing include limestone and silica fines such as silica flour [Sf], silica fumes [SF] and nano-silica [nS].

Sakka and Kosuko [2000] note that in cement and concrete, the effect of micro-silica includes the chemical and physical interactions. Dunster [2009] and Qing *et al.* [2007] state that, nano-silica increases material density and reduces porosity as well as chemical reactivity. This is because of the enhancement of the bond strength between cement and aggregate. A dense microstructure due to use of nano-silica is likely to prevent and/or retard water evaporation [Qing *et al.* 2007]. This is because nano-silica alters the material pore structure. Wynand [2011] establishes that increasing material tensile strength at an early stage minimises the occurrence of shrinkage and the resultant cracking.

2.5.6 Laboratory Measured Shrinkage

Shrinkage cracking is an inevitable characteristic that causes the majority of pavement failures. Despite this fact, its evaluation is not usually considered. A crack width of 3.0 mm to 6.0 mm wide cause poor load-transfer and localised damage, [Bofinger *et al.* 1978; Pretorius and Monismith, 1971; George 1973]. A number of shrinkage test methods are in place and every test method uses different specimen geometry, measurement criteria, curing procedures and setup. The following literature provides insight into the evaluation of material shrinkage:

a) Nakayama and Handy [1965] considered cylindrical specimens that were dynamically compacted whereby the measurement of shrinkage uses a sophisticated microscopic slide.
b) Bofinger *et al.* [1978] considered cylindrical specimens and deduced that there was some degree of anisotropy attributable to the differences in the total shrinkage measured on the specimens.
c) Grobler [1994] preferred beam specimens to cylindrical specimens and states that the cylindrical specimens as well as the compaction criteria employed do not simulate the field criterion. Horizontally placed and vertically compacted beam specimens are

preferred. Grobler [1994] shares similar insights with George [1970]; both measured shrinkage based on rectangular beam specimens.

Measurement of shrinkage perpendicular to the direction of compaction is usually preferred. This is because the majority of researchers consider shrinkage is greater in the direction perpendicular to compaction, [Nakayama and Handy, 1965]. Bofinger *et al.* [1978] establish that the method of compaction influences the extent of shrinkage. Specimens that were compacted using dynamic, impact and kneading compaction methods registered higher shrinkage than those compacted using static. Material density and moisture content influenced the total resultant shrinkage, [Grobler, 1994].

Bofinger *et al.* [1978] studied shrinkage of fine-grained soil-cement materials and established the following regarding laboratory measured shrinkage:

a) shrinkage of laboratory prepared specimens is anisotropic and its measurement is influenced by the method of compaction
b) autogenous shrinkage in the direction perpendicular to compaction varies with cement content
c) the initial condition of soil prior to compaction [moulding] along with the moisture content at compaction and density influence the resultant total shrinkage
d) volume and/or specimen dimensional changes are caused by an interaction of material-moisture suctions, re-orientation of water, expansion of the cement gel as it hydrates, self-desiccation caused by the hydration of cement and an increase in strength due to cement-material skeleton
e) the longer the exposure of specimens to drying conditions, the higher the total resultant shrinkage but with sealed-off specimens [before subjecting them to dry conditions] the resultant measured shrinkage is smaller than that of the exposed specimen

Several laboratory studies related to shrinkage measurement consider different curing conditions and measuring criteria; studies by Nakayama and Handy, [1965], George [1968], Pretorius and Monismith, [1971], Wang [1973], Dunlop [1973] and Grobler [1994] show different principles and criteria in measuring laboratory shrinkage. Bofinger *et al.* [1978] assert that evaporation from unprotected surfaces causes larger volume changes compared to sealing off surfaces; resultant volumetric changes are dependent on the curing conditions and level of exposure.

Volumetric changes are normally less than the corresponding loss of moisture; this is due to the capillary phenomena. Drying shrinkage obeys the capillary tension theory, [Wang 1973; Dunlop 1973; Bofinger *et al.* 1978]. Bofinger *et al.* [1978] elaborates that in curing cement paste under sealed conditions, there is an initial expansion during the first period before recrystallisation set in. Recrystallisation leads to a loss of intra-crystalline or absorbed water, which results in a reduction in volume of the cement paste, [Dunlop 1973; Bofinger *et al.* 1978].

Curing conditions have a significant influence on the total shrinkage. George [1968] elaborates that curing at high humidity results in the capillary tension effect predominating compared to intermediate humidity levels. At intermediate humidity, a decrease in the absorbed water film causes shrinkage. Nakayama and Handy [1965], George [1968] and Bofinger *et al.* [1978] establish that the prevailing humidity influences the loss of water from the material crystal lattice. Wang [1973] emphasises that drying shrinkage only occurs as soon as evaporation starts. Regarding the expansion of the specimen, Wang [1973] and Bofinger *et al.* [1978] establish that the cement gel expands when it hydrates which results in the overall expansion of the specimen.

A good understanding of shrinkage necessitates an examination of the specimen anisotropic response during the test. A number of researchers consider axial shrinkage of cylindrical

specimens compacted in moulds developed for producing compression-strength test specimens. George [1968] and Bofinger et al. [1978] state that specimens prepared and monitored in this way do not simulate the critical shrinkage criteria experienced by the stabilised layer. Bofinger *et al.* [1978] elaborates that shrinkage in the axial direction only causes changes in the layer thickness, but remains of no significance to the formation of cracks.

Nakayama and Handy [1965], George [1968] and Bofinger *et al.* [1978] state that shrinkage related research is concentrated on the measurement of the drying shrinkage of specimens initially cured in moist conditions for a specified period. Nakayama and Handy [1965] and Bofinger *et al.* [1978] note that this approach does not enable measurement of the volumetric changes that occur immediately after compaction is completed or during the early stages of curing. Bofinger *et al.* [1978] clarifies that the behaviour and early stages of the curing period have a significant influence on the subsequent shrinkage measurement. This suggests that shrinkage measurements should commence immediately after compaction of the specimen.

Figure 2-7 illustrates a cylindrical shrinkage test method by Pretorius and Monismith, [1971]; the test measures axial shrinkage. In this method, a reference point at the extreme ends of the cylinder purposed for refining the accuracy in measuring shrinkage is applied. Figure 2-8 illustrate the beam shrinkage-test method by George [1971]. With the linear shrinkage method, compaction of the beam is a major challenge and of concern. Frictional forces at the interface between the beam and base retard the 'actual' measure of shrinkage. If the specimen develops a crack, the measurement of shrinkage is erroneous; the measuring instrumentation does not register 'actual' shrinkage. These are major limitations to linear shrinkage method. The linear shrinkage method used by George [1971] comprises of a U-shaped plexiglass as illustrated in Figure 2-8.

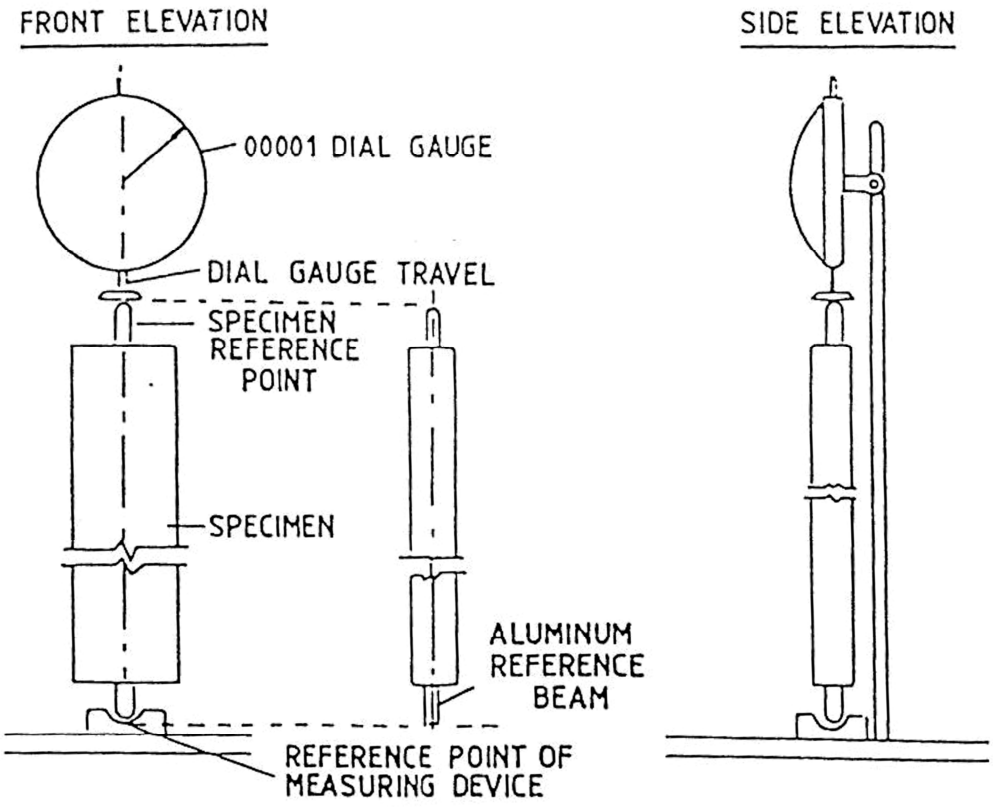

Figure: 2-7 Shrinkage Testing Equipment and Configuration based on a Cylindrical Specimen [Pretorius and Monismith, 1971]

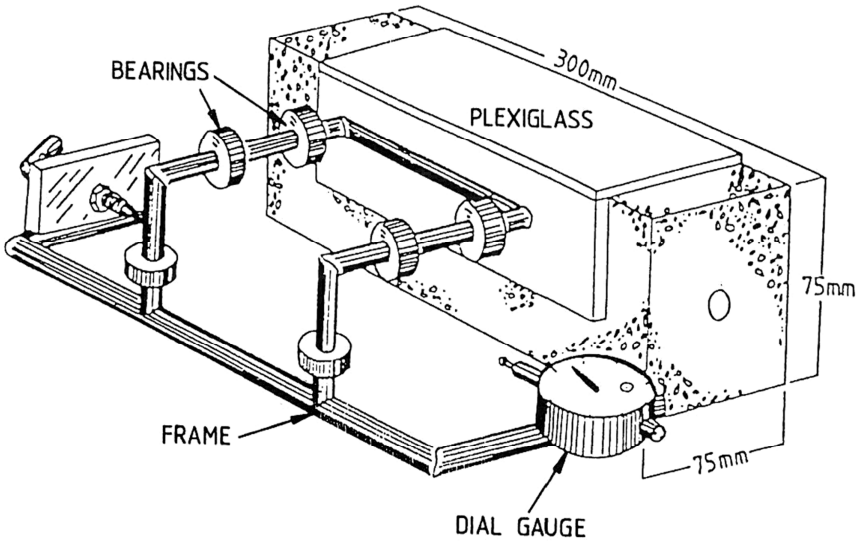

Figure: 2-8 Shrinkage Testing Equipment and Configuration based on a Rectangular Beam Specimen [George 1971]

The plexiglass has a frame, which fits in the beam; the frame rests on the plexiglass at one end while at the other end of the frame is a set of ball bearings. The contact pressure at both ends of the beam is maintained constant with the help of the spring-action of the dial gauge. Grobler [1994] states that it is difficult to attach the reference points to the beam; the test setup is complex and laborious. Figure 2-9 shows the alternative method of measuring shrinkage manually by placing a measuring instrument mounted with a dial-gauge device onto the studs. The distance between the studs was 100 mm.

Figure: 2-9 Shrinkage Testing Equipment and Measurement on Beam Specimen [Long and Ventura, 2004]

2.5.7 Prediction of Shrinkage Crack Patterns

Prediction of the shrinkage crack pattern, which refers to crack width, direction and spacing within a stabilised pavement layer, is essential. The detrimental effects emanating from shrinkage cracking predominantly in the region of crack include poor load-transfer. Detrimental effects related to resultant crack pattern are dependent on the individual crack width, direction and spacing, [Little *et al.* 1995; George, 2001; Wayne and Luhr, 2004]. Wide cracks usually greater than 6 mm wide result in poor load-transfer and increased stresses

within the pavement structure, [Little *et al.* 1995; Kota *et al.* 1995]; this eventually leads to a combination of performance and durability related distresses.

Several factors, including material characteristics, construction procedures and restraint imposed on the stabilised layer by the underlying layer influence the resultant crack pattern, [Wayne and Luhr, 2004; George, 2001; Little *et al.* 1995]. Environmental conditions, particularly thermal effects and seasonal ranges along with the time of construction influence resultant shrinkage crack pattern, [Houben, 2008; 2009]. Adaska *et al.* [2004], Little *et al.* [1995], Houben, [2008; 2009] typify shrinkage crack pattern as a resultant effect of a combination of factors related to material characteristics, interlayer restraint [friction at the interlayer] and environmental and/or seasonal effects. Adaska *et al.* [2004] states that the generated stress concentrations in the stabilised layer give rise to cracks if and/or when not relieved. The restraint at the interlayer between the stabilised layer and underlying layers in addition to material characteristics play a significant role in the resultant crack pattern.

Adaska *et al.* [2004], Little *et al.* [1995], George [1968] and Nakayama and Handy [1965] report that material characteristics, compaction, curing procedure and cement content influence shrinkage. A few studies do examine material related factors and their influence to shrinkage. Limited studies assess the resultant crack pattern relative to material type. Field studies conducted by Little *et al.* [1995] and George [2001] on stabilised base layer sections focused on the resultant shrinkage and performance. The studies concluded that resultant shrinkage dictated the section's performance; the wider the crack width the more water infiltration and subsequent pumping of the underlying material fines occurred. The field studies also reported that because of increased load-induced stresses emanating from wide cracks, further secondary cracks occurred. However, the studies provide limited data regarding the resultant crack pattern.

For concrete pavements, several models formulated to examine resultant shrinkage crack pattern and probable detrimental effects are in place. Such models incorporate seasonal effects, material parameters, as well as the techniques employed to mitigate shrinkage cracking. Houben [2008, 2009] show that environmental and/or seasonal variation, material characteristics and frictional coefficient at the interlayer along with material stress relaxation influence the resultant crack pattern particularly the crack width and spacing. The *Houben-model* analyses crack pattern for concrete pavement layer with and without cuts or joints. The model requires various parameters, which include but is not limited to, the following:

a) material strength properties including tensile and compressive strength as well as modulus of elasticity
b) seasonal data, particularly temperature amplitude
c) material thermal coefficients, i.e. coefficient of linear thermal expansion
d) shrinkage related data
e) material stress relaxation
f) frictional coefficient

The *El-Rahim and George Model* [El-Rahim and George, 2001] assesses transverse cracks in cement-stabilised layers. The *El-Rahim and George Model* is a simple one-dimensional mechanistic model. Parameters required by this model include the following:

a) volumetric change [shrinkage] due to drying and/or temperature variation
b) material tensile strength
c) material stiffness and creep
d) layer restraint

Like most models, its reliability is dependent on the input parameters as well as the assumptions made. The *El-Rahim and George Model* considers that the pavement layer maintains complete contact with the underlying layer, [El-Rahim and George, 2001]. Amidst

such assumption, friction forces and tensile stresses are calculated. Comparison of the calculated tensile stresses to the layer tensile strength is undertaken. Theoretically, cracks emanate when the material tensile stresses exceed the material tensile strength. In long pavement slabs or layers, the friction forces cause overstressing which leads to the formation of a crack, [George 2001].

The *Houben-Model* assumes that cracks emanate in the middle of an intact slab or layer. This inherent concept suggests that an increase in drying shrinkage results in a corresponding increase in tensile stress. This theoretically suggests that the occurrence of cracks is in the middle zone of the slab. George [2001] state that as drying progresses an increase in tensile stresses emanates in the intact half-slab causing secondary or subsequent cracks in the midsection of each intact slab. Successive cracks emanate in the midsection of the remaining intact slabs until the tensile strength exceeds the developed tensile stresses. A number of models show that the restraint imposed by the underlying layer induces tensile stresses in the longitudinal direction of the slab and/or layer, [El-Rahim and George, 2001; Houben, 2008; 2009; 2011].

Houben [2008] examines the shrinkage crack pattern in concrete pavements and reveals the following principles and insights:

a) the first cracks occur after construction
b) seasonal periods, i.e. summer, winter as well as day and night temperature fluctuations influence resultant shrinkage and slab crack patterns
c) calculations were made for a duration of 360 days or 8640 hours starting at the time after construction; every series of cracks results in a reduction in stress
d) the material exhibits an expansion and contraction depending on temperature variations [expansion when temperature levels increase and contraction when temperature levels drop]
e) the material is considered homogenous and exhibits linear-elastic behaviour [an average material behaviour is assumed]
f) the occurrence of cracks emanate due to the development of tensile stresses [when resultant tensile stresses exceed the plain concrete tensile strength cracks appear]
g) the model includes plain concrete, underlying layer and/or overlying layer

Furthermore, the values and/or range of the input parameters into the crack pattern models are of significant importance to the outcome especially in characterising the crack pattern. Xuan [2012] shows the influence of stress relaxation on shrinkage crack patterns and deduces that the value of stress relaxation affects the induced tensile stresses and thus, the resultant crack pattern. Houben [2008] defines stress relaxation as an exponential function with a value of 1.0 at the time of construction; this gradually reduces as the material ages or gains strength. Table 2-2 lists the various the stress relaxation models.

Houben [2008] and Xuan [2012] mention that the time of construction, degree of compaction and cement and moisture contents are other fundamental factors influencing the crack pattern. In practice, the control of shrinkage cracking is a combination of the following, [Nakayama and Handy, 1965; George, 1968; Little *et al.* 1995; George, 2001; Adaska *et al.* 2004]:

a) appropriate selection of materials
b) use of low cement and moisture contents
c) high compaction of stabilised layers [high compaction densities]
d) employing suitable curing procedures

While some researchers suggest placement of an asphalt surface as early as possible others recommend a delay in placing asphalt surface. George [2001] asserts that considering that shrinkage is an inevitable occurrence, it is practically feasible to place the surface layer as

soon as possible. Current control measures of shrinkage in cement-stabilised layers concentrate on limiting fines content and/or plasticity index, [Nakayama and Handy, 1965; Little *et al.* 1995; George, 2001; Adaska *et al.* 2004]. Recent research studies and models show that increasing the underlying layer resistance and/or interlayer bonding promotes narrower crack width, [Adaska *et al.* 2004]. This infers that increasing the friction resistance at the interlayer reduces the crack width. The realisation of full bonding at the interlayer zone is essential.

Table 2-2: Stress Relaxation Models

Items	Models of stress relaxation	References
Model 1	$R(t) = \exp(-0.0003 \cdot t)$	(Houben, 2008)
Model 2	$R(t) = \frac{0.32 + 0.85 \cdot t}{0.32 + t}$	(Morimoto & Koyanagi, 1994)
Model 3	$R(\alpha(t), \alpha(\tau)) = \exp[-(\frac{\alpha(t)}{\alpha(\tau)} - 1)]$	(Lokhorst, 2001)
Model 4	$R(t) = 0.8265 \cdot \exp(-8 \times 10^{-5} \cdot t)$	(Pradena & Houben, 2012)

2.6 Durability of Cement-Stabilised Materials

Durability of cement-stabilised materials also depends on the quality of the original un-stabilised material and applied construction techniques, [Paige-Green, 2008, De Wet and Taute, 1985]. The permanence of stabilised materials changes with time. After construction, the stabilised layer is still intact but due to environmental and traffic effects its durability changes. The appearance of cracks in the stabilised layer not only reduces the structural capacity of the pavement but also accelerates its degradation. Trafficking of a stabilised layer with cracks not only leads to continual damaging [formation of secondary cracks] but also pumping of fines due to water ingress. Section 2.4 notes on the detrimental effects emanating from shrinkage cracking. In this section durability of cement-stabilised materials as related to other factors, including environmental effects [carbonation and moisture susceptibility] are stated.

In order to gain a better understanding regarding the durability of cement-stabilised layers cognisance of the deterioration of the pavement from a road user point of view is essential. The present serviceability index [PSI] that defines the riding quality of the pavement is considered. Figure 2-1 illustrates the typical deterioration curve of a stabilised layer. The riding quality decreases slowly up to a certain point thereafter the rate of deterioration rapidly increases. The rate of deterioration is primarily dependent on [Freeme, 1984; De Beer, 1985; Paige-Green, 2008]:

a) materials considered for stabilisation [gravels and soils]
b) overall design of the pavement structure
c) quality control during construction
d) traffic loads
e) maintenance and rehabilitation measures
f) external factors, including adverse environmental conditions

Typical deterioration mechanisms include shrinkage cracking [Section 2.4] and load associated cracking [fatigue]. De Beer and Visser [1989] note that pumping is a mechanism

that contributes to the majority of deterioration in a cement-stabilised layer. Erosion is a cause of failure in stabilised pavement. The erodibility of a stabilised layer involves pumping of fines to the surface through cracks. The pumping mechanism includes:

a) water ingress into the pavement structure through cracks
b) most moisture sensitive layer parts get wet – moisture sensitivity is dependent on poor mixing or due to the carbonation of the materials especially in the region of a crack
c) in the region of a crack poor load transfer allies with secondary cracking emanating from traffic loads
d) under load there is a development of pressure and the resultant pumping of water and fine material to the road surface

Carbonation is a chemical reaction between carbon dioxide in the atmosphere and materials with chemical products of cementation; [Ca (OH) $_2$] revert to $CaCO_3$. The resultant product [$CaCO_3$] has a minimal cementing ability, [Bagonza *et al.* 1987]. Tests using phenolphthalein or hydrochloric acid can determine whether carbonation has taken place. Phenolphthalein determines if the saturation pH of 12.4 exists. A high pH of 12.4 is possible because of the presence of calcium hydroxide in the material. A pH of 12.4 and above increases the solubility of silica and alumina whereby the reactions proceed to form calcium silicates and aluminates. Calcium silicates and aluminates are necessary for cementation. Hydrochloric acid determines whether lime or cement is present. Paige-Green *et al.* [1990] state that by ensuring that stabiliser content exceeds its initial consumption, carbonation is minimised.

Salt crystals and sulphate attack cement-stabilised layers, causing a loss in cementation and/or excessive expansion and swelling, [CSRA, 1986; 1997]. This leads to a loss of strength; the presence of deleterious organic components causes a rapid reduction in pH. South African technical specifications TRH13 [1986] stipulate limits for salt and sulphate. Several factors need to be satisfied to ensure long-term performance of stabilised layers, [Sampson and Paige –Green, 1990]:

a) using the appropriate cement content to maintain the required pH so that the cementation reaction continues
b) suitable durability tests must be performed to identify potential degradation criteria
c) identification of the possible material erodibility and pumping
d) a minimum residual UCS value should be achieved in order to ensure an adequate structural capacity under the most severe adverse environmental conditions

The wet-dry test is a commonly used test. Developed by the Portland Cement Association and incorporated into the South African Technical Methods for Highways number 1 [TMH1, 1986] this test method is used to assess the durability of stabilised materials. Ventura [2003] details its development and reliability in assessing material durability. The mechanical brushing test uses the abrasion criteria to remove loose particles from the specimen surface. Method A19 TMH1 [1986] details the wet-dry durability test protocol. In the wet-dry test, the specimens are subjected to 12 cycles of wetting and drying.

Traditionally the development of most erosion tests concentrates on evaluating erosion resistance of materials usually considered for construction of canals, earth dams and slopes. Ventura [2003] states that any erosion tests purposed for evaluating stabilised materials [erodibility] must realise the following aspects:

a) the test should simulate a wet state and stabilised layer behaviour
b) it must incorporate the aggregate to aggregate contact stresses which significantly contribute to surface crushing [compression stress] in order to produce erodible fines
c) it must provide a quick assessment of the potential erodibility of materials to be used in the stabilised layer
d) it must offer a simple and easy method for measuring erosion

Rotational shear devices [RSD] measure the material erodibility; RSD remains an experimental test method. Van Wijk [1985] describes a type of RSD. In the annular space, water surrounds the specimen. By encapsulating the top and bottom of the cylinder, rotation of the specimen takes place securely. After completion of the test, weighing of eroded material follows. With the RSD test, uniform shear forces develop on the lateral surface. The test is not suitable for non-cohesive materials such as sands.

Construction of the majority of South African roads follows the standard specifications for roads and bridges for road authorities [COLTO, 1998]. The durability requirements for natural gravel and crushed stone are stated. Evaluation of material durability follows various test methods with limits proposed by Weinert [1980], Paige-Green [1980], Venter [1980], Sampson [1990], Carde and Francois [1997]. Test methods specified include the 10% Fines Aggregate Crushing Value [10%FACT] and Durability Mill Index. The 10%FACT is a wet and dry crushing test. The Durability Mill Index is a wet abrasion, impact test. The test involves soaking. The wheel-tracking test is another durability test method not specified.

Primarily, loss of material particles after a series of abrasion and/or erosion tests characterises the durability of the material. Increasing the amount of cement in the mix usually enhances the particle bond strength and ultimately decreases particle loss, [Parsons and Milburn, 2002]. However, in the case of high cement contents, a decrease in the average pore size and permeability results; this makes it more difficult to saturate the specimen besides reducing the particle bond strength, [Neville, 1997]. The key objective of conducting durability tests is to assess the material's resistance to abrasion-erosion effects, [Parsons and Milburn, 2002].

2.7 Evaluation of Material Engineering Properties and Characteristics

Material engineering properties and characteristics such as strength, elastic modulus and fatigue are essential to material and pavement performance, [Austroads 2006]. The mechanistic design of pavement uses layer moduli and strength parameters as inputs in the design of pavements. However, this requires knowledge of the stress-strain [stiffness properties] and fatigue relationships of materials, [Arellano and Marshall, 1998].

SAPEM [2013] among other technical guidelines refer to the compressive strength test [UCS] and the tensile strength test [ITS] for the evaluation of cement-stabilised materials. Practice routinely uses the UCS and ITS tests to assess the suitability of cement-stabilised materials, [TRL, 1993]. Table 2-3 summarises the various specifications.

The Southern African practice seldom considers mechanical strength tests such as the flexural beam tests in the evaluation of stabilised materials. Practice usually uses UCS test data to correlate and derive the various material engineering properties including the elastic modulus besides material strength. TRH13 [1986] specifications provide correlations [models] to derive the equivalent elastic modulus and strain-at-break. The current concept of reliability in design necessitates accurate quantification of the design inputs. Several models relate the compressive strength value of the stabilised material to their elastic modulus.

Lim *et al.* [2003] developed an elastic modulus relationship based on the material compressive strength test. The model [Equation 2-5] considers the dry density [D] in its computation of material elastic modulus [Lim and Zollinger, 2003].

$$E = 6.72\ (UCS)^{1.5}\ (D)^{0.75} \qquad \text{Equation 2-5}$$

Where: D is the Dry density [kg/m^3]; E is the elastic modulus in MPa; UCS compressive strength in MPa

Table 2-3: South African and ORN 31 Specifications

South African Specifications Strength Requirements for Stabilised Materials					
Material Classifications	(COLTO, 1996) Minimum ITS (kPa)	4 Hours Soaked UCS (MPa) after 7 days, (TRH 14, 1985)			
		100% Mod.AASHTO Compaction		97% Mod.AASHTO Compaction	
		Minimum	Maximum	Minimum	Maximum
C1	-	6	12	4	8
C2	400	3	6	2	4
C3	250	1.5	3	1	2
C4	200	0.75	1.5	0.5	1
ORN 31 (TRL 1993)					
Pavement Layer		Strength Requirements (MPa)			
Cement or Lime Stabilised Sub-base (CS)*		0.75 to 1.5			
Roadbase 1 (CB1)		1.5 to 3.0			
Roadbase 2 (CB2)		3.0 to 6.0			
Note *For CS materials, i.e. CBR value of 70 after 7 days moist curing and 7 days soaking CB1: cemented sub-base in high traffic designs under asphalt wearing course and crushed rock road base CB2: road base material with design traffic up to 10 million cumulative equivalent standard axles Source: TRL 1993					
Correction Factors for Cylindrical Specimen (ORN 31 – TRL 1993)					
Size (mm)		Correction Factor			
200-diameter, 100-mm height		1.25			
115-mm diameter, 105-mm height		1.04			
152-mm diameter, 127-mm height		0.96			

2.7.1 Factors Influencing Stabilised Material Properties

Engineering properties of cement-stabilised materials, including strength and elastic modulus extensively vary. The factors of influence to the engineering properties of stabilised materials include:

a) moulding moisture relative to the achievable material dry density
b) material quality relative to cement content and its efficacy
c) variation in natural material properties and characteristics
d) curing procedure and conditions

Moisture at the time of mixing has a direct effect on the achievable density and ultimately resultant engineering properties including strength. Density and moisture content affect the compressive and tensile strength properties. Felt [1955], Davidson [1962] and Catton and Felt [1943] showed that fine-grained materials exhibit a parabolic moisture density curve when stabilised using Portland cement. Felt [1955] showed that for either sandy or clayey soils, an increase in density resulted in an increase in compressive strength. However, subsequent studies such as Kayyal [1965] establish that strength increases with density to a specific limit beyond which, a reduction in material strength occurs.

Moisture content plays a significant role regarding achievable density. At the material's optimum moisture content, maximum density is registered. Coarse aggregates exhibit maximum compressive strength at moisture contents slightly below their optimum. On the contrary, finer materials such as soils exhibit maximum compressive strength at moisture contents slightly above their optimum, [Martin, 1960]. Watson [1941] notes that material characteristics such as, gradation and Atterberg Limits, among others influence the resultant engineering properties and characteristics.

A proportion of cement added to material alters the plasticity, volume, elastic and strength properties. The effect of cement on material depends on the degree of treatment and type, [Watson, 1941; Felt, 1955; Terrel *et al.* 1979; Paige-Green, 2008]. Felt [1955] varied the cement percentage from 6% to 30% by dry mass of fine-grained soils that included sands, silts and clay. Every addition of cement to the material resulted in a corresponding increase in strength.

The physical-chemical reactions involving material and cement following the addition of water are responsible for the resultant engineering properties. Type and quality of material considered for stabilisation influence the efficacy of cement and ultimately engineering properties, [Terrel *et al.* 1979]. Felt [1955] showed that at the same cement content and curing conditions, sandy soils provide higher compressive strength than silty and clayey soil types. The type and quality of the natural material influenced the efficacy of cement more than any other factors. Cement and material interactions include chemical and physical properties and characteristics. Chemical properties include the mineralogical and geological characteristics. Fines content and general particle-size distribution influence the cement-material reactions. Additionally the presence of deleterious organic matter retards the cementation; this impedes on the resultant strength properties, [Clare and Sherwood, 1954]. Catton [1940] establishes that the gradation of material influences on the density, cementation effect and ultimately the resultant strength. Well-graded coarse aggregates exhibit higher densities and provide more strength than materials that contain large quantities of fines. Well-graded materials usually require small quantities of cement for stabilisation.

The type of cement, moisture content and temperature influence the resultant strength of cement-stabilised materials. The procedure adopted and the time allowed for curing influence the engineering properties of stabilised materials, [Terrel *et al.* 1979; Bredenhann *et al.* 2011]. Curing conditions determine the amount of moisture retained in the mix. Maner [1952] notes that as long as adequate moisture for both compaction and hydration is available, appropriate curing conditions will provide suitable strength. Dumbleton and Ross, [1960] establish that an increase in material strength relative to curing temperature is greater at higher temperatures than lower temperature ranges for the majority of cohesive materials.

Material relative density relates to specified compaction energy, [Das, 1990]. The Modified AASHTO method uses the impact compaction method, which involves dropping a weight from a specified height or level onto the surface of the material. A comparison of the impact method to the vibration method shows that the vibratory method is an effective method for compacting granular soils and aggregates. Material compacted on the moist side [beyond the OMC] of the density-moisture relationship provides lower cohesion values and strength than equivalent type compacted at optimum moisture. Compaction reduces the voids content and thus increasing the density; this ultimately influences the engineering properties of stabilised materials, [Austroads, 1992].

The preparation of cement-stabilised materials often includes mix-in-place procedures, [Terrel *et al.* 1979]. The first phase comprises of the pulverisation of material. Later on, the addition of a mixed amount of cement to the material as a means to complete the dry mixing is undertaken. Subsequent to dry mixing, addition of a measured quantity of water to material follows. Material pulverisation improves the uniformity of the mix but increases the fines content and surface area. Increasing the time of mixing decreases material strength, [Felt, 1955]. This suggests that prolonging the mixing time influences the workability and overall compaction of the mix.

2.7.2 Initial Consumption of Cement

The effects due to carbonation of the cement-stabilised layer lead to the loss of cementation, which results in the disintegration of the layer, [De Wet and Taute, 1985; Sampson *et al.* 1987; Bagonza *et al.* 1987]. Carbonation of the cement-stabilised layer takes place during the curing phase and/or after construction. Carbonation is due to the attack of carbon dioxide on the hydroxides and other stabilisation products. The effect of carbonation on lightly cement-stabilised layers is considerably greater compared to concrete or heavily cement-treated material types, [Paige-Green *et al.* 1990]. Carbonation affects cement-treated materials, which exhibit reduced strength and pH, [Paige-Green 1991]. This suggests that with increased strength and cement contents the effects emanating due to carbonation are reduced.

2.7.3 Engineering Properties and Drying Shrinkage

Curing conditions influence shrinkage and the engineering properties of cement-stabilised materials. Temperature and humidity levels contribute to moisture loss from the material matrix. Available moisture in the mix influences the material strength properties and the degree of shrinkage. The achievable density is dependent on the moulding moisture and particle-size distribution, [Felt, 1955]. Moulding moisture and density influence the degree of shrinkage, [Bofinger *et al.* 1978].

Addition of cement to the material results in an increase in their moisture content, but a decrease in their dry density, [Das, 1990]. An increase in moisture demand is due to the flocculating effect as well as the influence of the cement hydration process. The reduction in material density due to the addition of cement is caused by the development of early bond strength, [TRH13 1986]. One of the control measures to minimise shrinkage cracking is to limit the cement dosage. This also reduces the strength. Another control measure to minimise shrinkage cracking is reducing the moulding moisture. The moulding moisture contributes to the extent of drying shrinkage, [Bofinger *et al.* 1978]. This is because the degree of cracking is proportional to moisture loss on drying. Longer curing periods increase the total drying shrinkage, [George, 1971; Felt, 1955]. Equally, increasing the curing temperature increases the rate of drying shrinkage, [George, 2001]. This suggests that wetter materials lose more moisture resulting in increased total drying shrinkage. Drying shrinkage is due to the loss of water and is dependent on the pore structure [dictated by density] and the available moisture in the matrix.

The amount of cement in the mix determines the resultant engineering properties and characteristics. However, this is dependent on the physical-chemical material characteristics, moisture content and degree of compaction along with the curing conditions [Austroads, 1992; Bofinger *et al.* 1978; Terrel *et al.* 1979]. Similar factors influence the total resultant drying shrinkage. Variations in cement content influence the shrinkage characteristics as well as strength properties. A material's density defines the particle-to-particle linkages, which characterise the pore structure [void content]. A material's matrix that exhibits high voids content [interconnected pore structure] also portrays reduced mechanical strength properties, [Callister, 2003]. Interconnected pores form passages to moisture loss during drying. This indicates that rate of shrinkage depends on the characteristics of the pore structure. Theories pertaining to the effect of cement include:

a) the addition of cement to material results in a corresponding increase in compressive and tensile strength properties but a reduction in flexibility [increase in brittleness or stiffness properties]
b) the addition of cement to material results in a reduction in density but an increase in moisture demand

c) increasing the cement in the mix contributes to drying shrinkage and resultant cracking, but this is dependent on the restraints and material characteristics

The resultant crack pattern, more importantly, the width of the cracks within a stabilised layer influences its overall performance and ultimately the engineering properties, [Freeme 1984; Bofinger *et al.* 1978]. Under ideal curing conditions, layer strength along with the imposed restraints influence the resultant crack pattern. However, during the early life of the stabilised layer [i.e. directly after construction], material shrinkage characteristics dictate on the resultant crack width, [Bofinger *et al.* 1978]. During the later life of the stabilised layer, variations in temperature and moisture influence the resultant crack width characteristics. The major factors that influence drying shrinkage in cement-stabilised materials ultimately influence the engineering properties of the materials [Barksdale and Vergnolle, 1968].

2.7.4 Strength Properties of Stabilised Materials

Hydration of cement contributes to the enhancement of its engineering properties. As the cement hydrates strong linkages [bond strength] develop between the material particles forming a hard material matrix [bound material]. Several factors influence the development of bond strength as listed in the previous sections. In general, the literature shows that strength increases with cement content, density, material characteristics and curing procedures. A number of factors influence material strength, [Terrel *et al.* 1979].

Compressive strength characterises the load capacity of a stabilised material. The test involves subjecting all the fibres to a compressive force. Strain is the change in length under applied compressive stresses, [Callister, 2003]. The compressive stresses are characterised by negative strains. In practice, the registering of the compressive strength value includes the curing period and compactive effort. Table 2-3 provides the specifications for compressive strength. Figure 2-10 exemplifies the relationship of UCS value and curing time as well as cement content. Sherwood [1968] defines the cement content and a UCS value relationship as linear. Several factors, including cement content and material as well as the degree of compaction influence the cement-UCS linearity. Kolias and William [1984] and TRH13 [1986] note that material mineralogy along with aggregate strength and gradation influence the resultant compressive strength. Curing conditions also influence the strength development of cement-stabilised materials.

Tensile strength is a significant material property because it measures the force required to break or cause fracture in tension. It defines the maximum tensile stress a given material can sustain before failure. Tensile strength characterises the structural capacity of a stabilised material to endure tensile stresses and strains when loaded, [Mindess *et al.* 1981]. Tensile strength testing and evaluation of cement-stabilised materials involve the consideration of the flexural beam test, a direct tension test and indirect tensile test.

Several researchers consider the direct tension test as a test that provides a better reliability and measure of the material tensile strength. Mindess and Young [1981] note that the direct tension test has no standard test protocol. The technique used to hold the specimen [i.e. in the direct tension test] generates secondary stresses, which influence the data. The repeatability of the tension test is challenging which is its primary disadvantage to its reliability.

The splitting tension test [ASTM, C496] and the flexural test [ASTM, D1635 and C78] are the two indirect tension tests considered for the characterisation of the material tensile strength. William [1986] provides the following demerits regarding the test procedure of the splitting tension test:

a) The test considers unrealistic assumptions pertaining to material behaviour under load; the test does not simulate field behaviour of the layer under wheel loading.

b) The influence of the wedges on the maximum load applied determines the measure of the material tensile strength properties. Due to this resistance the maximum applied load is initially distributed an aspect that influences the measure of 'actual' maximum load required to induce a split.

Method 16T TMH1 [1986] provides the test protocol used by the South African practice. Several relationships approximate the indirect tensile strength test to the UCS test such as Equation 2-6.

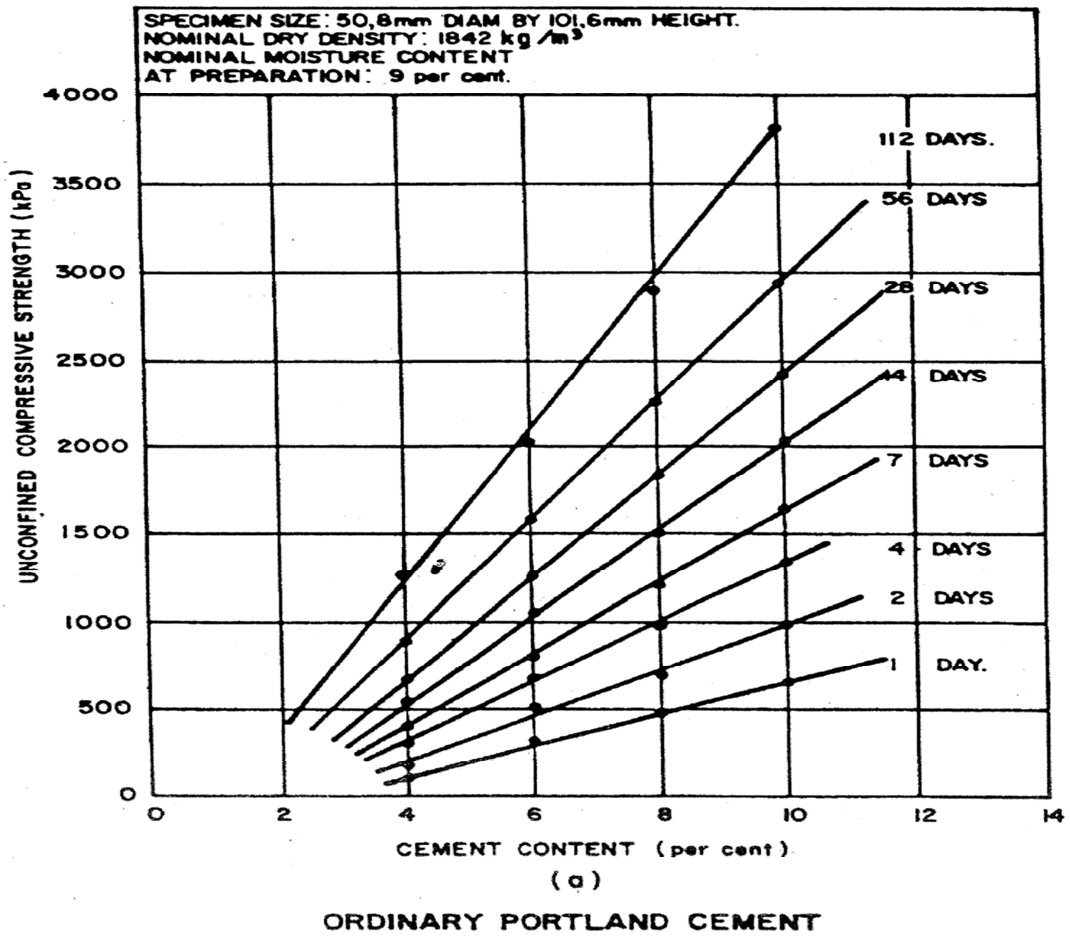

Figure 2-10: Relationship of Curing Time and Compressive Strength of Well-Graded Sand and Gravel [TRH13, 1986]

$$ITS = a\ UCS \quad \text{[TRH13, 1986]} \qquad \text{Equation 2-6}$$

Where: a is a coefficient dependent on the material [a = 0.13, TRH13, 1986]

The relationship between the tensile and compressive strength of cement-stabilised materials varies because of the variability between the material types. Sherwood [1968] concluded that split tensile strength was approximately 10% of the compressive strength for the same stabilised material type. Little [1995] state that for the same stabilised material the tensile strength was about 13% of the unconfined compressive strength. By comparing the tensile strength to the compressive strength, the validity of the analysis is subsequently characterised.

2.7.5 Flexural Strength Beam Test

The flexural strength tests determine the mechanical properties of the material. Flexural strength is a mechanical parameter, which defines the ability of the material to resist

deformation under load, [Callister, 2003; Hodgkinson, 2000]. Flexural strength testing includes two loading techniques viz. the three-point loading mode [also termed centre point loading] or a four-point loading [also termed third point loading]. Figure 2-11 illustrates the loading modes and the inherent principles of load distribution.

The four-point and three-point loading techniques determine the material flexural strength and modulus, [Theocaris *et al.* 1977; Baratta *et al.* 1987; Theobald *et al.* 1997]. From the principles of engineering mechanics, flexural modulus [also referred to as bending modulus] is the ratio of stress to strain in the flexural deformation. Several research studies establish that the flexural modulus is equivalent to modulus of elasticity or elastic modulus. By conducting a flexural strength test, material suitability can also be ascertained, [Baratta *et al.* 1987]; the flexural test is the primary source of the uniaxial strength data. However, the current impediment in considering the flexural strength test is due to the following aspects, [Arellano and Marshall, 1998; Baratta *et al.* 1987]:

a) lack of a standard test method or protocol
b) presence of experimental errors in the current practices which include accurate flexural strength and influence emanating from internal beam shear stresses

Baratta *et al.* [1987] declare that the simple beam theory assumptions adopted along with the ranges of specimen geometric ratios lead to an erroneous measure of the material flexural strength and the interpretation of test data. The beam theories and assumptions include:

a) transverse planes perpendicular to the longitudinal axis of the beam remain plane after the beam is deflected
b) the modulus of elasticity in tension is equal to the modulus of elasticity in compression
c) beam material is assumed to be isotropic and homogenous
d) maximum deflection can be small compared to the beam-depth
e) beam deflects normally under elastic bending stresses but not through any local collapse or twisting
f) stresses in the longitudinal direction are independent of those in the lateral displacements

The first two assumptions [as noted above] assert that transverse planes are intact after deflection, and that, the modulus in tension is equal to the modulus in compression. This suggests that:

a) Stresses and strains are proportional to the distance from the neutral axis, [Baratta *et al.* 1987; Arellano and Marshall, 1998]. This proposes that the bending stress is proportional to the distance from the neutral axis to the outer surface of the beam. Baratta *et al.* [1987] declares that the assumption is only valid if bending of the beam does not result in a localised force build up. Practically the flexure test requires direct contact of the fixtures [rollers] onto the beam in order to apply a load. At the point of contact, there is a compressive stress in the direction of the beam-depth. The compressive stress contributes to the local deviation of the bending stresses from its assumed linearity.
b) The stress does not exceed the proportional limit of the material, [Baratta *et al.* 1987].
c) Due to the first two assumptions, the influence of shearing resistance [shear stresses] within the beam will occur, [Baratta *et al.* 1987].

The assumption that the modulus of elasticity in tension equals modulus in compression [$E_t = E_c$] presents another internal error in the flexural beam testing, [Baratta *et al.* 1987; Arellano and Marshall, 1998]. Chamlis [1974] states that modulus in tension is not equal to the modulus in compression due to material heterogeneity. This suggests a variation in the material elastic modulus. Baratta *et al.* [1987] state that factors such as anisotropy and heterogeneity negate such assumptions made. If the beam is anisotropic then the bending

stress is equal to the elementary theory. However, the application of the bending moment produces a twisting moment within the beam as it deflects under load. For this fact, determining the shear stresses produced by bending the beam cross-section [beam deflection] is essential.

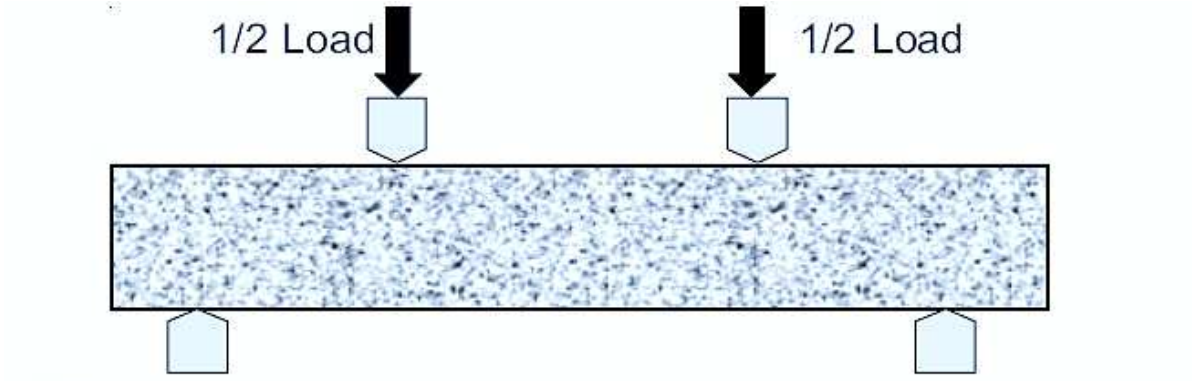

ASTM C 78 - Third-Point Loading - half the load is applied at each third of the span length. MR is lower than center-point loading. Maximum stress is present over the center 1/3 portion of the beam

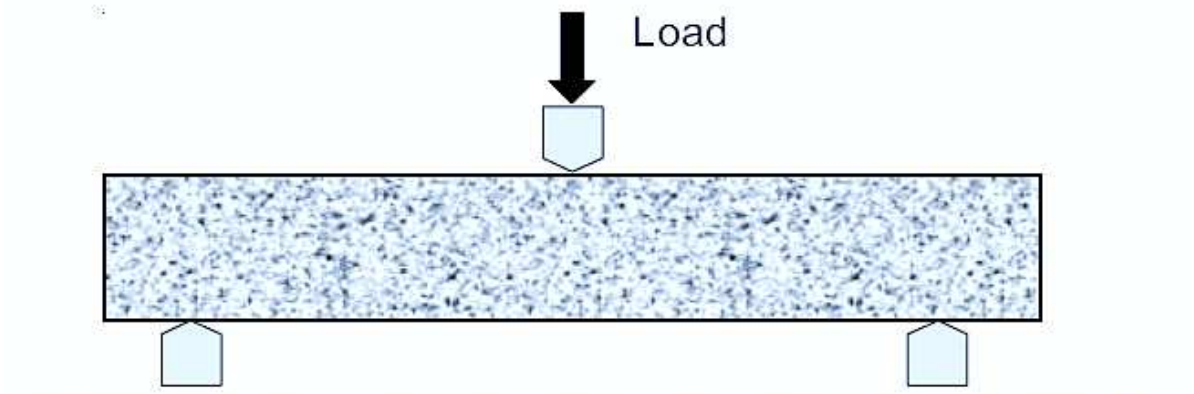

ASTM C 293 - Center-Point Loading - the entire load is applied at the center span. The MR will be greater than third-point loading. The maximum stress is present only at the center of the beam

Figure 2-11: Schematic Illustrations of the Flexural Loading Modes [ASTM C Specifications]

The bending moment in the four-point beam test is idealised as a constant; the assumption that there are neither horizontal nor vertical shear stresses within the inner span holds under such a criterion, [Chamlis, 1974]. In a three-point beam test, it is assumed that linearly is dependent upon the distance from the nearest support to the origin of fracture, however, this requires an additional distance in order to determine the fracture stress, [Baratta *et al.* 1987; Arellano and Marshall, 1998]. Shear stresses in a three-point beam test develop over the full span and thus, deviate from the uniaxial stresses in the four-point loading system.

Wedging stresses at the points of load application result in a deviation from the 'idealised' calculated constant stress at the two local regions in a four-point loading system, [Baratta *et al.* 1987; Arellano and Marshall, 1998]. In a situation where the ratio of half the distance between the outer span and inner span to the beam-depth is large enough, a minimal stress reduction takes place, [Chamlis, 1974].

Beam size plays a significant role when assessing brittle materials. The four-point beam test is preferred when determining the strength for design purposes, [Baratta *et al.* 1987; Arellano and Marshall, 1998]. Baratta *et al.* [1987] state that, the four-point beam test has its centre span uniaxially stressed and as a result, no shear stresses exist. The four-point and three-point tests are suited for specific applications and exhibit different advantages and disadvantages. External factors influence the accuracy of the test results. External factors are directly or indirectly caused by the loading application at the test fixtures; this leads to configuration constraints and/or errors, [Chamlis, 1974; Baratta *et al.* 1987; Arellano and Marshall, 1998].

The concept of reliability in the design of pavements following the prerequisite to appropriately quantify material properties and design inputs continues to intensify. Several road agencies continue to disregard the aspect of shear beam effects while undertaking material flexural strength measure. Publications reveal that because of the displacements and/or deflections, great span-depth ratios are preferred, [Timoshenko, 1921; Timoshenko, 1922; Timoshenko and Woinoswki-Krieger, 1970; Theocaris *et al.* 1977; Theobald *et al.* 1997]. A number of flexural strength evaluations consider different beam geometries and test configurations. Austroads [2014] applies a span-depth ratio of 3.0 in its flexural strength characterisation of cement-stabilised materials. Timoshenko [1921], Timoshenko and Woinoswki-Krieger [1970], Timoshenko [1978], Theocaris *et al.* [1977] and Theobald *et al.* [1997] reveal that:

a) for same material varying the support span in the flexural beam test changes the flexural strength; this suggests that test configurations have a significant influence on resultant material measure and the consequent interpretation of the test data
b) varying the beam geometric characteristics alters the flexural strength value; beam size and aggregate distribution are factors that also influence the measure of the flexural strength properties
c) the bending strength and modulus in the four-point loading is dissimilar to that in the three-point loading for the same material and beam geometric characteristics
d) a reduction in the support span occurs in the deformed configuration because of the rotation of the roller supports
e) beam-depth [beam height relative to loading-span, radius of the supports and loading noses also influence the measure of flexural strength properties

The strength tests such as the flexural beam test, split tensile test and compressive test measure different aspects of material strength, [Raad, 1976]. A number of strength test relationships link to the compressive strength test. Under applied wheel load, the stabilised layer experiences tensile stresses and strains. This recommends that the material evaluation process must consider some form of tensile strength measure. This refers to the indirect tensile strength [ITS] and flexural beam test. The flexural strength test simulates the mode of stress, which the stabilised layer experiences, [Arellano and Marshall, 1998]. Mindess and Young [1981] assert that the tensile strength acquired from the flexural beam test is normally higher than that obtained from the direct tension tests. In a stress-strain relationship, the slope of the straight line characterises the material elastic modulus. Likewise, assuming linear uniformity across the beam cross-section is erroneous as elaborated above. In the flexural test, the beam experiences compression [within the top portion] and tension stresses [within the bottom portion]. At the bottom middle section of the beam, a maximum tensile stress is reached; this is the zone of fracture.

A number of beam theories explain the dynamics of beam bending and deformation criteria, [Callister, 2003; Timoshenko, 1921; Timoshenko, 1922; Timoshenko and Woinoswki-Krieger, 1970]. The simplest beam theory is the Euler-Bernoulli beam theory. This theory assumes that straight lines normal to the mid-plane before deformation remain straight and normal to the mid-surface after deformation. This hypothesis negates the effects attributed to

transverse shear and transverse normal upon beam deflection. The Timoshenko beam theory relaxes the normality hypothesis as submitted by the Euler-Bernoulli beam theory. The Timoshenko beam theory integrates a constant transverse shear strain with respect to beam-depth and requires shear correction factors. The shear correction factors are dependent on the material type, specimen geometric parameters, loading and boundary conditions.

Raad [1976] demonstrated how various strength test procedures provide apparent strength differences because of negating the principles inherent to material behavioural response. The study considered the finite element theory and deduced that material modulus in compression is different from that, in tension. This deduction suggests that the flexural strength determined by different beam tests using simple beam theories assuming the stress-deformation characteristics of the material are linearly elastic is inaccurate. The study found that the moduli in tension compared to the moduli in compression almost doubled the true strength. However, pertaining factors such as beam geometric characteristics, particularly the span-depth ratio, degree of fixity at the supports and load applications influence the material property measure.

Despite this comprehension, development of the various strength test relationships is currently in place. Such relationships include:

a) Flexural strength to the tensile strength relation [Raad, 1976]
   f = 1.15 T [f – flexural strength and T – actual tensile strength] based on the simple beam theory assumptions.
b) Flexural strength to compressive strength [Mitchell and Freitag, 1977]
   $f = 0.5\ (UCS)^{0.88}$ [f – flexural strength in psi and UCS – compressive strength in psi compressive strength ranges of 500 psi to 3000 psi]

The elastic modulus expresses the stress-strain relationship of the material. For cement-stabilised materials, selection of an applicable elastic modulus value for design purposes is a challenging task owing to the difficulty in testing, [Scott, 1974]. Several researchers determine the material elastic moduli from the stress-strain curve. Roylance [2001] states that the stress-strain curves are the most fundamental material characterisation. Governing principles linked to Young's modulus of elasticity along with the stress-strain relationship are noted. Shen [1965], Bofinger [1970] and Chou [1977] investigated the stress-strain behaviour and concluded that the modulus in tension was lower than the modulus in compression. This recommends a new approach for evaluating the flexural strength and elastic modulus of materials.

2.7.6 Fracture Mechanics and Material Properties

The main objective in applying fracture mechanics is to predict the failure criterion of engineering materials, [Anderson, 1995; Hertzberg, 1995]. This technique provides insight into the material load-capacity besides crack propagation. The underlying assumption of fracture mechanics is that material breakup or crack when the resultant stress applied exceeds the bond strength. Fracture mechanics is a material failure theory which:

a) determines material failure by energy criteria feasibly with the material strength criteria
b) considers failure as a propagation throughout the structure rather than simultaneous throughout the entire failure region

The fatigue resistance of cement-stabilised materials decreases with increasing strength for a given strain level. This suggests that the stiffness properties of cement-stabilised materials dictate its fracturing behaviour. However the strains generated within the pavement structure of high stiffness [elastic modulus] are generally small, [Austroads, 1992].

Paris' law characterises the relationship between the rate of crack propagation under repeated cyclic loading and the range of stress intensity factor. Paris' law relates the stress intensity to sub-critical crack growth, [Paris and Erdogan, 1963]. Under fatigue loading the crack growth increases with the stress intensity factor. Figure 2-12 shows the schematic plot of the typical relationship between the crack growth rate and the range of the stress intensity factor. In order to model the linear interval calibration of the Paris' law is normally required.

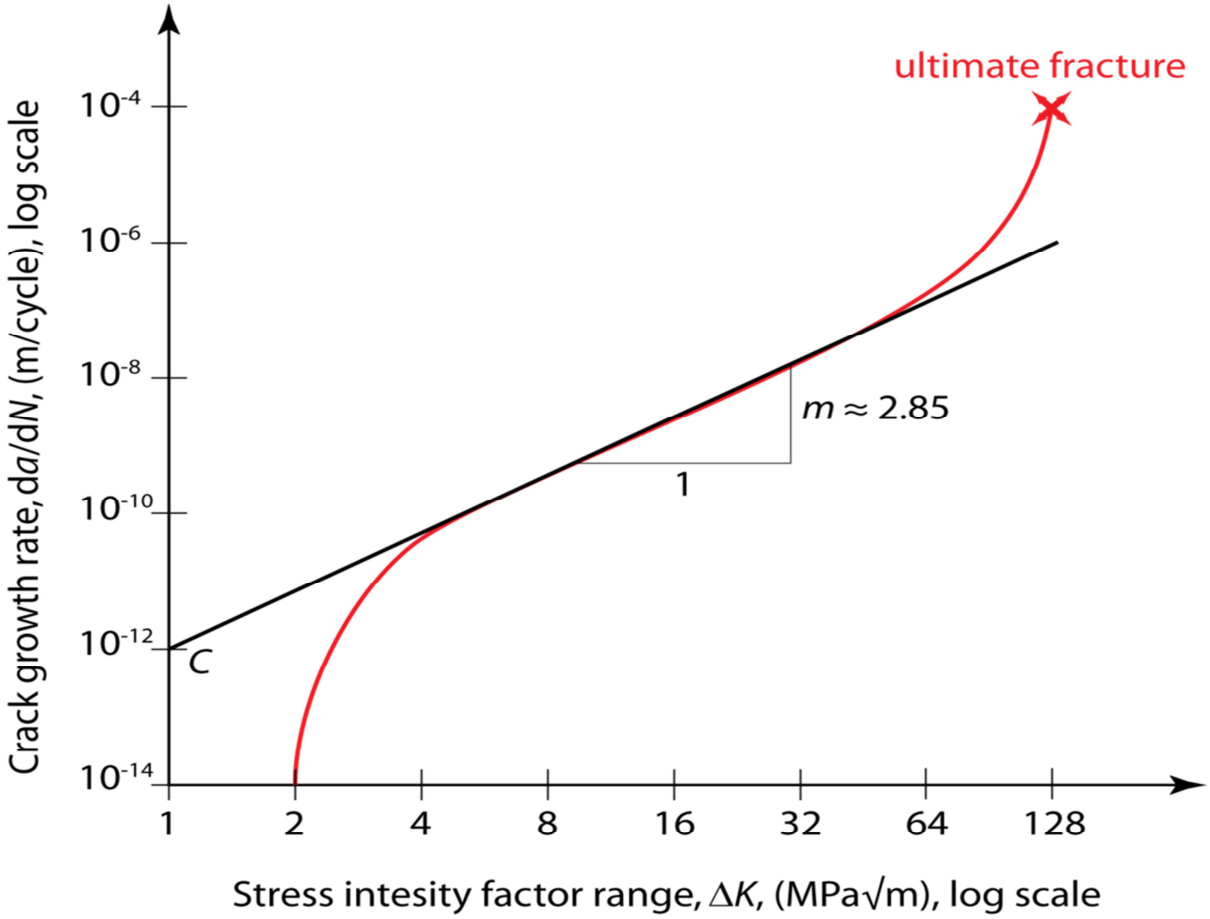

Figure 2-12: Schematic Plot of Crack Growth Rate versus Range of the Stress Intensity Factor [Roylance, 2001]

Roylance [2001] states that the use of Paris' law to quantify the residual life [in terms of load cycles] of a specimen for a given crack size is common. However, there is complexity in establishing a firm connection between Paris' exponent and microscopic parameters. For bodies under cyclic load with stress amplitude Paris' law governs their fatigue crack growth. Equation 2-8 denotes fatigue crack growth as related to Paris' law.

$$\frac{da}{dt} \sim (\Delta K)^{\beta} = C(\Delta\sigma\sqrt{a})^{\beta} \qquad \text{Equation 2-8}$$

Where: a – crack length, $\Delta K \sim \Delta\sigma\sqrt{a}$ – the stress intensity factor range and β is a material dependent exponent

The term fracture toughness refers to the ability of the material containing a crack to resist fracture, [Anderson, 1995; Hertzberg, 1995]. Fracture toughness characterises the resistance of the material to brittle fracture when and/or if the crack is present. A material that exhibits a high fracture toughness value undergoes ductile fracture. Various studies on fracture toughness, including Molenaar, [1983] [on asphalt mix types] as well as Bazant and Kazemi,

[1990] [on rock and concrete] reveal that the nature, type and quality of material significantly influence crack propagation and/or fracture behaviour.

The toughening mechanism emanating from the heterogeneous aggregates and the cement matrix influence crack propagation. For this fact, the heterogeneity, density relative to voids in the mix, will influence the Paris material exponent and thus, the crack growth rate. An increase in fracture resistance and/or toughness leads to a corresponding toughening mechanism and the ability to propagate a crack, [Bazant and Kazemi, 1990]. Fracture mechanics is an analytical tool, which provides insights regarding the mechanical behaviour of the material with reference to their fracturing criterion or crack behaviour under load.

The response of stabilised material to tensile and compressive strength loading is fundamental. This provides insight concerning their suitability for use in the construction of pavement layers. Concrete and cement-stabilised materials exhibit the best qualities in compression but are weak in tension; this suggests that cementitious materials can withstand considerable compressive loads but limited tensile stresses [Bazant and Kazemi, 1990]. For this reason, the evaluation of the stress-strain criteria along with the standard material property measure for stabilised materials provides a good indication of their behavioural response and properties. In the tensile loading criteria, induced tensile stresses result in the formation of cracks within the cement matrix, which reduces the bond strength and the elastic modulus. A cement matrix is essential because it binds the aggregate particles together. Equally, the occurrence of drying shrinkage cracks further reduces the bond-strength and elastic modulus; this ultimately decreases the fracture toughness of stabilised materials. Shrinkage cracks weaken the material load response, especially in the tensile loading criterion, [Thom and Cheung, 1999].

In order to evaluate the load-response and its fracture behaviour the fracture energy concept is normally applied, [Anderson, 1995]. Fracture energy is the energy required to fracture a unit area of surface. The following aspects characterise fracture energy:

a) it is a material property
b) it is independent of the size of the structure and thus, defined as a unit area of a surface
c) it is a function of displacement

In material science, the area under the stress-strain curve defines the energy required to result in a fracture. Unlike fracture toughness, fracture energy refers to either fractured or intact specimens. An increased fracture energy [area under the curve] value represents a material with a better load-response and/or typifies high resistance to cracking. Derivation of fracture energy includes the area from the start of the test to the peak [or the end of test], [Bazant and Kazemi, 1990; Anderson, 1995]. Figure 2-13 illustrates the different material types and their load-response and fracture energy. Different materials exhibit different stress-strain envelopes and ultimately different strain-at-break values.

Strain-at-break characterises material flexibility relative to the measure of loading capacity. When a material fractures, a reduction in its structural capacity results, but this is dependent on the resultant crack pattern and crack propagation. At its strain-at-break, the material is deformed, [Roylance, 2001]. Figure 2-13 typifies that material type (1) exhibits the greatest brittle character compared to the rest of the material types. This is attributable to the slope of the stress-strain curve. Material (1) also exhibits the lowest overall strain-at-break but highest overall peak force. Equally, material (1) reveals that a material can exhibit a high strength value and not necessarily signify good load-response and/or material performance.

For design purposes, a comprehension of both material elastic modulus and strength is essential, [Austroads, 2014; Anderson, 1995]. Unlike the rest of the material types, material (4) typifies good load response but low peak strength and material (2) portrays an almost similar stress-strain trend as material type (1) but slightly better load-response than material

(1). By observation, material (3) represents an ideal material type; strength measure is relatively closer to materials (1) and (2), the elastic modulus more or less comparable and certainly highest overall fracture energy [area under the stress-strain curve].

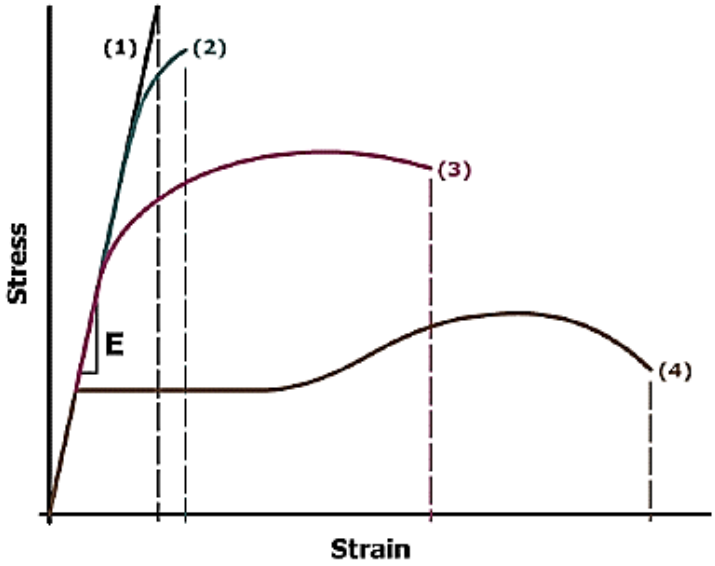

Figure: 2-13 Schematic Illustration of the Material Load-Response, Failure Criterion and Fracture Energy

2.8 Pavement Structures with Cement-Stabilised Layers

The use of stabilised materials extends from new flexible pavements to the rehabilitation of pavements. Determination of the layer thickness considers fatigue characteristics of stabilised materials, [Austroads, 2014]. The philosophy in pavement design presumes that treatment to a pavement layer [base, sub-base and even, subgrade] should provide increased service-life, [Austroads, 1992]. The major aim of pavement design is to select the most economical pavement thickness and composition. The resultant pavement design should offer a structurally feasible and economical pavement structure. The design of both flexible and rigid pavement types includes both empirical and mechanistic based procedures. Several roadway agencies continue to change from purely empirical to mechanistic-empirical design. Design of pavements using a mechanistic-empirical design is more of an interactive process that incorporates a number of design steps, which include the following:

a) determination of traffic - equivalent standard axles (ESALs) or load spectrum expected
b) computing load response using analytical or numerical models
c) determination of number of load cycles to failure by applying transfer functions and/or failure criteria
d) determining the damage ratio
e) determining layer thickness relative to damage ratio
f) ascertaining the final cross-section

The multilayer elastic design uses input parameters such as modulus values and strength. These input parameters must be determined with very reliable technique. In developing the conceptual procedures for designing pavements, a comprehension of the material characteristics and properties is needed, [Terrel *et al.* 1979; Papagiannakis and Masad, 2007]. Different design input parameters for the base, sub-base and subgrade material are required. The determination of the design moduli of cement-stabilised materials is essential. [Austroads, 2014] recommends the use of the flexural beam test.

Austroads [2014] recommends the consideration of the flexural beam test method based on concrete specification with a span-depth ratio of 3.0. South African practice does not include the flexural beam test. Several literatures, including Austroads [2014] mention various issues that hinder practice from considering a laboratory flexural beam method for the determination of the design modulus. Factors that limit the use of the flexural beam test include the following:

a) the equipment required to conduct the flexural beam test is relatively new and sophisticated
b) the laboratory determined flexural moduli are relatively higher than in situ moduli of pavements
c) practice applies low cement contents which present challenges to preparations of the beam
d) the lack of a standard test protocol to evaluate stabilised material moduli presents further challenges, including ambiguity in validating material moduli for design purposes

In the designing of pavements, the failure mode exhibited by stabilised material is essential. Theyse *et al.* [1996] and De Beer [1990] mention of two failure modes shown by cement-stabilised pavement materials as effective fatigue and crushing. The critical parameters of influence include:

a) maximum tensile strain at the bottom of the layer [controlling the effective fatigue-life]
b) vertical compressive stress on top of the cement-stabilised layer [controlling the crushing life]

An increase in traffic loading results in a gradual reduction in material elastic modulus. During effective fatigue-life when the stabilised layer is broken down into blocks, an assumption that the reduction in elastic modulus is half of its original elastic modulus value holds, [De Beer, 1990; Theyse *et al.* 1996]. Also assumed is that the stabilised pavement layer is further broken down into finer blocks similar to granular materials [equivalent granular phase]. Theyse *et al.* [1996] declare that under such circumstances, consideration of fatigue and equivalent granular in the prediction of stabilised pavement layer life is undertaken. De Beer [1990] establishes that the pre-cracked phase is very short and for this fact, the prediction of the layer life in the pre-cracked phase is not usually considered. A reduction in stiffness results in an increase in induced stresses and strains which lead to reduced layer life, [Freeme, 1984; De Beer, 1990; Theyse *et al.* 1996].

Table 2-4 presents the recommended elastic moduli for cement-stabilised materials, [De Beer 1994]. Figure 2-14 illustrates the reduction in stiffness following cumulative traffic loading, [Theyse *et al.* 1996]. Figure 2-15 illustrate the pavement structure and the phases as typified by Theyse *et al.* [1996]. Figure 2-15 also shows the different materials considered for the base layer; preference of a granular base in lieu of the cement-stabilised base is noted. Additionally, the cognisance of the effect of shrinkage cracking in the cement-stabilised base layer, which leads to reflective cracking, is also illustrated. Such illustrative measure of materials and the pavement structure offer insight regarding the design of pavements with and without cement-stabilised layers.

Table: 2-4 Recommended Elastic Moduli Values for Cement-Stabilised Materials [De Beer M 1994]

Original Code	UCS (MPa) for pre-cracked condition	Parent Material Code	Pre-cracked condition		Post-cracked condition			
			Phase 1		Phase 2	Phase 3		
			Stage 1: Intact (GPa)	Stage 2: Shrinkage cracking (MPa)	Stage 3: Traffic associated cracking, transitional phase with micro cracking (MPa)	Stage 4: Broken up in equivalent granular state (Mpa)		
						Dry condition	Wet condition	Equivalent code
C1	6 - 12	Crushed stone G1 Crushed stone G3	6 - 30	2500 - 3000	800 - 1000	400 - 600	50 - 400	EG1 EG2
C2	3 - 6	Crushed stone G2 Crushed stone G3 Gravel G4	3 - 14	2000 - 2500	500 - 800	300 - 500	50 - 300	EG2 EG3 EG4
C3	1.5 - 3	Gravel G4 Gravel G5 Gravel G6 Gravel G7 Gravel G8	2 - 10	1000 - 2000	500 - 800	200 - 400	20 - 200	EG4 EG5 EG6 EG7 EG8
C4	0.75 - 1.5	Gravel G4 Gravel G5 Gravel G6 Gravel G7 Gravel G8 Gravel G7 Gravel G8	0.5 - 7	500 - 2000	400 - 600	100 - 300	20 - 200	EG4 EG5 EG6 EG7 EG8 EG9 EG10

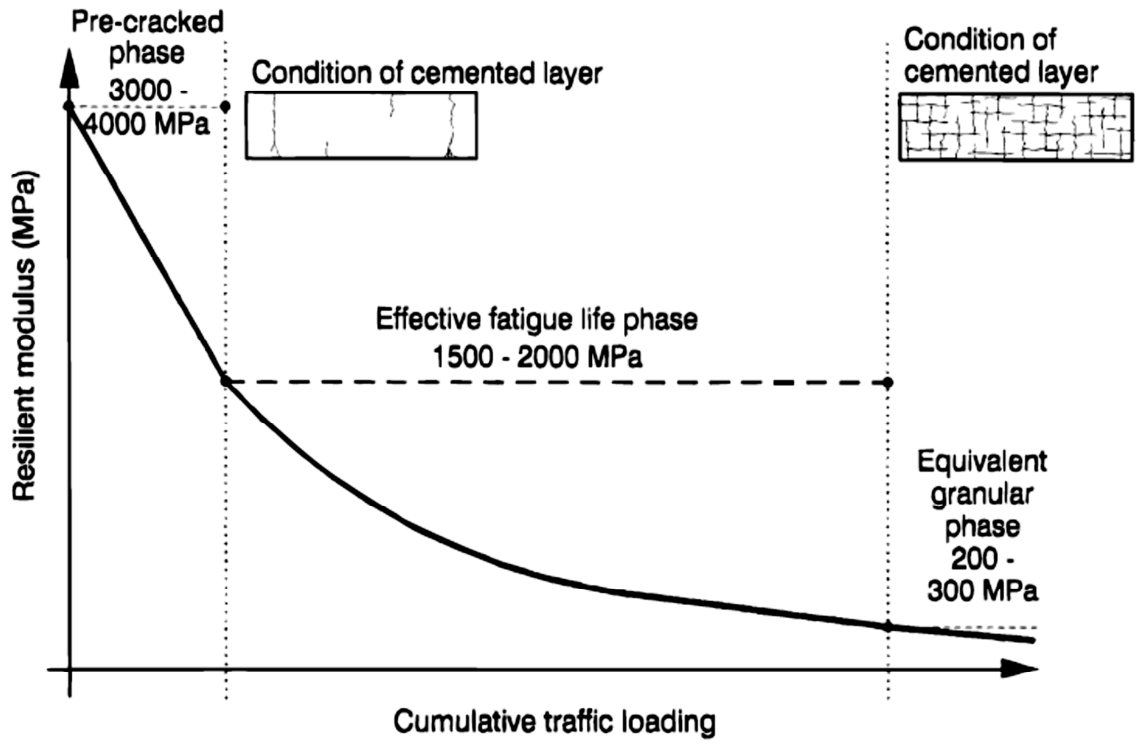

Figure: 2-14 Behaviour of a Lightly Cement Stabilised Pavement Layer [Theyse *et al.* 1996]

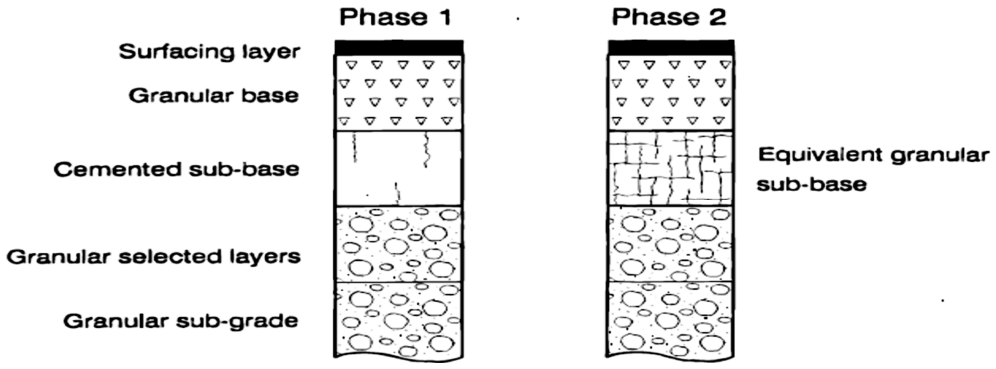

(a) Pavement structure with cemented sub-base

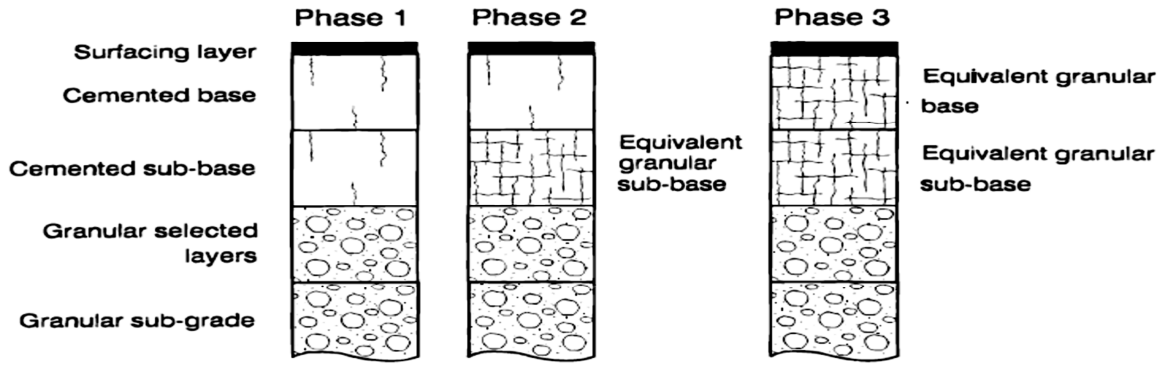

(b) Pavement structure with cemented base and sub-base

Figure: 2-15 Pavement Structure Life Phases [Theyse *et al.* 1996]

2.9 Summary of Chapter 2

In this chapter, the theoretical principles from previous research works concerning shrinkage, behavioural properties and durability of cement-stabilised pavement materials are stated. The fundamentals of cement stabilisation technology along with concepts concerning materials for stabilisation are also stated. Emphasis on the concepts regarding the resultant engineering properties and characteristics relative to probable material performance and durability is noted.

The concepts concerning shrinkage cracking in cement-stabilised materials and pavement structure are noted. This includes the mechanisms involved, resulting in shrinkage crack in a stabilised layer, the resultant crack pattern and related effects emanating from the manifestation of shrinkage cracks. Restraints, material characteristics and thermal effects are primary factors that influence the degree of shrinkage and the resultant crack pattern in a stabilised layer. The restraint at the interlayer between the stabilised and underlying layer is the causal factor for layer cracking. Thermal effects and temperature variations cause different shrinkage rates, which contribute to the development of cracks. The principles and benefits related to shrinkage mitigation techniques such as pre-cutting and pre-cracking of the stabilised layer are stated. The durability of the pavement structure relative to moisture ingress and poor load transfer attributed to shrinkage cracks is stated. The chapter lays out the significance of predicting shrinkage crack pattern along with the concepts adopted. Laboratory measured shrinkage along with the factors of influence that includes the procedure used to measure shrinkage, the specimen type and shape as well as the overall setup are stated.

The chapter provides principles and criteria regarding the behavioural properties and characteristics of cement-stabilised materials as well as pavement layer. The principles governing the flexural beam test and its evaluation of both material flexural strength and moduli are stated. The chapter emphasises the need for reliable design input parameters [concept of reliability] in the design of pavements; this includes the significance to establish a standard flexural beam test method. This chapter presents the theoretical principles adopted from previous literature; it provides the theoretical background to this research study.

2.10 References

ACI 223.98 (1998) *Standard Practice for the Use of Shrinkage-Compensating Concrete.* ACI Committee 223 American Concrete Institute, Farmington Hills Mich.

Anderson, T.L., (1995) *Fracture Mechanics: Fundamentals and Applications*, CRC Press.

Arellano, D. and Marshall, T.R., (1998) *Final Report: Stabilised Base Properties (Strength, Modulus, Fatigue) for Mechanistic-Based Airport Pavement Design,* Department of Civil Engineering, University of Illinois at Urbana-Campaign.

Asamoto, S., Tsuji, T. and Kurashige, I., (2012) *Study on Moisture Loss and Drying Shrinkage Behaviour of Mortar with Mineral Admixture Based on Pore Structure.* Central Research Institute.

ASTM Standards (1987) *Soil and Rock: Building Stones, American Society of Testing and Materials,* Annual Book of ASTM Standards Vol. 04.08, 1916.

Austroads (2014) *Cemented Materials Characterisation: Final Report,* AP-R462 ISBN 978-1-925037-72-2.

Austroads (2006) *Guide to Pavement Technology: Part 4D – Stabilised Materials.*

Austroads (2003) *Development of Performance-Based Specifications for Unbound Granular Materials – Part A: Issues and Recommendations*. AP-T29 ISBN 0 85588 678 1.

Austroads (1992) *Pavement Design: A Guide to the Structural Design of Road Pavements,* Publication No. AP-17/92.

Bagonza, S, Peete, JM, Freer, HR, and Newill, D., (1987) *Carbonation of Stabilised Soil-Cement and Soil-Lime Mixtures*, Seminar H, PTRC Transport and Planning Summer Annual Meeting, University of Bath, PTRC Education and Research Services.

Baratta, I. F., Mathews T. W. and Quinn, D. G., (1987) *Errors Associated with Testing of Brittle Materials,* US Army Laboratories Command, Materials Technology Laboratory.

Barksdale, R.D. and Vergnolle, R.R., (1968) *Expansive Cement Stabilization of Bases,* Highway Research Record 255 HRB pp. 30-41

Bazant, Z.P. and Kazemi, M.T., (1990) *Determination of Fracture Energy, Process Zone Length and Brittleness Number from Size Effect, with Application to Rock and Concrete,* International Journal of Fracture 44: Pp.111-131

Berke, N.S., Dallaire, M.P., Gartner, E.M., Kerkar, A.V. and Martin, T.J., (1996) *Drying Shrinkage Cement Admixture,* US Patent #5556460, US Patent and Trademark Office, www.uspto.gov.

Bentur, A., (1980) *Effect of Curing Temperature on the Pore Structure of Tri-calcium Silicate Pastes,* J Colloidal Interface Science Vol.74 1980 Pp.549-560

Bentur, A., (2002) *Early Age Cracking in Cementituos Systems,* RILEM State-of-Art Report TC-EAS, RILEM.

Bentz, D.P., Geiker, M.R. and Hansen, K.K., (2001) *Shrinkage Reducing Admixture and Early-age Desiccation in Cement Pastes and Mortars,* Cement Concrete Research 31 (7) pp.1075-1085

Bentz, D.P., Koenders, E.A.B., Monnig, S., Reinhardt, W.H., Van Breugel, K. and Ye, G., (2007) *Materials Science-Based Models in Support of Internal Water Curing* RILEM State-of-the-Art Report International Union of Testing and Research Laboratories for Materials and Structures, Paris pp. 29-42

Bisschop, J., (2002) *Drying Shrinkage Cracking at Early Ages,* RELIM TC 181-EAS: Final Report

Bisschop, J. and Van Mier, J.G.M., (2002) *Effect of Aggregates on Drying Shrinkage Microcrcaking in Cement Based Composites* Materials and Structures Volume 35, Pp. 453-461

Bofinger, H.E., (1970) *The Measurement of the Tensile Properties of Soil-Cement* RRL Report LR 365 Road Research Laboratory England

Bofinger, H.E., Hassan, H.O. and Williams, R.I.T., (1978) *The Shrinkage of Fine-Grained Soil-Cement,* TRRL Supplementary Report 398, Transport and Road Research Laboratory (TRRL).

Bouasker, M., Mounanga, P., Turcry, P., Loukili, A. and Khelidji, A., (2008) *Chemical Shrinkage of Cement Pastes and Mortars at Very early Age: Effect of Limestone Filler and Granular Inclusions* Cement and Concrete Composites Vol. 30, No.1 pp.13-22

Brandl, H., (1999) *Mixed in Place Stabilisation of Pavement Structures with Cement and Additives,* Proceedings of the 12th European Conference on Soil Mechanics and Geotechnical Engineering.

Bredenhann, S.J., Paige-Green, P. and Jenkins, K.J., (2011) *Cemented Materials: Accounting for Compaction Delays and Minimising Strength Loss with Time,* Marie Pave

Callister, W.D., (2003) *Material Science & Engineering: An Introduction* John Wiley & Sons ISBN 0-471-22471-5 A

Caltabiano, M.A. and Rawlings, R.E., (1992) *Treatment of Reflection Cracks in Queensland* 7th International Conference in Asphalt Pavements, pp.1-21

Carde, C. and François, R., (1997) *Effect of ITZ Leaching on Durability of Cement-Based Materials,* Cement and Concrete Research Vol.27 No.7 Pp. 971-978

Catton, M. and Felt, E.J., (1943) *Weight in Water Methods of Determining the Moisture Content of Soil-Cement Mixtures in the Field*, Proceedings, 23rd Annual Meeting of the Highway Research Board

Catton, M.D., (1940) *Research on the Physical Relations of Soil and Soil-Cement,* Proceedings 12th Annual Meeting on Highway Research Board

Chamlis, C.C., (1974) *Analysis of Three-Point Bend Test for Materials with Unequal Tension and Compressive Properties,* NASA TN D7572

Chou, Y.T., (1977) *Engineering Behaviour of Pavement Materials: State of the Art* Technical Report S-77-9 US Army Engineer Waterways Experiment Station

Clare, K.E. and Sherwood, P.T., (1954) *The Effect of Organic Matter on the Setting of Soil-Cement Mixtures, Journal of Applied Chemistry,* Vol.4 London

Clare, K.E. and Pollard, A.E., (1959) *Effect of Temperature on Soil-Cement* Geotechnique Vol.4

Croney, D. and Croney, P., (1998) *The Design and Performance of Road Pavements* 3rd Edition Published by McGraw-Hill

Colombier, G. and Marchand, J.P., (1993) *The Precracking of Pavement Underlays Incorporating Hydraulic Binders,* Proceedings of the 2nd International Conference RILEM Conference on Reflective Cracking in Pavements, E and FN Spon

Cohen, M.D., (1983) *Theories of Expansion in Sulfoaluminate – Type Expansive Cements: Schools of Thought,* Cement and Concrete Research Vol. 13, Pp. 809-818, Pergamon Press

Copeland, L.E., Kantro, D.L. and Verbeck G., (1960) *Chemistry of Hydration of Portland Cement,* Proceedings of the Fourth International Symposium Washington, D. C., 1960, held at the National Bureau of Standards (U.S. Department of Commerce) Monograph 43, Vol. I, Session N, Paper IV-3, 429-465

CSRA (1986) *Cementitious Stabilisers in Road Construction,* Draft TRH13, pp.64 Committee of State Road Authorities (CSRA)

CSRA (1997) *Standard Specifications for Road and Bridge Works,* Committee of State Road Authorities (CSRA) Department of Transport

Das BM (1990) *Principles of Geotechnical Engineering,* 2nd Edition PWS Kent

Davidson, D.T., (1958) *Use of Fly Ash with Portland Cement for Stabilisation of Soil* Highway Research Board Bulletin 198

Davidson, D.T., (1962) *Moisture-Density, Moisture-Strength and Compaction Characteristics of Cement-treated Soil Mixtures,* Bulletin 353, Highway Research Board

Davis, H.E., (1940) *Autogenous Volume Change of Concrete* Proceedings of the ASTM 40, 1103

De Beer, M., (1994) *The Evaluation, Analysis and Rehabilitation Design of Roads* Report IR93/296 South African Roads Board, Department of Transport

De Beer, M., (1985) *Behaviour of a Cementitious Subbase Layers in Bitumen Base Road Structures* Master's Thesis University of Pretoria

De Beer, M., (1990) *Aspects of the Design and Behavior of Road Structures Incorporating Lightly Cementituos Layers,* Ph.D. Dissertation University of Pretoria

De Beer, M. and Visser, A.T., (1989) *Erodibility of Cementitious Subbase Layers in Flexible Pavements.* Proceedings, 5th Conference on Asphalt Pavements for Southern Africa (CAPSA '89), Session VII, Swaziland, 5-9 June, pp VII-1-VII-15

De Beer, M., Fisher, C. and Jooste, F.J., (1997) *Determination of Tyre/Pavement Interface Contact Stresses Under Moving Loads and Some Effects on Pavements with Thin Asphalt Surfacing*, Technical Report No. TR-96/050, CSIR.

DETR Series 1000, (1998) *Road Pavements – Concrete and Cement Bound Materials*, Manual of Contract Documents for Highway Works (MCHW) Volume 1: Specifications for Highway Works, UK Dept. of Environment, Transport and the Regions

De Wet, L.F. and Taute, A., (1985) *Durability of Stabilised Materials* Proceedings of the Annual Transportation Convention, Volume FB Paper 1

Dixon, J.B. and Weed, S.B., (1989) *Minerals in Soil Environments,* 2nd Edition Soil Science Society of America,

Dolando, S.J., Griebel, M., Hamaekers, J. and Heber, F., (2010) *The Nano-Branched Structure of Cementitious Calcium-Silicate-Hydrate gel,* Institut fur Nemerische Simulation, Rheinische Friedrich-Wilhelms-Universitat Bonn

DOT UK (1995) *HA 26/94: Roadbase Materials Design Manual for Roads and Bridges* Volume 7 Section 2 Chapter 3 Department of Transport

Dumbleton, M.J., (1962) *Investigations to Assess the Potentials of Lime for Soil Stabilisation in the UK,* Road Research Technical Research Paper No. 64, HMSO

Dumbleton, M.J. and Ross, N.F., (1960) *Effect of Temperature in the gain of Strength of Soils Stabilised with Hydrated Lime and Portland Cement,* Research Note RN/3655, BS. 438 Road Research Laboratory

Dunlop, R.J., (1973) *Shrinkage and Creep Characteristics of Soil-Cement,* Ph.D. Dissertation University of Canterbury

Dunlop, R.J., (1978) *A Review of the Design and Performance of Roads Incorporating Lime and Cement Stabilised Pavement Layers,* Paper Presented at the NAASRA-ARRB Workshop on Stabilisation

Dunster, A., (2009) *Silica Fume in Concrete* Information Paper No IP 5/09 HIS BRE Press Garston

Elkhadiri, I., Marta, P. and Puertas, F., (2009) *Effect of Curing Temperature on Cement Hydration,* Eduardo Torroja Institute of Construction Sciences

Elkhadiri, I., Marta, P. and Puertas, F., (2008) *Construction and Building Materials*, Eduardo Torroja Institute of Construction Sciences

El-Rahim, A. and George, K.P., (2001) *Optimum Cracking for Improved Performance of Cement-Treated Bases* Proceedings 9th World Conference on Transport Research

Engstrand, J., (1997) *Shrinkage Reducing Admixtures for Cementituos Composition,* Con.Chem. Journal pp.149-151

Feldman, R.F. and Sereda, P.J., (1970) *A New Model of Hydrated Cement and Its Practical Implications,* Engineering Journal Canada Vol.53 Pp. 53-59

Felt, E.J., (1955) *Factors Influencing Physical Properties of Soil-Cement Mixtures,* Bulletin 108, Highway Research Board, 1955, Development Department Bulletin, D16, Portland Cement Association, Research and Development Laboratories

Filler, A., (2009) *The History, Development and Impact of Computed Imaging in Neurological Diagnosis*; CT, MRI and DTI Nature Proceedings

Freeme, C.R., (1984) *Symposium on Recent Findings of Heavy Vehicle Simulator Testing,* ATC 1984 NITRR

Frigioine, G. and Marra, S., (1976) *Relationship between Particle Size Distribution and Compressive Strength in Portland Cement,* Cement and Concrete Research Vol. 6 Pp. 113-128

Fuller, W.B. and Thompson, S.E., (1907) *The Laws of Proportioning Concrete* Trans. Am. Soc. Civ. Eng. 33 pp. 222-298

Gaitero, J.J., Campillo, I., Mondal, P. and Shah, S.P., (2010) *Small Changes Can Make a Great Difference,* Transportation Research Record, Journal of the Transportation Research Board, Transportation Research Board of National Academies, Pp. 1-5

Geogauge Brochure (2000) *Humboldt Management Company,* Norridge IL

George, K.P., (1968) *Shrinkage Characteristics of Soil-Cement Mixtures,* Highway Research Record 255

George, K.P., (1970) *Crack Control in Cement-Treated Bases* Final Report, Civil Engineering Department, University of Mississippi

George, K.P., (1971) *Shrinkage Cracking of Soil-Cement Base Theoretical and Model Studies* Highway Research Record 351

George, K.P., (1973) *Mechanism of Shrinkage Cracking in Soil-Cement Bases* Highway Research Record 442 HRB National Research Council pp. 1-10 1973

George, K.P., (1998) *Minimizing Cracking in Soil-Cement for Improved Performance* Technical Memorandum, Hitek Engineering Consultants Inc./PCA, Oxford

George, K.P., (1999) *Minimizing Cracking in Soil Cement for Improved Performance* Final Report Hitek Engineering Consultants Inc.

George, K.P., (2000) *Minimizing Cracking in Cement-Treated Materials for Improved Performance*, Final Report to Portland Cement Association Hitek Engineering Consultants

George, K.P., (2001) *Soil Stabilisation Field Trial* Interim Report 1 The Mississippi Department of Transportation, US Department of Transportation Federal Highways Administration and The Portland Cement Association

Goltermann, P., (1995) *Mechanical Prediction of Concrete Deterioration: Part 2 Classification of Crack Patterns* ACI Material Journal 92, Pp.58-63

Goto, T., Sato, T., Sakai, K. and Li, M., (1985) *Cement Shrinkage Reducing Agent and Cement Composition,* US Patent #4547223 US Patent and Trademark Office. www.uspto.gov.

Gray, W., Frobel, T., Browne, A., Salt, G. and Stevens (2011) *Characterisation and Use of Stabilised Basecourse Materials in Transportation Projects in New Zealand,* NZ Transport Agency Research Report 461

Gress, D., (2001) *Determination of Shrinkage Characteristics of Concretes with Type K Cement, Mineral and Chemical Additives,* University of New Hampshire and US Department of Transportation Federal Highways Administration

Grobler, J.A., (1994) *The Influence of compaction Moisture on Shrinkage in Stabilised Materials,* Master's Thesis University of Pretoria

Guthrie, W.S., Stephen, S. and Scullion, T., (2002) *Selecting Optimum Cement Contents For Stabilizing Aggregate Base Materials,* Texas Transportation Institute, The Texas A&M University System College Station, TX 77843-3135

Guthrie, W.S., Young, T.B., Blankenagel, J.B. and Cooley, D.A., (2005) *Early-Age Strength Assessment of Cement-Treated Base Material,* Transportation Research Record, Journal of

the Transportation Research Board, No. 1936 Transportation Research Board of the national Academies, Pp.12-15

Gutteridge, W.A. and Dalziel, J.A., (1990) *Filler Cement: The Effect of the Secondary Component on the Hydration of Portland Cement, Part 1: A Fine Non-Hydraulic Filler* Cement and Concrete Research, Vol.20 No.5 pp.778-782 1990

Hansen, W., (1987) *Drying Shrinkage Mechanism in Portland Cement Paste* Department of Civil engineering, University of Michigan, 48109-2125

Hertzberg, R.W., (1995) *Deformation and Fracture Mechanics of Engineering Materials,* 4th Edition Wiley ISBN 0-471-01214-9 1995

Hodgkinson, J.M., (2000) *Mechanical Testing of Advanced Fibre Composites,* Cambridge Woodhead Publishing Ltd, pg. 132-133

Houben, L.J.M., (2008) (A) *Transversal Cracking in Jointed Plain Concrete Pavements for Dutch Climatic Conditions,* Delft University of Technology

Houben, L.J.M., (2008) (B) *Model for Transversal Cracking (at Joints) in Plain Concrete Pavements,* Delft University of Technology

Houben, L.J.M., (2009) *Structural Design of Pavement Part IV Design of Concrete Pavements,* CT 4860 Delft University of Technology

Houben, L.J.M., (2011) *Model for Transversal Cracking in Non-Jointed Plain Concrete Pavements as a Function of the Temperature Variations and the Time of Construction,* Delft University of Technology

Husken, G. and Brouwers, H.H.J., (2008) *A New Mix Design Concept for Earth-Moist Concrete: A Theoretical and Experimental Study,* Cement and Concrete Research 38 pp. 1246-1259

Hwang, C.L. and Young, J.F., (1984) *Drying Shrinkage of Portland Pastes: Micro-cracking During Drying,* Cement Concrete Research Vol.14 Pp.585-594

Ingles, O.G. and Metcalf, J.B., (1972) *Soil Stabilisation: Principles and Practice* Published by Butterworth and Co. Ltd

Jayapalan R.A., Yeon, L,Y., Fredrich, M.S. and Kurtis, E.K., (2010) *Influence of Additions of Anatase TiO_2 Nanoparticles on Early-Age Properties of Cement Based Materials,* Transportation Research Record (TRB): Journal of the Transportation Research Board No. 2141, Transportation Research Board of the National Academies, pp.41-46 2010

Jennings, H.M., (2004) *Colloid Model of C-S-H and Implications to the Problem of Creep and Shrinkage, Materials and Structures/Concrete Science and Engineering* Vol. 37 Pp. 59-70

Junisbekov, T.M., (2003) *Stress Relaxation in Viscoelastic Material* ISBN 1-57808-258-7

Kadri, E. and Duval, R., (2002) *Effect of Ultrafine Particles on Heat of Hydration of Cement Mortars* ACI Materials Journal Vol.99 No.2 pp.138-142 2002

Kayyal, K.M., (1965) *Strength Characteristics of Soils Compacted by Four Methods,* unpublished Ph. D. Dissertation, University of Texas

Knudsen, T., (1984) *The Dispersion Model for Hydration of Portland Cement I. General Concepts,* Cement Concrete Res 14 Pp.622-630

Kolias, S. and William, R.I.T., (1984) *Estimation of the Modulus of Elasticity of Cement Stabilised Materials,* Geotechnical Testing Journal 7 (1) pp.109-117

Kovler, K. and Jensen, O.M., (2007) *RELIM Report 41: Internal Curing of Concrete* Ed. RILEM Publications SARL

Krauss, P.D., Rogalla, E.A., Sherman, M.R., McDonald, D.B., Osborn, A.E.N. and Pfeifer, D.W., (1995) *NCHRP Report 380: Transverse Cracking in Newly Constructed Bridge Decks,* TRB National Research Council

Kuhlman, R.H., (1994) *Cracking in Soil-Cement – Cause, Effect, Control* Concrete International, Vol.16 No.8 pp.56-59 1994

Lay, M.G., (1986) *Handbook for Road Technology* (Includes Chapter 10: Stabilisation – redrafted 1988). Published by Gordon and Breach

Larsen, T.J. and Nussbaum, P.J., (1967) *Fatigue in Soil Cement,* Bulletin D119, Portland Cement Association PCA

Lawrence, P., Cyr, M. and Ringot, E., (2008) *Mineral Admixtures in Mortars: Effect of Inert Materials on Short-Term Hydration* Cement and Concrete Research Vol.33 No. 12 pp.1934-1947

Lefort, M., (1996) *Technique for Limiting the Consequences of Shrinkage in Hydraulic-Binder-Treated Bases,* Proceedings of the 3rd International Conference on Reflective Cracking in the Pavements, E and FN Spon

Lim, S. and Zollinger, D.G., (2003) *Estimation of the Compressive Strength and Modulus of Elasticity of Cement Treated Aggregate Base Materials,* Transportation Research Record, TRB 1837 pp.30-38

Little, D.N., Scullion, T., Kota, P.B. and Bhuiyan, J., (1994) *Identification of the Structural Benefit of Base and Subgrade Stabilisation* TTI Report 1287-2 Texas Transportation Institute, Texas A & M University College Station

Little, D.N., Scullion, T., Kota, P.B. and Bhuiyan, J., (1995) *Guidelines of Mixtures Design of Stabilised Bases and Subgrades,* FHWA/TX-45/1287-3F Texas Department of Transportation, Austin Texas

Litwinowicz, A. and Brandon, A.N., (1994) *Dynamic Flexure Testing for Prediction of Cement-Treated Pavement Life* 17th Australian Road Research Board Ltd (ARRB) Conference Gold Coast, Queensland Australia Vol.17, No.2 1994, pp.229-247

Litzka, J. and Haslehner, W., (1995) *Cold in-place Recycling on Low Volume Roads in Austria,* Proceedings of the Sixth International Conference on Low Volume Roads, Minneapolis MN pp.189-194

Long, F.M. and Ventura, D.G.C., (2004) *Laboratory Testing for the HVS Sections on the N7 (TR11/1)* CSIR Technical Report

Lothenbach, B.G., Le Saout, G., Gallucci, E. and Scrivener, K., (2008) *Influence of Limestone on the Hydration of Portland Cements* Cement and Concrete Research Vol.38 No.6 pp. 848-860

Mack, E.C., (2006) *Using Internal Curing to Prevent Concrete Bridge Deck Cracking* Master's Thesis Cleveland University

Maher, M.H. and Ho, Y.C., (1993) *Behaviour of Fiber-Reinforced Cemented sand under Static and Cyclic Loads,* Geotechnical Testing Journal, GTJODJ Vol.16 No.3 Pp.330-338

Maner, A.W., (1952) *Curing Soil-Cement Bases* Proceedings 36th Annual Meeting of Highway Research Board

Maree, J.H. and Freeme, C.R., (1981) *The Mechanistic Design Method Used to Evaluate the Pavement Structures in the Catalogue of the Draft TRH14 1980 Technical Report RP/2/81,* National Institute for Transport and Road Research, CSIR

Martin, L., (1960) *Effect of Water Content on the Compressive Strength and Density of Various Aggregate-Cement Mixtures for Highway Cement Treated Bases,* Bulletin 251, Washington State University

Mehta, P.K., (1997) *Durability: Critical Issues for the Future,* Concrete International Conference Proceedings Pp. 27-33

Meyers and Chawla (1999) *Mechanical Behavior of Materials* ISBN 0-13-262817-1

Mindess, S. and Young, J.F., (1981) *Concrete* New Jersey Prentice Hall

Mitchell, J.K. and Monismith, C.L., (1977) *A Thickness Design Procedure for Pavements with Cement-Stabilised Bases and Thin Asphalt Surfacing* 4th International Conference on the Structural Design of asphalt Pavement, University of Michigan

Mitchell, J.K., Fossberg, P.E. and Monismith, C.L., (1969) *Behavior of Stabilized Soils under Repeated Loading Report 3: Repeated Compression and Flexure Tests on Cement and Lime Treated Buckshot Clay; Confining Pressure Effects in Repeated Compression for Cement Treated Silty Clay* Contract Report 3-145, US Army Engineer Waterways Experiment Station

Mitchell, J.K. and Freitag, D.R., (1959) *A Review and Evaluation of Soil-Cement Pavements,* Journal of the Soil-Mechanics and Foundations Division Vol.85 Part I, Proceedings of the American Society of Civil Engineers

Molenaar, A.A.A., (1983) *Structural Performance and Design of Flexible Road Constructions and Asphalt Concrete Overlays,* TU Delft University

NAASRA (1986) *Pavement Design: A Guide to the Structural Design of Road Pavements* National Association of Australian State Roads Authorities (NAASRA)

Naik, R.T., Kraus, N.R. and Kumar, R., (2011) *Influence of Types of Coarse Aggregates on the Coefficient of Thermal Expansion of Concrete,* Journal for Materials in Civil Engineering ASCE, 23:467-472

Nakayama, H. and Handy, R.L., (1965) *Factors Influencing Shrinkage of Soil-Cement* Highway Research Record 86 HRB National Research Council, pp.15-27

Neubauer, C.M. and Jennings, H.M., (2000) *The Use of Digital Images to Determine Deformation throughout a Microstructure,* Journal for Material Science Vol.35 2000 5751-65

Nmai, C.K., Tomita, R., Hondo, F. and Buffenbarger, J., (1998) *Shrinkage Reducing Admixture* Concr. Int. 4 pp.31-37

Nascimento, U., Castro, D.C., Lod, E. and Rodrigues, M., (1963) *Swelling and Petrification of Lateritic Soils* Proc. 3rd Reg. Coil! Afr. Soil Mech. Fdn Ellgng, Salisbury, (un-paginated).

Netterberg, F., (1987) *Durability of Lime and Cement Stabilisation,* National Institute for Transport and Road Research (NITRR) Unpublished Technical Note TS/9/87

Netterberg, F., (1975) *Self-Stabilisation of Road Bases: Fact or Fiction* Proceedings for 6th Reg. Conf. Afr. Soil Mech. Fdn Engng, Vol. 1, pp. 115-119.

Neville, A.M., (1997) *Properties of Concrete* John Wiley and Sons Inc.

Neville, A.M., (2000) *Properties of Concrete* 4th Ed. Pretence Hall/Pearson

Okamoto, P.A., (1990) *Non-destructive Tests for Determining Compressive Strength of Cement Stabilized Soils* Transportation Research Record 1295 TRB national Research Council

O'Flaherty, C.A., (1988) *Highway Engineering* 3rd Edition Volume 2 Published by Edward Arnold

Osbaeck, B. and Johansen, V., (1989) *Particle Size Distribution and Rate of Strength Development of Portland Cement,* Journal of American Ceram Society Volume 2 Pp. 197-201

Otte, E., (1978) *A Structural Design Procedure for Cement-Treated Layers in Pavements* DSc. (Eng.) Thesis Faculty of Engineering, University of Pretoria

Page, C. and Meyer, D., (2006) Applied Research Design for Business and Management, the MacGraw-Hill Companies Inc.

Paige-Green, P. and Netterberg, F., (2004) *Cement Stabilisation of Road Pavement Materials: Laboratory Phase 1,* CSIR Transportek

Paige-Green, P., Netterberg, F. and Sampson, L.R., (1990) *The Carbonation Chemically Stabilised Road Construction Materials: Guide to its Avoidance* CSIR Report No. PR 8/146/1

Paige-Green, P., (2008) *A Reassessment of Some Road Material Stabilization Problems,* Proceedings of the 27th Southern African Transport Conference (SATC) ISBN Number 978-1-920017-34-7

Papagiannakis, A.T. and Masad, E.A., (2007) *Pavement Design and Materials,* John Wiley and Sons Publishers

Paris, P.C. and Erdogan, F., (1963) *Basic Engineering* 85 London Press

Parrot, L.J., (2000) *Recoverable and Irrecoverable Deformation of Heat Cured Cement Paste,* Magazine of Concrete Research Vol.29 2000 Pp.101-116

Parsons, R.L. and Milburn, J.P., (2002) *Engineering Behavior of Stabilised Soils,* TRB 2003 Annual Meeting

Pera, J., Husson, S. and Guilhot, (1999) *Influence of Finely Ground Limestone on Cement Hydration of Portland* Cement and Concrete Composites Vol. 21 No.2 pp. 99-105 1999

Pretorius, P.C., (1970) *Design Considerations for Pavement Containing Soil Cement Bases* Ph.D. Dissertation, University of California Berkeley

Pretorius, P.C. and Monismith, C.L., (1971) *The Predication of Shrinkage Stresses in Pavements Containing Soil-Cement Bases,* Paper Presented at the Annual Meeting of the Highway Research Board

Qing, Y., Zenan, Z., Deyu, K. and Rongshen, C., (2007) *Influence of Nano-SiO_2 Addition on the Properties of Hardened Cement Paste as Compared with Silica Fume* Construction and Building Materials 21 pp. 539 - 545

Raad, L., (1988) *Behaviour of Cement-Treated Soils in Flexure,* Transportation Research Record 1190, TRB

Raad, L., (1976), *Design Criteria for Soil-Cement Bases* Ph.D. Dissertation, Department of Civil Engineering, University of California Berkeley

Road Note 29. (1970) *A Guide to the Structural Design of Pavements for New Roads,* Road Research Laboratory, Department of the Environment

Rajabipour, F., Sant, G. and Weiss, J., (2008) *Interactions Between Shrinkage Reducing Admixtures and Cement Paste's Pore Solution* Cement and Concrete Research Vol.38 No.5 pp.606 – 615

Raki, L., Beaudoin, J., Alizadeh, R., Makar, J., Sato, T., (2010) *Cement and Concrete Nanoscience and Nanotechnology,* National Research Council Canada, Institute for Research in Construction, Materials Journal ISSN 1996-1944

Reinhardt, H.W., (1998) *Beton als Constructiematerial* Delfse Universitaire Pers. Delft The Netherlands (English Translated)

Richardson, I.G., (1999) *The Nature of C-S-H in Hardened Cements* Cement and Concrete Research 29:1131-1147

Road Research Laboratory, (1952) *Soil Mechanics for Road Engineers,* Department of Scientific and Industrial Research, H. M. Stationary Office

Roylance, D., (2001) *Stress-Strain Curves* Department of Material Science and Engineering, Massachusetts Institute of Technology

Sakka, S. and Kosuko, H., (2000) *Handbook of Sol-Gel Science and Technology* Volume I: Sol-Gel Processing Kluwer Academic Publisher pp.9-10

Sampson LR and Paige-Green, P., (1990) *Recommendations for Suitable Durability Limits for Lime and Cement Stabilized Materials*, Transportek CSIR Research Report DPVT 130

Sastry, D., (1998) *Improving Soil Cement Characteristics with Fly Ash,* Master's Project Department of Civil Engineering, The University of Mississippi, University MS

Scott, J.L.M., (1974) *Flexural Stress-Strain Characteristics of Saskatchewan Soil Cements,* Technical Report 23, Saskatchewan Department of Highways and Transportation

Scullion, T. and Saarenketo, T., (1996) *Using Suction and Dielectric Measurements as Performance Indicators for Aggregate Base Materials,* Transportation Research Record 1577 TRB, National Research Council, pp. 37-44

Selvan, P.R., Hall, K.D., Subramani, J.V. and Murray, S.J., (2011) *Application of Nanoscience Modelling to Understand the Atomic Structure of C-S-H,* Nanotechnology in Civil Infrastructure Pp. 85 – 102

Senff, L., Labrincha, J.A., Ferreira, V.M., Hotza, D. and Repette, W.L., (2009) *Effect of Nano-Silica on Rheology and Fresh Properties of Cement Pastes and Mortars* Construction and Building Materials 23 pp.2487-2491

Singh, L.P., Agarwal, S.K., Bhattacharyya, S.K., Sharma, U. and Ahalawet, S., (2011) *Preparation of Silica Nanoparticles and its Beneficial Role in Cementituos Materials,* CSIR

Shalid, M.A. and Thom, N.H., (1996) *Performance of Cement Bound Bases with Controlled Cracking,* Proceedings 3rd International RILEM Conference on Reflective Cracking in Pavement

Shen, C.K., (1965) *Behaviour of Cement Stabilised Soils under Repeated Loading,* Ph.D. Dissertation, Department of Civil Engineering University of California

Sherwood, P.T., (1993) *Soil Stabilisation with Cement and Lime,* Transport Research Laboratory State of the Art Review Published by HMSO

Sherwood, P.T., (1968) *The Properties of Cement Stabilized Materials* RRL Report LR 205, Road Research Laboratory

Skinner, L.B., Chae, S.R., Benmore, C.J., Wenk, H.R. and Monteiro, P.J.M., (2010) *Nanostructure of Calcium Silicate Hydrates in Cements,* University of California Berkeley

Sobhan, K., Jesick, M.R., Dedominicis, E.J., McFadden, J.P., Copper, K.A. and Roe, J.R., (1999) *Soil-Cement-Fly Ash Pavement Base Course Reinforced with Recycled Plastic Fibers,* 78th Annual Meeting of the Transportation Research Board

State-of-the-Art Report on Soil Cement (1990) *ACI Materials Journal* Vol.87, No.4, 1990 Pp.395-417

Sebesta, S., (2005) *Use of Microcrcaking to Reduce Shrinkage Cracking in Cement-Treated Bases,* Transportation Research Record TRB Journal of the Transportation Research Board No. 1936, Transportation Research Board of the National Academies, pp. 3-11 2005

Shilstone, J.S.M., (1990) *Concrete Mixture Optimization,* Concrete International Vol.12 No.6 pp.33-39

Stutzman, P., (1999) *Chemistry and Structure of Hydration Products,* national Institute of Standards and Technology, Cement Research Progress

Syed, I. and Scullion, T., (1998) *Performance Indicator for Moisture Susceptible Stabilised Base Material in Pavements,* Proceedings of the Texas Section, American Society of Civil Engineers, Fall Meeting, pp. 213-222

Tao, J., (2005) *Preliminary Study on the Water Permeability and Microstructure of Concrete Incorporating Nano-SiO_2* Cement and Concrete Research 35 pp. 1943-1947

Taylor, P., Kosmatka, S. and Voigt, G., (2004) *Integrated Materials and Construction Practices for Concrete Pavements: State of the Art Manual,* Federal Highway Administration Publication No. HF-07-004, US Department of Transportation, Washington DC 2004

Taylor, H.F.W., (1997) *Cement Chemistry,* Thomas Telford Ltd, London UK

Taylor, H.F.W., (1986) *Proposed Structure for Calcium Silicate Hydrate Gel,* Journal of the American Ceramic Society Volume 69, Issue 6 Pp. 464-467

Tazawa, E. and Miyazawa, S., (1995) *Influence of cement and Admixture on Autogenous Shrinkage of Cement Paste,* Cement and Concrete Research 27(9) pp.281-287

Tazawa, E. and Miyazawa, S., (1992) *Autogenous Shrinkage of Cement Paste with Condensed Silica Fume,* 4th CANMET-ACI International Conference on Fly Ash, Silica Fume, Slag and Natural Pozzolans in Concrete Pp. 875

Tazawa, E. and Miyazawa, S., Sato, T. and Konishi, K., (1992) *Autogenous Shrinkage of Concrete,* Transactions of the Japan Concrete Institute Pp.139

Terrel, R.L., Epps, J.A., Barenberg, E.J., Mitchell, J.K. and Thompson, M.R., (1979) *Soil Stabilization in Pavement Structures, A User's Manual, Volume 2 Mix Design Considerations,* Report No. FHWA-IP-80-2, Federal Highway Administration

Tennis, P. and Jennings, H., (2000) *A Model for Two Types of Calcium Silicate Hydrate in the Microstructure of Portland Cement Pastes,* Cement and Concrete Research, Pergamon, pp. 855-863

Terzaghi, K. and Peck, R.B., (1948) *Soil Mechanics in Engineering Practice,* John Wiley and Sons

Theocaris, P.S., Paipetis, S.A. and Paolinelis, S., (1977) *Three-Point Bending at Large Deflections,* Journal of Testing and Evaluation 5 (6) Pp. 427–436.

Theobald, D., McClurg, J. and Vaughan, J.G., (1997) *Comparison of Three-Point and Four Point Flexural Bending Tests,* International Composites Expo 1997, Pp. 1–9.

Theyse, H.L., De Beer, M. and Rust, F.C., (1996) *Overview of the South African Mechanistic Pavement Design Analysis Method,* Transportek CSIR

Thom, N.H. and Cheung, L.W., (1999) *Relating Insitu Properties of Cement-Bound Bases to their Performance,* Transport Research Record, No. 1673, Pp. 3-8

Thomas, J.J. and Jennings, H.M., (2004) *A Colloidal Interpretation of Chemical Aging of the C-S-H gel and its Effects on the Properties of Cement Paste,* Cement and Concrete Research 36 (2006) 30-38

Thomas, J.J. and Jennings, H.M., (2003) *Changes in the Size of Pores during Shrinkage (or Expansion) of Cement Paste and Concrete,* Cement, Concrete Research Vol.33 2003 1895-900

Thomas, J.J., Jennings, H.M. and Chen, J.J., (2009) *Influence of Nucleation Seeding on the Hydration Mechanisms of Tricalcium Silicate and Cement,* Journal of Physical Chemistry, Vol. 113 2009 Pp.4327-4334

Timoshenko, S.P., (1921) *On the Correction Factor for Shear of Differential Equation for Transverse Vibrations of Bar of Uniform Cross-section,* Philosophical Magazine Pp.744,

Timoshenko, S.P., (1922), *On the Transverse Vibrations of Bar of Uniform Cross-section,* Philosophical Magazine 43,

Timoshenko, S.P. and Woinoswki-Krieger, S., (1970) *Theory of Plates and Shells,* McGraw-Hill

Timoshenko, S.P., (1978) *Strength of Materials,* Part 2 English Edition

TRH13., (1986) *Cementitious Stabilisers in Road Construction,* Technical Recommendations for Highways, ISBN 0 7988 3647 4 Draft TRH13, pp. 1-64

TRL., (1993) *Overseas Road Note 31: A Guide to the Structural Design of Bitumen-Surfaced Roads in Tropical and Sub-tropical Countries,* Transport Research Laboratory TRL

TRRL., (1978) *A Guide to Concrete Road Construction* 3rd Edition HMSO

Ventura, D.F.C., (2003) *Durability Testing of LCD and CTB Materials Supplied by Caltrans,* Technical Memorandum No.TM-UC-PRC-2003-2 Pavement Research Center, Institute of Transportation Studies, University of California

Wakasugi, S., Sakai, K., Shimobayashi, S. and Watanabe, H., (1984) *Properties of Concrete Using Balite-based Cement with Different Fineness,* O.E. Gjov (ed.), Concrete Under Severe Conditions 2, E & FN Spon, Pp. 2161-2169

Wang, J.W.H., (1973) *Use of Additives and Expansive Cement for Shrinkage Crack Control in Soil-Cement,* Highway Research Record 442 Washington DC, Highway Research Board Pp.11-20

Wainwright, P.J., (2005) *Portland Cement,* School of Civil Engineering University of Leeds

Watson, J., (1994) *Highway Construction and Maintenance,* 2nd Edition. Published by Longman Group

Watson, J., (1941) *The Unconfined Compressive Strength of Soil-Cement Mixtures,* Proceedings, 21st Annual Meeting of the Highway Research Board

Wayne, S.A. and Luhr, R.D., (2004) *Control of Reflective Cracking in Cement Stabilised Pavements,* 5th International RILEM Conference

Weinert, H.H., (1980) *The Natural Road Construction Materials of Southern Africa,* National Institute For Transport and Road Research, Council for Scientific and Industrial Research

Weiss, J. and Berke, N.S., (2002) *Shrinkage Reducing Admixtures* In Early Age Cracking in Cementitious Systems (A. Bentur Ed.) RILEM State-of-the-Art Report, International Union of Testing and Research Laboratories for Materials and Structures

William, R.I.T., (1986) *Cement-Treated Pavements: Materials, Design and Construction,* Elsevier Applied Science Publisher

Wynand, J.S., (2011) *Applications of Nanotechnology in Road Pavement Engineering,* Nanotechnology in Civil Infrastructure a Paradigm Shift, ISBN 978-3-642-16656-3

Xuan, D., (2012) *Cement Treated Recycled Crushed Concrete and Masonry Aggregates for Pavements,* Ph.D. Dissertation TU Delft

Yamanonchi, T. and Ihido, M., (1982) *Laboratory and In-situ Experiments on the Problem of Immediate Opening of Soil-Cement base to General Traffic,* Proceedings of the 4th Australia-New Zealand Conference

Zelic, J., Rusie, D., Veza, D. and Krstulovic, R., (2000) *The Role of Silica Fume in the Kinetics and Mechanism During the early Stage of Cement Hydration,* Cement and Concrete Research Vol.30 No.10 pp.1655-1662 2000

Chapter 3: Research Methodology

3.1 Background

Chapter 1 states the problem, objectives, the significance of the research, limitations to the study and the research outcomes. Chapter 2 provides the theoretical principles and related concepts in evaluating and design of stabilised materials. In this chapter, the procedures and/or techniques adopted in this research study are stated. Figure 3-1 provides a schematic illustration of the overall research approach.

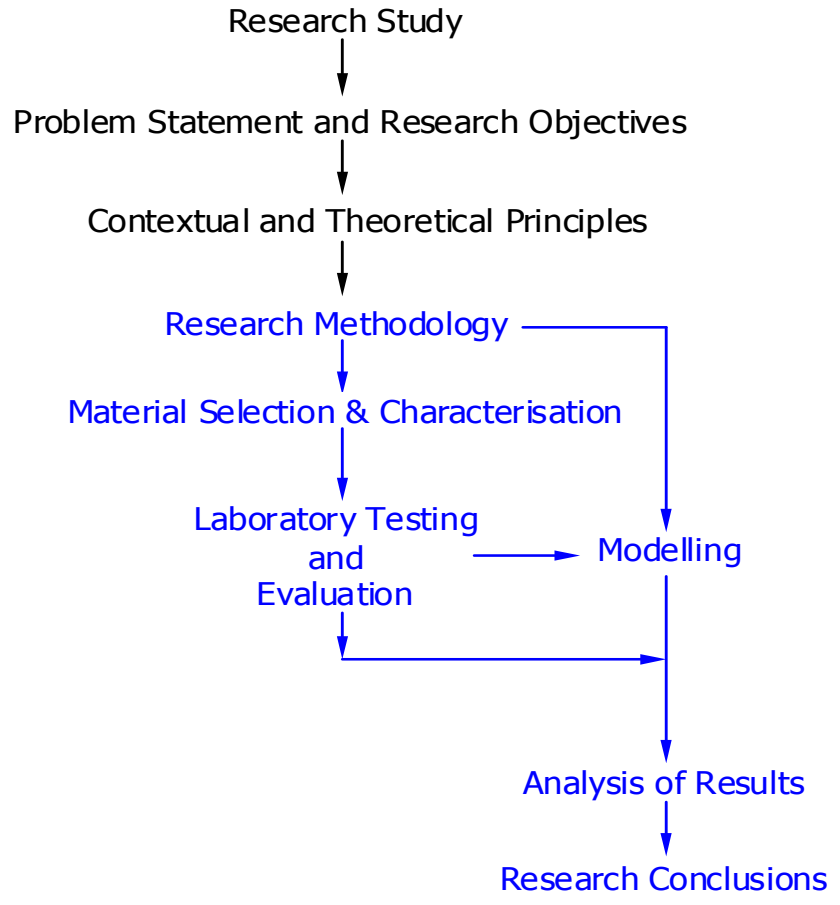

Figure 3-1 Schematic Layout of the Research Study

3.2 Experimental Program

For the characterisation of materials the South African material specifications TRH14 [1985] and TMH1 [1986] were adopted. TMH1 [1986] and TRH 13 [1986] provide standard tests pertaining to cement-stabilised materials. The research methodology includes:

a) *Material selection and characterisation*: a selection of materials along with the assessment of their characteristics and properties is undertaken. The assessment includes the use of index testing and related analysis. This encompasses material gradation, Atterberg limits, CBR testing, determination of the maximum dry density [MDD] and optimum moisture content, [OMC]. The objective of conducting index testing and related analysis is to obtain preliminary insight concerning the suitability of materials. For the assessment of material suitability reference to TRH14 [1985] and TMH1 [1986] is made.
   Apart from the standard tests and related analysis, additional testing is undertaken. The X-Ray Fluorescence [XRF] analysis of cement and selected materials is undertaken. The

purpose of the XRF analysis is to establish the mineralogy of the materials. The experimentation also considers the computerised tomography [CT] scanning of stabilised specimens. The purpose of the CT scanning is to study the internal morphology of the materials as to gain further insight regarding particle distribution and overall quality of the material.

b) *Cement treatment and material strength evaluation*: this phase encompasses the tensile and compressive strength evaluation. The purpose of this step is to investigate cement effectiveness after stabilisation as well as to ascertain the strength properties following specific cement contents. This phase provides the measure of material strength. TMH1 [1986] and TRH13 [1986] provide the test protocols for the evaluation of material strength specifically Methods A14 and A16T TMH1 [1986]. In this research, a minimum strength range equivalent to material class C4 based on the South African Material classification system is set. For stabilisation, 6.0% cement content is the highest possible treatment level in addition to two low cement contents.

c) *Evaluation of material durability*: this followed Method A19, TMH1 [1986] and includes soaked and un-soaked specimens.

d) *Set-up of flexural beam test criteria*: This section encompasses the study, analysis and formulation of flexural beam testing criteria. This includes the establishment of beam geometry relative to maximum aggregate particle size and test configurations. A study of the effect of the maximum particle size relative to the beam geometric characteristics, loading-span and effect of shear stress, is undertaken. Considering the lack of a standard flexural beam test and pure bending principles the establishment of a suitable flexural strength test method is essential. The experimentation considers the four-point loading technique in lieu of the three-point loading technique.

e) *Formulation of a shrinkage test criteria*: because no standard test method exists for the evaluation of material shrinkage at the laboratory level, formulation of a shrinkage test method is crucial. The proposed test method must be simple, user friendly and of good repeatability. This suggests that the instrumentation and overall set-up has to confirm and provide good reliability in the measure of shrinkage. Prioritisation of aspects such as test sensitivity, precision and accuracy are paramount. Additionally, because the test has to provide a quick insight of the material shrinkage, accelerated curing is preferred to ambient conditions. In order to validate the shrinkage test method, consideration of various trial runs on cement paste and stabilised materials is necessary. Trial runs provide insight regarding the test method in terms of its repeatability, reliability and usability.

f) *Modelling of shrinkage crack pattern:* this phase involves the consideration of the laboratory-acquired data, the coefficients of materials as well as the thermal parameters among others to model the crack width and spacing in a stabilised layer.

Figure 3-2 provides an outline of the experimental program showing the research sectors and their relationship to overall research scope. The research variables include:

a) *Cement and material types*: the experimentation considers hornfels and ferricrete material types. Ferricrete [also referred to as laterite] is a hard erosion-resistant layer within the earth-crust and has a reddish-like appearance. This is due to a high concentration of iron oxide. Hornfels is a metamorphic rock. Figure 3-3 shows the appearance of the two material types. For stabilisation purposes, cement type CEMII A-M 42.5N a Portland cement type is considered. This consideration is based on recent trends within the road industry and related research. Bredenhann *et al.* [2012] reports that CEMII A-M 42.5N conforms to both ITS and UCS specifications at only 2.0% stabiliser content compared to 3.0% with CEMII A-L 32.5R. Besides the stabiliser requirements, CEMII A-M 42.5N was preferred because it allows time to compact considering the tasks involved at the laboratory level.

b) *Cement contents*: a maximum cement content of 6% is set along with two lower cement contents. The minimum cement content is that which provides the least strength equivalent to stabilised material class C 4 as per South African specifications.

c) *Polymer cement-additive contents*: Being a new product and a cement additive, the application rate of the polymer to cement forms a good basis to initiate its suitability with stabilised materials. The experimentation considered shrinkage based evaluation and analysis of cement and polymer as the most feasible option to establish the application rate of the polymer to cement and stabilised materials. The Polymer-Cement experimentation includes varying the polymer content over a fixed water/cement ratio. At approximately highest shrinkage reduction, the application rate of the polymer relative to cement is determined. The Polymer-Cement experimentation considers a water/cement [*w/c*] ratio of 0.5. From the shrinkage experiment using cement paste, a ratio of cement to polymer is determined. The Polymer-Cement ratio is considered during the stabilisation of materials at varying cement contents.

d) *Mix types*: the experimentation, not only used mix types of varying cement contents, but also mix types of varying polymer contents. In this research study, all reference mix types had no polymer.

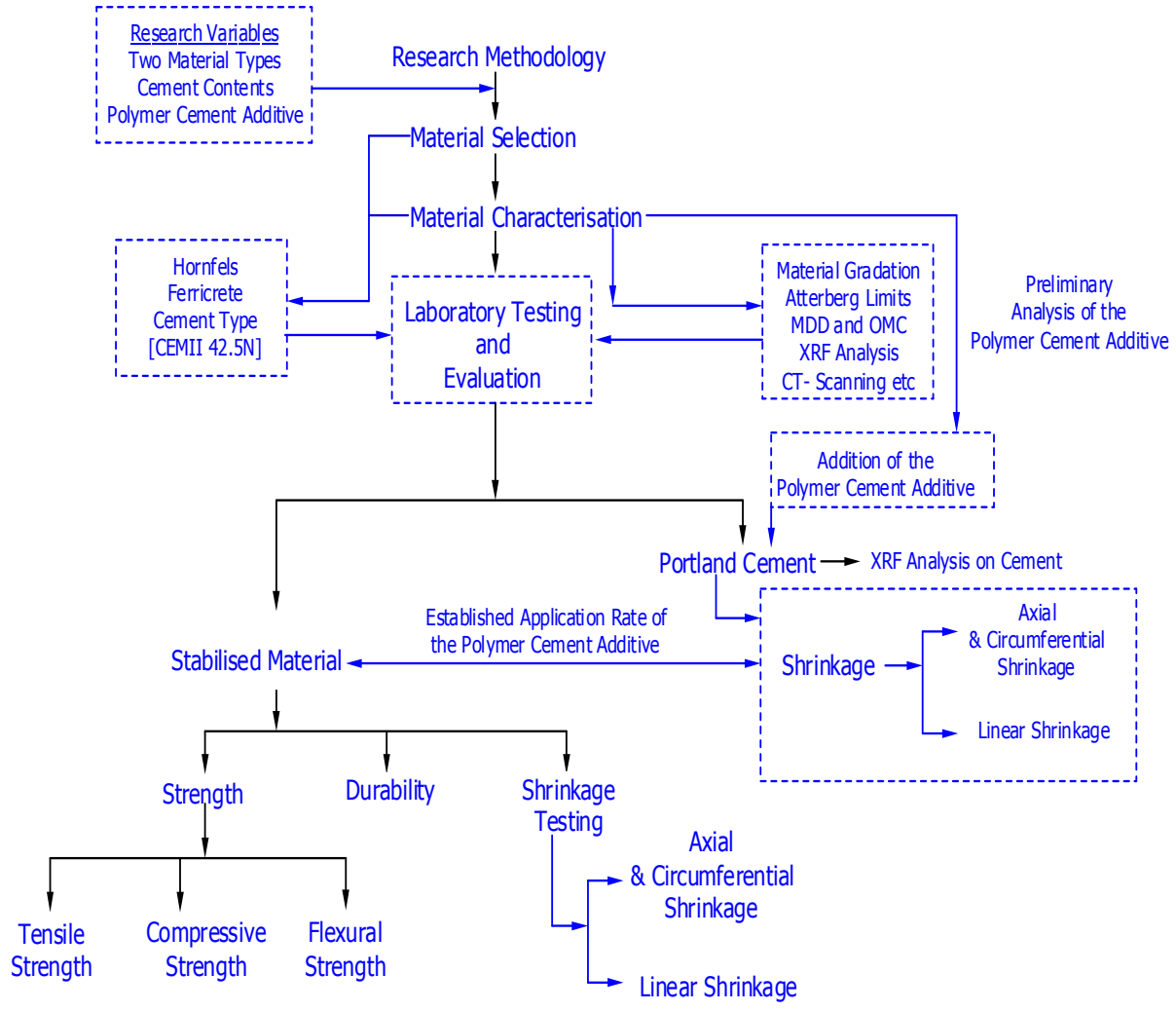

Figure 3-2 Outline of the Experimental Program

e) *Curing periods and procedures*: For the compressive and tensile strength evaluations, the experimentation considers a curing period of 7 days at an ambient temperature of 25ºC. For strength evaluation of cement-stabilised materials, the South African specifications specify curing for 7 days at ambient temperature or at accelerated conditions of 70ºC to

75ºC for 24 hours. For flexural strength evaluation, all beams were cured at 25ºC for 28 days. On the 28th day, all beams are tested. Some selected beams were soaked for 4 hours before testing in order to assess the effect of water ingress on flexural strength properties. Regarding the evaluation of shrinkage, the experimentation considers a conditioning temperature of 70ºC based on the accelerated strength development curing temperature range of 70ºC to 75ºC as specified for stabilised material, [TRH13, 1986]. The shrinkage experimentation considers a drying [curing] period of 3 days at 70ºC.

Figure 3-3 Hornfels and Ferricrete

3.3 Polymer [Nanoterra Soil®]

Nanoterra Soil® [NTS®] is a polymer dispersion of nano-silica dioxide. The term polymer shall refer to Nanoterra Soil®. Chapter 2 offers the theoretical principles and insight regarding nano-silica and nanotechnology. Figure 3-4 is a pictorial illustration of the polymer, which is a white emulsion-like solution.

Figure 3-4 White Emulsion-like Polymer

Based on the manufacturer's manual the polymer comprises of water, butadiene, nano-silica fines and cellulose. The percentages of each of these components could not be established using normal laboratory facilities, which became a limitation of this research. A variation in moisture content results in corresponding differences in not only density but also total

shrinkage. In order to control moisture in the mix, the amount of water in the polymer needs to be determined. An experiment conducted at a test temperature of 110ºC was undertaken. This testing included the use of a draught oven set at 110ºC as specified in the determination of material moisture, [TMH1, 1986]. The procedure to assess the amount of water [including other evaporating components] included:

a) placing the polymer sample in a container at ambient temperature
b) weighing and recording the mass of the polymer sample and the container
c) conditioning the sample at 110ºC for 1 day [24 hours]
d) weighing and recording the polymer and container after oven drying for 24 hours

Calculation of the amount of water contained in the polymer considered Equation 3-1.

$$\text{Percentage of evaporating components [\%]} = [[A - B]/[B - C]\,]\ x\,100 \qquad \text{Equation 3-1}$$

Where: A - Mass of the container and the NTS® polymer before oven drying [grams]
B - Mass of the container and NTS® polymer after oven drying [grams]
C - Mass of container [grams]

Figure 3-5 illustrates the appearance of the polymer before and after oven drying the polymer for 24 hours. As the polymer dried out in the draught oven, a layer formed at the top of the container. This layer was intentionally broken and sample returned to the oven to observe if any changes in mass resulted. With the findings from the first experiment, a second experiment was undertaken. The second experiment made use of a petri-dish and followed similar procedures but the layer remained undamaged.

Figure 3-6 shows the second experimentation after oven drying with an intact surfacing formed on the top of the petri-dish. An analysis of the two experiments provided insight regarding the polymer and the evaporants.

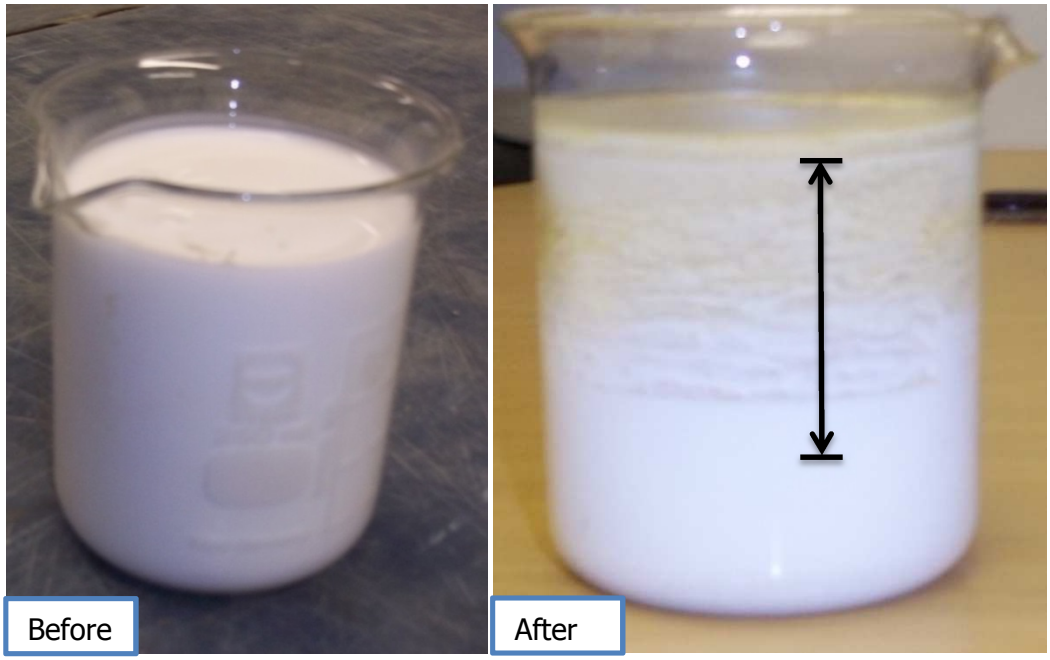

Figure 3-5 Effect of Heat on NTS® Polymer [Conditioning Temperature @ 110ºC]

Following the insight obtained from the two experiments as related to the polymer and its evaporants, a series of compaction trial runs using the modified AASHTO compaction method was undertaken. The purpose of the compaction experimentation was to determine the effect of polymer [water and solvents] on the material density. This compaction

experimentation comprised both stabilised and natural mix types with and without the polymer. Method A7 TMH1 [1986] details the standard compaction method.

Figure: 3-6 Effect of Heat on NTS® Polymer with formed Surface Cover [Conditioning Temperature @ 110ºC].

3.4 Material Characterisation

Material characterisation is essential to the overall evaluation process. This provides fundamental data regarding the suitability of materials. The characterisation process uses various techniques and index tests to identify specific material characteristics and properties.

3.4.1 Material Grading

Gradation of material is a classification process, which identifies the particle size distribution. The grading of material offers insight related to the particle packing which influence density. The packing of particles is a fundamental characteristic because it influences the material engineering properties. By analysing the sieve analysis results, aspects concerning material particle distribution are realised. For the sieve analysis, Method A1 (a) TMH1 [1986] and Method A1 (b) TMH1 [1986] are considered. Wet sieving provides a reliable particle distribution assessment since the particles are broken down into individual sized ones by the water. The consideration of dry sieving is to ration the material into individual particle size ranges.

3.4.2 Atterberg Limits

Atterberg limits provide a measure of the critical water contents of the materials. This includes the liquid limit, plastic limit and shrinkage limit. The shrinkage limit characterises the water content at which no further volumetric changes result, even if a loss in moisture takes place. The shrinkage limit is the minimum water content at which the material is still fully saturated. The test to assess the material shrinkage potential follows the bar linear shrinkage measurement. This remains an indicator test since fine particles are considered. Methods A2 and A3 TMH1 [1986] describe the test protocols for liquid and plastic limits respectively. The plasticity index [PI] provides a measure of the material plasticity. As PI = LL – PL also the plastic limit [PL] is required for the determination of the PI.

3.4.3 Material Dry Density and Moisture Content

Density and moisture content are significant factors that influence the mechanical properties of materials. Equally, the strength and permeability of a material are dependent on the

packing characteristics. Packing of material particles characterises the void ratio because of the particle size and shape. A comprehension of the material gradation is important while assessing the resultant material dry density [MDD] and optimum moisture content [OMC]. For the determination of MDD and OMC Method A7 TMH1 [1986] is followed.

3.4.4 California Bearing Ratio [CBR]

The California bearing ratio [CBR] is a penetration test for evaluating the mechanical strength of road layers. The test allows a comparison of the material bearing capacity to that of a well-graded crushed stone. This provides insight into the material quality but does not affirm their suitability. However, further testing and correlations are necessary. The procedure for determining the CBR of material is contained in Method A8 TMH1 [1986]. Figure 3-7 shows the CBR test equipment used. The recording of the test data is undertaken manually, which requires at least two persons.

Figure 3-7 CBR Equipment

3.4.5 X-Ray Fluorescence [XRF] Analysis

The X-ray fluorescence [XRF] analysis determines the chemical elements present in the material. By inducing XRF radiation, the photons of high energy emitted by the X-ray source impinge on the material, thereby transmitting radiation, [Gauglitz *et al.* 2003; Koen, 2004]. The XRF method uses radiation to assess the behaviour of atoms contained within the materials. The X-ray spectrometer illuminates using an intense X-ray beam, some of the energy is scattered, while some is absorbed within the sample in a manner, which is dependent on its chemistry. By undertaking an XRF analysis on ferricrete, hornfels and cement, the major and minor trace elements are determined. Establishing the chemical elements contained in the materials offer insight into the material reactivity and chemical behaviour. This provides a better understanding regarding their suitability for use in the pavement structure.

3.4.6 X-Ray Computerised Tomography [CT Scanning]

Any Industrial computerized tomography [CT] scan uses a series of 2-dimensional images taken at specific intervals around the entire sample to provide a holistic image of the material morphology. The CT system uses three principal components which include an X-ray tube, X-ray detector and rotational stage, [Julien, 2008]. Through CT scanning, the internal structure of the material is analysed. This provides further insight into the material particle and structural layout that is its morphology. The CT scanning on ferricrete and hornfels materials is undertaken.

3.5 Strength Test and Wet-Dry Brushing

The tensile and compressive strength tests are material property standard tests. Since the initial consumption of cement is dependent on the strength [i.e. cement content in the mix], a minimum strength equivalent to material class C4 is considered.

3.5.1 Unconfined Compressive Test (UCS)

The material compressive strength testing follows Method A14 TMH1 [1986]. The method considers cylindrical specimens measuring a height of 127 mm and a diameter of 152 mm. Material testing system [MTS] with testing parameters set for monotonic loading and at a loading rate of 140 kPa/s or 153 kN/min as defined by the specifications are adopted. The computation of the UCS value follows Equation 3-2. The UCS specimens were cured for 7 days.

$$\text{UCS [kPa]} = [\text{Peak Force} / \pi r^2] \qquad \text{Equation 3-2}$$

Where: Peak Force in kN and r is radius in m

3.5.2 Indirect Tensile Strength Test (ITS)

The determination of the tensile strength includes measuring the load required to cause failure in tension. For the tensile strength evaluation, consideration of cylinder specimen measuring a height of 127 mm and a diameter of 150 mm as stipulated by Method A16T TMH1 [1986] are adopted. The tensile strength testing considers the universal testing machine [UTM-25] with 40 kN/min loading rate until failure. The computation of the material tensile strength value follows Equation 3-3. The ITS specimens were cured for 7 days.

$$\text{Tensile Strength (kPa)} = [2\text{P}/\pi\text{hD}] \qquad \text{Equation 3-3}$$

Where: P - Peak force in kN; h - Height of the specimen in m; D - Diameter in m

3.5.3 Durability Test Method

Durability is an important material property to assess while ascertaining the suitability of the materials. However, durability remains an assessment of the present state of material at the time of testing. Figure 3-8 shows the wet-dry brushing test following procedures for specimen preparation as stipulated in Method A19 TMH1 [1986]. Method A19 is for hand brushing. In this research, machine brushing is preferred to hand brushing because of its consistency in 'brushing power'. The specimens were cured for 7 days before subjecting to 12 cycles of wetting and drying.

Figure 3-8 Automated Brushing Test

3.5.4 Procedure for Specimen Preparation

The preparation of specimens for evaluation requires the establishment of appropriate measures aimed at ensuring an acceptable quality. In order to gain proficiency in preparing as well as testing the specimens, the consideration of trial runs to familiarise oneself with the tasks and procedures is a priority. It is only after undertaking such trial runs that adjustments and/or competence is achievable. Reliability of test data is dependent on the quality control measures adopted, curing conditions and test configurations. After the characterisation criteria, preparation of specimens for the various tests followed. The following steps describe the preparation procedure in brief:

a) Determination of optimum moisture content [OMC] and maximum dry density [MDD] are undertaken using the modified AASHTO compaction method at 100% Modified AASHTO as compactive effort.
b) Following the addition of cement to the material, dry mixing is undertaken. The purpose of dry mixing is to mix cement particles evenly within the material. After 'dry-mixing' the material with cement, addition of water to the mixture [with the cognisance of the hygroscopic moisture] follows. Based on the OMC of the natural material, the computation of the required water is undertaken.
c) The application of the polymer to either cement or stabilised materials is a percentage of the dry mass of cement, i.e. is dependent on the cement content in the mix. However, this requires the mixing of the polymer in water. As a mixture in water, application of the polymer to a cement or stabilised mix is undertaken. In order to control the mix moisture a reduction of mixing water is necessary.
d) The compaction of test specimens makes use of the vibratory hammer following the moisture and density data obtained from the modified AASHTO experimentation. With reference to the material MDD and OMC, an adjustment to the mix water is necessary. By undertaking compaction trial runs with the vibratory hammer, the maximum achievable density and its corresponding moisture content are registered. The compaction trials enable the determination of an appropriate compaction time and moisture content while using the vibratory hammer.

3.6 Flexural Strength Evaluation and Test Configurations

Flexural strength is a mechanical strength evaluation, which studies the ability of the material to resist deformation. The beam-bending test characterises the measure of the material flexural strength. The three-point or four-point loading techniques are commonly considered. Flexural strength represents the maximum stress experienced within the material during the moment of rupture or fracture.

3.6.1 Contextualisation of the Beam Bending Principles

Cognisance of the classical Euler-Bernoulli beam theory [engineer's beam theory] along with the Timoshenko theory is realised. The fundamentals of engineering mechanics relative to the beam bending theories are also realised. Figure 3-9 shows the four-point and three loading techniques, which typify different loading mechanisms and beam bending criteria.

3.6.2 Flexural Strength Beam Test and Experimental Layout

Although the flexural strength beam testing is preferred, no test protocol is set within the South African specifications. Beam geometric characteristics in relation to dimensional specifications and maximum particle size remain unregulated. The current beam dimensional characteristics adopted for flexural strength negate the influence of beam shear stresses. This affects the actual measure of the material flexural strength properties and the consequent interpretation of test data. Figure 3-10 summarises the experimental process.

The selection of feasible beam geometry and test configurations in order to evaluate the flexural strength and elastic modulus while using the four-point loading technique is undertaken. Two variables related to the span-depth ratio are introduced as shown below.

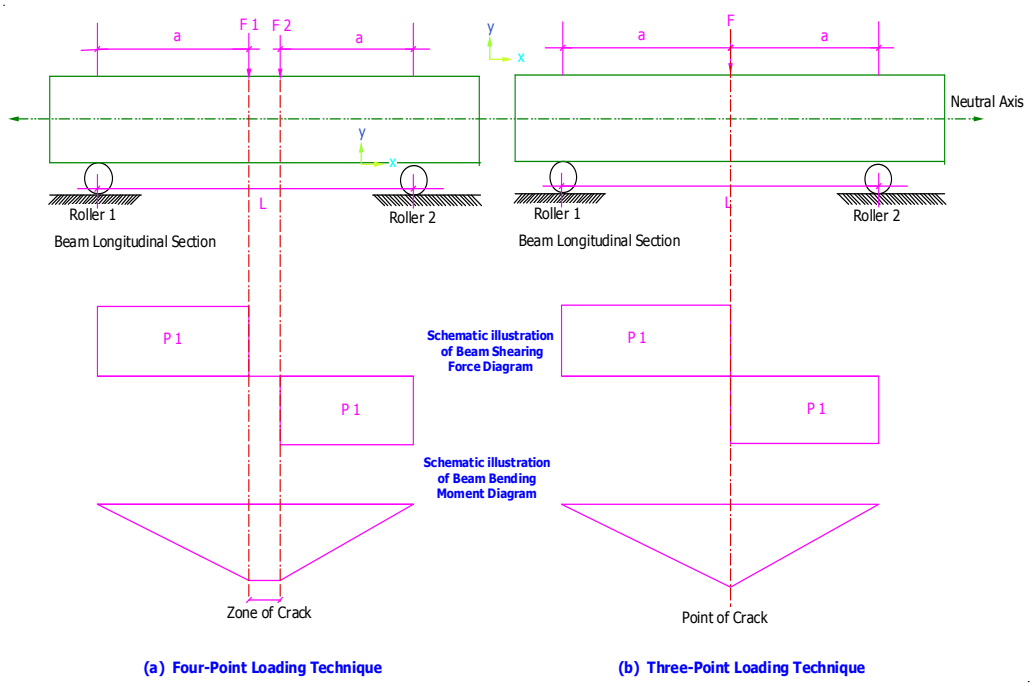

Figure: 3-9 Illustrating the Four-Point [a] and Three-Point [b] Loading Technique

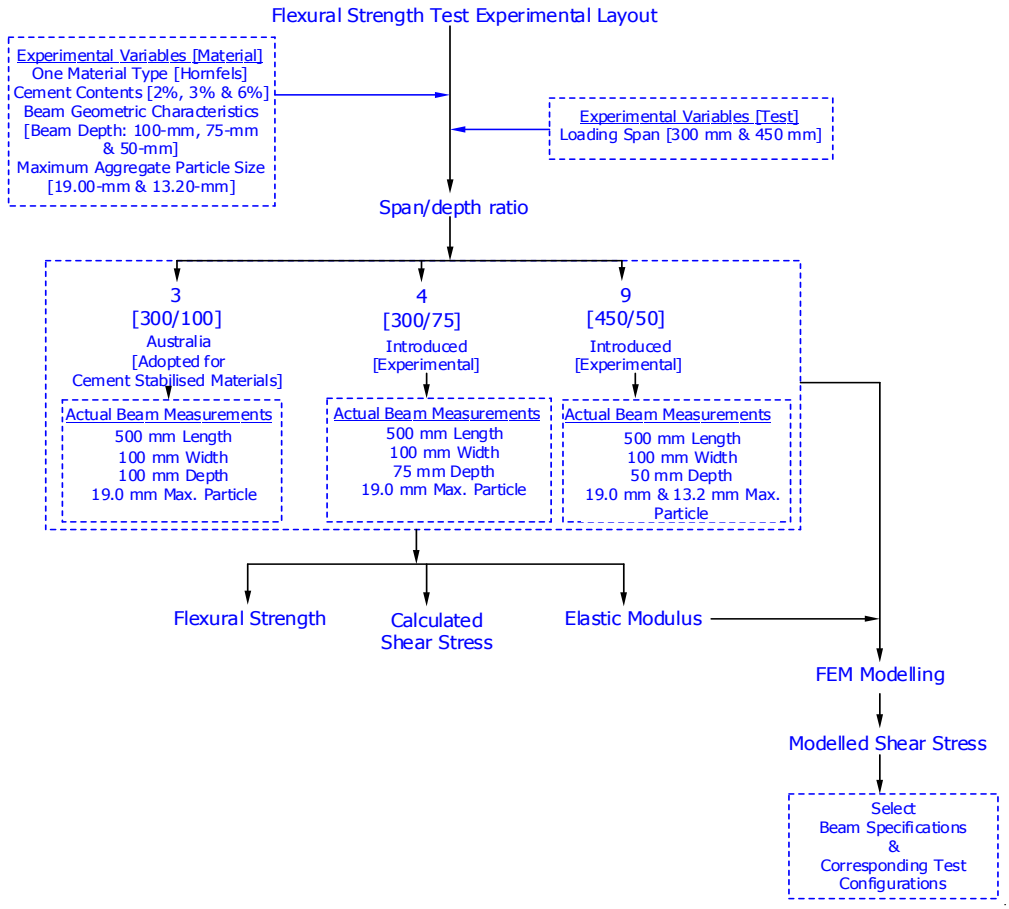

Figure: 3-10 Process of Determining an Appropriate Beam Geometry and Test Configurations [Four-Point Loading Technique]

From the fundamentals of engineering mechanics, shear stress typifies the component of stress co-planar of the beam cross-section. This emanates parallel to the beam cross-section. Equation 3-4 defines shear stress calculations.

$$\text{Shear Stress} = [F/A] \qquad \text{Equation 3-4}$$

Where: F - Force applied
A – The cross-sectional area of the material with area parallel to the applied force vector

Calculation of the beam shear follows the Zhuravskii shear stress formula, Equation 3-5. The beam shear is the internal shear stress due to the shear force applied to the beam.

$$\text{Beam Shear} = [VQ/It] \qquad \text{Equation 3-5}$$

Where: V – Total shear force at the location in question
Q – Statistical moment of area
t – Thickness of the beam perpendicular to shear
I – Moment of inertia of the entire cross sectional area

From engineering mechanics, shear modulus is the ratio of shear stress to shear strain, Equation 3-6. In engineering mechanics, the pure shear stresses and strains relate.

$$\text{Shear Modulus} = [E/2[1 + V] \,] \qquad \text{Equation 3-6}$$

Where: E – Modulus
V – Poisson ratio

3.6.3 Four-Point Loading Test Parameters and Test Configurations

The experimentation considers 300 mm and 450 mm as loading span length. The beam deflection is measured using 20 mm linear variable displacement transducer [LVDT] positioned at mid-span of the beam. Other test input parameters include:

a) type of loading i.e. monotonic type of loading, displacement controlled
b) displacement rate, i.e. 0.025 mm/second = 1.5 mm/min
c) 100 mm as inner loading span length
d) two loading spans, i.e. 300 mm and 450 mm
e) termination of the test at 35% of the maximum peak force [test-run]
f) 10 mm after initial test-run as safety travel

Figure 3-11 illustrates the four-point loading test and beam response. Beam geometric characteristics and bending criteria at mid-span are illustrated. At the support rollers, the beam rotates freely in the X-direction. L is the loading-span and a is the arm-length from the roller to the inner loading-span. The beam is loaded monotonically at a controlled displacement rate and bent until fracture. Upon loading, the beam deflects from its original shape to a deformed shape. At the beam mid-span, measurement of the maximum deflection [δ] using the LVDT is undertaken. L_i is the inner loading-span fixed at 100 mm.

Upon deflection at mid-span, the beam forms a curve. Mathematically, the radius of curvature [R] at a specific point is the radius of the circle that is in immediate contact and of similar tangent at a point. A material at distance y from the neutral axis is in tension and Equation 3-7 mentions of the resultant length of the layer; θ denotes the arch of the circle [deformed circle].

$$L_{\text{tension}} = (R + y)\,\theta \qquad \text{Equation 3-7}$$

Applying the principles of engineering mechanics, material modulus of elasticity [E] relates to the direct stress [σ] and strain [ε]. Equation 3-8 denotes of the relationship between the radius of curvature, material at distance y from the neutral axis, stress and elastic modulus.

$$\sigma = \frac{Ey}{R}$$ Equation 3-8

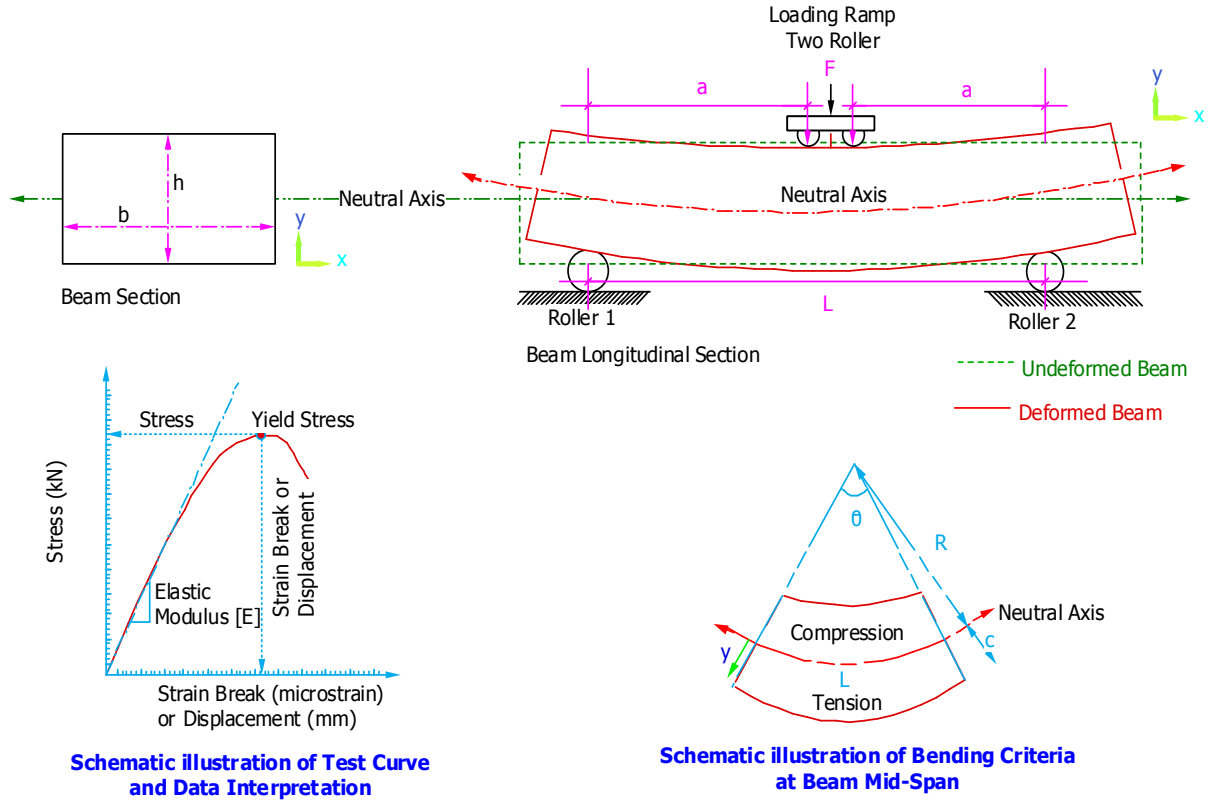

Schematic illustration of Test Curve and Data Interpretation

Schematic illustration of Bending Criteria at Beam Mid-Span

Figure 3-11 Schematic Overviews of the Four-Point Loading Test Technique and Bending Relations

The moment of area [I] of a beam cross-section is a significant property to consider when determining its deflection. The moment of area relates to the beam cross-section dimensions and remains specifically influenced by beam-depth. In the 4-point-loading flexural beam test, the rollers simply support the beam that is transversely loaded at mid-span. The beam deflects when loaded. At the mid-span of the beam, the maximum deflection [δ] is registered. By applying the principles of engineering mechanics and the centre loaded beam deflection formulae, derivation of Equation 3-9 results where F denotes the force. Equation 3-10 relates to the beam geometry and determines the elastic modulus [E] of the material.

$$\delta = \frac{Fa^2(3L-4a)}{6EI}$$ Equation 3-9

$$E = \frac{2Fa^2(3L-4a)}{\delta bh^3}$$ Equation 3-10

For the determination of flexural strength while using the four-point loading test technique Equation 3-11 is applied, [Hodgkinson, 2000]. Equation 3-10 is considered if the loading-span is neither half nor a third of the loading inner span.

$$f = \frac{3F(L-L_i)}{2bd^2}$$ Equation 3-11

Where: f – Flexural strength in MPa
F – Peak force at a point of fracture in N
L – Length of the support span in mm

L_i – Length of the inner loading span in mm
b – Width of the beam in mm
d – Depth [or height] of the beam in mm

3.6.4 Specimen Preparation [Flexural Strength Test]

The material rationing and mixing criteria followed is similar to the preparation of specimens for standardised tests. The compaction of the beams requires the modification of the vibratory hammer footing. Three categories of beams with different beam geometry are prepared. Table 3-1 shows the beam types against the loading span and span-depth ratio as considered in the flexural beam test experimentation. The compacting of the beam types varied depending on the beam height relative to the maximum aggregate particle size. Chapter 4 lists the beam compaction results. The beam type with a height of 50 mm is compacted in one layer. For beam types with 75 mm and 100 mm heights, compaction is carried out in two layers. Curing of the beams carried on at ambient temperature of 25ºC for 28 days. At 28 days, flexural strength testing is undertaken.

Table: 3-1 Summary of the Beam Specimens

Beam Type[1] [mm]	Loading Span [mm]	Span-Depth Ratio
500 x 100 x 100	300	3
500 x 100 x 75	300	4
500 x 100 x 50	450	9
[1]Length x Width x Height		

3.7 Development of Shrinkage Test Method and Protocol

Figure 3-12 illustrates the experimental program for the evaluation of shrinkage. Variables within the experimentation include hornfels and ferricrete material types in addition to one cement type CEMII A-M 42.5N and the polymer. The experimentation includes the beam linear and cylinder circumferential-axial methods. The evaluation of material shrinkage encompasses three maximum particle sizes that include 19.0 mm, 4.75 mm and 2.36 mm. This section of the research methodology explains the phases pertaining to the development of a shrinkage test-method. Factors and parameters include, but are not limited to, the following:

a) It is essential that the method provide a good reliability and reasonable repeatability in order to provide a better comprehension of material shrinkage criteria. The main objective of the experimental trial is to obtain first-hand experience with the test procedures and overall setup for the evaluation of material shrinkage. Trials also assess the practicality of the tasks pertaining to specimen preparation and specimen safeguarding until the start of the test.
b) The conditioning temperature for evaluating shrinkage has to offer a quick but reliable test result. With the knowledge gathered regarding temperature and rate of shrinkage, it became apparent that a high temperature or high humidity is appropriate. A test temperature of 70ºC based on the UCS accelerated strength increase temperature is selected. However, the effects pertaining to high humidity and resultant shrinkage are recognised. This includes computing its equivalent shrinkage to period based on the temperature relationships, i.e. the test temperature of 70ºC relative to 25ºC [the ambient temperature]. In general, the test method has to be simple and quick to undertake in any ordinary laboratory.
c) The precision of the measuring instrumentation, metal moulds, compaction and mixing procedure as well as materials gradations have to exhibit proficiency but also have to be

user-friendly. The precision of the measuring devices typifies the sensitivity of the device in measuring infinitesimal shrinkage.

The beam linear shrinkage is a commonly used approach in research. In this research, inclusion of beam linear shrinkage is to assess its suitability compared to the alternative cylinder circumferential-axial method. With improved instrumentation, it is crucial that comparison of the two approaches is undertaken. This comparison provides insight regarding the test suitability and reliability. All shrinkage specimens were tested immediately after their compaction.

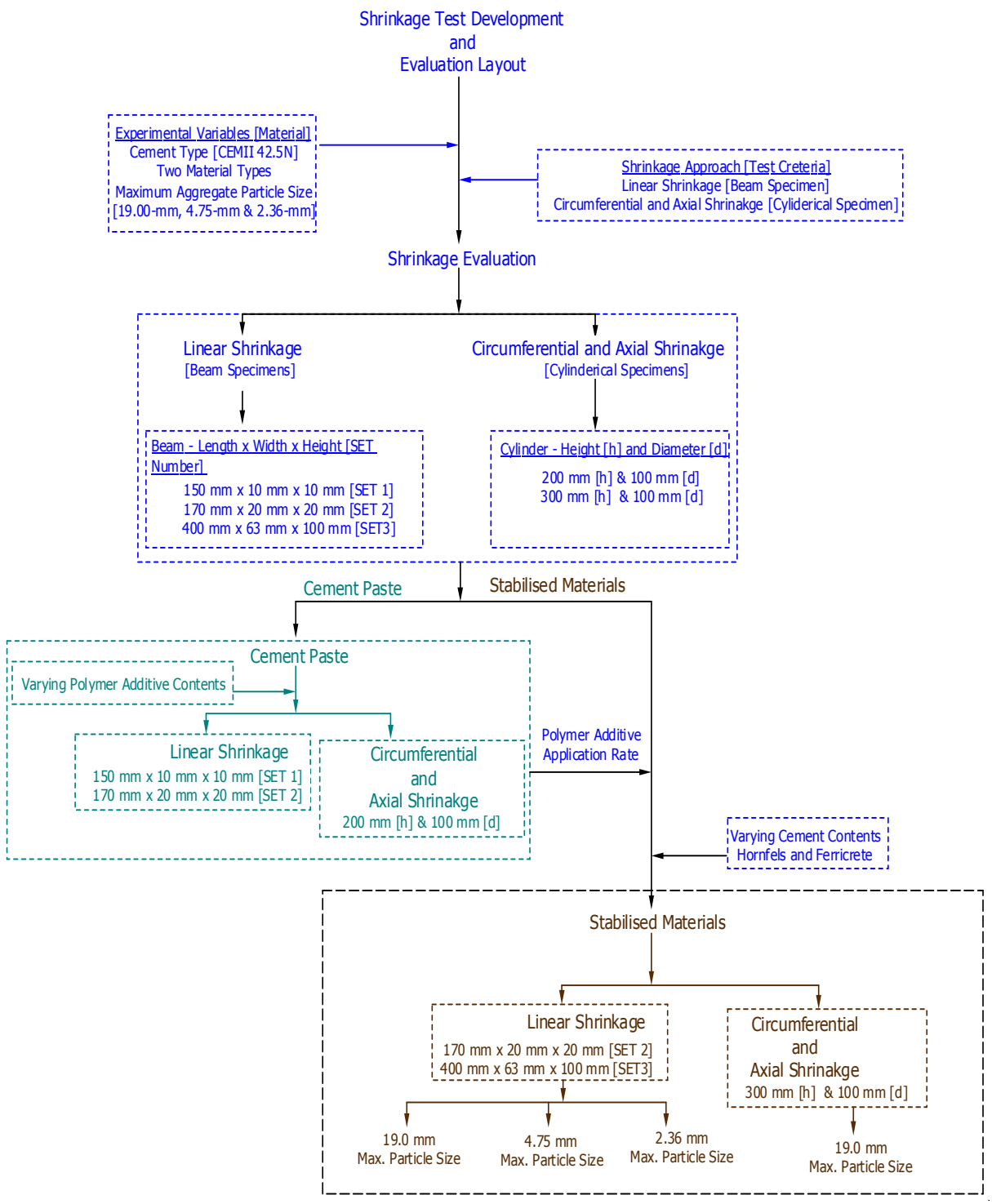

Figure 3-12 Schematic Overview of the Experimental Program to Evaluate Shrinkage

3.7.1 Beam Linear Shrinkage Method [Cement Paste]

In this experimental phase, shrinkage evaluation on cement-paste is undertaken. The purpose of evaluating the cement-paste is to obtain insight regarding the mechanism of shrinkage when considering the beam specimen. The experiment considers a water/cement ratio of 0.5. In the first phase, no waxing of the internal surfaces of the mould is undertaken. In the second phase of the experiment, in order to reduce friction waxing of the internal surfaces is undertaken. The two experiments [waxed and un-waxed] provide insight regarding friction and the resultant crack pattern.

The cement-paste shrinkage experimentation considers two types of mould sizes as shown in Figure 3-13. The experiment first considers rectangular moulds measuring internal dimensions of 150 mm in length, by 10 mm in width and 10 mm in height. The choice of this mould size is to study the effect of slenderness and/or specimen size on shrinkage. Size and shape play a significant role in the evaluation of material shrinkage and the resultant crack pattern. Figure 3-13 shows the beam specimens in the 150 mm mould type after 24 hours in a draught oven at 70ºC. Four specimens in total are prepared per mix variable. The specimens are compacted using a vibratory table at low amplitude in order to avoid the possible discharge or splashing out of the cement-paste. Figure 3-13 illustrates the shrinkage criterion and resultant crack pattern. Transverse shrinkage cracks develop along the length of the beam. There was no use of wax in the cement paste experiment in Figure 3-13.

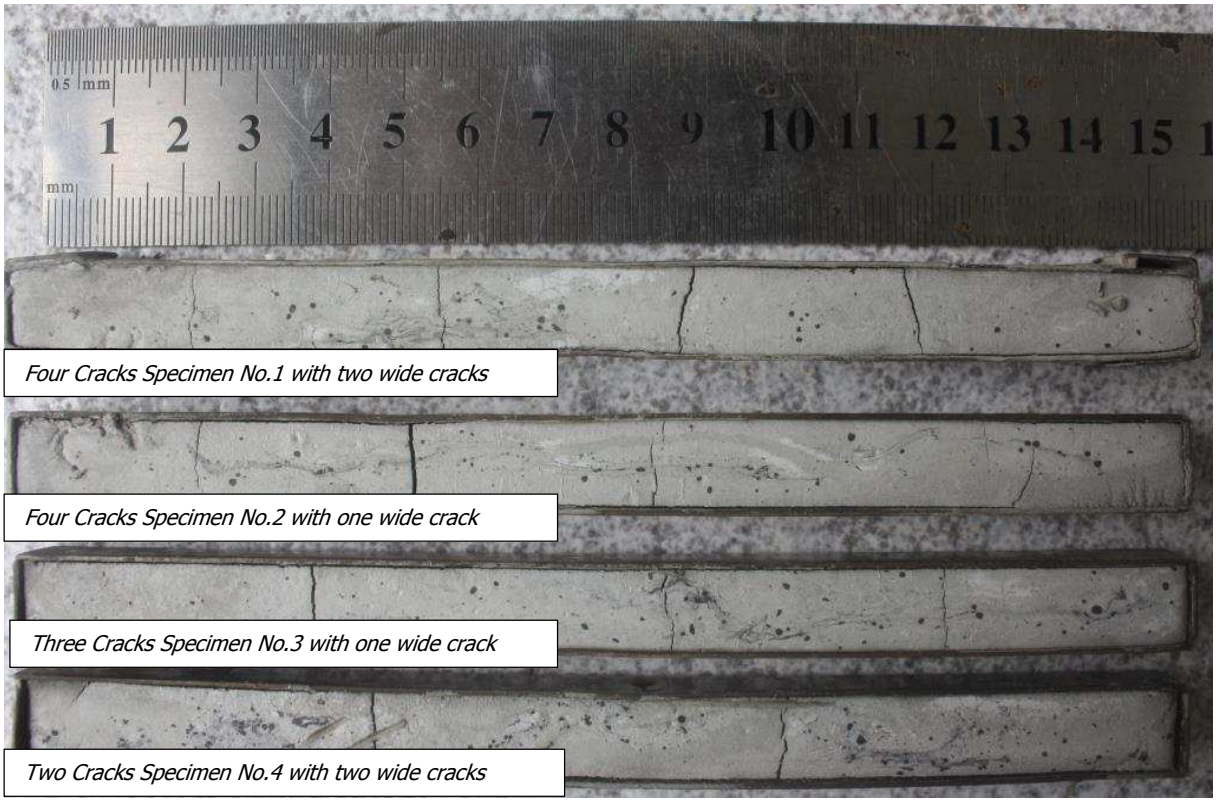

Figure: 3-13 Resultant Crack Pattern [Cement-Paste Mould: 150 mm x 10 mm x10 mm]

On average, three cracks resulted per specimen but at different crack spacings and widths. On average, crack spacing of approximately 34 mm is registered. All specimens displayed a characteristic 'wide' crack width. As observed in the field, cracks appear along the length of the beam in the transverse direction.

Following this first experiment, the occurrence of cracks within a specimen negates any reliable measure of shrinkage without data on the evaluation of crack width. The shape and size of the specimen [slenderness of the specimen] are essential to assess. Figure 3-14

illustrates the layout of the second experiment, whereby waxing of the internal mould surfaces is undertaken. The second experiment considers mould size measuring internal dimensions of 170 mm in length, 20 mm in width and 20 mm in height. The application of wax to the internal surfaces resulted in the specimen shrinking holistically and no visible cracks appeared. By gently sliding the whole specimen to one end of the mould, measured of shrinkage was undertaken using a steel ruler. The assessment of linear shrinkage followed Equation 3-12.

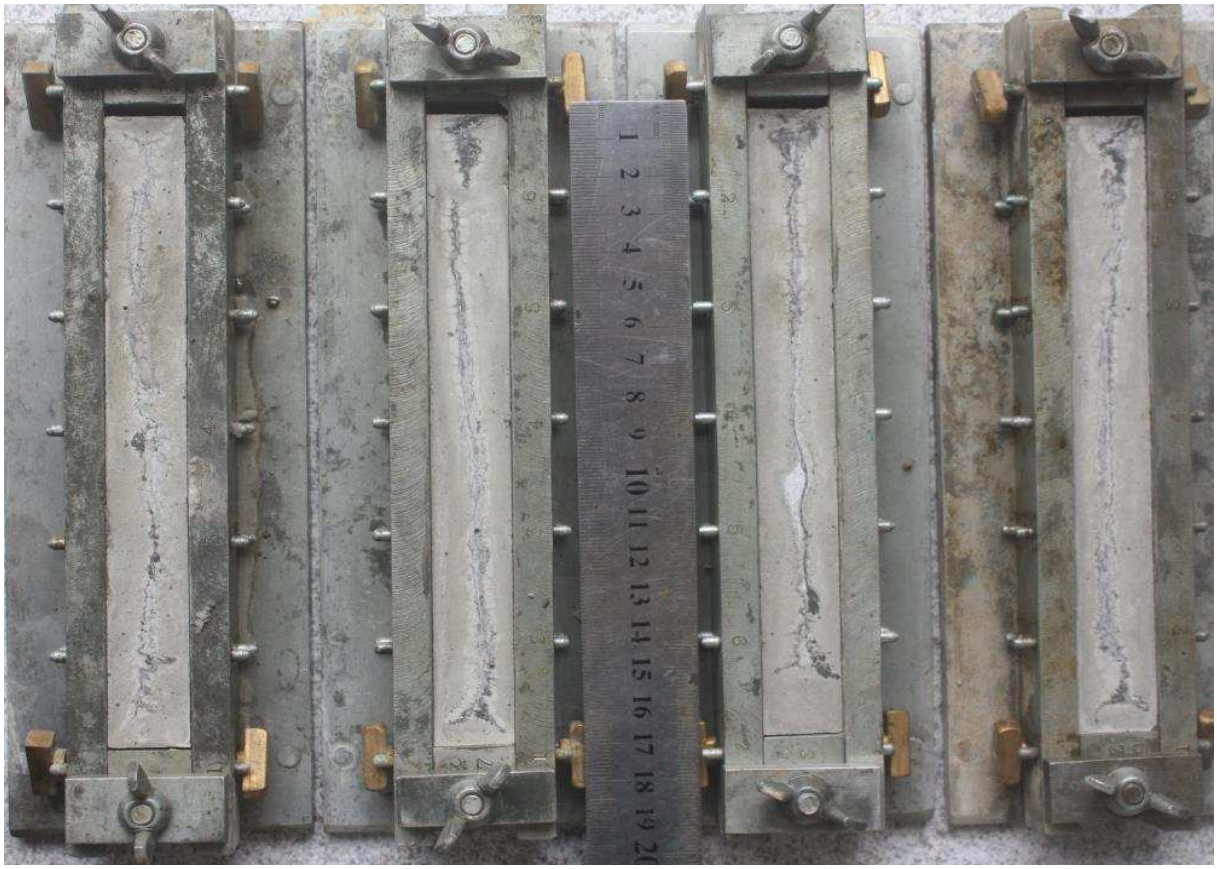

Figure: 3-14 Linear Shrinkage Method on Cement-Paste [Mould-170 mm x 20 mm x 20 mm]

Figures 3-13 and 3-14 illustrate the following principles regarding laboratory-measured linear shrinkage:

a) The application of wax reduces friction at the interface between the beam and mould surfaces. This characterises that the influence of friction on cracking.
b) Manifestation of cracks hinders the effective measure of shrinkage
c) Adjustment of the mould size results in an increased total shrinkage because of surface exposure
d) For the effective measure of shrinkage a friction reducing agent such as wax or moulding oil should be applied

$$\text{Linear Shrinkage } [\%] = [L_f/L_o] \times 100 \qquad \text{Equation 3-12}$$

Where: L_f – difference between the original length L_o and the final measured length of the specimen at the end of the test L_m i.e. $L_f = [L_o - L_m]$

3.7.2 Linear Shrinkage Method [Stabilised Materials]

With the knowledge gathered from the cement-paste analysis along with the cognisance of the low cement contents as applied in stabilising materials, shrinkage measurement for stabilised materials commenced. A consideration of the following factors is essential:

a) *Specimen geometry relative to maximum particle size categories*: The specimen geometry has to provide good packing for all particle sizes. Of the three maximum particle size categories, the 19.0 mm maximum particle size dictates the specimen geometry particularly its height and width. The experiment includes a metal mould measuring internal dimensions of 400 mm in length, 63 mm in width and 100 mm in height.
b) *Specimen compaction for maximum achievable density*: Compaction is initiated by using the vibratory table with a 20 kg weight placed on top of the material. The resultant material dry density obtained using the vibratory table is lower than that obtained using the vibratory hammer compaction. Following this realisation the experiment considers the vibratory hammer for compacting of the beam specimens of stabilised materials.
c) *Handling and demoulding of the specimen*: This is a crucial step in the preparation of the specimen. It is essential that the general preparation of the beam does not lead to any form of damage since this creates zones of discontinuity within the beam. A discontinuity in the beam has a direct influence on the measure of linear shrinkage. Demoulding of the beam involves removing the sides of the mould within the ambient temperature environment. The demoulding comprises of bolting off the nuts. The application of mould oil to the surfaces of the mould prevents sticking of the material. The beam remains undisturbed on the baseplate of the mould.
d) *Measuring instrumentation*: The experiment makes use of the linear variable displacement transducer [LVDT] and a set of surface mounted strain gauges. At each rear end of the beam, an LVDT mounted on plexiglass [which is glued to the end of the beam], measure shrinkage. Surface mounted strain gauges placed on top of the beam measure shrinkage over a length of 90 mm. Figure 3-15 illustrates the concept used.
e) *Reduction of friction between base plate and bottom surface of the beam*: In order to reduce friction at the interface between the base plate and the bottom surface of the beam, mould oil is applied.
f) *Test data acquisition and recording of the test results*: Two sets of data are essential for this setup. LVDT measurements provide the overall linear shrinkage of the beam. The strain gauge provides shrinkage measurement at specific zones of the beam. Both require a computer set and data acquisition devices. The Spider8 registers the LVDTs measurements and the strain gauge data acquisition box registers the six strain gauge measurements. The results are captured using CATMAN software for the LVDT and EXCEL for strain gauge recordings.

Figures 3-15 and 3-16 show the pictorial description of the specifics concerning the beam linear shrinkage test. A series of trial runs are undertaken. From the trial runs, careful consideration to a number of factors results in some significant adjustments to the test. The adjustments include the following:

a) Increasing the number of surface mounted strain gauges from three strain gauges to six in order to obtain a higher degree of reliability. Strain gauges mounted in pairs and parallel to each other are located at the two ends and the middle of the beam.
b) A rigid system is essential to clamp the LVDTs firmly in place for the rest of the test duration. Consequently, a magnetized stand with clamps to secure the LVDTs helps realise this. The magnetic stands, clamp the LVDTs firmly in position. To avoid the LVDT from 'digging' into the beam, a squared plexiglass glued onto the middle of the rear ends of the beam help realise this.
c) Due to the sensitivity of the strain gauges to temperature variations, conditioning of the strain gauges at the test temperature before commencing with the testing is necessary. In order to maintain the test temperature constant throughout the test the draught oven is kept closed throughout the test duration.

Despite the various adjustments made, several limitations while measuring the beam linear shrinkage resulted. Major limitations include the following:

a) *Compaction and beam edge effects*: Even by changing from the vibratory table to the vibratory hammer in addition to tampering the material before compaction, some degree of edge effects resulted. The beam type with 4.75 mm and 2.36 mm as maximum particle sizes and compacted in 2 successful layers, exhibited no beam edge effects. The beam type with 19.0 mm as maximum particle size exhibited the worst edge effects for both ferricrete and hornfels. Efforts to compact the beam type with 19.0 mm in two successive layers proved futile as the 19.0 mm aggregate protruded outwards preventing the holistic compaction of material. An effort to reduce the beam edge effects by increasing the compaction time also proved futile.
b) *Prevailing friction at the interface*: even with mould oil applied to the base plate, it became apparent that the mould oil does not completely reduce friction. This is because the bottom surface of the beam is rough, particularly with 19.0 mm particle size.

Figure 3-15 summarises the aspects of the linear shrinkage method and the beam edge effects with stabilised materials. Cement-stabilised materials were prepared at the OMC of the natural materials. The vibratory hammer was used to compact the stabilised material specimens. With the knowledge gained and the related limitations associated with the beam linear shrinkage method, consideration of alternative options for measuring shrinkage led to the cylinder specimen.

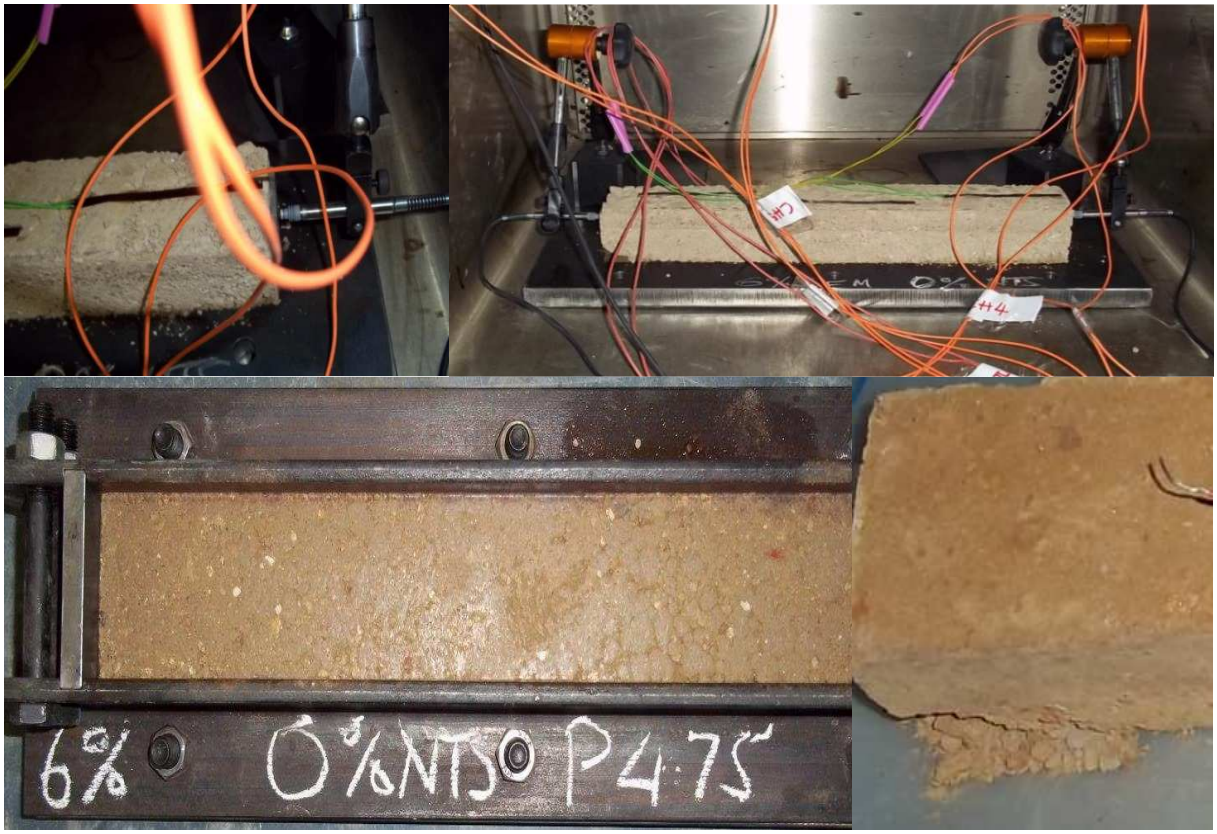

Figure: 3-15 Setup and Beam Edge Effects with the Linear Shrinkage Method on Stabilised Material [Mould- 400-mm x 63-mm x 100-mm]

Figure: 3-16 Beam Preparations and Linear Shrinkage Method on Stabilised Material [Mould-400-mm x 63-mm x 100-mm]

3.7.3 Axial and Circumferential Shrinkage Method [Cement-Paste]

With a good understanding of the beam shrinkage mechanism, development of a test method began based on the insight from the cylinder specimen. The objective of the test is to provide a good understanding of shrinkage as part of a material property evaluation. Similar to the beam linear shrinkage method, the experiment first considers cement-paste. The experiment makes use of a cylindrical mould measuring internal dimensions of 100 mm in diameter and 200 mm in height as shown in Figure 3-17.

In this experiment, four specimens per mix variable are prepared using a water-cement ratio of 0.5. Compaction of the cement-paste in the cylindrical moulds proceeds, using a vibratory table as shown in Figure 3-17. With mould oil smeared onto the internal surfaces of the mould, a reduction in friction is realised. After filling up the cylindrical moulds with the cement-paste, compaction of the specimen using a vibratory table, followed at low amplitude for a fixed duration. The compaction time was determined by undertaking trial runs. The extra cement-paste is scrapped-off to level with the top of the mould as is done with the beam specimens. Retained within their individual moulds, the conditioning of the specimens in the draught oven at a test temperature of 70^0C for 24 hours follows. Measurement of shrinkage is undertaken manually.

Figure 3-17 Cylindrical Cement Paste Specimens [100 mm in Diameter, 200 mm in Height]

From the cement-paste experimentation, cognisance of the semi-plastic state of the cement-paste at the time of compaction is realised. The tendency of the cement-paste to shrink more in the axial direction than in the circumferential direction is mainly attributable to the semi-plastic state. The particles of cement settle in the axial direction as the specimen shrinks. A scrutiny of the sides of the cement-paste exhibits some tendency to detach from the mould [slight decrease in diameter]. This observation only suggests that there is some form of circumferential shrinkage.

3.7.4 Axial and Circumferential Shrinkage Method [Stabilised Materials]

The two cement-paste experiments, i.e. the beam and cylinder specimens provide a good understanding of the shrinkage criteria relative to the specimen and measuring benchmarks. This includes specimen shape and size in addition to surface exposure. Following this investigation based on cement-paste, the following considerations are noted:

a) *Specimen geometric characteristics*: It is essential that the entire specimen completely dry out when subjected to 70ºC. This suggests that the cylinder specimen height has to be long enough and the diameter of the specimen has to be small enough to allow complete drying out, feasible for compacting and enabling the inclusion of the 19.0 mm particle size. The experiment involves a specimen with a diameter of 100 mm and a height of 300 mm.
b) *Compaction of specimen:* Having established the specimen geometry the compaction of the specimen is essential. The experiment includes the vibratory hammer fitted with a 100 mm diameter footing. Compaction proceeds in five layers of 60 mm in height. After

every layer compaction, scarification is undertaken. By conducting trials at different compaction periods for the same compactive effort per layer, the compaction time was determined. Figure 3-18 shows the overall criteria, including preparation and demoulding.

c) *Handling of the specimen after compaction:* To prevent damage to the specimen, demoulding and moving it to the draught oven has to be carefully planned. A split-mould proves an effective means to demoulding without damage. With mould oil, smeared onto the internal surfaces of the mould removal of the specimen is realised. At an ambient temperature of 25ºC, demoulding of the specimen takes place. By placing the specimen onto plexiglass assisted in carrying it around with ease. Before conditioning the specimen, its wet mass is registered.

d) *Measurement of shrinkage*: the measure of shrinkage encompasses both the axial and circumferential. The dial gauge and LVDT measure the axial shrinkage while the chain-linked extensometer measure the circumferential shrinkage at the mid-height of the specimen. In this experiment, shrinkage is assessed in the axial as well as the circumferential directions. For the axial shrinkage measurement, the dial-gauge and LVDT measure shrinkage co-currently. On top and at the bottom of the specimen, plexiglass provides a firm and stable area for the instrumentation. The top plexiglass provides a stable area for the dial-gauge and LVDT. On the bottom plexiglass, mould oil was smeared onto it to reduce friction at the interface between the specimen and plexiglass. On the top of the specimen, epoxy-glue was applied to secure the plexiglass in place. The top plexiglass is where the dial gauge and LVDT were placed. While positioning the extensometer at mid-height of the specimen it is crucial to align the extensometer horizontally. The extensometer comprises of a chain made up of individual rollers intertwined with each other. The clip device fastens into the chain and possesses a zeroing set-in-pin for calibration purposes. The spring holds the clip device to the chain and in position. The chain and the clip device link with the stand-alone display unit. The unit registers the changes in specimen dimensions. Before using it, calibration of the extensometer is necessary. The extensometer is set to measure within the range of +/- 2.0 mm with zero set as its datum point.

In general, manufacture of the chain-linked extensometer remains a specialised field of instrumentation and its calibration for use requires a certified ISO specialist. This was undertaken. The reliability of the chain-linked extensometer that is its range of sensitivity under the specified test conditions is also fundamental. This laid a firm understanding in selecting the instrumentation for use in this study. Universally, dial gauges and LVDTs are common instrumentation used to measure dimensional changes. However, it is vital to comprehend not only its measuring criteria, but also its calibration and range of measurements. In terms of practicality and usability, the dial gauge is preferred to the LVDT.

3.8 Summary of the Research Criteria

The layout of the research study and the specifics concerning the experimental program are included in this chapter. This research study encompasses both standard and non-standard tests. The experimental layout of the flexural beam test is detailed. The shrinkage experimental program is illustrated. With the comprehension of the principles gathered from Chapter 2 establishment of a research methodology followed.

Stabilisation of materials requires both compressive and tensile strength tests. The experimentation considers maximum cement content of 6.0% and a minimum content capable of providing a material strength equivalent to at least C4 material class. Hornfels is stabilised at cement contents of 2%, 3% and 6%. Ferricrete is stabilised at cement contents of 3%, 4% and 6%. Based on cement-paste shrinkage experimentations the polymer application rate is established.

Figure 3-18 General Setup for Circumferential-Axial Shrinkage Method

3.9 Analytical Procedure

The results obtained from both standard and non-standard tests are analysed. Analytical tools applied in this research include modelling. FEM modelling is a numerical analysis, which entails the development of models and requires input data. FEM modelling conducted in the research focuses on the four-point beam flexure technique to assess the effect of beam-depth relative to the effective loading-span [span-depth ratio]. This analysis together with the laboratory analysis assists in the formulation and selection of an appropriate flexural beam test for the evaluation of stabilised materials. For the computation of the fracture energy MathLab as an analytical tool and the stress-strain data from the flexural beam testing is used.

For the prediction of the shrinkage crack pattern in a stabilised pavement layer, the Houben model is preferred. The Houben model requires the development of the input parameters and data. These parameters and data include:

a) thermal coefficients for aggregates and cement paste
b) stress relaxation factors
c) annual temperature variations, seasonal ranges and diurnal trends
d) pavement temperatures

The outputs from the Houben model include crack spacing and crack-width data [crack pattern], which is fundamental to the performance of the pavement particularly for load transfer. Application of the cncPave software to assess probable layer trends and related performance is undertaken. Figure 3-19 is a schematic layout of shrinkage modelling criteria.

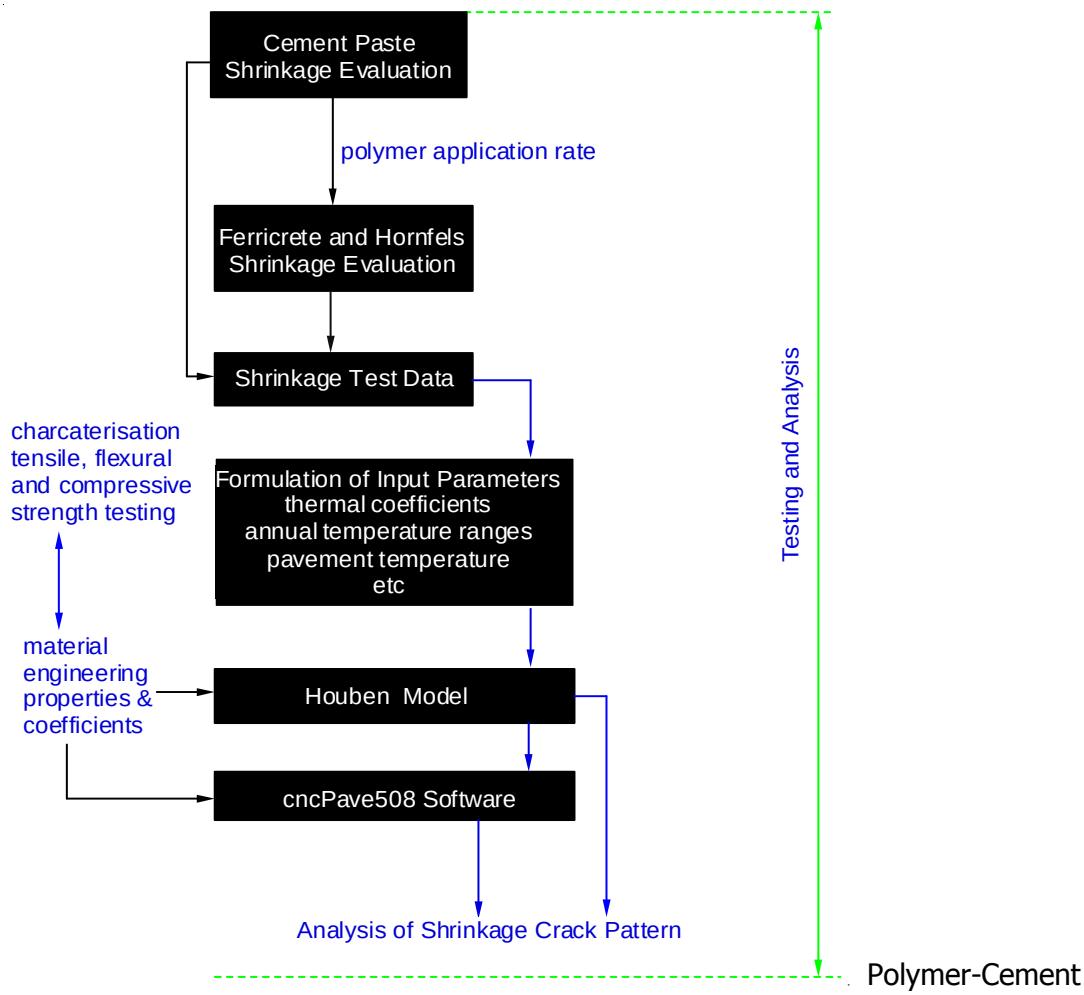

Figure 3-19: Schematic Layout of Shrinkage Analysis

3.10 References

Bredenhann, S.J. Paige-Green P. and Jenkins K.J., (2012) *Cemented Materials: Accounting for Compaction Delays and Minimizing Strength Loss with Time*, 7th International Conference on Maintenance and Rehabilitation of Pavements and Technological Control (MAIREPAV7)

Gauglitz, G. and Vo-Dinh, T., (2003) *The Handbook of Spectroscopy* Wiley-VCH, 2003, ISBN 3-527-29782-0

Julien, N., (2008) *Advantages of CT in 3D Scanning of Industrial Parts,* North Star Imaging Inc. Vol. 1, No. 3

Koen, H.A.J. and Van Grieken, R.E., (2004) *Non-destructive Microanalysis of Cultural Heritage Materials,* Elsevier, Amsterdam, The Netherlands, 2004 ISBN 0-444-50738-8.

Hodgkinson, J.M., (2000) *Mechanical Testing of Advanced Fibre Composites,* Cambridge Woodhead Publishing Ltd, pg. 132-133, 2000

Draft TRH4., (1996) *Structural Design of Flexible Pavement for Interurban and Rural Roads,* ISBN 1-86844-218-7 pp. 1-101

Geology Rocks and Minerals., (2005) *The Geology of Auckland,* University of Auckland

Philip, L., (2007) *Ferricrete Classification, Morphology, Distribution and carbon-14 Age Constraints in Environmental Effect of Historical Mining,* Animas River watershed, US Geological Survey Paper 1651 pp.726 2007

Standards Australia., (2000) *Methods of Testing Concrete: Method 11: Determination of the Modulus of Rupture,* AS 1012. 11

TMH1., (1986) *Standard Methods of Testing Road Construction Materials,* 2nd Edition ISBN 0-7988-3653-9 pp. 1-232

TRH13., (1986) *Cementituos Stabiliser in Road Construction,* ISBN 0-7988-3647-4

TRH14., (1985) *Guidelines for Road Construction Materials,* Technical Recommendations for Highways

Chapter 4: Material Characterisation, Strength and Durability Results

4.1 Background

The characterisation of materials should provide reliable insight regarding their suitability and probable performance. Strength is a key material property required for design and quality control during the construction phase. This chapter includes a summary of the South African specifications for G4 and G5 material types. The analysis of the compressive and tensile strength properties of cement-stabilised materials with and without the polymer is also included. The primary objective of cement stabilisation is to increase the quality and thus, the performance of the natural materials.

4.2 Material Characterisation Results

The South African specifications stipulate gradation, Atterberg limits, maximum dry density and CBR as part of the material characterisation and classification system. However, the same specifications do not consider material mineralogy and the assessment of their internal morphology. In this research, the characterisation process includes XRF analysis and CT scanning. The characterisation of the polymer and the determination of its application rate are also included. The polymer characterisation comprised of the following:

a) determining the amount of water and other evaporating components within the polymer
b) the effect of polymer on the material properties
c) ascertaining the application rate of the polymer

Table 4-1 presents a summary of the characterisation results based on the South African material specifications. Figure 4-1 illustrates the grading of hornfels and ferricrete materials. The wet sieve analysis was preferred because the water separates the conglomerates into individual particles. With the vibratory hammer, a higher maximum dry density is obtained for the same material compared to the modified AASHTO. The vibratory hammer possesses a higher compactive effort than the modified AASHTO.

An investigation of the physical and chemical properties of the natural materials is necessary. This is because the physical and chemical properties influence the engineering properties of the cement-stabilised materials. A comparison of the material grading shows that ferricrete contains more fines than hornfels. Furthermore, Table 4-2 and Figure 4-2 present the XRF results of cement, ferricrete and hornfels. Ferricrete is an indurated material type that contains iron oxides and other elements such as Aluminium [Al]. The iron rich particles in ferricrete typically exhibit a specific particle size, [Landon 2014]. Due to their high densities, the particles do not plot on a smooth curve; this is illustrated in Figure 4-1. The difference in the fine content between ferricrete and hornfels provides insight regarding the efficacy of cement, resultant and the general material quality.

The Atterberg limits indicate that hornfels is a non-plastic material type while ferricrete is plastic material with a plasticity index [PI] of 2.8. The maximum dry density [MDD] of hornfels is higher than that of ferricrete. This is indicative of the amount of fines in ferricrete, which is also typified by the moisture demand. An excess amount of fine particles results in a reduction in the material density, however, this also leads to an increase in moisture demand. Fines present a larger surface area than medium or coarse particles.

The CBR results in Table 4-1 [based on un-stabilised materials] indicate that hornfels has a higher bearing capacity than ferricrete. This suggests that ferricrete has a lower material quality compared to hornfels. With reference to the South African material classification system, ferricrete classifies as a material class G5 and hornfels as G4. Ferricrete is a typical natural soil and hornfels is a crushed aggregate material type. The road industry prefers material class G4 for stabilisation. The South African specifications stipulate a grading

envelope for material class G4, but not for the G5. However, compliance with specific material parameters such as the grading modulus, minimum CBR and PI is mandatory for material class G5.

Table: 4-1 Summary of Standard Material Characterisation

Sieve Size (mm)	Hornfels	Ferricrete
26.00	100.0	100.0
19.00	90.0	100.0
13.20	70.0	92.1
9.50	60.0	83.5
6.70	53.0	79.0
4.75	44.0	65.6
2.36	31.5	42.0
1.180	26.0	38.2
0.600	21.0	36.8
0.425	17.5	27.6
0.300	15.0	24.4
0.150	12.0	12.6
0.075	6.0	8.6
Property	**Hornfels**	**Ferricrete**
Maximum Aggregate Size (mm)	37.5	63
Grading Modulus	2.45	2.218
Liquid Limit (%)	Non-Plastic	17.9
Plastic Limit (%)	Non-Plastic	15.1
Plasticity Index	Non-Plastic	2.8
Bar Linear Shrinkage (%)	Non-Plastic	2.9
[1]Maximum Dry Density (MDD) (kg/m^3)	2346	2023
[2]Maximum Dry Density (MDD) (kg/m^3)	2352	2171
[3]Optimum Moisture Content (OMC) (%)	5.3	8.8
CBR @ 100% Mod.AASHTO	93	73
Swell @100% Mod.AASHTO	0.1	0.2

[1] Dry Density based on the AASHTO Modified Compaction Method
[2] Dry Density based on the Vibratory Hammer
[3] Optimum Moisture Content based on the AASHTO Modified Compaction Method

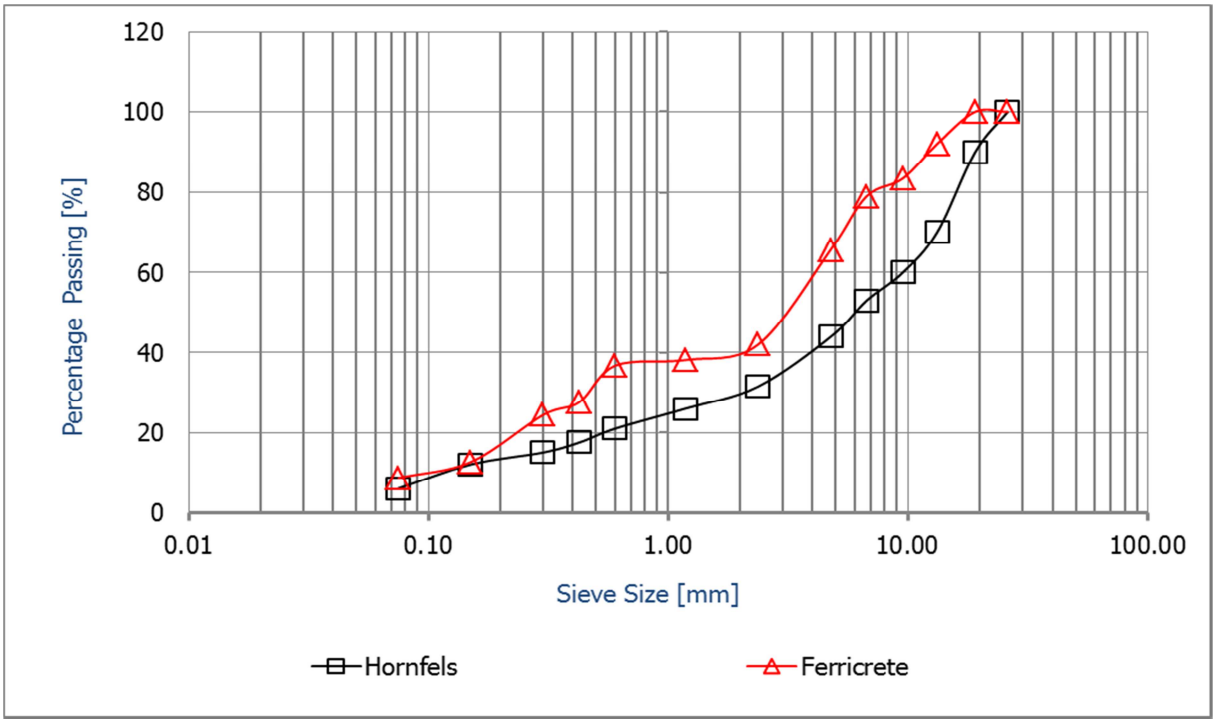

Figure: 4-1 Hornfels and Ferricrete Grading Curves

4.2.1 X-Ray Fluorescence [XRF] Results

The chemical compositions of the natural materials influence the engineering properties even after stabilising with cement. The XRF analysis provides the chemical composition of the materials. This provides insight into their probable reactivity, the effectiveness of cement, quality and to an acceptable degree, their durability criteria after stabilisation. The low sum of concentration [i.e. 97.7%] of cement is more due to the inability to test the sulphur trioxide [SO_3]. The optimum SO_3 content in cement is usually between 2.1% and 2.8% depending on the cement type, [Taylor, 1993]. The measurable quantity with which the gypsum is regulated is the percentage of the SO_3 content in the cement.

Table: 4-2 XRF Results for Cement, Ferricrete and Hornfels

Property (%)	Cement	Ferricrete	Hornfels
Al_2O_3	6.50	13.55	13.55
CaO	56.23	0.03	1.65
Cr_2O_3	0.00	0.03	0.01
Fe_2O_3	2.76	21.03	5.56
K_2O	0.59	0.15	3.24
MgO	3.78	0.12	2.47
MnO	0.04	0.01	0.11
Na_2O	0.26	0.00	2.25
P_2O_5	0.12	0.06	0.17
SiO_2	23.37	54.76	67.54
TiO_2	0.31	0.48	0.79
L.O.I.	3.74	10.60	2.24
Sum Of Concentration [%]	97.70	100.82	99.58
Note: L.O.I - Weight Loss or gain at 1000ºC			

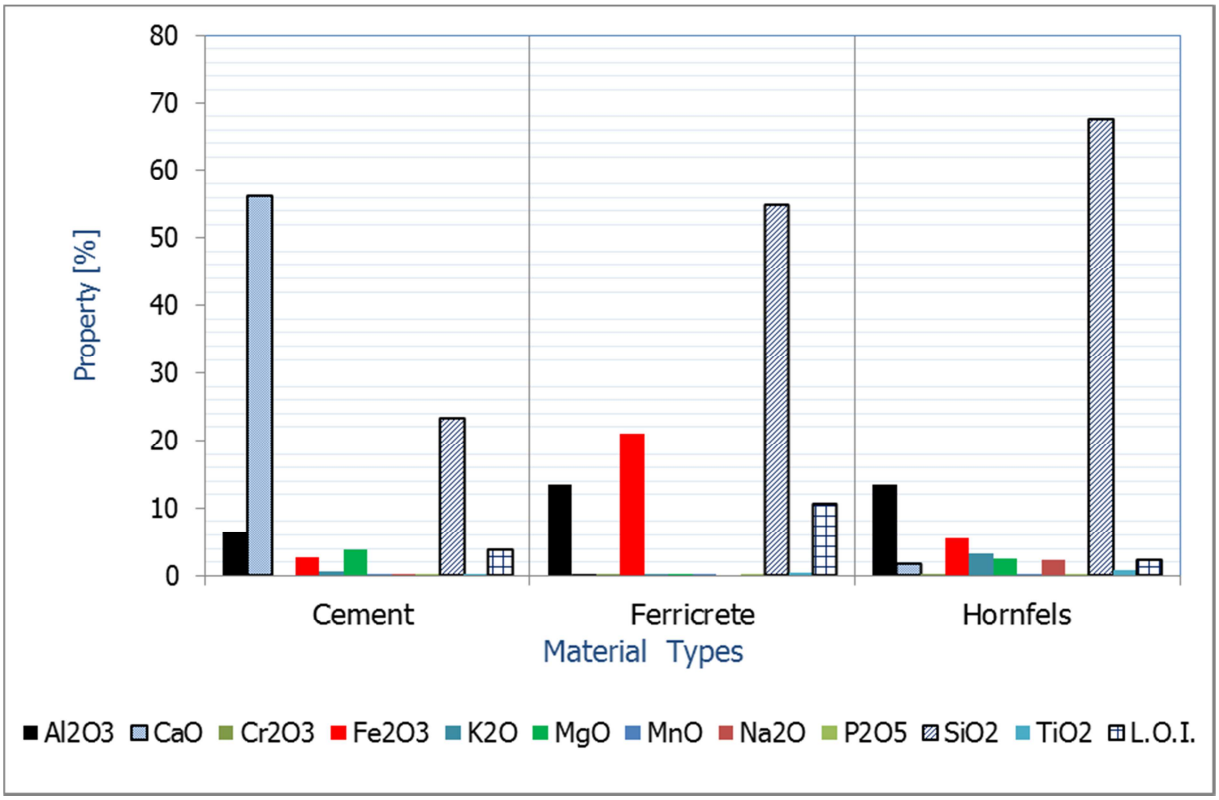

Figure: 4-2 XRF Results for Cement, Ferricrete and Hornfels

The mineral elements present in each material, including cement provide insight into their physical and chemical characteristics of the stabilised material. Several mineral elements show trace, typically less than 1.0%. However, specific elements show high concentrations in particular material types. Aluminium oxide [Al_2O_3], calcium oxide [CaO], iron III oxide [Fe_2O_3] also referred to as ferric oxide, potassium oxide [K_2O], magnesium oxide [MgO], sodium oxide [Na_2O] and silicon dioxide [SiO_2] show high concentrations. The Portland cement type CEMII A-M 42.5N exhibits oxides of aluminium and calcium in addition to silicon dioxide. All Portland cements should exhibit a calcium oxide to the silicon dioxide ratio of not less than 2.0. The cement type i.e. CEMII A-M 42.5N exhibits a calcium oxide to silicon dioxide ratio of 2.4. The magnesium oxide in Portland cement should never exceed 5.0% by mass. The cement type CEMII A-M 42.5N registers about 3.8% of magnesium oxide. Cement shows the highest overall percentage of calcium oxide [CaO] compared to ferricrete and hornfels. Calcium oxide is responsible for the exothermic reaction [produces heat energy in the presence of moisture]. Calcium oxide is one of the key components of cement.

Ferricrete exhibits the highest overall percentage of ferric oxide compared to hornfels and cement. Ferric oxide is responsible for the reddish pigmentation exhibited by ferricrete. Additionally, the amount of silica in the materials, including cement influences the resultant engineering properties, the long-term durability and shrinkage criteria. Silica content in ferricrete and hornfels is higher than that in cement. Silica exists naturally in several material types. In cement, silica combines with calcium in the presence of water to form calcium silicates hydrate [C-S-H] during the hydration process. An assessment of the silica content relative to the material provides the following ratios:

a) silica - cement ratio 0.2
b) silica - ferricrete ratio 0.5
c) silica - hornfels ratio 0.7

In general, each concentration of the individual elements is likely to influence the properties and quality of the stabilised materials. The XRF analysis does not register any traces of sulphates from the material types including cement. Cement contains alumino silicates, which could have been registered. Sulphates and organic matter hinder the cementation effect and thus, reduce the quality of the cement-stabilised materials.

4.2.2 Polymer Characterisation Results [Cement Shrinkage Approach]

The characterisation of the polymer concentrated on establishing its application rate to cement in addition to verifying the amount of water and other solvents. The amount of water added to the mix has an influence on the resultant moisture content and thus, varies the dry density. No further analysis was conducted on the polymer because of the contractual agreement with the stakeholders. This became a limitation to the study. The experiment to determine the amount of free water and other evaporating components provides the following interpretations:

a) The polymer comprises of more than 60% free water and other solvents; an average of about 64% of evaporants is assessed.
b) As the free-water and other components vaporised, a sheath or coating was formed at the top of the container. This was not entirely conclusive regarding the polymer mechanism in inhibiting further evaporants.

Subsequent to the findings, additional experimentations aimed at determining the application rate of the polymer followed. Being a cement additive that is purported to reduce shrinkage, a cement paste experiment commenced to determine the required polymer content to provide the least shrinkage. A series of trial runs were conducted to gain a good understanding of the factors influencing shrinkage. After two series of the cement paste trial runs, it became apparent that additional moisture due to the application of the polymer to the cement mix resulted. Preliminary results show that about 1% increase in moisture

content results for every 2% of polymer content added to the cement mix. As a result, a reduction of 1% of the mix-water was undertaken in the subsequent trials. Figures 4-3 and 4-4 illustrate the moisture variation and beam linear shrinkage at a fixed water-cement ratio [*w/c*] of 0.5 but different polymer contents. In this experiment, a mould size with internal dimensions measuring 170 mm in length by 20 mm in height as well as 20 mm is width, was used. Figure 4-5 illustrates the axial shrinkage method using a cylinder mould with an internal dimension of 200 mm in height and 100 mm in diameter.

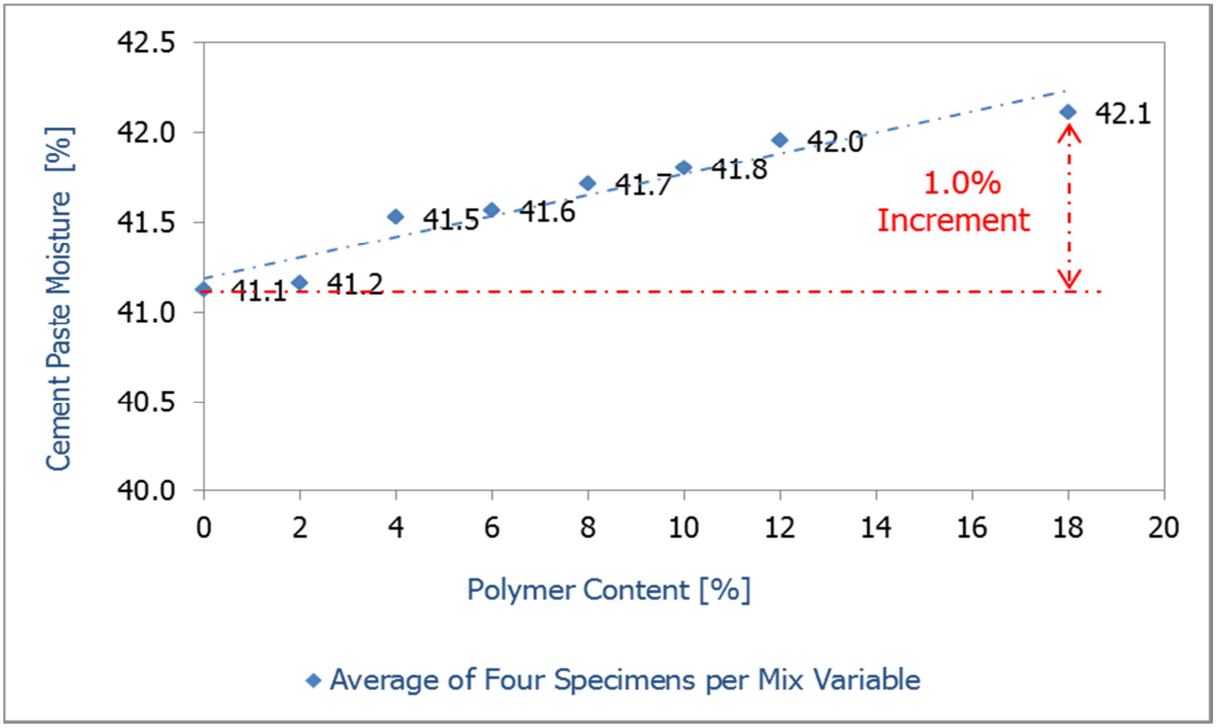

Figure: 4-3 Cement-Paste Moisture versus Polymer Content

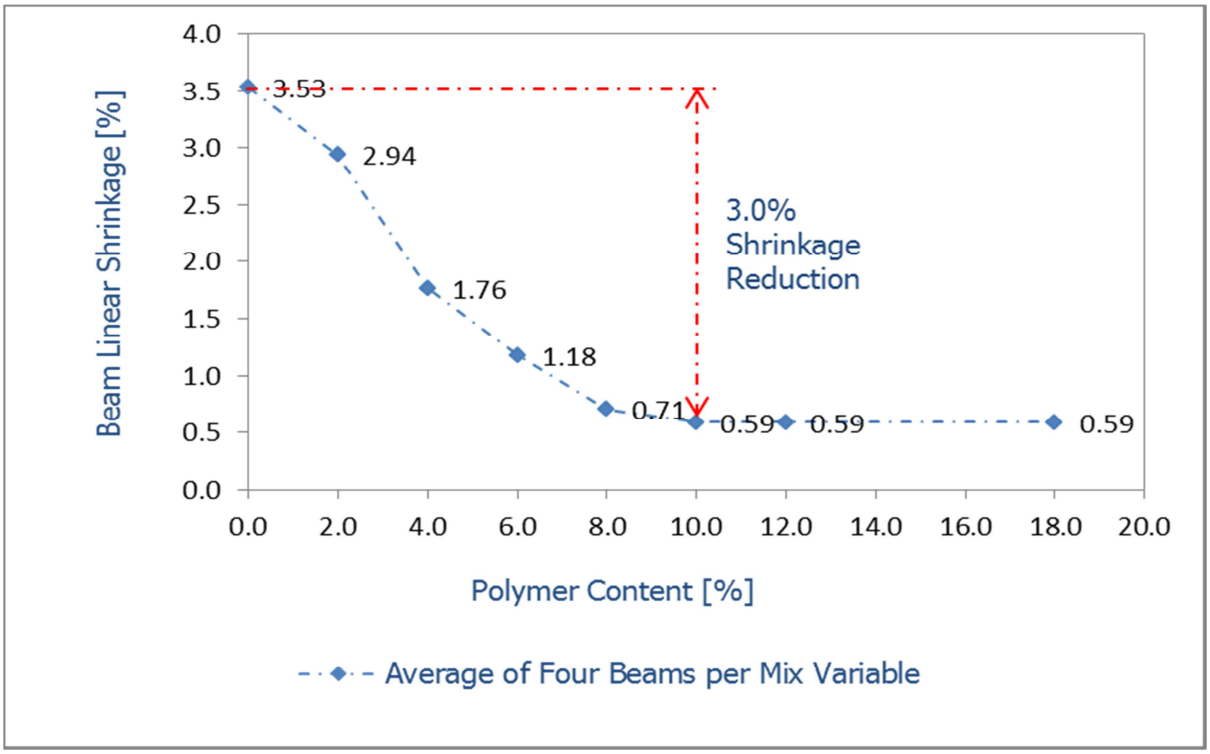

Figure: 4-4 Beam Linear Shrinkage versus Polymer Content

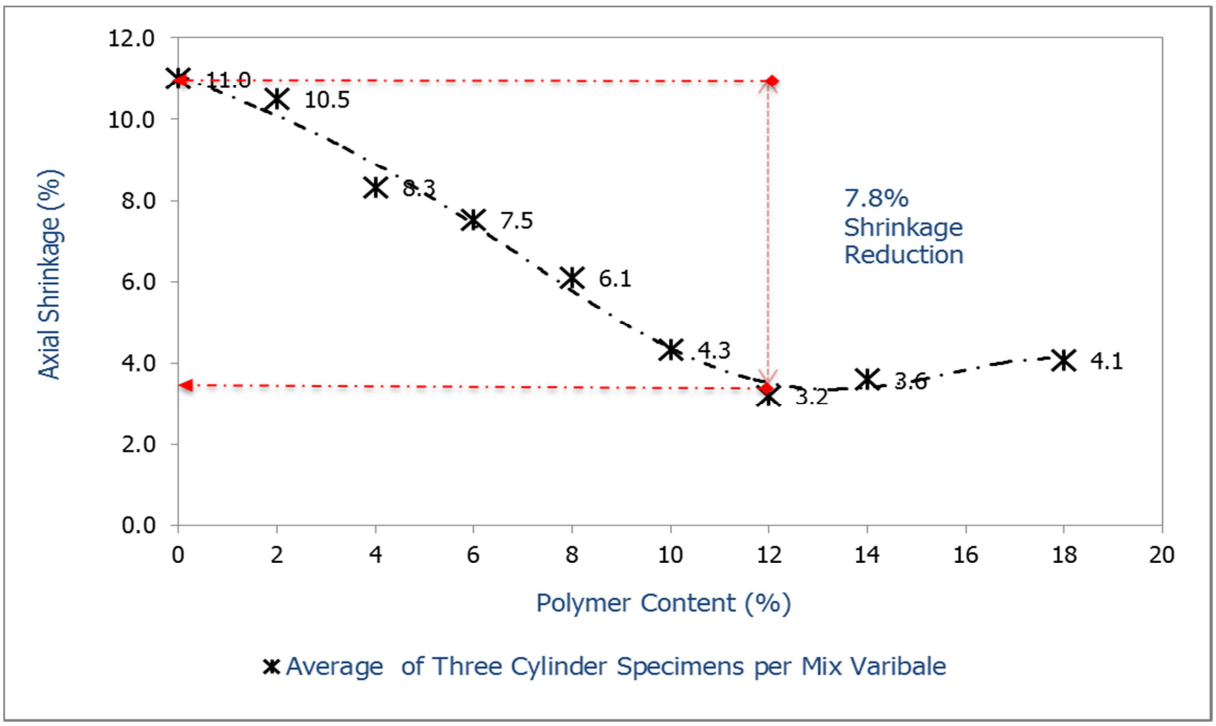

Figure: 4-5 Axial Shrinkage versus Polymer Content

Findings from the experiments suggest that the polymer increases the moisture content of the mix even after a reduction of 1.0% of the mix water. The mix types with without the polymer show the least overall moisture content but a significant shrinkage. Figures 4-4 and 4-5 show the results obtained using the two shrinkage methods. In interpreting these results cognisance of the different specimen sizes and measuring criteria must be noted. The size of the specimen particularly its slenderness ratio relative to its length influence the rate of drying, the resultant stress development and thus, the total measured shrinkage. As a result, the cylinder axial shrinkage and the beam linear shrinkage methods report different total shrinkage for the same mix type.

With the beam linear shrinkage method, least shrinkage corresponded with 10% polymer content. The cylinder shrinkage method shows least shrinkage with 12% polymer content in the mix. A percentage corresponding to the least shrinkage percentage defines the polymer application rate to cement. Considering the measuring criteria used to assess shrinkage, the beam method exhibits higher friction at the interface than the cylinder approach. From the two approaches, the cylinder method is preferred to the beam approach. This is because of the measuring criteria relative to the possibility of friction influencing the measurement of shrinkage in the cylinder method is avoided. Considering cement paste as 100% cement content, a Polymer-Cement ratio of 0.12 is computed based on the cylinder method. This ratio defines the relationship between the polymer and cement contents during the stabilisation of the materials.

4.2.3 Polymer Effect on the Moisture and Density [Modified Compaction Method]

With the computed Polymer-Cement ratio of 0.12, the influence of the polymer on the density and moisture content of the material was another fundamental factor to establish. The polymer-material density experiment included natural [un-stabilised] and stabilised mix types. For this experiment, hornfels stabilised using 6.0% cement content with and without the polymer is considered. With 6.0% cement content in the mix, a polymer content of 0.72% is applied. Compaction proceeded at 100% modified AASHTO using the modified

compaction method. Figure 4-6 illustrates the dry density results of hornfels [as a representative] based on the modified AASHTO.

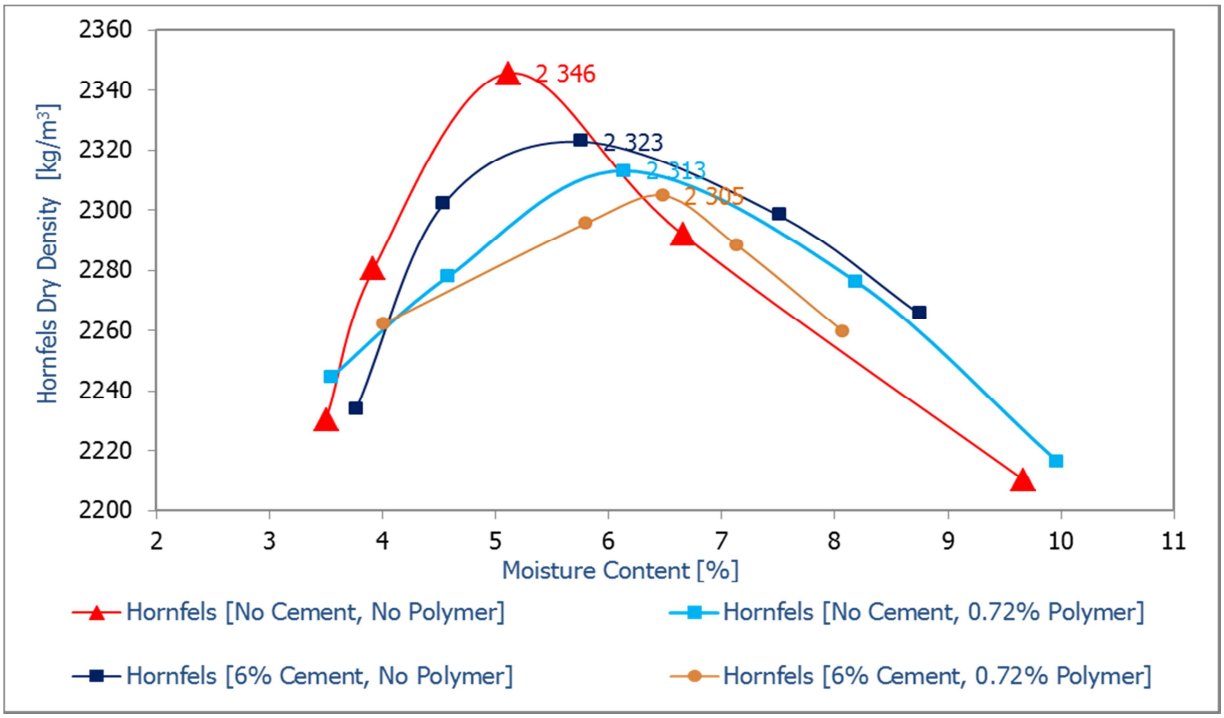

Figure: 4-6 Hornfels Dry Density versus Moisture Content [with and without Polymer]

From the compaction experimentation, the following interpretations are made:

a) The reference mix type [without cement and polymer] exhibits the highest overall MDD and the least OMC. The hornfels mix with 6.0% cement content shows an increase in moisture content but a reduction in the dry density. This observation is attributed to the effect of cement fines on material density. Cement fines increase the moisture demand as well as alter the gradation of the material. Fine particles present a large surface area. Adding cement to material also increases the water required for the hydration process.
b) By applying, the polymer to the natural material i.e. without cement shows a reduction in dry density from its reference mix. The resultant dry density is lower than that obtained by the stabilised mix with no polymer. This provides insight into the effectiveness of the polymer with cement than natural materials. The mix type stabilised with 6.0% cement content and polymer registers the least MDD but highest overall OMC. This suggests that the cement fines and nano-particles along with the polymer and cement interactions influence the resultant dry density.

Compared to the effect of cement fines to the material, the nano-particles reduce the dry density and increase the optimum moisture content. The addition of cement and polymer to material register the lowest density because an increase in fines results. The cement fines and nano-particles alter the material gradation and thus, reduce its dry density but increase its optimum moisture content. The exclusion of cement from the hornfels mix indicates that the polymer works with cement and that, its solvent components increase the moisture thereby reducing the material density. The interaction of the polymer and material without cement is more of a physical than a chemical effect.

4.2.4 CT Scanning and Internal Material Morphology

The packing of aggregates does not only influence the dry density, but also the engineering properties, especially the mechanical strength of the stabilised materials. In order to study the particle size distribution, CT scanning on stabilised specimens was conducted. Figure 4-7

shows [as a representative] the CT-scans of hornfels [A] and ferricrete [B] respectively. Hornfels exhibits a uniform particle distribution compared to ferricrete. Hornfels shows a well-graded material characterised by an even distribution of fine, medium and coarse aggregate particles. Ferricrete exhibits a material type with mainly fine and medium particles but limited amount of coarse particles. The ferricrete scan typifies that the material contains more fines in its matrix than hornfels. Figure 4-8 displays the air voids in the hornfels mix type with 6% cement content.

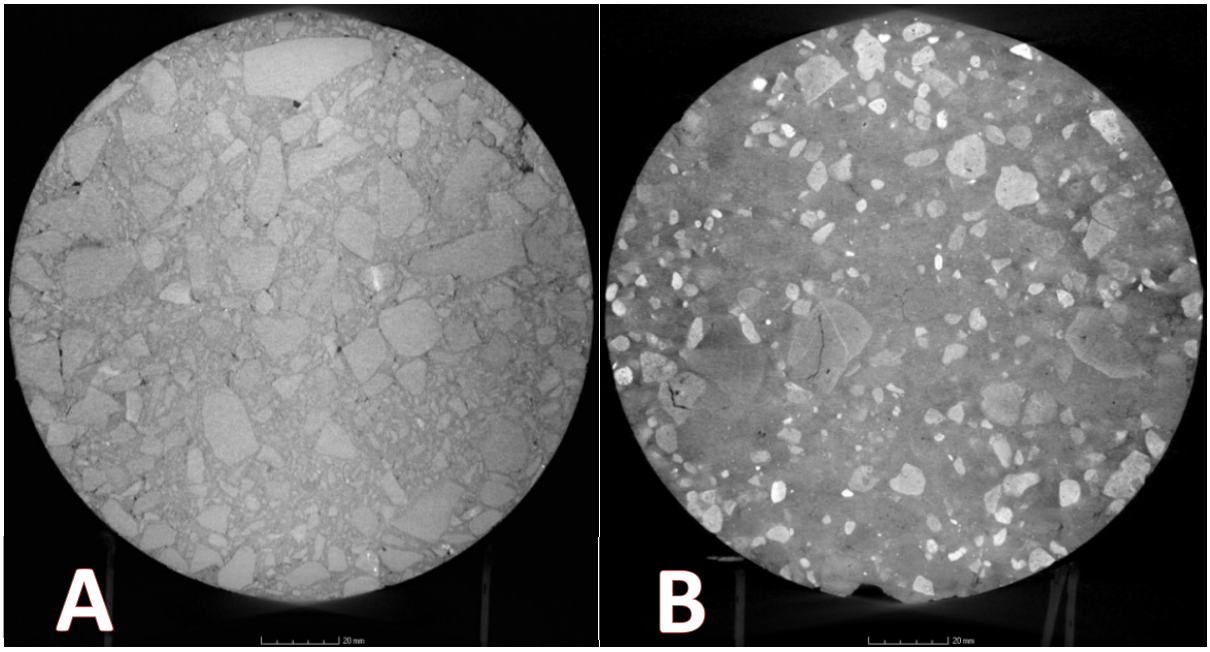

Figure: 4-7 Morphology of Hornfels [A] and Ferricrete [B] Cylindrical Specimen

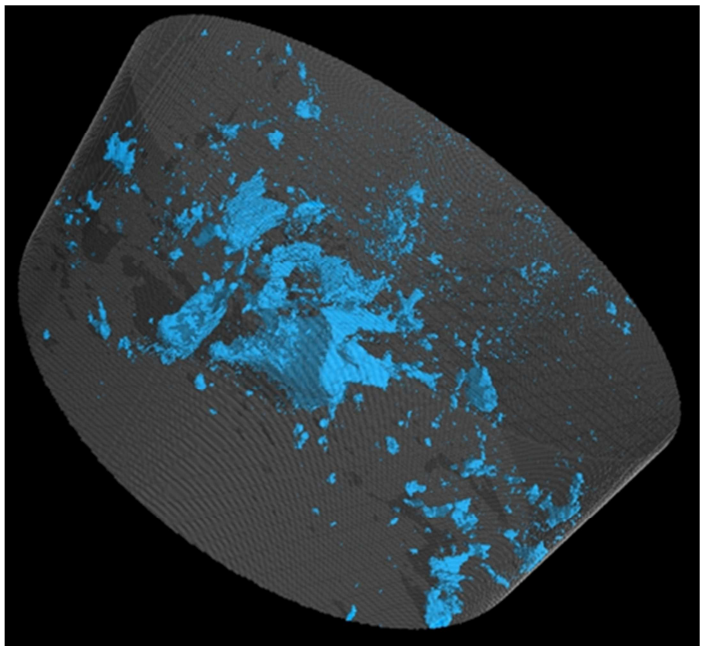

Figure: 4-8 Isometric View of Hornfels Cylindrical Specimen Displaying the Voids in the Mix

The material scans provide a better understanding regarding the distribution of particles, which relates to the effectiveness of cement and mechanical properties. The Unconfined Compressive Strength [UCS] test characterises the cement effectiveness [treatment of the materials]. By using the CT-scanning software, an estimation of the void content as shown in Figure 4-8 is undertaken. With 6.0% cement content in the mix, hornfels void content

ranged from 2.5% to almost 4.0%. Ferricrete void content ranged from 1.9% to nearly 3.6%. Both materials were compacted at 100% modified AASHTO using the vibratory hammer.

4.3 Compressive Strength Results and Compression Modulus

The Unconfined Compressive Strength [UCS] test is a commonly used method to evaluate the material compressive strength. The design of pavement layers requires a strength parameter such as the compressive strength as an input. The stabilisation of hornfels and ferricrete considered low cement contents in addition to 6% as the highest set level of stabilisation. Table 4a and 4b in the appendix to Chapter 4 lists the cement and moisture content, dry density and the resultant compressive strength values for hornfels and ferricrete without the polymer. Figures 4-9 and 4-10 illustrate the dry density and the resultant compressive strength properties of hornfels and ferricrete without the polymer, respectively.

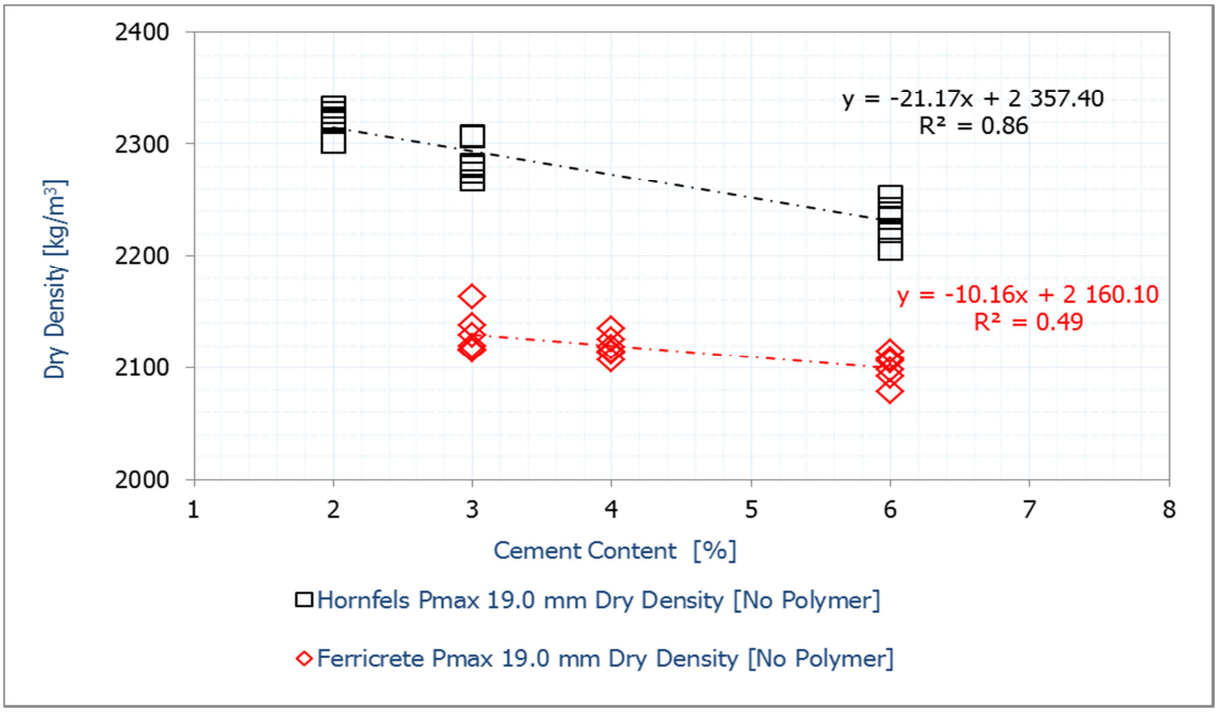

Figure: 4-9 Dry Densities of the Individual Compressive Strength Specimens [Ferricrete versus Hornfels]

The coefficient of determination [R^2 value] denotes the proportion of variability in the dry density data relative to the cement content in the mix. The reliability of the dry density data in terms of mix compaction relative to cement content is presented. Hornfels exhibited higher dry density values than ferricrete. The fines in the mix influence the moulding moisture and resultant dry density. Differences in material characteristics such as the level of weathering and plasticity also influence the moulding moisture and thus, dry density. The dry density of material is a function of its particle size distribution and moulding moisture content at a specific compactive effort. Therefore, the particle size distribution, moisture content and the applied compaction effort influence the resultant dry density and ultimately, the compressive strength.

A material's plasticity is usually associated with a high fine content and variant mineralogical characteristic that include clay minerals. Plasticity is a result of deleterious minerals owing to weathering. This involves the material particle breakdown and the formation of fines. Fines contribute to the increase in material plasticity. This is dependent on the level of weathering and material type. Excess of fines in the mix, increase the difficulty of mixing and, thus lead

to a high demand for cement. This suggests that extremely weathered materials with a high PI value and fine content are most likely to provide a low compressive strength at moderate and even, high cement contents. This is because excessive fines in the mix influence the effectiveness of cement.

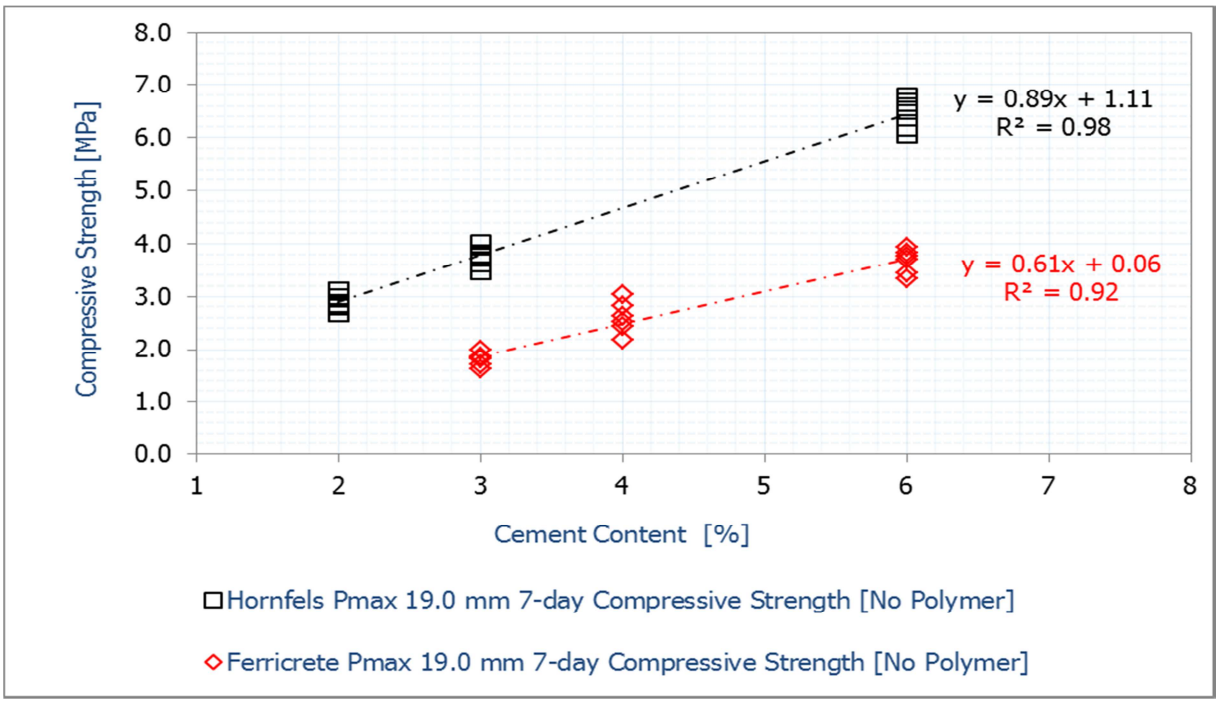

Figure: 4-10 7-Day Compressive Strength Results [Ferricrete versus Hornfels]

Ferricrete mix with 2% cement content could hardly provide the minimum UCS strength of 0.75 MPa. Ferricrete mix stabilised using 3% cement content provided an average UCS value of 1.81 MPa. This was still significantly lower than the UCS value obtained by the hornfels with 2% cement content. Ferricrete with 6% cement content registers an average UCS value of 3.66 MPa. This is comparable to hornfels mix stabilised using 3% cement content.

Linear regression equations of ferricrete and hornfels used to estimate the dry density [DD] and 7-day compressive strength [UCS] for cement content up to 6% are denoted by Equations 4-1 to 4-4.

$DD = 2357.40 - 21.17(CC)$ [Hornfels: $R^2 = 0.86$] Equation 4-1

$UCS = 1.11 + 0.89(CC)$ [Hornfels: $R^2 = 0.98$] Equation 4-2

Where: CC – cement content in the mix [%] and DD – dry density [kg/m^3]
UCS – compressive strength using the UCS test [MPa]

The regression models offer insights regarding the influence of cement content, dry density and compressive strength. Due to the material variability in terms of particle distribution and level of weathering, these models remain estimations. Figure 4-11 shows a plot of the 7-day compressive strength and the achievable dry density of ferricrete and hornfels stabilised at different cement contents. The regression models obtained by plotting the compressive strength against the dry density provide insight regarding the achievable density relative to the resultant strength properties. However, cognisance of factors such as cement and moisture contents, curing conditions, play a significant role in influencing the trends observed. The compressive-density relationship only shows that low dry density provides a higher compressive strength; this is a partial interpretation. The reduction in dry density and an increase in compressive strength properties provide insights into the effect of cement

content and the hydration process. Even though, the application of cement to materials leads to a reduction in the dry density, an increase in their compressive strength results. This suggests that cement stabilisation, which provides an improvement of material strength also result in negative effects such as a reduction in dry density.

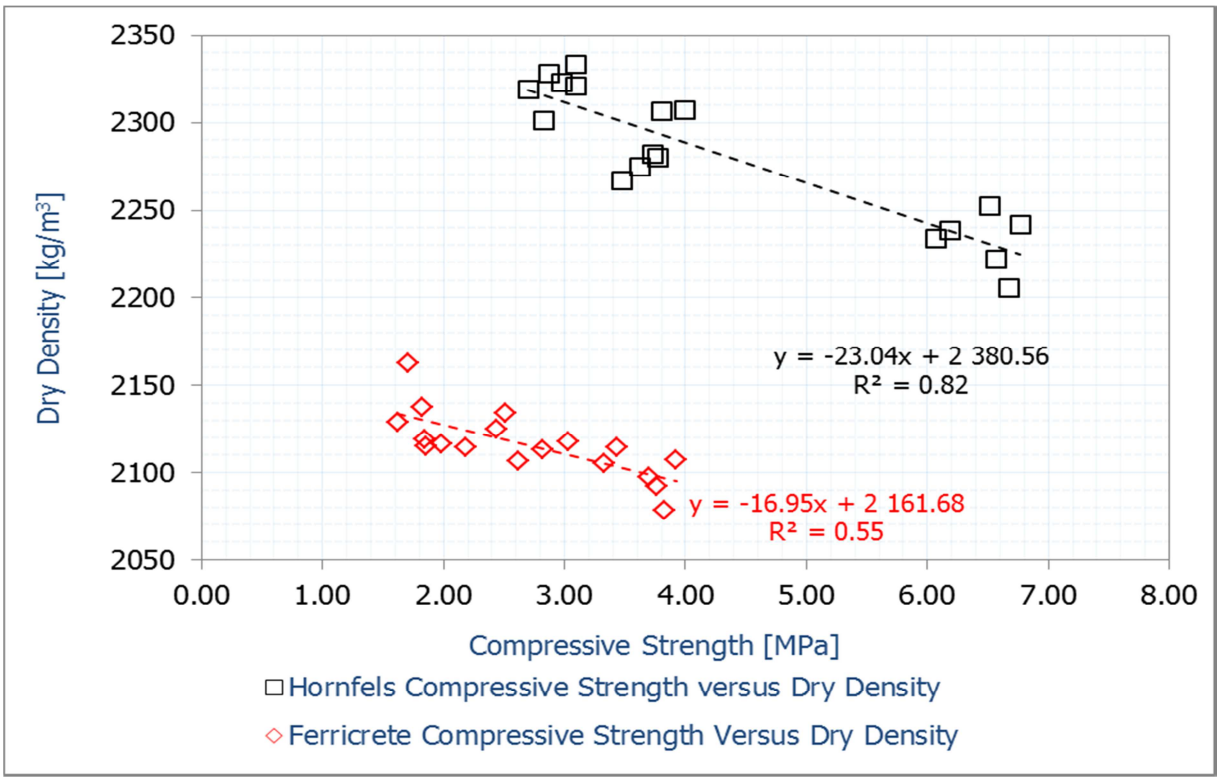

Figure: 4-11 Dry Density versus the 7-day Compressive Strength [Ferricrete and Hornfels]

The stress-strain behaviour of any pavement material type is usually expressed in terms of elastic modulus. For cement-stabilised materials, the selection of a suitable modulus value for design purposes is complex, partly because of the difficulty in testing and a lack of a standard test method. Different test methods provide dissimilar modulus values for the same material and/or mix type. Various procedural measures provide different relationships. As a result, the modulus value is estimated using the unconfined compressive strength test data.

By assessing the stress-strain curves of the various mix types computation of the compression modulus follows two procedural measures as shown in Figure 4-12. As a background, stress relates to applied force over an area and strain is the response of the material to stress. The modulus of the material is defined as a ratio of the stress to strain and it measures the stiffness properties of the material. It is essential to know the strength and stiffness properties of the stabilised layer. This is because the two parameters provide a good indication of the layer's response to traffic loads. A stabilised layer might be very stiff but not significantly strong to withstand heavy traffic.

Secant modulus [E_{se}] is taken at two particular points on the stress-strain curve [i.e. corrected curves]. This suggests that the secant modulus is for a particular stress limit. The tangent modulus [E_t] is taken at a specific point along the stress-strain curve before failure. The initial tangent modulus is taken at the initial portion of the stress-strain curve. In this research, the initial tangent modulus is not considered. This is because the effects emanating from the top wedge and the specimen influence the initial portion of the curve. Figure 4-13 shows typical force-displacement curves [i.e. corrected curves]. The linear regions, particularly with 4.0% and 6.0% cement content in the mix are not fully defined on the force-displacement curve, which caused variability amongst the mix types. With good

understanding of the concepts related to secant and tangent modulus and their determination. In this analysis, secant modulus is taken origin to the peak or maximum force. The tangent modulus varied depending on the mix type and the resultant curve; Figure 4-13 illustrates as example.

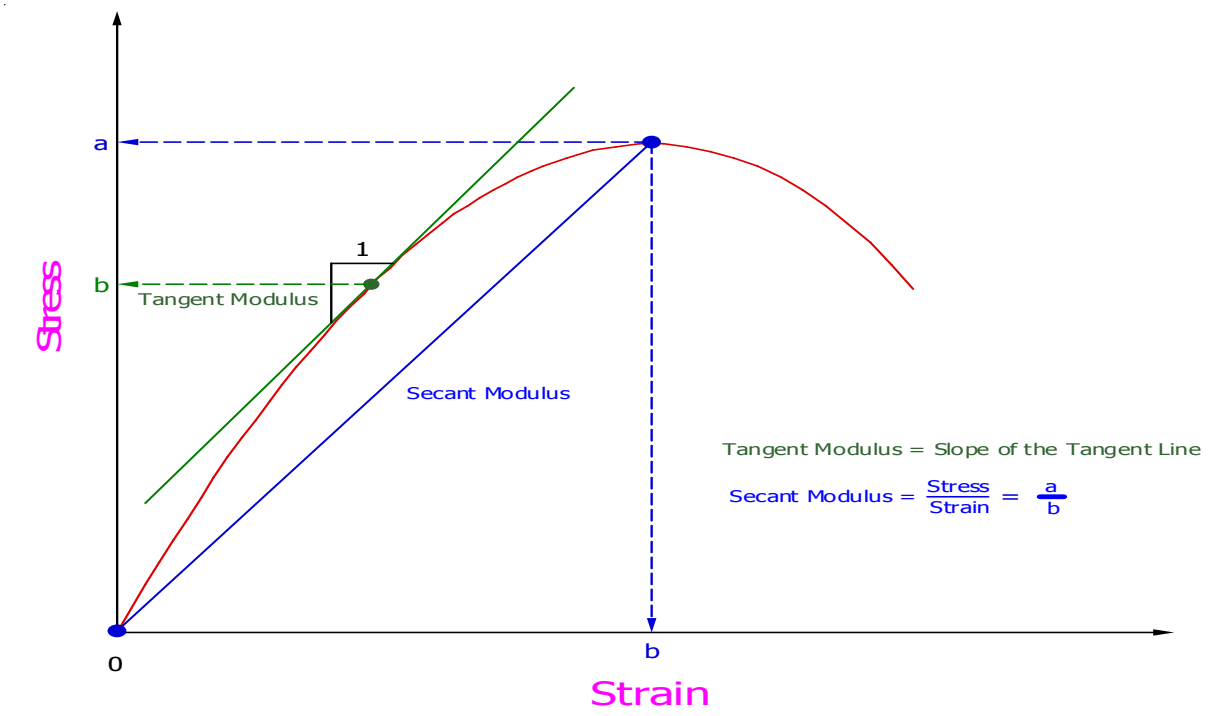

Figure 4-12 Defining the Compression Modulus [Secant Modulus and Tangent Modulus]

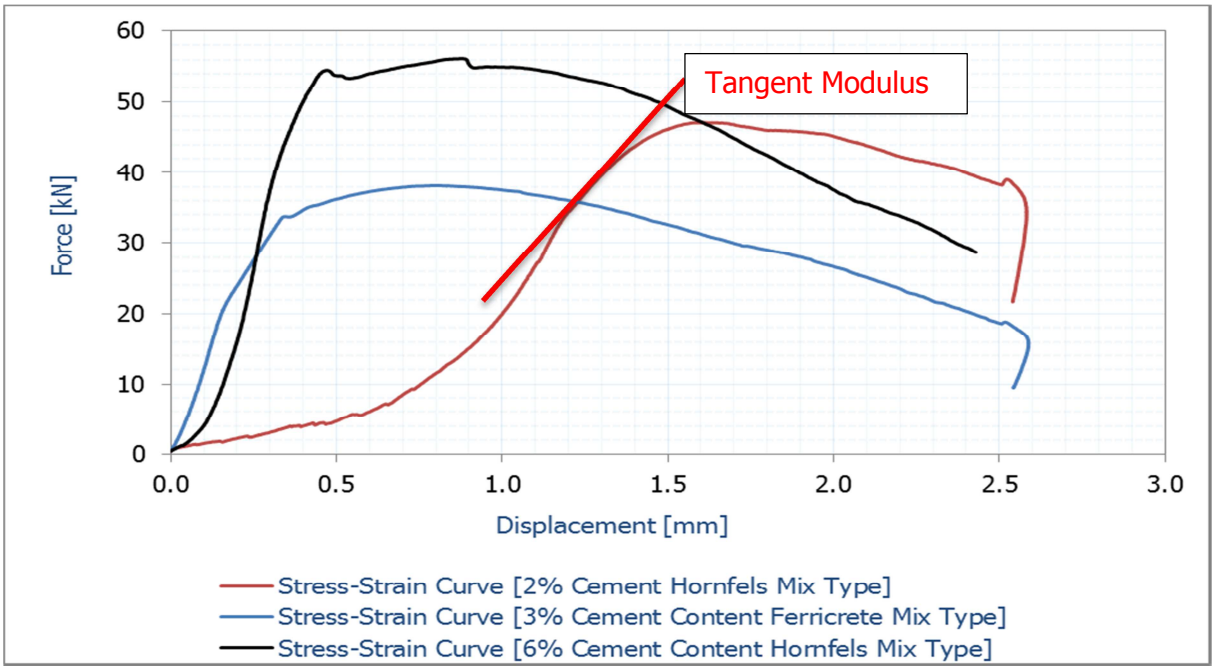

Figure 4-13 Typical Force-Displacement Curves

Figure 4-14 illustrates the UCS test specifications, mainly the applied loading rate and specimen height, the effect of the compression force on the material matrix. The rate of loading influences the behavioural trend of the force-displacement curve. A low loading rate influences the rate of rupture for a given displacement. Figures 4-15 to 4-16 show the secant and tangent modulus of ferricrete and hornfels respectively. The variability of the data points

exhibited by the mix types with 6.0% cement content indicate the influence of high cement dosages and the behavioural response of the stabilised material to compression forces. This also suggests stabilising a material with high cement contents results in an increase in stiffness [brittleness]; see Figure 4-13. Cognisance of the influence of voids in the mix, particle size distribution and material characteristics is noted; see Figure 4-14. For same material and mix type, the tangent modulus was lower than the secant modulus. This accounts for the procedural differences in computing the two-compression modulus as shown in Figure 4-12.

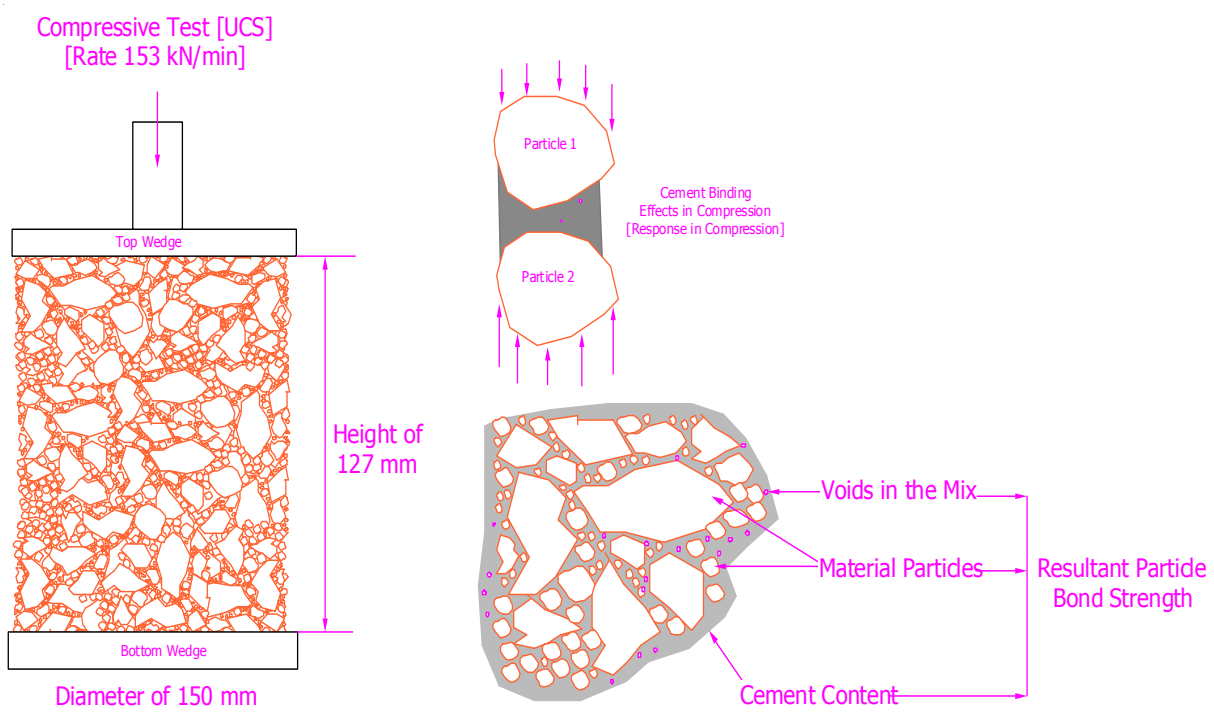

Figure 4-14 UCS Test Specifications, Particles in Compression and Components in the Mix

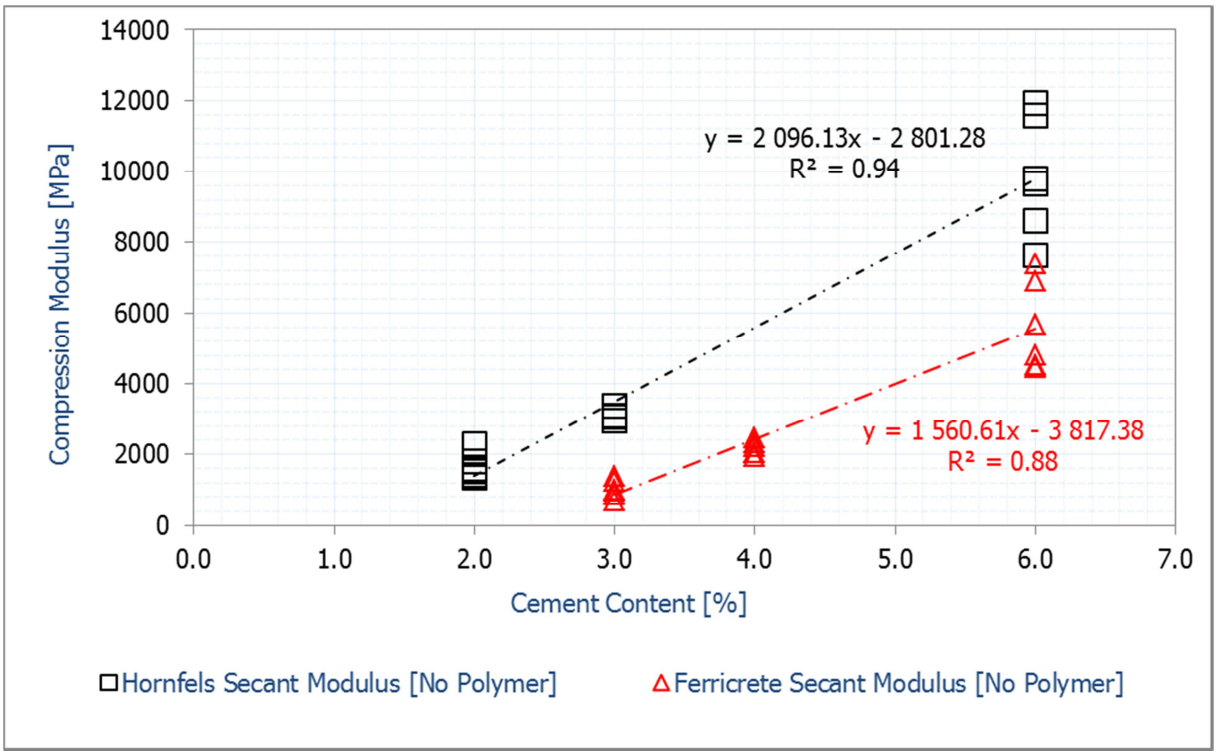

Figure 4-15 Compression Moduli [Secant Modulus, E_{se}] of Ferricrete and Hornfels

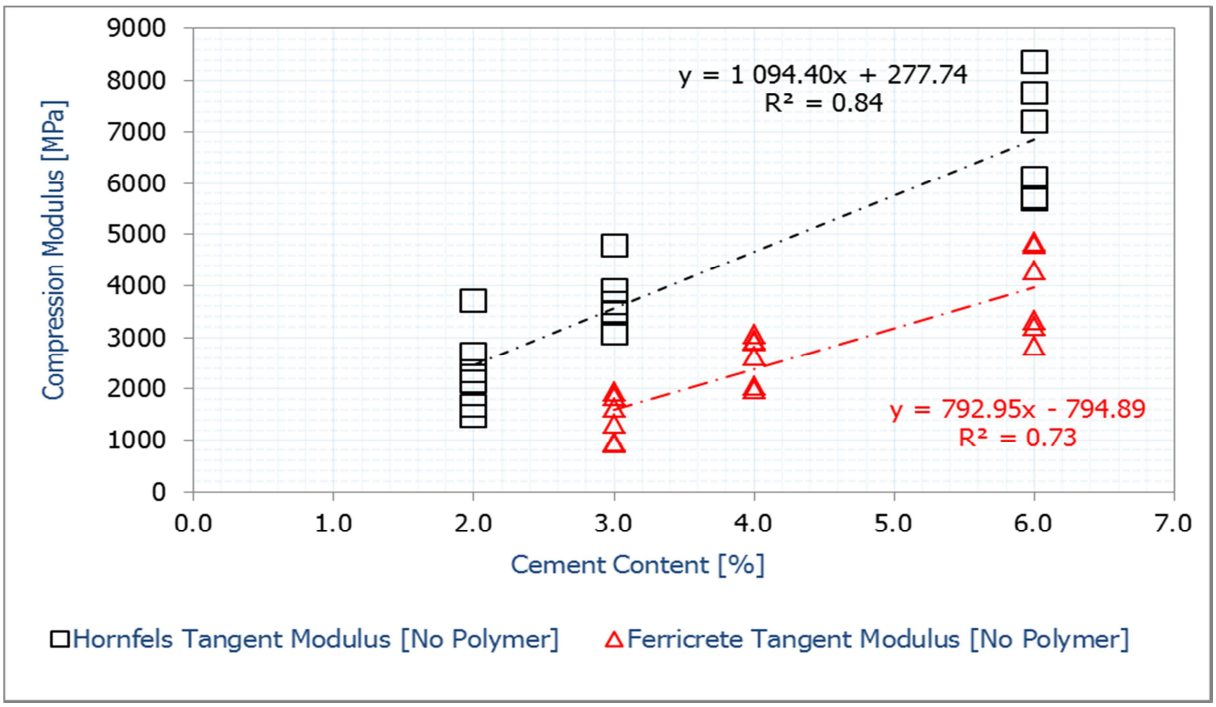

Figure 4-16 Tangent Moduli [E_t] of Ferricrete and Hornfels

Figure 4-17a compares the tangent modulus [Y-axis] to secant modulus [X-axis]; the inverse of this plot would provide a negative Y intercept i.e. in the form of y = mx + b as the linear equation. The gradients of the line [ferricrete and hornfels slope] are comparable despite the differences between the materials. By setting the intercepts to zero, Figure 4-17b is obtained; the secant modulus [E_{se}] is not equal to the tangent modulus [E_t]. At low stiffness [stabilised ferricrete using low cement contents], the secant modulus is comparable to the tangent modulus. However, this does not apply to hornfels; the secant modulus is higher than the tangent modulus. This criteria exhibited by ferricrete and hornfels show that behavioural properties are predominately influenced by the quality and type of the material.

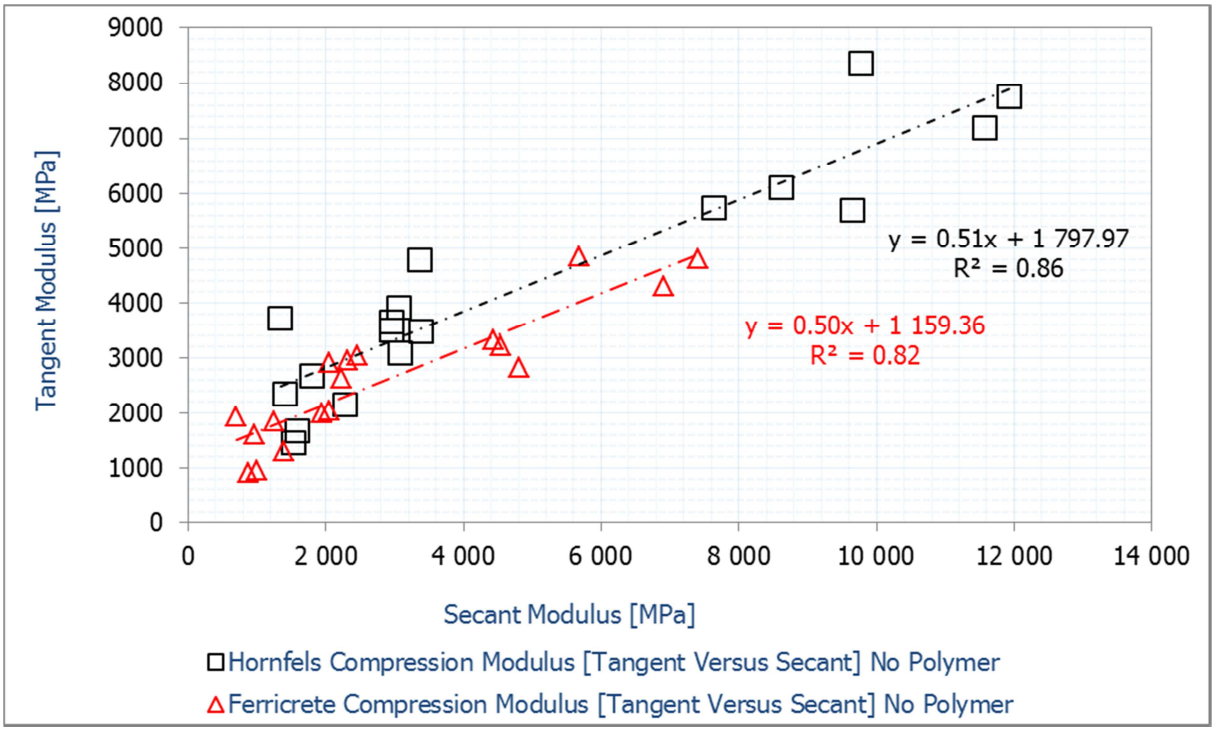

Figure 4-17a Tangent Modulus [E_t] versus Secant Modulus [E_{se}] of Ferricrete and Hornfels

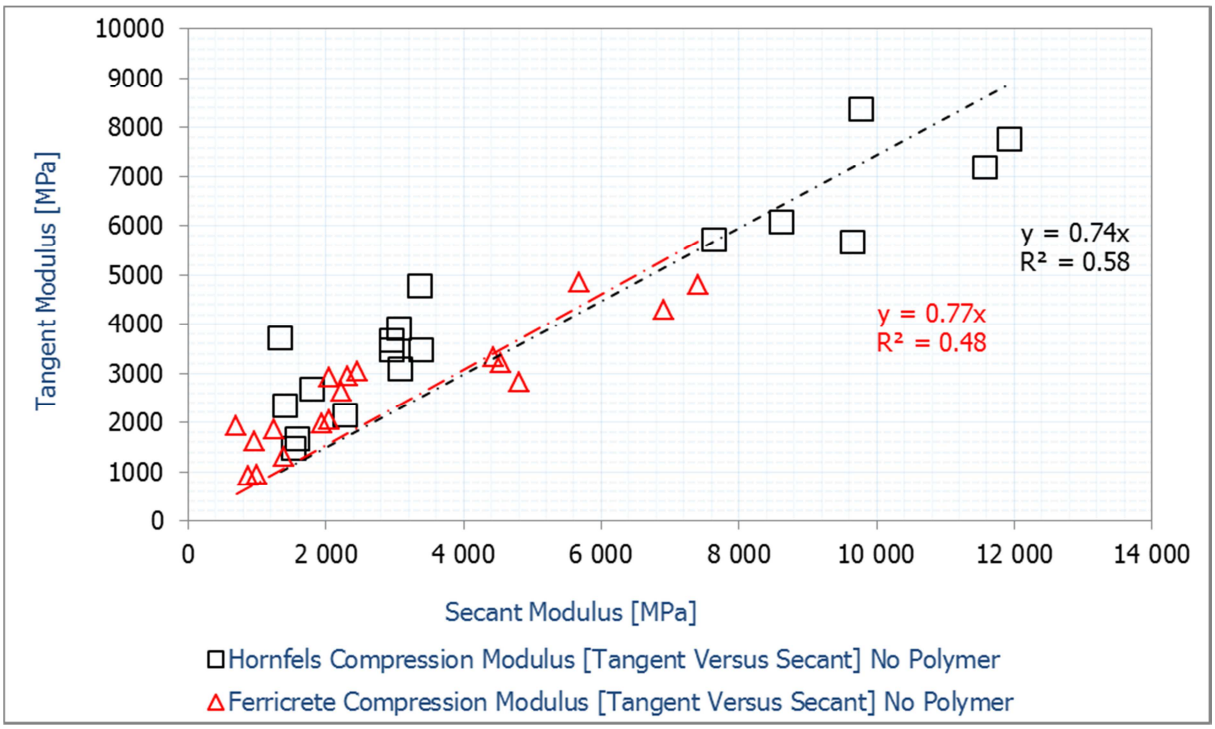

Figure 4-17b Tangent Modulus [E_t] versus Secant Modulus [E_{se}] of Ferricrete and Hornfels [Intercept = 0]

Figure 4-17c illustrates the relationship of compression modulus [secant modulus] to the compressive strength of the material. The secant modulus is about 1200 times the compressive strength of the materials. The material property relationships provide insight regarding the suitability of the material for use in the pavement structure. For a better understanding, each of the figures must be interpreted with the cognisance of the factors of influence as previously stated.

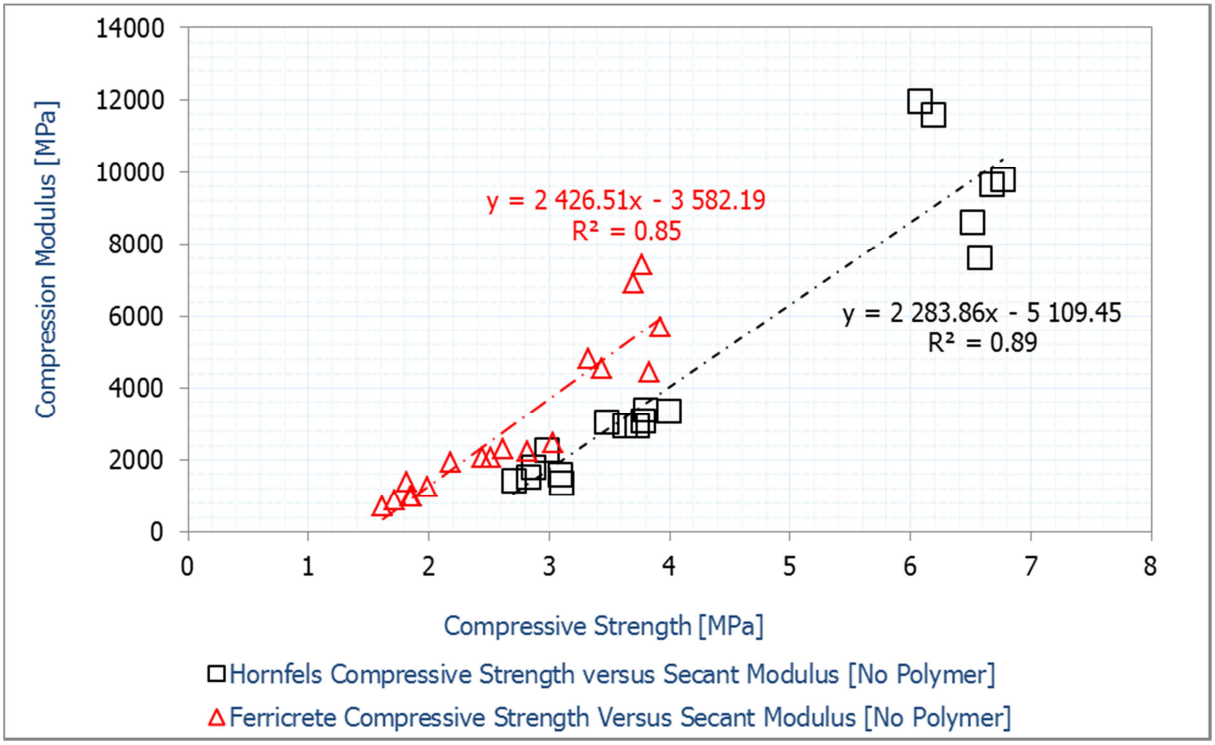

Figure 4-17c 7-Day Compressive Strength versus Compression Modulus [E_{se}] of Ferricrete and Hornfels

4.4 Tensile Strength Results and Strength Relationships

An evaluation of the tensile strength properties of cement-stabilised materials is essential to assess since stabilised sub-base and base layers endure tensile stresses and strains under wheel loading. In the appendix, the cement and moisture content, dry density and the resultant tensile strength values for hornfels and ferricrete without the polymer are provided. Figures 4-18 and 4-19 illustrate the dry density and the resultant tensile strength results. A linear regression relationship typifies the effect of cement content to the tensile strength as well as the dry density. Hornfels exhibits higher tensile strength properties and dry density than ferricrete. This is attributed to the differences between the material types that include the particle size distribution and the level of weathering. Cement alters the plasticity, volume change, elastic properties as well as strength of natural materials. However, the degree of alteration is dependent on the quality and type of the materials. In Figures 4-18 and 4-19, differences due to cement effectiveness with ferricrete and hornfels are illustrated.

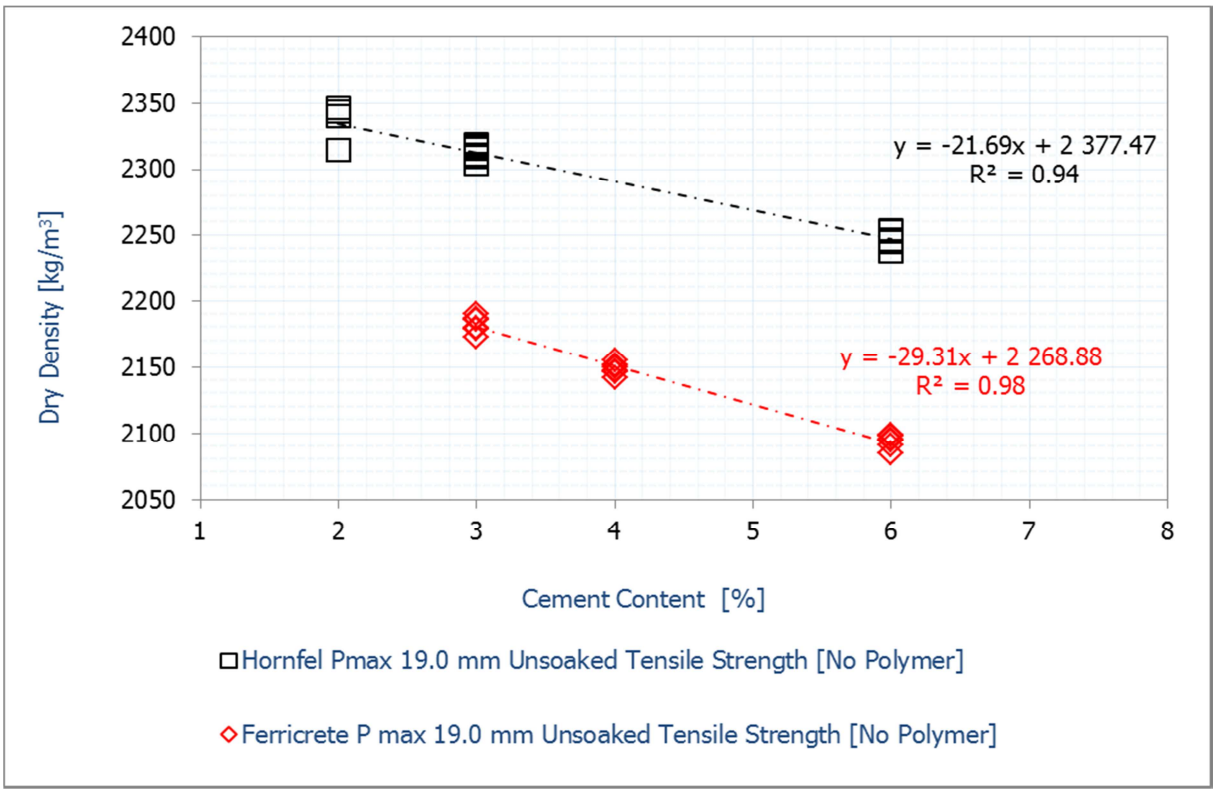

Figure: 4-18 Dry Densities of the 7-Day Tensile Strength Specimens [Ferricrete versus Hornfels]

Figure 4-20 presents the relationship between the dry density and tensile strength. The relationship of dry density to the strength of stabilised materials provides insight into the influence of cement in altering the physical and chemical properties of the natural materials. The differences between ferricrete and hornfels that include the moulding moisture and gradation contribute to the resultant strength properties and dry density. The physical-chemical reactions between the materials, cement and water dictate the resultant quality of stabilised material at a given compactive effort. Hornfels, which exhibits as a well-graded coarse type of material shows higher dry density and strength than ferricrete. Generally, the type of the natural material influences the quality and strength properties of the cement-stabilised materials. Equation 4-3 defines the tensile strength of hornfels without the polymer; reference to Figures 4-18 and 4-20.

$$\mathrm{ITS} = 152.9(\mathrm{CC}) + 278.9 \quad [\text{Hornfels } R^2 = 0.85] \qquad \text{Equation 4-3}$$

Figure 4-21 illustrates the relationship between compressive strength and tensile strength properties of ferricrete and hornfels stabilised at different cement contents. Insights into the compressive strength relative to the tensile strength properties are provided. The slope of the trend lines indicates the behavioural criteria and quality of ferricrete and hornfels following cement stabilisation. However, cognisance of the testing mode and loading rate as well as specimen dimensions, must be noted.

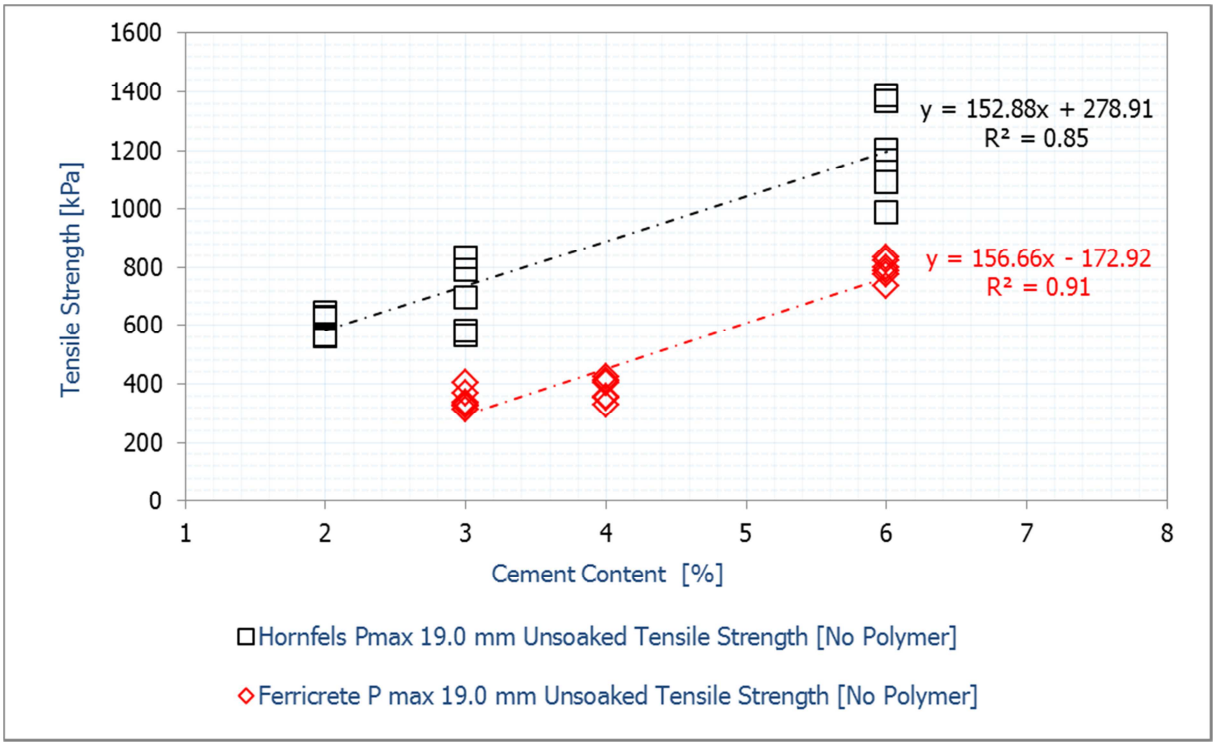

Figure: 4-19 7-Day Tensile Strength Results [Ferricrete versus Hornfels]

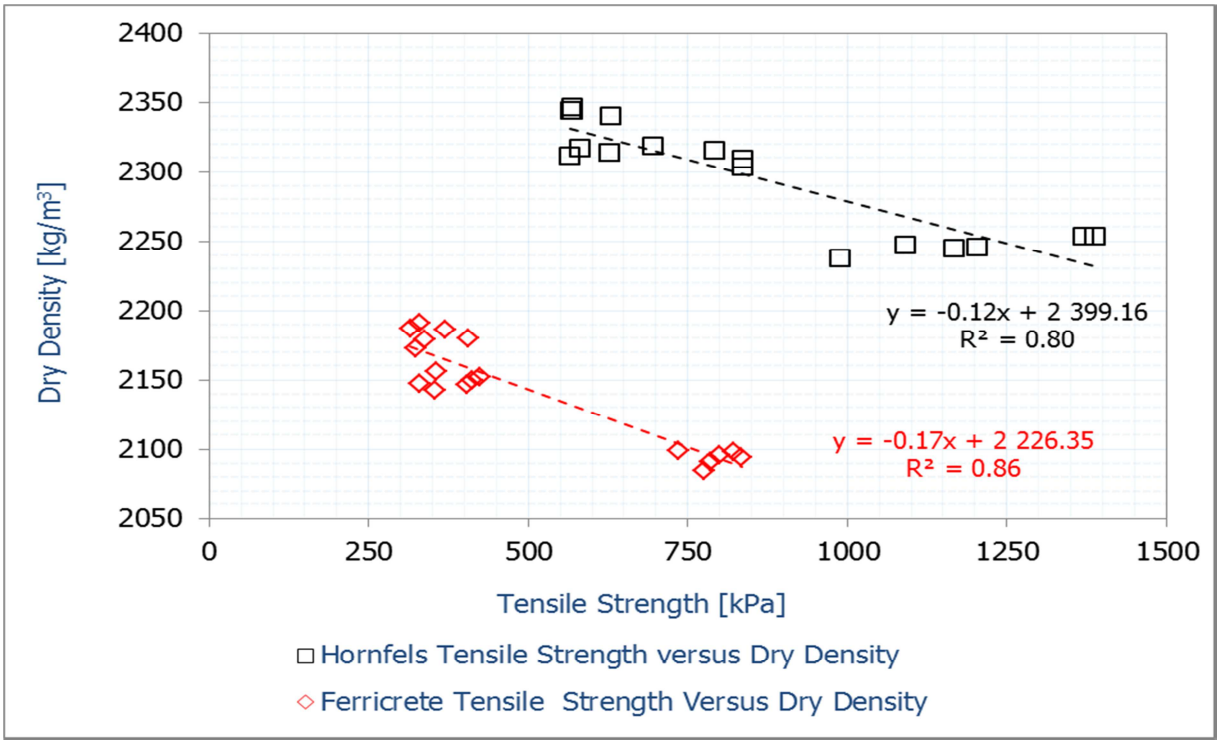

Figure: 4-20 Dry Density versus 7-Day Tensile Strength Results [Ferricrete versus Hornfels]

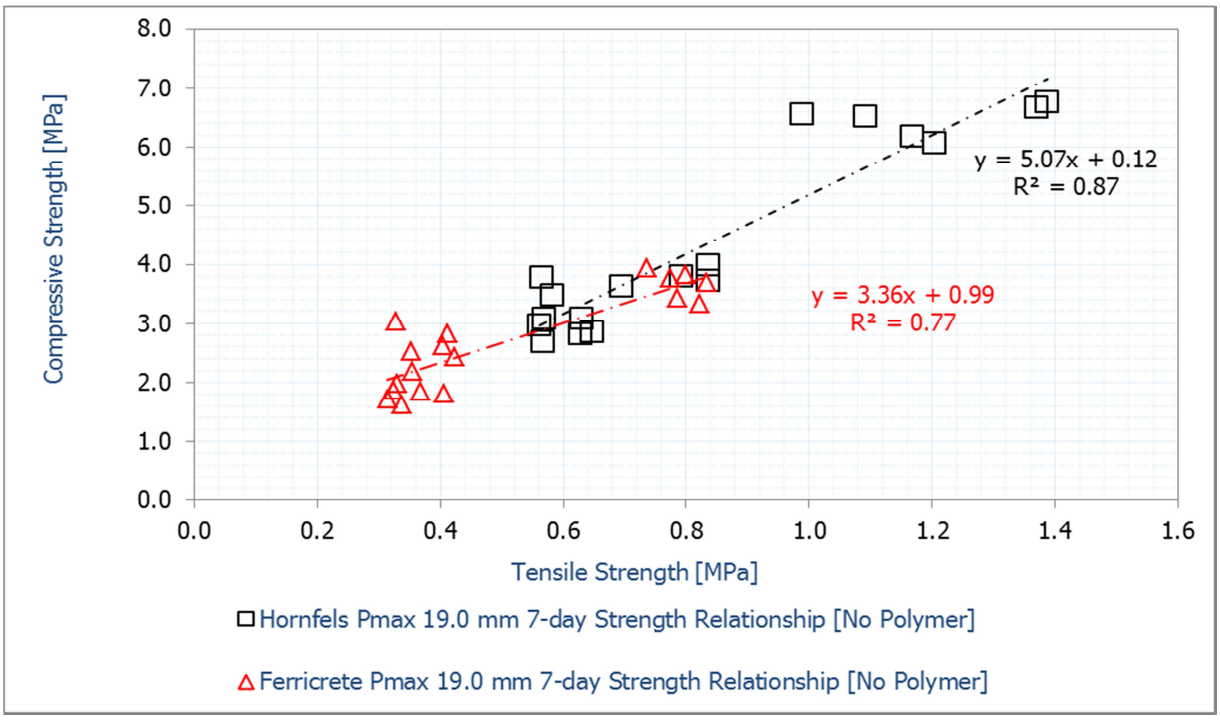

Figure: 4-21a 7-Day Compressive Strength versus 7-Day Tensile Strength Results [Ferricrete versus Hornfels]

The commonly used strength parameters for the design of the stabilised layers include the unconfined compressive strength and indirect tensile strength. The linear regression equations in Figure 4-21b [intercept = zero] suggests that, the unconfined compressive strength of hornfels is about 5 times the indirect tensile strength. Table 4-3 shows that the average indirect tensile strength and unconfined compressive strength. The tensile strength of hornfels is about 20% of the compressive strength.

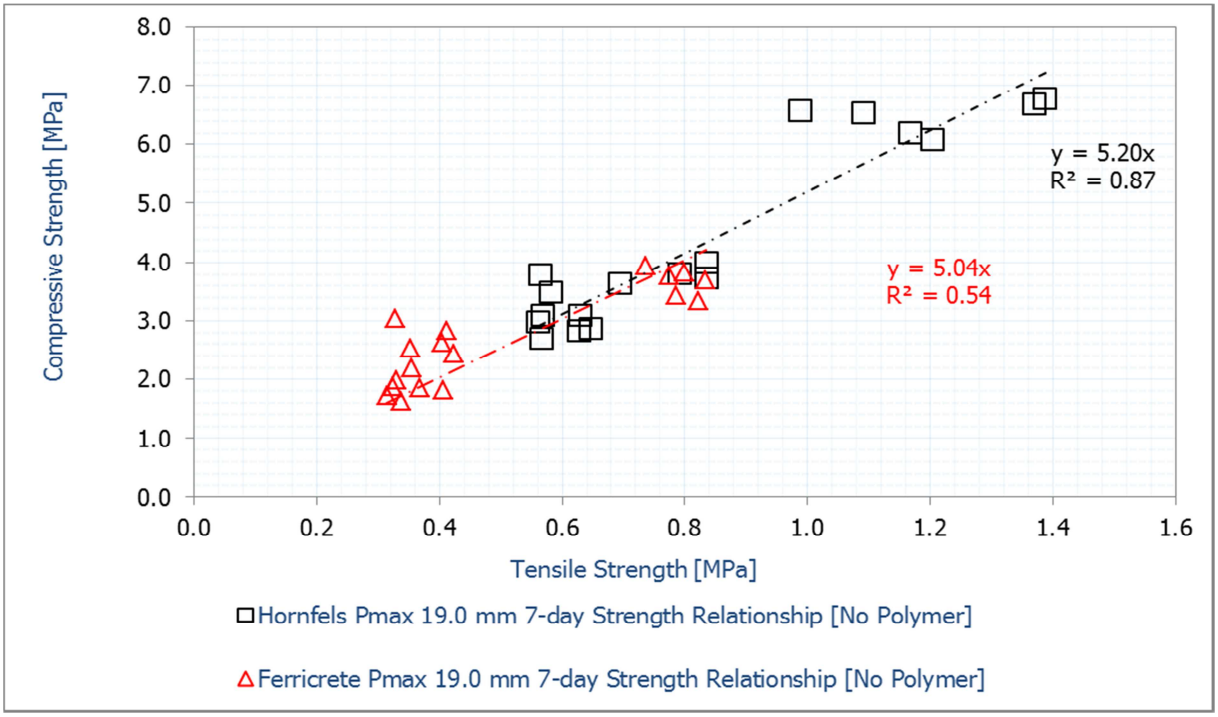

Figure: 4-21b 7-Day Compressive Strength versus 7-Day Tensile Strength Results [Ferricrete versus Hornfels]

Table 4-3 Compressive Strength and Tensile Strength Relationship

7- Day Strength Hornfels Cement Content (x) [%]	No Polymer Tensile Strength [MPa]	Compressive Strength [MPa]	(ITS/UCS) x 100 [%]
2	0.59	2.89	20
3	0.74	3.78	20
6	1.20	6.45	19
7- Day Strength Ferricrete Cement Content (x) [%]	No Polymer Tensile Strength [MPa]	Compressive Strength [MPa]	(ITS/UCS) x 100 [%]
3	0.30	1.89	16
4	0.45	2.50	18
6	0.77	3.75	20
Material Type	Regression Equation	Coefficient [R^2]	Relationship
Hornfels Mix Type	y = 5.07x +0.12	R^2 = 0.87	$UCS_{hornfels}$ = 5.07[ITS] +0.12
Ferricrete Mix Type	y = 3.36x +0.99	R^2 = 0.77	$UCS_{ferricrete}$ = 3.36 [ITS]+0.99
ITS - Indirect Tensile Strength in MPa and UCS - Unconfined Compressive Strength in MPa			

Ferricrete mix types show a low R^2 value of 0.77 [Figure 4-21a] and 0.54 [Figure 4-21b]; this denotes the reliability of the data points. For hornfels materials, the following strength relationship is proposed; see Equation 4-4.

$$ITS_{hornfels} = 0.2\ UCS_{hornfels} \qquad \text{Equation 4-4}$$

Characteristically, the strength of the cement-stabilised materials increases following the addition of cement to the natural material. However, the rate of strength-gain is dependent on the quality and type of the natural materials, moulding moisture and other factors.

4.5 Estimation of Material Durability Criteria [Wet-Dry Brush Test]

Durability is an essential material property required to ascertain the suitability of materials for use in the pavement structure. The wet-dry durability test protocol as specified in Method A19 TMH1 [1986] was followed. During the preparation of specimens for the wet-dry brushing test, the control the specimen's height was a priority. Figures 4-22 and 4-23 show the total mass loss of the three evaluated specimens per mix variable and material type. Hornfels and ferricrete exhibited a reduction in mass loss following an increase in cement content.

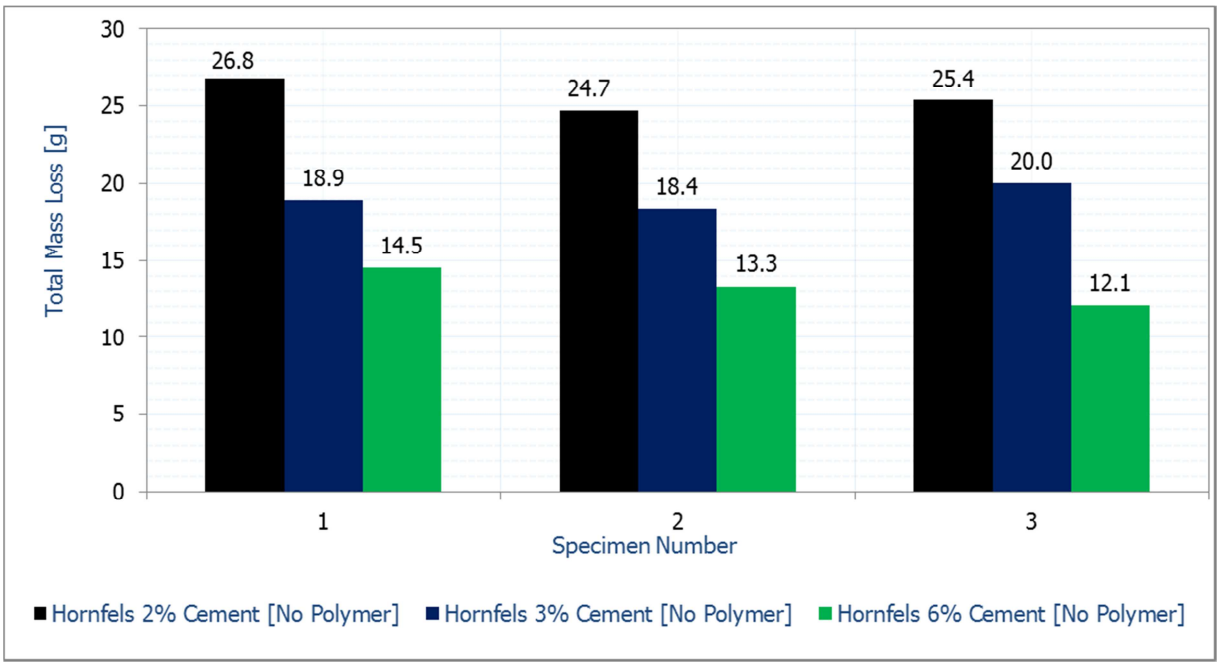

Figure: 4-22 Hornfels Results [Total Mass Loss per Specimen per Mix Variable]

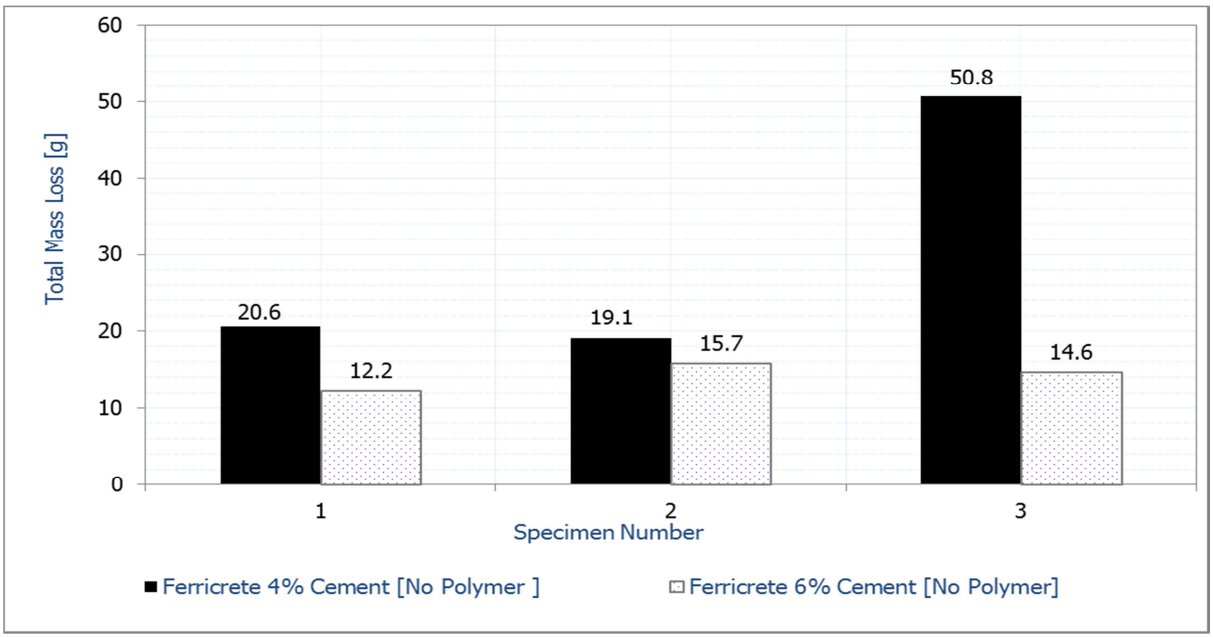

Figure: 4-23 Ferricrete Results [Total Mass Loss per Specimen per Mix Variable]

The ferricrete mix with 3.0% cement content did not survive the completion of 12 cycles of wetting and drying with brushing as stipulated in the protocol. After nearly 7 cycles, the specimens became too fragile to clamp in the wet-dry machine. One specimen crumbled while being transferred from the water-bath while the other two disintegrated while being soaked. From the performance of the ferricrete mix type with 3.0% cement content, the following conclusions are drawn:

a) the damage is due to moisture ingress and poor particle bonding because of the amount of fines [low cement effectiveness]
b) a higher cement content than 3.0% is required
c) the amount of fines content of ferricrete influences the capillary suction characteristics resulting in increased water ingress particularly at low cement contents

Ferricrete mix types with 4% and 6% cement contents survived the 12 cycles of wetting and drying conditions with brushing. This suggests that applying high cement contents results in improved particle bond strength. An increase in bond strength leads to enhanced material strength. However, the compaction of the specimen, which is characterised by its resultant density, has a significant influence the particle bond strength and ultimately, material loss. A variation in the specimen density results in a corresponding difference in the material loss. This provides insight regarding the significance of material density and bond strength on its durability criterion.

ASTMD 560-98 requirements stipulate standards for the soil-cement mixture [in this case, ferricrete]. In order to satisfy the durability requirements, the soil-cement mixtures must tolerate the 12 wetting-drying cycles and the abrasion must not exceed 14% weight loss [referred to as cement loss]. Figure 4-24 illustrates the specimen's mass loss as a percentage. The wet-dry test trends, illustrate a decrease in the loss of material following the addition of more cement. The trends characterise improved bond strength due to increased cement usage. An increase in particle bond strength results in reduced material loss following the ingress of moisture and abrasion. In terms of the material type, ferricrete exemplifies a higher material loss due to its low particle bond strength compared to hornfels. Hornfels mixes with 2% and 3% cement contents exhibited lower bond strength compared to that with 6% cement content. This provides insight regarding cement effectiveness, cement and material compatibility. The resultant particle bond-strength and degree of stabilisation relative to the resultant material properties are realised.

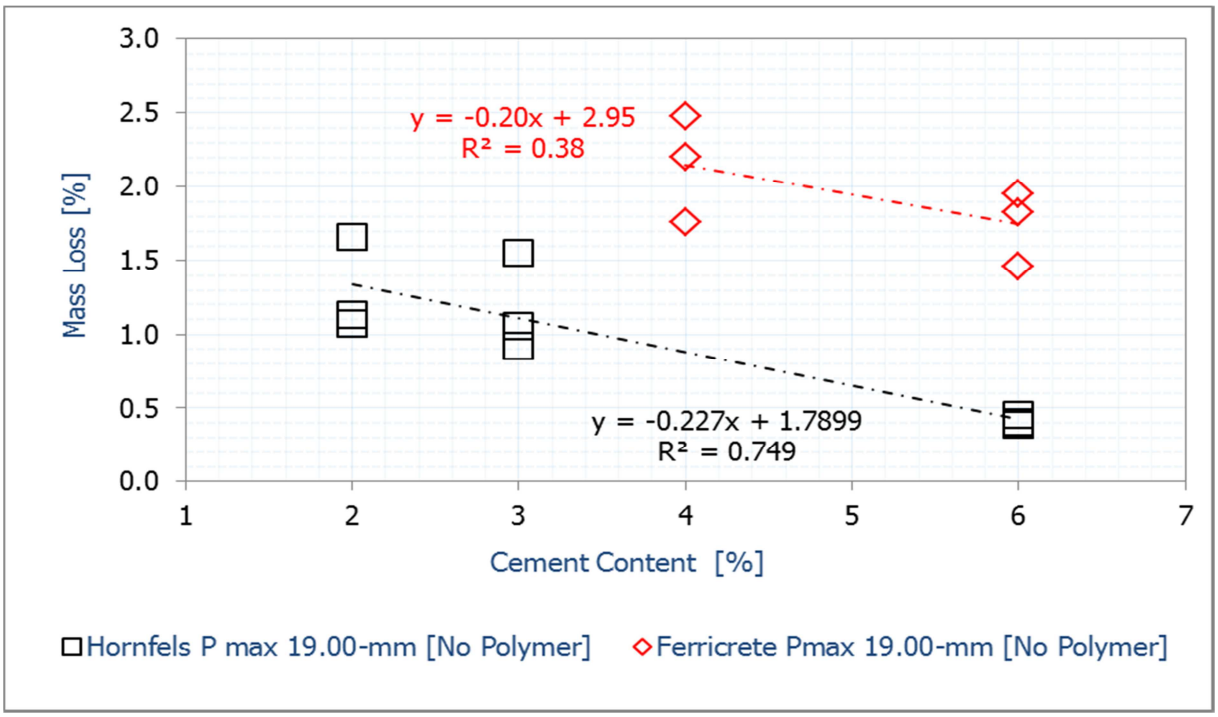

Figure: 4-24 Ferricrete versus Hornfels Wet-Dry Abrasion Results

4.6 Effect of Polymer on Material Properties

This section assesses the effect of the polymer on the material strength properties and probable durability. The polymer is a cement additive. This suggests that the polymer is dependent on the cement content. The following present the cement content and the resultant polymer application:

a) 2.0% cement content [0.24% polymer content]
b) 3.0% cement content [0.36% polymer content]
c) 4.0% cement content [0.48% polymer content]
d) 6.0% cement content [0.72% polymer content]

4.6.1 Effect of the Polymer on the Dry Density [Vibratory Hammer]

Figures 4-25 and 4-26 illustrate the effect of the polymer on hornfels and ferricrete dry density respectively. For both ferricrete and hornfels, the application of the polymer resulted in a reduction in dry density at increasing cement contents. Hornfels mix types with 2.0% and 3.0% cement contents without the polymer showed a slightly higher dry density than the mix types with the polymer. Hornfels mix stabilised at 6% cement without the polymer [i.e. the reference mix type] exhibited higher dry density ranges than the mix type with the polymer.

All ferricrete mixes with polymer exhibited a lower general dry density criterion than their reference mix types. This indicates that the polymer reduces the achievable dry density of stabilised materials. The reduction of material dry density is due to the effect of nano-particles and solvents including water contained in the polymer rather than the interaction of polymer and material and/or cement. The application of the polymer to stabilised materials required a reduction in mix water. An approximate 1% reduction of mix-water is realised as a means to satisfy the required moisture variations. Variations in moisture influence the material density, particularly bond strength.

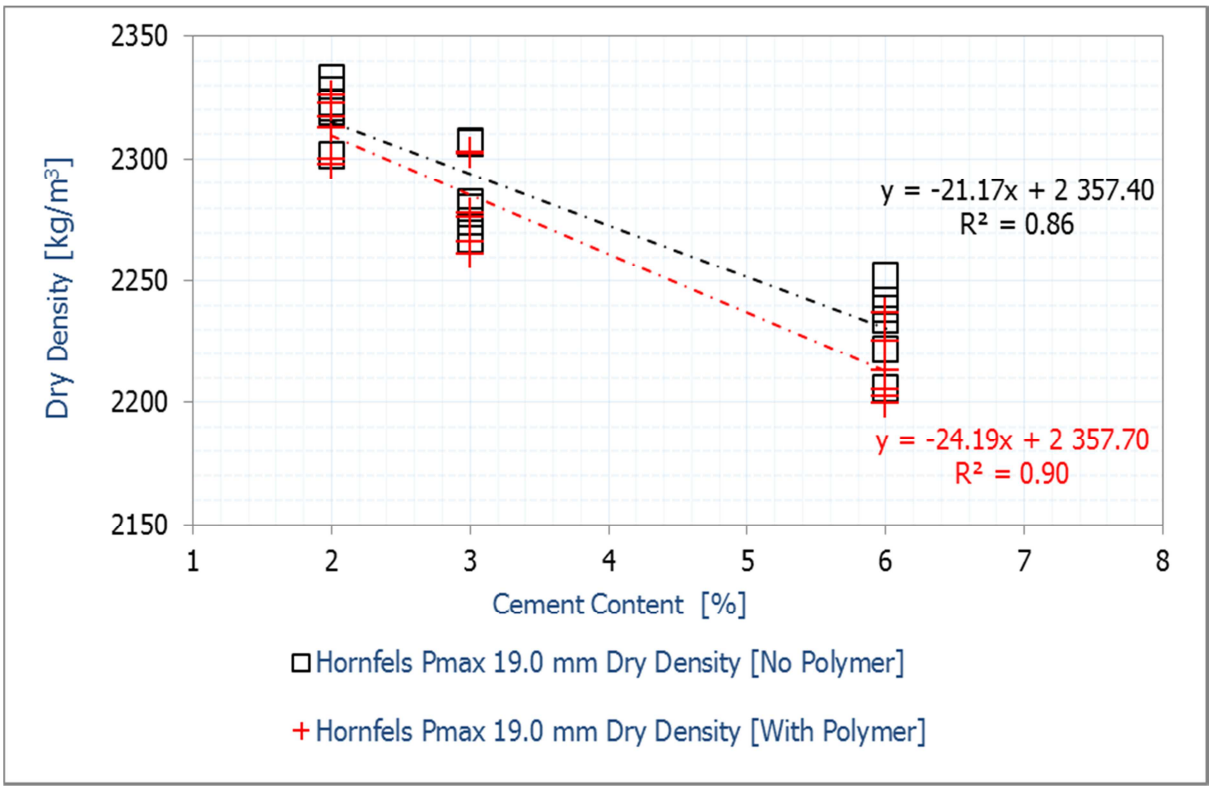

Figure: 4-25 Polymer Effect on Material Dry Density [Hornfels]

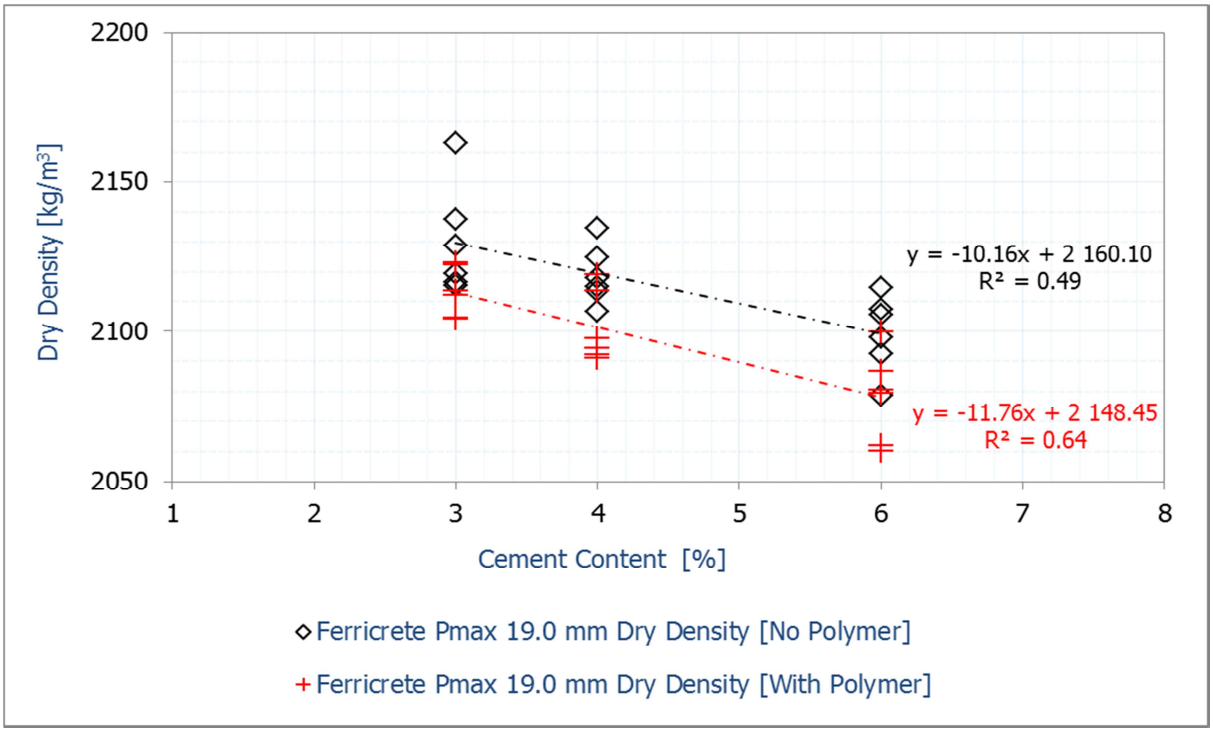

Figure: 4-26 Polymer Effect on Material Dry Density [Ferricrete]

4.6.2 Effect of the Polymer on the Compressive Strength and Modulus [E_{se}]

Figure 4-27 and 4-28 illustrate the effect of the polymer on the material compressive strength properties. For hornfels, the application of the polymer resulted in a general reduction in compressive strength with all cement contents. With ferricrete, the application of the polymer was beneficial, particularly at cement contents above 4%. Ferricrete mix

types with 6.0% cement content exhibited a significant increase in compressive strength following the application of 0.72% polymer to the mix. The regression equations along with the R^2 values denote the significance of the data points, which indicates the effectiveness of the polymer with the material and cement.

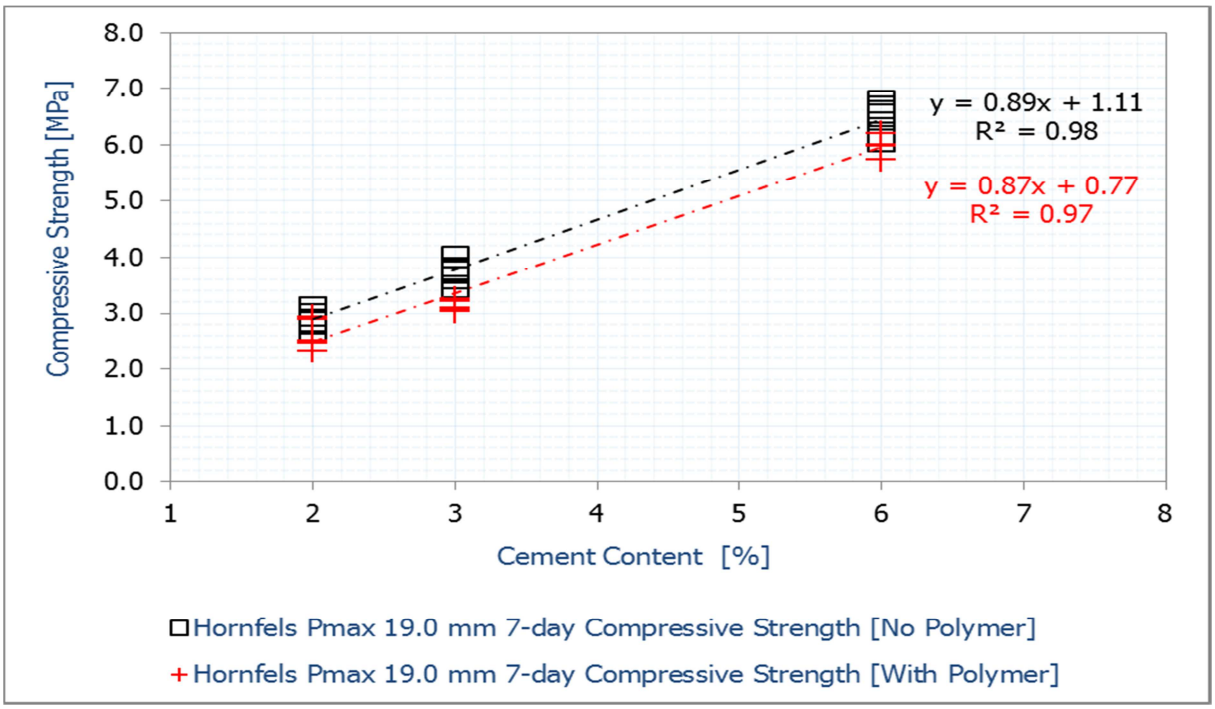

Figure: 4-27 Polymer Effect on Compressive Strength [Hornfels]

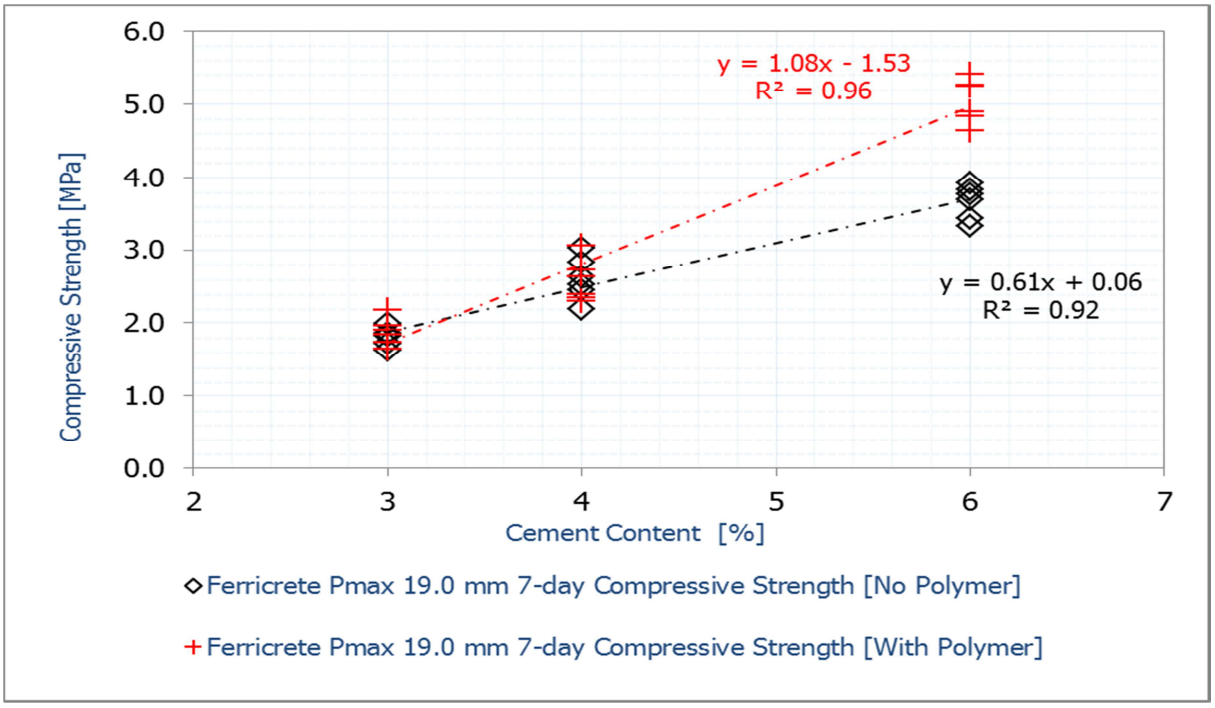

Figure: 4-28 Polymer Effect on Compressive Strength [Ferricrete]

The observed trends exhibited by ferricrete and hornfels indicate the compatibility and the efficacy of the polymer with stabilised materials. This suggests that the efficacy of the polymer is dependent on the material characteristics and properties. The trends obtained with ferricrete mix types suggest that the effectiveness of the polymer is dependent on the

cement content [preferably high cement dosages] and the quality of the material. In order to gain further insight regarding the effect of the polymer on the material properties, analysis of its effect on the compression modulus [E_{se}] relative to the compressive strength is undertaken. The compression modulus of the ferricrete and hornfels mix types [with and with the polymer] are plotted against that the resultant compressive strength. Figure 4-29 shows that the polymer not only reduces the compressive strength properties of hornfels but also a decrease in the compression modulus. Figure 4-30 shows that applying the polymer to ferricrete improves the compressive strength properties as well as compression modulus. The findings illustrated in Figures 4-28, 4-29 and 4-30 provide insight regarding the effectiveness of the polymer with a soil material type compared to a crushed gravel material type.

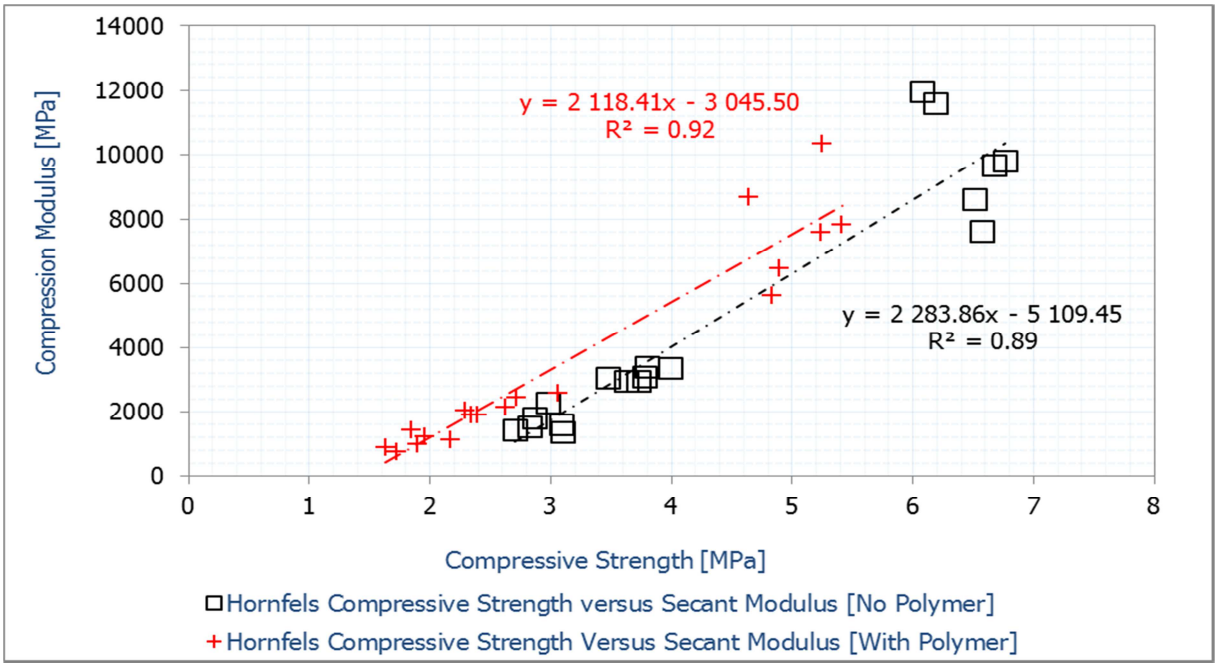

Figure: 4-29 Polymer Effect on the Modulus and the 7-Day Compressive Strength [Hornfels]

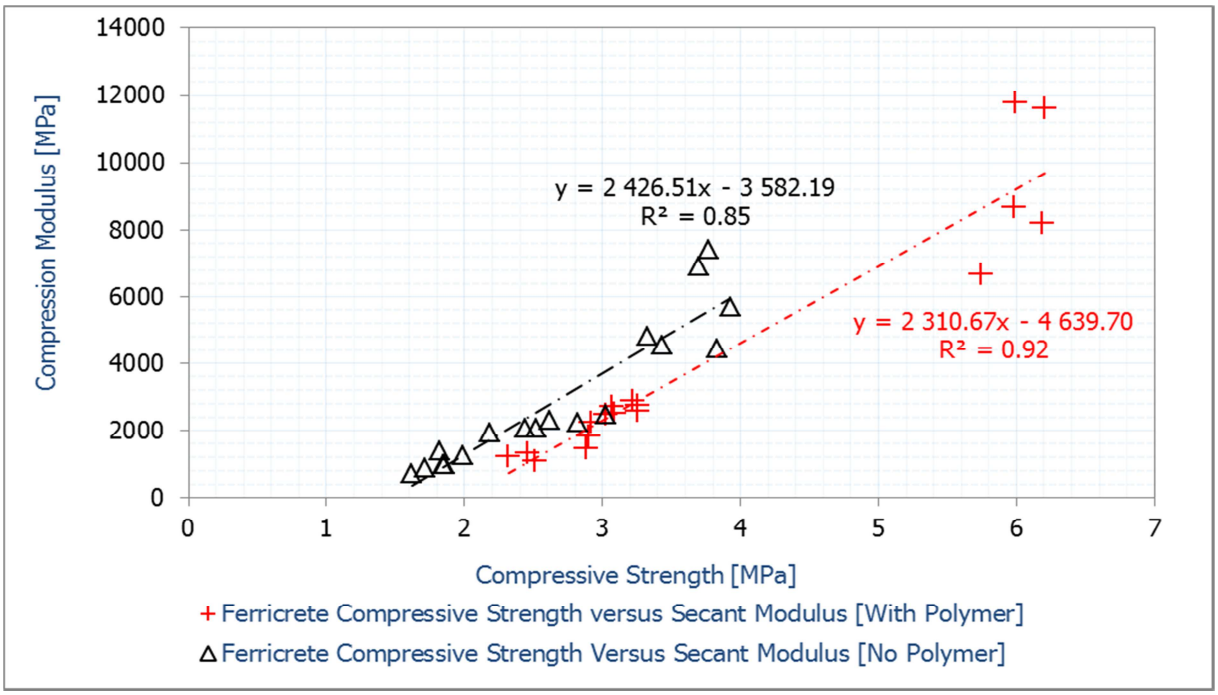

Figure: 4-30 Polymer Effect on the Modulus and the 7-Day Compressive Strength [Ferricrete]

4.6.3 Polymer and Tensile Strength Properties

Figures 4-31 and 4-32 illustrate the effect of the polymer on the material tensile strength properties. The application of the polymer in hornfels exhibited a comparable tensile strength criterion at low cement contents but a slightly lower tensile strength criterion with 6.0% cement. The regression equations model the effect of polymer on the material tensile strength properties at varying cement contents. A numerical calculation using the regression equations typifies a slightly higher tensile strength result following the application of the polymer with high cement contents. This suggests that the addition of the polymer to a hornfels mix stabilised using high cement contents slightly reduces the material tensile strength properties.

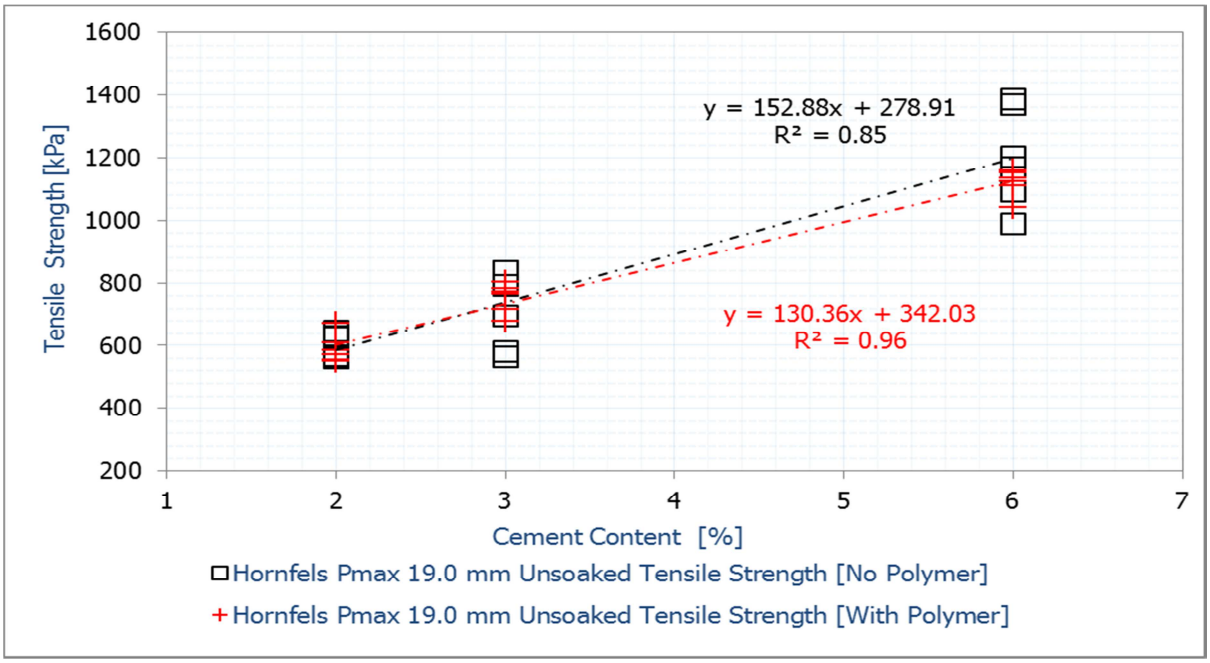

Figure: 4-31 Polymer Effect on Tensile Strength [Hornfels]

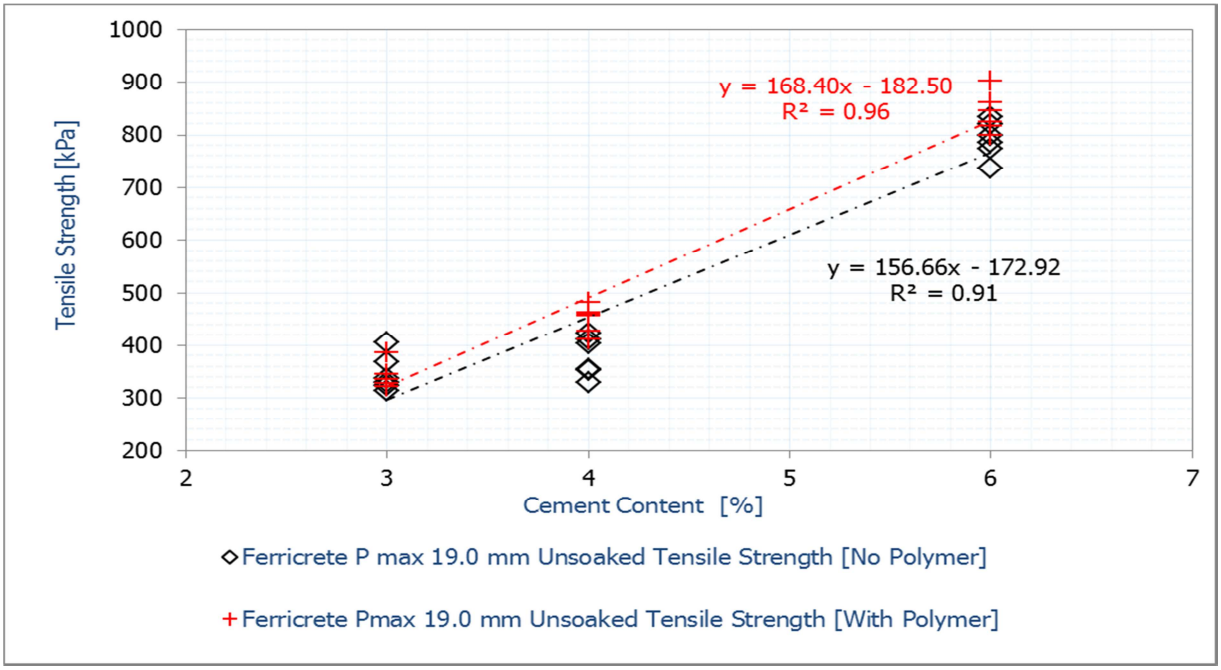

Figure: 4-32 Polymer Effect on Tensile Strength [Ferricrete]

Ferricrete exhibited a slight increase in tensile strength following the addition of the polymer to the material. The trends exhibited by ferricrete mixes with polymer further suggested that the efficacy of the polymer was associated with high cement usage, but was also significantly dependent on the material type and quality. The tensile strength trends showed a slight but a gradual increase, which corresponds to the addition of cement and polymer to ferricrete. Ferricrete mix types with 3% cement content exhibited a comparable tensile strength measure with and without polymer. Ferricrete mix stabilised using 4% cement content exhibited a gradual increase in tensile strength following the application of polymer. Ferricrete mix types with 6.0% cement content exhibited a distinct difference in tensile strength. The polymer effectiveness with ferricrete exhibited an increase corresponding to the addition of cement.

The polymer is purported to contain butadiene, which is known to enhance the tensile and flexural properties of materials. However, the inability to determine the components in the polymer is one of the research limitations. Figures 4-33a and 4-33b relate to Figures 4-21a and 4-21b and illustrate the effect of the polymer on the strength properties of the material types. Ferricrete mix types show an improvement in strength following the application of the polymer. Hornfels mix types show a general reduction in strength following the application of the polymer.

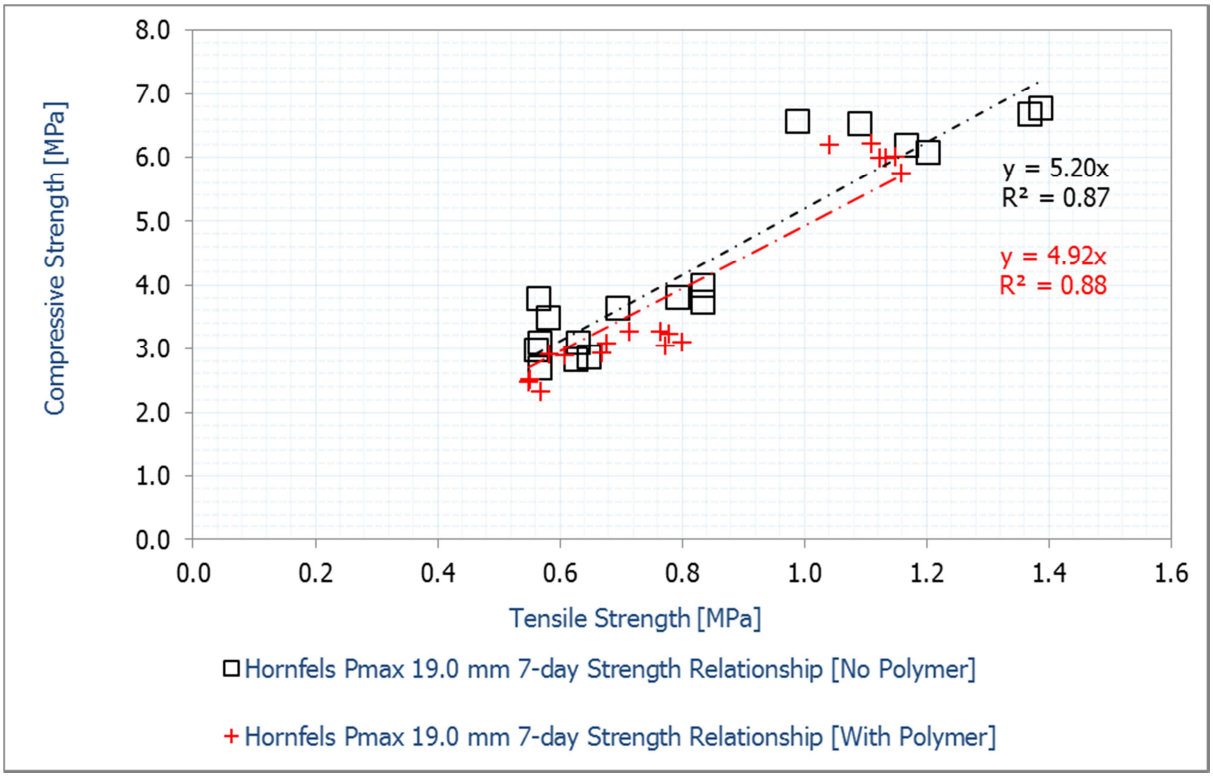

Figure: 4-33a Hornfels 7-Day Compressive Strength versus 7-Day Tensile Strength

The scattered data plots show the variables among the mix types, which include cement content, dry density and the effects related to stabilising materials. The low strength values relate to the low cement dosages used. The high strength values are associated with the 6% cement content in the mix. For hornfels mix types, with and without the polymer, show that the compressive strength is five times the tensile strength. The application of the polymer to ferricrete results in an increase in compressive strength. Ferricrete compressive strength is 6 times its tensile strength; this indicates that the polymer effect of the strength properties. At low cement contents [i.e. low strength values] the consideration of the polymer in improving strength is not economical; see Figures 4-33a to 4-33f. The application of the polymer to material results in either a reduction [hornfels, Figure 4-33c] or comparable strength

properties [ferricrete, Figure 4-33e]. At high cement contents, application of the polymer to hornfels results in a reduction in strength; see, Figure 4-33d. With 6% cement content in ferricrete, the application of the polymer enhances the strength properties, i.e. Figure 4-33f. These findings, based on the ITS and UCS tests establish that the efficacy of the polymer is dependent on high cement contents and the quality of the materials. The Southern Africa road industry usually considers low cement contents for stabilisation owing to the need to control shrinkage cracking.

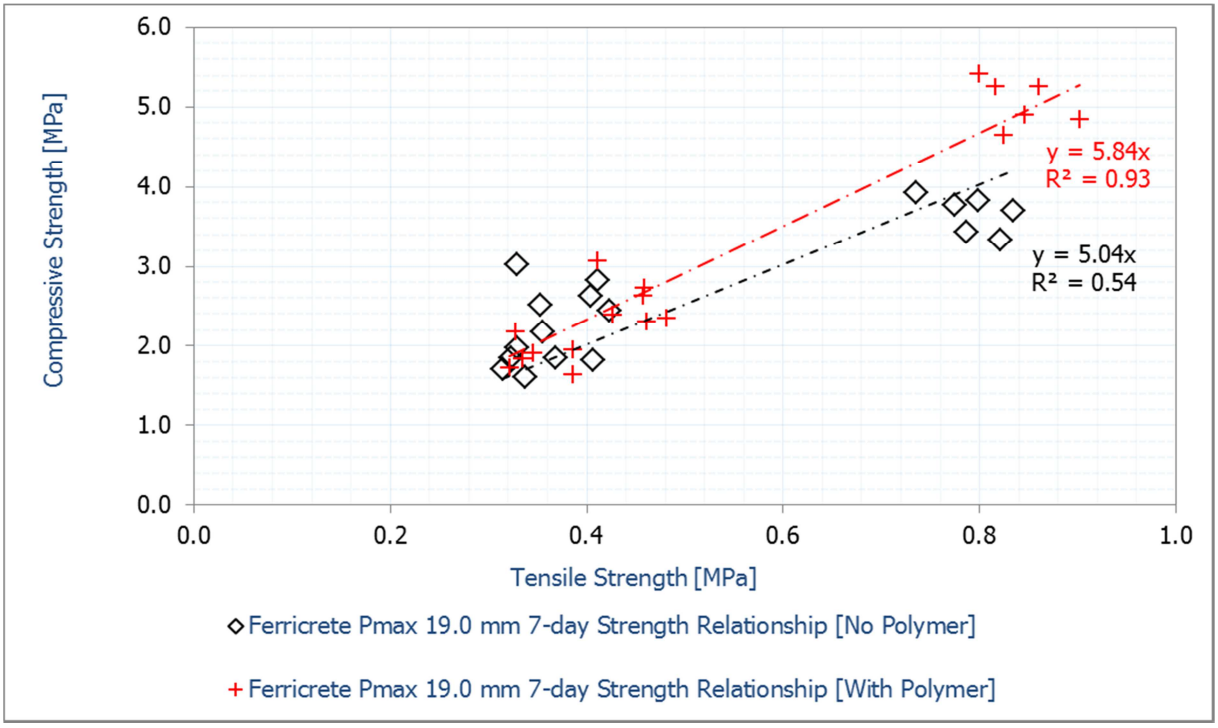

Figure: 4-33b Ferricrete 7-Day Compressive Strength versus 7-Day Tensile Strength

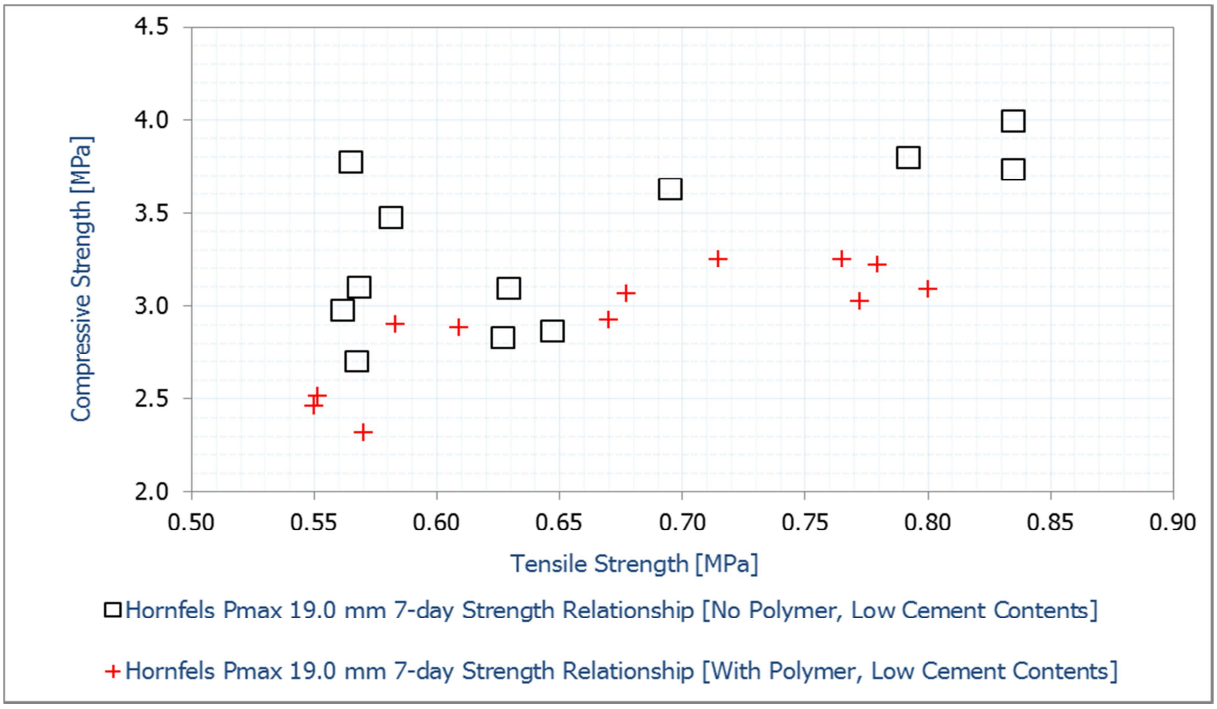

Figure: 4-33c Hornfels 7-Day Compressive Strength versus 7-Day Tensile Strength [2% and 3% Cement Contents]

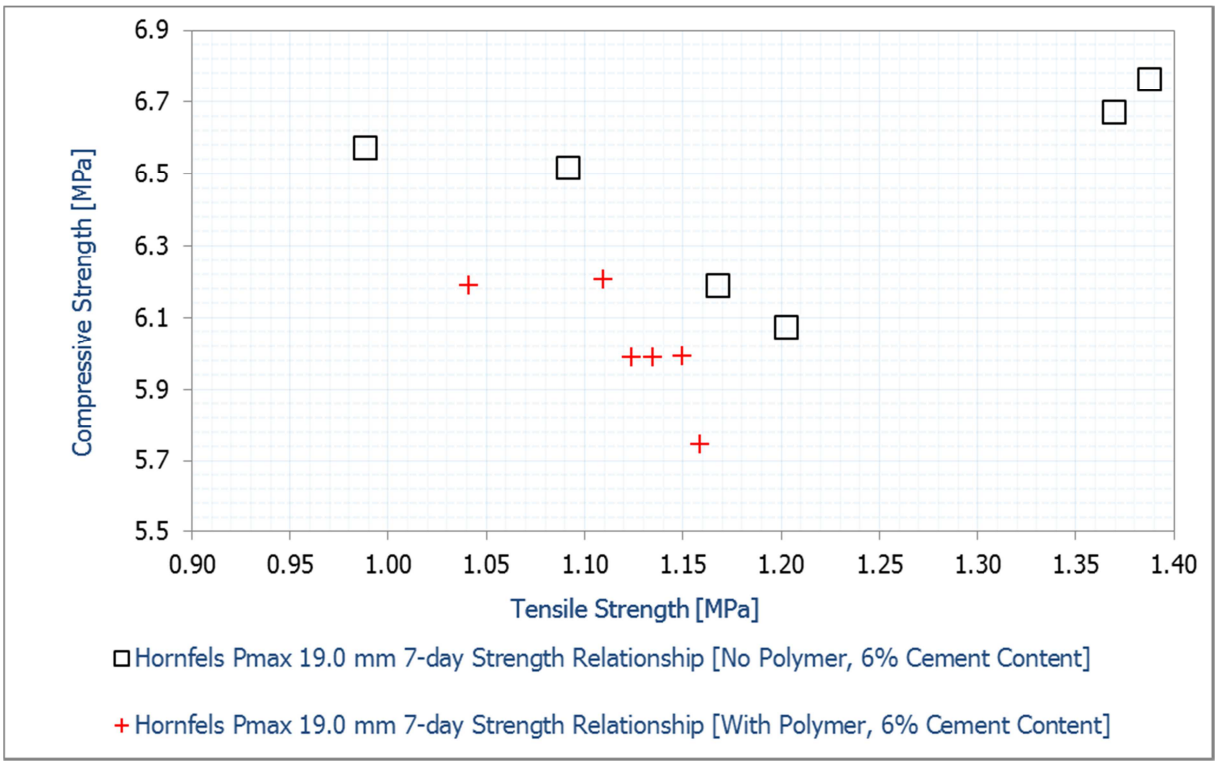

Figure: 4-33d Hornfels 7-Day Compressive Strength versus 7-Day Tensile Strength [6% Cement Content]

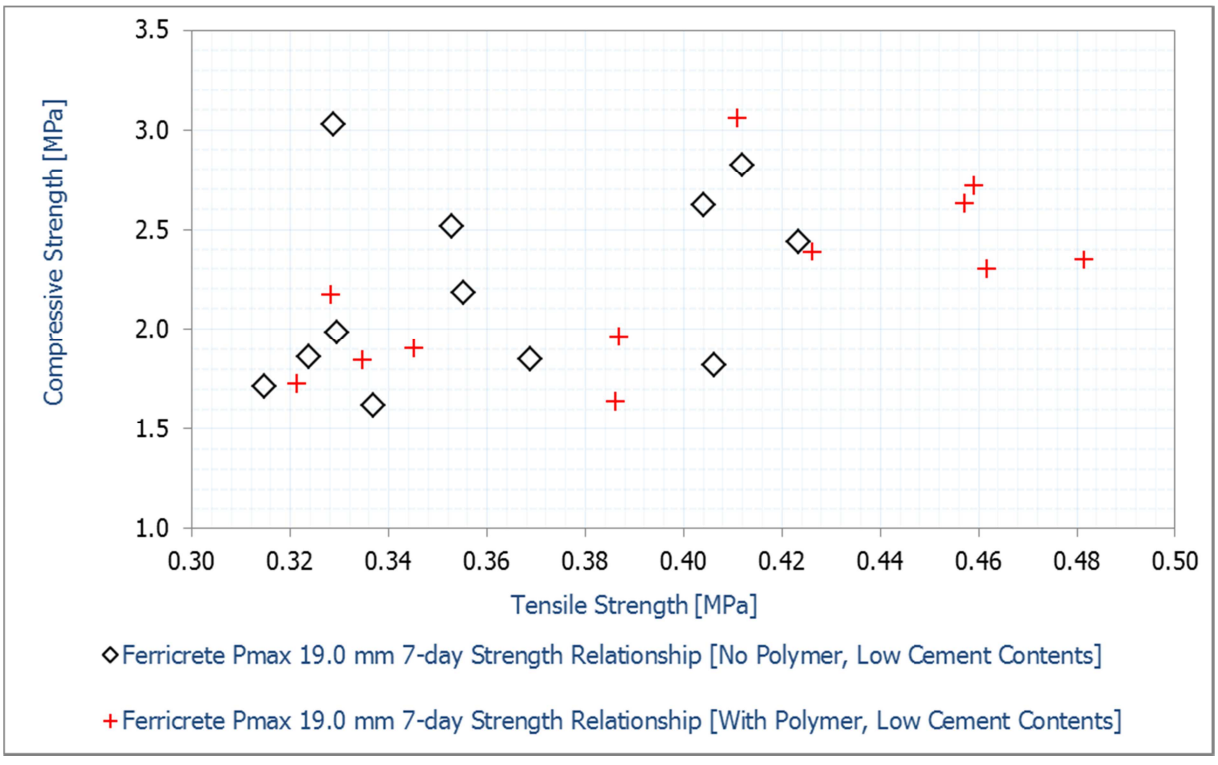

Figure: 4-33e Ferricrete 7-Day Compressive Strength versus 7-Day Tensile Strength [3% and 4% Cement Contents]

Figures 4-33g and 4-33h show the relationship of dry density to the compressive strength and tensile strength of the materials with the polymer. Equations 4-5 and 4-6 define the compressive strength [UCS] and tensile strength [ITS] of hornfels in terms of the cement content with the polymer. These equations relate to Equations 4-2 [UCS] and 4-3 [ITS]

without the polymer. DD denotes the dry density. The use of these equations is specified for hornfels mix types stabilised using cement contents of 2% to 6.0%.

$$\text{UCS} = (2373.91 - (DD))/27 \ [MPa] \ [R^2 = 0.83] \quad \text{Equation 4-5}$$

$$\text{ITS} = (2415.25 - (DD))/178[kPa] \ [R^2 = 0.86] \quad \text{Equation 4-6}$$

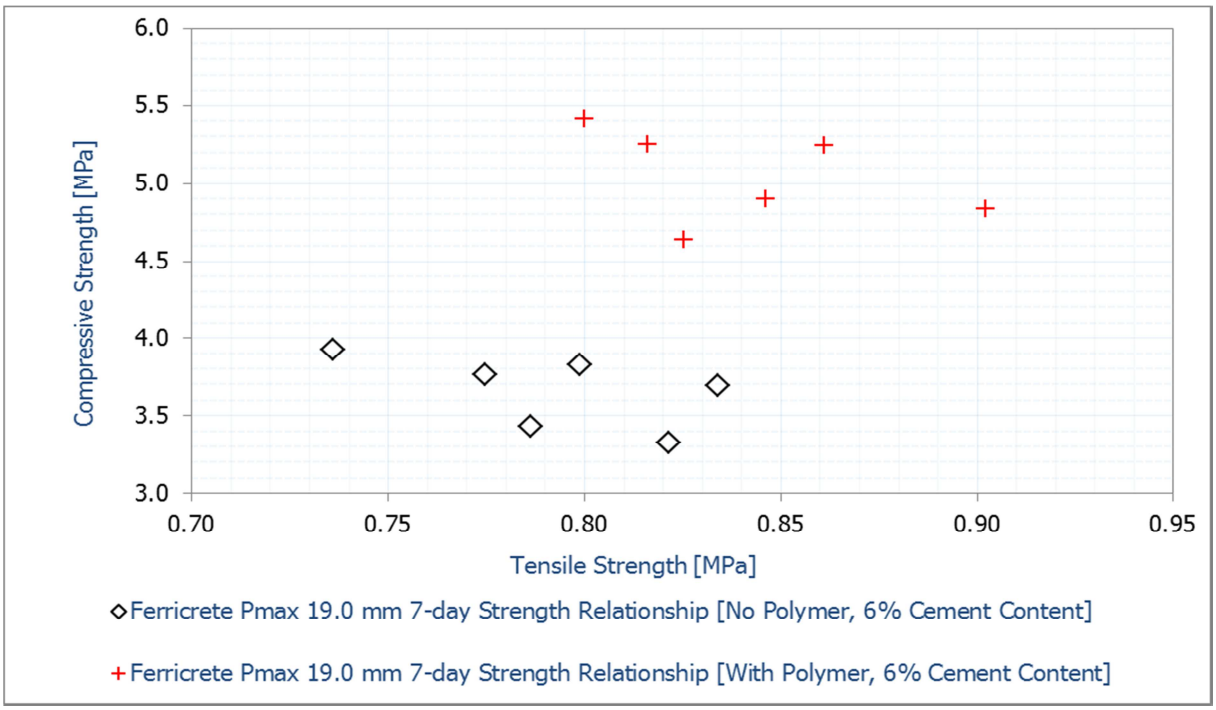

Figure: 4-33f Ferricrete 7-Day Compressive Strength versus 7-Day Tensile Strength [6% Cement Content]

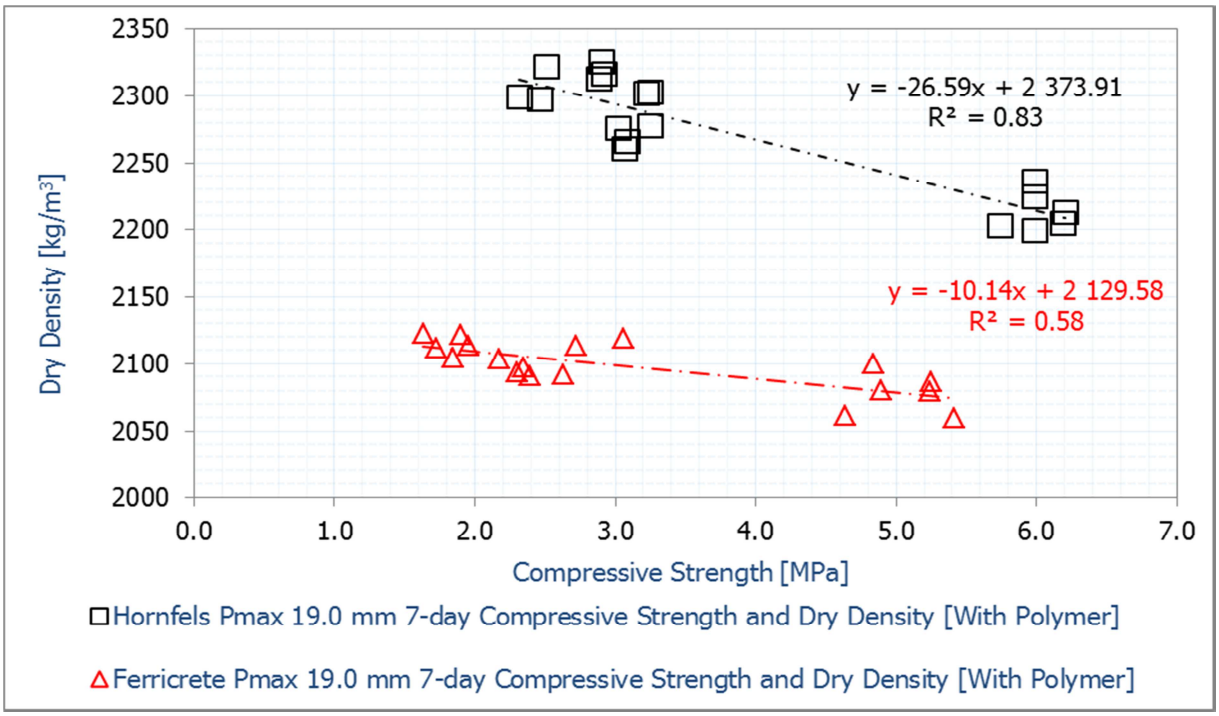

Figure: 4-33g 7-Day Compressive Strength versus 7-Dry Density

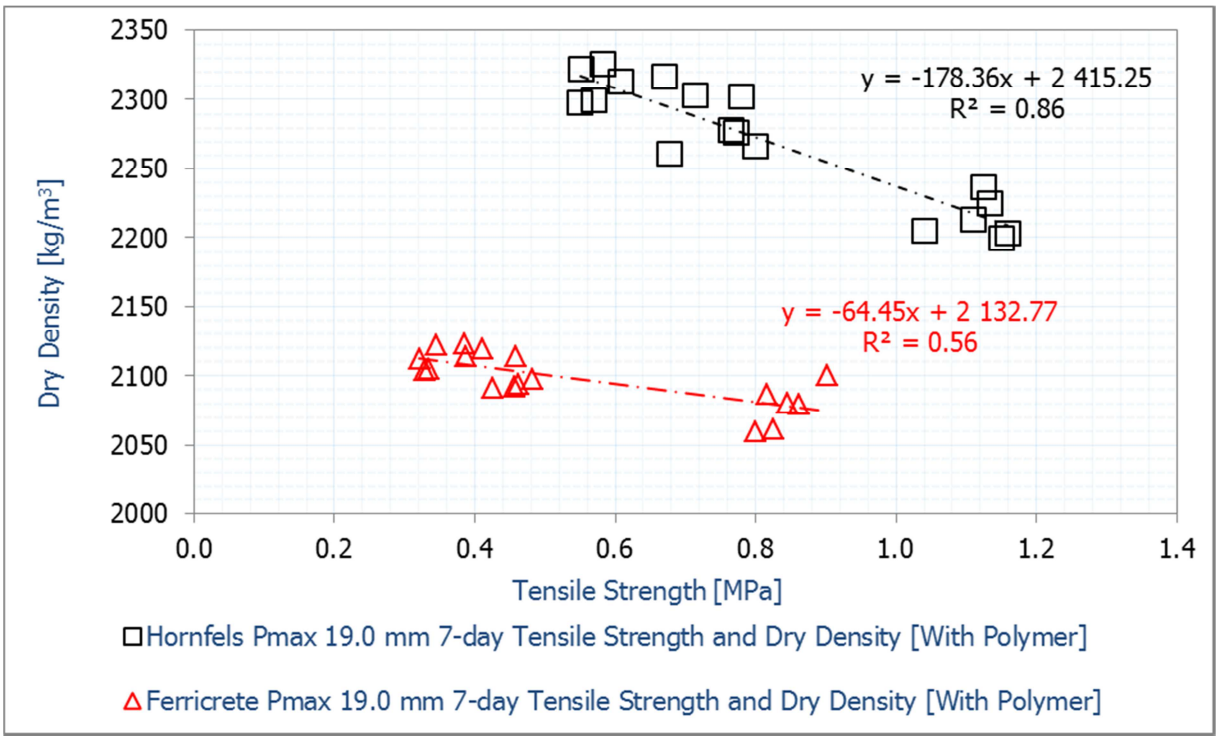

Figure: 4-33h 7-Day Tensile Strength versus 7-Dry Density

4.6.4 Polymer and Particle Resistance [Wet-Dry Test Criteria]

Figures 4-34 and 4-35 illustrate the wet-dry resulted with and without the polymer. The addition of the polymer in a hornfels mix results in an increase in the loss of material. This indicated that the polymer, which reduces density and strength, made the material more liable to loosen particles when brushed. This suggested that the abrasion on the specimen along with the effects emanating from soaking and drying conditions might exacerbate a mix, which is characterised by a low density and reduced strength properties.

A reduction in material density following the addition of polymer showed that its inclusion in the hornfels mix influenced the material gradation and the particle bond strength. Particle bond strength contributes significantly to the overall material strength properties. The strength results of hornfels typified the differences in strength with and without the polymer. The wet-dry results indicated the influence of the polymer on the strength properties of hornfels particularly particle bond strength.

Figure 4-34 illustrates that the hornfels mix types with the polymer exhibited higher material loss than their reference mix types [i.e. without the polymer]. This indicates that the overall effect of the polymer on the material density and strength had a significant influence on the resultant engineering properties. An increase in material loss following the abrasion test provided insight regarding the durability of hornfels with and without the polymer. Ferricrete mix types with and without the polymer were comparable. This suggests that the application of the polymer to ferricrete neither enhanced nor reduced its particle loss. This provides insight into the effect of the polymer on the particle bond strength.

From the wet-dry results, the efficacy of polymer with material indicated its dependency on cement content and properties of materials. This further established that the cement content and material characteristics as factors influencing the effectiveness of the polymer. The suitability of the polymer is dependent on certain specific material characteristics. The inclusion of other material types was necessary. Furthermore, the application of the polymer encompasses an evaluation of the material relative to the cement content under which the

best benefits are achievable. The objective of the material's evaluation with polymer or any other cement additive is to ascertain its compatibility with the material at specific cement contents for the required strength.

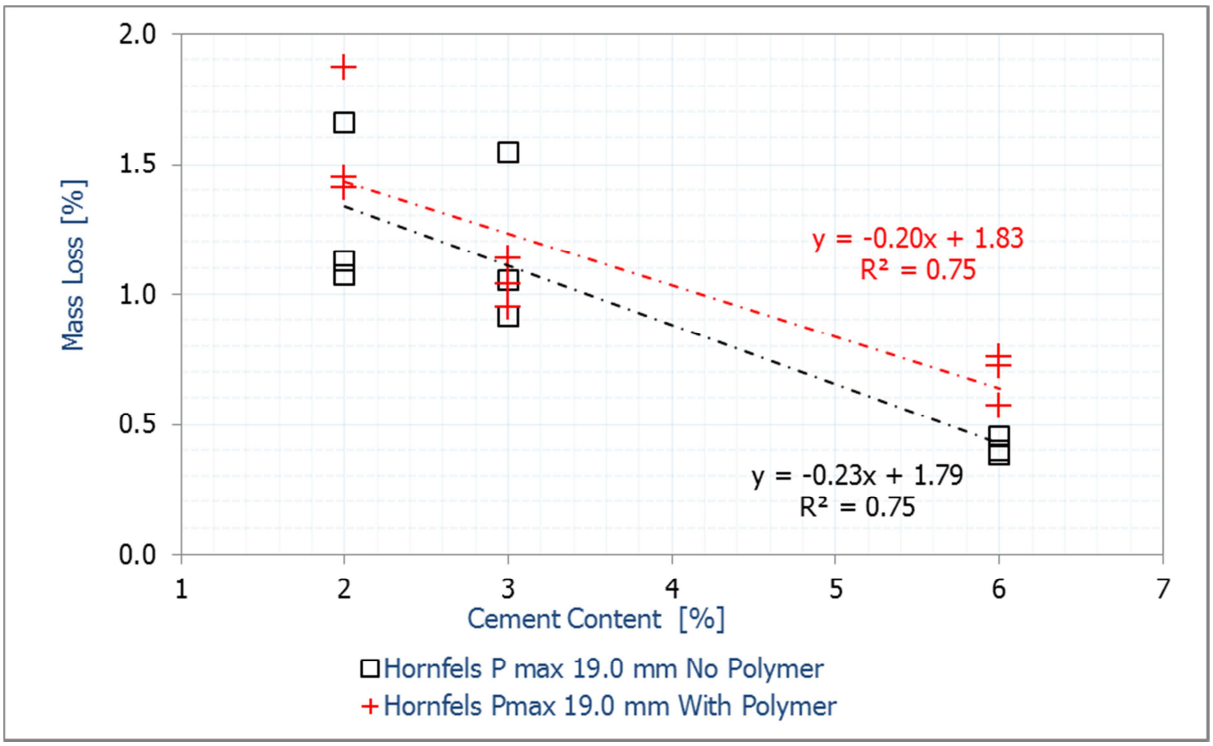

Figure: 4-34 Polymer Effect on Durability [Hornfels]

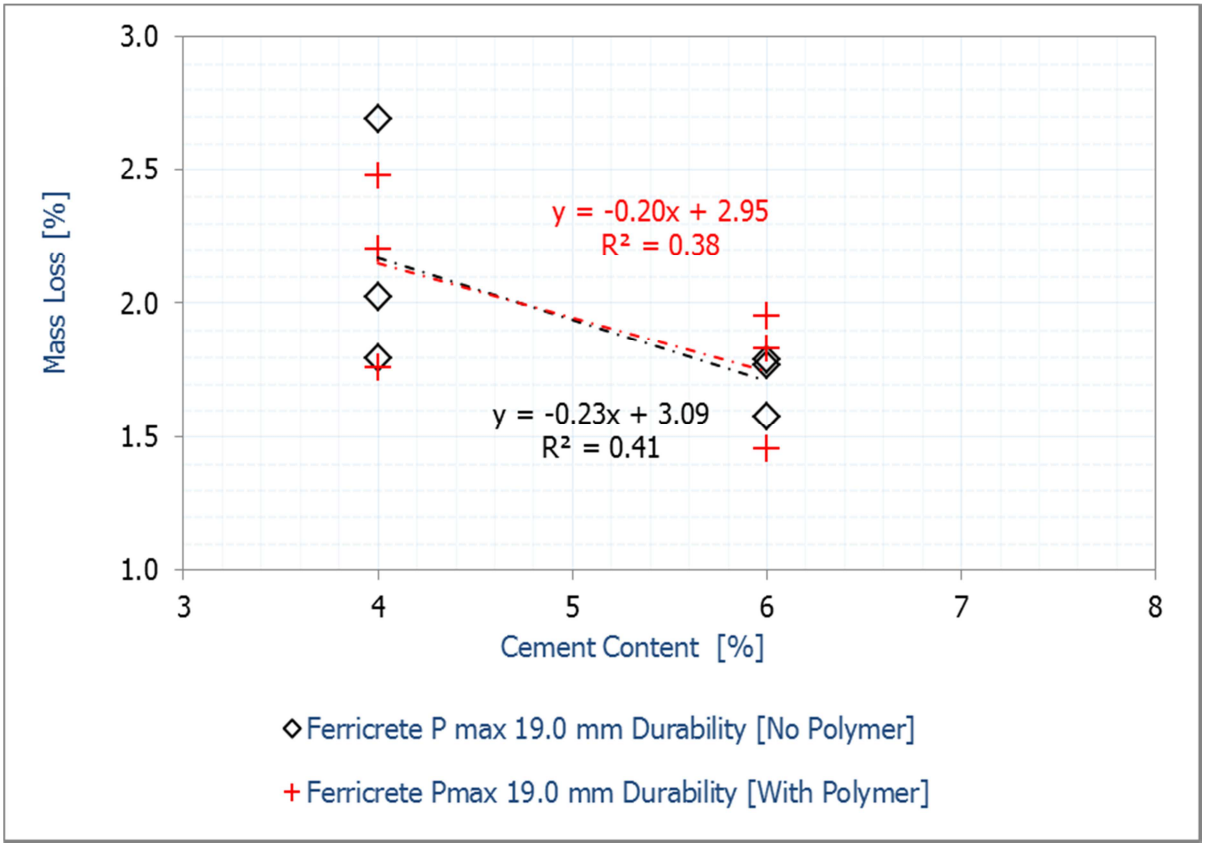

Figure: 4-35 Polymer Effect on Durability [Ferricrete]

4.7 Material Classification

With reference to the South African material classification system as stipulated in TRH14, [1985] along with the UK material specifications the quality and probable application of ferricrete and hornfels stabilised materials were analysed. Table 4-4 provides the material classification based on the average UCS strength of six specimens per mix variable.

Table: 4-4 Material Compressive Strength Classification

		7-day Hornfels Materials	TRH14 [1985]	TRL ORN31 [1993]
Cement Content	Polymer Content	Average UCS Value [MPa]	SA Material Strength Class	UK Material Strength Class
2	0%	2.928	C3	CB2 [stabilised roadbase]
3	0%	3.734	C2	CB1 [stabilised roadbase]
6	0%	6.466	C1	above CB1 [stabilised roadbase]
2	0.24%	2.666	C3	CB2 [stabilised roadbase]
3	0.36%	3.151	C2	CB1 [stabilised roadbase]
6	0.72%	6.018	C1	above CB1 [stabilised roadbase]
		7-day Ferricrete Materials	TRH14 [1985]	TRL ORN31
Cement Content	Polymer Content	Average UCS Value [MPa]	SA Material Strength Class	UK Material Strength Class
3	0%	1.806	C3	CB2 [stabilised roadbase]
4	0%	2.601	C3	CB2 [stabilised roadbase]
6	0%	3.662	C2	CB1 [stabilised roadbase]
3	0.36%	1.872	C3	CB2 [stabilised roadbase]
4	0.48%	2.573	C3	CB2 [stabilised roadbase]
6	0.72%	5.046	C2	CB1 [stabilised roadbase]

All mix types stabilised at the same cement contents registered similar material class with and without the polymer. This provided insight regarding the effect of the polymer and the resultant material strength ranges. For high quality sub-base pavement layers the Southern Africa road industry considers a material class C2. For the lower pavement layers of low volume roads, material classes C3 and C4 are considered. The South African road industry seldom considers C1 within the flexible pavement structure. The consideration of material classes C1 and C2 within rigid pavements is common. Some of the reasons for not considering C1 within the flexible pavement structure include their stiffness properties and propensity to break up because of their brittleness. The formation of wide shrinkage cracks in flexible pavements is one of the main reasons why material class C1 are certainly not considered. The UK road industry considers CB1 and CB2 for road base layers. Material class CB1 is comparable to C2 and C1. The UK specifications consider linear shrinkage results as an indicator test of the material shrinkage potential. This assists in ascertaining their suitability for use in the pavement structure.

4.8 Discussion of Results

The characterisation phase provides insight regarding the strength properties and characteristics of cement-stabilised materials with and without the polymer. The approach adopted to establish the polymer application rate takes into consideration of the following aspects:

a) the polymer is a cement additive, so its application rate is more allied with cement than material, i.e. its functionalities are associated with the amount of the cement in the mix
b) by considering that the polymer is purported to reduce shrinkage a simple test approach to evaluate shrinkage is deemed suitable in establishing its efficacy
c) in order to evaluate shrinkage as a material property measure the cylinder method is preferred to the beam method due to compactability of the beam edges and influence of friction at the interface between the base plate and the bottom of the beam

The characterisation phase establishes the differences between ferricrete and hornfels that include particle distribution, level of plasticity and even, shrinkage [based on the bar linear

method with material passing the 0.425 mm sieve]. The plasticity of the material influences the requirements of cement to produce a stabilised layer with viable strength. Ferricrete could hardly result in a variable mix of adequate strength [i.e. minimum of a C4] with 2.0% cement content.

Considering that, the polymer is a nano-silica, there is a tendency for it to react extremely fast with cement [or specifically with the free lime in the cement] and then react with the lime generated by the hydration of C_2S and C_3S. The rapid setting is likely to contribute to the reduction in the dry density compared to other influential factors such as higher cement contents.

Factors that influence the strength properties of cement-stabilised materials, such as dry density and moisture content, material type and gradation are illustrated. The physical-chemical effects emanating from combining material, cement and water have been illustrated to result in a reduction in density [physical effect] but with an increase in strength [chemical effect].

Ferricrete and hornfels exhibit an increase in in strength following the addition of more cement to the materials. However, the rate of increase varied with the type of material. Hornfels exhibited a higher increase than ferricrete, which is exemplified by the strength-cement relationship. The differences in strength increase following the addition of cement is attributed to the quality of ferricrete relative to hornfels. This suggests that ferricrete reacts differently with cement compared to hornfels. The mineralogical and physical makeup of ferricrete influences the cementation reactions [hydration process]. However, none of the materials exhibit traces of deleterious organic compounds, which are known to act as retarders causing low strengths. The dry density and strength properties of hornfels are significantly higher than ferricrete. The amount of fines in the mix, contribute to the low dry densities and strength properties.

The density results of ferricrete and hornfels show a decrease due to the addition of cement to the material but a strength increase. This indicates that although cement reduces the material's density, the cementation effects emanating from the hydration reaction result in a strength increase. Strength properties of cement-stabilised materials are dependent on the quality and type of the natural material before stabilisation.

In order to analyse the cementation and the strength properties, a scrutiny of the particle distribution [gradation] particularly its fines content relative to the coarse and medium particles is essential. This is because the particle distribution and characteristics of the material influence their bond strength. Bond strength contributes to the behavioural properties of the stabilised materials. Figure 4-36 illustrates the influence of bond strength relative to the particle interaction. Three situations A, B and C are conceptualised.

Situation A illustrates the same sized particles, which do not comprise of fines and medium particles. This leads to poor or no bond strength. Situation A is dependent on the particle size and material type. The importance of fines and medium particles in a coarse skeleton is illustrated. Without the fines and medium particles, more cement is required to achieve good bond strength and ultimately, meet the required strength properties. The addition of more cement to such a coarse skeleton results in a lean mix. Lean mixes are characterised by their high stiffness properties and brittleness. Lean mixes are prone to suddenly crack upon loading. Such mixes also exhibit increased shrinkage due to the high cement contents applied.

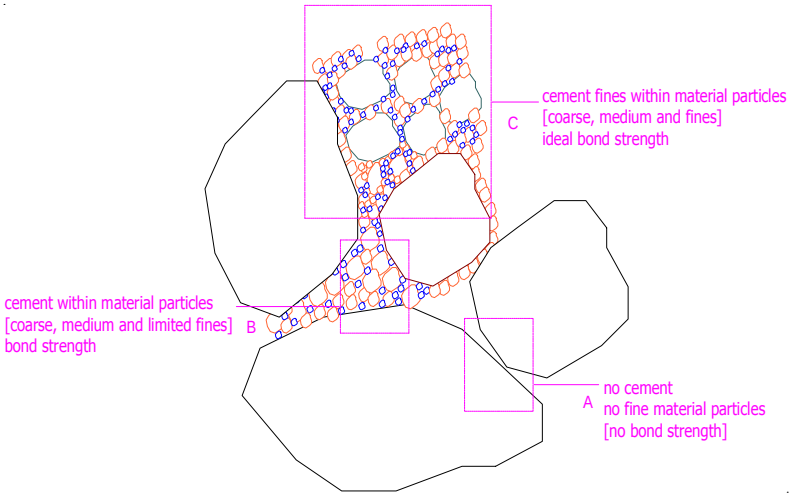

Figure: 4-36 Particle Bond Strength with and without Cement

Situation B occurs when there are more coarse and medium particles but limited fines and cement. The blue dots signify cement. Such mix types possess some degree of bond strength. A lack of suitable particle distribution influences the effectiveness of cement in the material matrix and thus, strength properties. A well-graded material, usually exhibits a suitable distribution of fines, medium and coarse particles, which enhances the cement effectiveness. This suggests that the degree of bond strength is dependent on:

a) the cement content and particle distribution
b) achievable density, which characterises the particle-to-particle contact and a reduction in void content [i.e. pore structure and interconnection]

The relationship between the particle distribution and the bond strength is essential. This influences the material properties, particularly strength. The particle bond strength is dependent on several factors including the material gradation, cement content and the achievable density. An increase in cement content results in a corresponding 'reinforcement' of the particle-to-particle interaction, which improves the bond strength. The addition of cement to material results in a corresponding increase in the particle bond strength. This ultimately influences the behavioural properties, particularly the material's load response and its fracturing behaviour. Equally adding more cement to material not only improves its particle bonding strength, but also reduces its material loss due to abrasion. This suggests that an increase in the particle bond strength reduces the erodibility of the materials and ultimately, increasing their durability.

The test method, particularly its the loading mode [in this case monotonic loading] and other test configurations relative to the specimen geometry play a significant role on the measure of the strength properties. The UCS and ITS test follow different property measure using different specimen geometry and test configuration. A relationship of UCS to ITS is presented. However, a number of factors, including the dry density, cement and moulding moisture as well as the curing conditions, influence the compressive strength and tensile strength relationship. A variation of any of the factors results in a corresponding difference in the material properties. The UCS and ITS tests provide a different measure of the strength properties of the cement-stabilised materials. Therefore, developing the relationship between the UCS and ITS as well as the material properties, is useful to the design of pavement layers.

Furthermore, the concepts behind the force-displacement analysis [as related to stress-strain curves] for the computation of the compression modulus are essential to this research. This provides a better understanding of the performance of the material i.e. load response and load-spreadability. Understanding the stress-strain criterion provides insights into the elastic

modulus of the material in the compression mode. However, cement-stabilised materials exhibit better performance in compression mode than in tension; this explains to an acceptable degree, differences between ITS and UCS values. In this research, the ITS value of hornfels is about 20% of its UCS value.

In this research, the effect of the polymer additive on the strength properties of cement-stabilised material is investigated. Findings show that the inclusion of the polymer to either ferricrete or hornfels resulted in a shift [i.e. from the reference mix] of the compressive strength and tensile strength relationship. This identified the suitability of the polymer with the material types [i.e. ferricrete and hornfels] at varying cement contents. It is deduced that the efficacy of the polymer is dependent on the quality of the material and cement content.

Furthermore, a reduction in the density results due to the application of the polymer to cement-stabilised materials. Being a cement additive, the polymer interacts with the cement and the resultant effect influences the particle bond strength of the stabilised materials. The interaction of the polymer with cement-stabilised materials depends on high cement contents such as 6.0 in the mix, as well as on the quality of the material. In terms of the quality of materials, the plasticity of the natural material, amount of fines in the mix and other intrinsic properties influence the efficacy of the polymer. The effect of the polymer on the dry density and moisture content of the cement-stabilised materials provides insight regarding its components and their influence. An increase in the moisture content from its optimum results in a reduction in dry density. A reduction in the dry density due to the polymer is indicative of its composite nano-particles and to an extent its solvent effect. Similar to the effect of cement on material, the polymer exhibits a physical-chemical effect i.e. a reduction in density [physical effect] and increase in strength at high cement contents [chemical effect]. In general, a negative effect of any additive or stabiliser on the particle bond strength affects the engineering properties of cement-stabilised materials, particularly strength.

4.9 Summary of Chapter 4

This chapter provides the material characterisation, strength and durability results. The evaluation of the cement-paste shrinkage, as part of the characterisation phase for establishing the efficacy of the polymer and its application rate, is provided. Additionally, the wet-dry brush test, which provides a good indication of the particle resistance of the material, is dealt with in this chapter. The wet-dry brush test data offer insight into the durability criterion of the various mix types i.e. with and without the polymer. A classification system based on South African and United Kingdom specifications is provided. This establishes the probable application of the stabilised materials with and without the polymer in the pavement structure. While the Southern Africa road industry uses low cement contents for stabilisation the European and American practice reports high cement dosages for stabilisation. With high cement dosages, the material becomes more rigid and prone to suddenly crack as well as being susceptible to shrinkage cracking. The following chapters provide additional evaluation and related analysis regarding the mechanical strength and shrinkage of cement-stabilised materials with and without the polymer. Chapter 5 provides the flexural strength results and the related analysis.

4.10 References

Landon, J.R., (1991) *Booker Tropical Soil Manual: A Handbook for Soil Survey and Agricultural Land Evaluation in the Tropical and Subtropics*, Longman Scientific and Technical Group.

Taylor, H.F.W., (1993) *Cement Chemistry*, London, UK, Academic Press Limited

Chapter 5: Flexural Strength Results

5.1 Background

This chapter provides results and analysis pertaining to the material's flexural strength, elastic modulus, strain-at-break, fracture energy and other related aspects. Section 1.6 introduces the flexural beam test with a focus on the need to evaluate the flexural strength properties of stabilised materials. Section 2.6.4 provides the principles and allied test techniques pertaining to flexural strength testing. The need to standardise the flexural beam test is to aid in the evaluation of stabilised materials with a good reliability.

Section 3.6 provides the criterion adopted by this research towards the standardisation of the flexural beam test. Chapter 4 provides the compressive and tensile strength results along with the material characterisation. This chapter provides insight regarding the material types and their quality relative to the resultant compressive and tensile strength properties. This chapter provides a background for the flexural strength evaluation.

5.2 Flexural Beam Testing Technique and the Factors of Influence

As part of the research objectives, the establishment of a flexural beam test procedure with defined beam geometric characteristics and test configurations is essential to the road industry. The standardisation of the flexural beam test helps to interpret the material's mechanical strength properties and elastic criterion using a similar protocol. The usually considered test protocols and their related measure of the flexural strength properties provide an obscure interpretation for the same material. This ambiguity in the measure emanates from the fact that the flexural strength measure of cement-stabilised material is unregulated. The use of different test configurations and beam geometry result in a different measure of flexural strength for the same material type.

A number of road agencies and even, research centres consider the concrete test procedures for the measurement of the flexural strength and elastic moduli of cement-stabilised materials. Limited [if any] cognisance regarding the effect of the beam geometric characteristics relative to test configurations is given. With a good comprehension of the beam theories along with the principles related to pure beam bending theories, an experiment to standardise the flexural beam test is undertaken. Section 3.6 provides the experiment and the specifics regarding the flexural beam testing of cement-stabilised materials.

5.2.1 Maximum Aggregate Size, Beam Geometry and Dry Density

Density is a function of the moisture content, particle size distribution and compactive effort applied to the material. Density is a key material parameter that provides insight regarding its quality and suitability for use in the pavement structure. In order to study the effects of the beam geometric characteristics relative to the test configurations, cognisance of the maximum aggregate size is crucial. The maximum aggregate size dictates the specimen geometry because of its influence on the particle packing and the overall compaction of the material. Particle packing plays a significant role on the achievable density and to a significant degree, on the strength properties.

The experimentation considered hornfels materials for its initial study. Evaluation of ferricrete material followed in the last phase of the investigation because:

a) unlike hornfels, ferricrete does not have a categorised grading envelope
b) hornfels is readily available at several quarries within the Western Cape of South Africa
c) ferricrete is a scarce material

d) the findings obtained using the standard strength tests characterise hornfels as a better material type to benchmark other materials including ferricrete

Following the standard strength testing, stabilisation proceeded at 2%, 3% and 6% cement contents for hornfels. The stabilisation of ferricrete followed at 3%, 4% and 6% cement contents. In this experiment, only one set of ferricrete beam type with a height of 50 mm is considered. Figure 5-1 illustrates the effect of maximum aggregate size on the dry density of the material. The experiment also included different beam types of varying heights and loading spans [span-depth ratios].

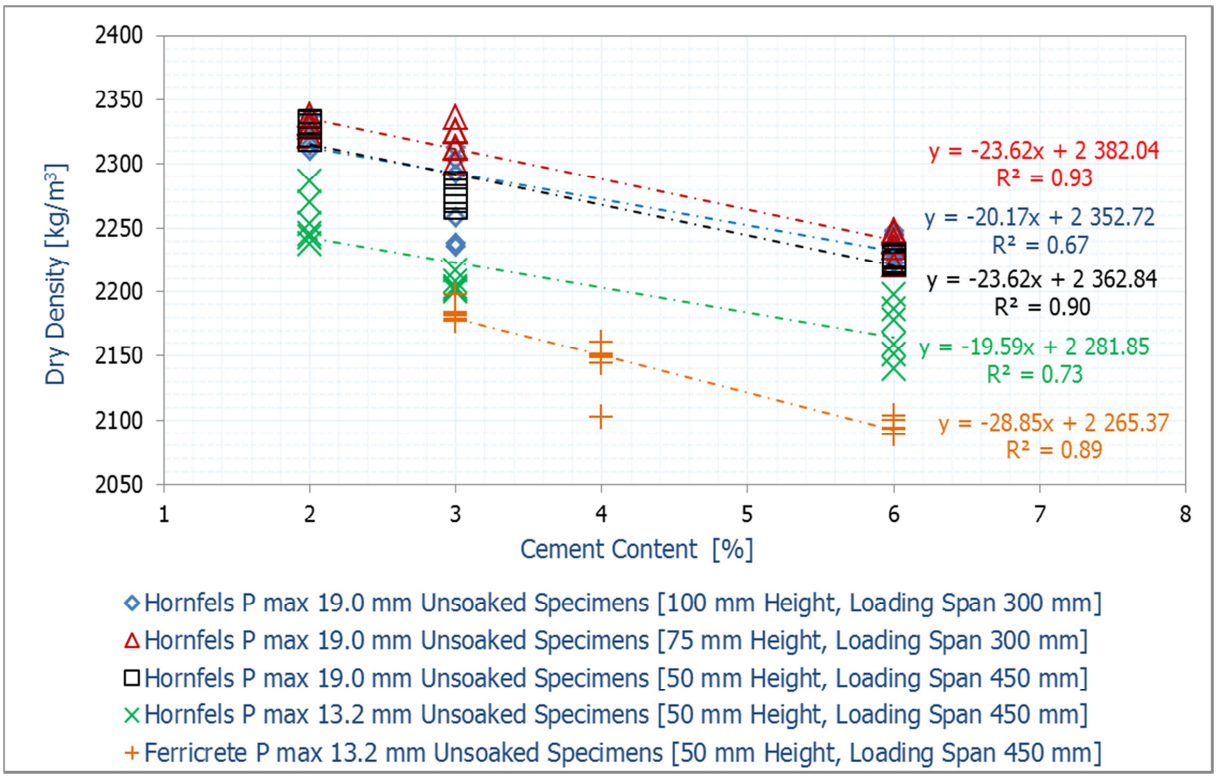

Figure: 5-1 Effect of Maximum Aggregate Particle Size on Material Density

Tables 5k to 5o in the Appendix to Chapter 5 list the various material parameters and the differences. The dry density results of hornfels exhibit a reduction due to the exclusion of the 19.0 mm aggregate size from the mix. Hornfels mix types with 13.2 mm as the maximum aggregate size register a lower overall dry density than hornfels mix types with 19.0 mm. By changing the beam height, there is no significant difference in the dry density. This is because dry density is a function of moisture and particle size in the mix than the physical shape and size of the specimen. All beam types with 19.0 mm as the maximum aggregate size showed slight variations; this was within acceptable dry density ranges. A number of factors, including the adopted compaction procedures, the packing of the aggregate particles among others influence the resultant dry density.

After a series of compaction trials using the vibratory hammer, the compaction procedure per beam type was determined. All specimens were compacted at the optimum moisture content of the natural materials. Mix types with the 19.0 mm as the maximum aggregate size showed an optimum moisture content of 5.3%. Mix types with the 13.2 mm as the maximum aggregate size registered an optimum moisture content of 5.7%. Beam types with a height of 100 mm and 19.0 mm as maximum particle size were compacted in two layers of 75 mm [first layer] and 25 mm [second layer]. After compaction of the first layer, scarification of the compacted layer, followed; this aimed at ensuring the bonding of the next layer is achieved. The beams with heights of 75 mm and 50 mm were compacted in one

layer. This was also determined after a series of compaction trials using the vibratory hammer.

Due to the variation of the maximum particle size, the moulding moisture also changed. Moulding moisture [OMC] is dependent on the particle size distribution; this is due to the effect of surface area availability. An increase in the size of the particle ultimately results in a reduction in moulding moisture.

The coefficient of determination [R^2 value] represents the variance amongst the beam types including the different cement contents among other experimental variables. In Figure 5-1, the R^2 value exhibits the compaction and resultant density of the individual beam types at varying cement contents. Insight into the quality and type of material are provided. Hornfels mix type with a height of 100 mm and 19.0 mm as maximum particle size registered the lowest R^2 value with a significantly low density with 4% cement content in the mix. Cognisance to the differences between the mix types such as the compaction procedure and the maximum aggregate size in the mix must be noted. To an acceptable degree, the maximum particle size dictates the geometry of the beam. However, depending on the height of the layer to be compacted, the maximum aggregate size could influence the compaction of the specimen and the mechanical properties of the material.

In terms of the material differences [ferricrete and hornfels], a comparison of the beam mix types with similar maximum particle size of 13.20 mm revealed that ferricrete registered a lower dry density than hornfels. Depending on the quality and type of the material, the moulding moisture and particle size distribution will vary; this influences the resultant dry density. Insight into the effect of the maximum aggregate size and moulding moisture on the dry density of the material are illustrated.

Statistically, beam types with 19.0 mm as maximum aggregate size compared well in terms of dry density. Hornfels beam type with a height of 50 mm and 19.0 mm as the maximum aggregate size registered the lowest dry density. The dry density results of the beam type with 19.0 mm and 13.20 mm as maximum aggregate size further indicate the significance of maximum aggregate size on the dry density. The beam type with 13.20 mm as maximum particle size shows a significant difference in dry density when compared to its reference type with 19.0 mm. This shows the influence of the maximum particle size on the dry density of the material.

5.2.2 28-Day Flexural Strength

The influence of the beam geometric characteristics relative to the maximum aggregate size and test configurations are essential to evaluate. These factors have a significant influence on the measure of the flexural strength properties of stabilised materials. Section 3.6 provides the flexural beam test variables and related equations for the calculation of the material's flexural strength. The influence of varying the maximum aggregate size on the density is established. Figure 5-2 shows the effect of varying the maximum aggregate size, beam height and loading span while using the four-point bending beam test technique. The R^2 values signify the variations amongst the mixes. The regression equations model the flexural strength properties and cement content. A linear relationship characterises the flexural strength and cement relationship.

The hornfels beam type with a maximum aggregate size of 19.0 mm and a height of 50 mm provided the lowest overall R^2 value. A 19.0 mm as the maximum aggregate size in small sized beam geometry with a height of 50 mm forms localised zones of weakness that contribute to a reduction in flexural strength, see Figure 5e in the Appendix. A maximum aggregate size in small sized beam geometry influences the packing. This usually leads to creation of weak zones, which influence the fracturing of the beam upon bending.

With low cement contents of 2% and 3%, hornfels beam types 75 mm and 100 mm in height and a loading span of 300 mm exhibited comparable flexural strength criteria. This was because of the low cement contents and the bond strength. This indicated that at low cement contents such as 3%, the influence of beam height on the measure of the flexural strength is not significant. However, with high cement contents such as 6% there is a difference due to variation in the beam height. A hornfels beam with a 75 mm height exhibited a higher flexural strength than its reference type of 100 mm. This also indicates that an increase in the beam span-depth ratio from three to four resulted in a significant rise in the material flexural strength properties particularly at high cement contents.

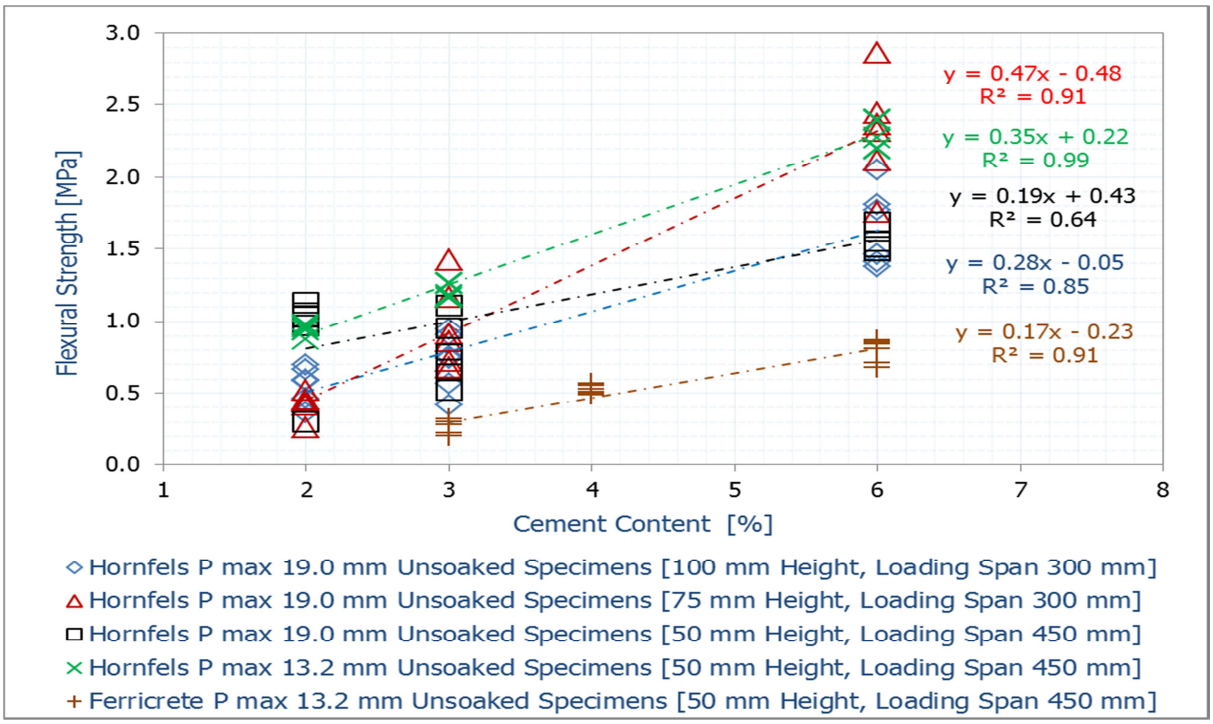

Figure: 5-2 Effect of Maximum Aggregate Size, Beam Geometry and Test Configurations on Material Flexural Strength

The application of high cement contents such as 6% for stabilising materials usually exhibits a tendency similar to lean mixes. Hornfels mix type with 6% cement content registered a compressive strength value higher than that required for C1 material class. The UCS value indicates the effects of over-stabilising a material. The testing of lean mixes [hornfels mix with 6% cement content] using low span-depth ratios of three or four usually result in an increased peak force value over a short range of displacement. This indicates its fracture behaviour and to a degree characterises the material's brittleness. The span-depth ratio and the maximum aggregate size in the mix influence the beam bending criteria [displacement] and its fracture characteristics. The extent to which the beam can resist the applied force is dependent on the particle bond strength, the span-depth ratio and the maximum aggregate size in the mix.

The hornfels beams stabilised using 2% cement with a span-depth ratio of nine, but different maximum aggregate sizes [19.0mm and 13.2 mm] showed comparable flexural strength values. However, upon increasing the cement content in the mix, a significant reduction in flexural strength for the hornfels beam with a maximum aggregate particle size of 19.0 mm and span-depth ratio of nine is realised. A comparison of the beam types with 13.2 mm and 19.0 mm as the maximum aggregate sizes provides insight regarding the effect of cement [particle bond strength] relative to the maximum aggregate size of the flexural strength.

The influence of the span-depth ratios at low and high cement contents is also studied. Varying the span-depth ratios from three to nine, results in an increase in the material's flexural strength. However, this variation ought to be realised along with the maximum aggregate size relative to the beam geometry. The ferricrete beam with 13.2 mm as maximum aggregate size and a span-depth ratio of nine exhibited the lowest overall flexural strength. This was largely due to the quality and type of material. A comparison of the hornfels and ferricrete beams with 13.2 mm as maximum aggregate size and a span-depth of nine showed the differences in flexural properties of the two materials.

5.2.3 Elastic Modulus [28-Day Flexural Modulus]

Using the flexural beam test, the material's elastic modulus was determined. This required the recording of the peak force and its corresponding displacement at the mid span of the beam. Equation 3-10 computes the flexural modulus [i.e. beam flexure mode]. Figure 5-3 illustrates the effect of maximum aggregate size, beam geometric characteristics and test configurations on the elastic modulus of stabilised materials.

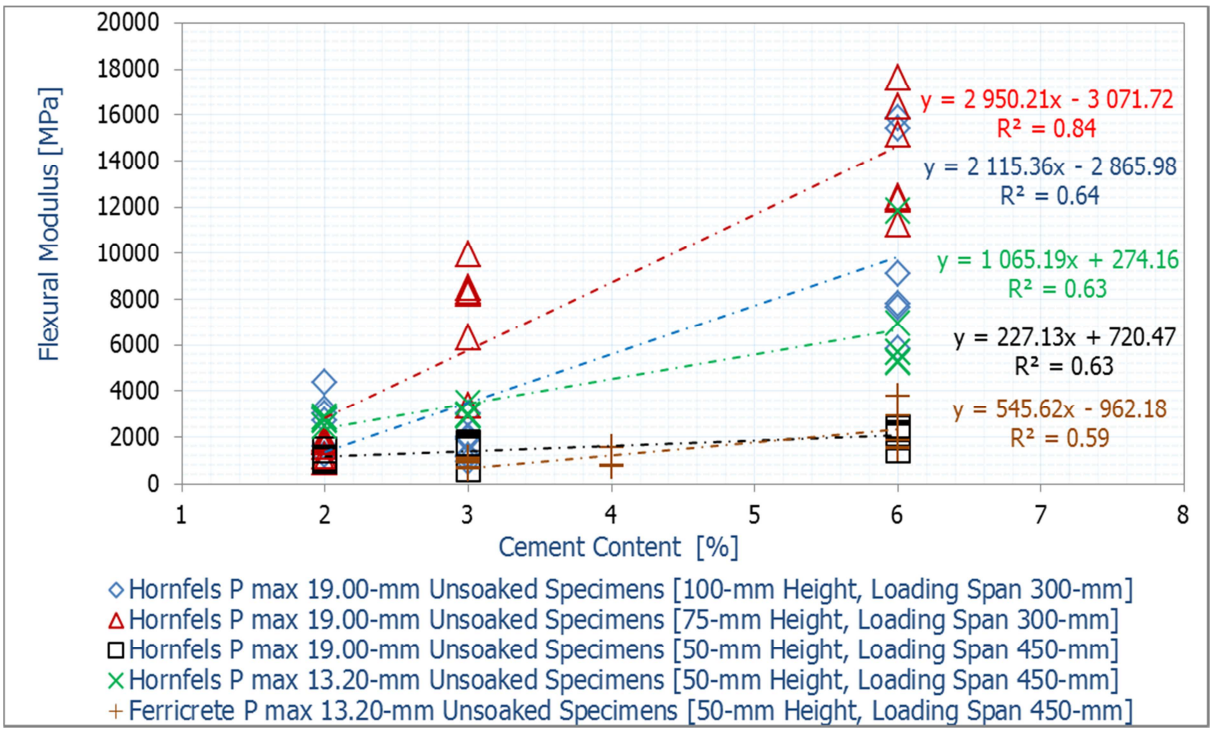

Figure: 5-3 Effect of Maximum Aggregate Size, Beam Geometry and Test Configurations on Material Flexural Modulus

A hornfels beam with a height of 75 mm, span-depth of four and 19.0 mm as its maximum aggregate size exhibited a high overall elastic modulus. This was significant with 3% and 6% cement in the mix. With 2% cement content in the hornfels mix, a comparable elastic modulus criterion is realised. With 2% cement content in the hornfels mix, all beams showed comparable elastic modulus values despite the significant differences in their geometry, maximum aggregate sizes and test configurations. The addition of cement to the hornfels resulted in a corresponding increase in its elastic modulus. Following the use of cement content higher than 2%, differences in elastic moduli were realised. This provides insight regarding the low particle bond strength relative to the cement content and material as well as its fracture characteristics.

With higher cement contents than 2%, differences in the elastic modulus and flexural strength values are realised. This indicates that with low binder content in the mix the mechanical strength and modulus are more or less comparable despite the differences in

beam geometry and test configurations. With 3% cement in the hornfels mix, the beam with a height of 100 mm and span-depth ratio of three compared well with the beam with a height of 50 mm and a span-depth of nine. With 6% cement in the mix, significant differences in elastic moduli between the beam types are realised. This is due to the resultant effect emanating from the differences in the span-depth ratio and maximum aggregate size at high cement content. The consideration of low span-depth ratios of three and four as test configurations provide higher elastic modulus values than span-depth ratio of nine. This is dependent on the level of stabilisation i.e. amount of cement in the mix relative to the quality of material, beam geometric characteristics and loading rate among others. With 6% cement in the hornfels mix, the beam with a span-depth ratio of four and a height of 75 mm exhibited a higher general increase in elastic modulus than the beam type with a span-depth ratio of three and a height of 100 mm. However, at low cement content of 2.0% the beam types with a height of 75 mm and 100 mm exhibit a comparable elastic modulus criterion. This indicates that amount of cement used to stabilise the material influences the resultant elastic moduli. Other influential factors such as the achieved density of the beam play a significant role on the resultant flexural strength and ultimately, the elastic modulus.

The hornfels beam with a height of 50 mm comprising of 19.0 mm as the maximum aggregate size and a span-depth of nine showed no significant increase in elastic moduli even with high cement contents. The hornfels beam with 13.2 mm as the maximum aggregate size and a span-depth ratio of nine shows increased elastic moduli trends compared to the beam type with 19.0 mm and of similar span-depth ratio of nine. The influence of the maximum aggregate size, beam geometric characteristics on the mechanical properties of the cement-stabilised materials is illustrated. The presence of 19.0 mm as the maximum aggregate size of a beam type with a height of 50 mm generates localised zone of weakness. These localised zones certainly influence the fracture criterion particularly as the beam deflects upon loading. The localised zones of weakness due to the effect of the maximum aggregate particle size provide easy-channelled paths where cracks can propagate.

The ferricrete and hornfels beam types with a height of 50 mm and 13.2 mm as maximum aggregate size tested at a span-depth ratio of nine characterise the elastic moduli of the materials. Similarly, the differences between the materials in terms of the elastic moduli are depicted. The R^2 values signify the significance of the test data. An increase in cement content to the mix shows intensified scattering of the data points. The scattering of data points is significant with high cement dosages. These trends indicate the fracture criteria of the various mix types relative to their cement content, beam geometric characteristics, maximum aggregate size, density and loading span.

5.2.4 Beam Shear Stresses and Measure of Engineering Properties

In this research, the application of Equation 3-4 is to assess the influence of beam shear stress. The derivation of the equation results from the fundamentals of engineering mechanics. Figure 5-4 shows the resultant shear stresses using Equation 3-4. The results illustrated that there was an increase in beam shear stress corresponding to a decrease in the span-depth ratio; this corresponded with an increase in cement content to the mix. An increase in the span-depth ratio resulted in a corresponding reduction in the beam's shear stress. All beam types with a span-depth ratio of 9.0 exhibited the lowest shear stress. This was significant with high cement contents added to the mix.

The beams with span-depth ratios of three and four showed comparable shear stress with 3% cement content in the mix. With 2% cement in the mix, all beams exhibited statistically similar shear stress values. However, at higher cement contents than 2% a variation in shear

stress occurred. This further provides insight regarding the application of low cement content and the resultant material behavioural properties.

The beam types loaded at a span-depth ratio of nine and 50 mm in height, with either 19.0 mm or 13.2 mm illustrated the influence of the maximum aggregate size relative to the beam geometry. The inclusion of 19.0 mm as the maximum aggregate size reduced the shear stress. The inclusion of 19.0 mm as the maximum aggregate size also reduced the flexural strength and elastic modulus values compared to when 13.2 mm was the maximum aggregate size. The ferricrete and hornfels beam types with a height of 50 mm loaded at a span-depth ratio of nine containing a 13.2 mm as the maximum aggregate size, show the influence of the material's quality on the shear stress. This indicates that the quality of material plays a significant role on the resultant flexural strength, elastic moduli and shear stress.

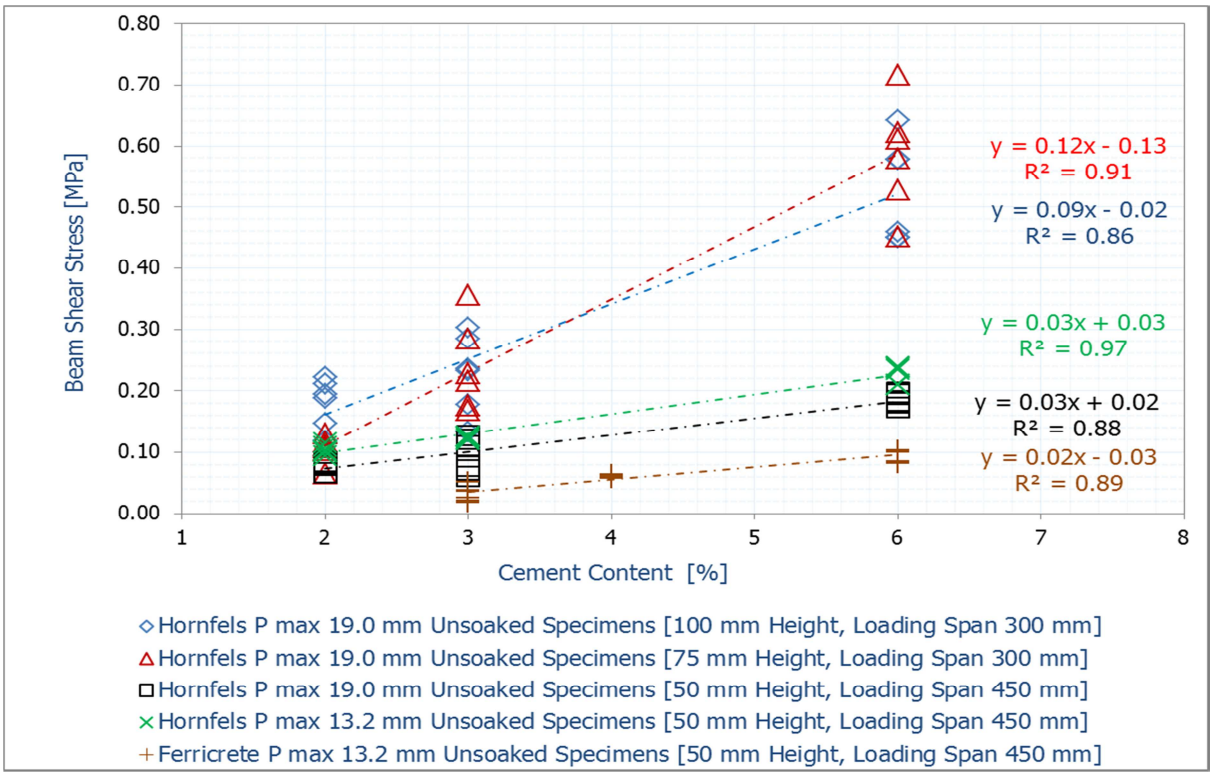

Figure: 5-4 Resultant Beam Shear Stresses [Beam Geometrics and Test Configurations]

The quality of particle distribution as illustrated by the CT scans of ferricrete and hornfels provided insight regarding the probable mechanical properties and particle interlock. Particle interlock influences the crack propagation. This also influences the resultant magnitude of the beam shear stress. The addition of more cement to material resulted in a corresponding increase in the shear stress of the beam. This implies that an increase in mechanical strength for specific test configurations and beam geometric characteristics resulted in a corresponding rise in the shear stress in the beam. A number of factors influence the material mechanical strength and include [but are not limited to]:

a) particle size distribution, i.e. maximum aggregate size and fines content
b) cement content, i.e. particle bond strength
c) span-depth ratio, i.e. loading span and height of the beam
d) general material characteristics and properties

In order to analyse the influence of shear stress in a beam, finite element modelling [FEM] was undertaken. The objective of the FEM analysis was to investigate beyond the laboratory-acquired test ranges in order to gain insight regarding the beam deflection and its load

response. By considering the elastic modulus of the material as an input into the FEM model, an investigation of the shear stresses in the beam was undertaken. From the laboratory testing, the addition of cement to material indicated that there was a corresponding increase in the material's elastic modulus and its flexural strength. Figure 5-4 shows that the addition of more cement to the material resulted in a corresponding increase in the shear stress. Figure 5-5 illustrates the modelled results and assumes that the material is homogeneous. The inner loading rollers were free rotating while one of the seating rollers is fixed and another is allowed rotate freely. Figure 5-4 provides different trends compared to Figure 5-5. Several factors related to the heterogeneity of the stabilised materials and the adopted testing criteria influence the outcomes shown in Figure 5-4. Figure 5-5 exhibits linearity trends, which characterises the assumptions made, including considering that the material is homogeneous besides the boundary conditions adopted in the model.

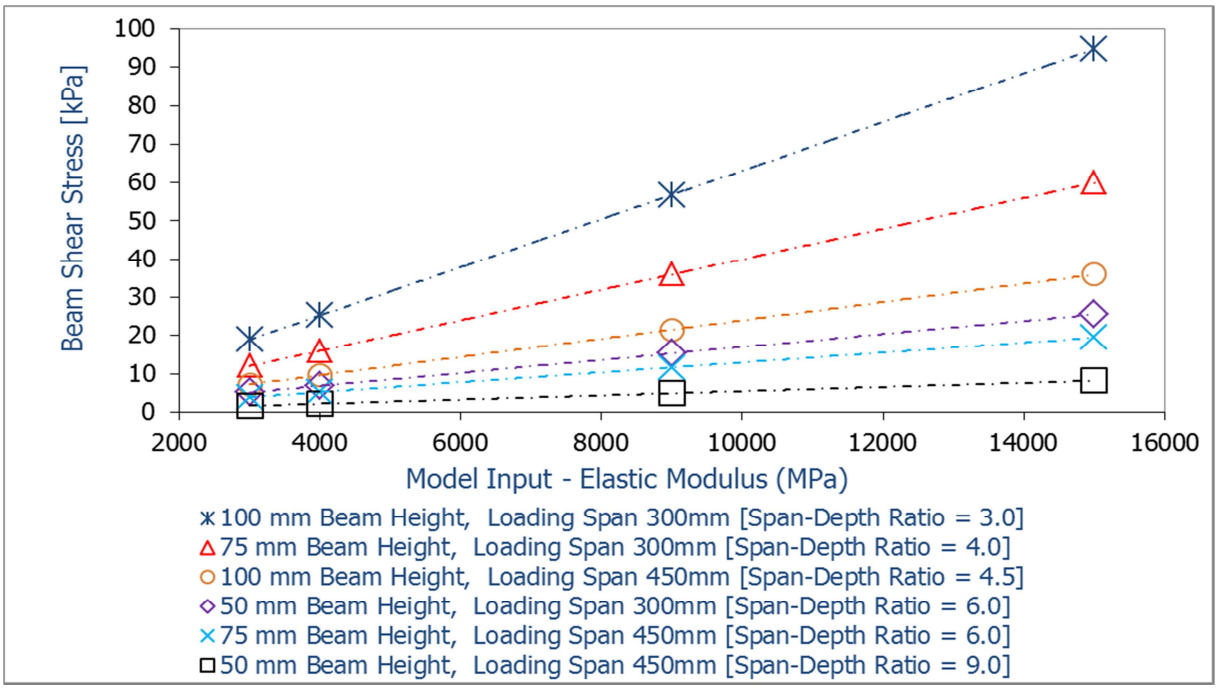

Figure: 5-5 Influence of Span-depth Ratio and Resultant Beam Shear Stresses [FEM Modelling]

Figure 5-5 illustrates that an increase in the material's elastic moduli resulted in a corresponding rise in the shear stress. Cognisance of the boundary conditions along with the assumptions made, are noted. The increase in shear stress corresponded with a decrease in the span-depth ratios. The beam types with a span-depth ratio of three exhibited high overall shear stresses at increasing elastic moduli. The beam types with a span depth ratio of nine registered the lowest overall shear stress values at increasing elastic moduli. The beam types with a similar span-depth ratio of six exhibited differences in the shear stress due to the effect of the beam height. A beam height of 75 mm showed lower shear stress than one with a height of 50 mm loaded at a span-depth ratio of six. The beams with heights of 75 mm and 50 mm loaded at the span-depth ratio of six illustrated the influence of the beam geometric characteristics on the measure of the engineering properties of stabilised materials.

Figures 5-6 and 5-7 show the models with span-depth ratios of three and nine respectively following the four-point loading technique. A visual insight regarding the influence of the beam height relative to loading span and the resultant deflection criteria is illustrated. As the beam deflects, cracking emanates from its bottom end located at mid-span where the exterior fibres experience maximum tensile stress. This is the region of the crack. In comparison, Figure 5-8 shows the laboratory testing criteria. The measurement of the

deflection of the beam at mid-span made use of the linear variable displacement transducers [LVDTs]. Figures 5-8 and 5-9 show the beam types and the region of crack. During the flexural beam testing, the fracture criteria exhibited by hornfels differed from that characterised by the ferricrete. Hornfels exhibited a staggered crack while ferricrete exhibited a clean crack. This observation provides insight regarding the aggregate interlock relative to material quality and their fracture behavioural properties between crushed aggregate and soil.

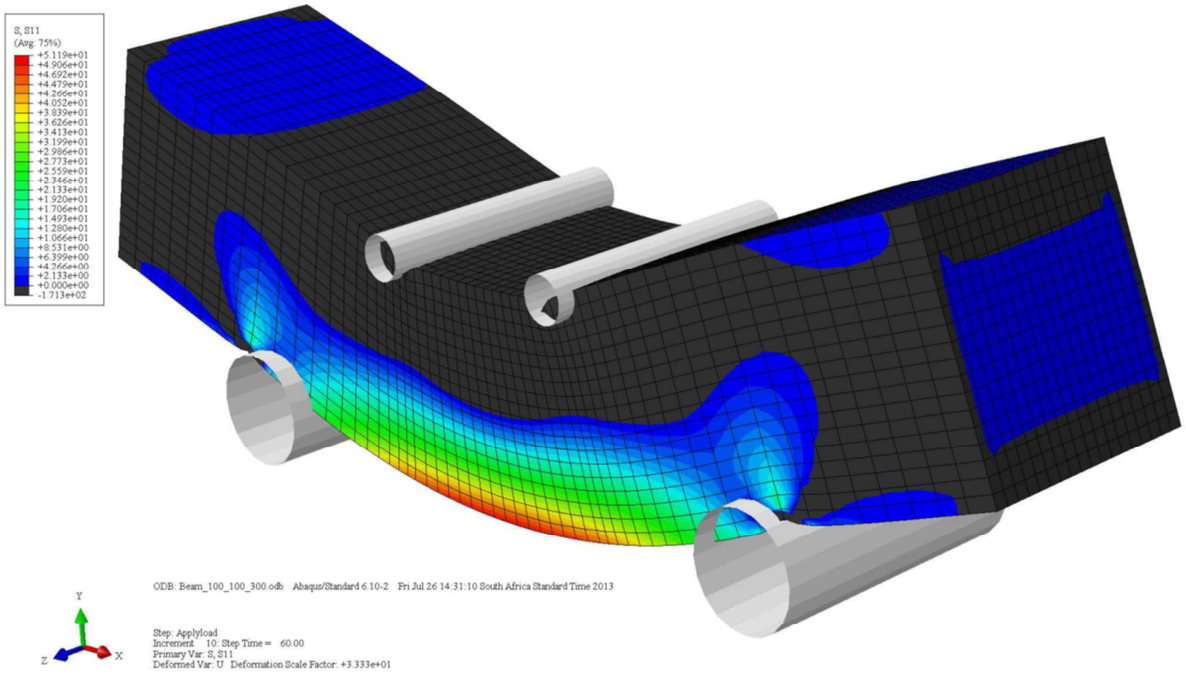

Figure: 5-6 Beam Type with Span-depth Ratio of 3 [Beam Type of 100 mm Height, 300 mm Loading Span - FEM Modelling]

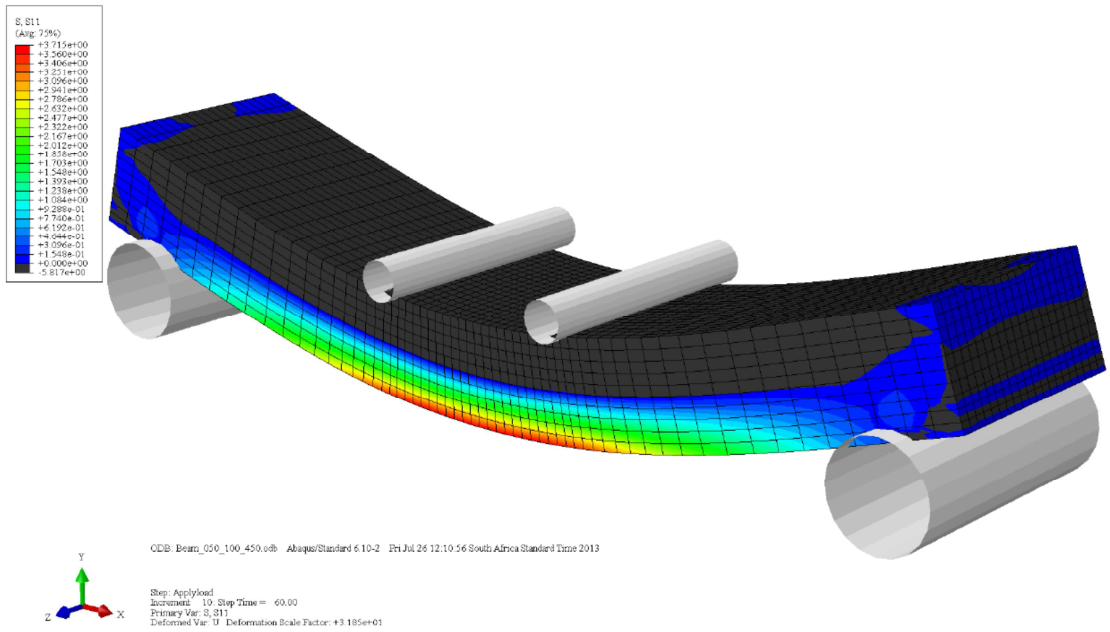

Figure: 5-7 Beam Type with Span-depth Ratio of 9.0 [Beam Type of 50 mm Height, 450 mm Loading Span - FEM Modelling]

Figure: 5-8 Flexural Beam Testing Criteria [Beam Type with Span-depth Ratio of 9.0 i.e. 50 mm Height, 450 mm Loading Span]

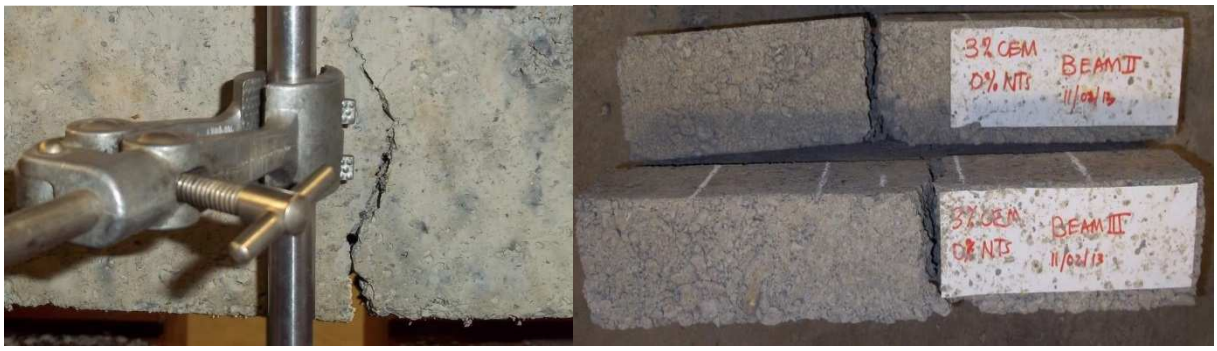

Figure: 5-9 Defection Measurement LVDT and Cracking Criteria [Region of Crack]

In order to gain further insight into the influence of beam geometry, maximum aggregate size and test configurations an assessment of the shear modulus was necessary. Shear modulus quantifies the material's shear stiffness. This provides further insight regarding the beam response to shear stress. By applying Equation 3-6, the shear modulus of the various beam types was determined. This required the determination of the flexural modulus [as the elastic modulus, E value] and an assumed Poisson ratio of 0.25. Figure 5-10 shows the shear modulus trends at varying cement contents. The addition of more cement to the material resulted in an increase in the shear modulus.

Hornfels beam type with a height of 75 mm loaded at a span-depth of 4 provided the highest overall shear modulus. Hornfels beam type with a height of 50 mm and 19.0 mm as the maximum aggregate size provides the least shear modulus of the hornfels mixes. This illustrates the influence of the maximum aggregate particle size on the resultant shear modulus. The particle-to-particle interaction relative to the maximum aggregate size is realised. The influence of the maximum aggregate size and the span-depth on the shear modulus is illustrated. Hornfels and ferricrete beam types with 13.2 mm as the maximum

aggregate size evaluated using a span-depth ratio of nine, illustrate the differences between the material types such as particle size distribution.

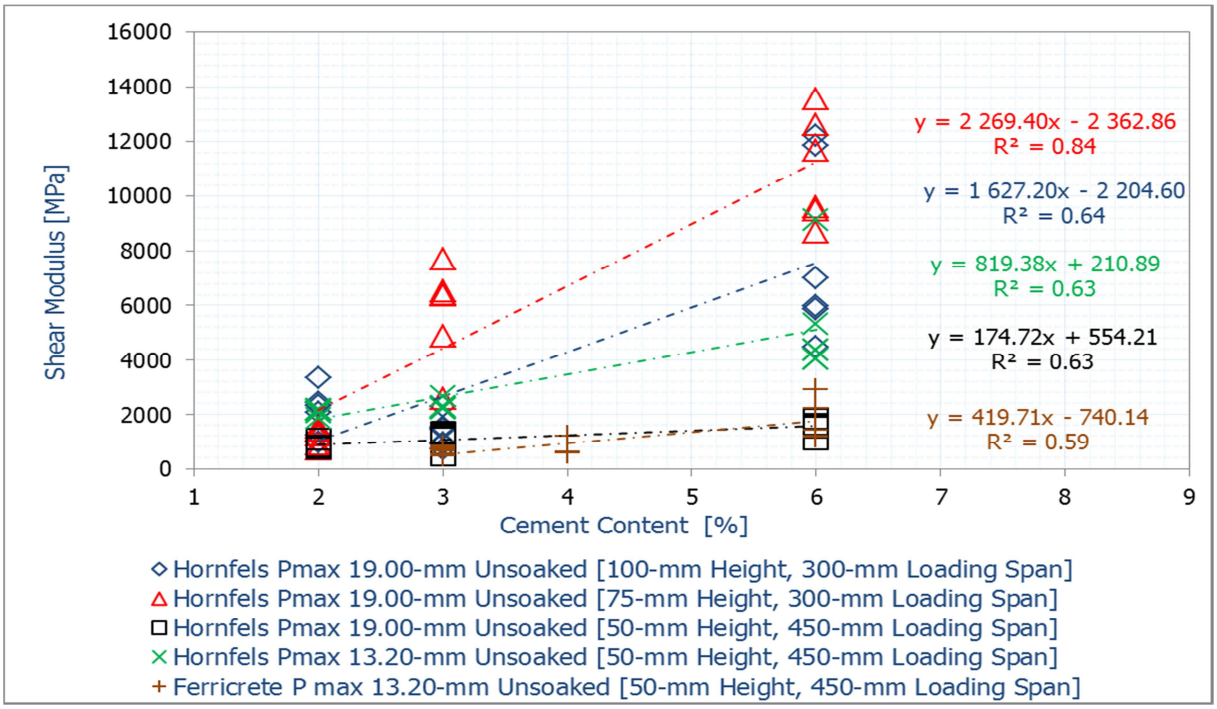

Figure: 5-10 Shear Moduli [Stiffness and Deformation Criteria]

An increase in the span-depth ratio resulted in a corresponding decrease in the beam's shear modulus. However, this was dependent on the maximum aggregate size and cement content in the mix. With low cement contents in the mix, the resultant shear modulus values were comparable. The addition of more cement to the material resulted in an increase in shear modulus. The ferricrete and hornfels beam types with 13.2 mm as the maximum aggregate size and evaluated using a span-depth ratio of nine characterise the effect of material type and test configurations on the flexural strength and modulus.

The standardisation of the flexural beam test must define the test configurations relative to the beam geometric characteristics including the maximum aggregate size. Variations of the beam geometry and test configurations influence the actual measure of the engineering properties of the stabilised materials. This eventually influences the design input parameters into the mechanistic pavement design. The need to quantify the actual properties of the stabilised materials and design input parameters remains the essential focus of both research and the road industry. This research considers the beam type with a span-depth ratio of nine, comprising of 13.20 mm as the maximum aggregate size for further analysis. This beam type not only exhibits a reduced shear stress criterion, but also provides a realistic measure of the engineering properties of cement-stabilised materials.

5.2.5 Strain-at-Break [28-Day Cured Beams]

The calculation of the tensile strain-at-break uses the deflection data obtained from the flexural beam test. Figure 5-11 illustrates the strain-at-break results of the various beam types at varying cement contents. A corresponding increase in strength and stiffness resulted following the addition of more cement to the material. However, the rate of strength increase is dependent on the material quality and type. Factors such as density, the amount of cement and the overall strength contribute to the degree of fracture. This is because the particle bond strength is dependent on several factors including the achieved density relative to the cement content in the mix. Addition of more cement to the material results in a

reduction in strain-at-break. In Figure 5-11 all beam types exhibit a reduction in the strain-at-break corresponding to the addition of more cement to the material.

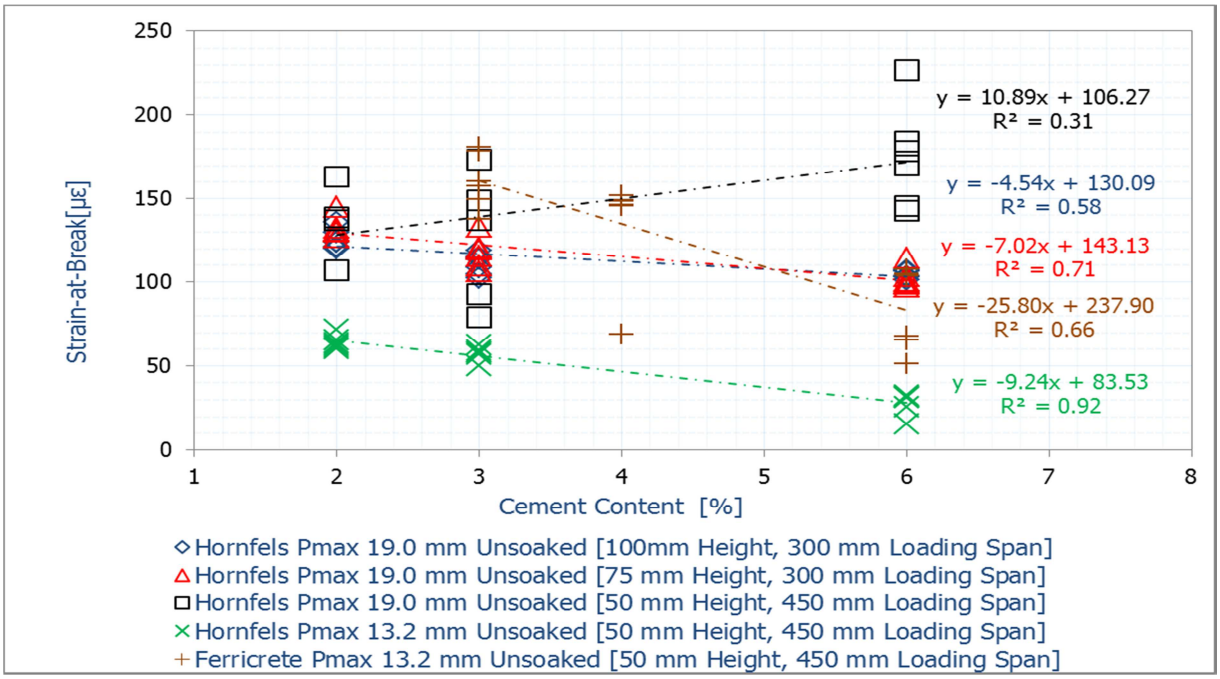

Figure: 5-11 Strain-at-Break [Brittleness versus Flexibility Properties]

On the contrary, the hornfels beam type with a 50 mm height and loaded at a span-depth ratio of nine with a maximum aggregate size of 19.0 mm showed an increase in strain-at-break. An assessment of trend and the R^2 value of this hornfels beam type with 19.0 mm display scattered data points. The scattering of the data points increased following the use of high cement dosages. This established that a beam type with 19.0 mm and loaded at a span-depth ratio of nine lacked the particle bond strength to undertake the monotonic load and the required stiffness to resist fracture. However, the observed trend could lead to an erroneous interpretation of its strain-at-break. A statistical assessment of the individual mix types was required to account its variance at the specified cement contents. Six specimens per mix variable were prepared. Statistically, this beam type with 19.0 mm as the maximum aggregate size and loaded at a span-depth ratio of nine did not exhibit any significant change in the strain-at-break values. The observed increase was due to the interaction of the aggregate-to-aggregate contact amidst a cement matrix.

The beam types with span-depth ratios of three and four with different beam heights of 75 mm and 100 mm showed comparable strain-at-break criteria. Both beam types contained a maximum aggregate size of 19.0 mm. The hornfels beam type with 13.2 mm as the maximum aggregate size and a span-depth of nine showed a gradual reduction in the strain-at-break at increasing cement contents. The ferricrete beam type with 13.2 mm as the maximum aggregate size and span-depth ratio of nine showed the lowest strain-at-break trend. This indicated that the maximum aggregate size relative to the beam geometric characteristics and material quality influenced the fracture behavioural properties. The particle bond strength, density of the beam and cement content also influenced the fracture behavioural properties.

To an acceptable degree, the strain-at-break value provides insight into the load response and the level of brittleness exhibited by a mix. Cement alters the material's strength and elastic properties, which influences its load response and fracture characteristics. The ferricrete beam type exhibited higher strain-at-break values at varying cement contents than its equivalent hornfels beam type. This indicates the effect of the material's quality on the

strain-at-break criteria, particularly its plasticity, particle size distribution and cement effectiveness.

5.2.6 Fracture Energy [28-Day Cured Beams]

This section assesses the fracture energy as the area under the stress-strain curve. For the calculation of the fracture energy, MATLAB software was applied as shown in Figure 5-12. Figure 5-13 illustrates fracture energy calculation criteria obtained from the MATLAB software. The stress-strain curve does not start from zero because a minimum seating is required in order to test using this machine. The area under the curve i.e. from the start of the test to the peak force represents the fracture energy. For each beam type, the fracture energy is calculated. Figure 5-14 presents the fracture energy results at varying cement contents.

```
% Import your data
file=importdata('BeamData/Beam_2_6CEM_G5_Unsoaked_50mm_450mm_13.20mmMax_Ferricrete.txt');
x_data=file(:,2);
y_data=file(:,1);

format long

% Plot Data
hold on
plot(x_data,y_data,'.r')

% Integrate up to y_max
y_max=max(y_data(:,1));
index=find(y_data(:,1)==y_max);
FE=trapz(x_data(1:index,1),y_data(1:index,1))
area(x_data(1:index,1),y_data(1:index,1))

% Find x&Y 35% of y_max
y_35=0.35*y_max;
index=find(y_data(:,1)>y_35,1,'first');
y_upper=y_data(index,1); x_upper=x_data(index,1);
y_lower=y_data(index-1,1); x_lower=x_data(index-1,1);
x_35=interp1([y_upper y_lower],[x_upper x_lower],y_35)
plot(x_35,y_35,'.g')
y_lower=y_data(index-1,1)
```

Figure: 5-12 Calculation of the Fracture Energy using the MATLAB Software [Python]

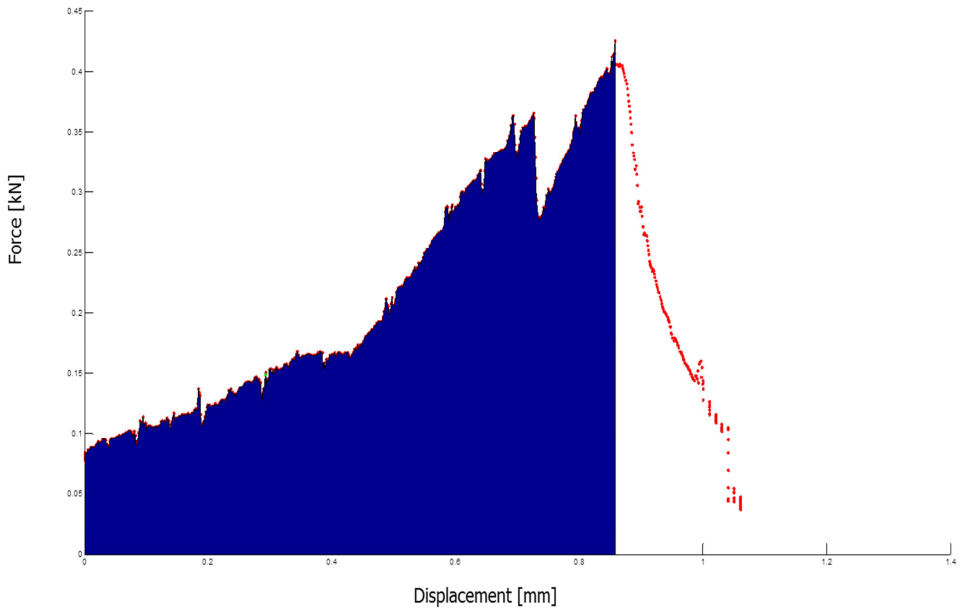

Figure: 5-13 Fracture Energy Calculation Criteria using the MATLAB Software

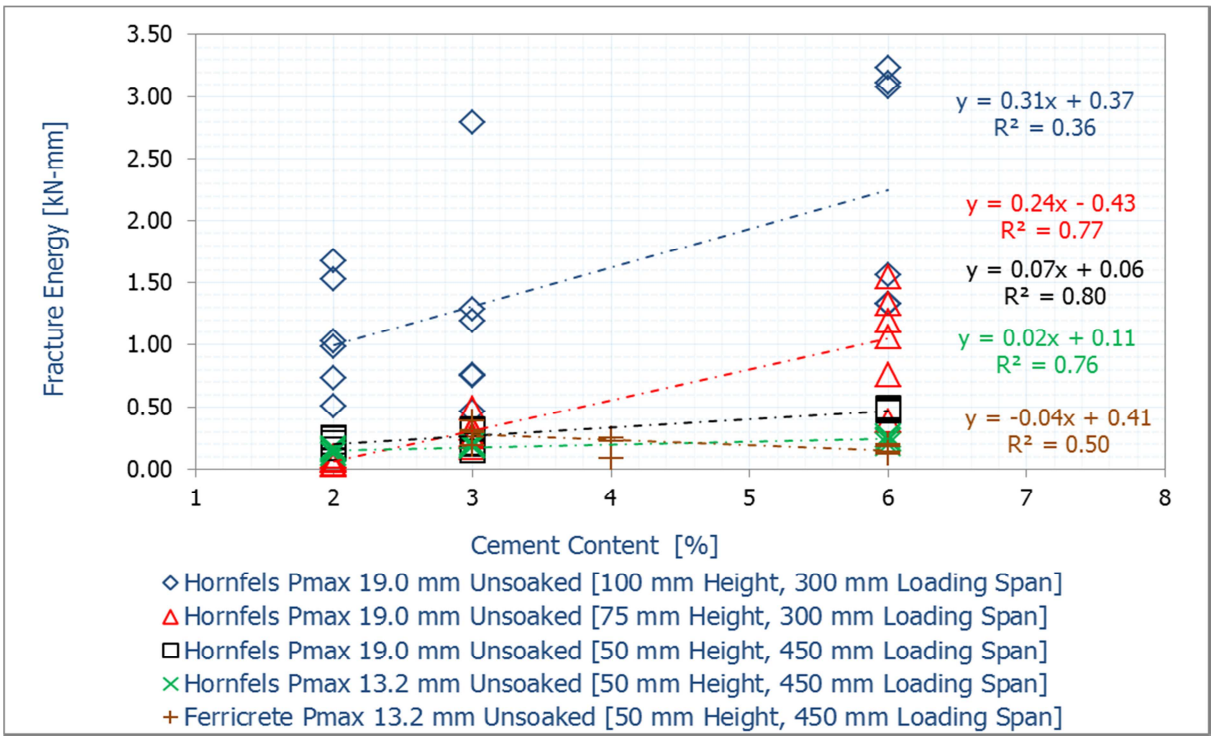

Figure: 5-14 Fracture Energy [Fracture Behaviour]

From the various fracture mechanics research including Mindess [1996], the propagation of cracks in cementitious materials, usually exhibits a low regression coefficient [R^2 value]. Cement-stabilised materials are brittle. Under compression, the stabilised materials exhibit great compressive values but under tension behave differently. A number of factors, including the particle bond strength and shrinkage cracking influence the material's resistance to fracture when loaded. The R^2 values range from 0.8 to as low as 0.36 depending on the mix type, test configurations relative to the beam geometry and maximum aggregate size.

Modern materials science considers fracture energy is a tool applied to assess the mechanical performance of stabilised materials. From the fracture energy results, the following interpretations are made:

a) reducing the span-depth ratio [typically the loading length and beam height] results in an increase in the fracture energy, however this should be undertaken in proportionate to the maximum aggregate size
b) the maximum aggregate size relative to the beam geometry significantly influence the resultant fracture energy

In characterising the fracture behavioural properties of stabilised materials, an assessment of the adopted test configurations relative to the specimen geometry is essential. This is because an erroneous consideration of any of these factors could lead to misinterpreting the material behavioural properties and thus wrongful application. For instance, the inclusion of a large aggregate size in a small specimen not only reduces the strength and elastic modulus properties but the fracture energy. The misinterpretation could lead the designer to consider high cement content or alternative material types. Significant differences between the beam types with 13.2 mm and 19.0 mm as maximum aggregate size are realised. Similarly, the consideration of low span-depth ratios not only results in a low flexural strength and high elastic modulus with increased internal beam shear stress but also leads to intensified fracture energy. This might erroneously indicate that the material possesses a substantial degree of fracture toughness and thus, a good performance criterion. Figure 5-15 displays

the mid-span of the hornfels beam type with a 50 mm height and comprising 19.0 mm as the maximum aggregate size.

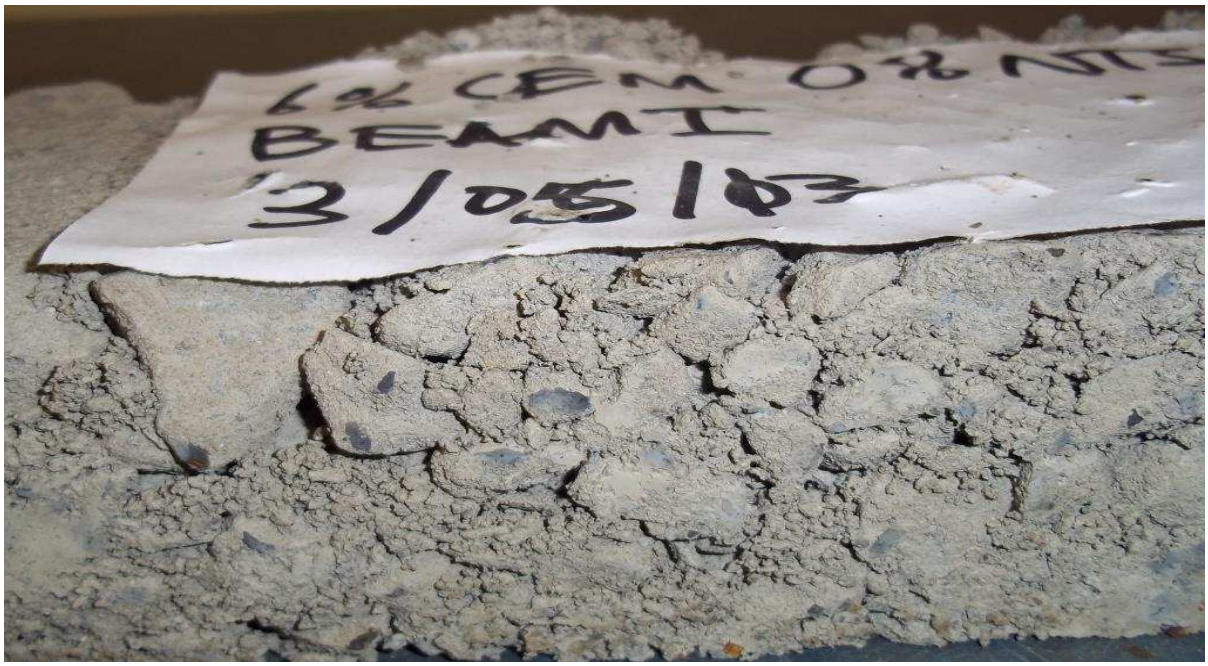

Figure: 5-15 Effect of Maximum Aggregate Particle Size and Beam Geometry [Hornfels 50 mm Height with Pmax 19.0 mm Beam Type]

5.2.7 Moisture Susceptibility

Moisture influences the stability and properties of stabilised materials. The effect of moisture ingress on the flexural strength and overall mechanical properties was undertaken. The objective of the evaluation was to provide improved insight regarding the material and test data interpretation. This experimentation considered beam types with the highest dry density. Hornfels beam type with a 75 mm height and 19.0 mm as the maximum aggregate size loaded at 300 mm was undertaken. The experimentation included soaking the beams for four hours before testing after 28 days of curing. Figure 5-16 shows the effect of moisture ingress on the flexural strength properties of stabilised materials. Figure 5-17 shows the effect of moisture ingress on the elastic modulus [stiffness properties]. Figure 5-18 illustrates the effect of moisture ingress on the strain-at-break.

By comparing soaked and un-soaked beam types, insight regarding moisture ingress and the resultant engineering properties of stabilised materials are obtained. Soaking, the beams for four hours in a water bath showed a variation in the engineering properties. From this experimentation, the following interpretations were gathered:

a) with the ingress of moisture into the beam a reduction in the flexural strength resulted and this was significant at high cement contents
b) an assessment of the soaked and un-soaked beams showed that the resultant elastic modulus was comparable
c) in terms of the strain-at-break criterion, water ingress into the beams resulted in an increase in the strain-at-break

The moisture and/or water ingress into the material matrix reduced the stability, particularly the particle bond strength. The addition of more cement to material enhanced the particle bond strength but the counteracting effects from moisture ingress contributed significantly to low strength levels. As a result, a reduction in the mechanical strength properties attributed to the ingress of moisture into the material matrix occurred. A reduction in the particle bond strength led to decreased brittleness within the material matrix. This changed the fracture

behavioural properties as characterised by the elastic modulus criteria and the significant increase in the strain-at-break.

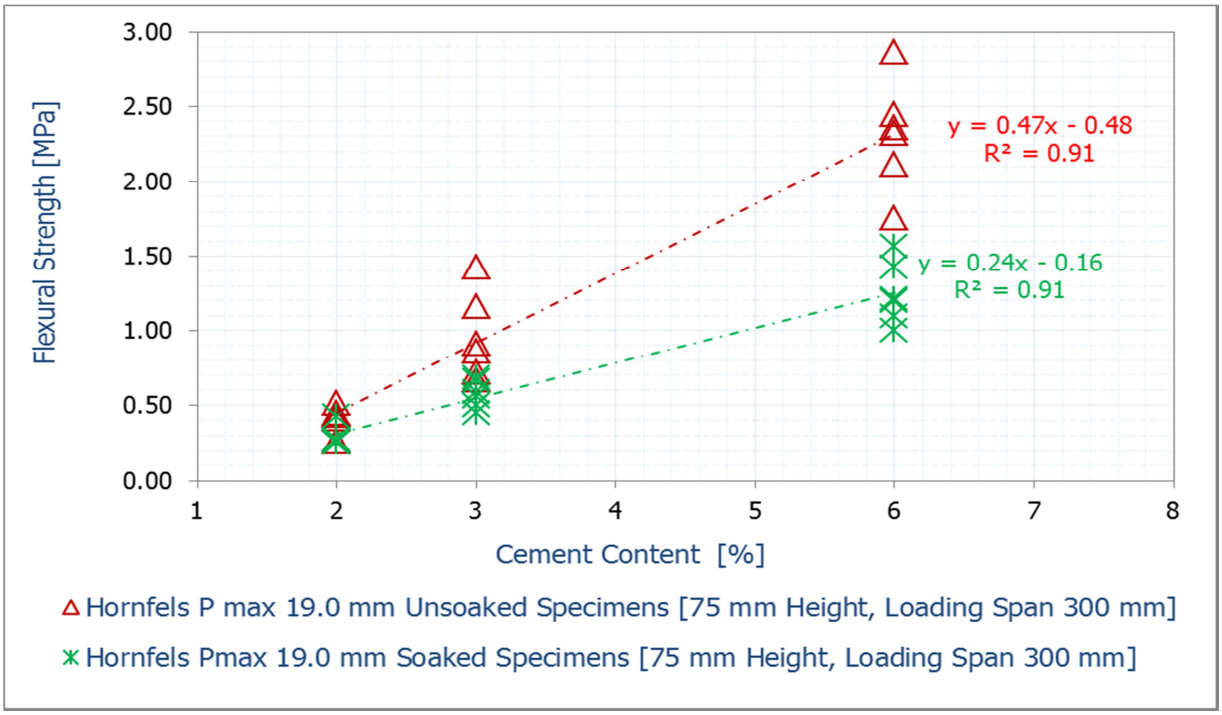

Figure: 5-16 Effect of Moisture on Material flexural Strength Properties

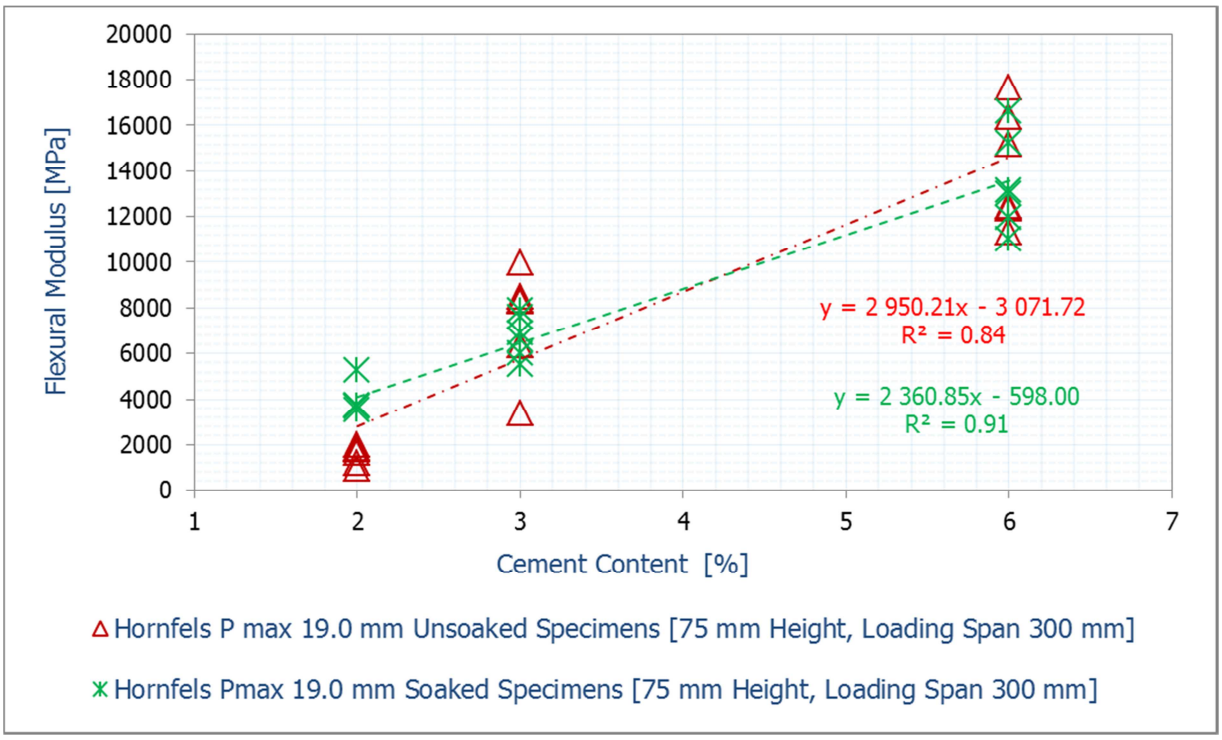

Figure: 5-17 Effect of Moisture on Material Elastic Moduli Properties [Stiffness Properties]

The exhibited trends of soaked and un-soaked elastic moduli were due to the interaction between the cement and the material particles with and without moisture. The resultant particle bond strength following the ingress of moisture was dependent on the curing conditions, cement content in the mix and the quality of the material. The amount of voids in the beam influenced the infiltration of water into the inner matrix. A low density is usually associated with a high amount of pores in the mix. An interconnected pore structure allows

quick saturation of moisture leading to the instability of the material and other durability related distresses.

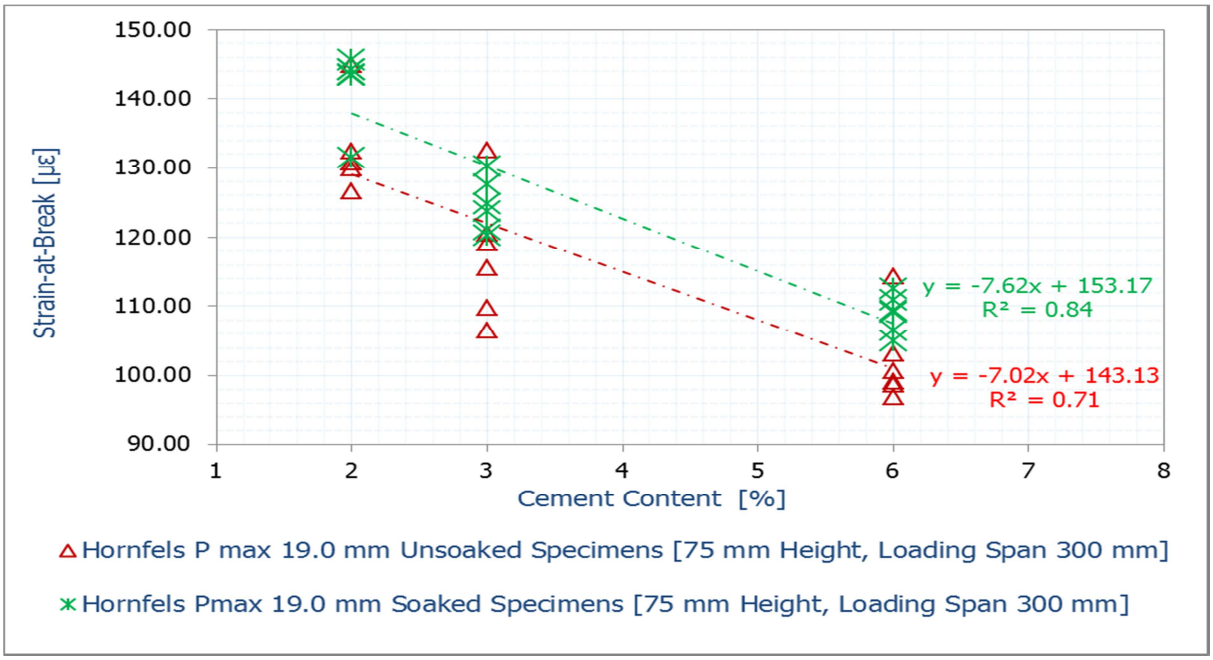

Figure: 5-18 Effect of Moisture on Strain-at-Break

The moisture within the matrix contributes to the cement hydration process. In excess moisture could affect the stability of the material. The level of strength increase due to continued hydration is dependent on cement content and the available moisture in the mix. The elastic modulus, which measures the resistance of material to deform, is dependent on the nature of particle bond strength after 28 days of curing. A stiffer material exhibits higher elastic modulus. Additionally, a stiffer material usually undergoes some degree of shrinkage and result in cracks depending on the imposed restraints. This influences the flexural strength measure, fracture behavioural properties, as well as the infiltration of water. Moisture ingress into the stabilised material contributes to the instability [i.e. deterioration] of the cement-stabilised layer; this could lead to durability related distresses.

By applying the regression equations in Figures 5-16, 5-17 and 5-18, the retained flexural strength, modulus and strain-at-break are assessed as a ratio of soaked and un-soaked values at varying cement contents.

a) A reduction in the retained flexural strength at an increasing cement content, result; 70% [2% cement], 60% [3% cement] and 54% [6% cement] is assessed. The retained flexural strength results indicate a loss in mechanical strength following an increase in cement content. This attributed to a number of factors, including the resultant microstructure of the stabilised material following an increase in cement content. This suggests that there is a possibility to alter the microstructure at high cement contents resulting in a capillary pore structure, which enhances the ingress of water i.e. the effect of meniscus.
b) An increase in the retained flexural modulus is observed at low cement contents of 2.0% and 3.0%. With a cement content of 6.0%, retained flexural modulus is 93%. This provides insight into the effect of moisture on the mechanical properties of cement-stabilised materials.
c) A general increase in the retained strain-at-break of about 7% is computed. This indicates that as water infiltrates the matrix of the cement-stabilised layer, its mechanical strength is reduced. However, the stabilised layer flexural modulus [i.e. stiffness properties] is more or less affected depending on the cement content in the mix. The

effect of water ingress on the mechanical strength and stiffness properties suggests that moisture affects the particle bond strength and the resultant effect is dependent on amount of cement in the mix.

5.3 Factors for the Selection of Beam Geometry and Test Configurations

The understanding gathered from the Timoshenko beam theory and experimentation provides insight regarding the factors influencing the flexural beam test and its measure of the properties of materials. The need to standardise the flexural beam test does not require any further emphasis. This is because maximum aggregate sizes relative to the beam geometry significant influenced on the measure of the flexural strength, elastic moduli, strain-at-break value, as well as the fracture behavioural properties. The maximum aggregate size directly influences the dry density of the material. Dry density influences the material's permeability, shrinkage, strength and other engineering properties. Therefore, specifying the beam geometry with a maximum aggregate size along with the appropriate test configuration was necessary. The Appendix provides the flexural beam test configurations along with beam geometry and maximum aggregate particle size in the mix.

Following the insight gathered such as the resultant shear stresses relative to the span-depth ratio, additional evaluation and analysis considers the beam type with heights of 50 mm and 100 mm with different maximum aggregate size and span-depth ratios. The beam type with a height of 100 mm and a span-depth of three is used by the Australian practice to characterise cement-stabilised materials. The introduced beam type with a height of 50 mm comprising of a 13.20 mm as the maximum particle size and evaluated at a span-depth ratio of 9.0 provides the least shear stresses. Figure 5-19a compares the flexural modulus of the beam types to the compression modulus [secant modulus].

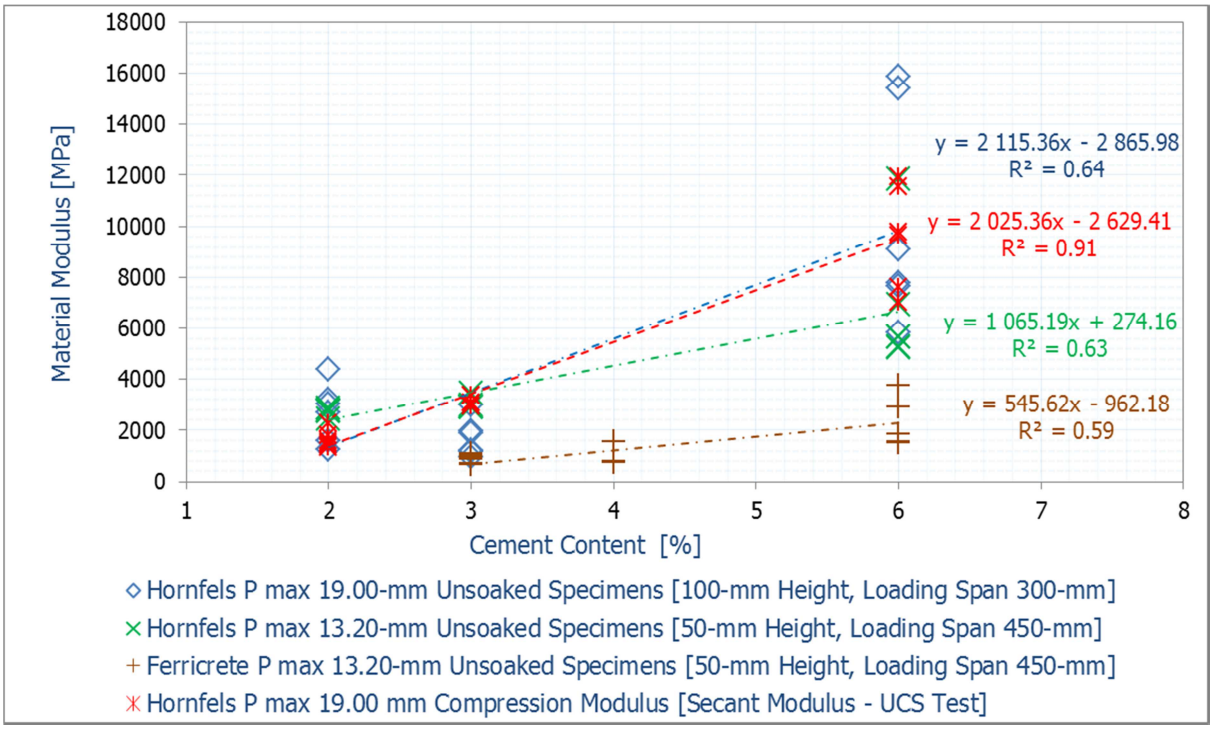

Figure: 5-19a Flexural Modulus versus Compression Modulus

The compression modulus [secant modulus] is comparable to the flexural modulus when using the 100 mm beam type with a span-depth ratio of three. Figure 5-19b illustrates that at low cement contents, the flexural modulus is comparable to the compression modulus. However, at high cement contents such as 6.0% scattered data points are obtained. This indicates the differences between the flexural strength and UCS test i.e. the applied test

mode relative to specimen geometry and aging. Cement-stabilised materials characteristically show an increase in strength with time. This is dependent on the cement content as well as the type and quality of the natural materials considered for stabilisation. Figure 5-19c illustrates the comparison between the compressive and flexural strength.

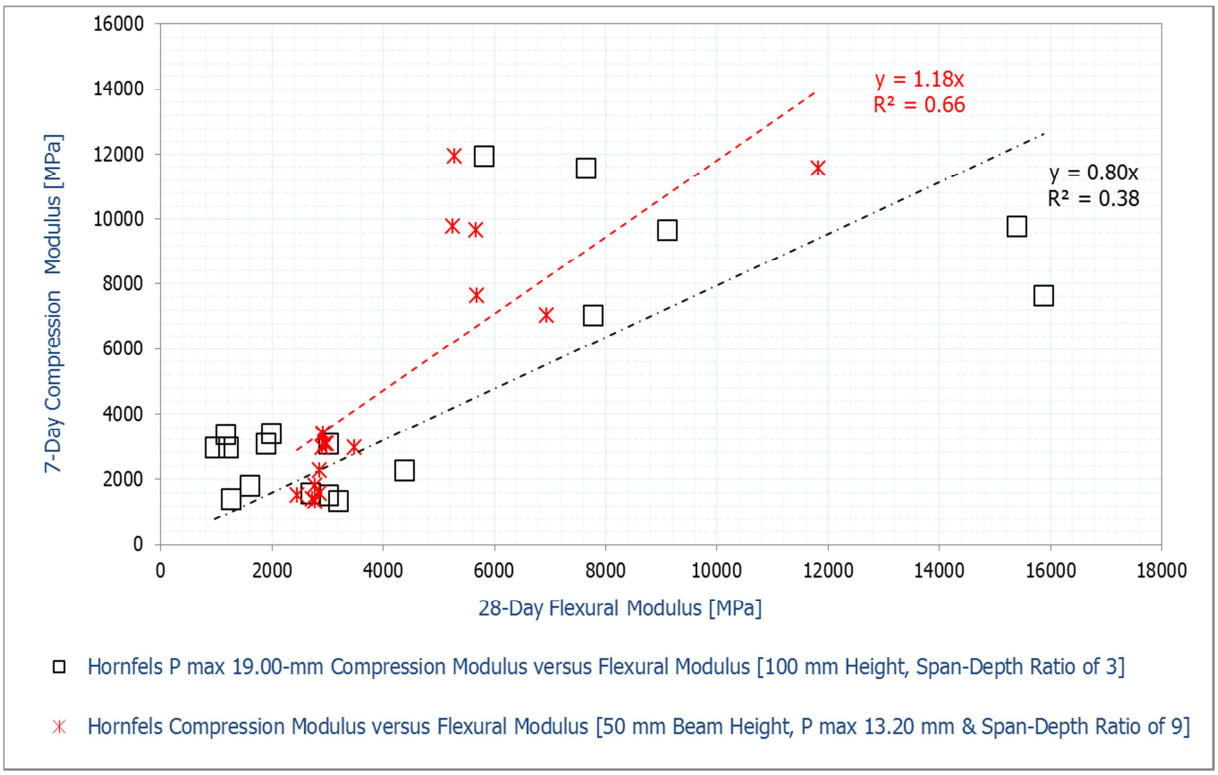

Figure: 5-19b 7-Day Compression Modulus versus 28-Day Flexural Modulus

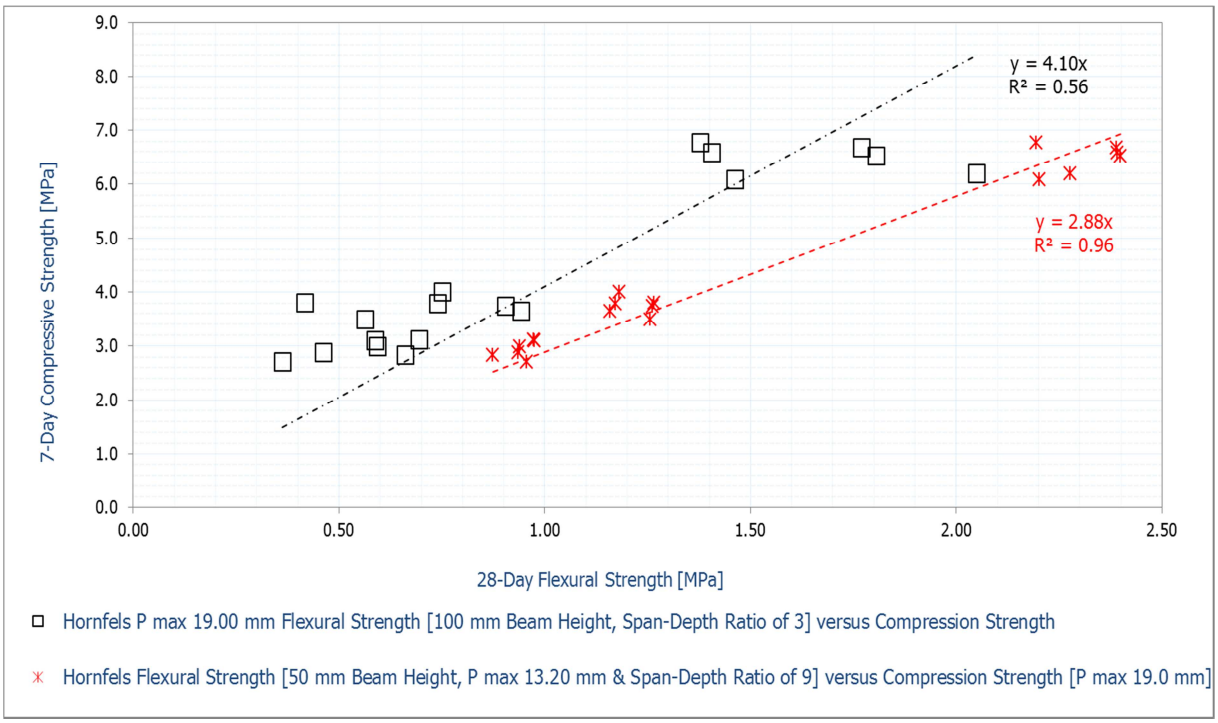

Figure: 5-19c 7-Day Compression Strength versus 28-Day Flexural Strength

With high cement content in the mix, an increase in the bond strength results and the specimen begins to behave as a lean mix. This suggests that with high cement contents, the

hornfels mix becomes stiffer [brittle] than at low cement contents. The differences in the R^2 values illustrated in Figures 5-19b and 5-19c indicate the differences such as, the test mode [i.e. compression versus flexural mode], specimen geometry, the stiffness properties owing to high cement usage as well as aging effects [i.e. 7-day versus 28-day cured specimens]. This explains the low R^2 as well as strength values between the compressive and flexural strength. For same cement content in hornfels, the 7-day compressive strength is higher than the flexural strength values despite the 28-day curing period for the beams. This shows the effect of the test mode on the behavioural properties of cement-stabilised materials; see Figure 3-11. In flexural mode, the beam experiences a combination of compression [above the neutral axis] and tension [below the neutral axis].

Equation 5-1 presents the relationship between the 7-day compressive strength [$UCS_{7\text{-day}}$] and the 28-day flexural strength [$f_{28\text{-days}}$] of hornfels beam with a height of 50 mm comprising of a 13.20 mm maximum aggregate size evaluated at a span-depth ratio of nine without the polymer. The 7-day tensile strength can be used to approximate the 28-day flexural strength, see Figure 5-19c.

$$f_{28\text{-days}} = 0.35\ UCS_{7\text{-day}}\ [\text{Beam Span-Depth Ratio of 9 and 13.20 mm } P_{max}] \qquad \text{Equation 5-1}$$

Figure 5-19d shows the 7-day tensile strength versus the 28-day flexural strength. With the cognisance of the R^2 values, the 7-day tensile strength is about 0.6 to 0.8 times the 28-day flexural strength for the same mix type at different span-depth ratios. In view of the resultant beam shear stresses and the reliability of test data, beam type with a height of 50 mm, span-depth of nine and comprising of a 13.20 mm as the maximum aggregate size is selected for further analysis.

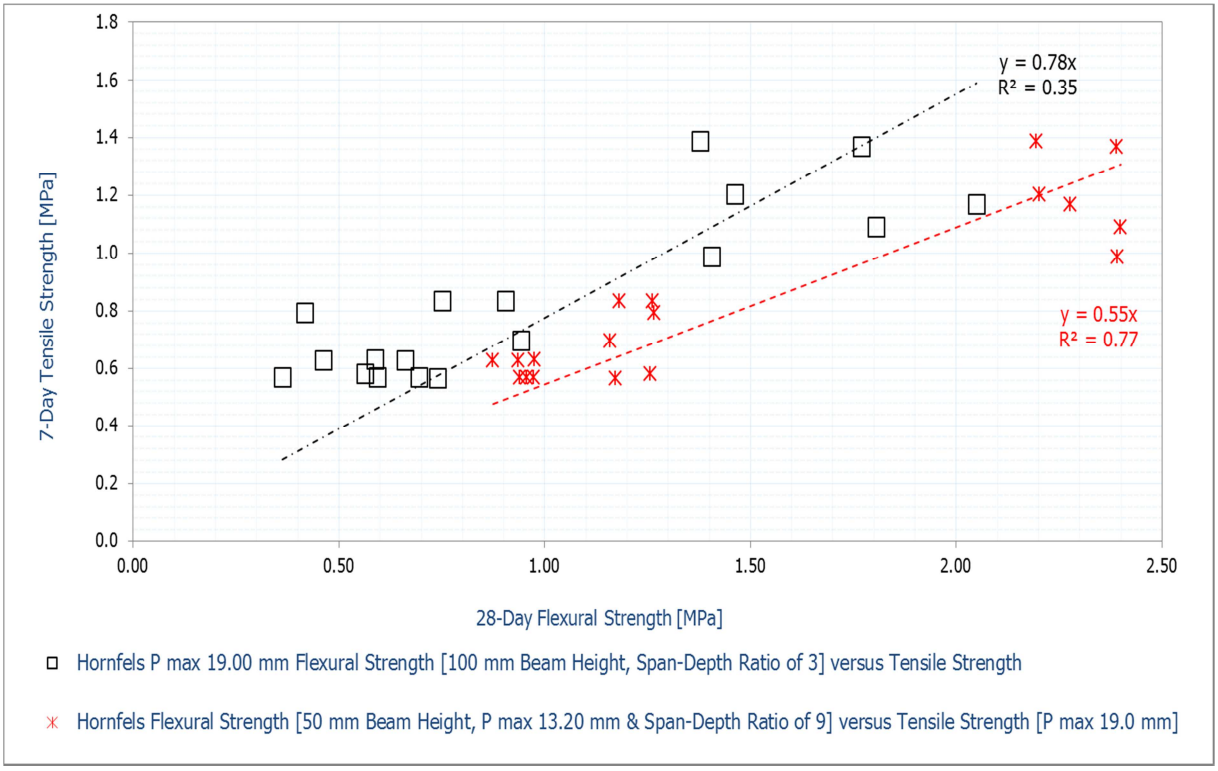

Figure: 5-19d 7-Day Tensile Strength versus 28-Day Flexural Strength

5.4 Effect of Polymer on Material Properties [50 mm Beam Type]

The application rate of the polymer to the stabilised materials is determined in Chapter 4. This section provides further results on the effect of the polymer on the flexural strength, elastic modulus, fracture energy and strain-at-break criteria. The effect of polymer on the

material's dry density was realised. Figure 5-20 confirms the effect of the polymer on the dry density of the stabilised materials. In Figure 5-20, the beam compaction relative to the type and quality of material at varying cement and polymer contents is illustrated.

In terms of the quality and type of material, ferricrete exhibited the overall lowest dry density criteria at varying cement contents with and without the polymer in the mix. Both hornfels mix types, i.e. with and without the polymer in the mix, are comparable, especially with 6% cement content. Ferricrete mix types with the polymer showed a general reduction in dry density. This is attributable to the effect of cement fines and nano-particles in the polymer as established in Chapter 4.

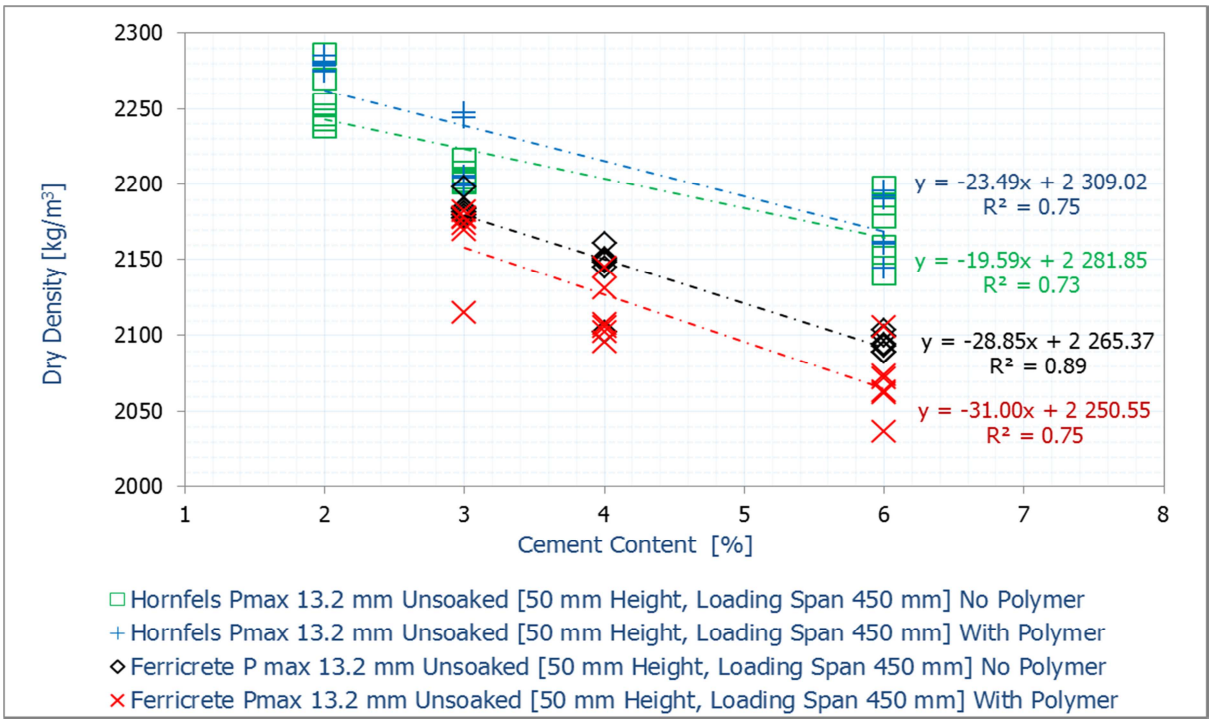

Figure: 5-20 Effect of Polymer on Material's Dry Density

5.4.1 Effect of the Polymer on the Flexural Strength Properties

Figure 5-21 shows the effect of the polymer on the material flexural strength properties. Sections 4.6.2 and 4.6.3 reported on the effect of polymer on the material's compressive and tensile strength properties. The addition of the polymer to hornfels resulted in a reduction in the flexural strength.

A reduction in flexural strength at increasing cement content following the addition of the polymer to the hornfels mix resulted. At a cement content of 2%, adding the polymer to the hornfels mix resulted in a reduction of approximately 20% in flexural strength. The hornfels mix with 6% cement content a reduction of about 40% flexural in strength. At low cement contents, the hornfels mix with the polymer exhibited scattered flexural strength data points but these were comparable to its reference mix. This indicates that the low cement contents [i.e. reduced particle bond strength] and material characteristics play a more significant role than the polymer effect. This confirms the efficacy of the polymer with cement.

Similar to the tensile strength criteria as illustrated in Figure 4-23, adding the polymer to ferricrete improved its flexural strength properties at cement contents of 4% and higher. At low cement contents, both ferricrete mix types with and without polymer were comparable. These trends also confirmed the efficacy of the polymer with the material. The polymer effectiveness is dependent on the type and quality of material in addition to high cement

contents. With low cement contents, adding the polymer to a ferricrete mix resulted in a flexural strength increase of less than 5.0% [i.e. 3% cement content]. With a cement content of 6% in a ferricrete mix, the application of the polymer resulted in an increase of approximately 35.0% in the flexural strength compared to its reference mix type [i.e. without the polymer].

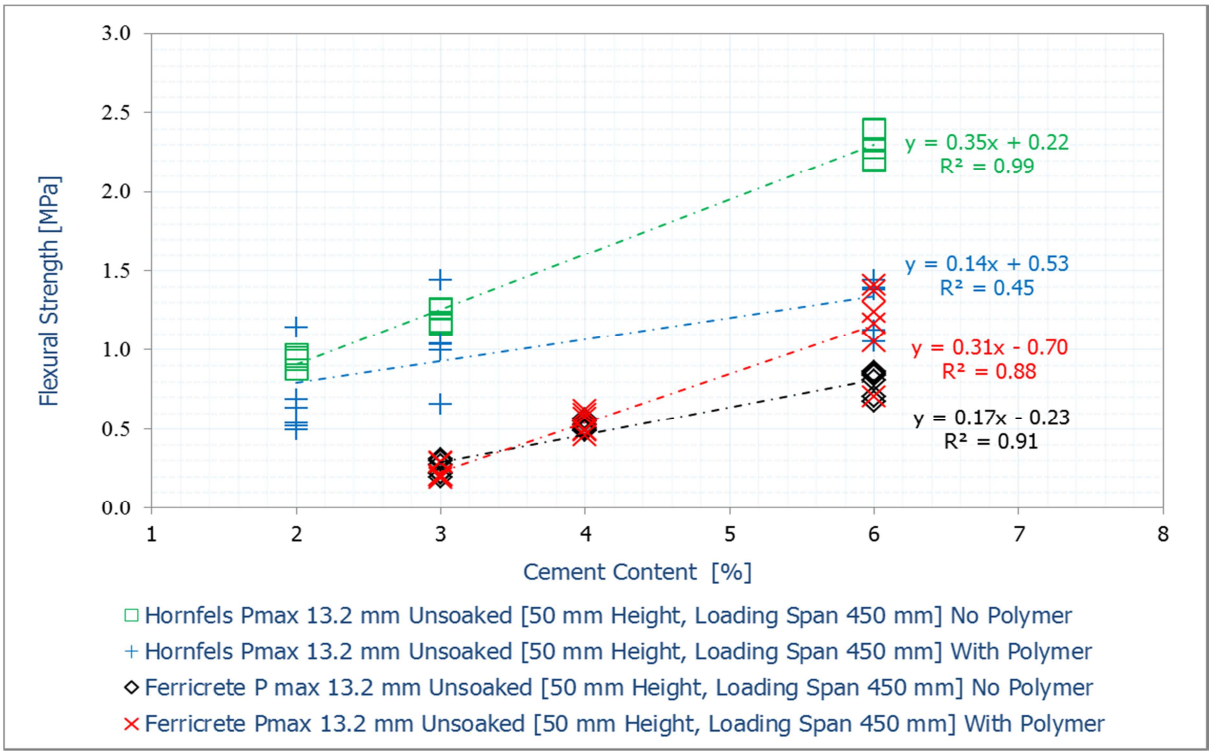

Figure: 5-21 Effect of Polymer on Flexural Strength

Despite the reduction in the dry density, the application of the polymer to ferricrete stabilised using more than 4.0% cement content yielded an increase in mechanical strength. This was significant with high cement contents such as 6% and with a specific material such as ferricrete. Hornfels mix type with 6% cement content and no polymer showed flexural strength values comparable to ferricrete mix type with the polymer. The use of the polymer with hornfels does not offer beneficial outcomes in terms of strength. The addition of the polymer to ferricrete provided benefits and this was significant at high cement contents. Considering the amount of fines contained in ferricrete the application of such high cement contents makes the material more prone to shrinkage cracking. Chapter 6 provides the shrinkage results and related analysis.

5.4.2 Effect of the Polymer on the Beam Flexural Modulus

Figure 5-22 illustrates the effect of the polymer on the material elastic modulus. The addition of polymer to ferricrete resulted in an increase in elastic modulus. The increase corresponded to the addition of more cement content to the mix. The application of polymer to hornfels resulted in a general reduction in elastic modulus.

For hornfels materials, adding the polymer resulted in a general decrease of less than 25% in elastic modulus as measured from the reference mix types [without the polymer]. Compared to its reference mix, ferricrete mix with the polymer showed a gradual increase in the elastic modulus. The elastic modulus increase corresponded with high cement contents in the ferricrete mix. The addition of the polymer registered the following increases with ferricrete in terms of the elastic modulus i.e. compared to their reference mix types:

a) with 3% cement content about 25.0% increase in elastic modulus was registered
b) 4% cement content registered less than 30.0% increase in elastic modulus
c) less than 35.0% increase in elastic modulus was registered with 6% cement content in the mix

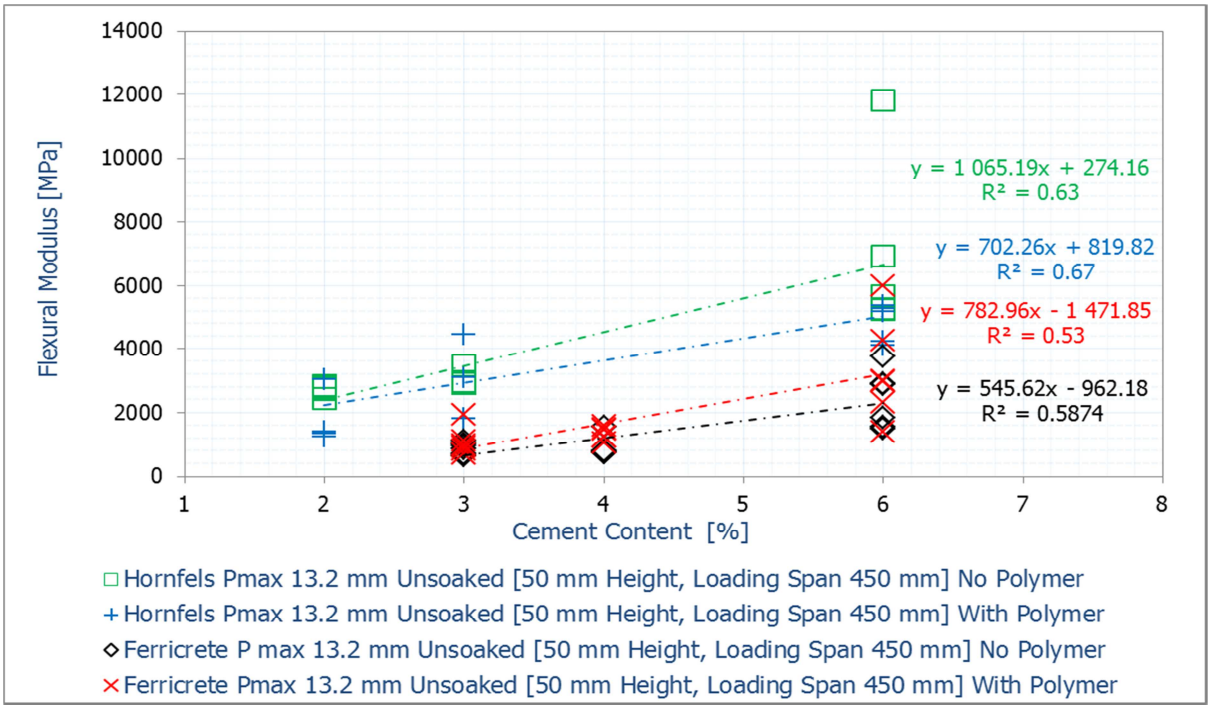

Figure: 5-22 Effect of Polymer on Flexural Modulus

5.4.3 Effect of the Polymer on the Beam Strain-at-Break

Figure 5-11 illustrates the effect of cement content on the strain-at-break. An increase in cement content resulted in a reduction in strain-at-break. This is due to the effect of cement on the stiffness properties of the material. Stabilised materials of high stiffness [brittleness] tolerate minimal deflections i.e. reduced ability to bend when loaded. An increase in cement content ultimately results in a corresponding increase in the material's stiffness. At high cement contents, the strain-at-break values reduced. This characterises that the materials become stiffer and more brittle at high cement content compared to using low cement contents. Figure 5-23 shows the effect of the polymer on the strain-at-break.

The application of the polymer to the hornfels mix shows a general trend in its strain-at-break, which provides insight on the effect of the polymer on the stiffness properties of hornfels. This observation provides insight regarding the fracture behavioural properties of the stabilised materials with and without the polymer. Figure 5-22 illustrates that there was a reduction in the elastic modulus with hornfels i.e. reduced stiffness properties. Figure 5-21 shows a reduction in hornfels flexural strength following the application of the polymer. Figures 5-20 to 5-23 provide insight into the polymer effect on the particle bond-strength, the engineering and the behavioural properties of cement-stabilised materials. By assessing the material fracture characteristics further understanding regarding the quality and general properties of hornfels relative to the polymer effectiveness are realised.

The application of the polymer to ferricrete material showed no significant reduction in strain-at-break value. Ferricrete mix types without the polymer exhibit a decrease characterised by a negative slope. The trend shown by ferricrete mix with polymer provides insight into the polymer effectiveness relative to the fracture characteristics of ferricrete.

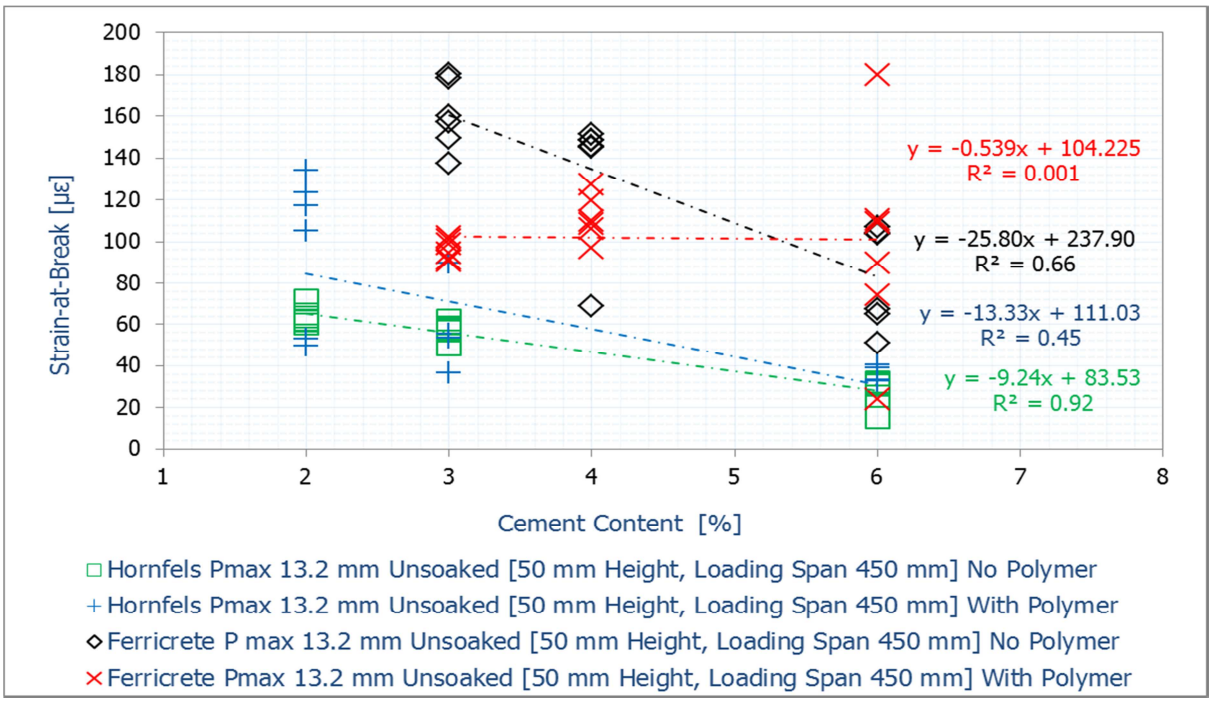

Figure: 5-23 Effect of Polymer on Strain-at-Break

5.4.4 Effect of the Polymer on the Fracture Energy

Section 5.2.6 provides the quantification of the fracture energy, which relates to the load response and fracture criteria of the material. Figure 5-24 illustrates the effect of the polymer on the fracture energy of hornfels and ferricrete with and without the polymer.

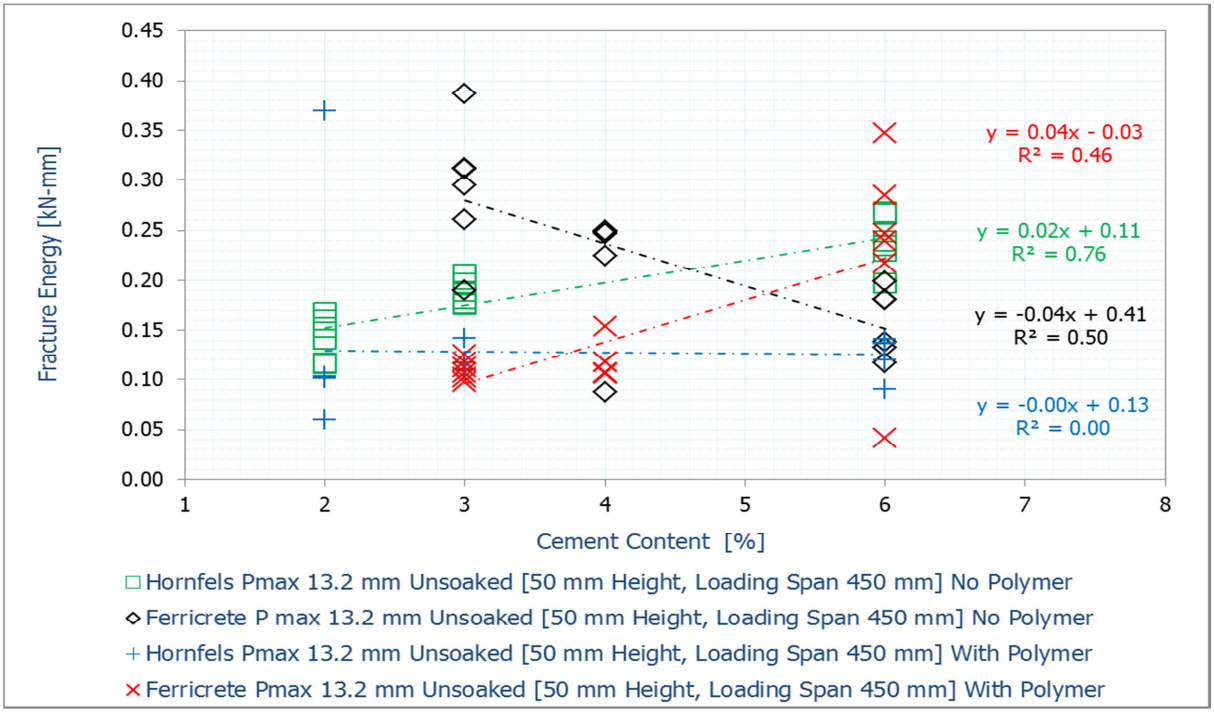

Figure: 5-24 Effect of Polymer on Fracture Energy

The hornfels mix with the polymer exhibits no significant change in fracture energy. The reference hornfels mix type [without the polymer] showed an increase in fracture energy at increasing cement content. The fracture energy results displayed scattered data points, which characterise the variability of the stabilised materials and their behavioural

characteristics relative to cement content. The influential factors such as mix components [gradation], cement content and curing conditions relative to the resultant effects emanating from shrinkage influence the fracture behavioural properties. The scattered data points for mix type with 6% cement content characterise the influence of cement content on the fracture behaviour of cement-stabilised materials.

The ferricrete mix with the polymer yielded an increase in fracture energy at increasing cement contents. The ferricrete mix without the polymer showed a reduction in fracture energy at increased cement content. The ferricrete mix types, i.e. with and without the polymer, provide insight concerning the fracture behavioural properties as well as the material's load response. Even though the polymer reduced the dry density of ferricrete, its application showed benefits corresponding with high cement contents. The polymer mechanism in increasing the strength and fracture energy of ferricrete encompasses its interaction with fine particles of material and cement to enhance the bond strength. The particle bond strength plays a key role to the overall strength and its fracture characteristics of the stabilised materials.

5.5 Discussion of Results

The importance of standardising the flexural beam test is to evaluate the stabilised materials in a more reliable manner. The experimentation provides viable insight related to the evaluation of the engineering properties of cement-stabilised materials and their related analysis. The effect of beam geometry, maximum aggregate size and the span-depth ratio relative to the measurement of the engineering properties of stabilised materials is realised. The effect of the beam shear stresses relative to the span-depth ratio is established. The assessment of the engineering properties for the same material type using different span-depth ratios and maximum aggregate size shows a variation. This leads to inconsistencies and deviations from the 'actual' material property measure. This suggests that the standardisation of the flexural beam test is necessary. The experimentation adopts a span-depth ratio of nine because of its minimal beam shear stress.

Stabilising materials using low cement contents results in reduced particle bond strength. However, this is dependent on the material type and quality. A reduction in particle bond strength ultimately leads to a decrease in the strength and stiffness properties of the material. The effectiveness of the particle bond strength is dependent on:

a) the achievable density
b) amount of fines in the mix
c) cement content and the quality and type of material to be stabilised
d) curing conditions

However, the amount of fines in the mix influences the effectiveness of cement. A poor cementation results due to the amount of fines in the mix. In order to achieve a material class C1, the addition of more cement to ferricrete is required. The trends of strength increase with the hornfels mix types are higher than with ferricrete. The addition of more cement to hornfels without the polymer results in an increased fracture energy and strength. The ferricrete mix without the polymer shows that the addition of more cement results in a rapid reduction in the fracture energy. This indicates the interaction of cement and material particles in yielding an increased fracture behaviour and strength. This provides insight regarding the cement and material interaction relative to the resultant particle bond strength. The resultant particle bond strength influences the strength, elastic modulus and fracture behavioural properties.

Strain-at-break and fracture energy results provide insight into the fracture characteristics and mechanical behaviour of the stabilised materials. The strain-at-break trends show a reduction in the value corresponding to an increase in cement content. This indicates that an

addition of more cement content results in a corresponding increase in the material's stiffness [brittleness] properties. The degree of stiffness exhibited by a stabilised material characterises its fracture criteria. The development of the stiffness properties of stabilised materials is dependent on a number of factors, including the interaction of the cement and material particles to result in suitable particle bond strength. The scattered data points and R^2 values show the variability that characterise cement-stabilised materials, particularly the factors that influence its particle bond strength. Moisture ingress, curing conditions and the packing of the particles influence the resultant bond strength.

The flexural strength results confirm that the polymer is not only dependent on the quality and type material but also on the amount of cement in the mix. Characteristic trends as obtained under the compressive and tensile strength test are realised with the flexural beam test despite the test mode. The application of the polymer to ferricrete exhibits an increase in fracture energy. The application of the polymer to hornfels shows no significant change in fracture energy; this corresponds with its reduction in flexural strength properties and flexural modulus. The interpretations suggest that the efficacy of the polymer is dependent on high cement contents as well as the type and quality of the material.

5.6 Summary of Chapter 5

This chapter provides additional insight concerning the engineering properties and behavioural characteristics of stabilised materials. Insight regarding the behavioural properties, fracture characteristics and polymer effectiveness with materials stabilised at varying cement contents are realised. This chapter proposes flexural beam test protocol and beam geometry along with the factors of influence. This experiment shows the effect of varying the test configurations relative to the beam geometry and proposes a test method. The experimentation adopts the proposed test method to evaluate the efficacy of the polymer. This chapter provides insight regarding mechanical and behavioural properties of stabilised materials with and without a nanotechnology polymer. Chapter 6 provides the laboratory shrinkage measured results and the related analysis.

5.7 References

Mindess, S., (1996) *Fracture Mechanics of Cementituous Materials*, Canadian Journal of Civil Engineering 23(5): 1138, 10.1139/196-922

Chapter 6: Shrinkage Results

6.1 Background

Shrinkage cracks are a distress to the cement-stabilised layer and the pavement structure as a whole, particularly if left to occur in an uncontrolled manner. The previous chapters provide a literature review, methodology and the strength results. The fundamental philosophies, theories and factors contributing to the cracking of a cement-stabilised layer, are also included in the previous chapters. In this chapter concept adopted for the measurement of laboratory-based shrinkage are provided along with the results.

The significance of evaluating shrinkage at laboratory level in order to ascertain the suitability of the cement-stabilised materials for use in the pavement structure has already been emphasised. One of the key objectives of this research is to develop a shrinkage test method that provides a good indication of the material shrinkage potential. This suggests that the test method should be user friendly as well as inexpensive, but provide a reliable measurement of shrinkage.

6.2 Moulding Moisture, Specimen Dry Density and Compaction Method

The influence of moisture content of the mixture on the shrinkage of the cement-stabilised materials is extensively studied. Additionally, the influence of the specimen dry density relative to the method of compaction is widely documented. For this research, the cement-stabilised specimens were prepared at the optimum moisture content of their natural material type as reported in Chapter 4. Two types of specimen geometry are considered in this research, i.e. the beam and the cylinder specimen types.

By varying the moisture content of the material while, applying the same compactive effort for specimen compaction results a change in its dry density. A variation in moisture content influences the total shrinkage of the specimens. The dry density and moisture content have a significant influence on the measurement of shrinkage. Tables 6-1 and 6-2 provide the moisture content and dry density results. Figure 6-1 illustrates the dry densities of the different specimens using the vibratory table and hammer.

Table 6-1 Moisture Content, Dry Density and Compaction Method [Beam Specimens]

Hornfels Mix Type	[Pmax = 19.00 mm]	Beam Specimen	MDD* = 2346 kg/m^3
Cement Content [%]	Moisture Content [%]	Vibratory-table Method Dry Density [kg/m^3]	Vibratory-hammer Method Dry Density [kg/m^3]
2	5.2	2211	2301
2	5.2	2201	2274
2	5.2	2209	2254
3	5.0	2132	2207
3	5.0	2115	2228
3	5.0	2148	2266
6	4.6	2000	2198
6	4.6	2028	2159
6	4.6	2084	2174
Ferricrete Mix Type	[Pmax = 19.00 mm]	Beam Specimen	MDD* = 2023 kg/m^3
Cement Content [%]	Moisture Content [%]	Vibratory-table Method Dry Density [kg/m^3]	Vibratory-hammer Method Dry Density [kg/m^3]
3	7.8	2000	2089
3	7.8	2007	2083
3	7.8	2002	2085
4	7.6	1968	2011
4	7.6	1970	2018
4	7.6	1987	2022
6	7.2	1901	2001
6	7.2	1905	1989
6	7.2	1915	1980
MDD* denotes	Maximum Dry Density	using the Modified AASHTO	

Table 6-2 Compaction Dry Densities and Moisture Results [Cylindrical Specimens]

Hornfels Mix Type	[Pmax = 19.00 mm]	Cylindrical Specimens
Cement Content [%]	Moisture Content [%]	Vibratory-hammer Method Dry Density kg/m^3]
2	5.1	2295
2	5.1	2301
2	5.1	2322
3	5.0	2298
3	5.0	2294
3	5.0	2303
6	4.7	2234
6	4.7	2245
6	4.7	2237
Ferricrete Mix Type	[Pmax = 19.00 mm]	Cylindrical Specimens
Cement Content [%]	Moisture Content [%]	Vibratory-hammer Method Dry Density [kg/m^3]
3	8.0	2129
3	8.0	2134
3	8.0	2126
4	7.6	2108
4	7.6	2121
4	7.6	2129
6	7.4	2090
6	7.4	2092
6	7.4	2096

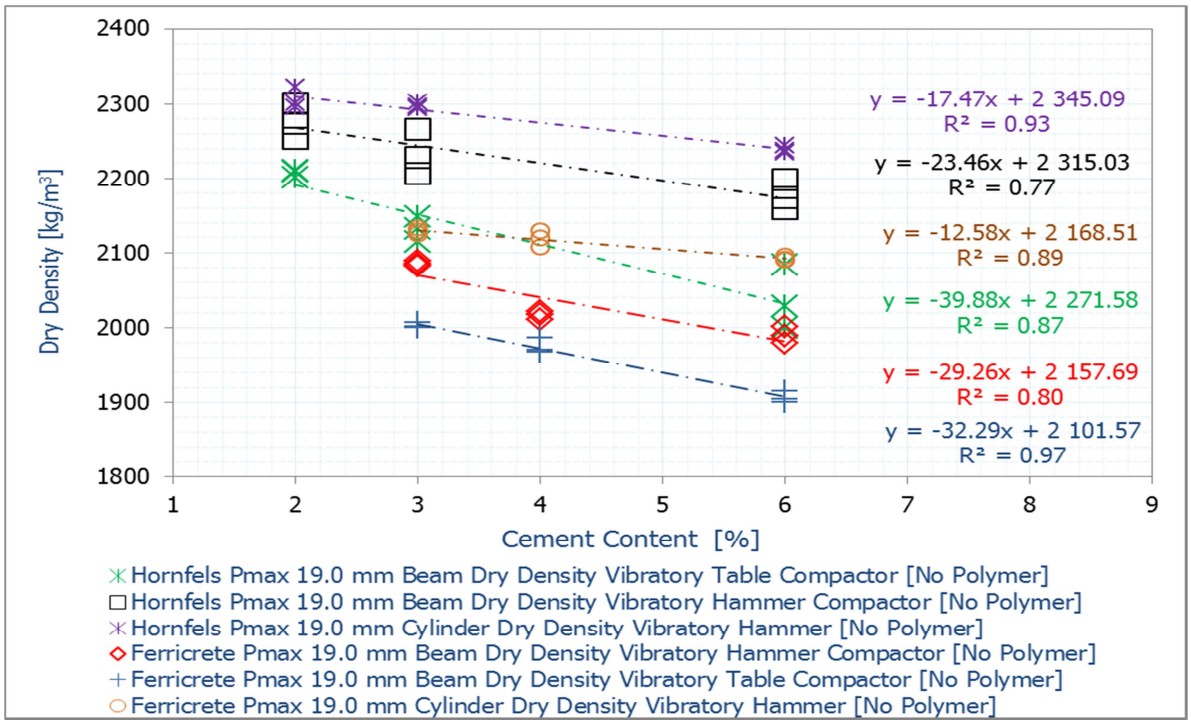

Figure 6-1 Dry Density Results at varying Cement Contents [Beam versus Cylinder]

Compaction of the beams using a vibratory hammer results in higher dry density values compared to using the vibratory table. The Bosch hammer is deemed to offer higher amplitudes and particle re-orientation for better packing than the vibratory table. This suggests that the vibratory hammer provides a higher compactive effort than the vibratory table for the same mix type and specimen geometry. For each mix type, mixing occurred in one batch in order to control moisture. With the insight gathered from the dry density values of the beams relative to the selected compaction method, the vibratory hammer was considered for the compaction of the cylinder specimens. The cylindrical specimens exhibit higher dry density values compared to the rectangular beam specimens. Figure 6-2 provides a conceptual illustration of the beam versus the cylindrical specimen compaction.

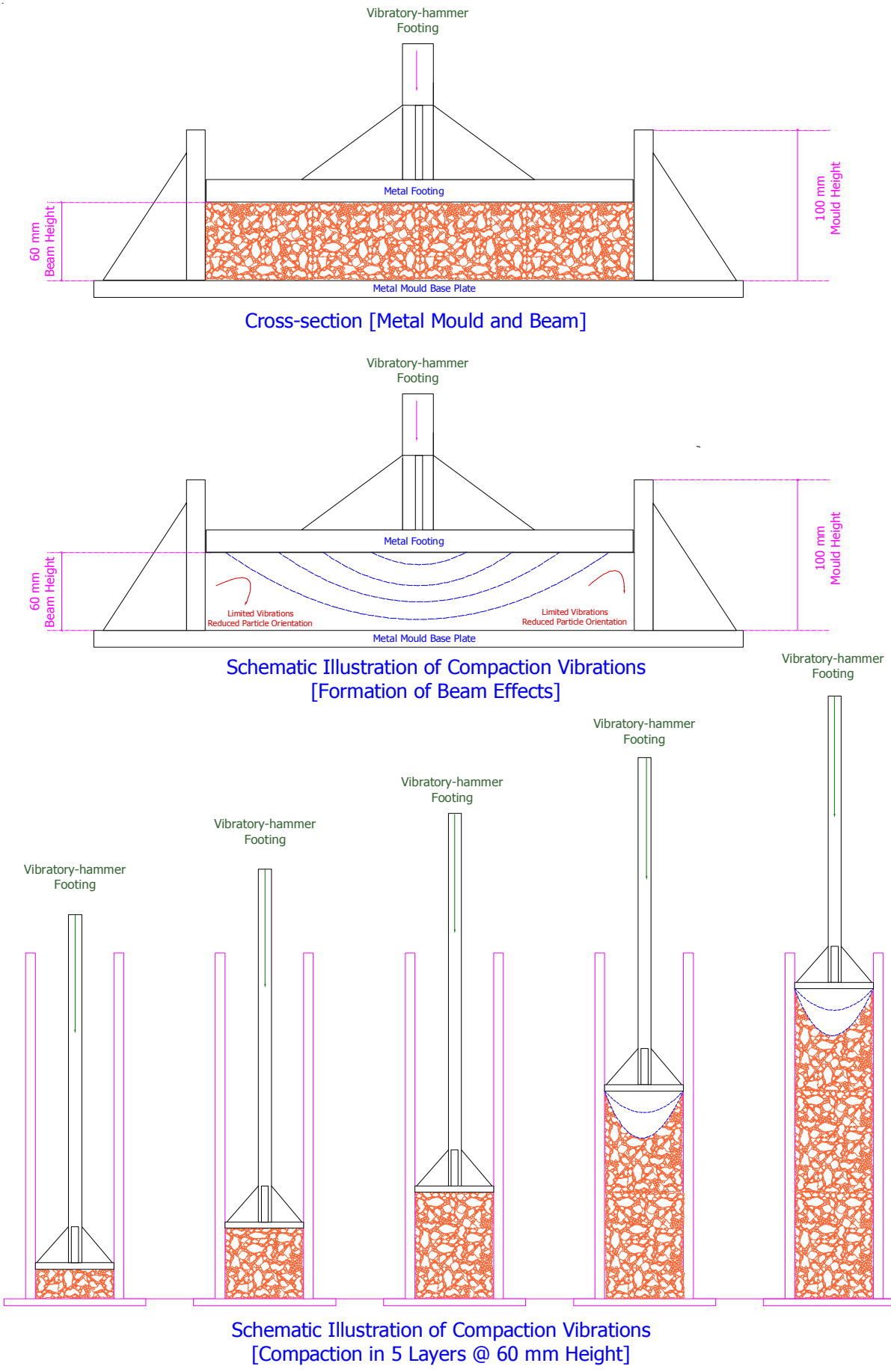

Figure 6-2 Conceptual Illustration of Beam versus Cylinder Compaction [Vibratory-hammer]

From Figure 6-2, insights regarding the degree of applied compactive effort relative specimen geometric characteristics are realised. The factors, particularly related to the effect of the compactive effort relative to the particle packing in order to achieve a maximum feasible density are conceptualised. The compaction technique [i.e. compacting in 5 layers of 60 mm height] relative to the length of the footing illustrates the distribution and effectiveness of the vibrations. In order to achieve a maximum feasible density, the material particles need to be re-oriented so that packing results in a dense matrix. The practical technique of realising this is to subject the particles to high vibrations. Vibrations must effect vigorous re-orientation of the particles for appropriate packing [reduced voids]. A uniform distribution of the applied vibration forces [compactive effort] is essential for particle re-orientation. The applied compactive effort must be of such nature that the vibrations result in particle re-orientation over the entire specimen depth and length.

The vibrations emanating from the Bosch hammer relative to the length of the footing influence the particle re-orientation and packing. A low re-orientation with the vibratory hammer contributes to a low density [i.e. poor packing of the particles]. A poor packing of the particles with a material matrix is usually associated with high voids.

The pore structure of a material matrix typifies the degree of particle packing and ultimately the density. The pore structure has a significant influence on the rate of moisture loss, particularly when the matrix exhibits an interconnected void structure. This ultimately influences the rate of moisture loss and thus, the resultant shrinkage. The cylindrical specimens present a concentric-like geometry whereby the vibratory-hammer footing evenly distributes the compactive effort over the entire surface of the specimen. Compaction of the cylindrical specimens in five layers, each measuring 60 mm height results in the achievement of high density. A high particle packing is usually associated with a dense matrix i.e. reduced voids.

For any compaction method, the distribution of its compactive effort over the specimen is fundamental. Beam compaction exhibit reduced density at the edges [i.e. referred to as 'beam-edge' effects as illustrated by Figure 3-15. The 'beam-edge' effects typify that the beam exhibits a non-uniformity compaction. This indicates that a low compaction [reduced density] prevails at the rear ends while a high compaction [an increased density] occurs in the middle section of the beam. This explains the difference between the cylinder and beam specimens.

6.3 Trends of the Shrinkage Test Curves and Results

The shrinkage-time curves of the various mix types indicate the response of the material to moisture loss [dimensional changes] as well as characterise their shrinkage criterion. A test temperature of 70ºC [accelerated curing] was set to increase the rate of moisture loss. All specimens were tested immediately after compaction and demoulding from their respective metal mould types. Demoulding of the beam involves the removal of the mould sides while that of the cylinder involves the splitting of the metal mould; this is detailed in Chapter 3 of this dissertation. Figures 6-3a and 6-3b illustrate the overall beam linear as well as cylinder axial and circumferential shrinkage setup.

With the beam shrinkage technique, three pairs of surface mounted strain gauges placed at the two rear ends as well as the middle section of the specimen measured the dimensional changes. Each surface mounted strain gauge with a length of 90 mm was placed in parallel along the top surface and the length of the beam. Figure 6-4a shows a typical strain gauge measurement for the first 13 hours [46800 seconds]. The test was run for 3 days. A computer set connected to a 'strain box' capture the dimensional changes [as strain data] for every 10 minutes. It became apparent that after 24 hours of testing there was no significant change in the strain gauge values despite the mix and/or material type. For each beam type,

an LVDT was mounted to the rear end. The initial and final readings of the LVDT were recorded and the difference is considered as the beam linear shrinkage i.e. the dimensional change along the entire length [400 mm] of the beam.

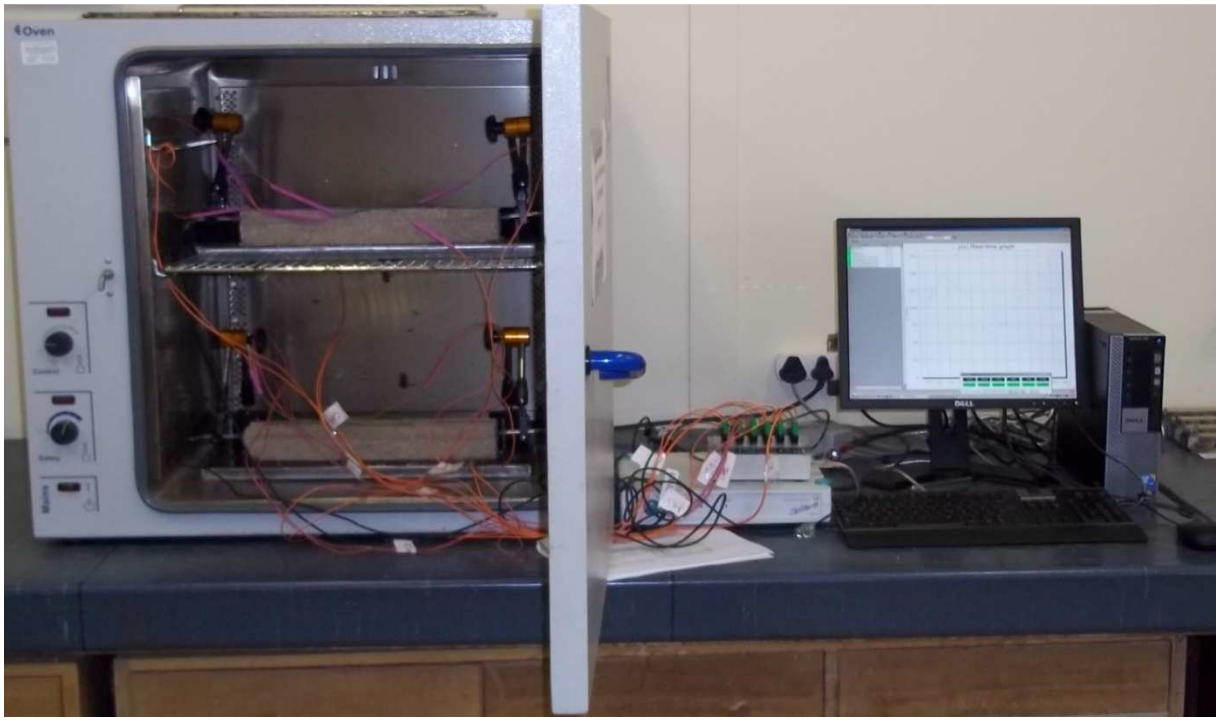

Figure 6-3a Beam Linear Shrinkage Setup [Surface Mounted Strain Gauges and LVDT, Data Acquisition Devices and Computer]

Figure 6-3b Cylinder Axial and Circumferential Shrinkage Setup in the Draught Oven at 70ºC

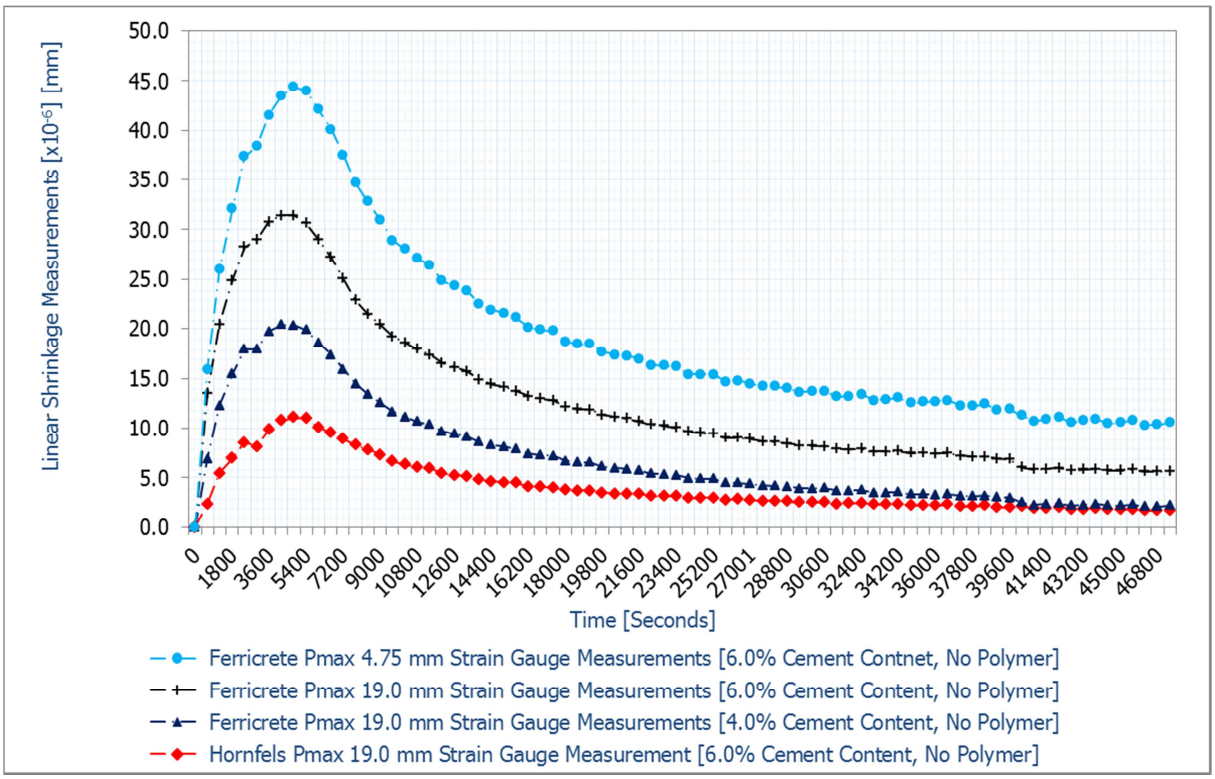

Figure 6-4a Typical Beam Linear Shrinkage Test Curves [Readings for the first 13 hours of Testing]

Figure 6-4b presents the axial shrinkage recordings measured in the direction of compaction on the cylinder specimen for 72 hours [4320 minutes] using a dial gauge. The dial gauge was mounted on plexiglass; the plexiglass was glued onto the cylinder top [see, Figure 6-3b] using epoxy glue. Figure 6-4c presents the axial shrinkage recordings for the ferricrete material. A comparison of the shrinkage-time curves of Figures 6-4b and 6-4c reveals insights into the shrinkage criterion of the mix type as well as the type and quality of material.

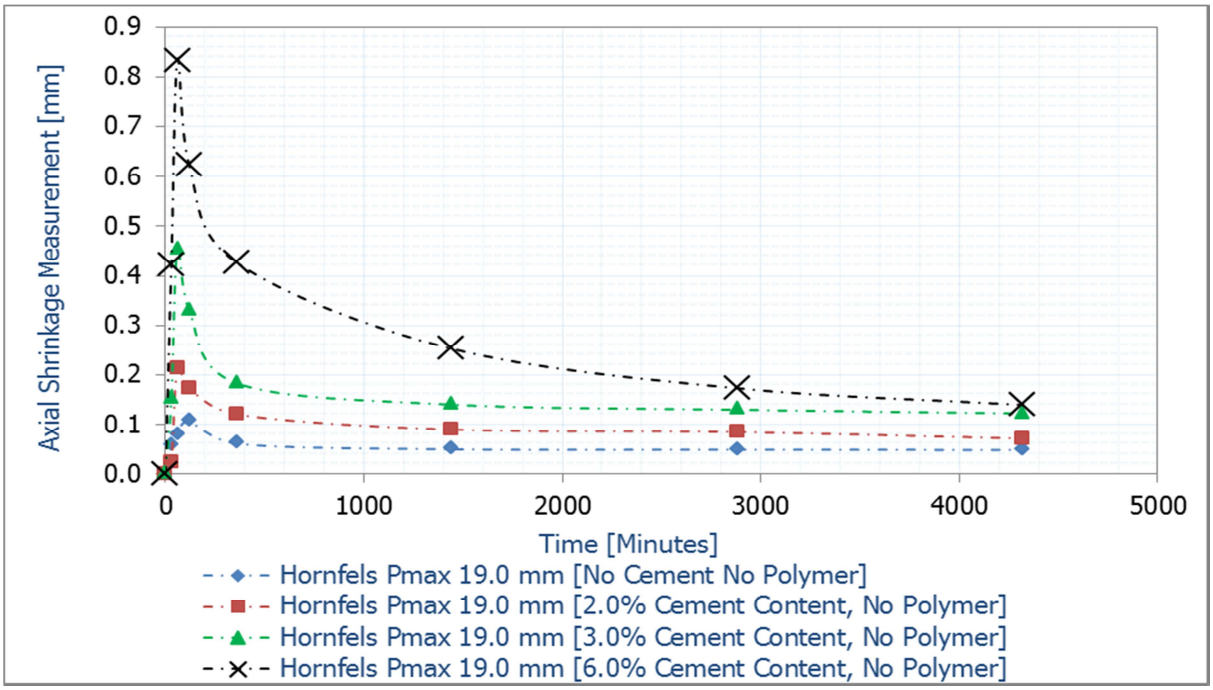

Figure 6-4b Typical Hornfels Axial Shrinkage Curves at Varying Cement Content [Dial Gauge]

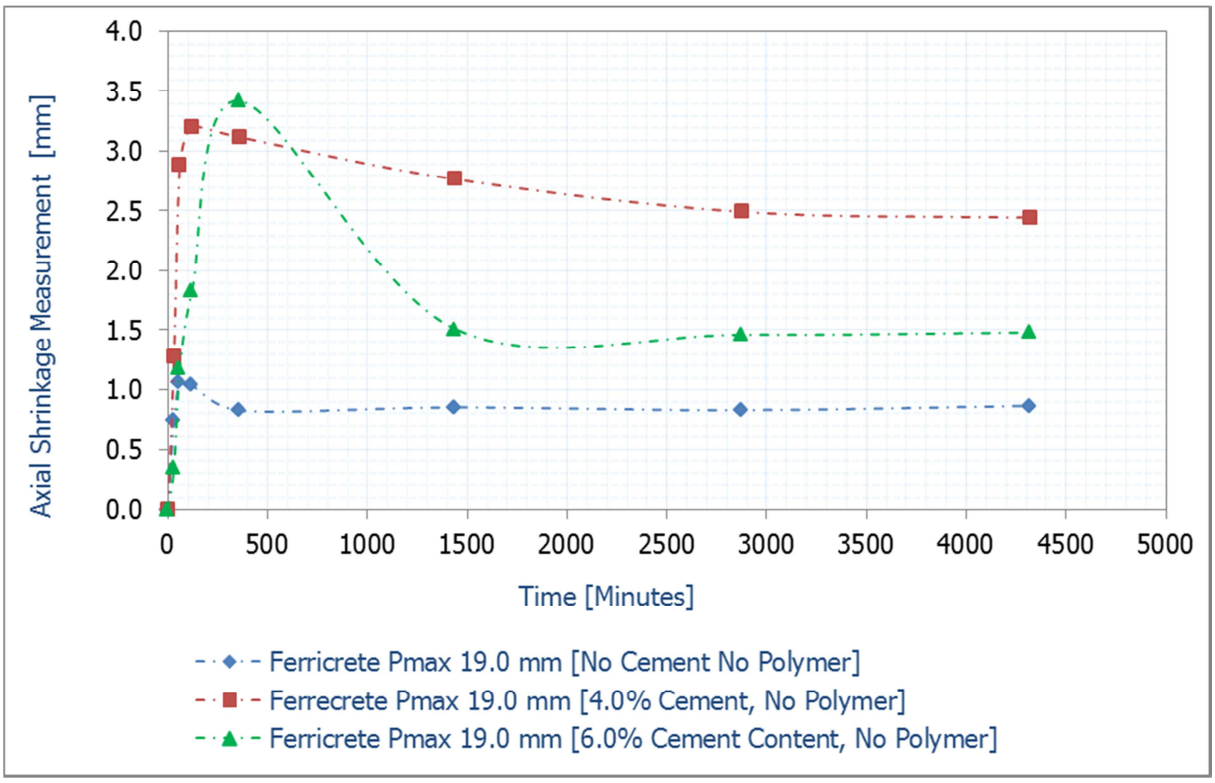

Figure 6-4c Typical Ferricrete Axial Shrinkage Curves at Varying Cement Content [Dial Gauge]

The surface mounted strain gauges and the dial gauges reveal that material initially expands. However, the amount of cement content in the mix, quality and type of the material in addition to the maximum aggregate size [gradation of the mix] influence the initial expansion, i.e. the peak of the shrinkage-time curve in the first period of testing. It should be noted that the dial gauge measure in the direction of compaction while the strain gauges measure in the direction perpendicular to compaction. The initial beam linear and cylinder axial expansions suggest that the initial expansion exhibited by the specimen is independent of the direction compaction.

In order to investigate the effect of the initial expansion on the specimen geometry, an extensometer was considered to record the circumferential shrinkage as illustrated with the cylinder specimen in Figure 6-4b. Figures 6-4d and 6-4e reveal that as the specimen expands in the axial direction, a reduction in its circumferential dimension [diameter] results. This provides insight into the specimen response to thermal effects. This suggests that its shape relative to the measuring method adopted influences the shrinkage of the laboratory specimen. The extensometer is calibrated to measure shrinkage as a negative value and expansion as a positive value; Chapter 3 provides the precision of the extensometer and other instrumentation used.

Figures 6-1 to 6-4e suggest that the prediction of the shrinkage potential of cement-stabilised materials based on the laboratory prepared specimens must consider the following among others:

a) the geometric characteristics of the specimen relative to the measuring criterion
b) its preparation, particularly the resultant density
c) the direction in which shrinkage is measured relative to the direction of compaction
d) its repeatability, reliability as well as its usability
e) the measuring range, sensitivity and precision of the instrumentation used

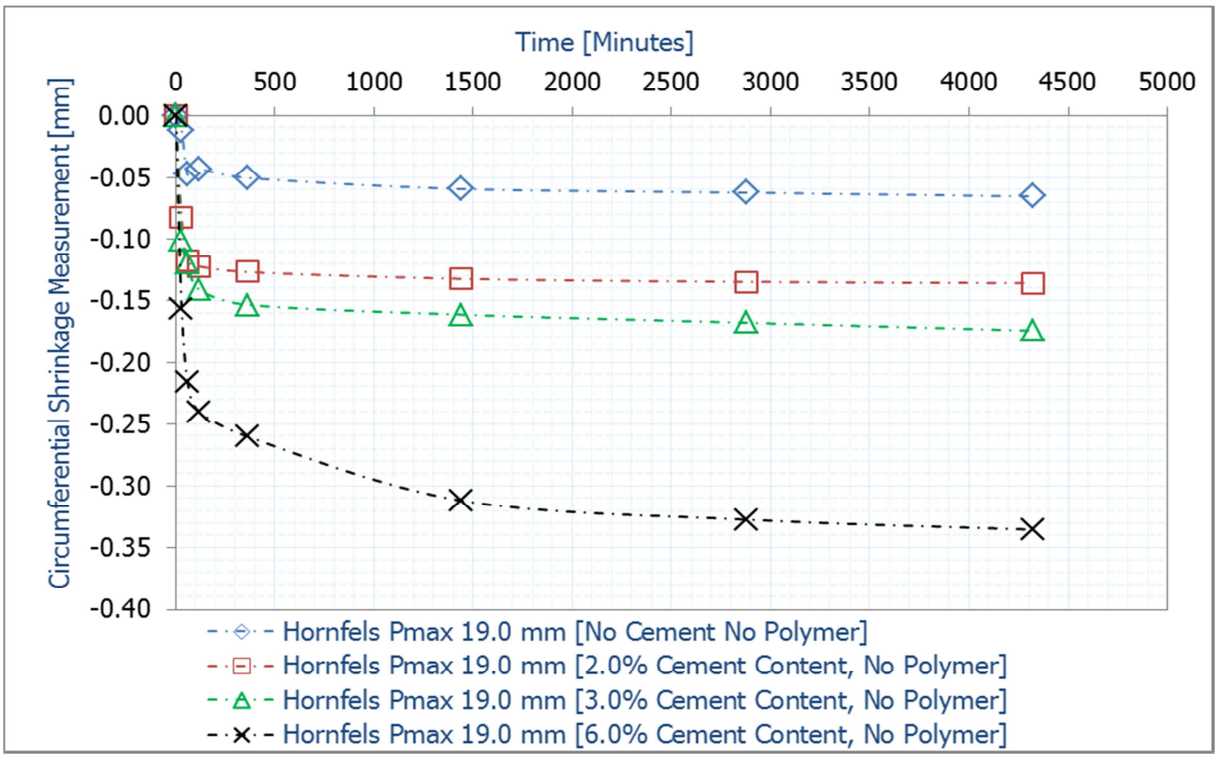

Figure 6-4d Hornfels Average Circumferential Shrinkage Measurements [Extensometer Readings]

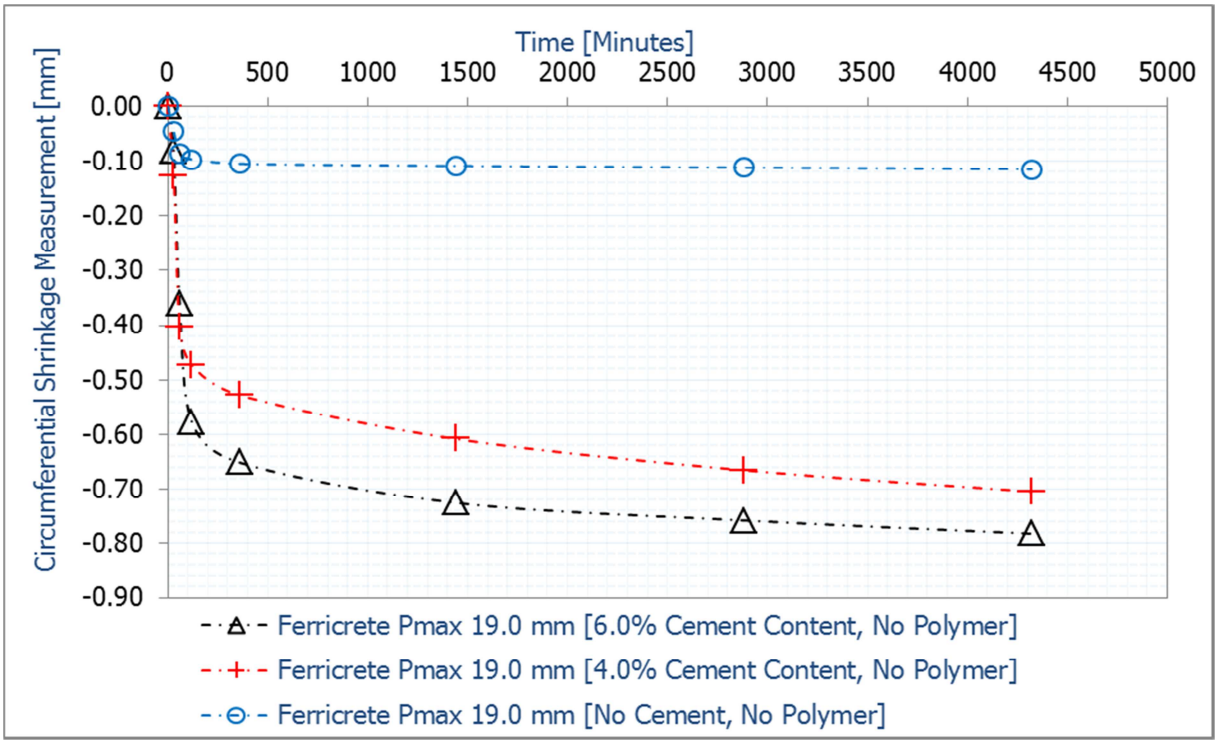

Figure 6-4e Ferricrete Average Circumferential Shrinkage Measurements [Extensometer Readings]

In order to account for the shrinkage behaviour, good investigation and knowledge regarding the shrinkage-time curve relative to the phenomenological factors portrayed by the curve is essential. This is because the trend defines the dimensional changes and behavioural response to thermal effects. Reference is made to cement paste experimentation illustrated in Figures 3-13, 3-14 and 3-17.

6.3.1 Trends of the Shrinkage-Time Curves and Interpretations

Characteristically, shrinkage of cement-stabilised materials consists of autogenous shrinkage [due to the hydration process], thermal shrinkage [due to low temperature contraction] and drying shrinkage [due to the loss of moisture]. However, drying shrinkage dominates the shrinkage strain of cement-stabilised layers and causes the majority of cracking. Autogenous shrinkage usually results in small volumetric changes compared to drying shrinkage. Autogenous shrinkage is considered as a macroscopic volumetric reduction, which does not lead to any moisture exchange to and from the specimen under a constant temperature, [Tazawa and Miyazawa, 1995]. Autogenous shrinkage depends on the extent of the hydration process, [Neithalath *et al.* 2005]. Tazawa and Miyazawa, 1995 indicates that autogenous shrinkage is not proportional to the volumetric change of the chemical reaction.

Several researchers approve that the volumetric changes due to autogenous shrinkage in cement-stabilised materials are small compared to those caused by the drying shrinkage. Bofinger *et al.* [1971] shows that shrinkage strain in a soil stabilised slab exhibits no cracks after more than 3 hours of curing at ambient temperature.

In a cement-stabilised layer, drying shrinkage is defined as the loss of moisture from the internal matrix of the material. This leads to the development of tensile stresses which cause the majority of cracking in stabilised layers, [Bofinger *et al.* 1971; Neithalath *et al.* 2005]. As moisture is drawn out [through the process of evaporation], the stabilised material begins to shrink. As a requisite to equilibrate with the surrounding thermal environment, a loss of moisture occurs which leads to changes in the moisture gradient. A change in the moisture gradient leads to the development of the tensile stresses in the stabilised material.

When a cement-stabilised material is subjected to high thermal environments, the rate of shrinkage is assumed as rapid in the first phase of the test. The rapid shrinkage is attributed to the effect and dominancy emanating from the pore suction when moisture is extruded from the specimen. As the pore suction dissipates, the resultant shrinkage also diminishes; the flattening-off of the shrinkage-time curve depicts this. However, Figures 6-4a to 6-4b show that there is an initial expansion. In this research the terms, *beam linear expansion* and *cylinder axial expansion* are used to differentiate between the shrinkage measuring criteria and the specimen type.

During the first phase of the shrinkage-time curve, an expansion that lasts less than 90 minutes [*beam linear expansion* with the strain gauge] and about 2 hours [*cylinder axial expansion* with the dial gauge] is shown. The expansion reaches a peak and then rapidly reduces before changing to a gradual trend and then flattening off. The trend of the shrinkage-time curve is dependent on the mix as well as the type and quality of the material. In modern material science, a number of factors such as the hydration of material as well as the physical-chemical effect are considered to explain the materials behaviour and response.

Concerning cement-stabilised materials, a number of factors, including the natural material characteristics, pore suction [due to the hydration of cement] and the expansion of the cement paste [C-S-H gel], will contribute to the dimensional changes during a shrinkage test. Differences due to the cement content affect the degree of hydration and moisture loss as well as the pore suction characteristics within the specimen. Other pertaining factors considered to contribute to the initial expansion on the shrinkage-time curve include the hydration of the natural materials, aggregate expansion due to the increase in temperature [i.e. 25ºC to 70ºC] and the internal distribution of moisture in the specimen.

For this research, the following assumptions are made in order to interpret the shrinkage-time curve of the cement-stabilised materials:

a) Autogenous shrinkage starts immediately after mixing the cement and materials in the presence of a measured quantity of water [i.e. at the OMC of the natural materials]. Autogenous shrinkage continues until the end of the hydration process. This suggests that the initial expansion supersede the prevailing autogenous shrinkage in the 'cylinder axial' and 'beam linear' directions in the initial phase of the shrinkage-time curve.
b) The expansion of the specimen continues until no further expansion occurs. This indicates the lessening of the hydration process whereby shrinkage is assumed to supersede the expansion; a change after the shrinkage-time curve is observed with a peak and a rapid reduction. Additionally, the dissipation of the residual compaction stresses [in combination to the pore water] can also lead to some expansion after compaction.
c) The rapid reduction after the peak of the shrinkage-time curve is assumed to indicate the withdrawal of water from the large pores and is exacerbated by the high-test temperature used. The rapid reduction is deemed less significant than the withdrawal of water from the small pores.

After the initial expansion, withdrawal of water from large pores [mainly from the exterior of the specimen] follows. There is no complete drying out of the exterior of the specimen. Instead, water diffuses from the liquid water in the specimen to water vapour to evaporate at the edges of the specimen. This results in a diffusion gradient with a slight change continuously from wet to dry. Depending of the specimen pore structure [typically, the connectivity of the pores] and test temperature [curing conditions] moisture is in a continuous equilibrium with the adjacent water. The resultant moisture gradient causes a differing between and the need to equilibrate with the exterior; this results in an outward flow of water vapour. In general, there is a continued flow of inner water to vapour until no further free water available.

The withdrawal of water from the small pores causes a large build-up of the suction pore pressures, which cause the development of tensile stresses. Large pore suction pressures cause 'detrimental' shrinkage that leads to cracking of the cement-stabilised layer. However, the resultant of cracks is also dependent on the restraints such as the prevailing friction imposed by the underlying layer. Figure 6-5 conceptualises the shrinkage-time curve and the factors of the influence. In this research, a change in the shrinkage-time curve between point A and C [see Figure 6-5] defines the withdrawal of water from the internal core pores [small pore] of the specimen. It is assumed the resultant tensile stresses are significant to cause detrimental shrinkage in the field.

The boundary between the end of autogenous shrinkage and the start of drying shrinkage is not evidently demarcated by the curve; further work is required. In this analysis, drying is located at point B. By using tangential relationships, i.e. connecting point A [peak of the curve] to point C [end of the test] an arc AC is formed. The peak of the arc AC defines point B. By drawing a horizontal line from point C, the difference between points B and C values typifies the detrimental shrinkage that causes the majority of cracking is estimated.

The circumferential shrinkage undertaken using the extensometer positioned at mid height of the cylinder shows no initial expansion occurs, but a significantly rapid reduction is observed; see Figure 6-4d and 6-4e. Figure 6-6 conceptualises the detrimental shrinkage assessed from the circumferential shrinkage. Similar factors to the axial shrinkage are deemed to affect the circumferential shrinkage measurement. It is presumed that the expansion of the specimen in the axial direction supersedes the likely expansion in the circumferential direction. This assumption holds because a response of a material in one direction results in an opposite response in another.

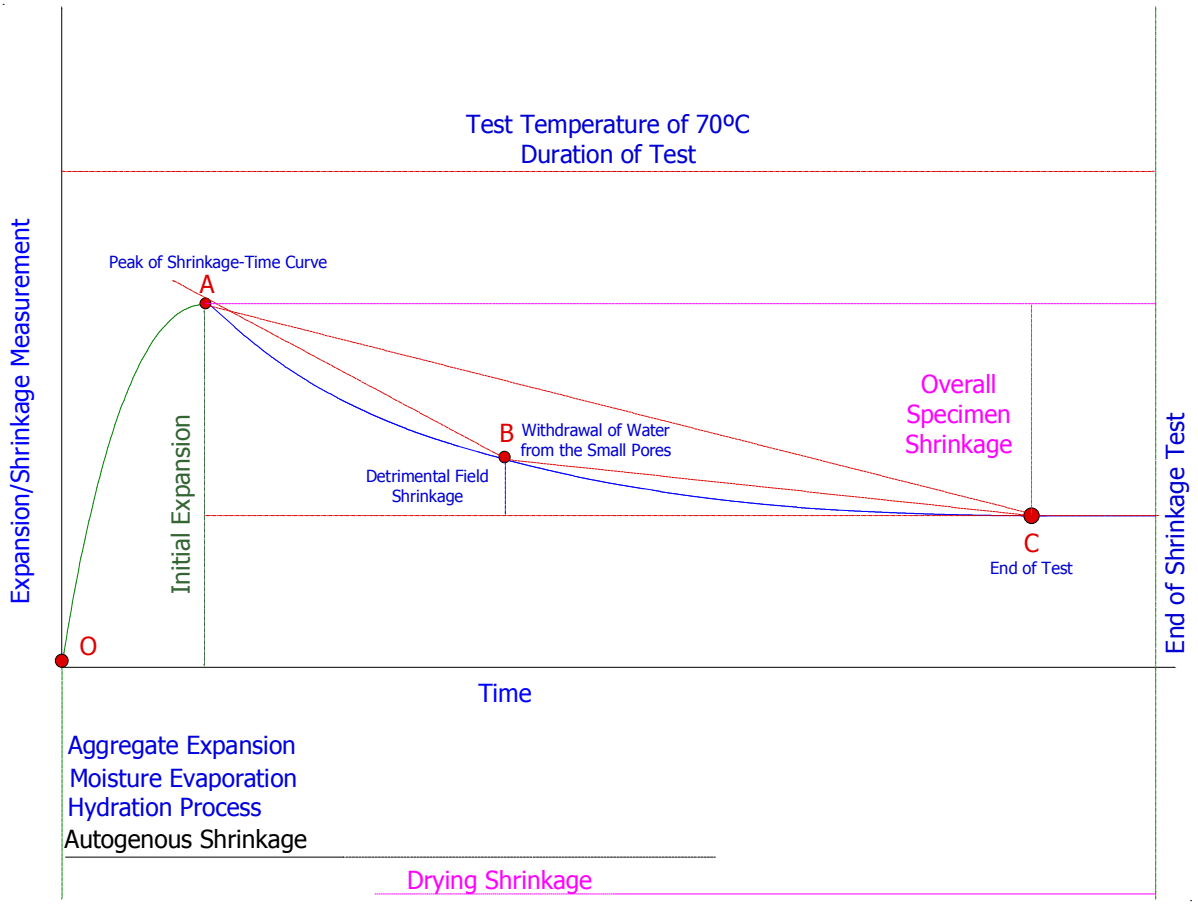

Figure 6-5 Conceptualisation of the Shrinkage-Time Curve and Factors of Influence

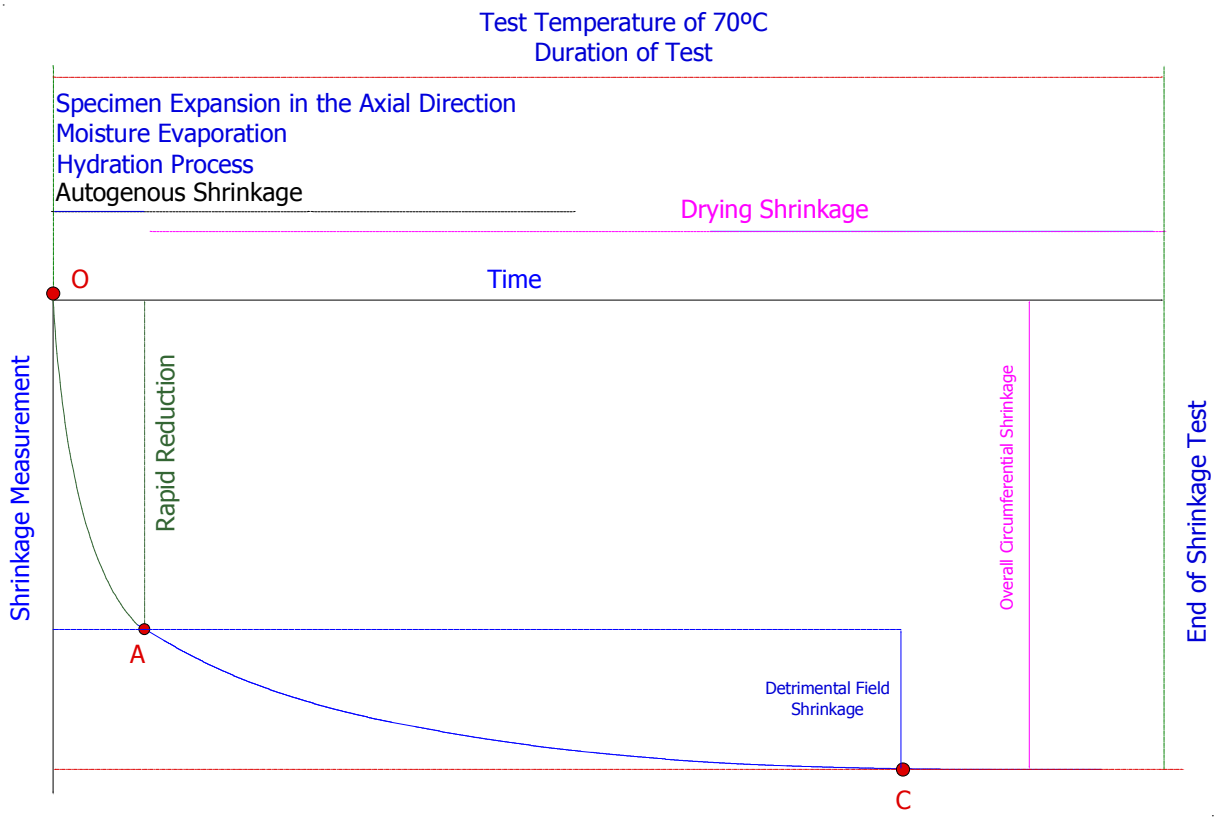

Figure 6-6 Conceptualisation of the Shrinkage-Time Curve and Factors of Influence [Circumferential Shrinkage – Extensometer]

Furthermore, the concentric nature of the cylindrical specimen does not foster an 'outward' response [dilation in the circumferential] but rather an axial relaxation. An axial relaxation could be positive [expansion] or negative [shrinkage]. Figure 6-7a and 6-7b provide a conceptualisation of the cylinder specimen relative to moisture loss [shrinkage] and response. This suggests that the rapid reduction observed in the circumferential shrinkage-time curve is more attributed to the initial axial expansion than the loss of moisture from the specimen.

Figure 6-8 shows the beam linear measurement and conceptualises the factors of influence to the shrinkage-time curve. Owing to the beam 'edge-effects' and the prevailing friction at the interface between the bottom of the beam and base plate, the measurement of the overall beam shrinkage is obstructed. This indicates that measurement by the LVDT [positioned at the rear ends] and surface mounted strain gauges will differ.

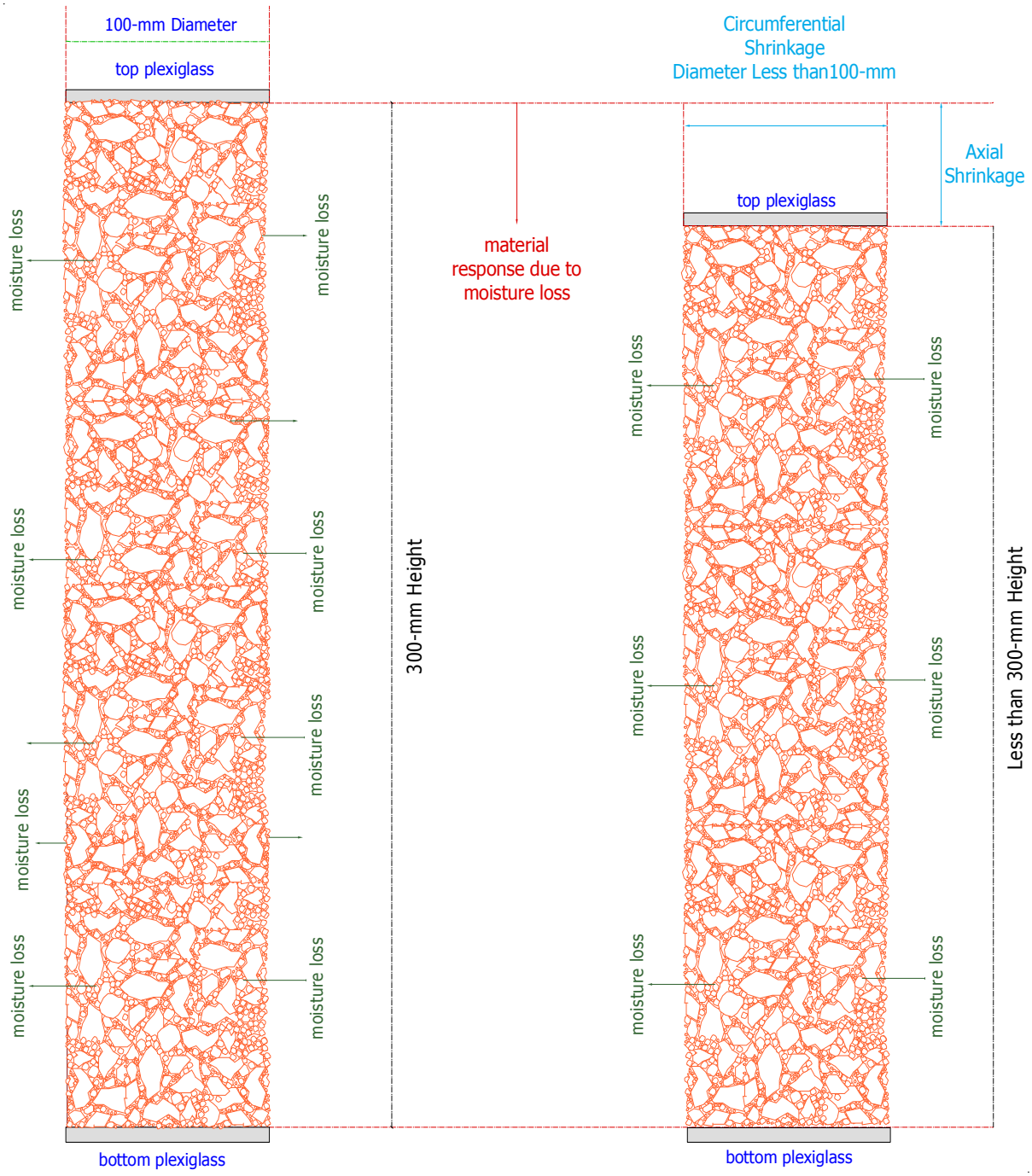

Figure 6-7a Overview of Axial and Circumferential Shrinkage Measurements

The cylinder specimen uses a different measuring criterion compared to the beam. The axial shrinkage measurement is not influenced by friction [if any]. Equally measuring the circumferential shrinkage at the mid height of the specimen also negates the influence of friction. Unlike concrete mix types, cement-stabilised materials contained low cement contents; in this research, a maximum of 6.0% cement content is considered. At such low cement contents, the behavioural properties, particularly in response to shrinkage are different from those observed with concrete. Heterogeneity of the cement-stabilised materials plays a significant role in characterising shrinkage. The appearance of cracks is dependent on the imposed restraints relative to the tensile strength of the material.

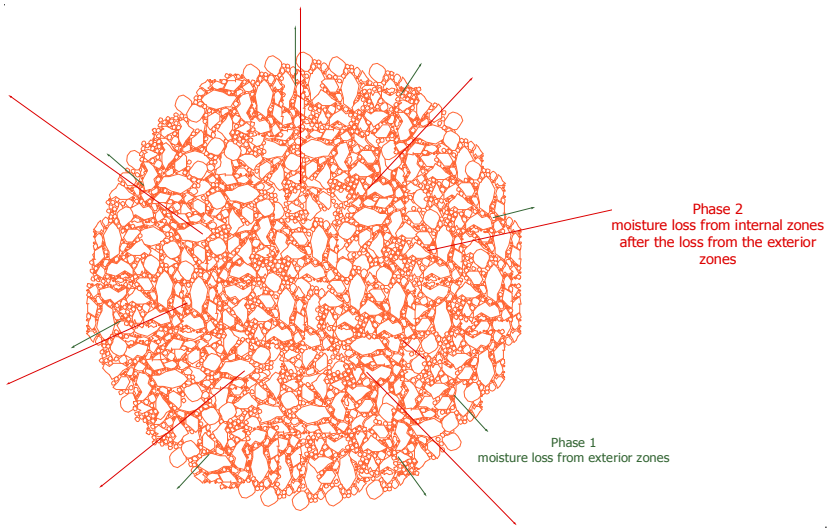

Figure 6-7b Concept of Specimen Moisture Loss [Exterior versus Internal Core]

Figure 6-8 Overview of the Beam Linear Shrinkage Measurements [Effect of Material Matrix, Surface Exposure and Friction to Dimensional Change]

6.3.2 Linear Shrinkage Results [Strain Gauge and LVDT]

Table 6-3 as well as Figures 6-6a and 6-6b provide the average shrinkage results assessed from the middle section of the beam using a pair of strain gauge with a length of 90 mm. A pair of the strain gauges was positioned on the middle section of the beam as well as its two rear ends. Considering the beam 'edge-effects' only strain gauge reading of the middle section of the beam were considered. The shrinkage results characterise the differences within the mix types relative to measuring criterion. The effect of the maximum aggregate size, cement content and type of material on the total shrinkage is illustrated. For identical material type, a reduction in the maximum aggregate size results in an increase in shrinkage. This is because an increase in surface area availability results leading to higher moisture demand.

Table 6-3 Average Linear Shrinkage Results [Strain Gauge – Middle Section]

Hornfels Mix Type	[Pmax = 19.0 mm]	Beam Specimens	Linear Shrinkage
Cement Content [%]	Moisture Content [%]	Vibratory-hammer Method Dry Density [kg/m^3]	Strain Gauge x10^{-6} [mm/mm]
2	5.2	2283	1.1
3	5.1	2209	2.3
6	4.4	2178	6.1
Hornfels Mix Type	[Pmax = 4.75mm]	Beam Specimens	Linear Shrinkage
Cement Content [%]	Moisture Content [%]	Vibratory-hammer Method Dry Density [kg/m^3]	Strain Gauge x10^{-6} [mm/mm]
2	6.3	2103	3.2
3	6.1	2088	4.2
6	5.7	2069	8.7
Ferricrete Mix Type	[Pmax = 19.0 mm]	Beam Specimens	Linear Shrinkage
Cement Content [%]	Moisture Content [%]	Vibratory-hammer Method Dry Density [kg/m^3]	Strain Gauge x10^{-6} [mm/mm]
3	7.9	2082	4.2
4	7.5	2012	5.0
6	7.2	1993	8.2
Ferricrete Mix Type	[Pmax = 4.75 mm]	Beam Specimens	Linear Shrinkage
Cement Content [%]	Moisture Content [%]	Vibratory-hammer Method Dry Density [kg/m^3]	Strain Gauge x10^{-6} [mm/mm]
3	10.3	1730	6.5
4	10.1	1743	9.2
6	9.7	1689	9.3

All mix types with 4.75 mm as the maximum aggregate size exhibit a higher overall shrinkage criterion than mix types with 19.0 mm as the maximum aggregate size. The effect of maximum aggregate size on shrinkage is attributable to the influence of particle size on the water demand and the reduced ability to retard further shrinkage. Large aggregate or particle size impedes the occurrence shrinkage. This provides insights regarding the field shrinkage whereby a maximum aggregate size in a cement-stabilised layer is usually more than double of the laboratory specimen. In the field, a maximum aggregate size of 37.5 mm or more depending on the type and quality of material is considered. Figures 6-6a and 6-6b illustrate the influence of maximum particle size on shrinkage as well as the type and quality of material.

Mix types with large aggregate size exhibit lower shrinkage than mix types with a small aggregate size. Large sized aggregates not only retard shrinkage but also reduce the amount of moulding moisture due to their reduce surface-area availability. Small sized aggregates present a large surface-area availability, which increases the moisture demand necessary for maximum dry density. An increase in moisture content results in a corresponding increase in shrinkage. The rate of shrinkage is dependent on the maximum aggregate size, moisture and cement as well as type of material. For the same mix type, addition of cement to material registers a corresponding increase in shrinkage. Adding fine cement particles to

material alters the gradation, thus increasing moisture demand and the rate of hydration. Moisture and hydration play a significant role on the resultant material shrinkage.

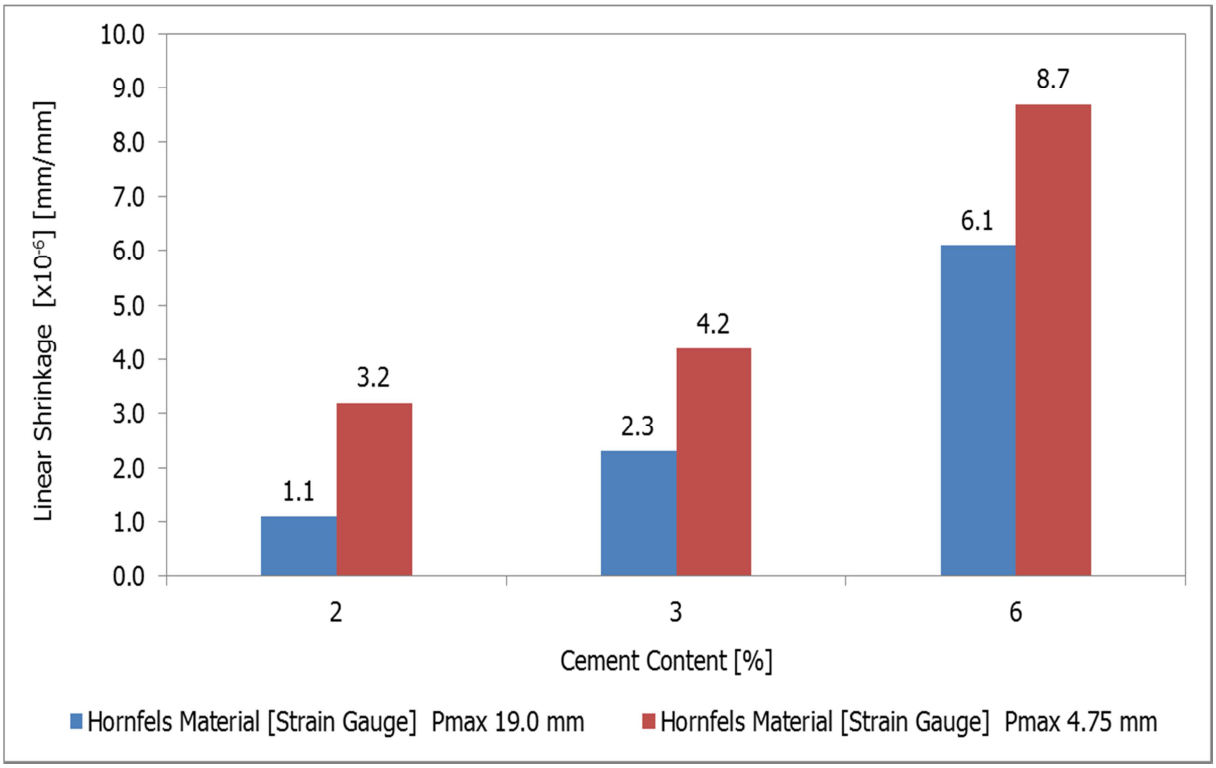

Figure 6-6a Influence of the Maximum Aggregate Size of Average Linear Shrinkage [Strain Gauge – Middle Section of the Hornfels Beam]

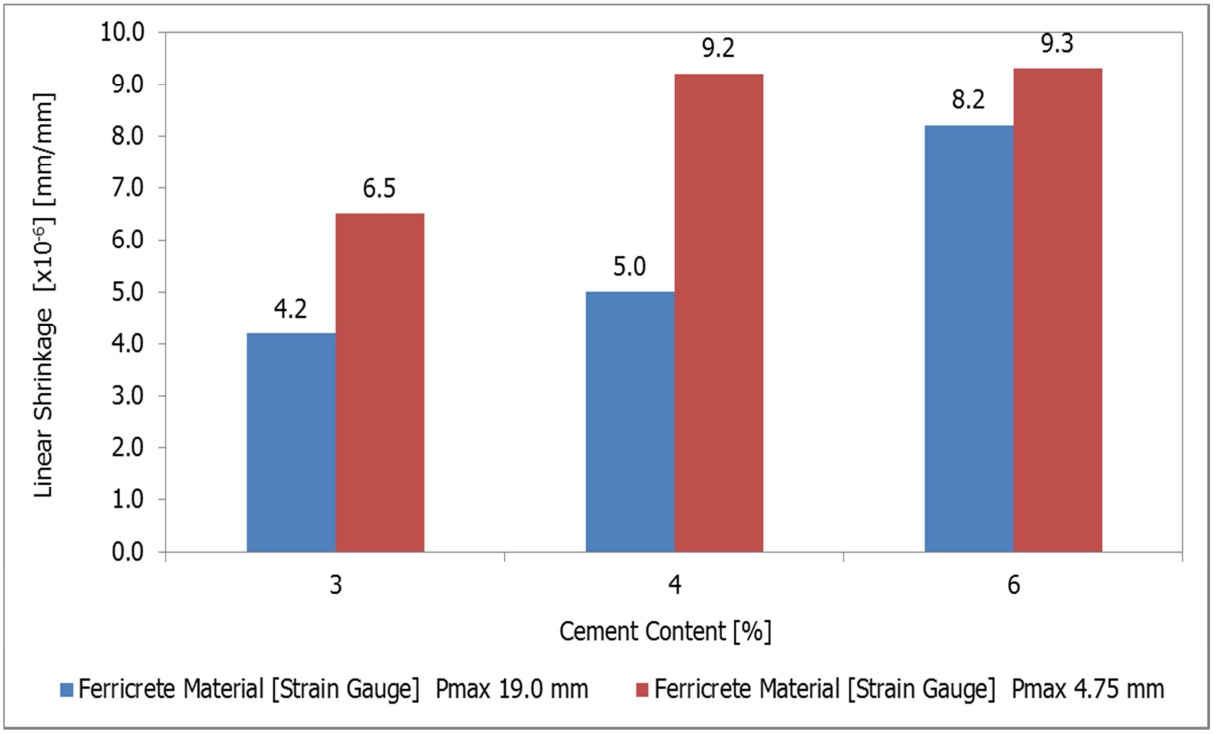

Figure 6-6b Influence of the Maximum Aggregate Size of Average Linear Shrinkage [Strain Gauge – Middle Section of the Ferricrete Beam]

Table 6-4 and Figure 6-7 present the absolute linear shrinkage values obtained using LVDT. One LVDT was positioned firmly to the rear ends of the beam. The LVDT measured the

dimensional changes over the entire beam length of 400 mm. The initial and final LVDT readings were recorded. The difference between the initial and final readings is the dimensional change value [LVDT value]. The LVDT measured over the entire beam length while the strain gauge measured over a length of 90 mm. The absolute value is the ratio of the dimensional change value [LVDT value] and beam length [400 mm].

A comparison between the strain gauge measurements [Figures 6-6a and 6-6b] to LVDT measurements [Figures 6-7a and 6-7b] typifies the differences in instrumentation and measuring criteria in determining the material shrinkage. Hornfels mix types with 2.0% cement content and ferricrete mix types with a cement content of 3.0% recorded infinitesimal shrinkage values with the LVDT compared to those registered by the strain gauges. The LVDT measured shrinkage values were lesser than those obtained using the strain gauges mounted in the middle section of the beam. With the strain gauges, the obtained results indicate a gradual increase corresponding to the addition of cement to the material. LDVT shrinkage results show an exponential increment, which indicates the influence of the beam edge effects [resultant density] relative to cement content in the mix.

Table 6-4 Ferricrete Beam Linear Shrinkage Results [Absolute Values]

	Ferricrete Material Pmax 19.0 mm [LVDT]		
Cement Content [%] [Beam Number]	Dimensional Change LVDT [mm]	Linear Shrinkage [mm/mm] [Absolute Value= (LVDT/Beam Length)]	Linear Shrinkage [x10^{-6}] mm/mm
3% [B.1]	8.96E-06	2.24E-08	0.22
3% [B.2]	9.87E-06	2.47E-08	0.02
3% [B.3]	7.12E-06	1.78E-08	0.02
4% [B.1]	6.57E-04	1.64E-06	1.64
4% [B.2]	5.75E-04	1.44E-06	1.44
4% [B.3]	5.96E-04	1.49E-06	1.49
6% [B.1]	2.45E-03	6.13E-06	6.13
6% [B.2]	3.19E-03	7.97E-06	7.97
6% [B.3]	3.50E-03	8.75E-06	8.75
	Ferricrete Material Pmax 4.75 mm [LVDT]		
Cement Content [%] [Beam Number]	Dimensional Change LVDT [mm]	Linear Shrinkage [mm/mm] [Absolute Value= (LVDT/Beam Length)]	Linear Shrinkage [x10^{-6}] mm/mm
3% [B.1]	1.91E-04	4.79E-07	0.5
3% [B.2]	2.45E-04	6.13E-07	0.6
3% [B.3]	2.13E-04	5.33E-07	0.5
4% [B.1]	6.01E-04	1.50E-06	1.5
4% [B.2]	6.89E-04	1.72E-06	1.7
4% [B.3]	6.98E-04	1.74E-06	1.7
6% [B.1]	4.28E-03	1.07E-05	10.7
6% [B.2]	5.01E-03	1.25E-05	12.5
6% [B.3]	4.11E-03	1.03E-05	10.3
	Ferricrete Material Pmax 2.36 mm [LVDT]		
Cement Content [%] [Beam Number]	Dimensional Change LVDT [mm]	Linear Shrinkage [mm/mm] [Absolute Value= (LVDT/Beam Length)]	Linear Shrinkage [x10^{-6}] mm/mm
3% [B.1]	3.61E-04	9.04E-07	0.9
3% [B.2]	4.48E-04	1.12E-06	1.1
3% [B.3]	4.45E-04	1.11E-06	1.1
4% [B.1]	8.91E-04	2.23E-06	2.2
4% [B.2]	9.98E-04	2.50E-06	2.5
4% [B.3]	1.13E-03	2.81E-06	2.8
6% [B.1]	5.68E-03	1.42E-05	14.2
6% [B.2]	6.81E-03	1.70E-05	17.0
6% [B.3]	6.15E-03	1.54E-05	15.4

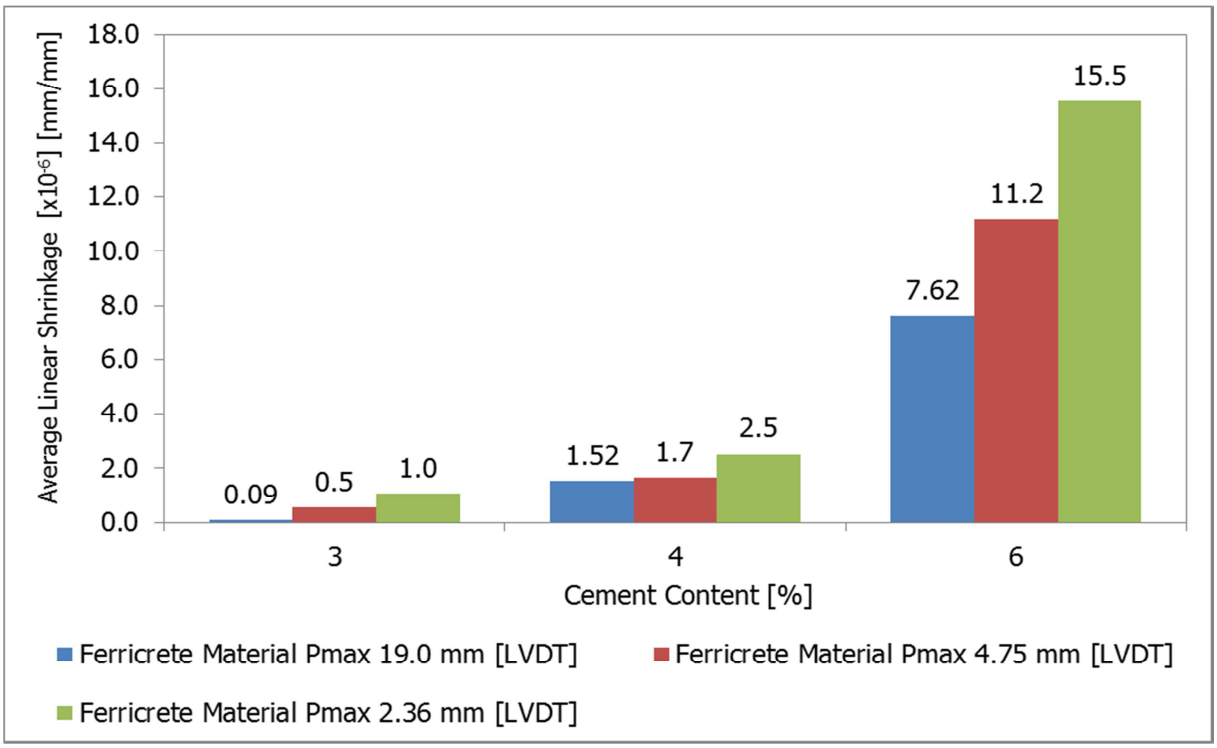

Figure 6-7a Influence of the Maximum Aggregate Size of Average Linear Shrinkage [LVDT – Rear End of the Ferricrete Beam]

Table 6-5 Hornfels Beam Linear Shrinkage Results [Absolute Values]

	Hornfels Material Pmax 19.0 mm [LVDT]		
Cement Content [%] [Beam Number]	Dimensional Change LVDT [mm]	Linear Shrinkage [mm/mm] [Absolute Value= (LVDT/Beam Length)]	Linear Shrinkage [x10^{-6}] mm/mm
2% [B.1]	8.15E-06	2.04E-08	0.02
2% [B.2]	6.21E-06	1.55E-08	0.02
2% [B.3]	1.54E-06	3.86E-09	0.00
3% [B.1]	1.54E-04	3.86E-07	0.39
3% [B.2]	1.25E-04	3.14E-07	0.31
3% [B.3]	1.13E-04	2.81E-07	0.28
6% [B.1]	7.25E-04	1.81E-06	1.81
6% [B.2]	8.80E-04	2.20E-06	2.20
6% [B.3]	9.71E-04	2.43E-06	2.43
	Hornfels Material Pmax 4.75 mm [LVDT]		
Cement Content [%] [Beam Number]	Dimensional Change LVDT [mm]	Linear Shrinkage [mm/mm] [Absolute Value= (LVDT/Beam Length)]	Linear Shrinkage [x10^{-6}] mm/mm
2% [B.1]	9.46E-05	2.36E-07	0.24
2% [B.2]	6.45E-05	1.61E-07	0.16
2% [B.3]	8.21E-05	2.05E-07	0.21
3% [B.1]	2.91E-04	7.28E-07	0.73
3% [B.2]	4.40E-04	1.10E-06	1.10
3% [B.3]	4.54E-04	1.14E-06	1.14
6% [B.1]	2.28E-03	5.70E-06	5.70
6% [B.2]	2.01E-03	5.03E-06	5.03
6% [B.3]	2.11E-03	5.28E-06	5.28
	Hornfels Material Pmax 2.36 mm [LVDT]		
Cement Content [%] [Beam Number]	Dimensional Change LVDT [mm]	Linear Shrinkage [mm/mm] [Absolute Value= (LVDT/Beam Length)]	Linear Shrinkage [x10^{-6}] mm/mm
2% [B.1]	1.46E-05	3.64E-08	0.04
2% [B.2]	2.56E-05	6.41E-08	0.06
2% [B.3]	1.57E-05	3.92E-08	0.04
3% [B.1]	4.46E-04	1.11E-06	1.11
3% [B.2]	4.69E-04	1.17E-06	1.17
3% [B.3]	4.67E-04	1.17E-06	1.17
6% [B.1]	3.28E-03	8.20E-06	8.20
6% [B.2]	3.01E-03	7.53E-06	7.53
6% [B.3]	3.11E-03	7.78E-06	7.78

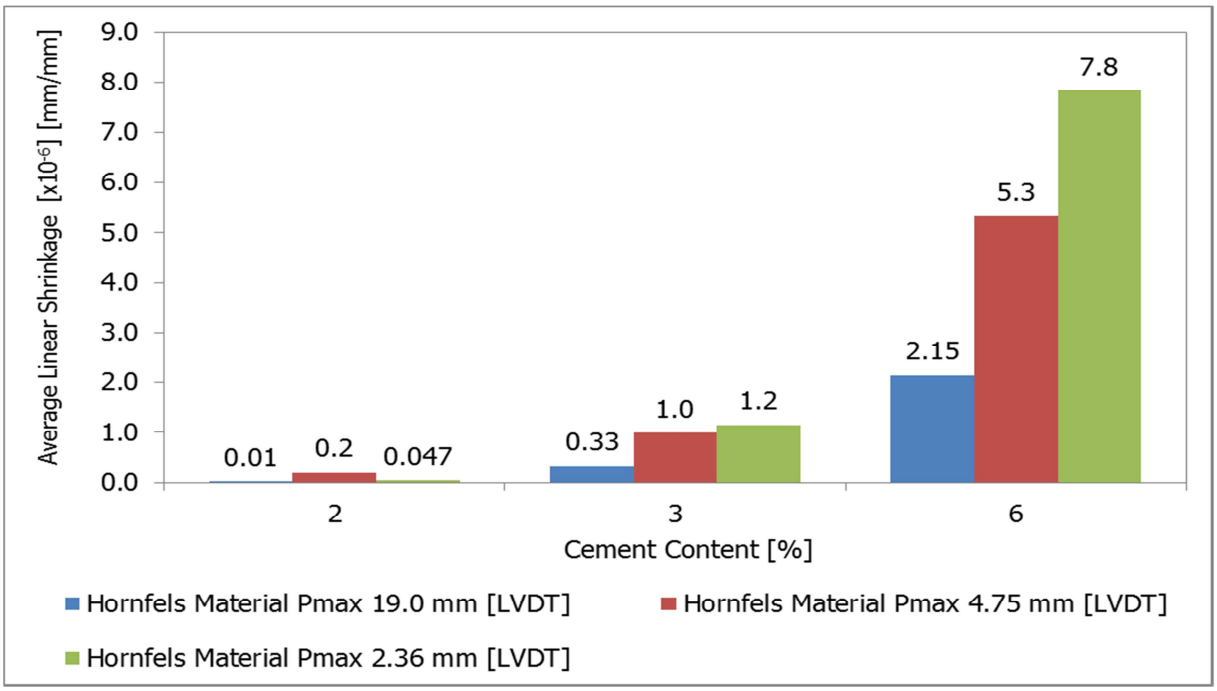

Figure 6-7b Influence of the Maximum Aggregate Size of Average Linear Shrinkage [LVDT – Rear End of the Hornfels Beam]

The beam linear shrinkage results provide the following interpretations:

a) a reduction in maximum aggregate size results in a corresponding increase of linear shrinkage; ferricrete and hornfels mix types with a maximum aggregate size of 2.36 mm exhibit the highest overall material shrinkage compared to their equivalent material mix types with larger maximum aggregate sizes of 4.75 mm and 19.0 mm
b) at low cement content of 2% and 3% minimal linear shrinkage values are registered; this provides insights regarding the degree of shrinkage relative to the cement content in the mix
c) material type and quality influence shrinkage; a material with high amount of fines requires a higher moisture content in order to its MDD however this increases shrinkage
d) the influence of friction and beam edge-effects on the measurement of shrinkage is realised; a combination of beam edge effects and friction lowered the LVDT shrinkage values

The results show that the resultant linear shrinkage is dependent on the cement and moisture contents, type and quality of the material as well as the maximum aggregate size in the mix. This supports earlier observations obtained using the strain gauge instrumentation. Ferricrete, which exhibits a higher plasticity index than hornfels, registered highest overall linear shrinkage. Despite the differences in the measurement of linear shrinkage, the obtained trends provide insights regarding the shrinkage potential of the cement-stabilised materials. This suggests that the instrumentation used, the adopted criterion of measuring shrinkage relative to the geometric characteristics of the specimen should be standardised. This will allow an acceptable range of consistency while evaluating shrinkage at laboratory level. Section 6.3.3 provides the axial shrinkage results.

6.3.3 Axial Shrinkage Results [Dial Gauge]

Table 6-6 lists the axial shrinkage measurements for the various mix types with a maximum aggregate size of 19.0 mm. Figures 6-8a and 6-8b illustrate the axial shrinkage results for ferricrete and hornfels mix types. Dissimilarities in shrinkage due to differences in mix types, specimen size and shape as well as the type and quality of material, are illustrated.

Table 6-6 Axial Shrinkage Measurements [Dial Gauge Readings]

	Ferricrete Material Pmax 19.0 mm		
Cement Content [%] [Cylinder Number]	Dimensional Change [Dial Gauge] [mm]	Axial Shrinkage [mm/mm] [Absolute Value= (Dial Gauge/Cylinder Height)]	Axial Shrinkage [$x10^{-6}$] mm/mm
0% [C.1]	2.00E-02	6.67E-05	66.7
0% [C.2]	2.70E-02	9.00E-05	90.0
0% [C.3]	1.00E-02	3.33E-05	33.3
4% [C.1]	2.70E-01	9.00E-04	900.0
4% [C.2]	5.14E-01	1.71E-03	1713.3
4% [C.3]	6.10E-01	2.03E-03	2033.3
6% [C.1]	1.14E+00	3.79E-03	3790.0
6% [C.2]	1.26E+00	4.20E-03	4200.0
6% [C.3]	1.16E+00	3.88E-03	3876.7
	Hornfels Material Pmax 19.0 mm		
Cement Content [%] [Cylinder Number]	Dimensional Change [Dial Gauge] [mm]	Axial Shrinkage [mm/mm] [Absolute Value= (Dial Gauge/Cylinder Height)]	Axial Shrinkage [$x10^{-6}$] mm/mm
0% [C.1]	3.75E-03	1.25E-05	12.5
0% [C.2]	2.80E-03	9.35E-06	9.3
0% [C.3]	3.44E-03	1.15E-05	11.5
2% [C.1]	6.55E-02	2.18E-04	218.4
2% [C.2]	6.98E-02	2.33E-04	232.6
2% [C.3]	9.00E-02	3.00E-04	300.0
3% [C.1]	1.48E-01	4.92E-04	491.8
3% [C.2]	1.46E-01	4.86E-04	485.7
3% [C.3]	1.56E-01	5.19E-04	519.4
6% [C.1]	2.50E-01	8.33E-04	833.3
6% [C.2]	3.34E-01	1.11E-03	1115.0
6% [C.3]	2.88E-01	9.61E-04	960.9

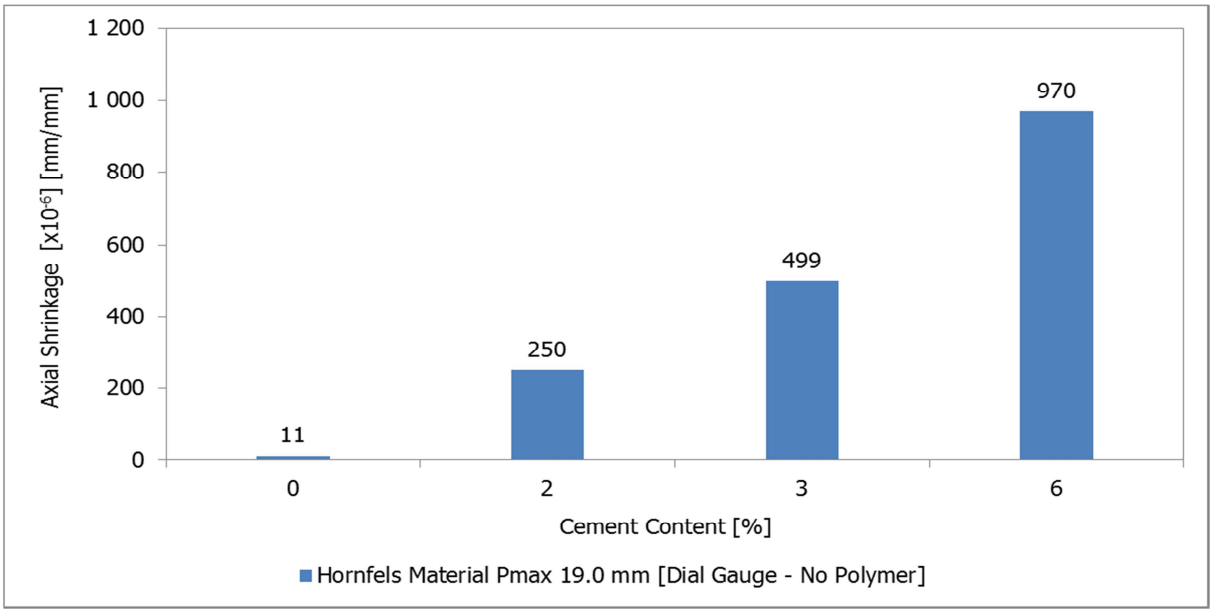

Figure 6-8a Hornfels Average Axial Shrinkage [Absolute Values - Dial Gauge]

Ferricrete exhibits higher overall axial shrinkage than hornfels. The differences between ferricrete and hornfels are significant at high cement contents. The axial results indicate similar trends of material shrinkage as shown with the beam linear approach. However, for the same mix type, the axial shrinkage values are significantly higher than the beam linear values. The axial shrinkage, which is a measurement taken in the direction of compaction and in line with the natural gravitational force over a length of 300 mm, is not impeded by friction. The beam linear shrinkage is a measurement perpendicular to the direction of compaction and is obstructed from free movement by the friction and to an acceptable degree, the self-weight of the beam, as well as, the heterogeneity of the material. As a result, there is a possibility of micro cracks manifesting within the beam specimen compared to the cylinder.

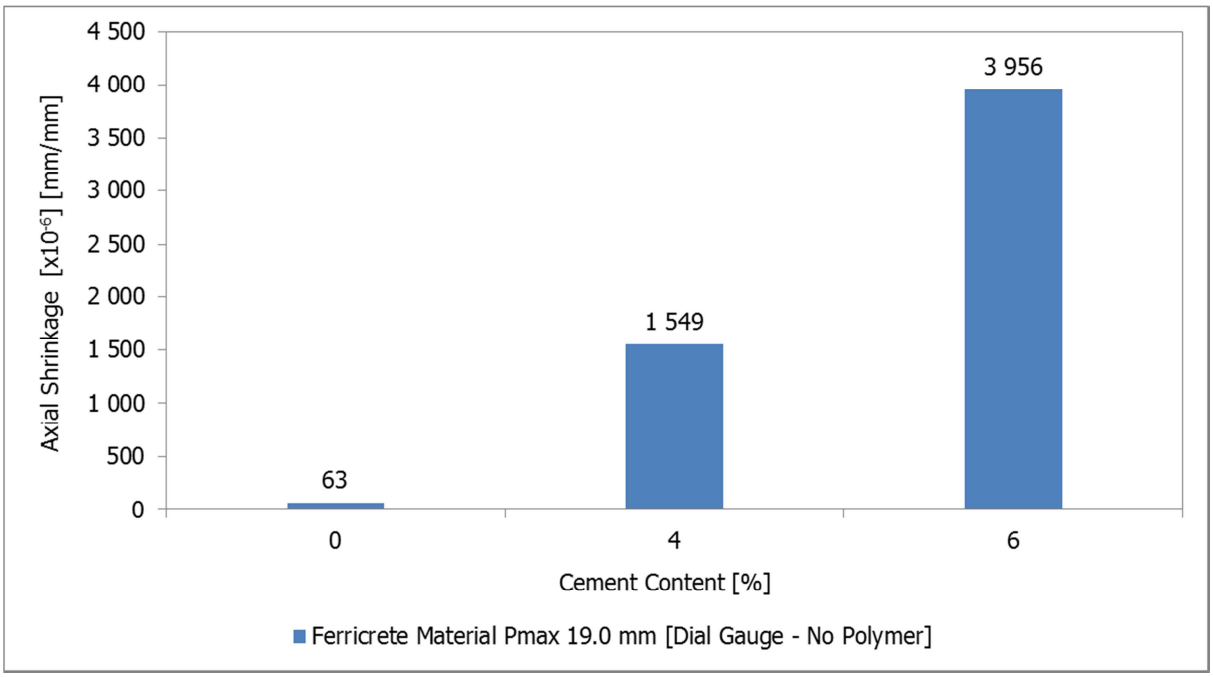

Figure 6-8b Ferricrete Average Axial Shrinkage [Absolute Values - Dial Gauge]

6.3.4 Circumferential Shrinkage Results [Extensometer]

Table 6-7 lists the circumferential absolute shrinkage values. Figures 6-9a and 6-9b illustrate the average circumferential shrinkage absolute values for hornfels and ferricrete. In interpreting the circumferential and axial shrinkage results, the direction of compaction relative to the 100 mm diameter and a height of 300 mm must be taken into consideration. This is because the slenderness ratio relative to the specimen surface exposure influences the rate of moisture loss and total measured shrinkage. The axial and circumferential values provide insights regarding the specimen volumetric shrinkage. Similar trends as observed with the axial and beam linear are observed.

Table 6-7 Circumferential Shrinkage Measurements [No Polymer]

	Ferricrete Material Pmax 19.0 mm		
Cement Content [%] [Cylinder Number]	Dimensional Change [Exten'l] [mm]	Circumferential Shrinkage [Absolute Value= (Exten'l/Cylinder Circum.)] [mm/mm]	Circumferential Shrinkage [x10^{-6}] mm/mm
0% [C.1]	2.20E-02	7.33E-05	73.3
0% [C.2]	3.30E-02	1.10E-04	110.0
4% [C.1]	3.16E-01	1.05E-03	1053.3
4% [C.3]	2.83E-01	9.43E-04	943.3
6% [C.1]	4.20E-01	1.40E-03	1400.0
6% [C.3]	4.21E-01	1.40E-03	1403.3
	Hornfels Material Pmax 19.0 mm		
Cement Content [%] [Cylinder Number]	Dimensional Change [Exten'l] [mm]	Circumferential Shrinkage [Absolute Value= (Exten'l/Cylinder Circum.)] [mm/mm]	Circumferential Shrinkage [x10^{-6}] mm/mm
0% [C.1]	2.20E-02	7.33E-05	73.3
0% [C.3]	1.30E-02	4.33E-05	43.3
2% [C.1]	1.90E-02	6.33E-05	63.3
2% [C.3]	1.80E-02	6.00E-05	60.0
3% [C.1]	4.80E-02	1.60E-04	160.0
3% [C.3]	6.20E-02	2.07E-04	206.7
6% [C.1]	1.25E-01	4.17E-04	416.7
6% [C.3]	1.14E-01	3.80E-04	380.0
Note: Exten'l - Extensometer ; Circum. - Circumferential			

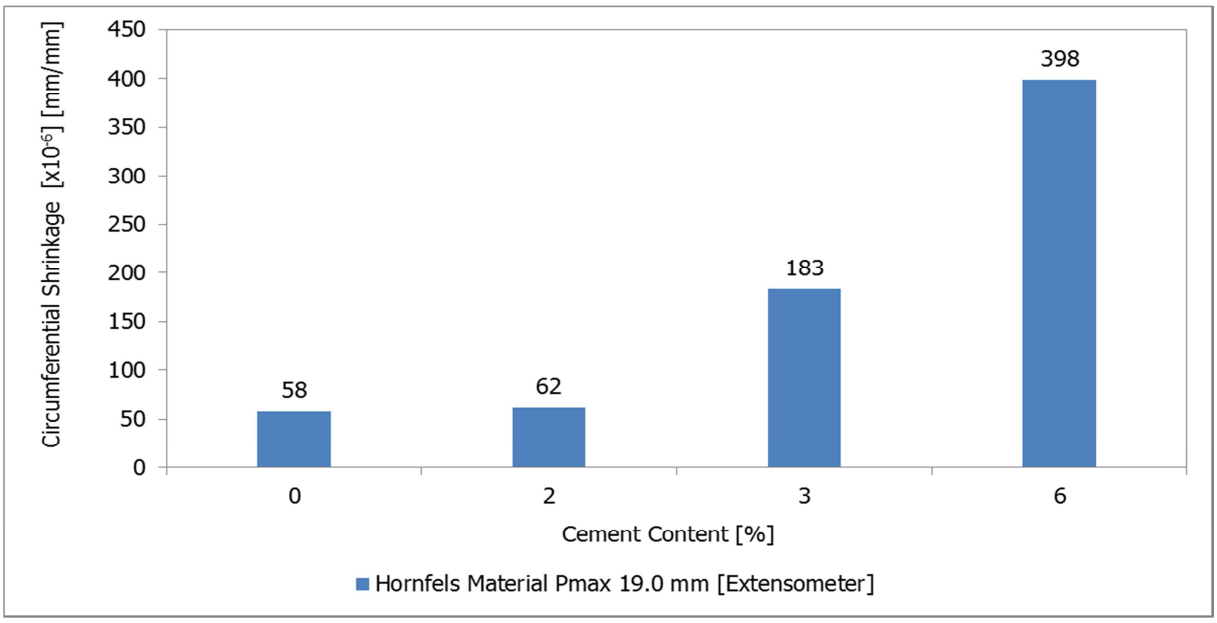

Figure 6-9a Hornfels Average Circumferential Shrinkage [Absolute Values – Extensometer]

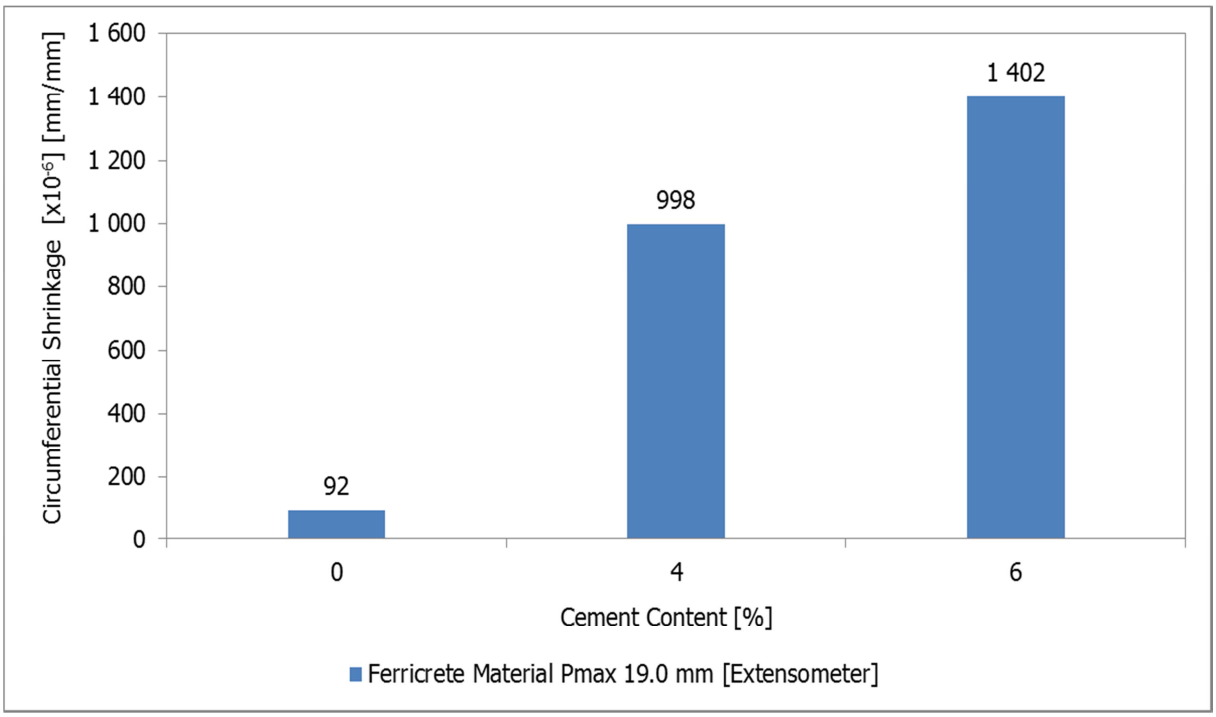

Figure 6-9b Ferricrete Average Circumferential Shrinkage [Absolute Values – Extensometer]

6.3.5 Assessment of Volumetric Shrinkage [Cylindrical Specimen]

Specimen size and shape influence the magnitude of shrinkage measured at laboratory level. The degree of shrinkage is proportional to the amount of moisture lost under specific environmental conditions. The distribution and rate of moisture loss are dependent on the size and shape of the specimen as well as the characteristics of the pore structure [i.e. achievable density]. The diffusion of moisture from the internal zones of the specimen is influenced by the specimen geometry and interconnectivity of the pore structure relative to the achievable density. The size and shape of the specimen are at times characterised relative to its slenderness ratio and surface exposure to the drying conditions.

Volumetric shrinkage takes into account of the shape and size of the specimen in computing shrinkage of the material. Analysing the volumetric provides additional data regarding the shrinkage potential of cement-stabilised material. The assessment involves using simple mathematical relations as shown in Table 6-8 as well as Figure 6-10a and 6-10b. Similar shrinkage trends as observed with axial and circumferential criteria are illustrated in Figures 6-10a and 6-10b. Ferricrete registered a higher volumetric shrinkage than hornfels.

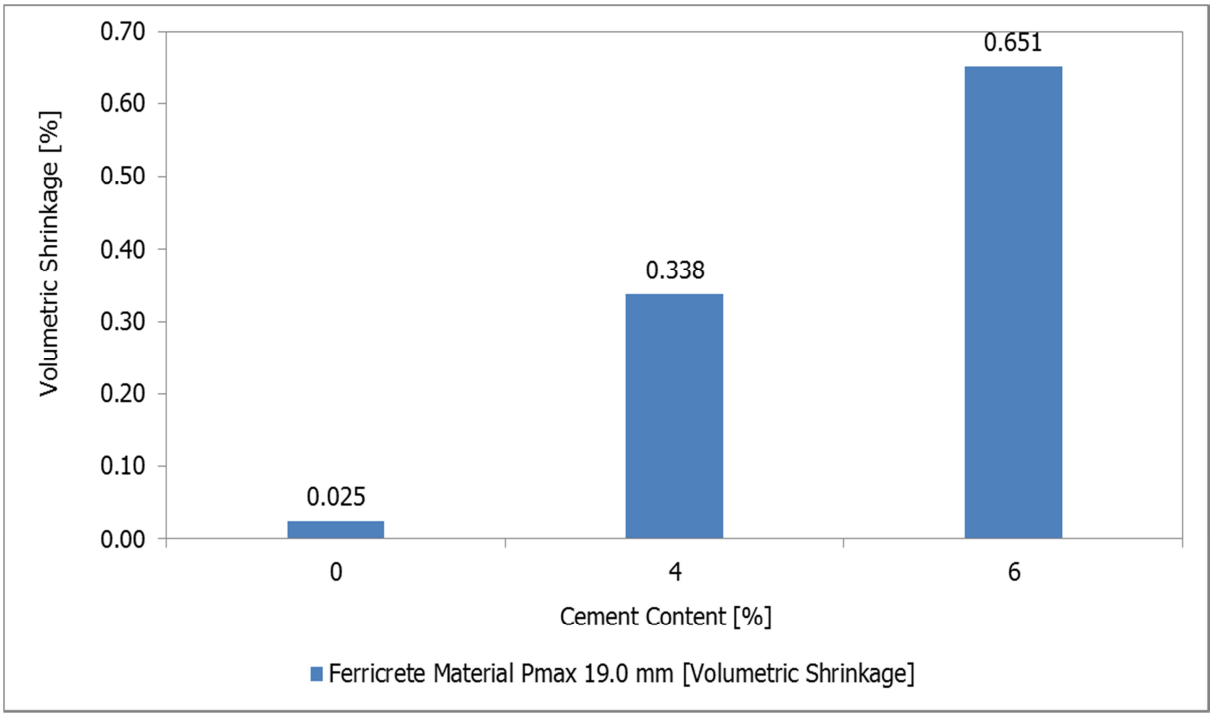

Figure 6-10a Average Volumetric Shrinkage Results [Ferricrete No Polymer]

Table 6-8 Volumetric Shrinkage Measurements [No Polymer]

Ferricrete Material Pmax 19.0 mm					R = 50 mm		
Cement Content [%] [Cylinder Number]	Circumferential Shrinkage [C_o] mm	Axial Shrinkage Change in Height [h] mm	Change in Radius [r = (C_o/(2 x 3.14)] [mm]	Specimen Height [H] [mm]	Original Volume Vo = 3.14R^2H [$x10^6$] [mm^3]	Final Volume Vf = 3.14 x $(R-r)^2$ x (H-h) [$x10^6$] [mm^3]	Volumetric Shrinkage V = ((Vo - Vf)/Vo) x 100 [%]
0% [C.1]	2.20E-02	2.00E-02	3.50E-03	304	2.386	2.386	0.021
0% [C.2]	3.30E-02	2.70E-02	5.25E-03	309	2.426	2.425	0.030
4% [C.1]	3.16E-01	2.70E-01	5.03E-02	292	2.292	2.285	0.293
4% [C.3]	2.83E-01	6.10E-01	4.50E-02	302	2.371	2.362	0.382
6% [C.1]	4.20E-01	1.14E+00	6.68E-02	304	2.386	2.371	0.640
6% [C.3]	4.21E-01	1.16E+00	6.70E-02	294	2.308	2.293	0.662
Hornfels Material Pmax 19.0 mm					R = 50 mm		
Cement Content [%] [Cylinder Number]	Circumferential Shrinkage [C_o] mm	Axial Shrinkage Change in Height [h] mm	Change in Radius [r = (C_o/(2 x 3.14)] [mm]	Specimen Height [H] [mm]	Original Volume Vo = 3.14R^2H [$x10^6$] [mm^3]	Final Volume Vf = 3.14 x $(R-r)^2$ x (H-h) [$x10^6$] [mm^3]	Volumetric Shrinkage V = ((Vo - Vf)/Vo) x 100 [%]
0% [C.1]	2.20E-02	3.75E-03	3.50E-03	299	2.347	2.347	0.015
0% [C.3]	1.30E-02	3.44E-03	2.07E-03	307	2.410	2.410	0.009
2% [C.1]	1.90E-02	6.55E-02	3.02E-03	308	2.418	2.417	0.033
2% [C.3]	1.80E-02	9.00E-02	2.86E-03	301	2.363	2.362	0.041
3% [C.1]	4.80E-02	1.48E-01	7.64E-03	297	2.331	2.330	0.080
3% [C.3]	6.20E-02	1.56E-01	9.87E-03	293	2.300	2.298	0.093
6% [C.1]	1.25E-01	2.50E-01	1.99E-02	304	2.386	2.383	0.162
6% [C.3]	1.14E-01	2.88E-01	1.81E-02	302	2.371	2.367	0.168

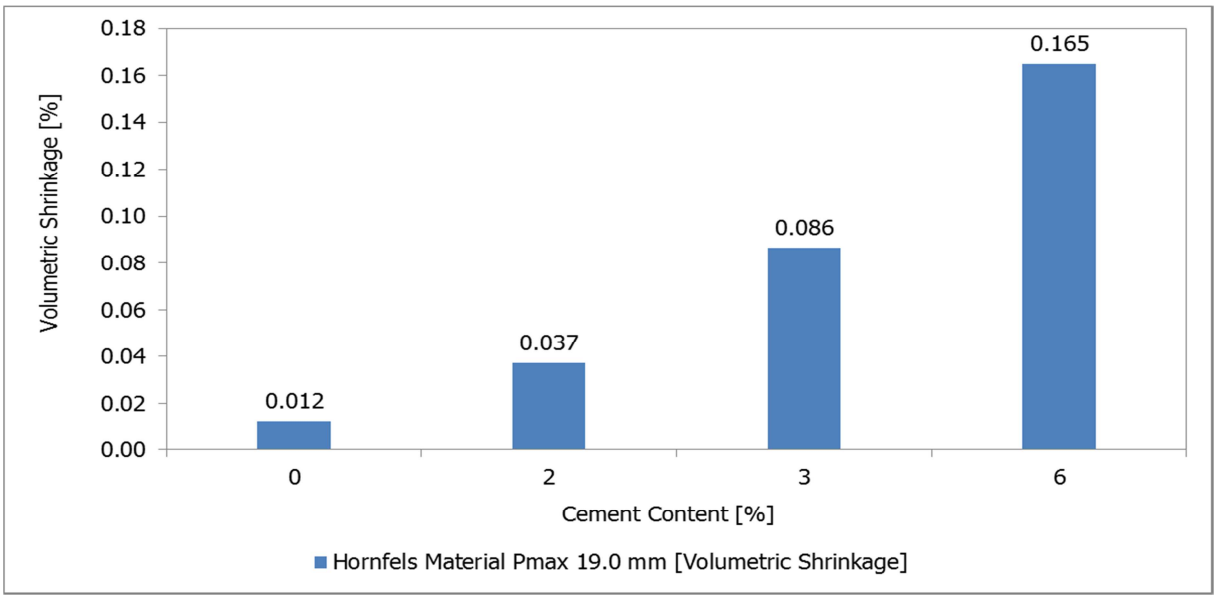

Figure 6-10b Average Volumetric Shrinkage Results [Hornfels No Polymer]

6.3.6 Comparison of Beam and Cylinder Shrinkage

Drying shrinkage is dependent upon several factors, which include aggregate properties, the amount of cement and moisture in the mix, mixing criteria, curing conditions and specimen size [geometric characteristics]. Under specific curing conditions, cement-stabilised material will undergo some volumetric change. Each specimen size exhibits different shrinkage criteria under specific curing conditions. The magnitude of the measured shrinkage is dependent on the curing conditions, particularly relative humidity, temperature and air circulation as well as the shape and size of the specimen. The type of specimen and the measurement criteria adopted influence the total shrinkage.

Figure 6-11 illustrates the effect of frictional forces [restraint], specimen size and shape relative to the measurement of material shrinkage. Cognisance of the compaction criteria and resultant density as well as specimen geometry is necessary when making comparisons. The beam exhibits a restraint at the interface between the base plate and the beam.

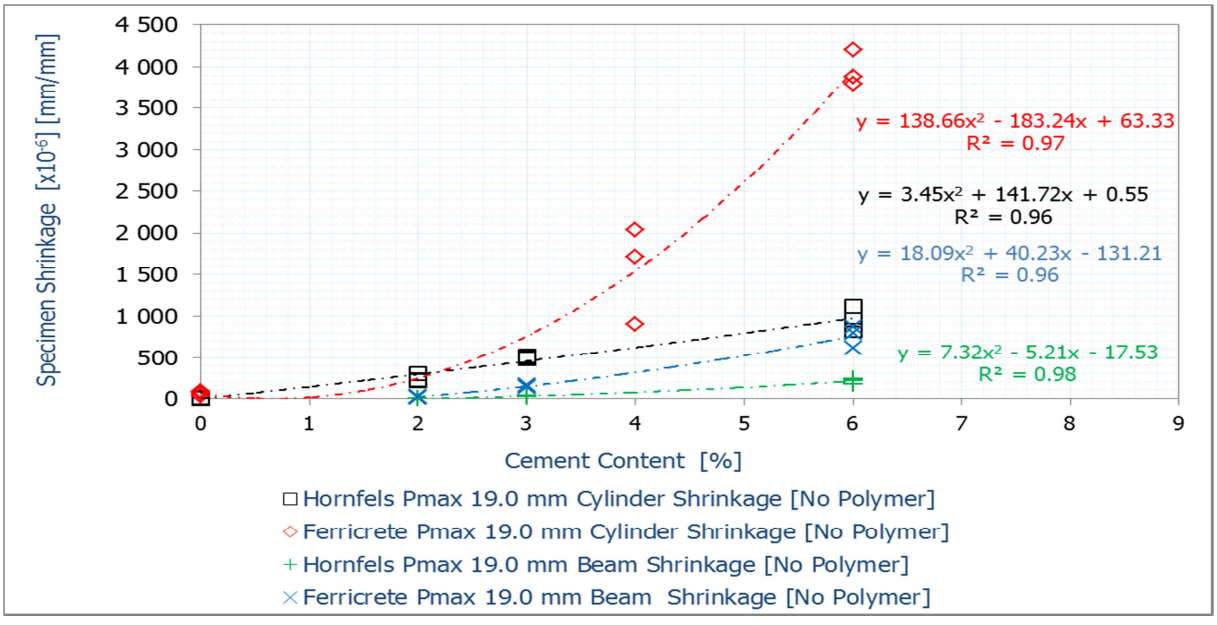

Figure 6-11 Beams versus Cylinders Shrinkage [Effect of Friction, Specimen Size and Shape]

Despite applying mould-oil to the base plate, the self-weight and roughness of the beam causes friction at the interface of the base plate and the underneath of the beam. The resultant friction retards the beam from freely moving as shrinks. The roughness of the underneath of the beam emanates from particle protrusion and unevenness; this increases the friction at the interface.

6.4 Effect of Polymer on Material Shrinkage

In the previous chapters, the influence of the polymer has been associated more to the amount of cement in the mix as well as the type and quality of the material. The interaction of polymer and cement is as either physical or chemical and even a combination of both. The cement and polymer interaction influences the hydration process, autogenous shrinkage and certainly the rate of evaporation. Table 6-9 lists the absolute shrinkage values. Figures 6-12a and 6-12b illustrate the effect of the polymer on the shrinkage of cement-stabilised materials

The shrinkage results reveal that adding the polymer to stabilised materials reduces shrinkage, particularly at high cement contents. Mix type stabilised at low cement content [with and without polymer] showed a slight reduction in shrinkage. This indicates that applying polymer to heavily stabilised materials is likely to result in a substantial reduction in shrinkage. This observation characterises the cement and polymer interaction in mitigating shrinkage in cement-stabilised materials. Table 6-10 lists the circumferential shrinkage with the polymer. Figures 6-13a and 6-13b provide the circumferential shrinkage results with and with the polymer.

Compared to the reference mix type [i.e. without the cement and polymer], insight into the quality and type of the material based on their shrinkage criteria is illustrated. Addition of cement to material results in an increase in shrinkage. The reduction in the absolute shrinkage value suggests a decreased moisture loss from the specimen. This proposes that use of the polymer results in reduced moisture loss. The mechanism in mitigating shrinkage in cement-stabilised materials encompasses cement and polymer interaction [chemical or physical] as well as the effect of nano-particles in influencing the pore structure of the material. By altering the pore structure, results in a change in the rate of moisture loss, which influences the total shrinkage. Hornfels mix type with the polymer stabilised using 2.0% cement content showed a higher circumferential shrinkage [average value] compared to its reference mix type. This suggests that for lightly cement-stabilised layers, the effectiveness of the polymer in mitigating shrinkage does not result in significant reductions compared to heavily stabilised layers.

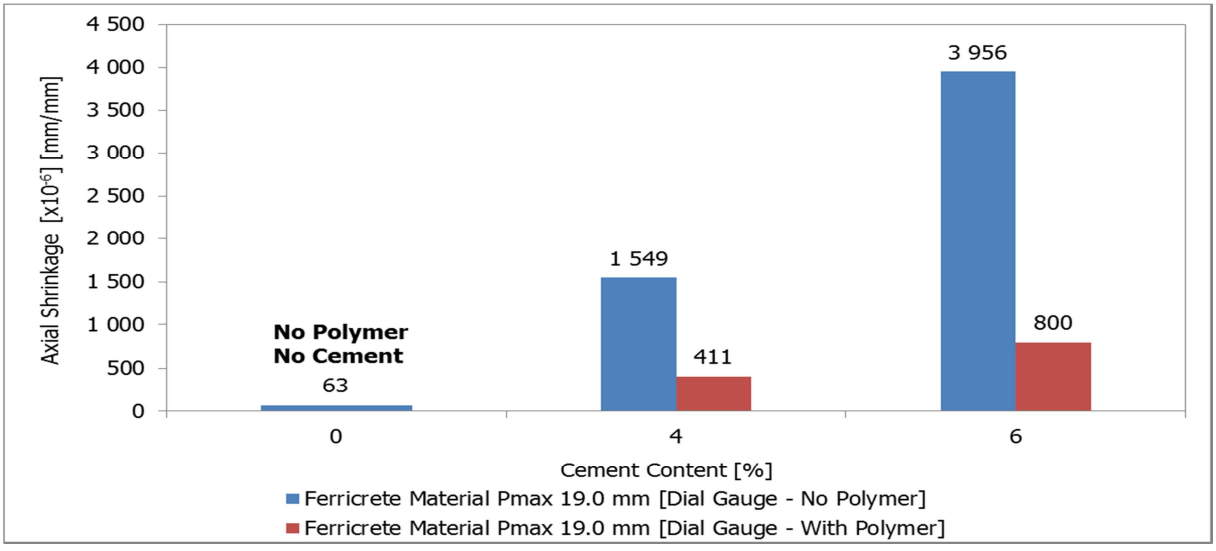

Figure 6-12a Average Axial Shrinkage Results [Ferricrete with and without the Polymer]

Table 6-9 Ferricrete and Hornfels Shrinkage Results [Mix Types with Polymer]

	Ferricrete Material Pmax	19.0 mm [With Polymer]	
Cement Content [%] Polymer [%]	Dimensional Change	Axial Shrinkage [mm/mm]	Axial Shrinkage
[Cylinder Number] Polymer Content	Dial Gauge [mm]	[Absolute Value= (Dial/Cylinder Height)]	[x10^{-6}] mm/mm
0% [C.1] No Polymer	2.00E-02	6.67E-05	66.7
0% [C.2] No Polymer	2.70E-02	9.00E-05	90.0
0% [C.3] No Polymer	1.00E-02	3.33E-05	33.3
4% [C.1] 0.48%	1.00E-01	3.33E-04	333.3
4% [C.2] 0.48%	1.60E-01	5.33E-04	533.3
4% [C.3] 0.48%	1.10E-01	3.67E-04	366.7
6% [C.1] 0.72%	2.50E-01	8.33E-04	833.3
6% [C.2] 0.72%	2.90E-01	9.67E-04	966.7
6% [C.3] 0.72%	1.80E-01	6.00E-04	600.0
	Hornfels Material Pmax	19.0 mm [With Polymer]	
Cement Content [%]	Dimensional Change	Axial Shrinkage [mm/mm]	Axial Shrinkage
[Cylinder Number]	Dial Gauge [mm]	[Absolute Value= (Dial/Cylinder Height)]	[x10^{-6}] mm/mm
0% [C.1] No Polymer	3.75E-03	1.25E-05	12.5
0% [C.2] No Polymer	2.80E-03	9.35E-06	9.3
0% [C.3] No Polymer	3.44E-03	1.15E-05	11.5
2% [C.1] 0.24%	7.00E-02	2.33E-04	233.3
2% [C.2] 0.24%	4.00E-02	1.33E-04	133.3
2% [C.3] 0.24%	7.89E-02	2.63E-04	263.0
3% [C.1] 0.36%	1.12E-01	3.74E-04	373.7
3% [C.2] 0.36%	1.05E-01	3.50E-04	350.0
3% [C.3] 0.36%	8.90E-02	2.97E-04	296.7
6% [C.1] 0.72%	2.20E-01	7.33E-04	733.3
6% [C.2] 0.72%	2.24E-01	7.46E-04	745.7
6% [C.3] 0.72%	2.33E-01	7.77E-04	776.7

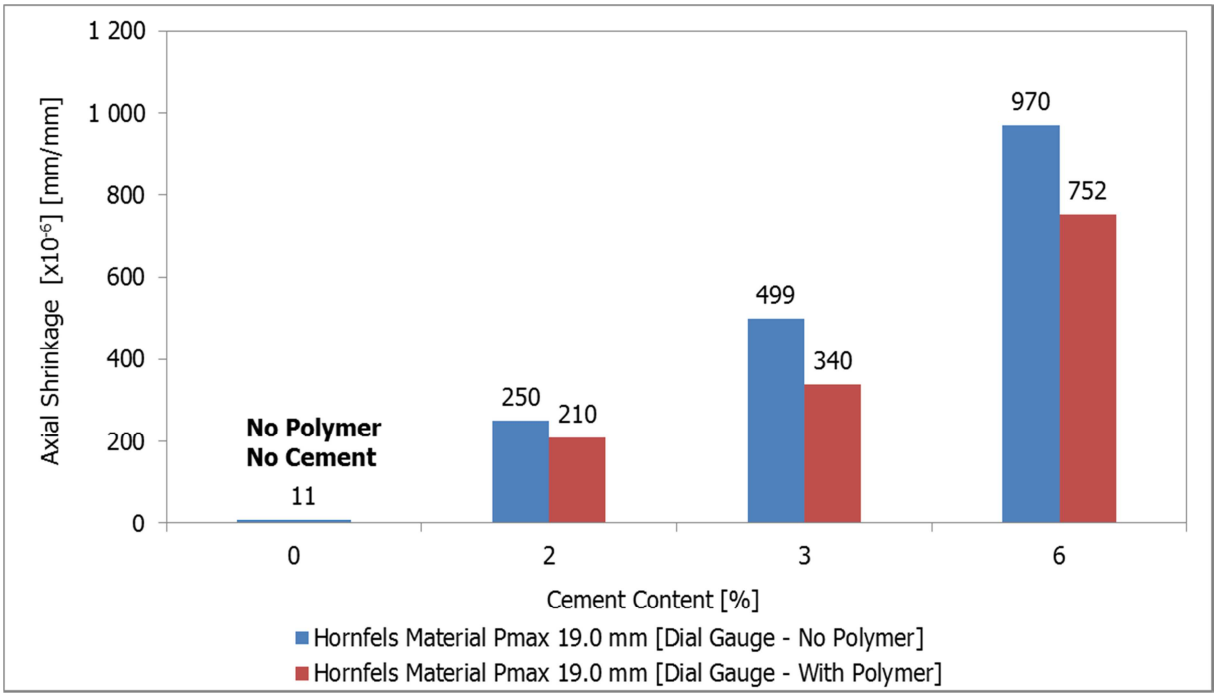

Figure 6-12b Average Axial Shrinkage Results [Hornfels with and without the Polymer]

Furthermore, the efficacy of polymer is also dependent on the quality and type of the materials. Ferricrete mix types stabilised using 4.0% and 6.0% cement contents show a significant axial and circumferential shrinkage reduction of more than 80% when compared to their reference mix types. The findings related to the cement content in the mix as well as the type and quality of the material provide insights regarding the efficacy of the polymer as well as its limitations and consideration. Aspects such as the suitability and compatibility of the polymer with material at specific ranges of cement content are shown.

Table 6-10 Circumferential Shrinkage Results [With Polymer]

Ferricrete Material Pmax 19.0 mm [With Polymer]			
Cement Content [%] [Cylinder Number] Polymer Content	Dimensional Change [Exten'l] [mm]	Circumferential Shrinkage [Absolute Value= (Exten'l/Cylinder Circum.)] [mm/mm]	Circumferential Shrinkage [x10^{-6}] [mm/mm]
0% [C.1] No Polymer	2.20E-02	7.33E-05	73.3
0% [C.2] No Polymer	3.30E-02	1.10E-04	110.0
4% [C.1] 0.48%	4.26E-02	1.42E-04	141.9
4% [C.3] 0.48%	3.21E-02	1.07E-04	107.1
6% [C.1] 0.72%	5.64E-02	1.88E-04	188.1
6% [C.3] 0.72%	5.03E-02	1.68E-04	167.7
Hornfels Material Pmax 19.0 mm [With Polymer]			
Cement Content [%] [Cylinder Number]	Dimensional Change [Exten'l] [mm]	Circumferential Shrinkage [Absolute Value= (Exten'l/Cylinder Circum.)] [mm/mm]	Circumferential Shrinkage [x10^{-6}] [mm/mm]
0% [C.1] No Polymer	2.20E-02	7.33E-05	73.3
0% [C.3] No Polymer	1.30E-02	4.33E-05	43.3
2% [C.2] 0.24%	2.80E-02	9.33E-05	93.3
2% [C.3] 0.24%	2.90E-02	9.67E-05	96.7
3% [C.1] 0.36%	4.15E-02	1.38E-04	138.3
3% [C.2] 0.36%	3.80E-02	1.27E-04	126.7
6% [C.1] 0.72%	6.00E-02	2.00E-04	200.0
6% [C.3] 0.72%	1.12E-01	3.73E-04	373.3
Note: Exten'l - Extensometer ; Circum. - Circumferential			

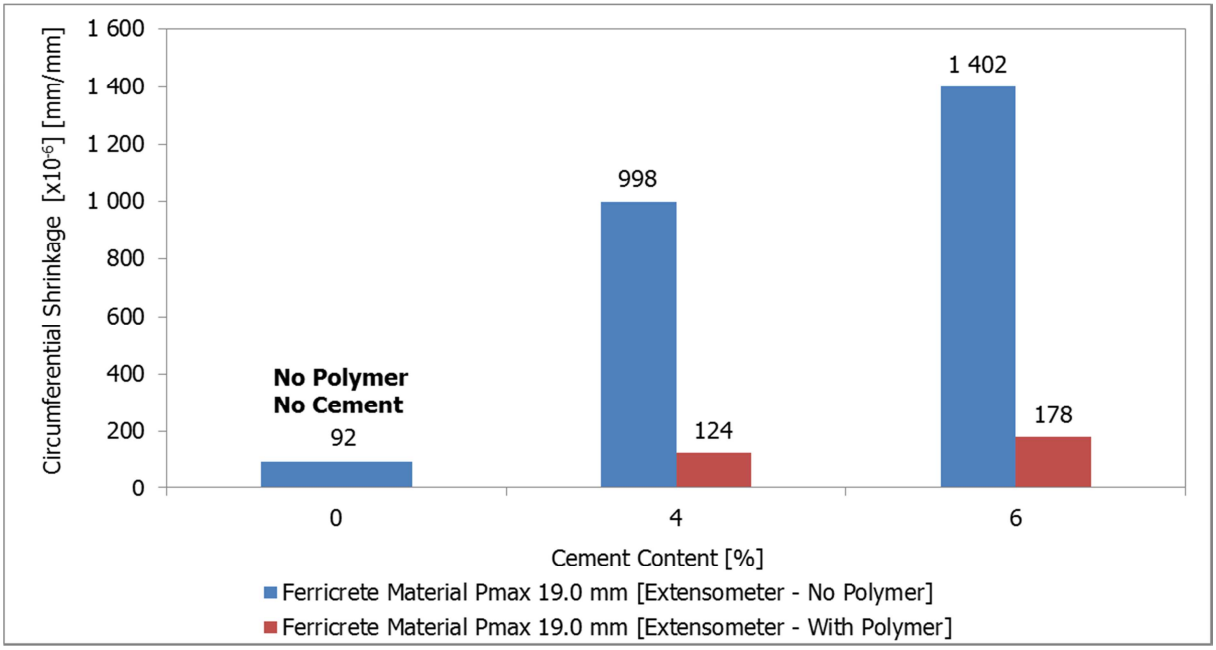

Figure 6-13a Average Circumferential Shrinkage Results [Ferricrete with and without the Polymer]

Based on the axial and circumferential shrinkage, hornfels stabilised using 2.0% cement content, does not show significant reduction; instead, an increase in the circumferential shrinkage is observed. Stabilising using 3.0% cement content in a hornfels mix does not provide strong shrinkage reduction trends compared to using 6.0% cement content. This indicates that the polymer possesses a lower limited beyond which its application does not result in any substantial reduction in shrinkage. This lower limit of the polymer effectiveness is dependent on the cement content in the mix as well as the type and quality of the natural material.

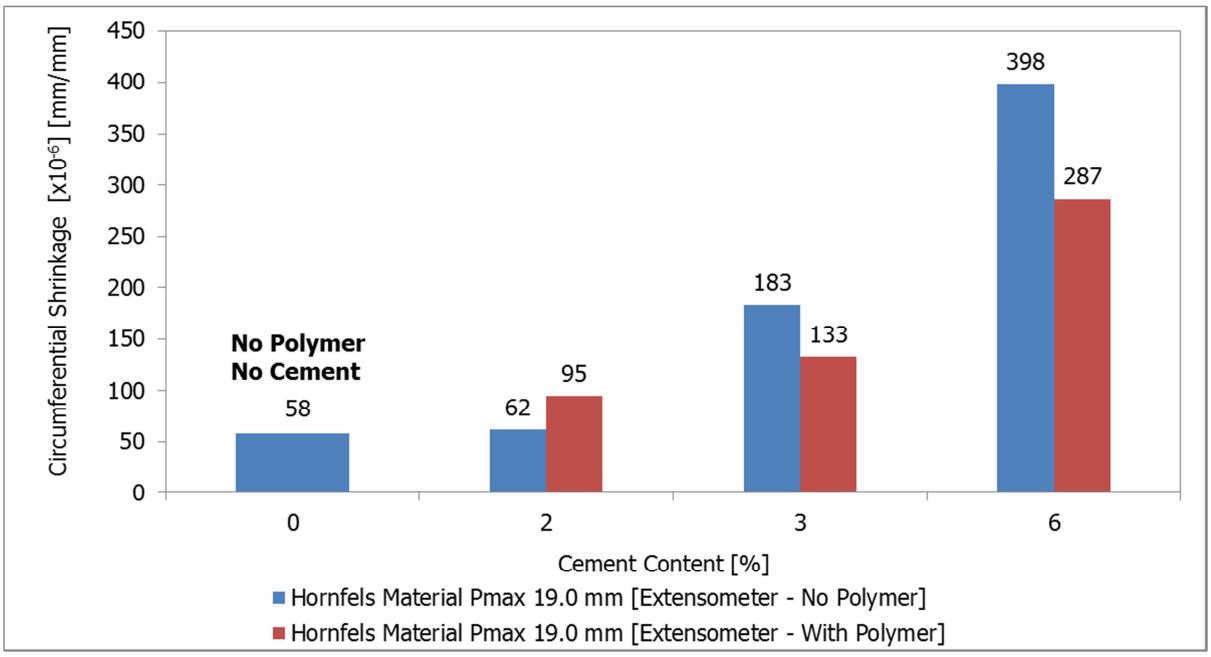

Figure 6-13b Average Circumferential Shrinkage Results [Hornfels with and without the Polymer]

6.5 Discussion of Shrinkage Results

Characteristically, the strength and durability of cement-stabilised materials increase following the addition of more cement. However, the addition of cement contributes to increase in shrinkage. The two conflicting outcomes following the addition of cement to material indicate that a balance between strength and shrinkage should form part of the evaluation process.

Several factors, including compaction, cement and moisture content, attainable density and drying conditions influence the rate of moisture loss and thus, the total shrinkage. The applied compactive effort and resultant dry density characterise the void content in the mix; this provides insight regarding the pore structure. The pore structure of the mix influences the strength of the cement-stabilised layers as well as its moisture loss. Strength and moisture loss are associated with the density of the stabilised layer. However, the amount of moisture in the mix significantly influences the resultant density and shrinkage of the cement-stabilised layer. Particle size distribution, particularly the amount of fines in the mix, has an influence on the moisture content required to realise the target density. In general, density plays a key role in characterising the suitability of a material for use. However, a high density does not suggest a good performance and long-term durability. As a result, an evaluation to determine the strength relative to shrinkage criteria of the selected material is necessary.

The possibility of shrinkage occurring in a cement-stabilised layer depends on a number of factors related to the characteristics of the materials, mix composition and environmental effects. As a result, evaluation of materials in relation to their shrinkage potential, layer restraint, as well as degree of stress relaxation relative to strength development of the material is important. To ensure that a stabilised layer has a long-term service life with viable capacity to withstand design traffic, a holistic yet relevant evaluation of materials must be undertaken with good reliability.

In establishing an appropriate shrinkage method, factors such as, specimen size and shape, measuring criteria and drying conditions remain the driving factors of influence. However, to evaluate the shrinkage potential of cement-stabilised materials, a standard technique is

required. This suggests that the curing test configurations and specimen geometry must be within good range to provide a good understanding of the material's shrinkage potential.

The beam linear method is assessed in this research. However, a number of factors including the influence of friction at the interface and the resultant beam density present a negative impediment to the measurement of reliable ranges of the material's shrinkage. The cylinder method [axial and circumferential shrinkage], provides a good measure of the shrinkage potential of cement-stabilised materials. With the cylinder method, the effects emanating from friction and the possibility of micro cracks within the specimen are negated. The axial shrinkage measurements, which are obtained in the direction of compaction and along the gravitational path, provide good and reliable shrinkage results. The instrumentation used to measure the axial shrinkage is easily available as well as interpreted by the technical staff. The circumferential shrinkage measurement, which applies a reliable but sophisticated and expensive device, remains a research-based type of analysis. However, the correlation between the circumferential to the axial shrinkage can be developed. Figure 6-14 correlates the circumferential shrinkage to the axial graphically.

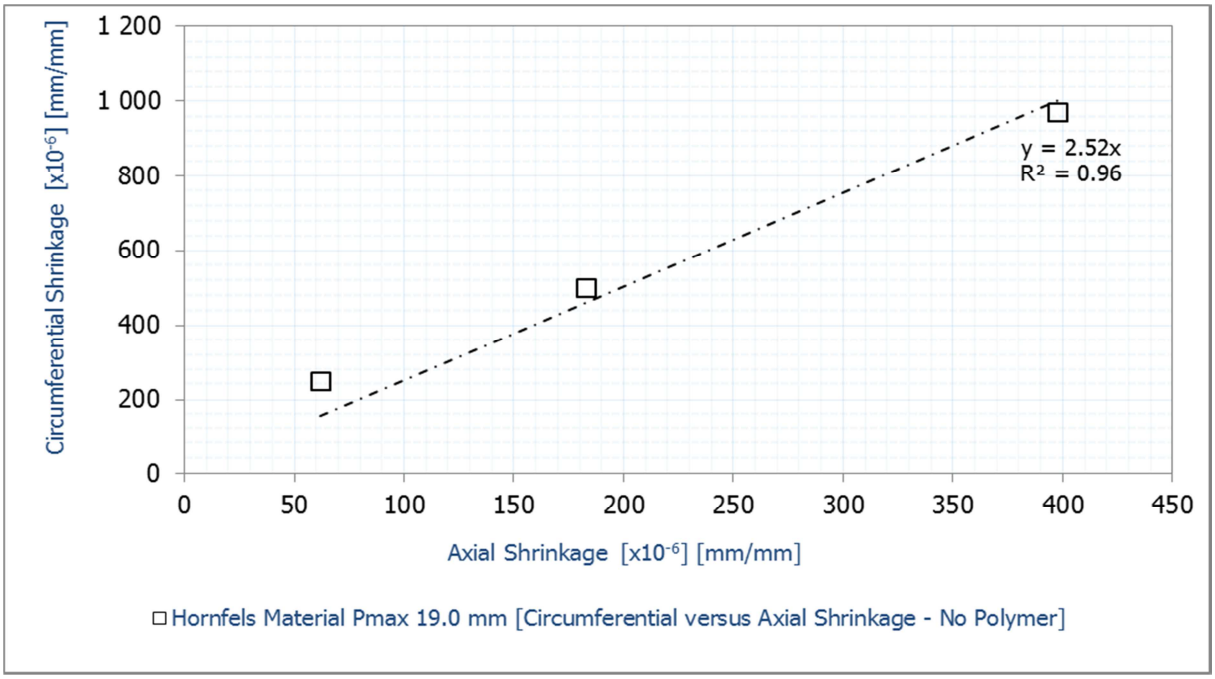

Figure 6-14 Average Circumferential versus Average Axial Shrinkage [Hornfels]

The circumferential shrinkage is about 2.5 times the axial shrinkage for the same material type. This provides further insight regarding the specimen shrinkage relative to the overall shrinkage. The cylinder method provides a good repeatability and usability. The axial shrinkage measurement provides a good indication of the shrinkage potential of the cement-stabilised materials. Testing at 70ºC using the cylinder method provides significant trends defining the influence of each factor on shrinkage. Factors attributed to the characteristics of the materials, the effect of cement content in the mix as well as, the effectiveness of the polymer on the resultant shrinkage of cement-stabilised materials are realised.

It is evident that the beam linear and cylinder axial expansion influence on the measurement of shrinkage at laboratory level. The concept developed to negate the effect of material expansion during the test provides a good indication of the detrimental shrinkage. The initial expansion and rapid reduction exemplify the cement and material interaction during the hydration process. The consideration of the circumferential shrinkage provides additional insight regarding the specimen response during its desiccation under the set conditions.

The shrinkage criteria exhibited by ferricrete and hornfels characterises, to a satisfactory degree, the suitability of materials for use in the pavement layer relative to the quantity of cement in the mix. Ferricrete exhibited high fine and moisture content, which contribute to its increased total shrinkage compared to hornfels. The influence of the particle size distribution and other intrinsic properties of the materials on shrinkage are realised. The cement and polymer interaction encompass a mechanism that mitigates shrinkage. This mechanism could include the alteration of the pore structure and/or supplying additional moisture to supplement on that, which is lost from the material matrix. The cement and polymer interaction exhibits a mutual relationship. This suggests that polymer effectiveness is dependent on high cement contents and material.

Although the use of low cement contents could reduce shrinkage, cracking in a stabilised layer an establishment of limits is essential. Low cement dosages result in reduced strength properties and probably the durability of the material. An adequate balance between material strength properties and its degree of shrinkage is necessary. Additionally, reduction of moisture content as a control measure to reduce shrinkage might affect the realisation of a higher density. A reduction of moisture [from its optimum content] could compromise the density, which influences the strength properties of a stabilised layer. By undertaking a shrinkage evaluation, better understanding regarding suitability of cement-stabilised materials relative to their strength properties and characteristics is realised. An understanding of the properties and characteristics of materials is the basis for a better design and thus, the construction of pavement structures.

6.6 Summary of Chapter 6

This chapter elaborates on a better understanding pertaining to material suitability. The chapter presents the need to establish a relationship between the engineering properties of the stabilised materials and the resultant shrinkage. The chapter probes the current approach to defining the suitability of materials based on the resultant engineering properties such as strength. This chapter provides the shrinkage results along with the applied cement contents, which provides insight into layer cracking. Conventional techniques applied for the mitigation of shrinkage along with the factors of influence are stated. The chapter reports on the influence of maximum aggregate size, moulding moisture, density and compactive effort in relation to material type and quality. Assessments and discussions of each factor relative to material shrinkage criteria along with the result are stated. The chapter also states results and findings pertaining to the use of polymer to mitigate shrinkage. This provides a better understanding of the efficiency of polymer along with its probable practical benefits.

6.7 References

Bofinger, H. E. and Sullivan, G. A., (1971), *An Investigation of Cracking in Soil Cement Bases for Roads,* Road Research Laboratory (RRL) Report LR 379, Road Research Laboratory, Crowthorne, Berkshire.

Neithalath, N., Pease, Moon, J.H. Rajabipour, F. Weiss, J. and Attiogbe, E., (2005), *Considering Moisture Gradients and Time Dependent Crack Growth in Restrained Concrete Elements Subjected to Drying,* NSF Workshop on High Performance Concrete, Westerville: American Ceramic Society, pp. 279-290.

Tazawa, E., S. Miyazawa, and T. Kasai, (1995), *Chemical Shrinkage and Autogenous Shrinkage of Hydrating Cement Paste,* Cement and Concrete Research, Vol. 25, No. 2, pp. 288-292.

Chapter 7: Analysis of Crack Pattern in Cement-Stabilised Layers

7.1 Background

Section 2.4.7 of Chapter 2 introduces concepts pertaining to the prediction of the shrinkage crack pattern in a cement-stabilised layer. Shrinkage is a natural material characteristic where the addition of cement produces volume reduction leading to tensile stresses. Depending on the characteristics of the individual shrinkage cracks and the related crack pattern, the extent of pavement degradation will vary. Wide shrinkage cracks not only lead to rough riding surfaces but also to the delamination of the layers and localised failure. Wide cracks influence the load-transfer mechanism, especially in the region of the crack. This eventually leads to increased stresses within the pavement structure.

Figure 3-13 examines the cracking behaviour and resultant crack patterns of cement-paste beams. The objective of this experiment was to provide insight regarding crack pattern and specimen geometry. Cracks run transverse to the length of the rectangular beam, which simulates shrinkage cracking criteria within a stabilised layer. Several factors influence the shrinkage crack pattern. These include [but are not limited to]:

a) frictional coefficient at the interlayer
b) daily and seasonal thermal variations
c) heterogeneity of material composition and layer thickness
d) material engineering properties

In this chapter, the analysis uses the laboratory obtained results along with the climatic data and other factors significant to shrinkage i.e. in predicting the crack pattern. The analysis considers the Houben model [a numerical analysis] to determine the crack width and spacing of the stabilised layer.

7.2 A Theoretical Background

Moisture plays a significant role in a number of chemical and physical processes in cement, concrete and other cementitious materials, including cement-stabilised materials. Variations in moisture content under a given relative humidity leads to shrinkage or swelling owing to a characteristic change of surface energy. At high relative humidity, cementitious materials tend to absorb water by capillary condensation; a reverse process occurs at low relative humidity. The capillary water is chemically reactive and is part of the pore solution. The interaction of the pore solution with the solid skeleton of the hydration products leads to the development of tensile stresses and/or disjoining pressures.

Fick's second law is commonly applied to describe the drying process of cementitious materials, [Alvaredo, 1994]. The law is applied to predict how moisture dissemination causes the concentration to change with time. The drying mechanisms in cementitious materials involve an initial period of a constant rate of moisture loss i.e. through evaporating from the surface. Moisture is transported onto the surface by flow and at the surface, the moisture vaporises. However, factors such as moisture content, drying time and the distance from the drying surface influence the drying process.

The primary mechanism of drying shrinkage is moisture loss from the material matrix. The mechanism of moisture loss include capillary stresses at high relative humidity levels due to stress induced by the meniscus in the pores, disjoining pressures and surface energy, [Alvaredo, 1994]. In order to simulate the drying process, consideration of factors such as the moisture flux normal to the exposed surface, must be accounted for. Moisture loss depends essentially on the surface exposure to thermal effects i.e. temperature and wind flow.

At a high moisture contents, liquid water movement governs the mass transport. Under these conditions, the water mass in the porous structure forms a continuous body; the moisture is transported by capillary action to the drying surface, [van Breugel 1991]. As the moisture content decreases, the remaining moisture is trapped in finer capillaries. The moisture in the finer capillaries evaporates and mass transport to the drying surface is essentially due to vapour diffusion. The surface diffusion contributes to the moisture transfer at low humidity levels. In other words, the diffusion coefficient decreases with the reduction in moisture potential.

In cement and concrete research, prediction of shrinkage involves some sort of measurement or numerical analysis. This analysis considers the numerous factors and approaches conducted using concrete but cognisance of the low cement contents as applied during the stabilisation of materials is recognised.

7.3 Modelling Concepts and Influencing Factors

The hydration, strength development and shrinkage of cement-stabilised materials involve interrelated processes i.e. chemical, physical and mechanical processes. A thorough understanding of these processes is an essential prerequisite for modelling the shrinkage crack pattern in a cement-stabilised layer. This proposes that the model must account to an acceptable degree the influence of the chemical, physical and mechanical characteristics of the cement-stabilised materials. The hardening of cementitious materials is considered as a multiphase interaction of the chemical, physical and mechanical phases, [Cervera *et al,* 2002; Schindler and Folliard, 2005].

Before developing any numerical modelling and/or make any consideration of one, it is important to assess the various influencing factors in terms shrinkage cracking and the related mechanisms. Several publications including van Breugel [1991] provide a comprehensive study of cement hydration. The composition of cement is one of the influencing factors to the hydration of cementitious materials. Two forms are used to describe the composition of cement i.e. the oxide composition and the chemical composition. The chemical composition significantly influences the degree of hydration.

The water-cement ratio and/or moisture influence the hydration characteristics but this only influences to a lesser degree in the early stages, [Taplin, 1969]. It is typically conceptualised that a higher water-cement ratio or moisture content an increased hydration rate results. In general, the water-cement ratio or moisture content determines the degree of hydration. Additionally, the fineness of cement influences the rate and ultimate degree of hydration, [Keienburg, 1976]. However, at low water-cement ratios or moisture contents the influence of cement fineness on the ultimate degree of hydration diminishes.

The curing temperature and/or thermal effects also influence on the rate of hydration. The hydration and reaction rates increase following an increase in temperature, [Schindler and Folliard, 2005]. The density of the hydration products at high curing temperatures is higher, [Keienburg, 1976]. This suggests that the chemical composition of cement influences the chemical affinity and thus, the strength properties and shrinkage criterion. However, the water-cement ratio or moisture content in the mix significantly contributes to the chemical affinity as well as the degree of shrinkage and strength development.

7.4 Material Properties and Input Parameters

Table 7-1 provides material property results [averaged values] with and without the polymer. The flexural strength and elastic moduli input parameters considered test data and results of the 50 mm beam type with a maximum aggregate size of 13.20 mm and loaded monotonically at a span length of 450 mm with a span-depth of nine. Table 6-6 provides drying shrinkage results. Chapter 4 provides the compressive and tensile strength results.

Table 7-1 Material Properties and Input Parameters

Ferricrete Mix type [Cement Content]	Polymer Content [%]	7-Day Compressive Strength [MPa]	7-Day Tensile Strength [MPa]	28-Day Flexural Strength [MPa]	Elastic Modulus [MPa]
3%	0	1.91	0.319	0.294	757
	0.36	1.83	0.347	0.277	1000
4%	0	2.41	0.426	0.422	1068
	0.48	2.56	0.469	0.461	1448
6%	0	3.84	0.761	0.867	2120
	0.72	5.12	0.858	1.288	3035
Hornfels Mix type [Cement Content]	Polymer Content [%]	7-Day Compressive Strength [MPa]	7-Day Tensile Strength [MPa]	28-Day Flexural Strength [MPa]	Elastic Modulus [MPa]
2%	0	2.95	0.594	0.948	2570
	0.24	2.63	0.604	0.742	2069
3%	0	3.57	0.704	1.180	3201
	0.36	3.25	0.702	0.862	2603
6%	0	6.31	1.173	2.283	6193
	0.72	6.10	1.104	1.352	5190

7.5 Modelling of Shrinkage Crack Pattern [Houben Model]

Figure 7-1 conceptualises the cracking criteria of the cement-stabilised layer. For this analysis, the Houben model a numerical analysis method is considered. The Houben model analyses the shrinkage crack pattern in concrete pavements. The model contains several formulae and coefficients based on rudimentary material property relationships allied with various engineering criteria. The formulae and coefficients numerically relate material properties to specific responses and behavioural characteristics. Material responses include the following [Houben 2008]:

a) daily and seasonal thermal fluctuations
b) stress reduction due to cracking, tensile strength and elastic modulus development over time
c) stress relaxation and development

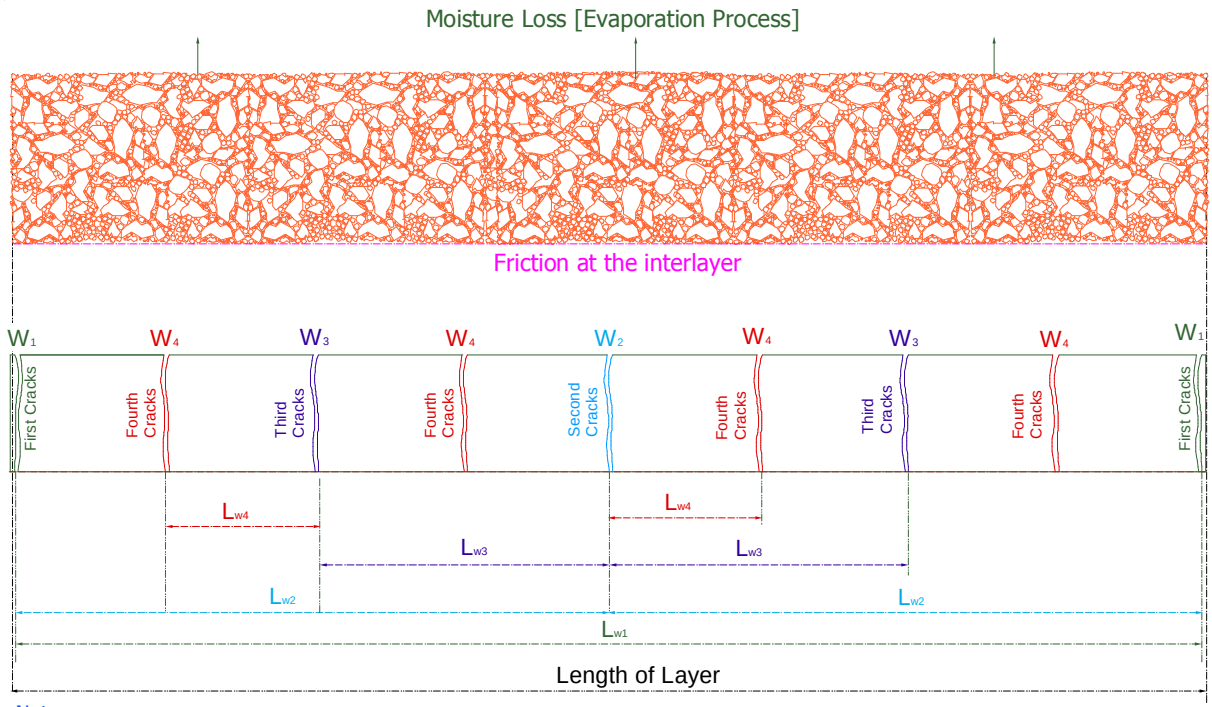

Note:
L_{w1} Crack Spacing Between First Cracks
L_{w2} Crack Spacing After Second Cracks
L_{w3} Crack Spacing After Third Cracks
L_{w4} Crack Spacing After Fourth Cracks

Note:
W_1 Crack Width of First Cracks
W_2 Crack Width of Second Cracks
W_3 Crack Width of Third Cracks
W_4 Crack Width of Fourth Cracks

Figure 7-1 Schematic Representation of the Concept of Cracking and Resultant Crack Pattern

The Houben model provides material trends related to tensile stress development after a series of subsequent transverse cracking for a specified period. The model considers one year, i.e. 360 days [8640 hours] as the duration of the analysis. The model provides the development of tensile stresses and strength, times of occurrence of transversal cracks and their individual spacing as well as widths. The progress of the cracking process is dependent on several factors, including the resultant crack pattern relative to stress development and tensile strength.

The Houben model assumes that all cracks appear at mid-span between already existing cracks in the layer. First cracks appear at a wider length L_{w1} than the second and subsequent series of cracks. The subsequent cracking within the layer is dependent on the material properties, climatic conditions and friction at the interlayer.

7.5.1 Concept for Cracking Behaviour and Load Transfer Mechanism

A good understanding the concept of crack pattern and load transfer mechanism provides essential insights regarding the structural performance of a pavement. Strauss *et al* [2001] shows that the maximum stress at a joint or crack in the pavement is dependent on the stiffness properties of the individual layers, the thickness of the layer and magnitude of the load. Load transfer is considered as a function of the relative vertical movement at the region of crack.

The magnitude of the load transfer is dependent on the aggregate interlock at the region of the crack. Walraven [1981] notes that, the relative vertical movement and thus, aggregate interlock is a function of crack width, aggregate shape and size in addition to its strength. This suggests that aggregate interlock influence the vertical movement at the region of the crack. Figure 4-7 shows the internal morphology of hornfels and ferricrete mix types. Figure 7-2 schematically illustrates the relationship between crack width and aggregate interlock in addition to their significance in terms of the load transfer mechanism.

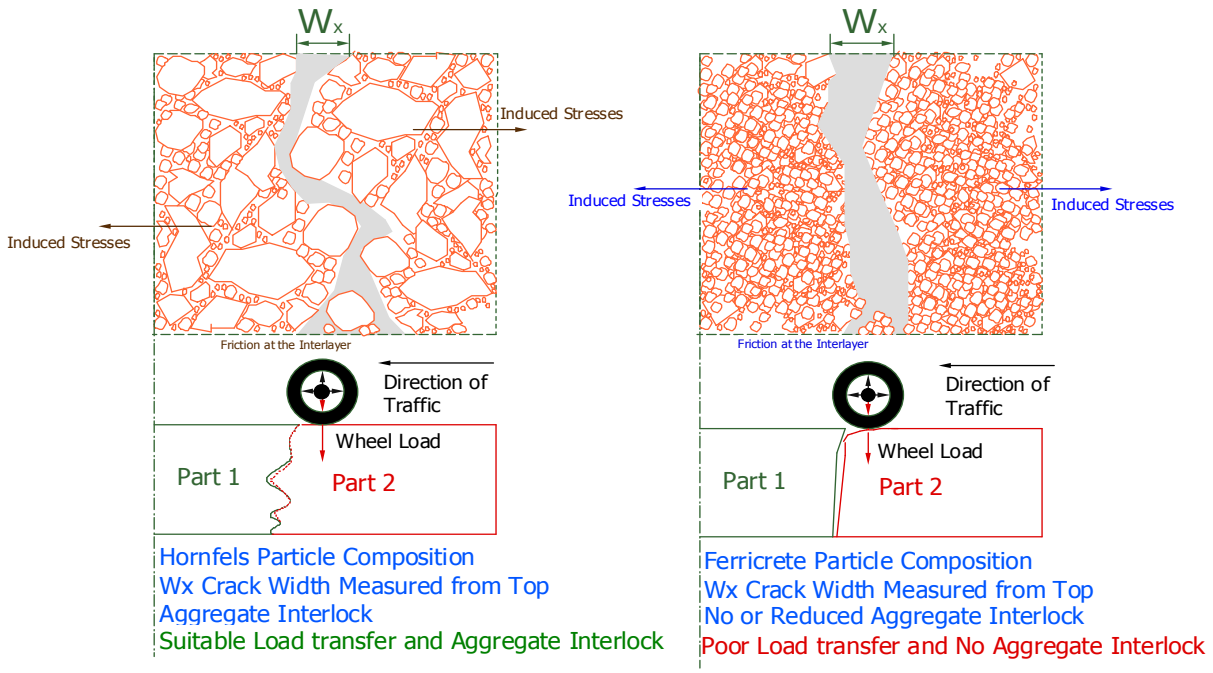

Figure 7-2 Aggregate Interlock and Load Transfer Mechanism for Hornfels and Ferricrete

Figure 7-2 uses insights based on the internal structure of the material and cracking behaviour to exemplify aggregate interlock and load transfer mechanism. Based on the physical observations during laboratory testing ferricrete typifies a clear type of cracking with

limited aggregate interlock. Hornfels exhibits some degree of aggregate interlock. The wider the crack the less effective the aggregate interlock becomes able to provide substantial load transfer particularly with heavy traffic. Wider shrinkage cracks exhibit zones of discontinuity and thus, increased traffic load stresses i.e. higher maximum stress at the region of crack. As the tyre moves over the region of the crack, the extent of deflection exhibited by Part 2 is dependent on the prevailing aggregate interlock as well as the crack width [W_x]. The contribution of the aggregate interlock is to maintain some degree of connection thus, preventing complete discontinuity within the cement-stabilised layer.

7.5.2 Calculations and Model Parameters

In order to use the model to predict the crack patterns in cement-stabilised pavements, adjustments to the input parameters were undertaken. This required a good understanding of the fundamental differences between concrete and cement-stabilised materials. Initial focus between concrete and stabilised materials involved establishing differences in cement content, engineering properties and behavioural response to thermal fluctuations.

In this analysis, the climatic influences of the Western Cape Province of South Africa are considered. The analysis considers the Cape Town meteorological data sourced from the South African Weather Services. Calculations related to daily, seasonal and annual climatic data are applicable to this region. Meteorological data include:

a) Annual average air temperature [$T_{aveyear}$] of 17ºC that is present on 1st May and 1st November at 10:00 a.m. with a maximum of 22ºC [1st February] and minimum temperature of 12ºC [1st August]
b) Annual average air temperature amplitude [$T_{ampyear}$] of 5ºC

Temperature Calculations:

Owing to the lack of field temperature measurements, the assumption that the temperature of the cement-stabilised layer is equal to the air temperature is assumed. For computing the average temperature [T_1] of the cement-stabilised layer on the day of construction, Equation 7-1 is considered. Since temperature over the year varies with time [t], a sine is considered. Equally, the air temperature varies over a range throughout the year with an average and amplitude.

$$T_1=T_{aveyear}+T_{ampyear} \times \sin(t_1) \quad (°C) \qquad \text{Equation 7-1}$$

Where: t_1 – time of construction [i.e. number of days after 1st February]

Regarding the daily variation of temperature, the following range of parameters is considered:

a) Averaging the daily temperature considers ranges between 10:00 a.m. and 10:00 p.m. with a maximum at 4:00 p.m. [$T_{aveyear}$ +$T_{ampyear}$] °C and minimum temperature at 4:00 a.m. using the following relationship [$T_{aveyear}$ -$T_{ampyear}$] °C
b) Daily temperature amplitude [T_{ampday}] of 4.5ºC is considered

In computing the temperature [T_2] at the hour of construction, Equation 7-2 is considered.

$$T_2=T_1+T_{ampday} \times \sin(15.(-10+t_2)) \ (°C) \qquad \text{Equation 7-2}$$

Where: t_2 = clock hour [from 0 to 24 hours] of construction [at day of constructing the layer]

In order to account for the climatic effects and shrinkage the climate-dependent temperature of cement-stabilised is computed as a function of the temperature at the hour of construction, annual and daily air temperature amplitudes over time. Equation 7-3 is derived

from the basis that pavement temperatures are influenced by several factors such as the air temperature, precipitation and wind speed as well as solar radiations, among others. Equation 7-3 defines the climate-dependent temperature [T_3] of the stabilised layer.

$$T_3 = T_2 + T_{ampyear.} \sin [(t/24) + t_1] - T_{ampyear}. \sin (t_1) + T_{ampday}. \sin (15.t) \ (°C) \qquad \text{Equation 7-3}$$

Where: t = time [number of hours] after construction

Owing to the hydration process, an increase in layer temperature occurs. Equation 7-4 computes the hydration temperature [T_4].

$$T_4 = c_1. f_1. f_2 \ (°C) \qquad \text{Equation 7-4}$$

$$\text{Where: } f_1 = t^{c2} \qquad \text{Equation 7-5}$$

With $c_2 = 2.0$

$$f_2 = e^{-c3.t} \qquad \text{Equation 7-6}$$

With $c_3 = 0.27$

For concrete, $c_1 = 1.0$ when assuming there is 375 kg cement per m³, [Houben 2008]. The hydration coefficient [c_1] is dependent on the cement content. Stabilisation technology considers low cement contents compared to 15% to 17%. As a result, the hydration coefficient [c_1] for cement-stabilised materials is calculated based on the cement content in the mix. Table 7-2 provides the calculated hydration coefficient [c_1] per mix type. Calculation of hydration coefficient included the maximum dry density [MDD] of material and their related volume weight.

Table 7-2 Calculation of Hydration Coefficient [c_1] and Volume Weight [γ]

Hornfels Materials	MDD = 2346 kg/m^3	c_1 =1.0 for Cement Content v= 375 kg/m^3	
Cement Content	Mass of Cement	Hydration	Volume Weight
c [%]	m [kg] = [c]x MDD	C_1 = [m/v]	γ [kN/m³]
2	46.92	0.125	23.92
3	70.38	0.188	24.16
6	140.76	0.375	24.87
Ferricrete Mix Types	MDD = 2023 kg/m^3	c_1 =1.0 for Cement Content v= 375 kg/m^3	
Cement Content	Mass of Cement	Hydration	Volume Weight
c [%]	m [kg] = [c]x MDD	C_1 = [m/v]	γ [kN/m³]
4	80.92	0.216	21.09
6	121.38	0.324	21.44

The resultant hydration coefficients of cement-stabilised materials are lower than that of concrete because of the low cement content in the stabilised mix types. Mix types with 6% cement content provide a higher hydration coefficient of 0.3, which is significantly lower than that of concrete. The amount of hydration products is proportional to cement reacted; this influences the resultant material properties such as stiffness and strength properties. The hydration reaction is exothermic chemical reaction i.e. generates heat [heat of hydration]. The heat generated by the hydration reaction increases the temperature of the stabilised layer.

Publications including Burg and Ost [1994] state of temperature rise of up to 55°C with high cement contents in the mix. The temperatures rises cause an expansion while the mix hardens. In this analysis, the temperature of the stabilised layer [T_5] is the sum of the two temperatures, i.e. climatic temperature [T_3] and hydration temperature [T_4]. For the computation of the temperature of the stabilised layer, Equation 7-7 is applied.

$$T_5 = T_3 + T_4 \quad (°C) \qquad \text{Equation 7-7}$$

Material Property Calculations:

In Chapter 4 and 5, an increase in cement content results in a corresponding increase in compressive and tensile strength. Cementitious materials have a relatively high compressive strength but significantly lower tensile strength. The elasticity of most cementitious materials is relatively constant at low stress levels but begins to reduce at higher stress levels as cracks develop. Several publications stipulate that concrete exhibit a very low coefficient of thermal expansion and as concrete matures, it shrinks. Equation 7-8 computes the characteristic 28-day cylinder compressive strength [$f_{ck\ 28\ day}$] as a function of the average 28-day cylinder compressive strength [$f_{cm\ 28\text{-}day}$].

$$f_{ck\ 28\text{-}day} = 0.8355 f_{cm\ 28\text{-}day}\ (MPa) \qquad \text{Equation 7-8}$$

Where: $f_{cm\ 28\text{-}day}$ - average 28-day cylinder compressive strength [MPa]

In computing the 28-day tensile strength value Equation 7-9, is considered.

$$f_{ctm\ 28\text{-}day} = 0.3(f_{ck\ 28\text{-}day})^{2/3}\ (MPa) \qquad \text{Equation 7-9}$$

Equation 7-10 computes the characteristic 28-day cube compressive strength [$f_{ck\ cube\ 28\text{-}day}$].

$$f_{ck\ cube\ 28\text{-}day} = 1.25 f_{cm\ 28\text{-}day}\ (MPa) \qquad \text{Equation 7-10}$$

Equations 7-8, 7-9 and 7-10 are adopted from the Houben Model but the inputs to these equations are based on cement-stabilised material parameters.

Drying Shrinkage Calculations:

In this research, drying shrinkage is characterised as the constricting of a hardened cement-stabilised layer owing to the loss of capillary moisture. The constricting causes an increase in tensile stresses, which lead to cracking. Drying starts after construction and is dependent on the mix type. In computing, the total shrinkage [S_t] Equation 7-11 is considered.

$$S_t = a.\ \ln((t/24)+1)\ \ (t\ –time) \qquad \text{Equation 7-11}$$

Where: a is a shrinkage coefficient [a is an optimised value obtained from the shrinkage test data and is mix dependent]

Due to the lack of field data, laboratory-measured shrinkage at 70ºC for 72 hours was assumed to being equal to 3 months in the field.

Coefficient of Linear Thermal Expansion [α]:

From a theoretical point of view, the heat generated by hydration process in a cement-stabilised layer depends on the cement content, hydration rate and the quality of the natural material stabilised. During the hydration process, cement-stabilised materials expand and then contract as established in Chapter 6.

The coefficient of linear thermal expansion is the magnitude of dimensional changes that results per unit length of a stabilised layer that results from a 1 degree change in temperature. In considering the coefficients of linear thermal expansion, an assessment regarding ranges of material types to ferricrete and hornfels was carried out. In computing, the coefficient of linear thermal expansion [α] Equation 7-12 is applied.

$$\alpha = C_8.\ E_{28\text{-}day} \qquad (°C^{-1}) \qquad \text{Equation 7-12}$$

Where: $E_{28\text{-}day}$ – 28-day Elastic Modulus [MPa] based on the flexural beam test

The coefficient of linear thermal expansion [α] is dependent on the modulus of elasticity. Houben [2008] considers C_8 = 3.095 x 10^{-10} whereby α is specified based on concrete grade. For cement-stabilised materials, computation of the coefficient of linear thermal expansion takes into account a series of similar materials. Xuan [2012] establishes that for cement treated recycled crushed concrete and masonry aggregates for pavement the coefficient of linear thermal expansion varied from 7.5 x 10^{-6} °C^{-1} to 10 x 10^{-6} °C^{-1}. An assumed coefficient for cement-stabilised materials of 8.0 x 10^{-6} °C^{-1} after 28 days is considered.

Shrinkage strain is caused by a variation in temperature and this concept is used to compute the thermal deformation [ε_T (t)], Equation 7-13 is applied.

$$\varepsilon_T (t) = -\alpha . \Delta T \qquad \text{Equation 7-13}$$

Where: $\Delta T = T_5 - T_2$ (°C)

Computation of the total deformation [ε (t)] considers Equation 7-14.

$$\varepsilon (t) = S_t + \varepsilon_T (t) \qquad \text{Equation 7-14}$$

Cement strength varies with fineness; in this model, the strength related coefficient [s] is established. Cement type CEMII A-M 42.5N which is used for material stabilisation has a coefficient of strength [s] of 0.25. The average modulus of elasticity [E_{cm} (t)] after 28 days correlates with the 28-day elastic modulus [$E_{28\text{-day}}$]. Equation 7-15 computes the average modulus of elasticity [E_{cm} (t)].

$$E_{cm}(t) = \text{exponential}\left[\left(s.\left(1-(672/t)^{0.5}\right)\right).E_{28\text{-day}}\right] \text{ (MPa)} \qquad \text{Equation 7-15}$$

The average tensile strength of the cylinder [$f_{ctm\ (t)}$] after 28 days correlates to the 28-day tensile strength [$f_{ctm\ 28\text{-day}}$]. Equation 7-16 computes the average tensile strength [$f_{ctm\ (t)}$].

$$f_{ctm\ (t)} = \text{exponential}\left[\left(s\ (1-(672/t)^{0.5})\right) f_{ctm\ 28\text{-day}}\right] \text{ (MPa)} \qquad \text{Equation 7-16}$$

Table 7-3 summarises the model input parameters using the equations stated. It is assumed that at a test temperature of 70ºC obtained shrinkage test data represents twelve months field shrinkage. This assumption correlates ambient temperature ranges relative to the laboratory test temperature used [accelerated curing].

Table 7-3 Summary of the Model Input Parameters

	Hornfels Material					
Cement Content [%]	Shrinkage Coefficient [a]	$f_{ck\ 28\text{-day}}$ [MPa]	$f_{cm\ 28\text{-day}}$ [MPa]	$E_{28\text{-day}}$ [MPa]	$f_{ctm\ 28\text{-day}}$ [MPa]	Assumed α = 8.0 x 10^{-6} °C^{-1} [C_8] =α/$E_{28\text{-day}}$
2 [No Polymer]	5.33E-05	3.14	3.76	2591	0.643	3.09E-09
2 [With Polymer]	3.32E-05	2.86	3.42	2065	0.604	3.89E-09
3 [No Polymer]	6.95E-05	3.99	4.78	3243	0.755	2.47E-09
3 [With Polymer]	6.54E-05	3.38	4.04	2597	0.676	3.08E-09
6 [No Polymer]	3.20E-04	6.93	8.30	6355	1.090	1.26E-09
6 [With Polymer]	1.45E-04	6.45	7.72	5163	1.040	1.55E-09
	Ferricrete Material					
Cement Content [%]	Shrinkage Coefficient [a]	$f_{ck\ 28\text{-day}}$ [MPa]	$f_{cm\ 28\text{-day}}$ [MPa]	$E_{28\text{-day}}$ [MPa]	$f_{ctm\ 28\text{-day}}$ [MPa]	Assumed α = 8.0 x 10^{-6} °C^{-1} [C_8] =α/$E_{28\text{-day}}$
4 [No Polymer]	7.46E-04	2.78	3.33	1312	0.593	6.10E-09
4 [With Polymer]	1.06E-04	2.76	3.30	1790	0.590	4.47E-09
6 [No Polymer]	2.56E-03	3.92	4.96	2247	0.746	3.56E-09
6 [With Polymer]	3.55E-04	5.41	6.48	3146	0.925	2.54E-09

Table 7-3 lists the various inputs including the calculation of C_8 as a ratio of the coefficient of linear thermal expansion [α] and the material elasticity at 28-day. The shrinkage coefficient defines the change in strain as a function of moisture and/or relative humidity. Table 2-2 in

Chapter 2 lists the models for computing stress relaxation factors. To account for the relaxation behaviour of hardening cement-stabilised materials the analysis primarily considered the Houben stress relaxation factor. Cognisance of the differences in cement content between concrete and cement-stabilised materials is considered. Besides the Houben stress relaxation factor, a sensitivity analysis using three other stress relaxation factors is carried out. The following equations define the various stress relaxation models [f_9] as a function of time.

a) Houben stress relaxation model: $f_9 = e^{-0.003t}$
b) Xuan high stress relaxation model: $f_9 = 2.59t^{-0.3}$
c) Xuan average stress relaxation model: $f_9 = 2.22t^{-0.25}$
d) Xuan low stress relaxation model: $f_9 = 1.89t^{-0.2}$

Equation 7-17 computes the occurring stresses [σ]. Occurring stresses [σ] are a function of total deformation [ε (t)], modulus of elasticity [$E_{cm\,(t)}$] and stress relaxation [f_9].

$$\sigma = f_9 .E_{cm}(t).\ \varepsilon\ (t)\ (MPa) \qquad \text{Equation 7-17}$$

Coefficient of Friction:

The analysis considered a coefficient of friction of 3.8 based on field pavement studies. A sensitivity analysis to evaluate the influence of coefficient of friction is undertaken.

First and Second Cracks Calculations:

Breathing length [L_{a1}] determines the distance between first cracks. Breathing length [L_{a1}] at the first cracks is determined using Equation 7-18.

$$L_{a1} = 1000E_{cm}(t).\ \varepsilon\ (t)/\ (\gamma f)\ (m) \qquad \text{Equation 7-18}$$

Where: ɣ (kN/m^3) is the volume weight of the stabilised layer [see Table 7-2]

The distance [L_{w1}] between the first cracks is twice the breathing length [L_{a1}]; Equation 7-19 denotes the relationship.

$$L_{w1} = 2L_{a1}\ (m) \qquad \text{Equation 7-19}$$

Equation 7-20 computes the initial width [w_{1i}] of the first cracks.

$$w_{1i} = 1000000E_{cm}\ (t).\ \varepsilon\ (t)\ ^2/\ (2\gamma f) \qquad (mm) \qquad \text{Equation 7-20}$$

Where: t – denotes the time of the first cracks

With the manifestation of the first cracks and thus the initial crack width [w_{1i}], a stress reduction [$\Delta\sigma_1$] of the maximum tensile stress at mid-span of the stabilised layer between the first cracks results.

Computation of the layer stress reduction [$\Delta\sigma_1$] after the first cracks appear, considers Equation 7-21.

$$\Delta\sigma_1 = 0.5\sigma\ x\ (1+w_{1i}/\ (1000\ x\ L_{a1})) \qquad (MPa) \qquad \text{Equation 7-21}$$

Where: σ – occurring tensile stresses in the stabilised layer at the time when the first cracks appear

With the manifestation of the first cracks, tensile stresses in the stabilised layer continue to develop until a maximum. For computing the maximum tensile stresses [σ_1 (t)] Equation 7-22 is applied.

$\sigma_1 (t) = \sigma - \Delta\sigma_1$ (MPa) Equation 7-22

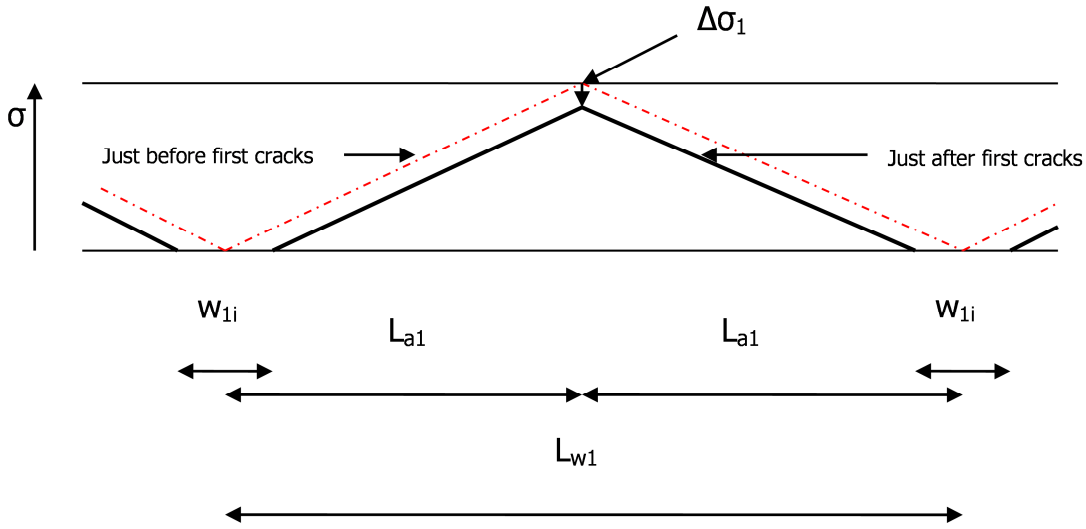

Figure 7-3 Tensile Stresses in a Stabilised Pavement at the Time the First Cracks appear [Houben 2008]

Equation 7-23 computes the maximum tensile strain [$\varepsilon_1 (t)$] in the stabilised layer at the time when the first cracks appear.

$\varepsilon_1 (t) = \sigma_1 (t)/E_{cm} (t)$ Equation 7-23

Figure 7-4 illustrates the tensile stress development in a stabilised layer between the first and second cracks.

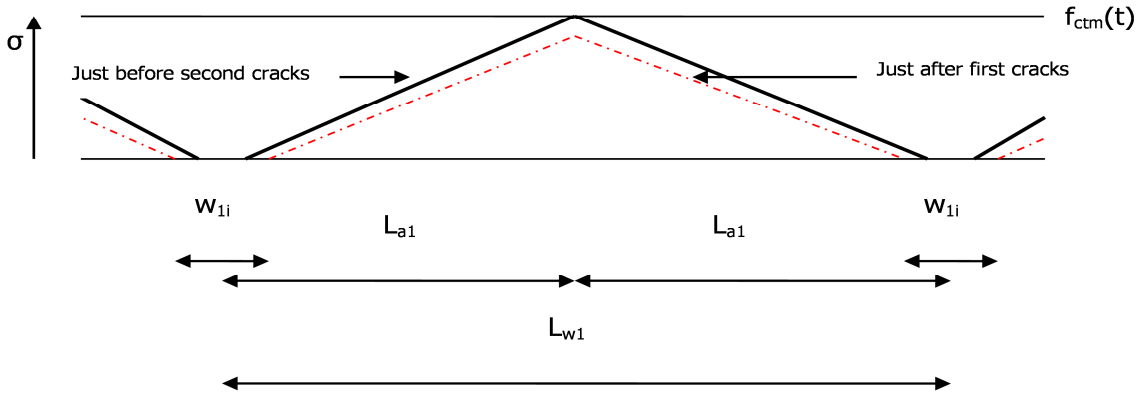

Figure 7-4 Development of Tensile Stresses in a Stabilised Layer between the First and Second Cracks [Houben 2008]

Equation 7-24 computes the change in crack width [$\Delta w_1 (t)$] for first cracks.

$\Delta w_1 (t) = 1000000 E_{cm} (t).\varepsilon_1 (t)^2 / (\gamma f) - x_{1i}$ (mm) Equation 7-24

Where: x_{1i} – initial value and t - the time when the first cracks appear

Equation 7-25 computes the width of the first cracks [$w_1 (t)$].

$w_1 (t) = w_{1i} + \Delta w_1 (t)$ (mm) Equation 7-25

Stress reduction due to the first cracks is dependent on the cement type and mix compositions. After the first cracks, tensile stresses continue to develop until maximum when stresses tend to exceed strength; this is when the second cracks appear at mid-span of the first intact sections of the stabilised layer. Figure 7-5 illustrates the tensile stress in a stabilised layer at the time the second cracks appear.

Equation 7-26 computes the breathing length [L_{a2}] due to the second cracks.

$$L_{a2} = 0.5L_{a1} \text{ (m)} \qquad \text{Equation 7-26}$$

Equation 7-27 computes the distance between the second cracks.

$$L_{w2} = 0.5\ L_{w1} \text{ (m)} \qquad \text{Equation 7-27}$$

The computation of stress reduction [$\Delta\sigma_2$] due to the second cracks uses Equation 7-28.

$$\Delta\sigma_2 = 0.5\ \sigma_1 \text{ (t) (MPa)} \qquad \text{Equation 7-28}$$

After the appearance of the second cracks, tensile stresses develop within the stabilised layer is the mid-span of the first and second intact sections. The development of the stresses continues reaching a maximum and thus exceeding the material strength, which leads to another series of cracks. Equation 7-29 computes the maximum tensile stress [σ_2 (t)] developed.

$$\sigma_2 \text{ (t)} = \sigma_1 \text{ (t)} - \Delta\sigma_2 \text{ (MPa)} \qquad \text{Equation 7-29}$$

Where: t – the time the second cracks appear

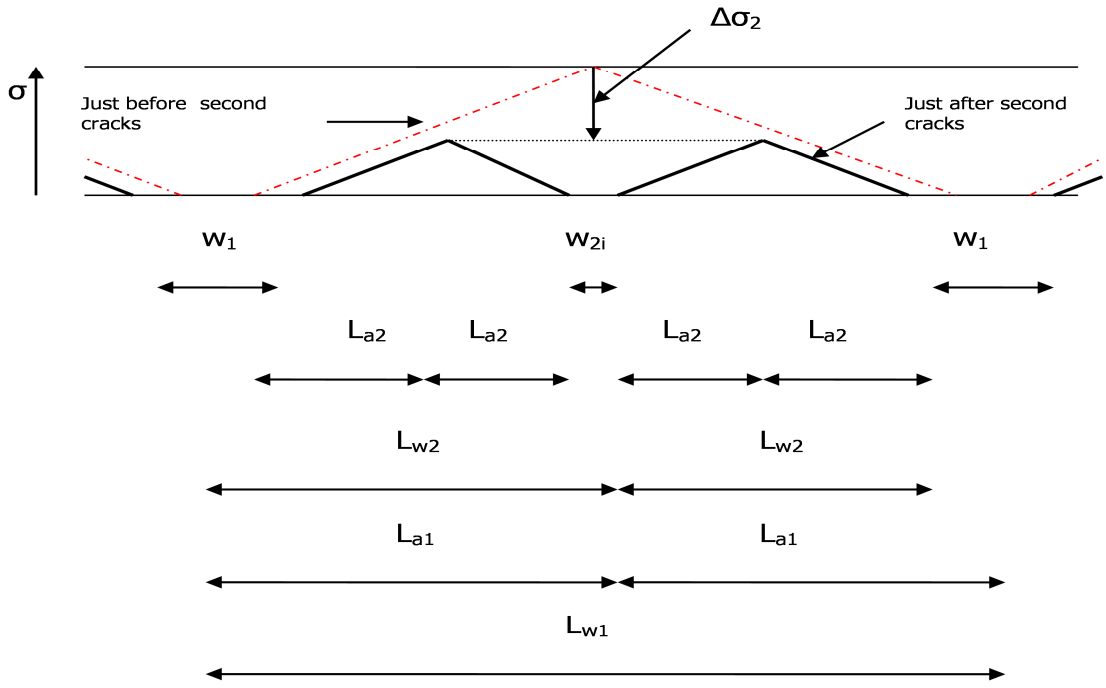

Figure 7-5 Tensile Stress in a Stabilised Layer at the Time the Second Cracks appear

Equation 7-30 computes the maximum tensile strain [ε_2 (t)] due to the second cracks.

$$\varepsilon_2 \text{ (t)} = \sigma_2 \text{ (t)} / E_{cm} \text{ (t)} \qquad \text{Equation 7-30}$$

Equation 7-31 computes the change in crack width for the second cracks [Δw_2 (t)].

$$\Delta w_2 \text{ (t)} = 1000000E_{cm} \text{ (t)}.\varepsilon_2 \text{ (t)}^2 / (\gamma f) - x_{2i} \quad \text{(mm)} \qquad \text{Equation 7-31}$$

Where: x_{2i} – initial value and t is the time the second cracks appear

Equation 7-32 computes the width of second cracks [w_2 (t)].

$$w_2 (t) = w_{2i} + \Delta w_2 (t) \quad (mm) \qquad \text{Equation 7-32}$$

Third and Fourth Cracks Calculations:

Manifestation of the first and second cracks leads to stress reduction. Depending on the mix type, there is continued stress development, which reaches maximum and other cracks manifest. When the tensile stress [σ_2 (t)] reaches its maximum, third cracks appear. Equation 7-33 computes the initial crack width of the third cracks.

$$w_{3i} = 1000000 E_{cm} (t).\varepsilon_2 (t)^2 / (\gamma f) \quad (mm) \qquad \text{Equation 7-33}$$

Equation 7-34 computes the breathing length of the third cracks [L_{a3}].

$$L_{a3} = 0.5 L_{a2} = 0.25 L_{a1} (m) \qquad \text{Equation 7-34}$$

Equation 7-35 relates the distance [L_{w3}] of the third series of cracks to the first and second cracks.

$$L_{w3} = 0.5 L_{w2} = 0.25 L_{w1} (m) \qquad \text{Equation 7-35}$$

Equation 7-36 computes the stress reduction [$\Delta\sigma_3$] due to the third cracks.

$$\Delta\sigma_3 = 0.5 \sigma_2 (t) (MPa) \qquad \text{Equation 7-36}$$

The appearance of the fourth cracks results when the tensile stress [σ_3 (t)] develops reaching a maximum. Equation 7-37 computes the maximum tensile stresses.

$$\sigma_3 (t) = \sigma_2 (t) - \Delta\sigma_3 (MPa) \qquad \text{Equation 7-37}$$

Where: $\Delta\sigma_3 = 0.5 \sigma_2$ (t)

Equation 7-38 computes the maximum tensile strain [ε_3 (t)] after the appearance of the third cracks.

$$\varepsilon_3 (t) = \sigma_3 (t) / E_{cm} (t) \qquad \text{Equation 7-38}$$

Equation 7-39 computes the change in crack width [Δw_3 (t)] after the third cracks.

$$\Delta w_3 (t) = 1000000 E_{cm} (t).\varepsilon_3 (t)^2 / (\gamma f) - x_{3i} \quad (mm) \qquad \text{Equation 7-39}$$

Where: x_{3i} – initial value and t - the time the third cracks appear

Equation 7-40 computes the width of the third cracks [w_3 (t)].

$$w_3 (t) = w_{3i} + \Delta w_3 (t) (mm) \qquad \text{Equation 7-40}$$

Equation 7-41 computes the initial crack width of the fourth cracks [w_{4i}].

$$w_{4i} = 1000000 E_{cm} (t).\varepsilon_3 (t)^2 / (\gamma f) \quad (mm) \qquad \text{Equation 7-41}$$

Equation 7-42 calculates the breathing length [L_{a4}] of the fourth cracks.

$$L_{a4} = 0.5 L_{a3} = 0.25 L_{a2} = 0.125 L_{a1} (m) \qquad \text{Equation 7-42}$$

Equation 7-43 computes length between the fourth cracks [L_{w4}].

$$L_{w4} = 0.5 L_{w3} = 0.25 L_{w2} = 0.125 L_{w1} (m)$$

Equation 7-44 computes stress reduction [$\Delta\sigma_4$] due to the fourth cracks.

$$\Delta\sigma_4 = 0.5\ \sigma_3\ (t)\ (MPa) \qquad \text{Equation 7-44}$$

Equation 7-45 computes the maximum tensile stress [$\sigma_4\,(t)$] in the stabilised layer.

$$\sigma_4\,(t) = = \sigma_3\ (t) - \Delta\sigma_4\ (MPa) \qquad \text{Equation 7-45}$$

Equation 7-46 computes the maximum tensile strain [$\varepsilon_4\ (t)$] in the stabilised layer.

$$\varepsilon_4\ (t) = \sigma_4\,(t)/\ E_{cm}\ (t) \qquad \text{Equation 7-46}$$

Equation 7-47 computes the change in crack width [$\Delta w_4\ (t)$] after the fourth cracks.

$$\Delta w_4\ (t) = 1000000E_{cm}\ (t).\varepsilon_4\ (t)^{\,2}/\ (\gamma f) - x_{4i} \quad (mm) \qquad \text{Equation 7-47}$$

Where: x_{4i} – initial value and t - the time the fourth cracks appear

In computing the width of the fourth cracks, Equation 7-48 is applied.

$$w_4\ (t) = w_{4i} + \Delta w_4\ (t)\ (mm) \qquad \text{Equation 7-48}$$

Fifth and subsequent cracks appear if the tensile stress [$\Delta\sigma_x$] develops and exceeds the material strength; the process continues until no further cracks appear.

7.5.3 Seasonal and Temperature Variations

According to the South African weather service, the official dates for the start of the seasons are as follows; summer [1st December], autumn [1st March], winter [1st June] and spring [1st September]. Figure 7-6 shows the variation in temperature along with the annual average air temperature from the 1st February to the 1st February [for 360 days]. The time of construction influences the rate of moisture loss and ultimately the resultant shrinkage. For this analysis, the time of constructing the stabilised layer is 1st of February at 10:00 am [i.e. at the average temperature on the hottest day of the year].

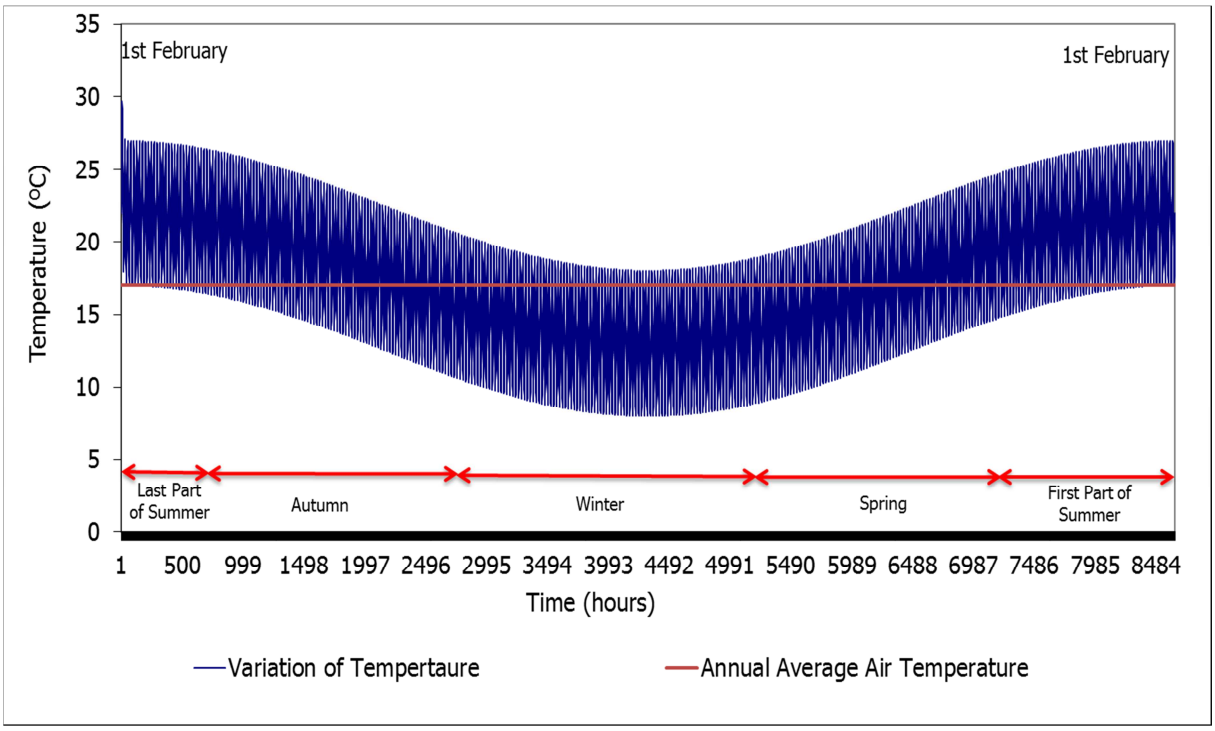

Figure 7-6 Typical Layer Temperature Variations over a Period of 360 Days

7.5.4 Trends from the Houben Model

The following figures illustrate typical trends obtained from the Houben model. The thermal strains and seasonal changes are significant factors influential to material shrinkage. The restriction of thermal strains causes thermal stresses. Figure 7-7 shows how the thermal strains [ε_T] vary with time i.e. for 360 days. Figures 7-8 and 7-9 illustrate how drying and total shrinkage varies over a period of 360 days. These trends provide insight regarding the shrinkage criteria relative to seasonal changes.

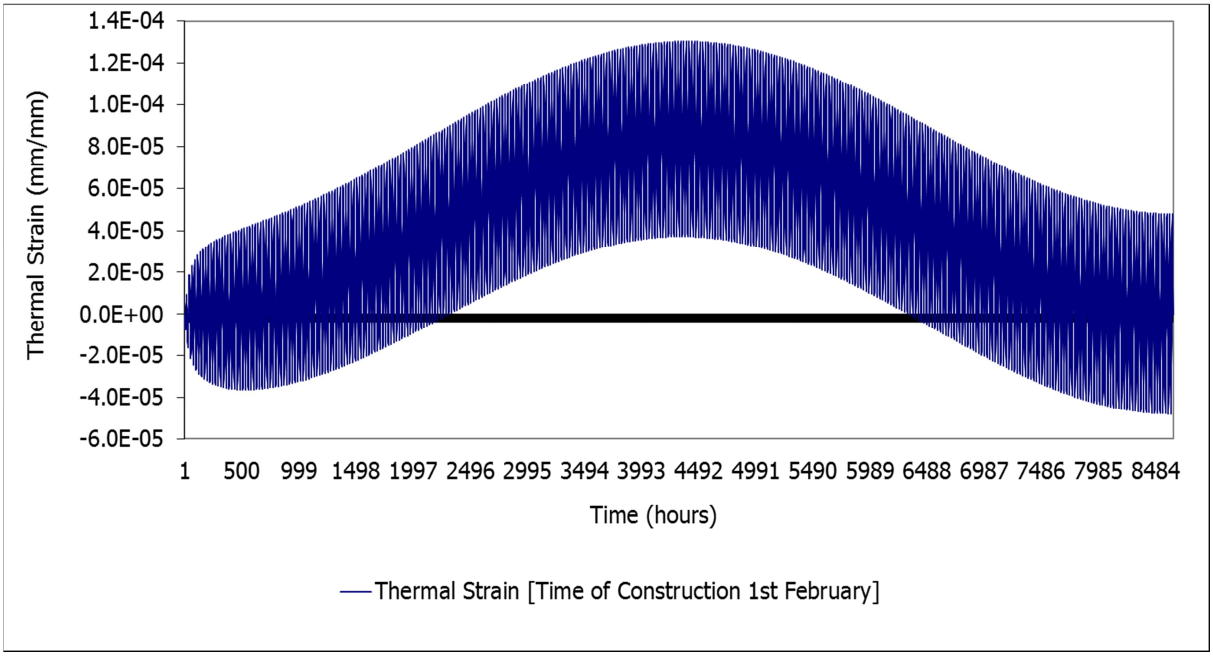

Figure 7-7 Typical Thermal Strain [ε_T] Variations over a Period of 360 Days

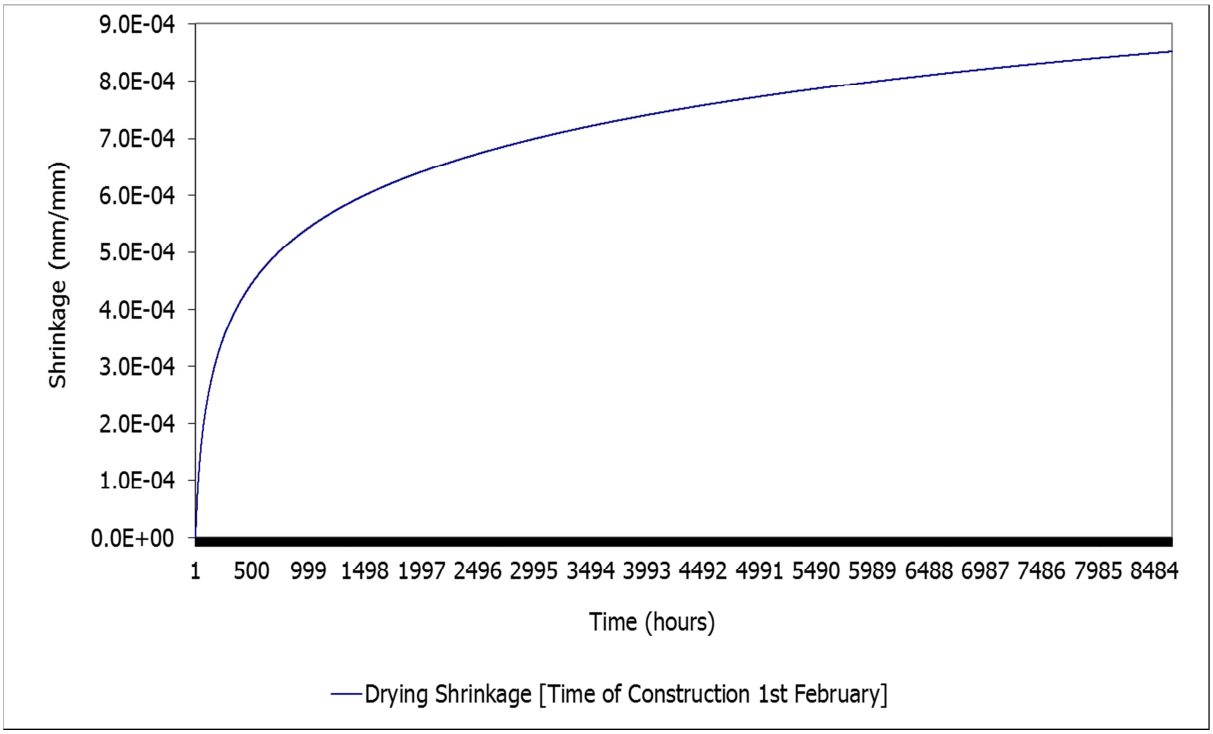

Figure 7-8 Typical Drying Shrinkage [S_t] Variations over a Period of 360 Days

Figures 7-10 and 7-13 illustrate how the tensile stresses with and without the consideration of the Houben stress relaxation factor varies over a period of 360 days [including the seasonal changes]. Figure 7-12 illustrates the trends of the Houben versus Xuan stress relaxation factors. Insight regarding the influence of the Houben stress relaxation factor concerning the development of the tensile stress within the stabilised layer is provided. Figure 7-11 shows the tensile strength increase over a period of 360 days. When the tensile stresses exceed the material strength, cracks appear within the stabilised layer. Figure 7-14 illustrates the relationship between tensile stress development and layer strength over a period of 360 days.

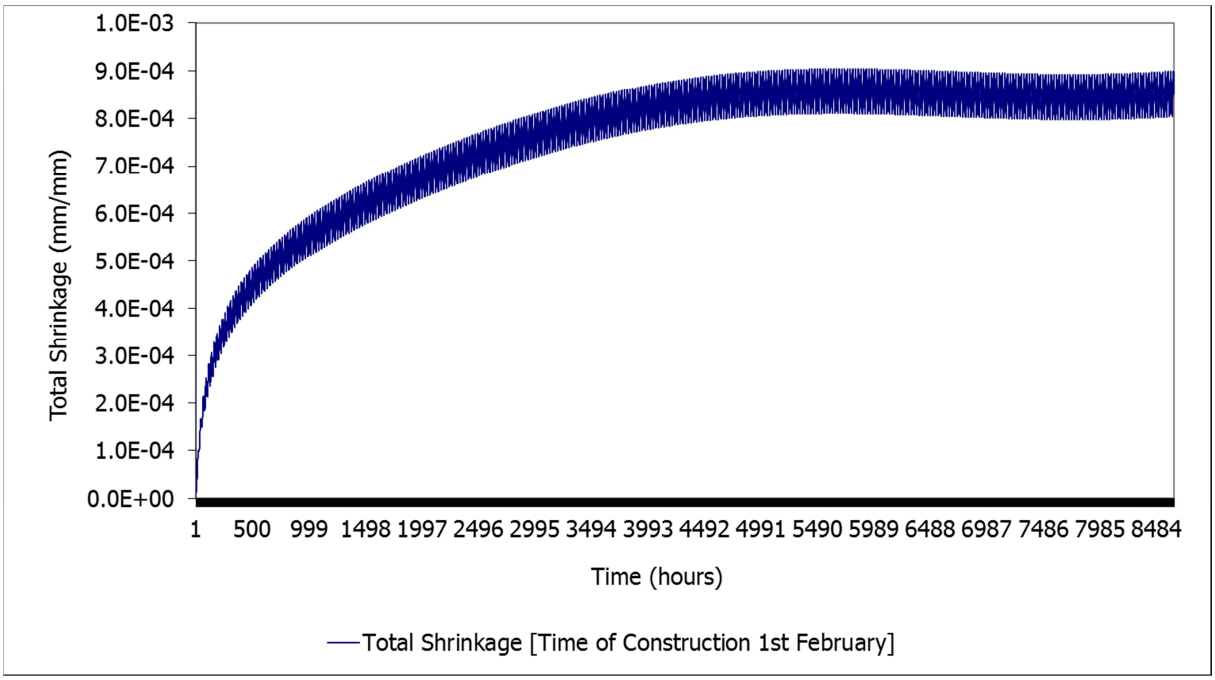

Figure 7-9 Typical Total Shrinkage Variations over a Period of 360 Days

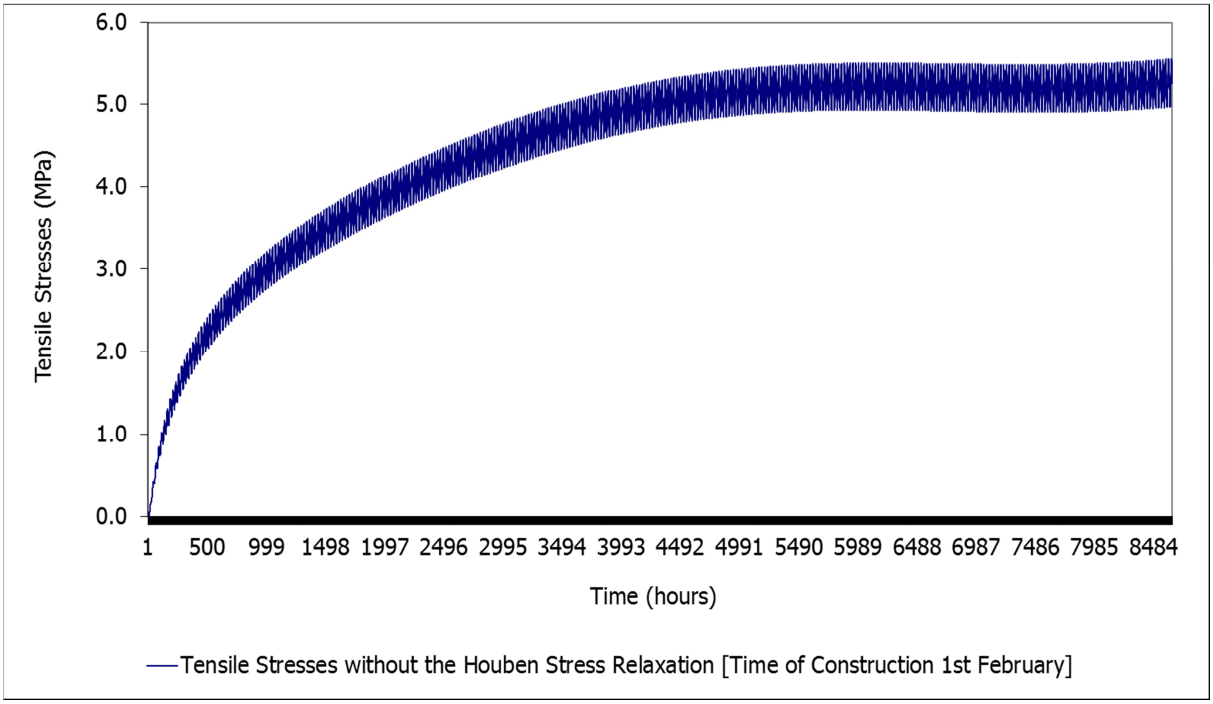

Figure 7-10 Typical Tensile Stress Development without the Houben Stress Relaxation over a Period of 360 Days

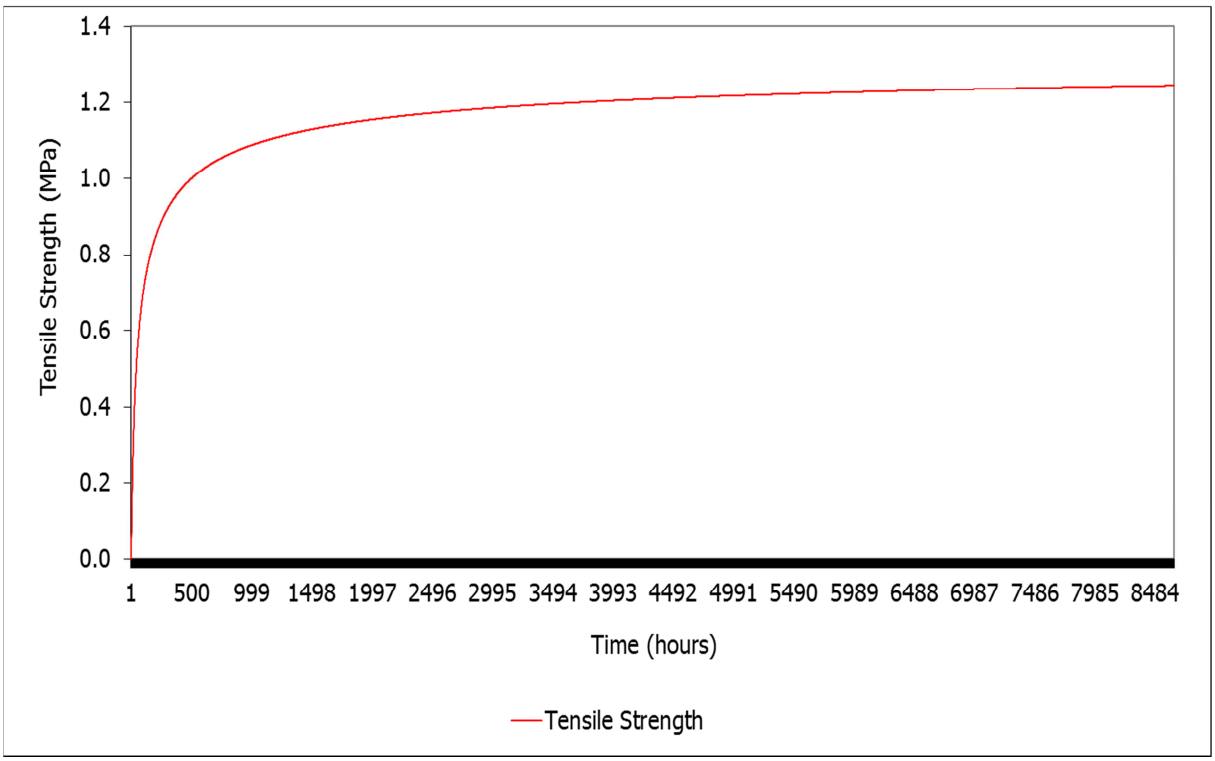

Figure 7-11 Typical Tensile Strength Variations over a Period of 360 Days

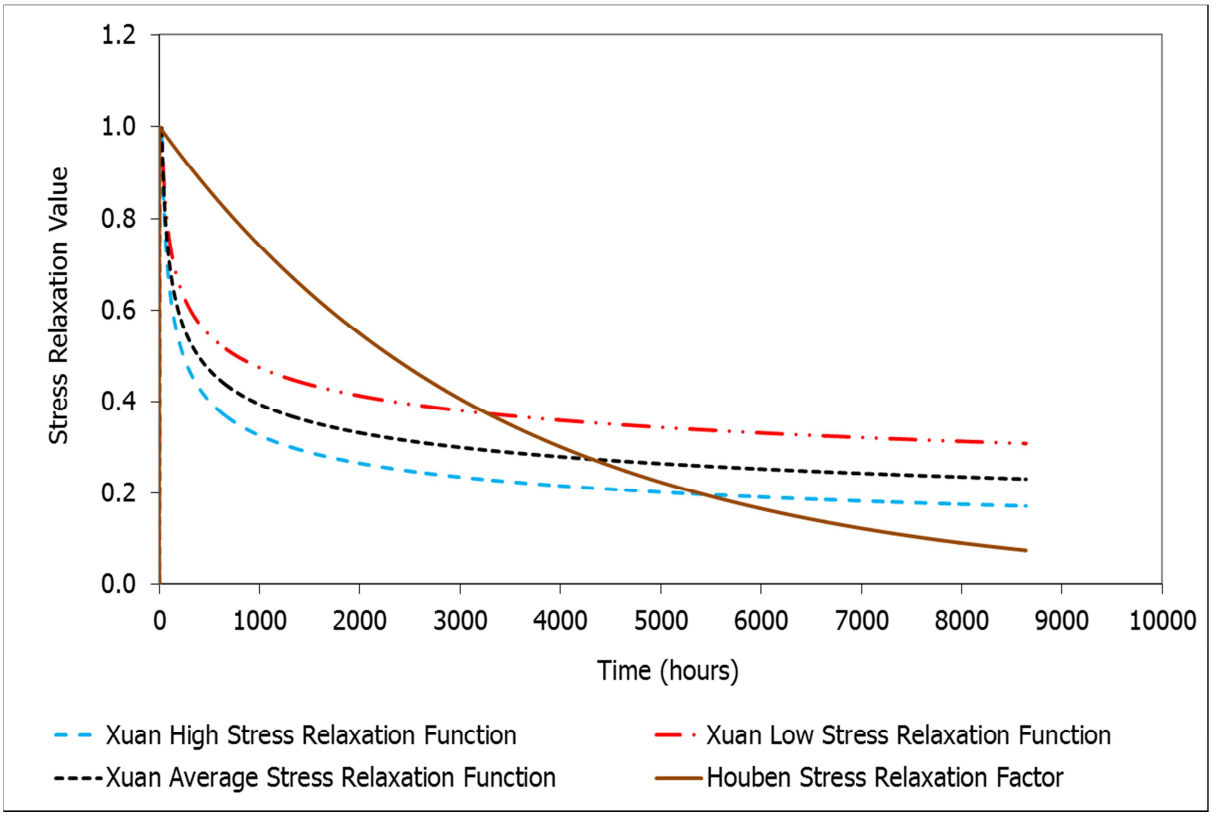

Figure 7-12 Typical Stress Relaxation Functions [Houben versus Xuan] Variations over a Period of 360 Days

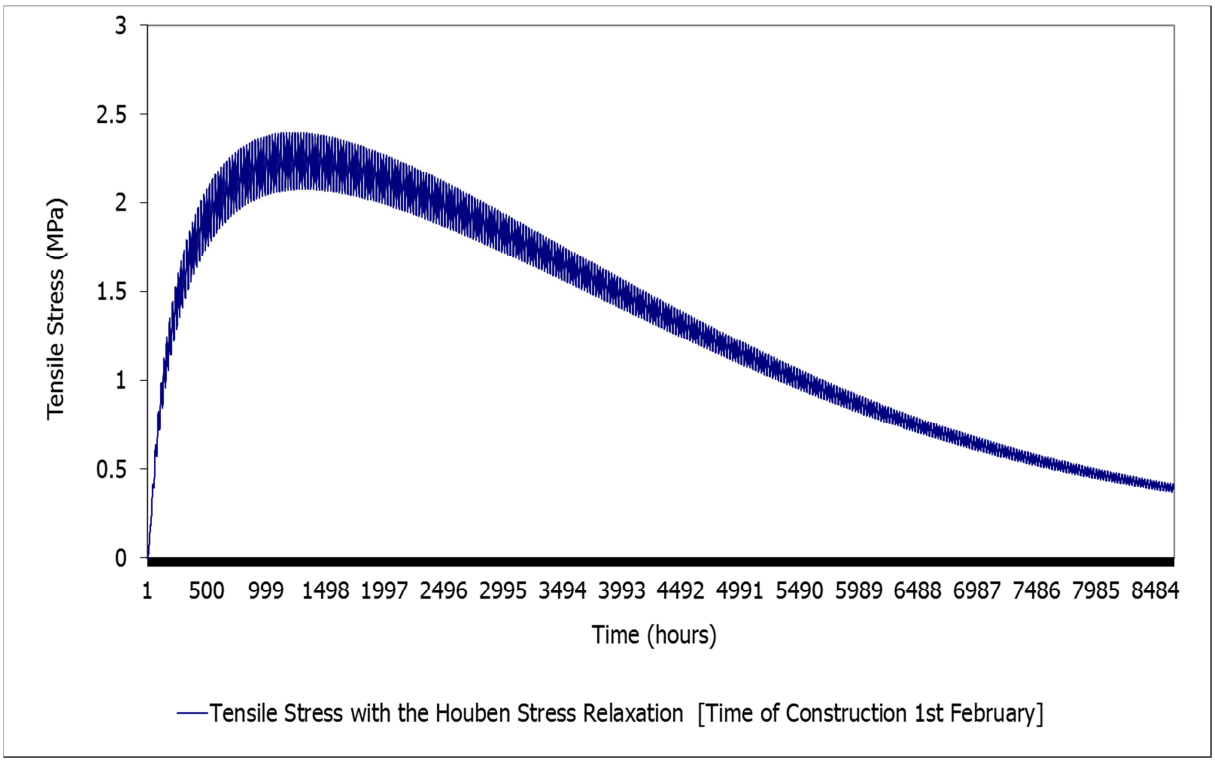

Figure 7-13 Typical Tensile Stress Development with the Houben Stress Relaxation over a Period of 360 Days

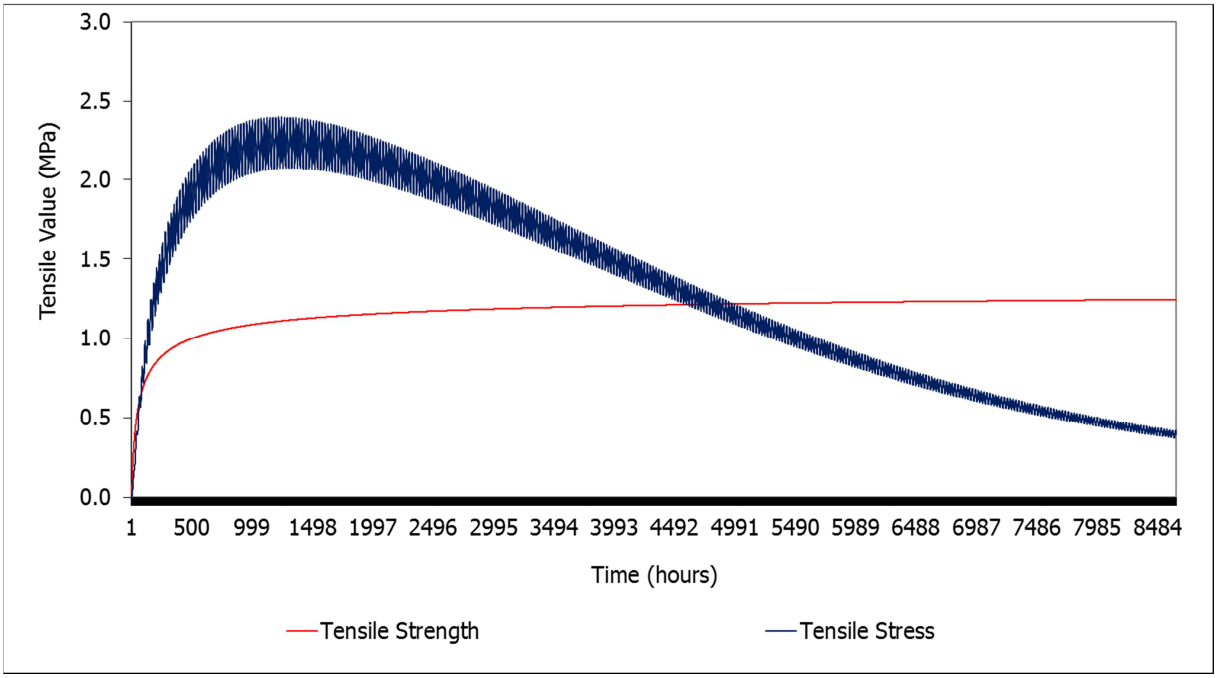

Figure 7-14 Tensile Stress with the Houben and Strength Increase over a Period of 360 Days

7.5.5 Tensile Stress Development and Material Strength

This section assesses the tensile stress development relative to material's strength. The Houben stress relaxation model along with a frictional coefficient of 3.8, are considered. In this phase of the analysis, no subsequent pre-cutting and cracking of the stabilised layer is considered. Figure 7-15 and 7-16 illustrate the tensile stress development along with the material's strength for a mix type stabilised with 6.0% cement content without and with polymer respectively.

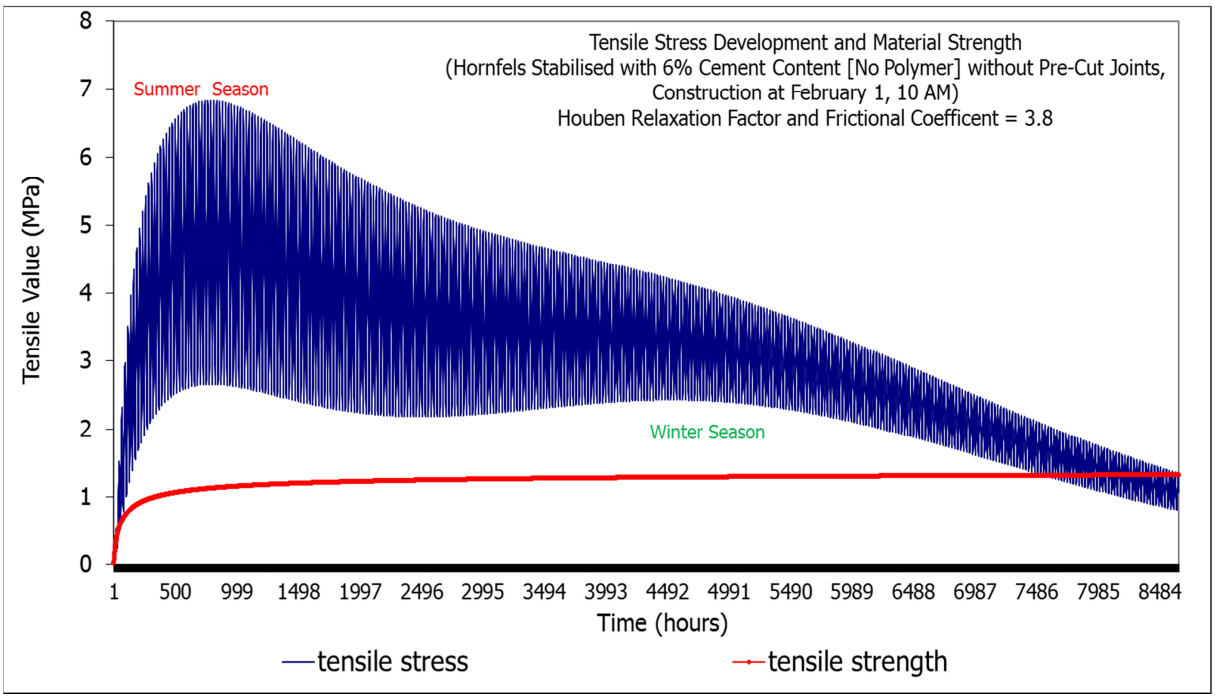

Figure 7-15 Tensile Stress and Strength with Hornfels 6% Cement Content [No Polymer]

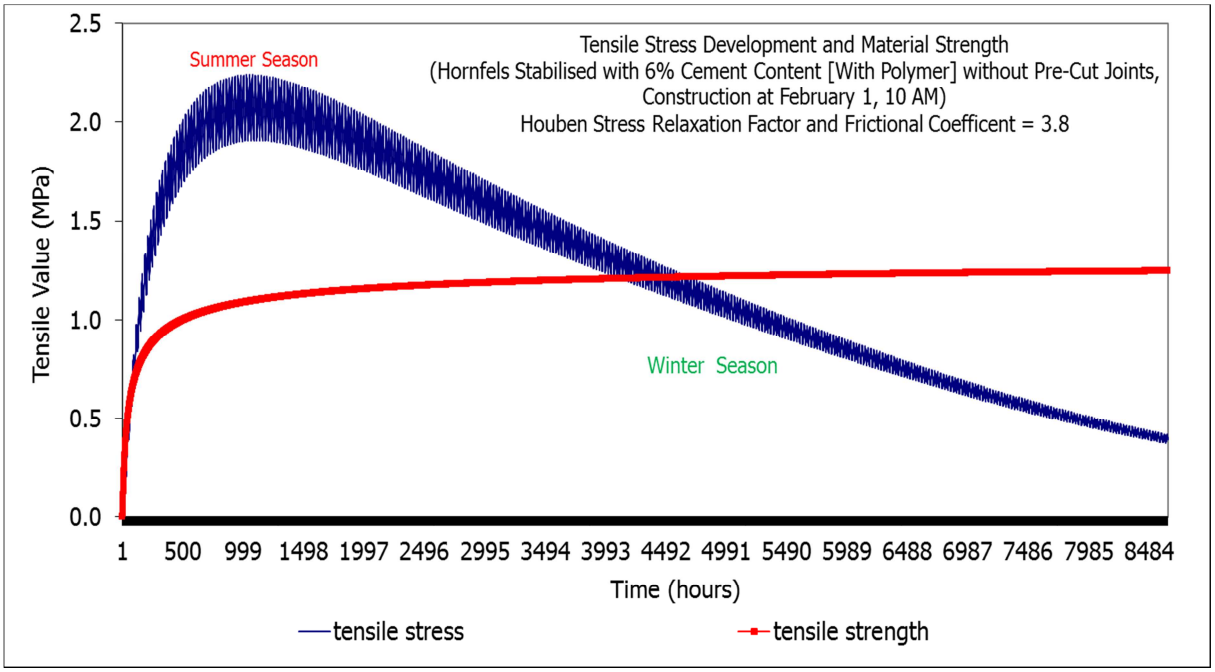

Figure 7-16 Tensile Stress and Strength with Hornfels 6% Cement Content [With Polymer]

A stabilised pavement layer develops tensile stresses as differences in temperature and moisture content take place. The cracking relieves the tensile stresses within a stabilised layer. Temperature differences contribute to the development of cracks in the pavement layer. The hydration process, through which the stabilised layer hardens, produces heat that causes the material to expand. However, exposure of the layer to air and ultra-violet rays leads to loss of moisture through evaporation; these factors contribute to cooling and shrinkage near the surface of the layer. The underlying layer material along with the interlayer bonding [i.e. friction at the interlayer] acts as external restraints to shrinkage of the top surface, which further induces the tensile stresses.

Thermal contraction comprises the primary causal factors of shrinkage cracking in cement-stabilised layers. Due to temperature fluctuations, variations in tensile stress development are illustrated. High summer temperature ranges not only increase the rate of moisture loss but also result in temperature differences within the layer. The upper exposed part of the stabilised layer experiences higher temperatures and as a result moisture loss through evaporation. Under such high summer temperatures, an increase in moisture loss and temperature differences induces internal restraints typified by the development of layer tensile stresses.

When the induced tensile stresses exceed the material's strength, cracking occurs. The external restraints such as interlayer friction and thermal effects also influence the cracking behaviour and crack pattern. As the winter season sets in, the high temperatures start to decline, which reduces the rate of moisture loss. With reduced moisture loss and temperature differences a decrease in the tensile stress results. Eventually the tensile stress in the stabilised layer diminishes as the stabilised layer reaches a point when cracking leads to a reduction in stress.

Hornfels mix type with 6.0% cement content exhibits an initial cracking in the first days after construction; the thermal effects attributed to the summer conditions contribute to the increased stress development. Adding the polymer to the hornfels mix type stabilised with 6.0% cement reduces shrinkage and thus the development of tensile stresses. The rate of strength increase between the mixes is comparable.

Polymer application to cement-stabilised layers results in reduced tensile stress development. Tensile stress peak values, particularly in the summer and winter season exhibit a reduction following the use of polymer. A number of factors, including thermal effects, moisture loss and material related characteristics contribute to the development of tensile stress. Therefore, the polymer mechanism in reducing shrinkage links to other factors, which contribute to lessening the resultant tensile stresses within the stabilised layer. Moisture control and material related characteristics are some of the factors most likely influenced by the polymer and that lead to the reduction in shrinkage. A reduction in shrinkage lessens the resultant tensile stress and their development. Drying shrinkage depends on the cement content, mix properties and characteristics as well as thermal effects and imposed restraints.

In order to analyse the effect of low cement contents and the development of tensile stresses along with the material strength increase hornfels mix types stabilised at low cement contents with and without polymer, were included. Figures 7-17 to 7-20 provide the tensile stress development and strength of hornfels stabilised at low cement contents of 2.0% and 3.0% with and without the polymer. For each figure, a maximum tensile stress value along its corresponding strength at that moment is illustrated.

The application of the polymer in stabilised materials results in a reduction in the maximum tensile stress values. This is significant with high cement contents such as 6.0%. Equally, the application of low cement content leads to reduced maximum tensile stress values. Resultant tensile stress at 2.0% and 3.0% are lower than the strength of the stabilised layer and thus, no cracking result. The use of low cement contents for stabilisation and polymer application contribute to the reduction of tensile stresses. However, at low cement contents the developed tensile stresses did not exceed the material strength, which suggests that, no cracks result. Therefore, use of the polymer at low cement contents with hornfels materials is an uneconomical undertaking since no cracking results in any case.

The complexity of quantifying shrinkage in cement-stabilised layers results from the numerous factors involved and their influence in cracking. Such factors include material stress relaxation, combination of thermal and hydration related effects, to note but a few. The use of high cement contents influences the hydration of material. This influences the

causal factors such as thermal effect and moisture loss that lead to stress development and layer cracking.

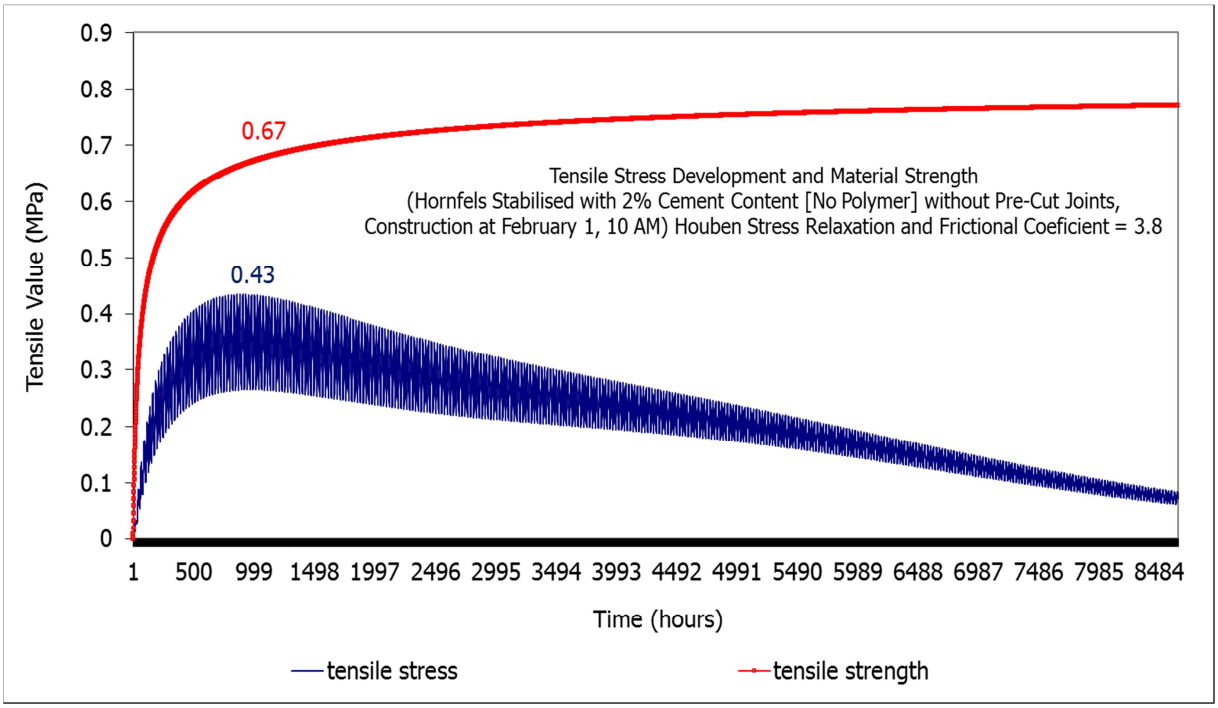

Figure 7-17 Tensile Stress and Strength with Hornfels 2% Cement Content [No Polymer]

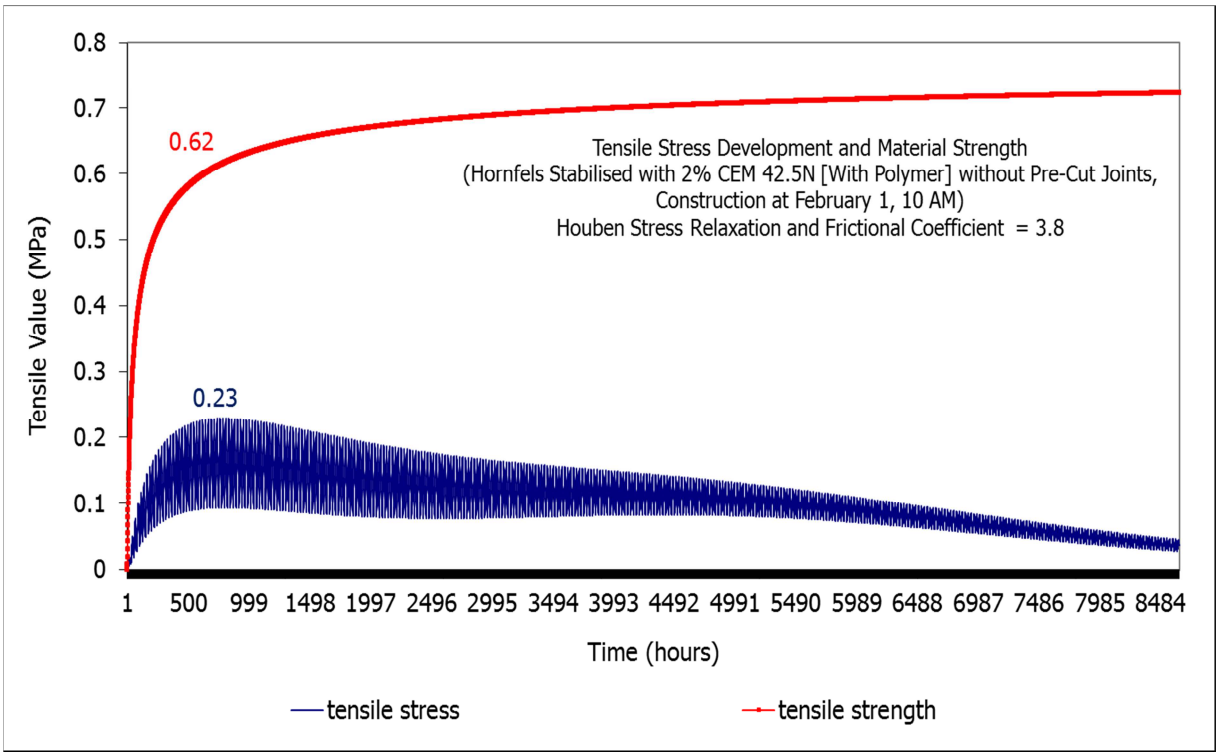

Figure 7-18 Tensile Stress and Strength with Hornfels 2% Cement Content [With Polymer]

All hornfels mix types gain the majority of their strength within the first 30 days after construction. Within the same period, the tensile stress reaches its peak value; this trend is dependent on the mix type. Tensile stress trends exhibited an increase corresponding to addition of cement content to hornfels. This suggests that the use of high cement contents contributes towards the increase in tensile stress development within a stabilised layer. High

summer temperatures increase the rate of moisture loss and as a result, contribute towards the development of tensile stress within the stabilised layer. This suggests that the severity of layer cracking occurs when one constructs in the summer and applies high cement contents.

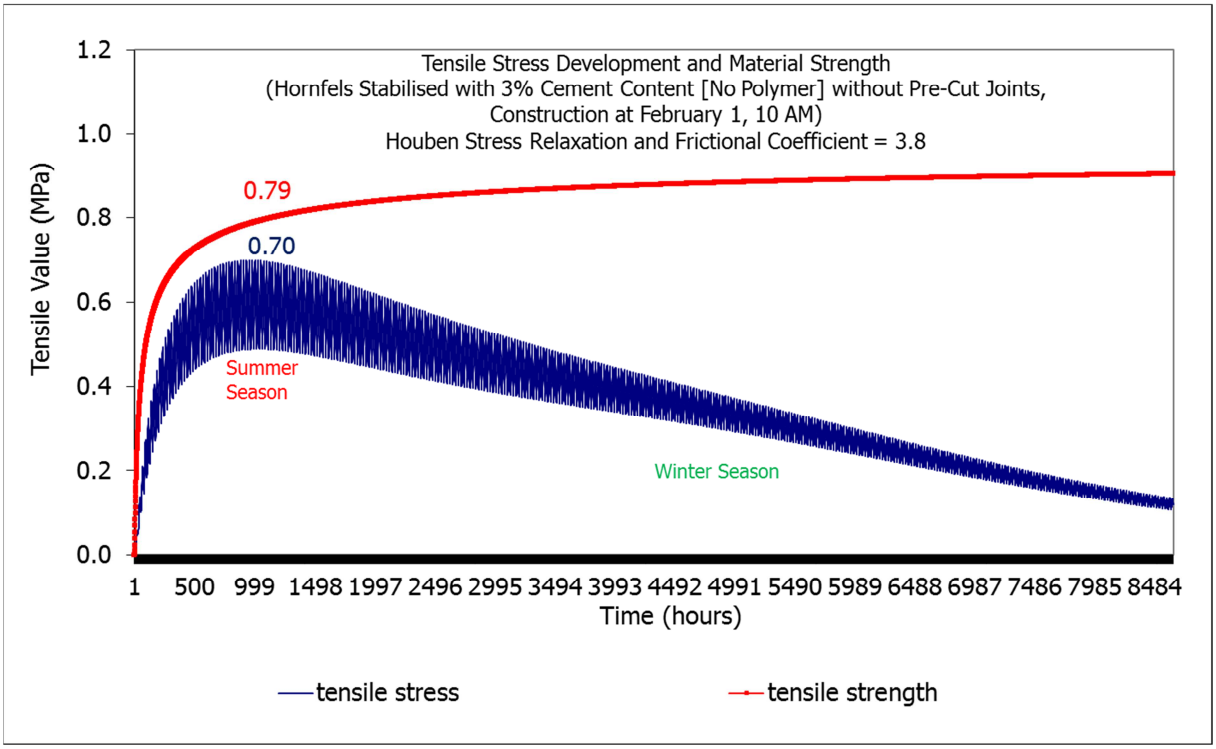

Figure 7-19 Tensile Stress and Strength with Hornfels 3% Cement Content [No Polymer]

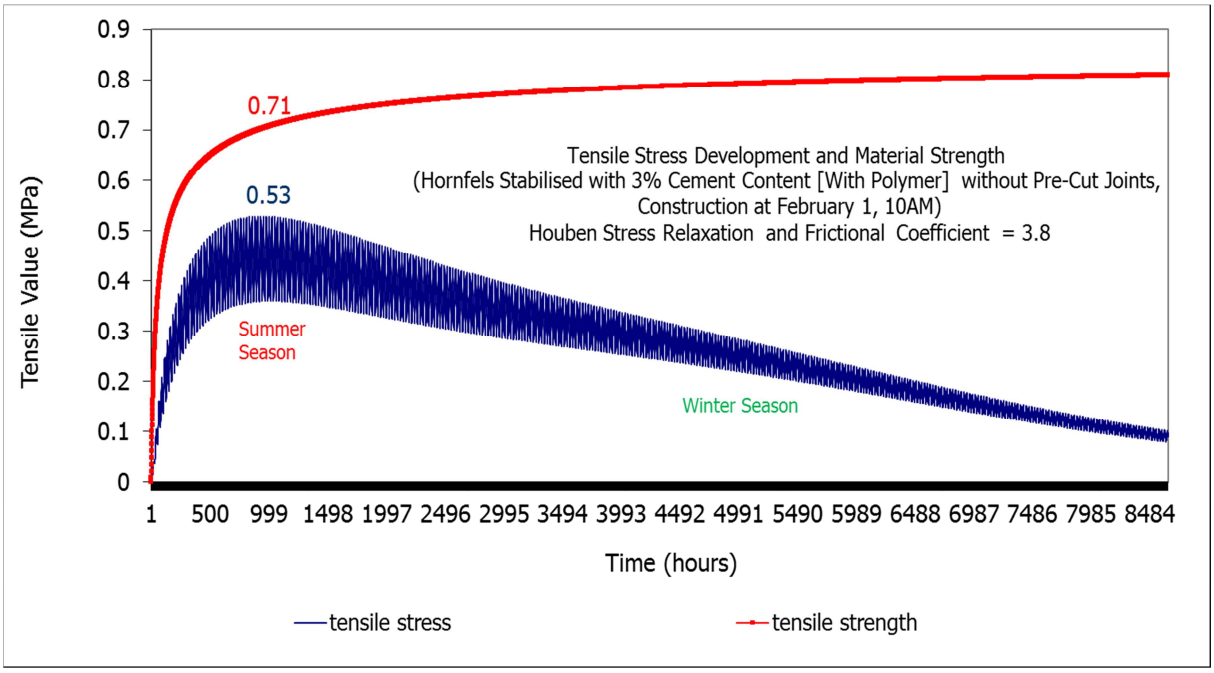

Figure 7-20 Tensile Stress and Strength with Hornfels 3% Cement Content [With Polymer]

Constructing under high temperatures requires the use of appropriate curing conditions aimed at minimising moisture loss from the stabilised layer. Application of the polymer to hornfels mix type stabilised with 6.0% cement content did not inhibit the developed tensile stress beyond the strength of the stabilised layer. A comparison of hornfels mixes stabilised with 6.0% cement content shows a reduction in tensile stress following the addition of the

polymer; the resultant tensile stress exceeded the material strength, which suggests layer cracking. The trends exhibited by hornfels mix types stabilised at 6.0% cement content suggest that the polymer reduces the stress development; however, it does not completely prevent the layer from cracking. At low cement contents, use of the polymer is not practically feasible since the layer does not initiate cracking.

External and internal restraints imposed on the stabilised layer contribute to cracking and the resultant crack pattern. An external restraint is the interlayer frictional force, which is dependent on the bonding between the stabilised and underlying layer. High interlayer bonding leads to increased frictional force thus a reduced tendency for layer to move as the constituent material dries out. Heterogeneity of the material influences the internal and external restraints. The influence of the interlayer friction depends on the internal tensile stress and mix quality. In quantifying shrinkage in a cement-stabilised layer, the induced tensile stress development relative to material strength and mix quality along with interlayer friction should be determined.

Figures 7-21 to 7-24 illustrate the tensile stress development and strength increase in ferricrete mixes. Ferricrete stabilised with 6.0% or 4.0% cement contents with or without the polymer provides insight related to mix quality as well as resultant material shrinkage and related strength. Compared to hornfels, ferricrete mixes exhibit lower strength levels even though they are stabilised with relatively higher cement contents. The high tensile stress values generated in the ferricrete mix stabilised with 6.0% cement content signifies severe cracking of the pavement layer. Even after a year, the tensile stresses generated are higher than the material's strength. The addition of the polymer to ferricrete reduced the developed tensile stress but still exceeded the material's strength signifying cracking in the stabilised layer. The ferricrete mix with 4.0% cement content and polymer yielded no shrinkage cracks in the stabilised layer. This suggests that the efficiency of the polymer is within specific limits beyond which no significant reduction result. These limits are mainly dependent on material and cement content. Ferricrete mix types reveal similar criteria pertaining to cement content and tensile stress development. The addition of cement to material results in a corresponding increase in tensile stress development. A high cement content in the material increases moisture consumption and leads to increased desiccation. Some mix water is required for cement hydration purposes.

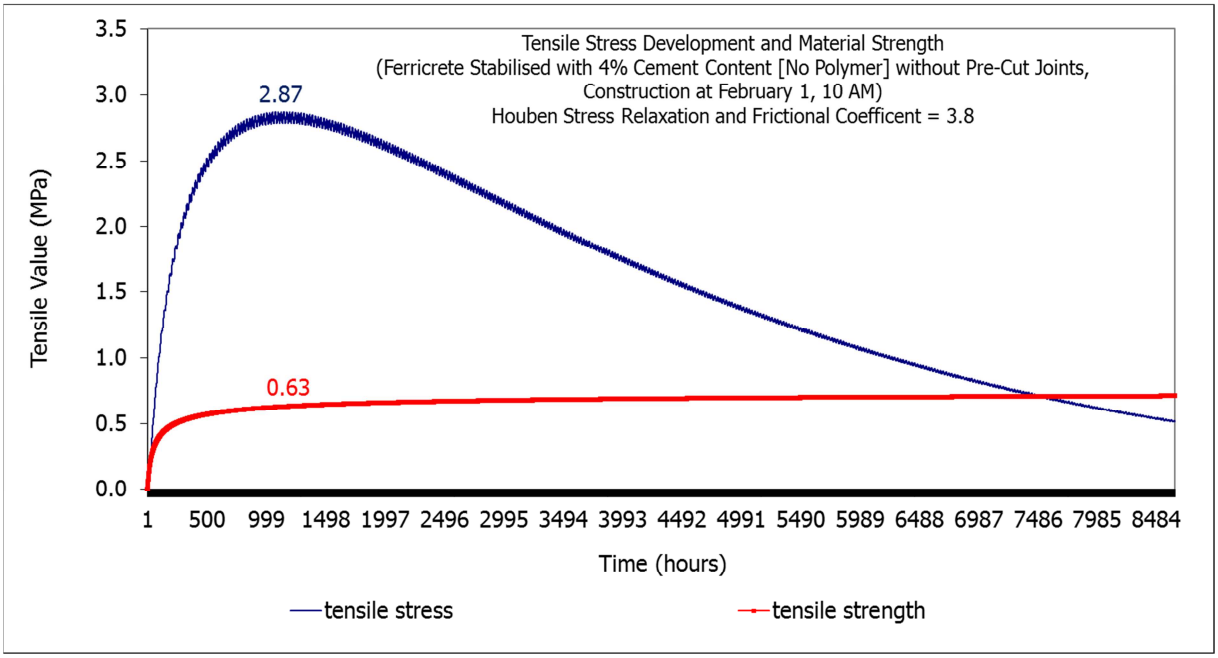

Figure 7-21 Tensile Stress and Strength with Ferricrete 4% Cement Content [No Polymer]

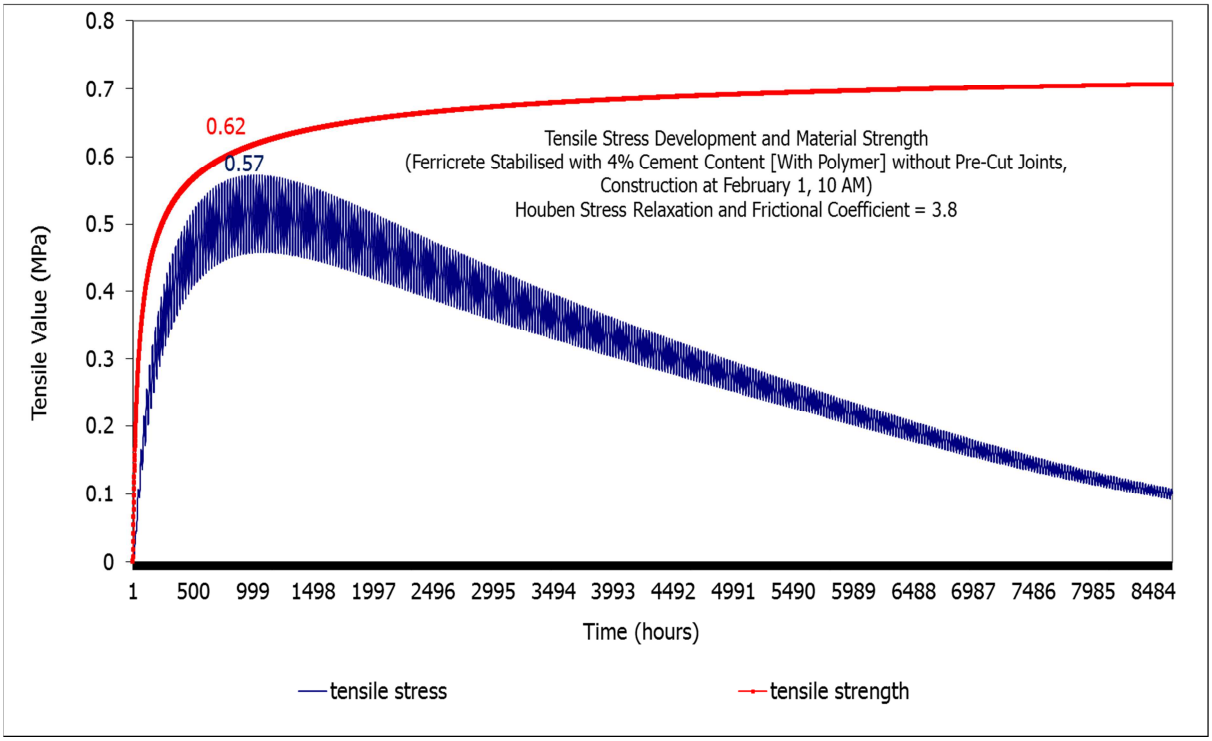

Figure 7-22 Tensile Stresses and Strength with Ferricrete 4% Cement Content [With Polymer]

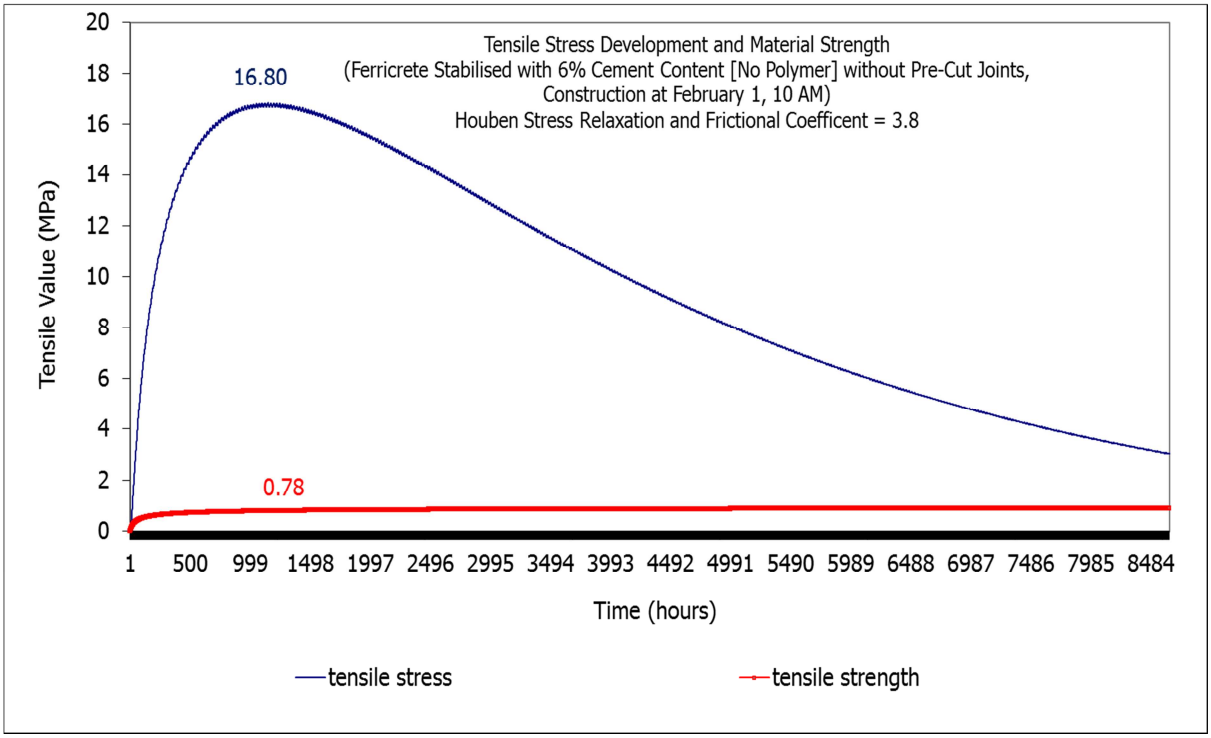

Figure 7-23 Tensile Stress and Strength with Ferricrete 6% Cement Content [No Polymer]

In order to analyse the polymer effectiveness and establish probable limits the average peak tensile stress values along with the corresponding material strength were registered. Table 7-4 lists the peak tensile stress values [summer season] along with the corresponding material strength of the various mix types. Figures 7-25 and 7-26 show the polymer limits relative to cement content versus the resultant tensile stress and strength. Ferricrete generates higher tensile stress but lower layer strength than hornfels. This is due to the dissimilarities between the material types.

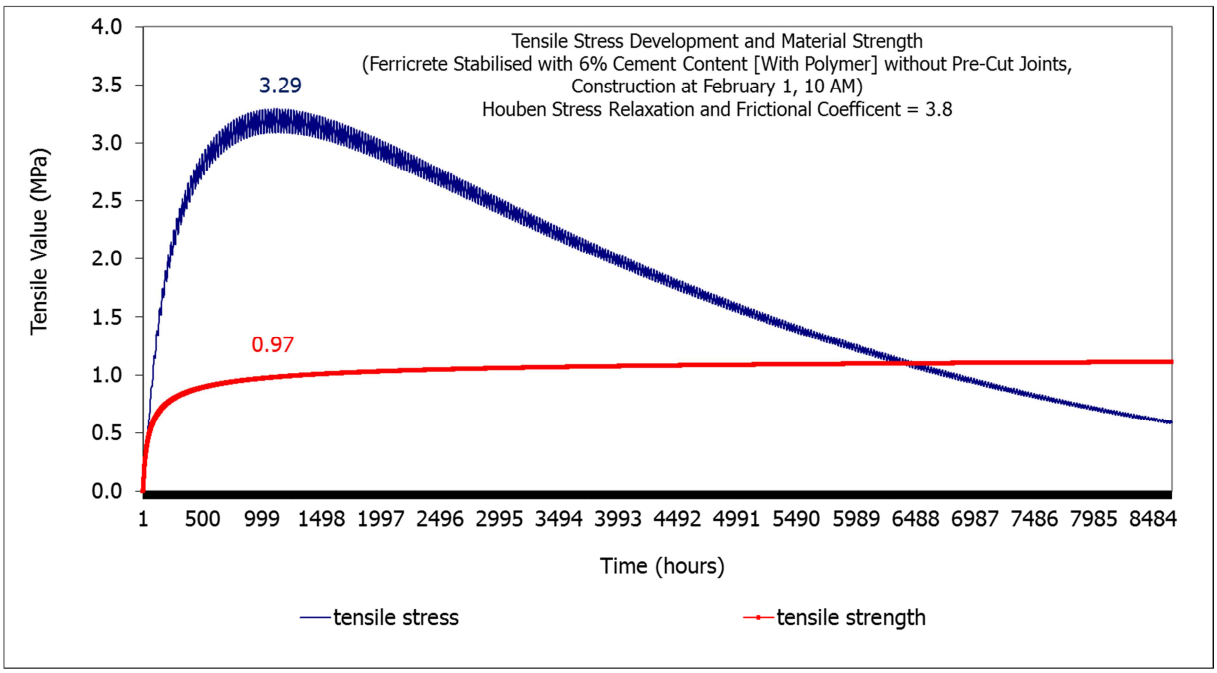

Figure 7-24 Tensile Stress and Strength with Ferricrete 6% Cement Content [With Polymer]

Table 7-4 Peak Tensile Stress Values and Corresponding Tensile Strength per Mix Type

	Houben Stress Relaxation	Construction at February 1, 10AM
Hornfels Mix Types	Friction coefficient [f]= 3.8	Tampyear = 5.0 ºC, Tampday = 4.5 ºC
Cement Content [%]	Peak Tensile Stress Value	Corresponding Tensile Strength
With and Without Polymer	[MPa]	[MPa]
2% Cement No Polymer	0.43	0.67
2% Cement With Polymer	0.23	0.62
3% Cement No Polymer	0.70	0.79
3% Cement With Polymer	0.53	0.71
6% Cement No Polymer	6.80	1.10
6% Cement With Polymer	2.21	1.12
	Houben Stress Relaxation	Construction at February 1, 10AM
Ferricrete Mix Types	Friction coefficient [f]= 3.8	Tampyear = 4.5C, Tampday = 5C
Cement Content [%]	Peak Tensile Stress Value	Corresponding Tensile Strength
With and Without Polymer	[MPa]	[MPa]
4% Cement No Polymer	2.87	0.63
4% Cement With Polymer	0.57	0.62
6% Cement No Polymer	16.80	0.78
6% Cement With Polymer	3.29	0.97

The use of ferricrete as layer material requires the application of the polymer. The low strength levels exhibited by ferricrete suggest a high cement content ought to be applied. While the use of high cement contents increases the tensile stresses, application of polymer to ferricrete significantly reduces the resultant stress. Hornfels mix types stabilised cement contents between 3.0% and 4.0% exhibited no layers cracking following the use of polymer. Beyond 4.2% cement content in the hornfels mix, the addition of the polymer results in reduced cracking as typified by lower tensile stress.

Owing to the variability of stabilised materials emanating from their gradation, characteristics and level of weathering the effectiveness of cement and polymer will vary. As a result, the regression equations only estimate the effect of cement content [with and without the polymer] relative to the tensile stress and corresponding material strength. The R-square values model the influence of tensile stress and corresponding strength with increasing cement content [with and without the polymer].

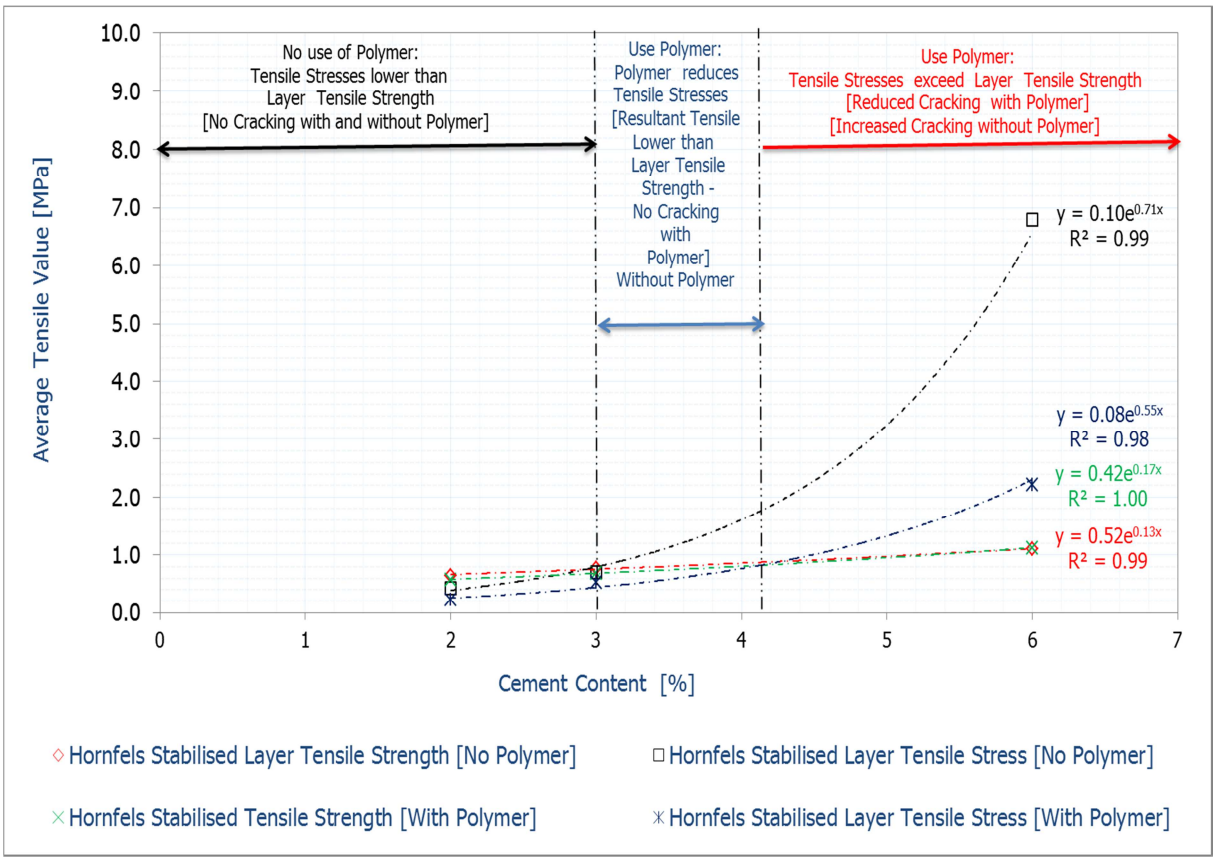

Figure 7-25 Peak Tensile Stress Values and Corresponding Tensile Strengths [Stabilised Hornfels Layer with and without Polymer]

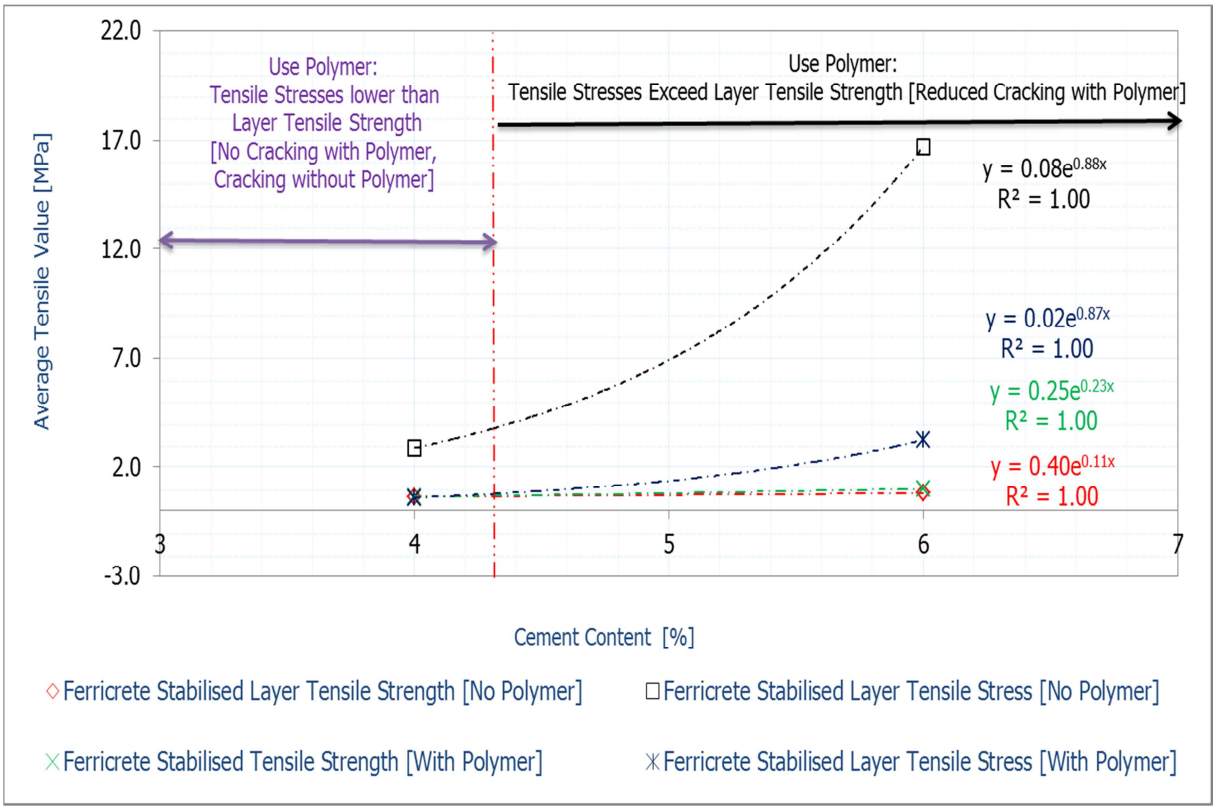

Figure 7-26 Peak Tensile Stress Values and Corresponding Tensile Strengths [Stabilised Ferricrete Layer with and without Polymer]

7.5.6 Shrinkage Crack Pattern Results

The development of tensile stress is due to several factors, including thermal effects and mix quality characteristics. The tendency of the layer to crack depends on the resultant tensile stress relative to material strength as a function of time. As a means to relieve stress, the layer cracks. Table 7-5 summarises the mix types crack pattern results.

For each series of cracks, there is a corresponding stress reduction because after cracking the layer relieves the induced tension forces. This section provides the crack spacing and width of the various mix types using the Houben stress relaxation factor and a frictional coefficient of 3.8. No pre-cutting is considered. Ferricrete mixes stabilised using 6.0% cement with and without the polymer showed a crack spacing of less than 0.5 m within a few days after construction. Ferricrete mixes stabilised using 6.0% cement without polymer exhibited the following crack pattern:

a) 20 hours after construction, the first cracks appeared with a crack spacing of less than 2.5 m and a width of 11.0 mm
b) the second series of cracks appeared 33 hours after construction with a crack width of 8.0 mm and spacing of 1.2 m
c) the third series of cracks appeared 84 hours after construction with a crack width of 5.4 mm and spacing of less than 0.7 m
d) the fourth cracks appeared 22 hours after the third cracks with a crack width of less than 3.0 mm and spacing of less than 0.3 m
e) the subsequent cracking is not analysed since the stabilised layer typifies severe cracking after four series of cracks

Table 7-5 Crack Pattern Results [Houben Stress Relaxation, f= 3.8, No Pre-cutting]

Hornfels Mix Type				
Cement Content [%] With & Without Polymer	Type of Cracks	Time After Construction [Hours]	Crack Spacing [m]	Initial Crack Width [mm]
2% No Polymer	No Cracks	N/A	N/A	N/A
2% With Polymer	No Cracks	N/A	N/A	N/A
3% No Polymer	No Cracks	N/A	N/A	N/A
3% With Polymer	No Cracks	N/A	N/A	N/A
6% No Polymer	Very Severe Cracking			
6% With Polymer	First Cracks	64	6.5	0.67
	Second Cracks	136	3.2	0.11
	Third Cracks	280	1.6	0.04
Ferricrete Mix Type				
Cement Content [%] With & Without Polymer	Type of Cracks	Time After Construction [Hours]	Crack Spacing [m]	Initial Crack Width [mm]
4% No Polymer	Very Severe Cracking			
4% With Polymer	No Cracks	N/A	N/A	N/A
6% No Polymer	Very Severe Cracking			
6% With Polymer	Severe Cracking			

The ferricrete mix stabilised with 6.0% cement and no polymer registered a crack spacing of less than 0.3 m in less than 4 days after construction. The initial crack width of 11.30 mm is detrimental to the pavement. For fine-grained materials, a crack width of 3.0 mm or more results in severe damage due to poor load transfer, particularly in the region of the crack since limited aggregate interlock occurs. With a crack spacing of less than 0.3 m, the ferricrete mix stabilised with 6.0% cement content exhibits a block crack pattern [very severe cracking]. The same mix with polymer showed no significant improvement. After the fourth series of cracks, which appeared in less than 6 days after construction, the ferricrete mix stabilised using 6.0% cement content with polymer registered a crack width of less than 0.2 mm but a spacing of 0.6 m [severe cracking]. The ferricrete mix stabilised using 4.0%

cement content without the polymer registered an initial crack width of 0.5 mm and a spacing of less than 3.0 m. In less than 5 days after construction, the ferricrete mix with 4.0% cement content and no polymer exhibited a block crack pattern with a crack spacing of less than 0.4 m. However, the equivalent mix type with the polymer registered no cracks.

Hornfels mix type with 6.0% cement content and no polymer registered a crack spacing of less than 0.4 m within 40 hours after construction, which is characterised as block cracking. The addition of the polymer to its equivalent hornfels mix type stabilised at 6.0% cement content showed an improved crack pattern. Table 7-6 details the crack pattern results for hornfels mix stabilised using 6.0% cement content and 0.72% polymer content.

Table 7-6 Crack Pattern Results for the 6.0% Cement Content Hornfels Mix Type with polymer [Houben Stress Relaxation, f= 3.8, No Pre-cutting]

Hornfels Mix	6% Cement Content	With Polymer	At the day with the maximum crack width		After One Year [at day 360]	
Type of Cracks	Crack Spacing [m]	Initial Crack Width [mm]	Maximum Crack Width [mm] [Critical Situation]	Minimum Crack Width [mm] [Variation of Crack Width]	Maximum Crack Width [mm]	Minimum Crack Width [mm]
First Cracks	6.5	0.67	1.9	1.6	1.1	1.0
Second Cracks	3.2	0.11	1.0	0.7	0.2	0.1
Third Cracks	1.6	0.04	0.5	0.2	-0.4	-0.4

Figure 7-25 shows the effect of layer cracking and stress reduction after a series of cracks. Figure 7-26 details the tensile stress development and reduction for the first two months after construction. The stress reduction is attributable to cracking within a stabilised layer, which leads to a release of tension forces. The process continues until the occurring tensile stress does not exceed the present tensile strength any more. Figure 7-27 provides the variation of crack width over a period of 360 days. Maximum crack width occurs in summer.

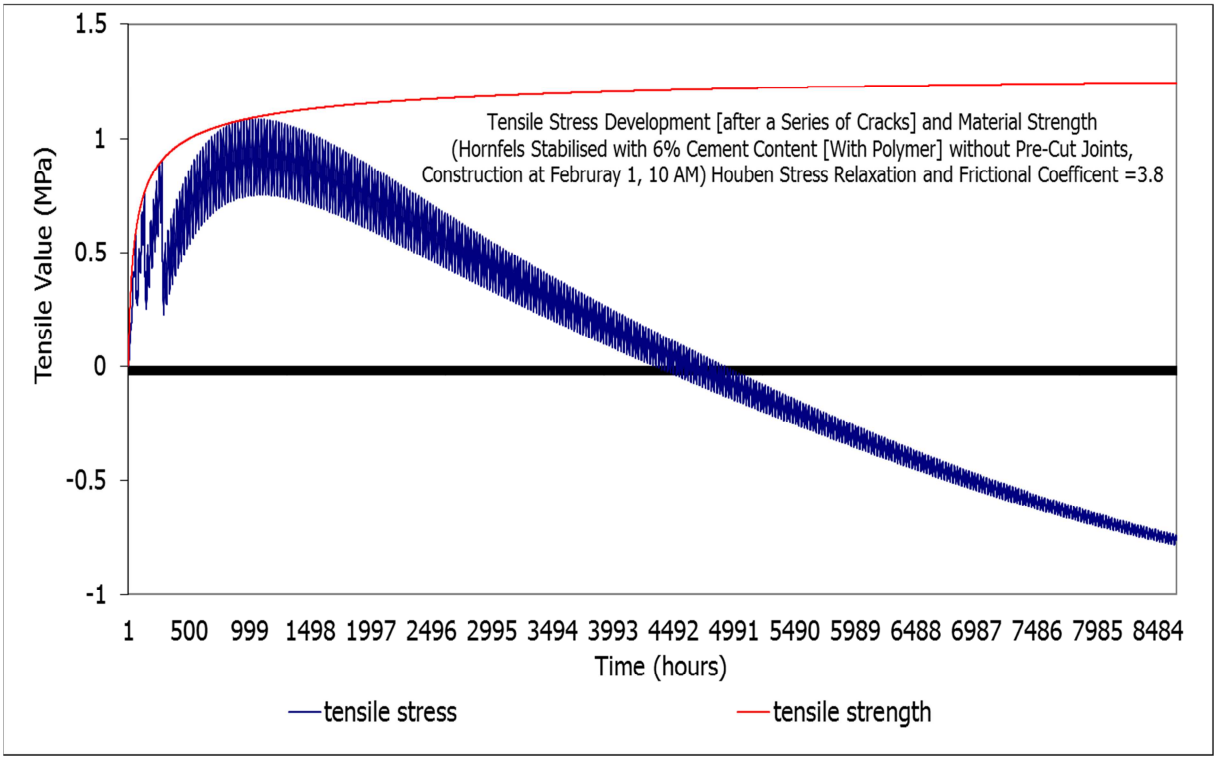

Figure 7-25 Maximum Tensile Stress due to Cracking and Material Strength [Hornfels Mix with 6.0% Cement Content and Polymer]

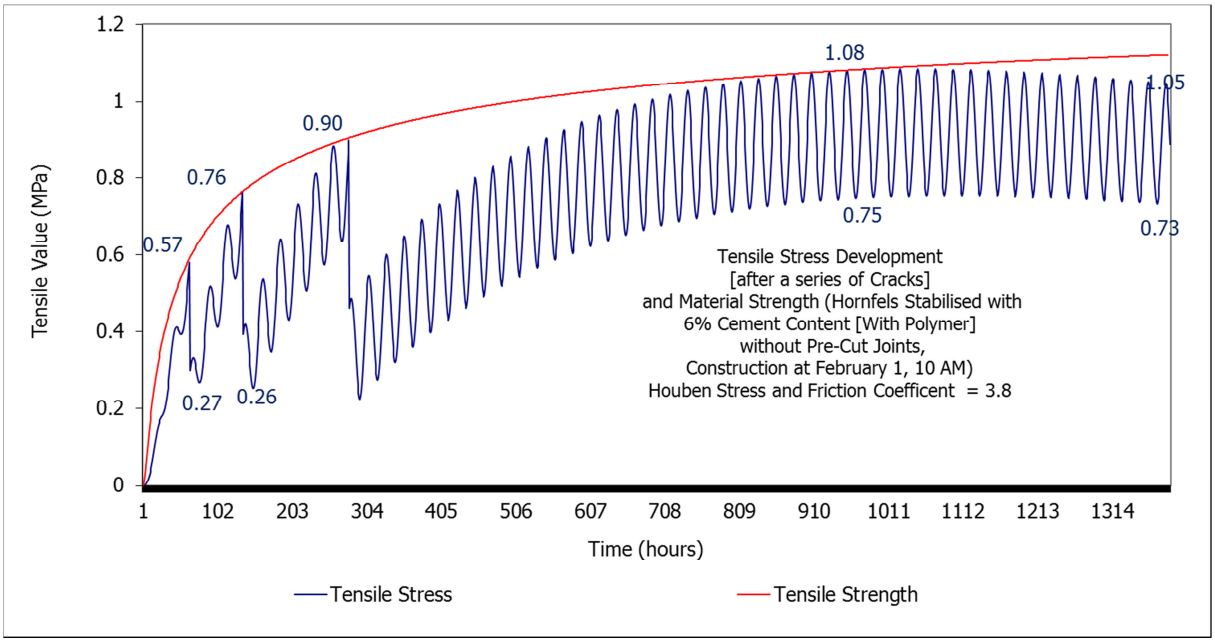

Figure 7-26 Maximum Tensile Stress and Material Strength [Stress Reduction for the First Two Months after Construction of the Hornfels Mix with 6.0% Cement Content and Polymer]

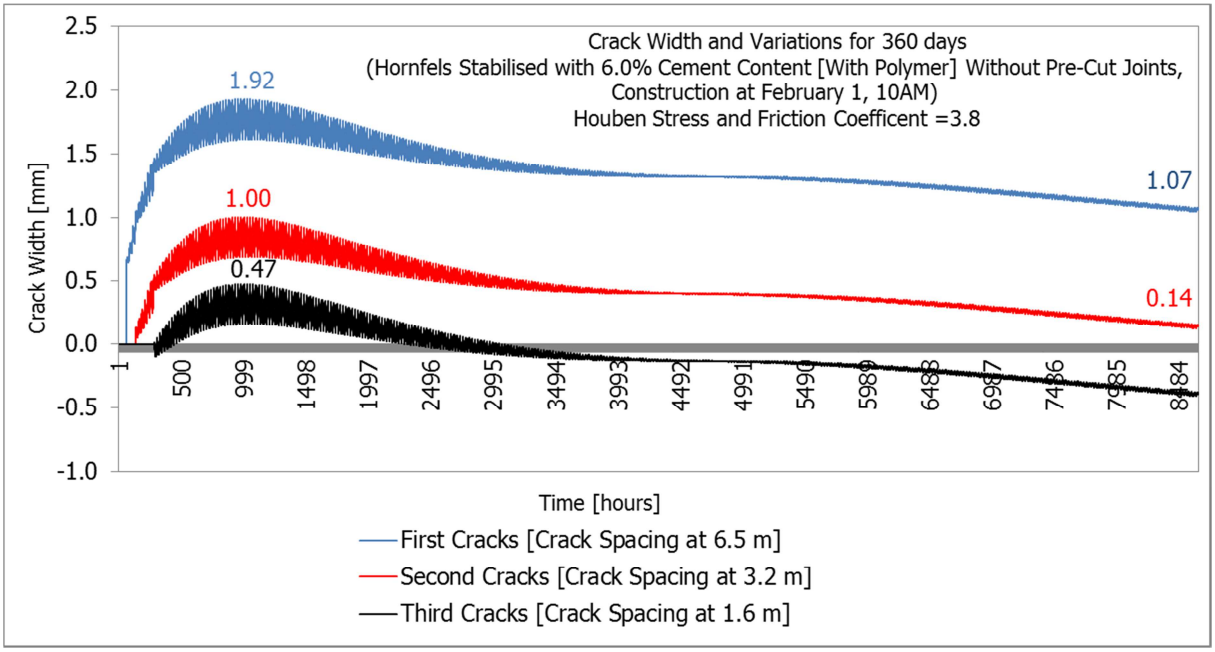

Figure 7-27 Appearance of Cracks Series and Maximum Crack Width [Hornfels Mix with 6.0% Cement Content and Polymer]

Seasonal changes influence shrinkage crack width. Maximum crack width occurs one to two months after construction of the stabilised layer. One would expect the largest crack width in the winter; however, this does not occur because of the influence emanating from the stress relaxation. After the closure of the third cracks, the two cracked layer sections begin to push against each other generating compressive stress in the region of the crack. However, because of the heterogeneity of the stabilised material the effects leading to compressive stress might not necessarily occur. The stabilised layer will integrate along the individual particles relieving the effect of crack space closure. Equally, the effect of warping as exhibited by concrete is dependent on the material homogeneity. Stabilised materials exhibit zones of weakness [due to heterogeneity] around the individual particles. Factors such as cement and moisture content as well as compaction influence particle bond strength and

ultimately the heterogeneity of the stabilised layer. A variation in crack width due to the thermal effect is dependent on the frictional coefficient at the interlayer as well as layer heterogeneity. Particle distribution and bond strength contribute to the heterogeneity of the layer. This influences the tensile stress dissemination and ultimately the crack pattern.

7.5.7 Pre-cutting the Stabilised Layer and Resultant Crack Pattern

Although pre-cutting of the stabilised layers is not a common practice in Southern Africa, from a theoretical perspective its impact in mitigation of shrinkage cracking is considered. For pre-cutting analysis, hornfels mix stabilised at 6.0% cement content with polymer is considered. In this analysis, the objective is to establish the effect of layer pre-cut on the resultant crack pattern. As a result, crack spacing and width following the pre-cutting of the stabilised layer should provide a better load transfer mechanism than the natural crack pattern illustrated in Section 7.3.6.

Pre-cut spacing and depth influence the resultant crack spacing and width. The pre-cutting technique induces the shrinkage cracks to appear in the region of cut. The stabilised layer exhibited initial crack spacing of 6.5 m with a 0.7 mm initial crack width; this forms the basis for the pre-cut spacing and depth. In Figure 7-28, the relationship between pre-cut spacing and depth relative to the thickness of the layer is illustrated. The analysis considered a stabilised layer thickness of 250 mm, Houben relaxation factor and a frictional coefficient of 3.8. The cut width is equal to the width of the saw blade. For the pre-cut analysis, all calculations are similar to the plain stabilised layer apart from the computation of the resultant tensile stress in the region of the pre-cut.

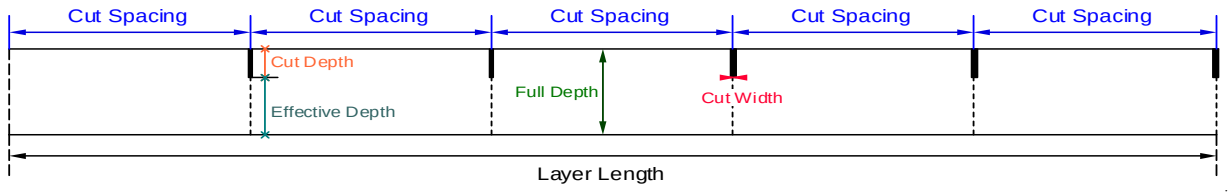

Figure 7-28 Relationship between Cut Spacing and Depth in a Stabilised Pavement Layer

Due to the pre-cut, the resultant tensile stress differs from the uncut layer. It is essential to compute the tensile stress under the cut; Equation 7-49 is applied.

$\sigma_{zs} = \sigma.g$ (MPa) Equation 7-49

Where: σ is the occurring stress in the plain layer and g is a multiplication factor for stress under a cut. For the computation of tensile stress under a cut, Equation 7-50 is applied.

$g = (h/ (h-zs))$ Equation 7-50

Where: h is the layer thickness and zs is the cut-depth; (h-zs) is the thickness under the cut depth [effective depth] in mm

The analysis considered a longer pre-cut spacing assumed at 2.5 m based on the 1.6 m final crack spacing after the third cracks; this helped assess the resultant crack width and spacing as well as established the practical pre-cut spacing for a given cut-depth.

a) 2.5 m Cut Spacing at 10% Cut Depth [250 mm Layer Thickness]:
With 10% cut depth of a 250 mm layer thickness the computed effective depth is 225 mm [g=1.111] at a pre-cut spacing of 2.5 m. Figure 7-29 shows the maximum tensile stress along with the material strength. Figure 7-30 illustrates the crack width with the pre-cut joints. Pre-cutting of the stabilised layer resulted in only two series of cracks with a final spacing of 17.5 m but a large maximum crack width of more than 5.0 mm.

Pre-cutting at 2.5 m spacing and 10% cut-depth, does not provide a practical solution because of the crack width after the first series of cracks. This is more than the crack width obtained under the natural cracking as presented in Figures 7-27 and 7-30. Figure 7-31 details the tensile stress development [stress reduction] after the first and second series of cracks along with strength increase. Figure 7-32 illustrates the two layer conditions with and without pre-cuts along with the final crack spacing and width. [Note: w1, w2 and w3 represent the maximum crack widths of the first, second and third crack respectively].

Pre-cutting at 2.5 m intervals with a cut depth of 10% provides insight regarding the significance of pre-cutting compared to natural cracking [without pre-cut joints]. This first iteration provides longer crack spacing but wider crack width. For the second iteration, an increase of the cut depth from 10% to 20% was undertaken.

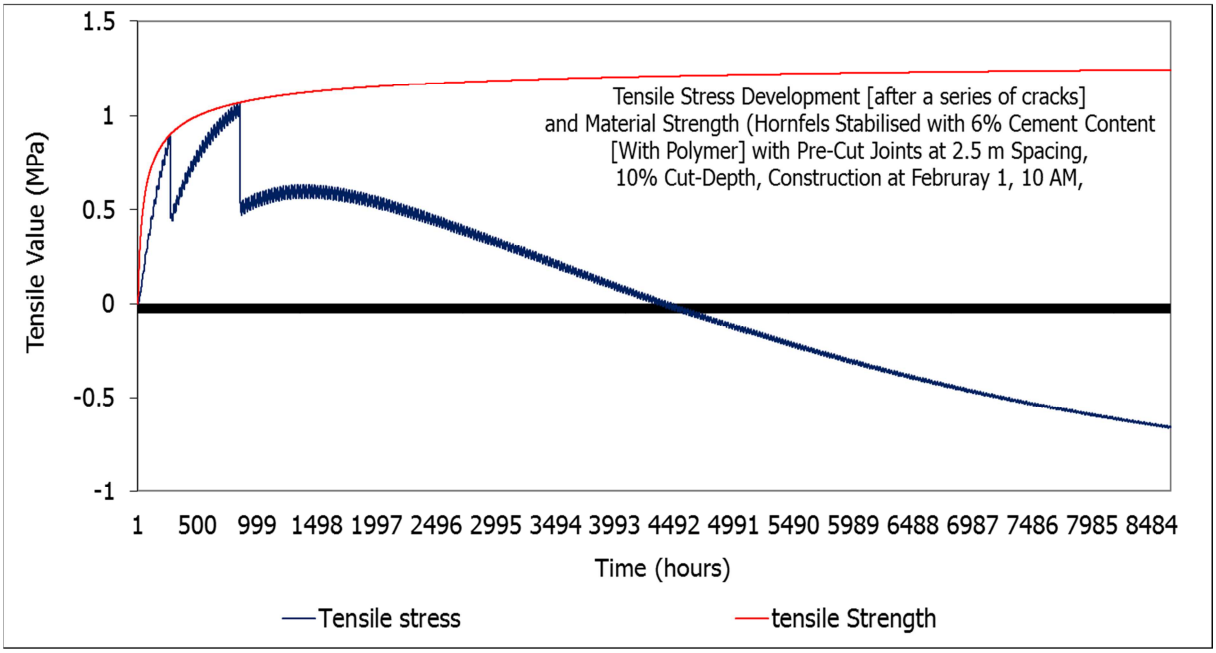

Figure 7-29 Variation in Tensile Stress and Strength at Pre-cut Joints at 2.5 m Spacing and Cut depth of 10% of the Layer Thickness

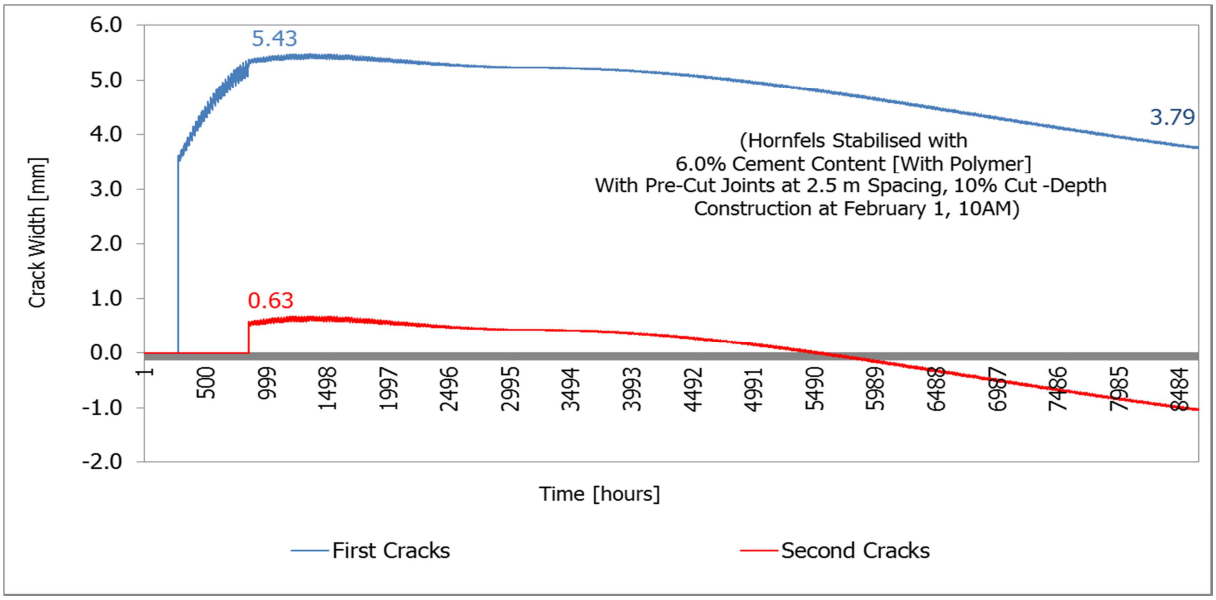

Figure 7-30 Variation in Crack Width at Pre-cut Joints at 2.5 m Spacing and Cut depth of 10% of the Layer Thickness

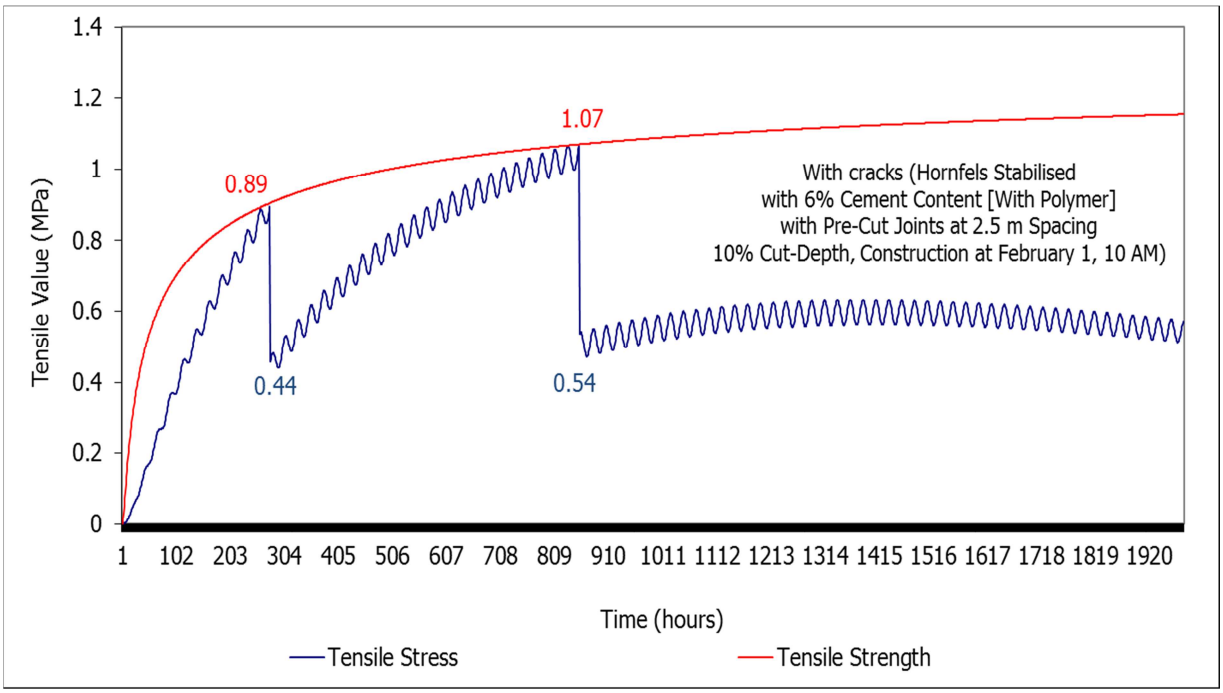

Figure 7-31 A Detailed Variation in Tensile Stress and Strength at Pre-cut Joints at 2.5 m Spacing and Cut depth of 10% of the Layer Thickness

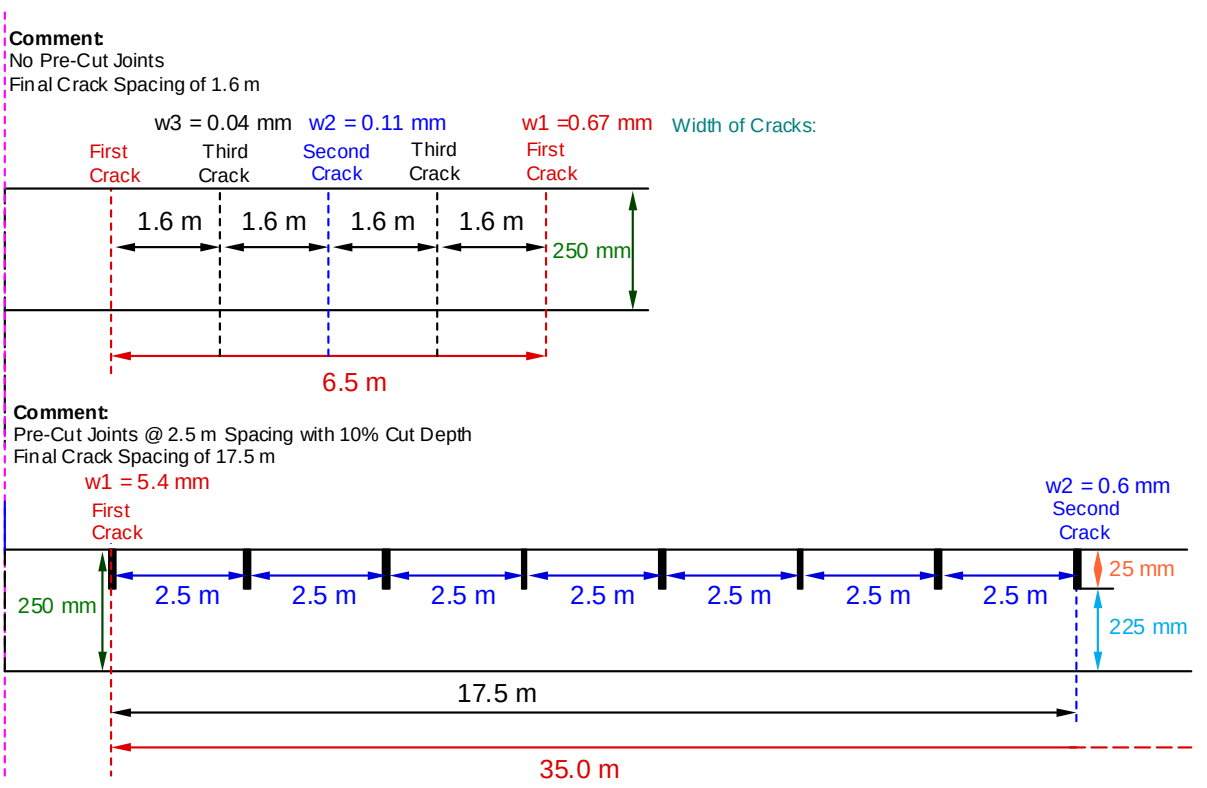

Figure 7-32 Stabilised Layers With and Without Pre-Cuts [2.5 m Cut Spacing at 10% Cut-Depth]

b) 2.5 m Cut Spacing at 20% Cut Depth [250 mm Layer Thickness]:

By increasing the cut-depth, the effective depth becomes 200 mm, which influences the crack propagation trends. With a 20% cut-depth, the final crack spacing was 12.5 m with a mid-cracked section of 2.5 m between the long layer sections. Similar to the 10% cut-depth, two crack series appeared but with a different crack pattern. The second cracks appeared

along the pre-cut joints. The occurring stress at the cuts influences the manifestation of the second cracks to appear at the cuts. Figure 7-33 illustrates the effect of pre-cutting at 2.5 m spacing with a cut depth of 20%. Even though the maximum crack width is slightly reduced to approximately 4.5 mm, following an increase in cut depth by 10% of the layer thickness, this still results in a poor load transfer.

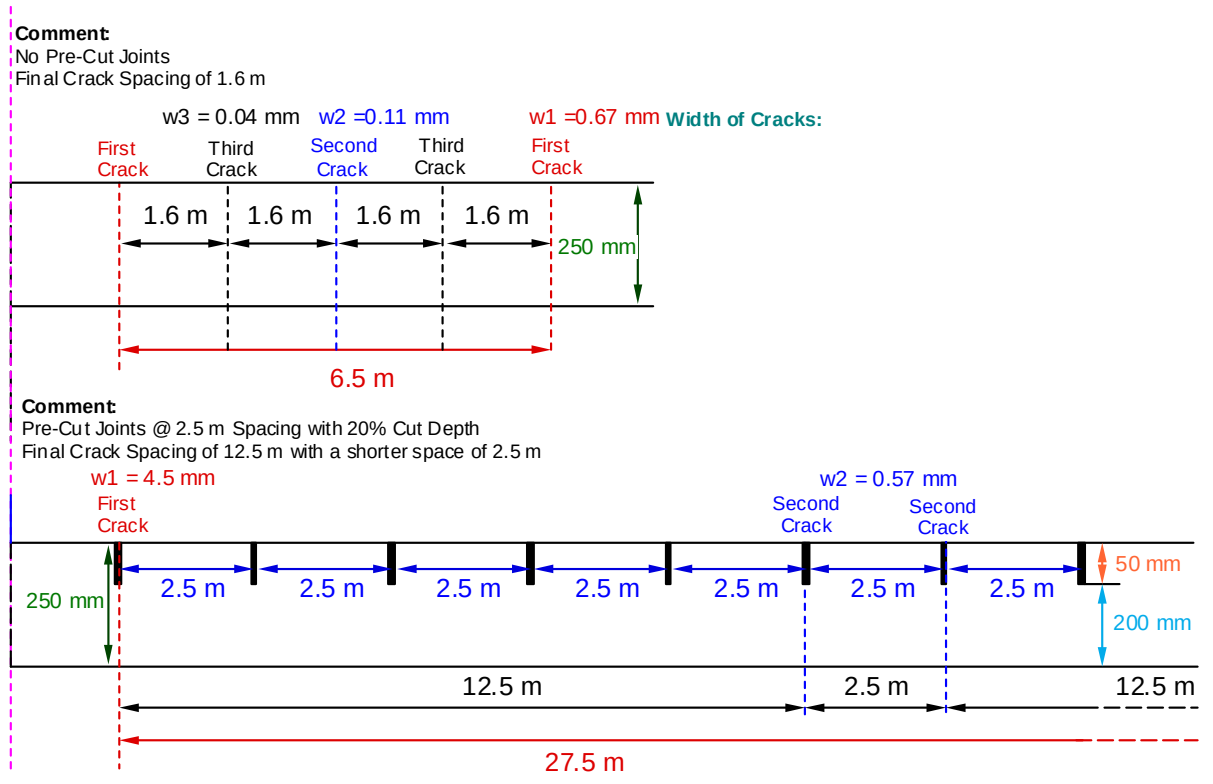

Figure 7-33 Stabilised Layers With and Without Pre-Cuts [2.5 m Cut Spacing at 20.0% Cut Depth]

c) 2.5 m Cut Spacing at 30% Cut Depth [250 mm Layer Thickness]:
When increasing the cut depth to 30% of the layer thickness, the final crack spacing is 10 m with the second cracks located at the cuts as illustrated by Figure 7-34. The maximum crack width after the first cracks is 5.6 mm with a spacing of 22.5 m. After the second cracks, the maximum crack width is 0.89 mm with a spacing of 10.0 m – 2.5 m – 10.0 m. For the second crack series, two narrower cracks occur simultaneously instead of one wider crack. Although the width of the second series of cracks is narrower, the width of the first cracks is 3.6 mm.

d) 2.5 m Cut Spacing at 40% Cut Depth [250 mm Layer Thickness]:
With a cut depth of 40% of the layer thickness, the final crack spacing is 7.5 m with second cracks located at the cuts as illustrated by Figure 7-35. The initial crack width was narrower than that obtained with a cut depth of 30%. Figure 7-36 illustrates the practical pre-cut spacing for specific cut depth whereby final crack spacing is equal to pre-cut spacing. Figure 7-37 shows cut depth and final crack spacing. Using the regression equation with R –square value of 0.93 a readjustment of the pre-cut spacing at a cut depth of 20% is realised.

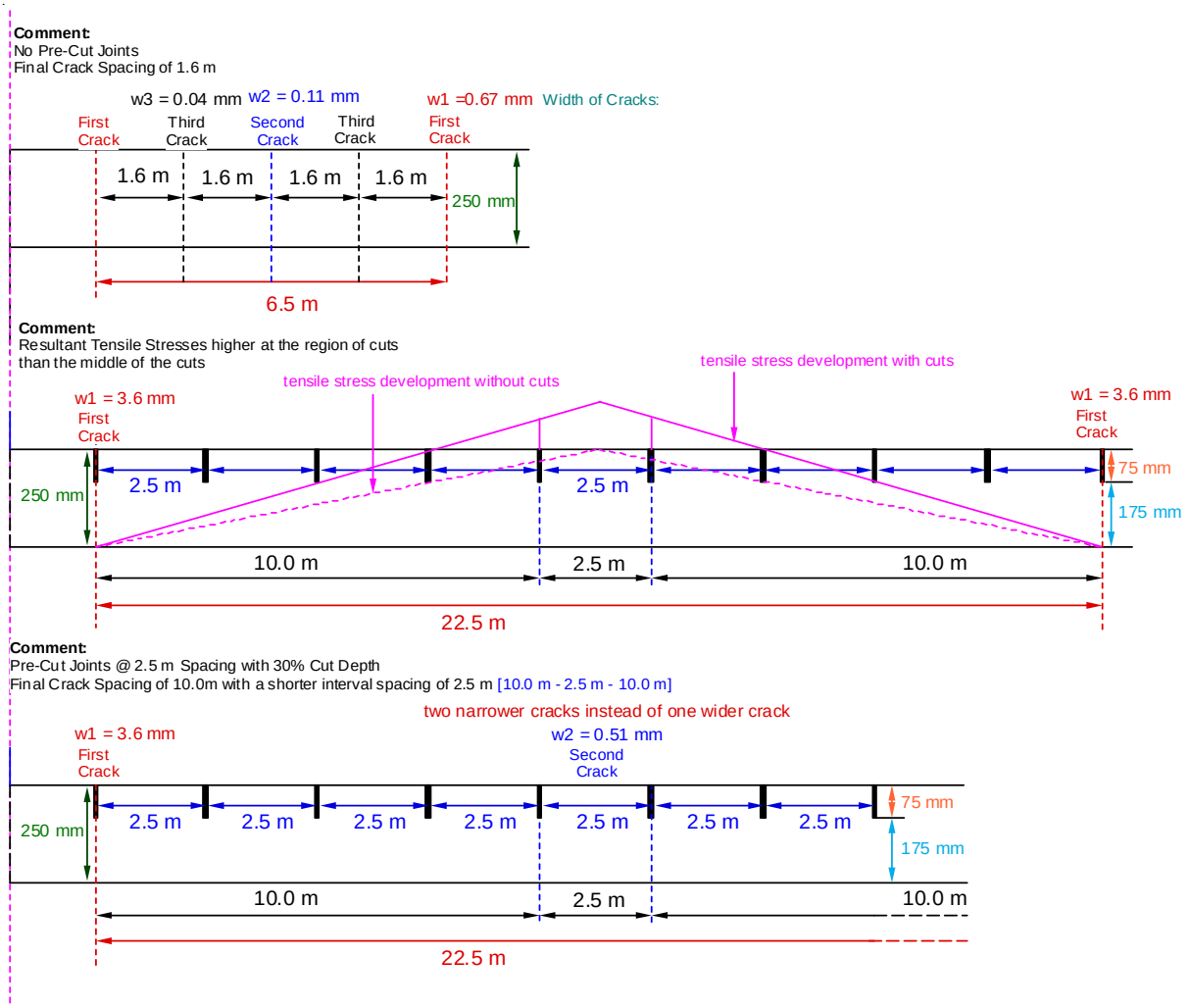

Figure 7-34 Stabilised Layers With and Without Pre-Cuts [2.5-m Cut Spacing at 30.0% Cut Depth]

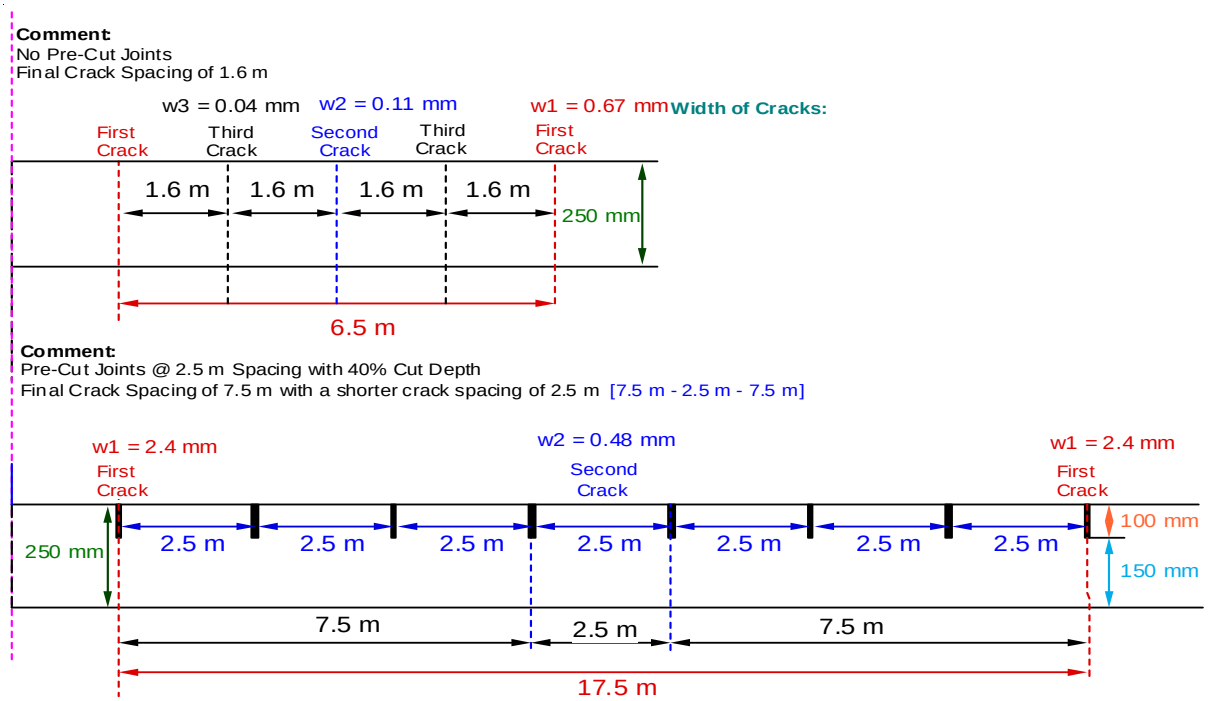

Figure 7-35 Stabilised Layers With and Without Pre-Cuts [2.5-m Cut Spacing at 40.0% Cut Depth]

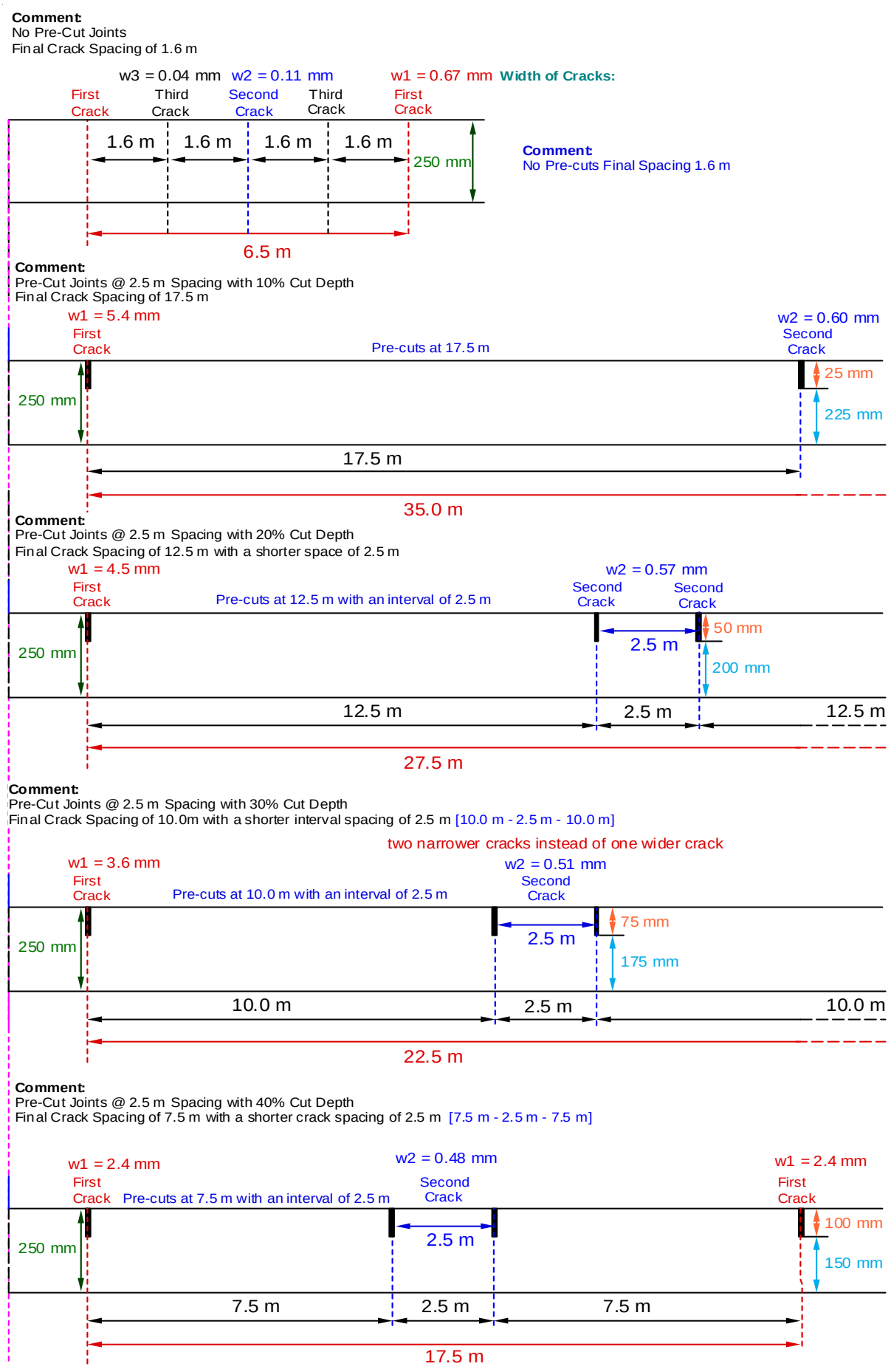

Figure 7-36 No Pre-Cut Joints versus Pre-Cut Joints

Figure 7-36 compares the option of pre-cutting the stabilised layer or not. By not pre-cutting the stabilised layer, the crack spacing is shorter and is comprised of three series of cracks. By pre-cutting the same layer at longer pre-cut spacing than the reference (without pre-cuts), only two crack series appear however the initial cracks are wider.

Note: For same material type, the resultant stresses at longer pre-cut spacing are usually higher than at shorter pre-cut spacing. As a result, the initial crack width (critical crack width) at longer pre-spacing is wider than at shorter pre-cut spacing.

Figure 7-36 offers insight regarding the effect of the pre-cut joints versus natural cracking [no pre-cut joints]. Additionally, the influence of cracking [pre-cut] spacing and crack width is realised. By increasing the pre-cut spacing [i.e. spacing between the joints] wider crack width result. The practical choice between pre-cutting and no pre-cutting must be undertaken with a good understanding of the initial crack width (critical crack width).

Table 7-7a lists the crack pattern details along with the cut depth, crack spacing and width. For practical crack spacing for the 20% pre-cut depth is 13.25 m [i.e. 12.5 -2.5-12.5], 30% is 11.25 m [10.0-2.5-10.0] and 8.75 m [7.5-2.5-7.5] as illustrated in Figure 7-37 and listed in Table 7-7b. Figure 7-38 illustrates the influence of cut depth on the width of first and second cracks. Increasing the cut depth reduces the pre-cut spacing and resultant crack width.

Table 7-7a Effect of Cut Depth on the Crack Pattern [Pre-cut Spacing 2.5 m]

		Hornfels Mix 6%	Cement Content	0.72% Polymer	Content		
Pre-Cut Spacing	of 2.5 m	Houben Stress Relaxation		At the Day	At the Day	At 360	At 360
Pre-Cut Depth [%]	Type of Cracks	Crack Spacing [m]	Crack Width [mm]	Maximum Crack Width [mm]	Minimum Crack Width [mm]	Maximum Crack Width [mm]	Minimum Crack Width [mm]
10%	First	35.0	5.4	5.56	5.30	4.07	4.05
	Second	17.5	0.60	0.76	0.60	-0.70	-0.73
20%	First	27.5	4.50	7.20	7.06	5.99	5.98
	Second	12.5-2.5-12.5	0.57	1.22	1.08	0.01	-0.01
30%	First	22.5	3.60	5.75	5.60	4.89	4.86
	Second	10.0-2.5-10.0	0.51	1.63	1.02	0.77	0.75
40%	First	17.5	2.44	5.23	5.05	3.70	3.70
	Second	7.5-2.5-7.5	0.48	1.76	1.59	0.84	0.82

Table 7-7b Uniform Crack Spacings [Practical Pre-cut Spacing]

		Hornfels Mix 6%	Cement Content	0.72% Polymer	Content		
Pre-Cut Spacing	[Practical]	Houben Stress Relaxation		At the Day	At the Day	At 360	At 360
Pre-Cut Depth [%]	Type of Cracks	Crack Spacing [m]	Crack Width [mm]	Maximum Crack Width [mm]	Minimum Crack Width [mm]	Maximum Crack Width [mm]	Minimum Crack Width [mm]
10%	First	35.0	5.4	5.56	5.30	4.07	4.05
	Second	17.5	0.76	0.76	0.60	-0.73	-0.70
20%	First	29.2	5.00	7.42	7.20	6.03	5.90
	Second	13.50	0.85	1.80	1.30	0.10	0.09
30%	First	23.8	3.80	6.02	5.80	5.54	5.50
	Second	11.25	0.73	2.02	1.60	0.97	0.96
40%	First	19.3	2.70	5.80	5.70	3.90	3.88
	Second	8.75	0.53	2.10	2.00	0.96	0.91

With a cut depth of 10% of the layer thickness, the crack width of the first series of cracks is large and positioned at a wider spacing. This is likely to lead to poor load transfer depending on the level of traffic. With a cut depth of 20%, a reduction in crack width results. The second series of cracks appear at the cuts and exhibit narrow crack width. However, the interval of 2.5 m between the 12.5 m spacing is quite tedious to realise in the field. This also applies to the 30% and 40% cut depths.

A practical cut depth must not involve different cut spacings or depths, as this is not only tedious to the executor but also unrealistic to achieve. The specified cut spacing and depth should be practically identical that is having one cut depth for a specific pre-cut spacing. With a cut depth of 20%, a spacing 13.75 m is feasible. However, a balance between feasible pre-cut spacing and resultant crack width is essential. This is because a wide crack will lead to poor load transfer, despite the final crack spacing. Figure 7-38 shows that with a cut depth of 35%, the widths of the first and second cracks are 3.0 mm and 0.5 mm respectively at a pre-cut spacing of about 10 m. With a 40% cut depth at a cut spacing of 7.5 m with an interval of 2.5 m, a crack width of less than 3.0 mm is registered.

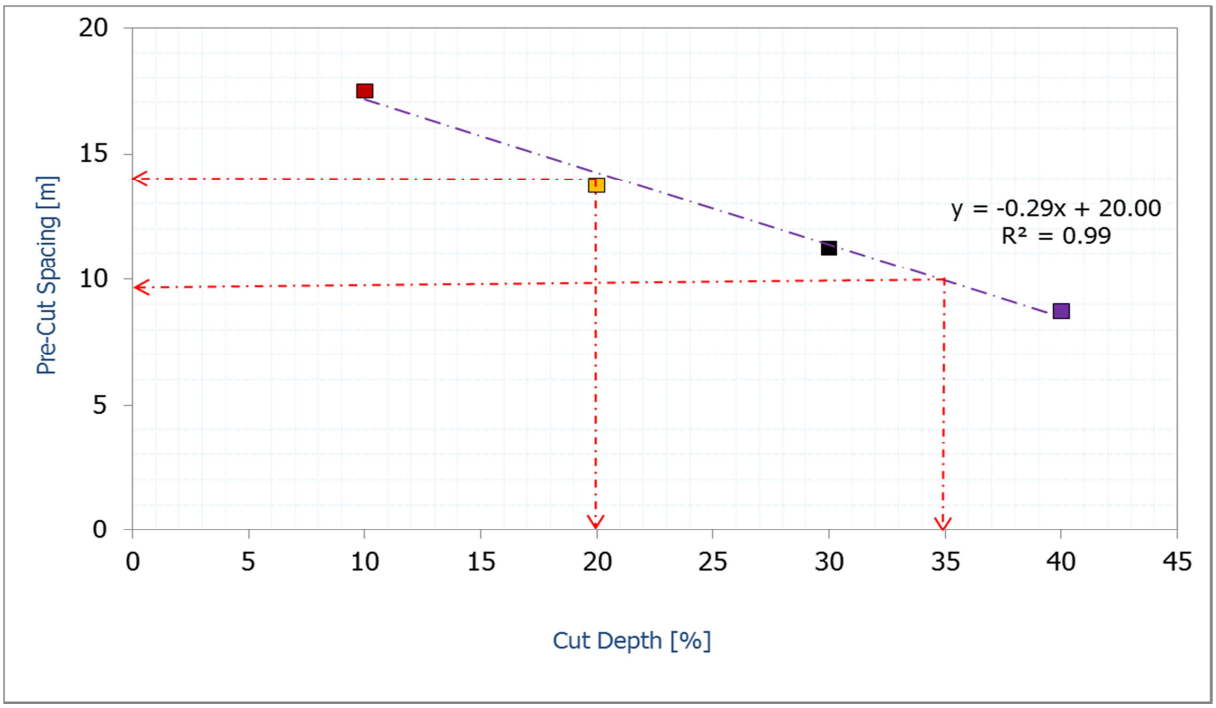

Figure 7-37 Relationship of Cut Depth and Pre-Cut Spacing [Final Crack Spacing]

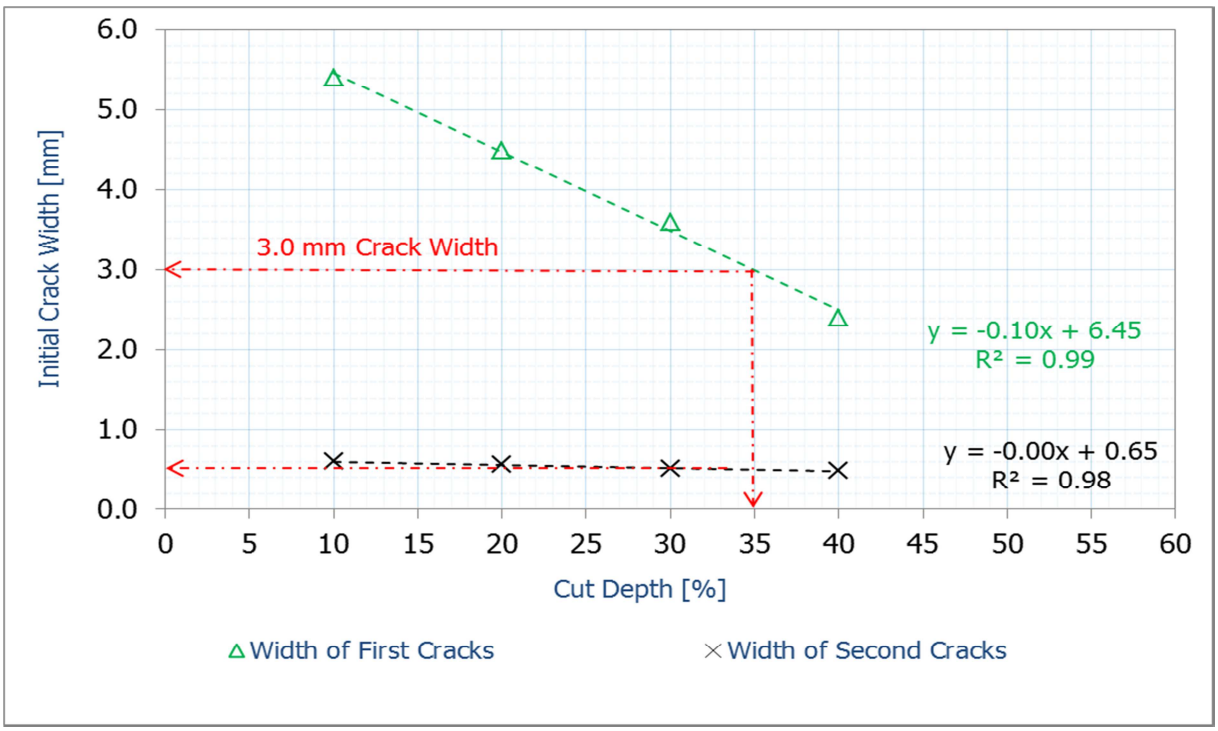

Figure 7-38 Effect of Cut Depth on the Initial Width of Cracks

Figure 7-39 shows the maximum crack width of the first and second cracks. At the cut depths of 20%, 30% and 40% the second cracks appeared at the cuts. With a cut depth of 35%, the width of first cracks is lesser than 3.0 mm. However, the maximum crack width of the first series of cracks is more than 5.0 mm. The trends shown in Figures 7-38 and 7-39 indicate that for a specific pre-cut spacing there is an optimum cut depth. By increasing the cut depth, a reduction in the initial crack width result. However, this does not suggest a reduction in the maximum crack width. Other factors influence the characteristics the crack pattern particularly the width. For instance, if the cracks appear at the cuts or not will significantly influence the resultant crack width.

For the estimation of the pre-cut spacing and crack width beyond the analysis ranges, the regression equations in Figures 7-37 and 7-38 are applicable. The modelling using a pre-cut spacing of 2.0 m and 3.0 m was also undertaken. Pre-cut spacing of 2.0 m did not provide a feasible option as cracks appeared alongside the cuts as well as between them. This resulted in a final crack spacing of 1.0 m, which is lower than that obtained without pre-cutting the stabilised layer. As a result, no further analysis was undertaken. Pre-cutting at 3.0 m spacing provided the following:

a) at a cut depth of 10% a few cracks appeared alongside the cuts and others outside
b) 20% cut depth resulted in more cracks appearing alongside the cuts
c) 30% cut depth many more cracks appeared alongside the cuts

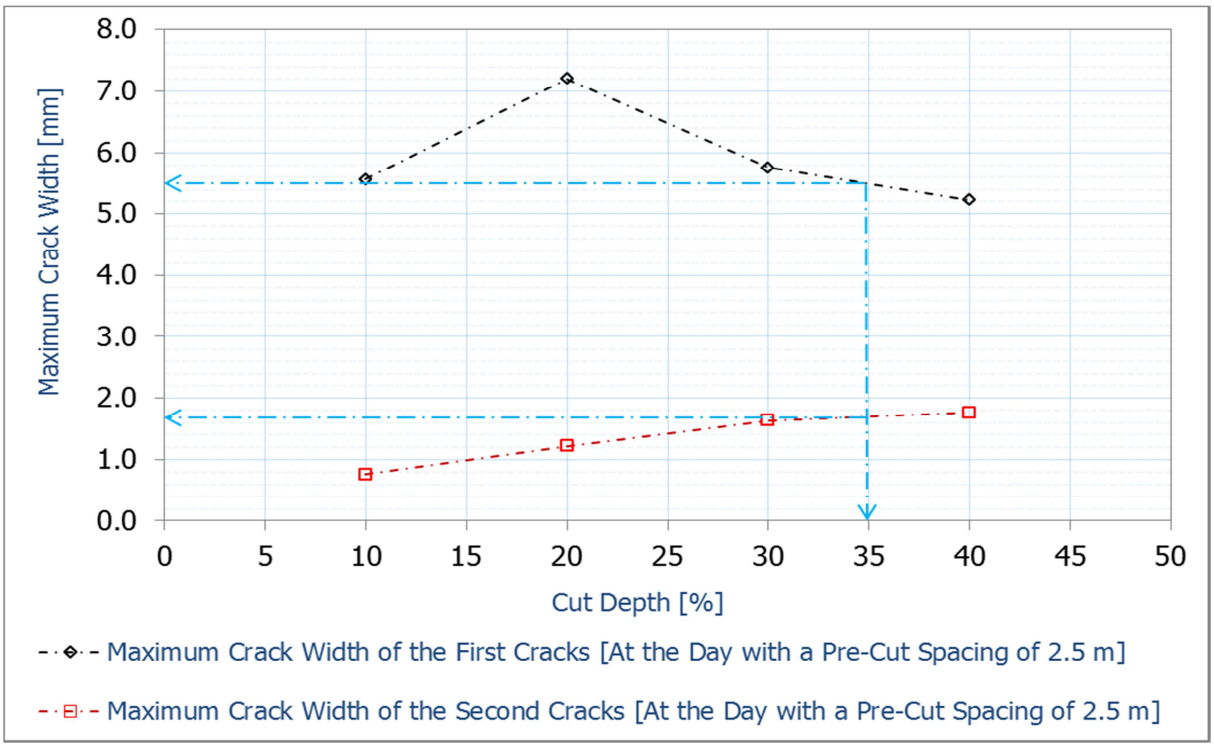

Figure 7-39 Effect of Cut Depth on the Maximum Crack Width of First and Second Crack Series

The underlying principle for using the pre-cutting technique to is to introduce grooves in order to provide a desirable crack pattern within the stabilised layer. This suggests that the cut depth and pre-cutting spacing must provide a minimal crack width. Viewed differently, the objective of the pre-cutting technique is to prevent the occurrence of occasional but relatively wide and damaging natural cracks. Therefore, selecting a wide pre-cutting spacing does not usually provide a desirable crack width.

A cut depth of 20% at a pre-cut spacing of 13.75 m [14.0 m] provides an initial crack width of 4.5 mm. In order to obtain a crack width of less than 3.0 mm a cut depth of 35 % is required. A cut depth of 35% provides a final spacing [pre-cut spacing] less than 10.0 m. The primary objective of pre-cutting a stabilised layer is not only to reduce the frequency of cracks but also to result in a suitable crack pattern particularly realising minimal crack width. A desirable crack pattern refers to achieving practical crack spacing with a suitable crack width that does not result in a poor load transfer.

A shrinkage crack width of less than 3.0 mm, does not usually result in poor load transfer since some degree of aggregate interlock exists at the interface of the crack. Aggregate interlock improves to an acceptable degree the performance of the pre-cut sections. However, the occurrence of wide cracks diminishes its effectiveness in realising some degree of load transfer at the crack interface. This proposes that the pre-cut spacing relative to the cut depth should result in minimal crack width. However to achieve aggregate interlock within the stabilised layer particularly at the zone of pre-cuts and cracks a suitable grading [particle distribution] must be followed. To achieve a minimal crack width of less than 3.0 mm at a feasible pre-cut spacing, a cut depth of 35% or more is required. This observation suggests that for minimal crack width a short pre-cut spacing is preferred. However, a suitable cut depth is necessary.

7.5.8 Influence of Interlayer Frictional Coefficient

Throughout the analysis, a frictional coefficient of 3.8 is applied. In order to analyse the effect of interlayer friction the 3.8 coefficient is varied:

a) multiplying 3.8 by 2 a frictional coefficient of 7.6
b) considering half of 3.8 for a frictional coefficient of 1.9

This part of the analysis considers a stabilised layer with pre-cut joints specifically a cut depth of 30% in order to continue with the practical approach as established in Section 7.3.5. Figures 7-40 to 7-42 show the variation of the frictional coefficient on the layer crack width using the Houben stress relaxation.

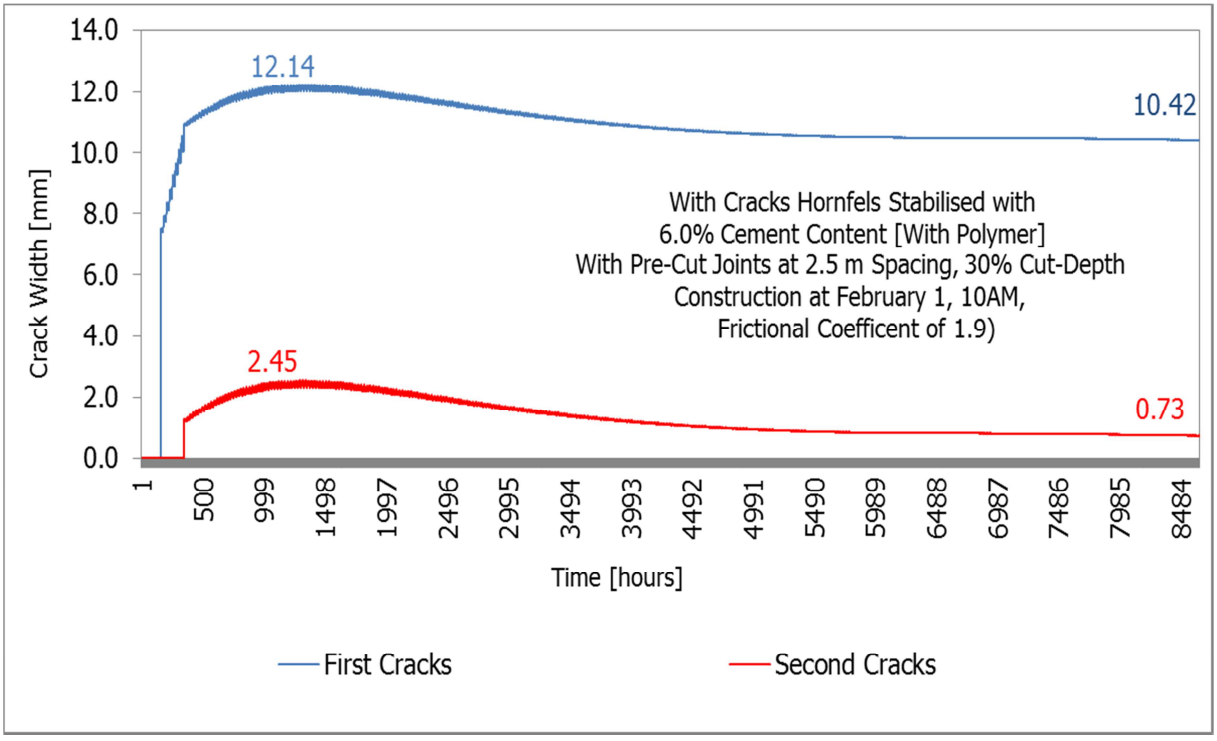

Figure 7-40 Variation of Crack Width at a Frictional Coefficient of 1.9 and Houben Stress Relaxation

The figures illustrate that increasing the frictional coefficient at the interlayer results in a reduction in layer crack width. Table 7-8 summarises the influence of the frictional coefficient on the layer crack width. Table 7-8 lists the following important aspects:

a) initial crack width [width of first cracks]
b) maximum crack width
c) crack width at the end of 360 days

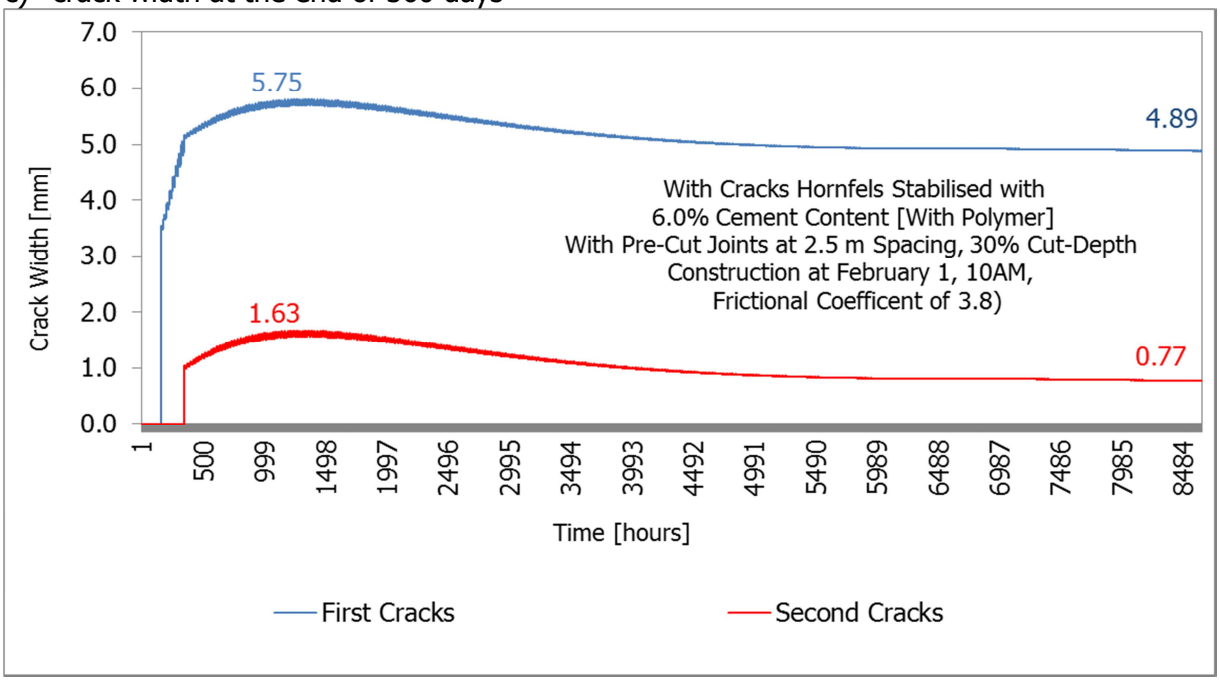

Figure 7-41 Variation of Crack Width at a Frictional Coefficient of 3.8 and Houben Stress Relaxation

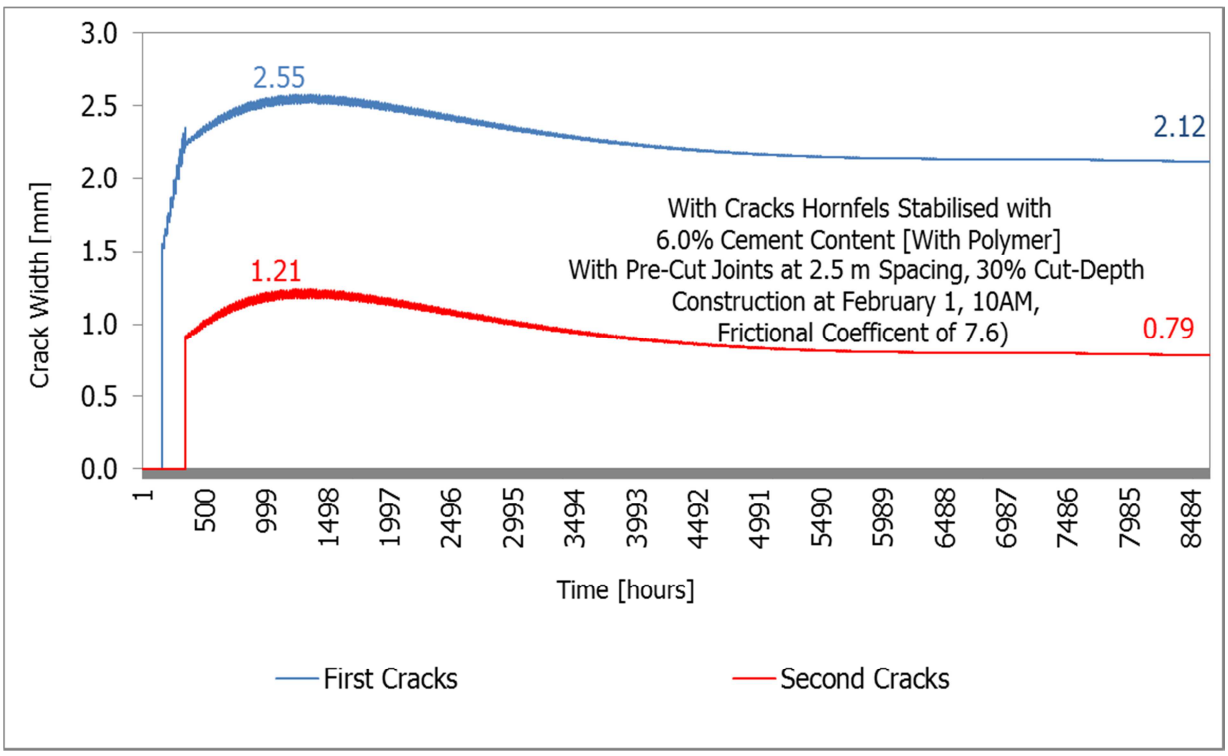

Figure 7-42 Variation of Crack Width at a Frictional Coefficient of 7.6 and Houben Stress Relaxation

Table 7-8 Summary of the Influence of the Frictional Coefficient on Crack Width

Hornfels Mix	6% Cement Content	With Polymer	Houben Stress Relaxation	
Frictional Coefficient	Type of Cracks	Initial Crack Width [mm]	Maximum Crack Width [mm] [Critical Situation]	Maximum Crack Width after 1 year [mm]
1.9	First Cracks	7.07	12.14	10.42
	Second Cracks	1.01	2.45	0.73
3.8	First Cracks	3.63	5.75	4.89
	Second Cracks	0.51	1.63	0.77
7.6	First Cracks	1.50	2.55	2.12
	Second Cracks	0.97	1.21	0.79

Figure 7-43 illustrates the influence of the frictional coefficient on the width of the cracks. Interlayer friction influences the resultant crack pattern. Friction is dependent on the bonding at the interlayer. A decrease in the restraint between the two layers results in layer free movement as a response to moisture loss and temperature changes.

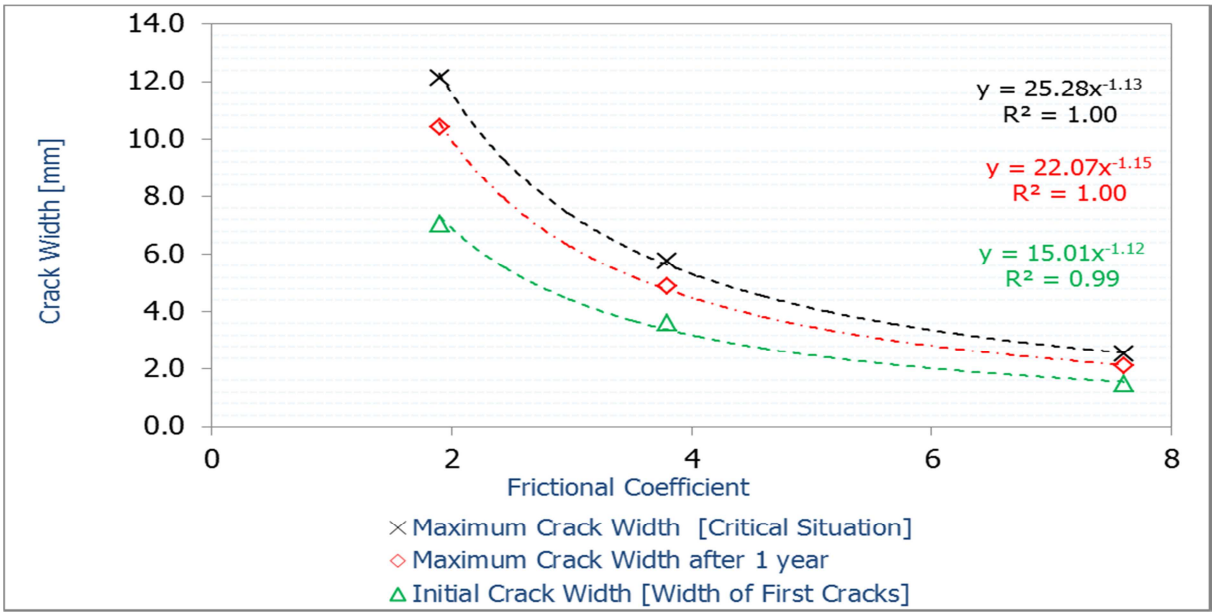

Figure 7-43 Influence of Frictional Coefficient on the Width of the First Cracks

Interlayer friction is a restraint that contributes to the cracking of the stabilised layer and has a significant influence on the resultant crack pattern. The relationship between the frictional coefficient and the width of the first cracks relates to the durability of the layer. At a low frictional coefficient, the width of the first cracks is wider than that obtained with a high coefficient. Equally, the maximum crack width for the critical situation is wider while using a lower frictional coefficient compared to a high. The regression equations model the influence of the frictional coefficient on the crack width. Using a polynomial regression, R-squared values of 1.0 are registered. This regression shows that the relationship of the interlayer friction or bonding to crack width is a nonlinear relationship, which suggests that there are other influential factors.

The material heterogeneity and pore structure of the stabilised layer influence the crack width characteristics and the friction at the interlayer. The presence of weak zones within the material matrix usually results in areas for crack propagation as the layer relieves the induced stresses. These weak zones are usually due to the heterogeneity of the materials as well as the interconnectivity of the pores [pore structure]. Depending on the friction at the interlayer, the resultant crack width will vary. The regression equations and trend lines indicate influence of low and high frictional coefficients on the crack width. The regression equations suggest that with high frictional coefficients reduced crack width result. Figure 7-44 illustrates the influence of frictional coefficient on the pre-cut spacing.

A reduction in crack spacing results due to increase in frictional coefficient at the interlayer. The frictional coefficient influences the crack spacing and width [crack pattern]. The observations in Figure 7-43 and 7-44 suggest that increasing the frictional coefficient [interlayer bonding] reduces the crack width and pre-cut spacing. This shows that the interlayer bonding between the stabilised and underneath layer has a significant influence on the shrinkage crack pattern. A reduction of interlayer bonding lessens the degree of friction restraint imposed on the stabilised layer. This leads to the stabilised layer to move as it constricts. The movement of the stabilised layer as it constricts leads to the manifestation of wide cracks at longer spacing.

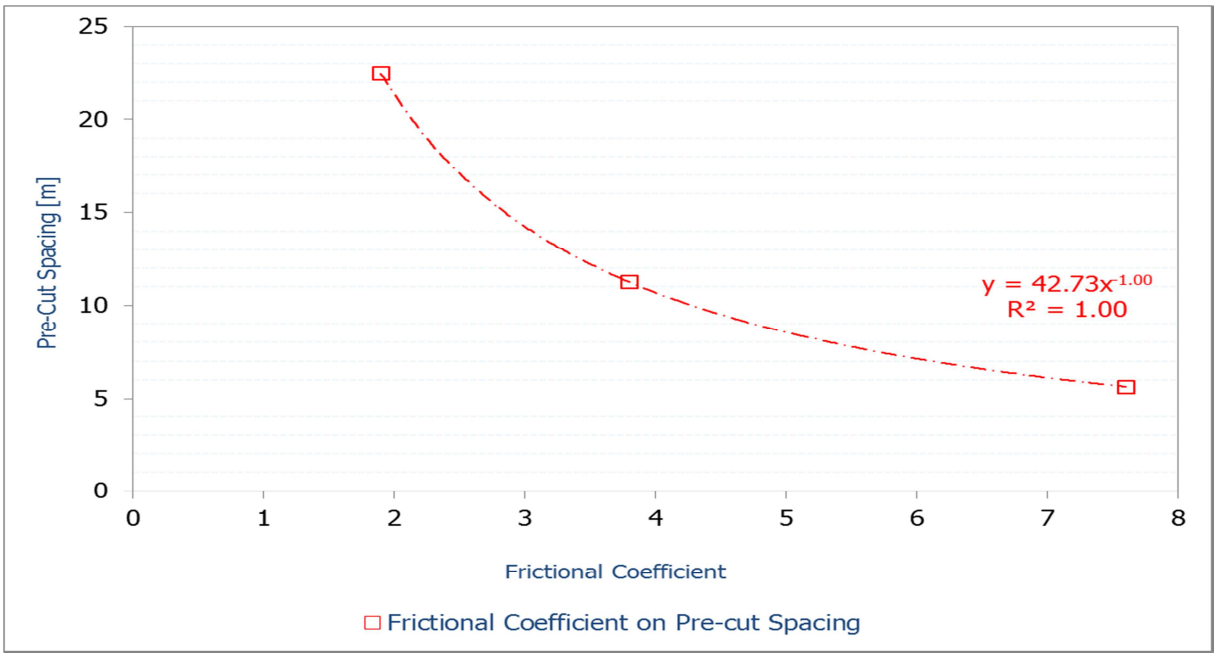

Figure 7-44 Effect of Frictional Coefficient on the Pre-cut Spacing

As the stabilised layer loses moisture, the layer particles move closer together, resulting in shrinkage as a response to moisture loss from the material matrix. Bearing in mind the exposure of the stabilised layer to air and ultra-violet rays while the underlying layer is sealed off, suggests that the rate of shrinkage between the two layers is different. As the stabilised layer dries, its tendency to shrink is higher than its underlying layer. When the layer shrinks, the constituent particles come closer together. The underlying layer retards free movement by acting as a restraint to the stabilised layer. Depending on the level of bonding at the interlayer [or interlayer friction], the tendency of the stabilised layer to shrink freely in response to the loss of moisture will vary. A higher restraint at the interlayer results in restricted movement and cracks will emerge at shorter spacing with reduced width. The layer cracks in order to relieve developed stress. The ability to relieve the induced tensile stress over the layer length is dependent on its ability to constrict relative to restraint at the interlayer.

A reduced frictional coefficient [low bonding at the interlayer] suggests that the layer moves freely and thus, wider cracks at increased spacing emerge. An increased frictional coefficient [high bonding at the interlayer] implies that layer movement is restrained. This suggests that because of the layer restriction to freely move, relieving of the stress takes place at short spacing resulting in small crack width.

Figure 7-45 conceptualises the interlayer friction or bonding and the resultant crack pattern. The concept of crack width and aggregate interlock is also illustrated. As the stabilised layer constricts in response to the induced tensile stresses, the degree of bonding at the interlayer dictates the resultant crack pattern. On a practical basis, ensuring the layers are well

bonded, the resultant crack width is minimised. This further suggests that without adequate interlayer bonding the shrinkage of the stabilised layer results in a large crack width at increased spacing.

Wide cracks are detrimental to the pavement layer. Control of shrinkage embodies the philosophy of ensuring that numerous fine cracks result at short spacing rather than wide cracks at larger spacing. Unfavourable load conditions accompanied with wide cracks may result in premature distress, which decreases the service life of the pavement structure. Scarifying the top of the underlying layer to provide a rough surface might increase the interlayer bonding. However, the compaction technique used also influences the resultant interlayer bonding.

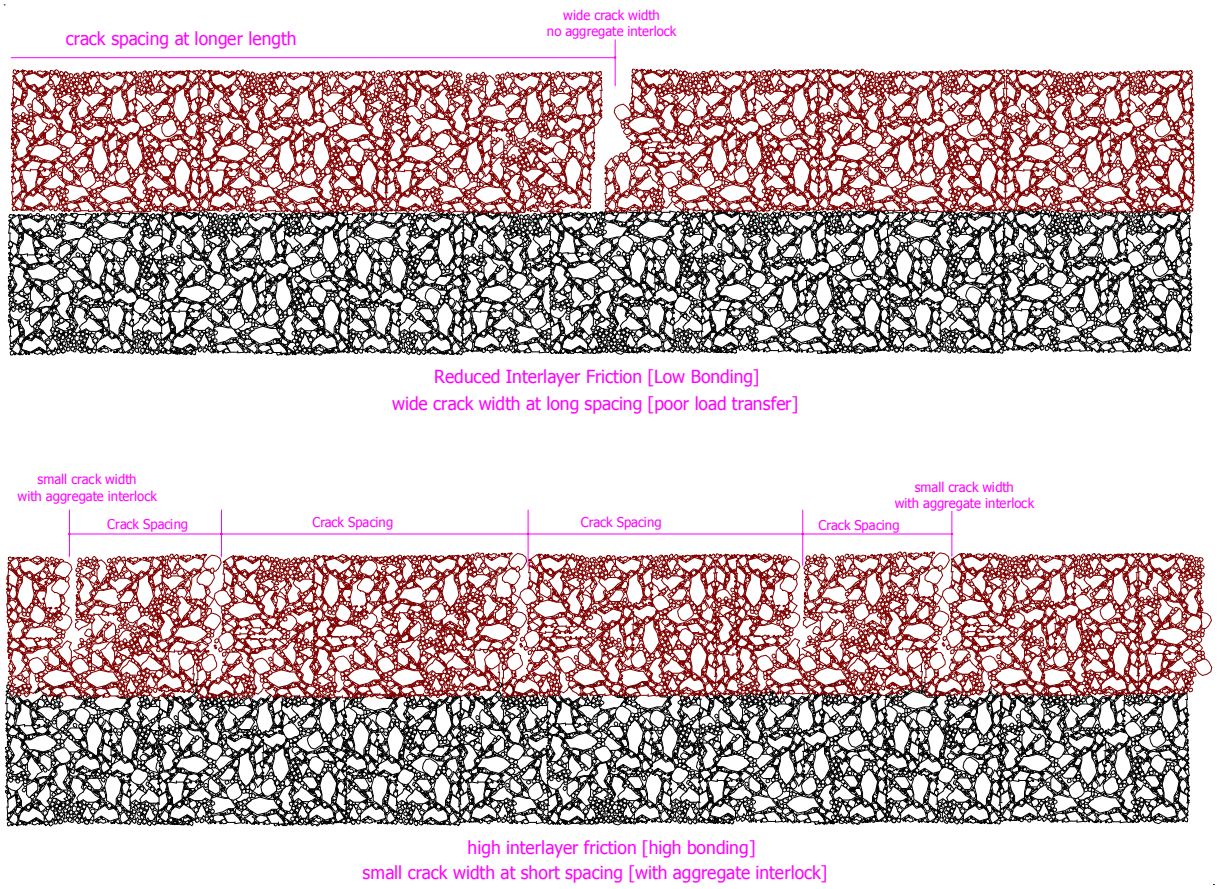

Figure 7-45 Conceptualisations of the Interlayer Bonding and Resultant Crack Pattern

7.5.9 Effect of the Stress Relaxation Factor

Stress relaxation relates to the behavioural response of a material to relieving stress imposed at a constant strain. In this analysis, the Houben stress relaxation function was used to assess the response of stabilised material in relieving the tensile stress under given restraints and conditions. Stress relaxation is the inverse of creep. Creep is a time dependent deformation due to induced stress. Figure 7-46 illustrates how each stress relaxation function computes the occurring stress. Figures 7-47 to 7-54 illustrate the Xuan stress relaxation that is the high, low and average types along with the tensile strength increase with and without cracks. The manifestation of cracks results in a stress reduction.

With the Xuan high stress relaxation, no cracks manifest because the occurring stress is lower than the layer tensile strength. Figure 7-47 and 7-48 detail the occurring stress and tensile strength increase for a year and the first 90 days [three months] after construction. Xuan low and average stress relaxation show that cracking occurs within the stabilised layer.

Figures 7-51 and 7-54 illustrate stress reduction that takes place following a series of cracks. Xuan stress relaxation functions assume that the occurring stress within the stabilised layer develop, reaching a maximum whereby they show about a constant variation with time.

The stress relaxation factor influences the trend and development of the tensile stress [stress behavioural trend] and ultimately the crack pattern of the stabilised layer. Figure 7-46 and Figure 7-12 characterise the effect of stress relaxation on the resultant stress and crack pattern. A comparison based on the Xuan functions show that applying a high stress relaxation factor not only affects the stress development but also the crack pattern.

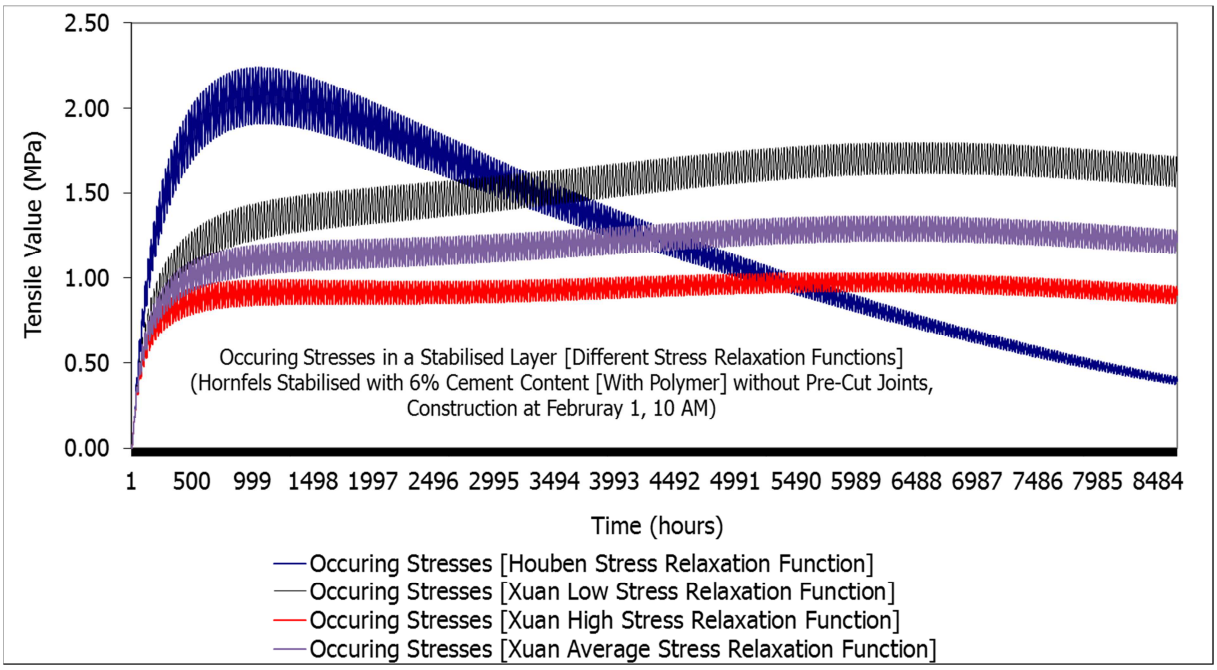

Figure 7-46 Stress Relaxation Functions and Occurring Stresses within the Stabilised Layer

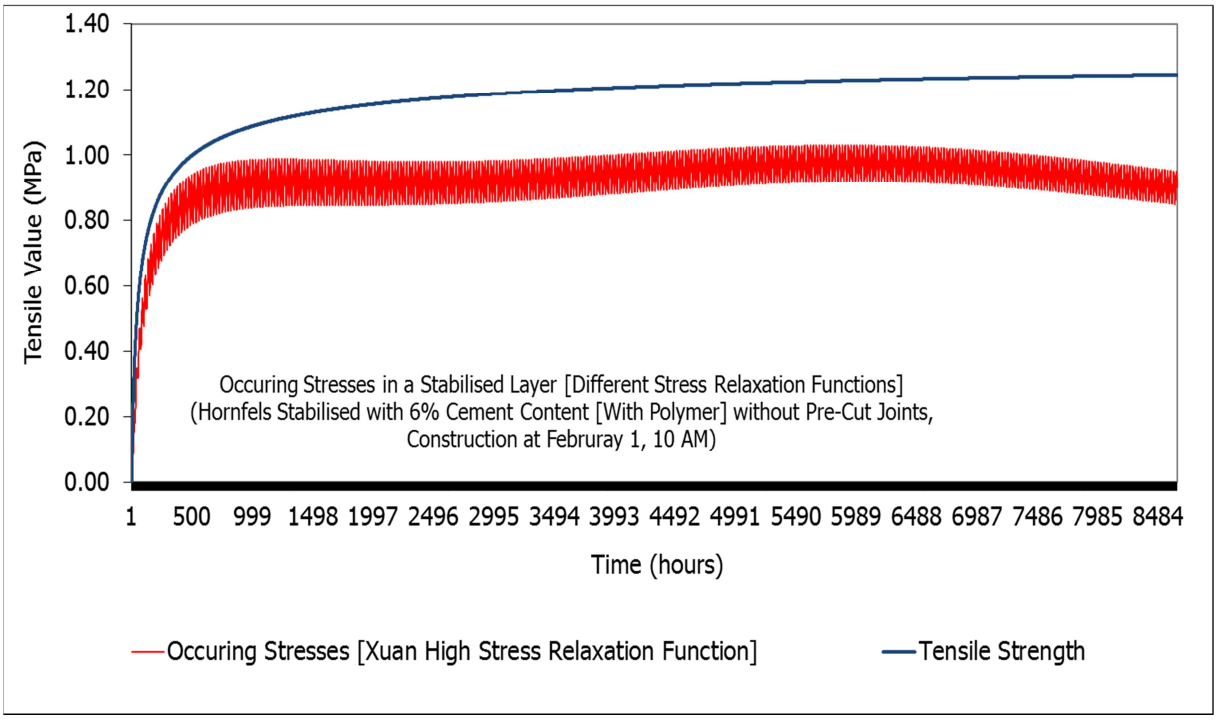

Figure 7-47 Xuan High Stress Relaxation, Stresses and Tensile Strength [For 360 days after Construction]

The low and average Xuan stress relaxation factors show that, 90 days after construction no further cracking occurs. For an identical mix, applying the Xuan low stress relaxation registers two crack series while the average function shows only first cracks and the Xuan high shows no cracking results. The Houben stress relaxation function registered three series of cracks.

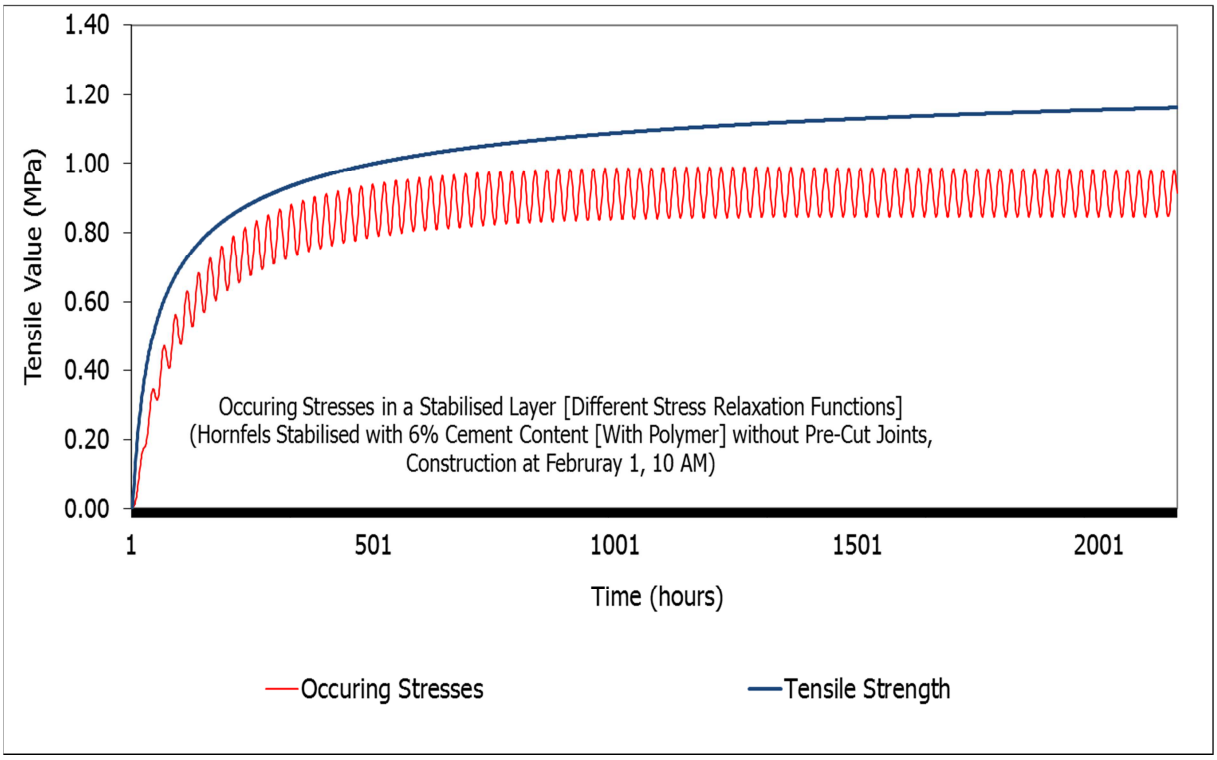

Figure 7-48 Xuan High Stress Relaxation, Stresses and Tensile Strength [For the first 90 days after Construction]

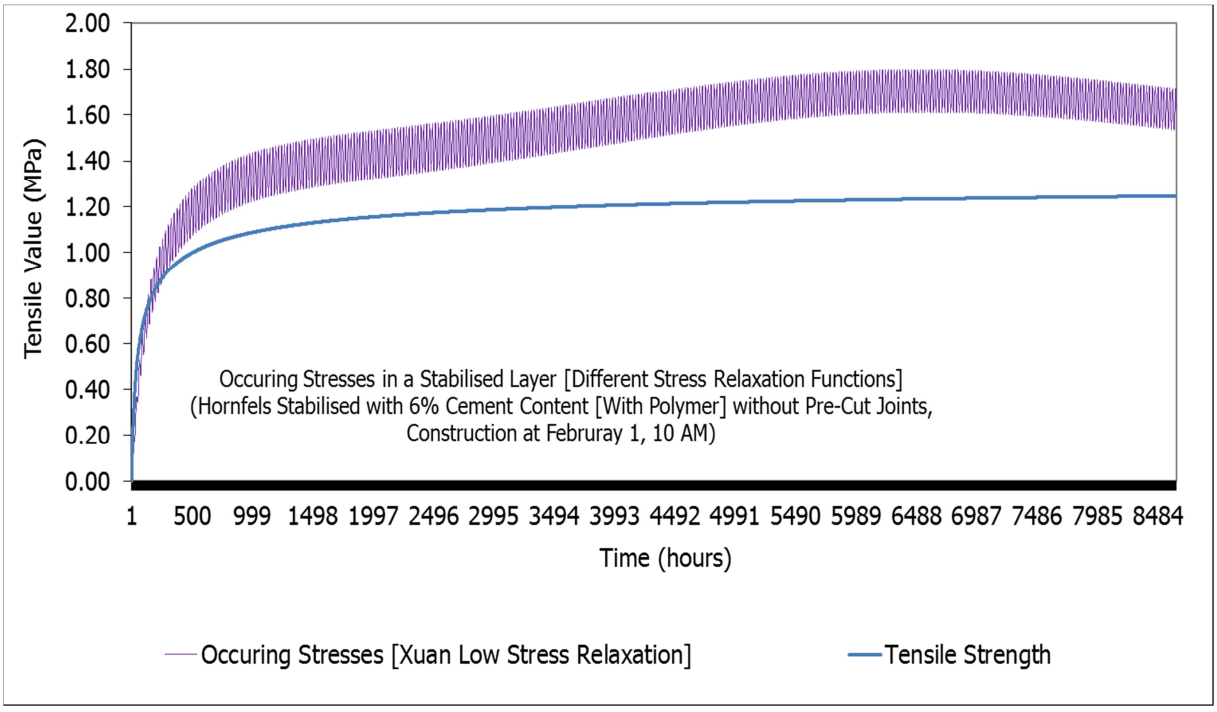

Figure 7-49 Xuan Low Stress Relaxation, Stresses and Tensile Strength [For 360 days after Construction]

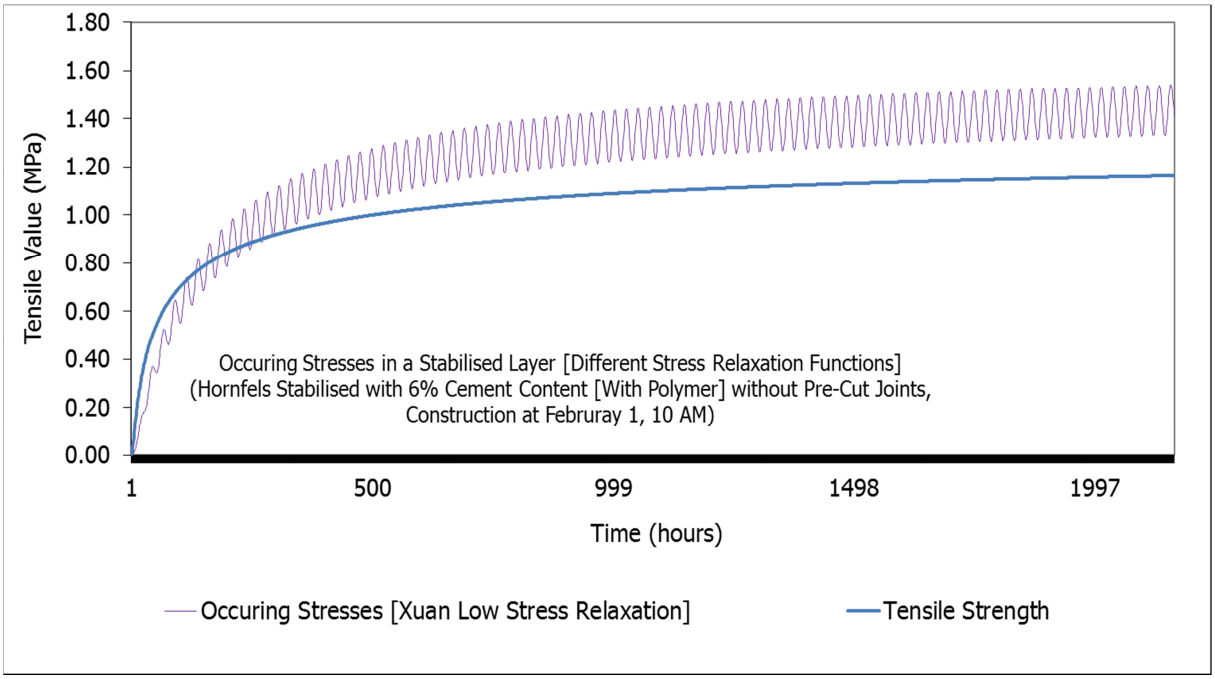

Figure 7-50 Xuan Low Stress Relaxation, Stresses and Tensile Strength [For the first 90 days after Construction without Stress Reduction Following Cracking]

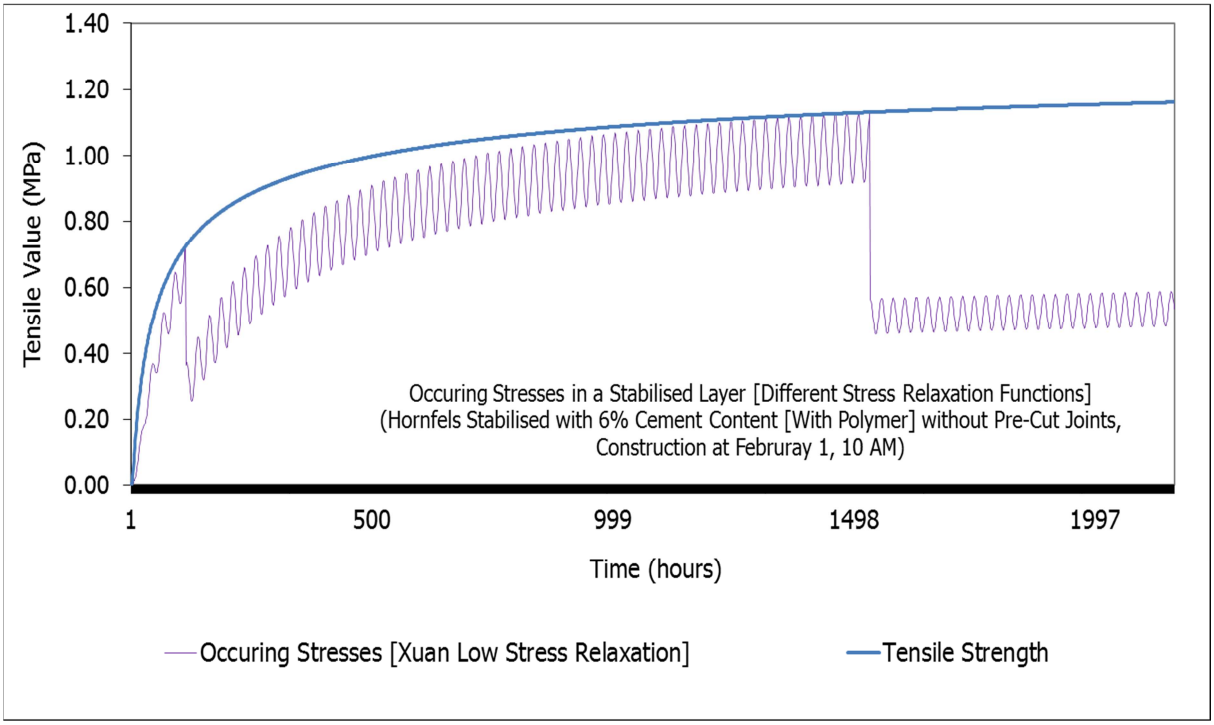

Figure 7-51 Xuan Low Stress Relaxation, Stress Development after a Series of Cracks and Tensile Strength [For the first 90 days after Construction with Stress Reduction Following Cracking]

The Houben stress relaxation function leads to an initial increase, reaching a maximum peak and then declines showing a reduction in occurring stress. Xuan stress relaxation shows an initial increase of tensile stress development reaching a maximum. Thereafter about a constant variation takes place. This characterises the behavioural properties of stabilised materials and their ability to relieve stress under constant strain [or restraint]. The amount of cement in the mix and achieved density contribute to the ability of the stabilised layer to relieve stress.

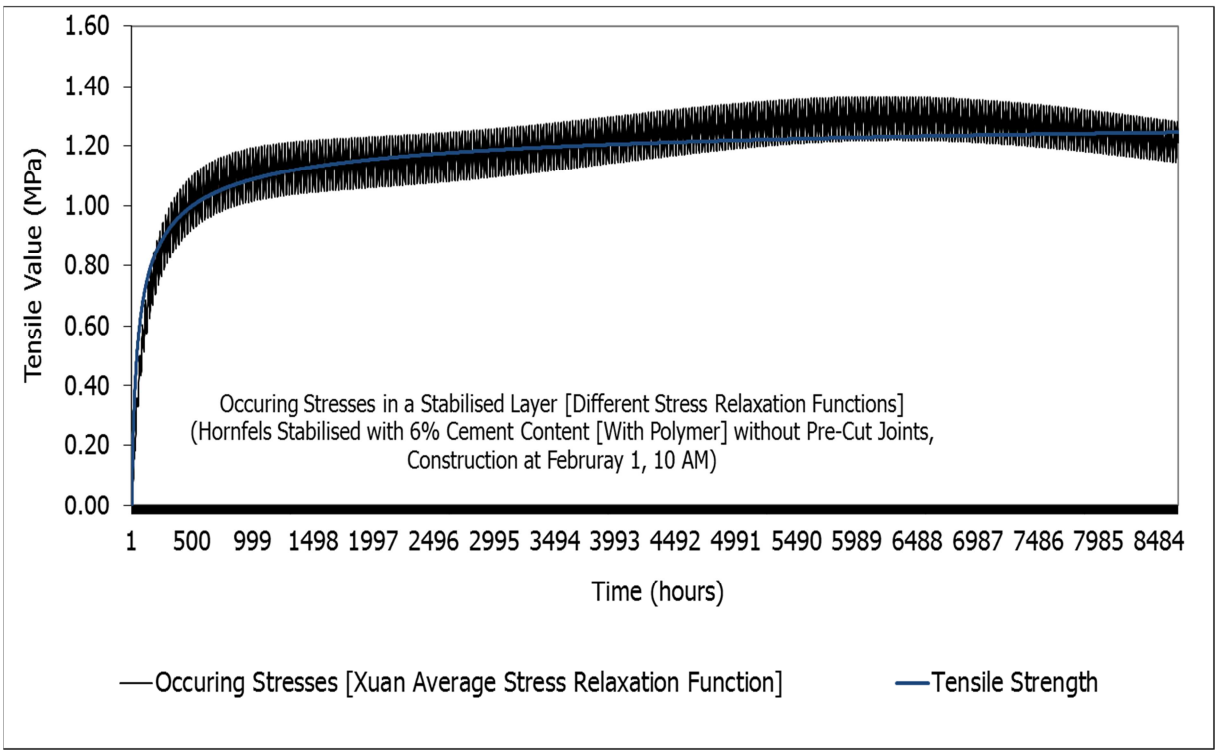

Figure 7-52 Xuan Average Stress Relaxation, Stresses and Tensile Strength [For 360 days after Construction]

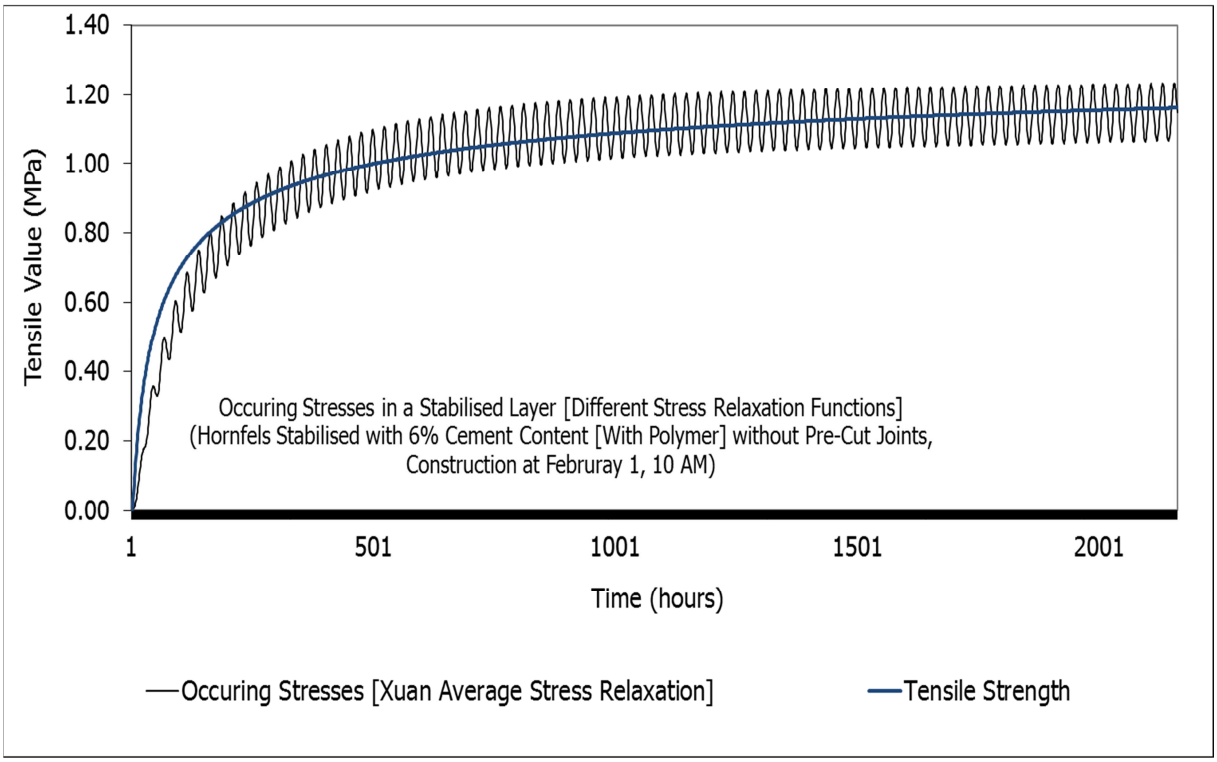

Figure 7-53 Xuan Average Stress Relaxation, Stresses and Tensile Strength [For the first 90 days after Construction without Stress Reduction Following Cracking]

Table 7-9 lists the crack pattern [particularly the crack width]. With the Houben stress relaxation function, reduced crack widths at short spacings result. The Xuan low stress relaxation registers two series of cracks but the width of the first cracks is wider than that obtained using the Houben function. The Xuan average function registers only first cracks with a larger width than the Houben function.

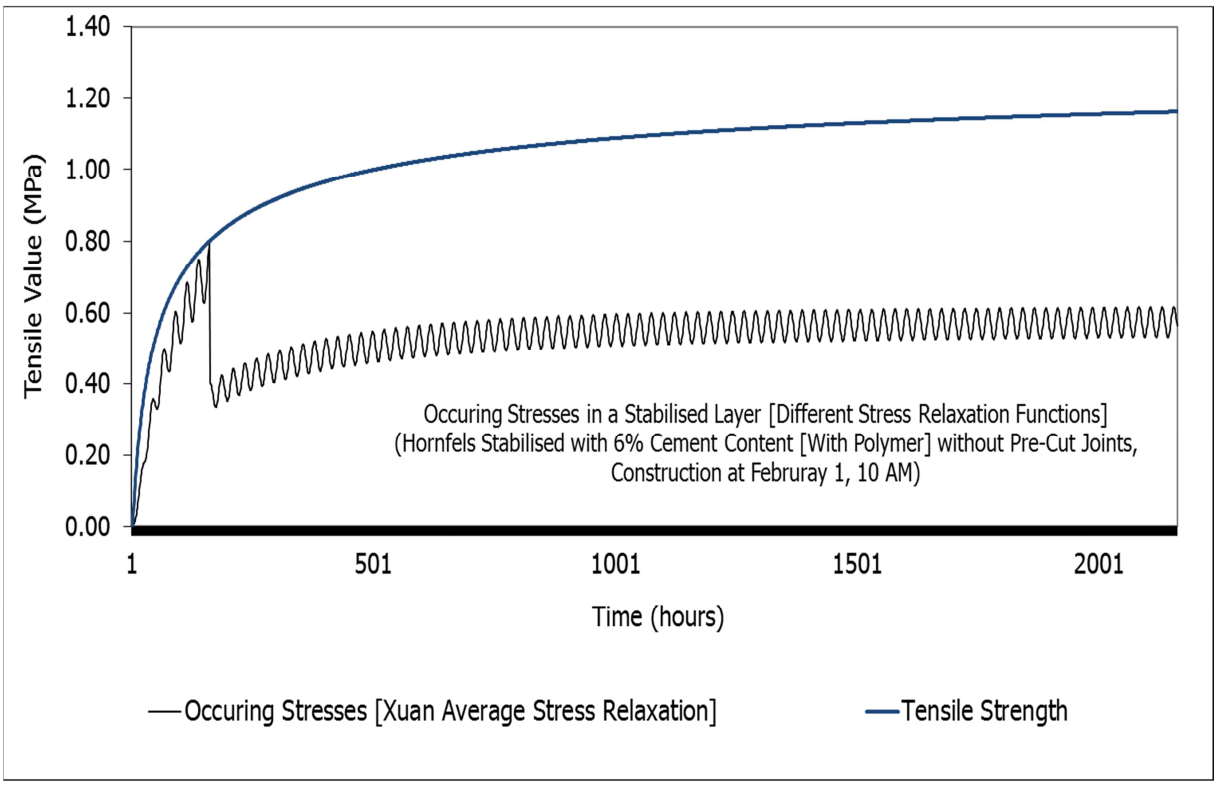

Figure 7-54 Xuan Average Stress Relaxation, Stresses and Tensile Strength [For the first 90 days after Construction with Stress Reduction Following Cracking]

Table 7-9 Effect of Stress Relaxation Function on the Resultant Crack Pattern

Hornfels 6.0% Cement Content With Polymer	Frictional Coefficient [f=3.8] No Pre-Cut Joints		
Stress Relaxation Function	Xuan [Low]	Xuan [Average]	Houben
Initial Width of First Cracks [mm]	1.46	2.21	0.67
Initial Width of Second Cracks [mm]	0.16	N/A	0.11
Initial Width of Third Cracks [mm]	N/A	N/A	0.04
Maximum Crack Width of First Cracks [mm]	2.19	5.60	1.92
Maximum Crack Width of Second Cracks [mm]	0.33	N/A	1.00
Maximum Crack Width of Third Cracks [mm]	N/A	N/A	0.47
Average Crack Width after 1 Year First Cracks [mm]	2.13	4.80	1.07
Average Crack Width after 1 Year Second Cracks [mm]	0.27	N/A	0.14
Average Crack Width after 1 Year Third Cracks [mm]	N/A	N/A	-0.40
Final Crack Spacing [m]	1.52	1.61	1.60

7.6 Shrinkage Crack Pattern [cncPAVE – Empirical Approach]

The South African concrete pavement design software [cncPAVE] makes use of concrete related empirical data and concepts to predict the resultant crack pattern. The consideration of cncPAVE software is to establish its suitability in predicting the shrinkage crack pattern in a cement-stabilised pavement layer. For the analysis, software version cncPAVE508 is applied. The software development and background includes 'rulebooks' principles which define its empirical methodology and limitations of its input variables as well as the constants. Several input variables and constants relate to concrete rather than to cement-stabilised materials.

Some design parameters in the cncPAVE were not adjustable outside the specified range, which is a limitation in analysing the stabilised materials. Specific limitations include:

a) Input variables such as the flexural strength input value that ranges from 3.5 MPa to 5.5 MPa, which is applicable to concrete rather than cement-stabilised materials, were not

adjustable. The specified range is higher than the 28-day flexural strength values listed in Table 7-1. As a result, a minimum of 3.5 MPa for mix types stabilised using 6.0% cement contents was used as input.

b) Principles defining the drying shrinkage criteria in addition to the computation of crack width and spacing make use of empirical methods with limited numerical analysis. Due to this fact, it was difficult to re-adjust the parameters to suit cement-stabilised materials.

Cognisance of the material differences between concrete and cement-stabilised materials is noted. In this analysis, stabilised hornfels with 6.0% cement content and polymer is considered as a very weak concrete mix. This analysis aims at obtaining trends from the software while it is realised that the numerical values are not valid for the stabilised hornfels under consideration.

7.6.1 Drying Shrinkage, Material Properties and Thermal Parameters

The software considers moisture loss as the causal factor in drying shrinkage and the resultant crack width. Even though links of drying shrinkage to the curing method and initial water content in the concrete mix are emphasised no computation and/or numerical analysis is included. Other notable links to drying shrinkage without any numerical analysis include:

a) age of the concrete
b) relative humidity [environment] and temperature
c) aggregate [mix proportions] as well as content and type
d) cement content and fineness
e) temperature at the time of construction

In terms of material quality, the fineness of the aggregate and its influence to drying shrinkage is emphasised. The software uses a factor linked to the material fineness to define the resultant drying shrinkage; the derivative of this factor is limited to concrete mix. Furthermore, only four materials and their related factors are registered. Other input constants along with their ranges as related to material quality and drying shrinkage include:

a) type of aggregate with a fineness factor range of 0.7 to 1.3
b) coarse aggregate content range of 0.65 to 0.75
c) aggregate size between 9.5 and 37.5 mm sieve size

Despite the significant influence of cement type and content on drying shrinkage, no numerical analysis is noted. As an alternative assumed factors ranging from 0.9 to 1.1 are noted. The input variables for cement content vary between 300 kg/m³ and 450 kg/m³. The input variable for water content varies between 170 l/m³ and 210 l/m³. The input variable for the daily temperature cycle ranges between 9ºC and 17ºC depending on the location and its climatic data. No further climatic relations are made.

Crack Pattern and Aggregate Interlock:

The software includes relationships that link the load transfer [C] with the pavement structure to the aggregate interlock. The significance of both aggregate interlock and crack width in the load transfer mechanism is noted. $D_x^{1.5}$/Agg links, crack width [D_x] and aggregate interlock, [Agg represents the size of the 15% biggest aggregate in the mix]. This relationship suggests that a theoretical sieve, which will retain 15% of the aggregate, defines the resultant aggregate interlock. This acknowledges the significance of material properties, drying shrinkage and the resultant crack pattern with limited numerical analysis to validate or include other alternative material types. The software computes the resultant crack width [D_x] using the spacing between joints/cracks times 0.00055 as a first approximation.

Load transfer [C] is a function of the vertical movement in the region of the crack when a load is applied. Equation 7-52 computes the load transfer [C].

$C = \text{function } (D_y)^{0.5}$ Equation 7-52

Where: D_y is the relative vertical movement in the region of the crack

Regarding concrete with joints [J], the assumption upheld submits that cracks only occur at the joints. This suggests that the input joint spacing is equal to the crack spacing. With such an assumption, it is suggestive that the crack width [D_x] is the only variable. Joint spacing is an input constant that is dependent on the slab thickness with a maximum input value of 4.5 m. This became another limitation to this analysis. In a cement-stabilised layer, field crack mapping have measured crack spacing of more than 4.5 m. The software input guide recommends crack spacing between 1.5 m and 2.0 m for good structural capacity.

Traffic Load:

The standard axle load is 80 kN, which corresponds to an axle mass of 8.2 tonnes. Equation 7-53 computes the equivalent standard axle load [ESAL].

$ESAL\ (= E80) = (A/8.2)^{b}$ Equation 7-53

Where: A is the axle load in metric tonnes and b is the damage exponent [b = 4.2 for flexible pavements]

The cncPAVE software analyses plain slabs with and without dowel bars at the transverse joints, continuously reinforced and ultra-thin reinforced. For any reinforced slabs, input constants that include a steel diameter and spacing are a prerequisite to running the software. The analysis only considered hornfels mix type stabilised using 6.0% cement content with polymer and pre-cut at specific spacing. The rest of the input variables and constants followed the recommended values as detailed in the input guide. The relevant input variables and constants included:

a) Computation of the water and cement contents
b) 250 mm layer height [exposed]
c) Elastic modulus value input from Table 7-1
d) Flexural strength of 3.5 MPa [defined as the minimum flexural strength input]
e) Cape Town Climatic data
f) Joint spacing [1.6, 2.0, 2.5 & 3.0]
g) Bond constants of 4.0, 6.0 and 8.0

7.6.2 Shrinkage Crack Pattern

Table 7-10 lists the crack pattern results along with the relevant data obtained from the cncPAVE analysis. Figure 7-55 illustrates the relationship between the crack pattern and interlayer bonding. An increase of the interlayer bonding results in a corresponding reduction in crack width. Increasing the joint spacing [pre-cut spacing] significantly widens the crack width in the region of pre-cut. This suggests that the resultant crack width is more dependent on the crack spacing than on the interlayer bond. An increase in interlayer bond does not significantly reduce the resultant crack width. Table 7-10 lists the resultant deflection relative to the crack pattern. A reduction in crack width results following an increase in interlayer bond. This suggests that the mitigation of shrinkage and the resultant crack pattern should focus on the following:

a) selecting a feasible pre-cut spacing which provides minimal crack width in order to allow for adequate load transfer at the region of pre-cut
b) ensuring that the maximum achievable interlayer bonding is attained

Table 7-10 Crack Pattern, Deflection and Load Induced Stress [Varying Bonding Levels]

Hornfels 6.0% Cement Content With Polymer	$E_{28\text{-day}}$ = 6193 MPa	Joint Spacing = 1.6 m	
Bond [0=No cohesion & 10 = Perfect Bond]	4.0	6.0	8.0
Crack Width [mm]	2.62	2.57	2.52
Pavement Structural Stress [MPa]	0.52	0.48	0.44
Hornfels 6.0% Cement Content With Polymer	$E_{28\text{-day}}$ = 6193 MPa	Joint Spacing = 2.0 m	
Bond [0=No cohesion & 10 = Perfect Bond]	4.0	6.0	8.0
Crack Width [mm]	3.28	3.21	3.16
Pavement Structural Stress [MPa]	0.74	0.67	0.60
Hornfels 6.0% Cement Content With Polymer	$E_{28\text{-day}}$ = 6193 MPa	Joint Spacing = 2.5 m	
Bond [0=No cohesion & 10 = Perfect Bond]	4.0	6.0	8.0
Crack Width [mm]	4.10	4.02	3.95
Pavement Structural Stress [MPa]	1.20	1.10	0.93
Hornfels 6.0% Cement Content With Polymer	$E_{28\text{-day}}$ = 6193 MPa	Joint Spacing = 3.0 m	
Bond [0=No cohesion & 10 = Perfect Bond]	4.0	6.0	8.0
Crack Width [mm]	4.90	4.80	4.70
Pavement Structural Stress [MPa]	2.00	1.70	1.44

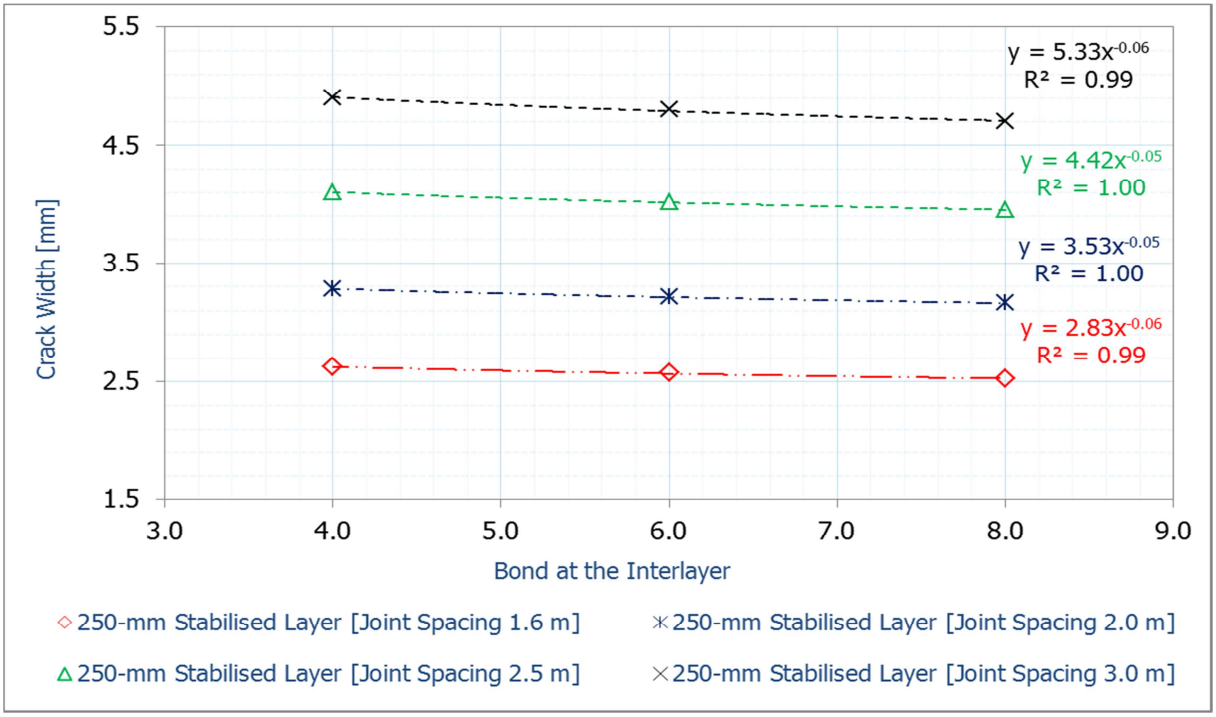

Figure 7-55 Crack Pattern versus Interlayer Bond

7.7 Discussion of Results

Due to the variations in temperature and moisture, the tensile stresses develop in a stabilised layer. Several factors, including the restraints influence the tensile stress development and crack pattern. The restraints imposed on the stabilised layer contribute to its cracking behaviour as well as influence the resultant crack pattern. A stabilised layer is composed of different particle sizes, which typifies that the material exhibits a degree of heterogeneity. Heterogeneity of the stabilised material has an influence on crack location and the resultant crack pattern. The variations in particle bonding strength and cement distribution typify the material heterogeneity within the stabilised layer. Particle bond strength contributes to the material tensile strength and ultimately influences the manifestation of the crack. For an aggregate interlock to provide suitable load transfer, the resultant crack width should be small enough in order to allow the aggregate connection.

The connection of the aggregates after the manifestation of the crack in a stabilised layer is dependent on:

a) the interlayer friction
b) particle distribution relative to cement content and resultant bond strength
c) the tensile strength of the material

The interlayer frictional coefficient influences the resultant crack pattern particularly, the crack width. The width of the crack and particles in the mix contributes to the aggregate interlock. The width of the crack is dependent on several factors, including material characteristics and interlayer friction. An increase in frictional coefficient results in a corresponding reduction in the crack width and spacing. Similarly, by increasing the bonding at the interlayer leads to a reduction in crack width. However, this is dependent on the joint spacing. Interlayer friction has a direct influence on the resultant crack pattern particularly crack width and spacing. Interlayer friction acts as a restraint to layer movement when it constricts. This shows that a high friction or increased bonding at the interlayer restricts layer movement as the composite materials constrict; this limits the width of the crack as well as influences the spacing between the cracks. Significant constriction of the layer begins when suction pressures result due to the withdrawal of moisture from the capillary pore spaces.

The quantity of cement and mix-water influence the hydration process. The hydration process consumes some of the mix-water. This process is responsible for the hardening of materials. Depending on the available mix-water and prevailing thermal effects the rate of moisture loss through evaporation will vary. This directly influences shrinkage. High temperatures lead to increased moisture loss from the layer particularly when the surface is exposed. The use of large quantities of mix-water leads to increased moisture availability in the material matrix. This increases the extent of constriction and thus, the degree of total shrinkage. Owing to the thermal effects and their variations, high rates of moisture loss, contribute to the increased constriction [total shrinkage] of the material. The rate of moisture loss is dependent on the level of exposure, temperature and material characteristics.

An exposed surface experiences higher rates of moisture loss [increased shrinkage] than a covered surface. This equates to sealing and complete exposure of the specimens at laboratory level. The differential shrinkage rates between the exposed and unexposed layer sections ultimately induce tensile stress within the stabilised layer. However, other factors, including the layer depth and its void content also influence moisture loss from the material matrix. Voids in the mix are dependent on the grading and compactive effort applied. This dictates the resultant density and interspaces between the particles.

Furthermore, the type of material [hornfels or ferricrete], cement content besides the thermal effects and moisture variations directly influence the degree of shrinkage. The quantity of cement added to either hornfels or ferricrete dictated the resultant crack pattern. Low cement dosages to material reduced the resultant shrinkage as typified by the resultant tensile stress and crack pattern characteristics. High quantities of cement added to material result in high moisture consumption during the hydration process. This contributes to drying shrinkage. High cement contents to material also results in increased rigidity and strength. Material with high tensile strengths exhibit cracks that are spaced far apart. However, the individual cracks are wide. This affects the load transfer mechanism since wide cracks do not usually possess aggregate interlock at the region of the crack.

The effect of cement content and the resultant shrinkage is dependent on a number of factors, including material type, quality and moisture content. Ferricrete mix types exhibited severe cracking at 4.0% cement content without the polymer. Stabilised soils [ferricrete] and crushed aggregates [hornfels] exhibit different shrinkage criteria. These stem from the

dissimilarities between the material type, including intrinsic properties and characteristics. Ferricrete exhibits a worse crack pattern than hornfels particularly at high cement contents and without the polymer. Ferricrete compared to hornfels exhibited higher tensile stress development [total shrinkage] due to the differences in materials. The fines content exhibited by ferricrete contributes to the increased stress development [severe crack pattern]. The fines in ferricrete possess larger surface areas than the hornfels particles. Equally, the fines in the ferricrete mix require higher moisture contents for compaction purposes than hornfels. Materials with fines require higher cement contents compared to well-graded coarse materials. The application of high cement contents to materials with substantial fines in their mix increases the optimum moisture content required to achieve maximum density. Increasing the moisture content along with using high cement dosages for stabilisation, results in an increase in the total drying shrinkage.

7.7.1 Practical Significance of the Trends [Houben Model versus cncPAVE]

In predicting the resultant shrinkage crack pattern, two analytical tools are applied. Houben model uses fundamental material properties, in addition to thermal and frictional coefficients. The basis of the Houben model is set on the fundamental relationships of the influential factors to shrinkage. Illustrations and results from the Houben model suggest the following:

a) reduced cement content results in reduced stress development and subsequently resultant total drying shrinkage
b) material quality and type influence shrinkage
c) mitigation of shrinkage through the use of polymer with and without joints exhibits significant relationships with material properties, technique and product influence

The Houben model results show that material characteristics relative to their stress relaxation behaviour, interlayer friction and thermal effects influence the resultant crack width and spacing. The model includes the various factors that influence drying shrinkage and cracking behaviour. Relationships of tensile strength relative to stress development along with the coefficient pertaining to interlayer friction and material stress relaxation are included. The integration of influential factors provides further understanding of shrinkage cracking and its mechanism. This requires the comprehension of the layer shrinkage along with the material properties and characteristics. The Houben model provided the following trends:

a) the addition of cement to material resulted in high tensile stress development along with increased strength
b) difference in the mix and material type exhibited dissimilarities in stress-strength trends and finally different crack pattern characteristics; the occurrence of cracks in the stabilised layer is dependent on the mix type
c) the use of polymer resulted in reduced stress development because of less shrinkage
d) manifestation of cracks in the stabilised layer resulted in a stress reduction
e) the cracks that occur first are the most critical and they exhibit a larger width than intermediate cracks which occur later
f) pre-cutting the stabilised layer offered a desirable crack pattern but this is dependent on the cut depth and pre-cut spacing
g) increasing the interlayer layer friction results in a reduction in crack width and spacing
h) the material stress relaxation criterion has a significant influence on the resultant crack spacing and width

The increasing tensile stress development following the addition of cement to material establishes the relationship between cement content and drying shrinkage. Practically, using high cement content leads to an increased demand of mix-water. The use of high cement dosages results in increased tensile strength and rigidity but also shrinkage. A balance between these properties has to be realised in order to obtain an optimal crack pattern [crack spacing and width].

The differences in the mix and material types typify the dissimilarities related to material gradation [material type differences] and cement content [mix type differences]. Fines content influence the amount of mix-water and finally drying shrinkage. The Effect of cement content and fines exacerbate the material susceptibility to shrinkage; these two factors increase the amount of mix water in the mix. The extent of moisture loss from the stabilised layer determines the degree of shrinkage and ultimately the crack pattern.

The efficiency and practical use of the polymer in mitigating shrinkage shows benefits associated with cement content and material. The efficiency of the polymer is dependent on the cement content and material type. At specific cement contents, dependent on the material type, benefits of polymer are realised. Despite the benefits associated with the polymer in mitigating shrinkage cracking, the consideration of other mitigation techniques such as pre-cracking of young stabilised layer and pre-cutting remain necessary.

Hornfels mix type stabilised at 6.0% cement content with polymer showed minimal crack width, reduced maximum width [critical situation] as well as a low width after 1 year. Pre-cutting the stabilised layer provides added benefits to the performance and longevity of the stabilised layer. The pre-cutting technique prevents the occurrence of occasional cracks. The practical benefits of the pre-cutting technique depend on the cut depth and spacing. In the end, the resultant crack width must be lower than the uncut condition. The objective is to obtain a minimal crack width using a feasible pre-cutting spacing and cut depth.

The cncPAVE software is restrictive in terms of the input ranges [input variables and constants]. Besides, its general conceptualisation remains based on empirical concrete-related data. The purpose of considering the cncPAVE is to assess the trends related to the shrinkage crack pattern rather than validate the actual values. The cncPAVE analysis also considered hornfels mix type stabilised using 6.0% cement content with polymer. The trends from the analysis reveal the following:

a) an increase in joint spacing [crack spacing] slightly results in the widening of cracks [larger crack width]
b) increasing the bonding at the interlayer [friction] reduces the crack width
c) reducing the joint spacing leads to a decrease in the load induced stresses within the stabilised layer

The analysis and conceptualisation of the Houben model reveal that cncPAVE software excludes influential aspects pertaining to material shrinkage besides its restricted applicability to concrete. The cncPAVE attempts to correlate drying shrinkage to gradation, cement and water content but factors such as stress relaxation as well as stress development and reduction are not numerically analysed as phenomena behaviour. Stress relaxation and development are fundamental parameters for material shrinkage behaviour and cracking damage. Different mix types exhibited different stress development and ultimately dissimilar cracking behaviour as exemplified by the resultant crack pattern. The inclusion of material properties, coefficients related to drying shrinkage, such as thermal and restraints imposed on the pavement layer will increase analytical reliability of the cncPAVE508 version.

7.7.2 Practical Implications

Stabilising hornfels using low cement contents results in tensile stresses, which are lower than the material strength. In the end, there is no cracking in the stabilised layer. Therefore, application of polymer to materials stabilised using low cement contents such as 2.0% and 3.0% is uneconomical. The feasible ranges under which the polymer application to material provides benefits are established. The current trend within the Southern African practice prefers the use of low cement contents for stabilisation. Consideration of reduced cement contents is to mitigate shrinkage and wide cracks, which are usually associated with the application of high cement dosages.

With increased technological innovations, the development of laboratory evaluation techniques aimed at ensuring product suitability with stabilised materials is necessary. A link between the benefits of shrinkage mitigation using the polymer to cement content and material type is established. This insight defines the importance of evaluating the polymer in proportion to cement content and material type in order to determine its suitability.

Mitigation of shrinkage is a unified approach to attain the desired crack pattern particularly, minimal crack width at short spacing. Consideration of reduced cement contents, application of shrinkage reducing products [polymer] and traditional mitigation techniques such as pre-cracking and pre-cutting might result in the desired crack pattern. In general, the primary objective of any mitigation technique or method is to result in narrower crack width at closer spacing.

7.8 References

Alvaredo, A.M., (1994) *Drying Shrinkage and Crack Formation*, Building Materials Reports No. 5, Aedificatio Publishers Freiburg

Burg, R.G., and Ost, B.W., (1994) *Engineering Properties of Commercially Available High-Strength Concrete (Including Three-Year Data)*, RD104, Portland Cement Association, Skokie, Illinois,.

Cervera, M. Faria, R., and Oliver, J., (2002) *Numerical Modelling of Concrete Curing; Regarding Hydration and Temperature Phenomena,* Computers and Structures 80 pp. 18-19 1511-1521

Houben, L.J.M., (2008) *Model for Transversal Cracking (at Joints) in Plain Concrete Pavements,* Faculty of Civil Technology and Geotechnical, Delft University of Technology

Keienburg, K.K., (1976) *Particle Size Distribution and Normal Strength of Portland Cement*, PhD Dissertation, Karlsruhe University

Schindler, A.K., and Folliard, K.J., (2005) *Heat of Hydration Models for Cementitiuos Materials,* ACI Materials Journal 102 (1) pp.24-33

Strauss, P.J., Slavik, M., and Perrie, B.D., (2001) *A Mechanistically and Risk Based Design Method For Concrete Pavements in Southern Africa*, Proceedings of 7th International Conference on Concrete Pavements, Session 3

Taplin, J.H., (1969) *A Method for Following Hydration Reaction in Portland Cement Paste*, Australian Journal of Applied Sciences 10 pp. 329-345

van Breugel, K., (1991) *Simulation of Hydration and Formation of Structure in Hardening of Cement-Based Materials*, PhD Dissertation, Delft University of Technology, The Netherlands

Xuan, D., (2012) *Cement Treated Recycled Crushed Concrete and Masonry Aggregates for Pavements,* Ph.D. Dissertation, Faculty of Civil Technology and Geotechnical, Delft University of Technology

Walraven, J.C., (1981) *Fundamental Analysis of Aggregate Interlock,* Journal of the Structural Division, ASCE, Vol. 107, No ST11, pp 2245-2270.

Chapter 8: Conclusions and Recommendations

Cement-stabilised materials are used for the construction of the base and/or sub base layers. Materials for the construction of roads ought to provide feasible engineering properties and characteristics capable of withstanding the applied traffic loads and endure the adverse environmental conditions. This suggests that the material properties should provide a good performance criterion as well as offer an acceptable durability range throughout the pavement design life.

Strength is one of the fundamental design inputs parameters apart from traffic and the environment. Through laboratory-based tests, a number of the design input parameters such as strength and elastic modulus are usually determined. However, the design input parameters should provide a good reliability for the designing of pavement structures.

In this research, a laboratory-based evaluation on ferricrete and hornfels stabilised at varying cement contents is undertaken. In order to confederate with the current research needs as related to materials, consideration of a nanotechnology product, a polymer cement additive, is included in this study. The assessment of the polymer cement additive focused on the verification its applicability and suitability with cement-stabilised materials.

This research is a two-pronged study i.e. laboratory-based evaluation followed by numerical modelling and analysis. The laboratory-based evaluation required the development of a shrinkage test method as well as the formulation of a flexural beam test protocol for the evaluation of cement-stabilised materials. The numerical modelling and related analysis made use of a finite element program and the Houben Model. An integral of the laboratory-based evaluation and the numerical modelling as well as analysis assisted in realisation of the key objectives of this study.

8.1 Conclusions

As a background, the application of cement to ferricrete and hornfels increases the strength properties [i.e. compressive strength, tensile strength, flexural strength as well as modulus of elasticity]. Equally, particle resistance following the wet-dry brushing evaluation is enhanced by cement stabilisation. However, the engineering properties of the cement-stabilised materials are dependent on the type and quality of the natural materials to be stabilised, curing criteria and age. Other factors such as mix components and proportions, mixing efficiency and resultant dry density influence the strength development of cement-stabilised materials. In this research, ferricrete exhibited a lower material quality compared to hornfels.

The research conclusions are categorised according to the specific evaluation sectors i.e. strength testing and shrinkage evaluation. The compressive, tensile and flexural strength results show that the strength properties of cement-stabilised materials increase with an increase in cement content. However, the rate of strength increase is dependent on the type and quality of the material stabilised.

In this study, each test i.e. unconfined compression [UCS], flexural beam and indirect tensile [ITS] provide a different measure of the strength properties of the cement-stabilised materials. Relationships between the different strength measures are presented in this dissertation in order to facilitate the use of different tests in the design process. However, an important characteristic of cement-stabilised materials is that strength continues to increase with time. This study considered 7-day strength for the compressive and tensile strength evaluation and the 28-day strength for flexural strength and elastic modulus. The stress-strain behaviour is expressed in terms of the elastic modulus [i.e. flexural modulus].

Using the flexural beam test an evaluation of the behavioural properties of cement-stabilised materials was assessed. However, this required reassessing the flexural beam test configurations relative to beam geometric characteristics in order to achieve reliable measure of the behavioural properties of the cement-stabilised materials. From this flexural beam test experimentation, the key conclusions include the following:

a) A maximum large aggregate size in a small-sized beam significantly reduces the actual flexural strength and moduli values as well as the overall mechanical strength. It is deductive that the presence of large aggregate sizes in a small-sized beam generates zones of weakness, which create 'easy paths' for cracks upon loading. This eventually leads to erroneous interpretation of the test data as well as the characterisation and application of the cement-stabilised material type.
b) In terms of the beam geometric characteristics and test configurations, an increase in the beam depth [or height] at a fixed loading span result in a decrease in the flexural strength but an increase in the shear stresses. An increase in the loading span at a fixed beam depth significantly lowers the shear stresses in the beam, especially at high elastic moduli or cement contents. The resultant effects significantly influence the flexural strength values as well as the related analysis and the overall interpretation of test data.
c) Beam type with a 50 mm depth tested using a span-depth ratio of nine and containing a maximum aggregate particle size of 13.20 mm provides the least beam shear stresses. It is deductive that an increase in the span-depth ratio results in a reduction in beam shear stresses. The flexural beam test protocol provides relationships between the beam geometry and test configurations.
d) The 28-day flexural strength [based on the beam type with 50 mm and span-depth ratio of nine with 13.20 mm as P_{max}] is about 35% of the 7-day compressive strength. Additionally, the 28-day flexural strength is about twice the 7-day tensile strength; this is based on R-square value of 0.77.

In terms of the laboratory shrinkage evaluation, the key conclusions from this study include the following:

a) The developed shrinkage test method provides a good repeatability and is user friendly. Owing to the high-test temperature of 70ºC, testing is quick and the outcomes provide a good indication of the material's shrinkage criteria. A full test protocol is provided in the appendix.
b) The method of compaction, material quality and type [i.e. including the moisture content and particle size distribution] contribute to the resultant dry density. The dry density obtained using the vibratory table is lower than that achieved using vibratory hammer. The achievable dry density typifies to an acceptable degree the nature of the pore structure. The nature of the pore structure along with the moisture in the mix and other pertaining effects such as temperature significantly influence the degree of shrinkage.
c) This research provides shrinkage results based on different sizes and shapes of specimens for cement paste and stabilised materials. The study shows that the method of measuring shrinkage at laboratory level requires a good understanding of a number of aspects including the restraints imposed in the direction of measurement on the specimen, the specimen size and shape relative to the maximum aggregate particle size as well as the ability of the specimen to completely dry out. The rate of drying is dependent on the test temperature relative to the specimen geometric characteristics as well as mix type. it is deductive the maximum aggregate size in the mix, moisture content and method of compaction, have a significant influence on the achievable dry density and thus, contribute to the magnitude of shrinkage.
d) The higher the proportion of cement in the mix the greater is the resultant drying shrinkage. Ferricrete, which exhibited a lower material quality than hornfels, showed a higher shrinkage potential compared to hornfels. Generally, the shrinkage test method provides a good measure of the influential factors pertaining to material shrinkage i.e.

thermal response due to drying relative to cement in the mix and material characteristics, among others.

e) The findings from the shrinkage evaluation confirm that curing conditions, cement content in the mix and the characteristics of the original materials before stabilisation have a significant influence. Without cement in both ferricrete and hornfels, the materials still exhibited some shrinkage. However, compared to their equivalent stabilised mix types the resultant shrinkage without cement in the mix is considerably lower.

The evaluation conducted on the polymer cement-additive reveals that the polymer is a shrinkage-reducing additive. However, the effectiveness of the polymer is dependent on the amount of cement in the mix as well as the type and quality of the materials. The key conclusions following both the laboratory shrinkage evaluation and numerical analysis include the following:

a) Similar to the effect of cement on material, the application of the polymer to stabilised materials reduces the dry density. A reduction in dry density could negatively influence on the resultant engineering properties and to an extent, their shrinkage criterion. Following the addition of the polymer to hornfels, results lower strength properties compared to its reference mix type [i.e. without the polymer additive]. Ferricrete exhibits increased compressive, tensile and flexural strength properties. The increase of ferricrete strength properties with the polymer is significant at higher cement contents of 4.0% and above, but comparable at low cement contents of 3.0 and lower.
b) In terms of material shrinkage, applying the polymer to the cement-stabilised materials decreases the resultant shrinkage compared to its reference mix type. The numerical analysis shows that use of the polymer lessens the development of tensile stresses in the stabilised layer. However, the reduction in tensile stress development following the application of the polymer is effective for specific mix ranges dependent on cement and material characteristics. Beyond these mix ranges, no significant reduction in shrinkage cracking provides benefits with the polymer; the resultant crack pattern is comparable to its reference mix.
c) Furthermore, with low cement contents, the application of the polymer to the stabilised materials is not be necessary since no cracks appear. A feasible and economical use of the polymer is associated to use of high cement contents but this is highly dependent on the quality and type of the materials to be stabilised.
d) With and without the polymer in the mix, there is need to consider other traditional mitigation techniques such as pre-cutting the stabilised layer. The application of polymer to a cement-stabilised layer in conjunction with pre-cutting provide suitable crack pattern, i.e. wider crack spacing with a characteristic minimal crack width. Findings based on both the laboratory and numerical analysis suggest that despite the 'upcoming chemical mitigation' techniques it is worthy to integrate the modern techniques with the conventional methodologies such as pre-cracking and pre-cutting methods along with applying appropriate curing procedures.
e) Regarding durability, use of the polymer prolongs the service life of the pavement structure by allowing substantial load transfer. The resultant layer crack width following the addition of the polymer was lesser than its reference layer [i.e. without the polymer].

Pertaining the shrinkage modelling and analysis of crack pattern, key conclusions include:

a) Material properties, mix characteristics and thermal effects among other factors influence the resultant shrinkage crack pattern. The Houben model, which uses fundamental concepts of material science, builds various relationships defining the influential factors related to material properties, mix components and compositions to shrinkage cracking in a stabilised layer. The increase of tensile strength relative to the development of the tensile stresses is typified. This is used to analysis the shrinkage crack pattern in a cement-stabilised layer.

b) The Houben model shows that an increase in interlayer friction coefficient results in a reduction in crack width of a stabilised layer. This is because a higher friction at the interlayer retards complete movement of the stabilised layer following the development of tensile stresses. Consequently, the cracks appear at short spacings and thus the crack width is minimised.
c) The influence of the stress relaxation factor to shrinkage crack pattern is illustrated. The stress relaxation, which relates to the response of the material at constant strain, is included in the Houben Model. The Houben stress relaxation provides a more reliable approach to the analysis of shrinkage crack pattern in a cement-stabilised layer.
d) The cncPAVE software, which is specifically configured for concrete design and analysis, does not offer reliable results pertaining to cement-stabilised layers. The inputs to the cncPAVE software do not allow input values for lower ranges of material properties; this are fixed based on specific concrete mix types. Furthermore, the cncPAVE software does not take account of fundamental material parameters such as stress relaxation in defining material shrinkage [i.e. even for concrete design].

8.2 Recommendations

In general, this research provides a good understanding of the level of shrinkage analysis and criterion as well as the characterisation of cement-stabilised materials. Aspects related to material characteristics, construction and environmental factors deemed to influence shrinkage crack pattern are provided. However, in order to achieve an improved evaluation and the analysis of cement-stabilised materials, the following are deemed necessary:

a) The development of any material property relationship must account the pertaining material factors relative to the laboratory method employed. The employed method must provide a reliable measure of the material property. This aids in accruing appropriate design inputs for the designing of pavements with a good understanding of the fundamentals.
b) The current characterisation procedure requires revision in terms of testing and the interpretation of the test data. The characterisation procedure, which involves the evaluation of strength as a measure the suitability of material, remains partial. A comprehensive characterisation method ought to include the evaluation of shrinkage as well as flexural strength properties of the stabilised material. The significance of evaluating shrinkage and flexural strength is provided in this dissertation. A comprehensive understanding of the material characteristics and properties relative to their load and environmental response provides reliable insights that aid in the designing of structurally sound and durable pavement structures.
c) In order to realise a complete characterisation and analysis of cement-stabilised materials and/or layers, an integrated approach comprising of both laboratory and field investigation is recommended. This will benefit the calibration of the Houben model and the revision of existing software packages such as the cncPAVE software. For Laboratory testing, studies could focus on the influence of test temperature on the aging process of cement-stabilised materials. This could include conducting shrinkage testing at ambient temperature of 25°C and comparing the obtained results to the elevated temperatures such as 70°C as considered in this research. Field investigation could include shrinkage crack mapping, stress relaxation tests, tensile strength development and stresses, moisture and temperature variations as well as other influential parameters deemed essential to measurement of shrinkage. The inclusion of other notable material types with and without the polymer other than ferricrete and hornfels could also be realised. The variability related to particle size distribution, moisture and cement contents could also be evaluated at field level and correlated to the laboratory criterion.

Appendences

Table 4a Cement and Moisture Content, Dry Density and Resultant Compressive Strength [Hornfels]

	Hornfels Mix Types [No Polymer]	Maximum Dry Density [kg/m^3] =	2352	Dry Density	Estimated Voids
Cement Content [%]	Moisture Content [%]	Dry Density [kg/m^3]	Compressive Strength [MPa]	as a Percentage of MDD	in the Mix [%]
2	5.1	2321	3.09	98.7	1.3
2	5.1	2323	2.98	98.8	1.2
2	5.1	2328	2.87	99.0	1.0
2	5.1	2319	2.70	98.6	1.4
2	5.1	2333	3.10	99.2	0.8
2	5.1	2301	2.83	97.8	2.2
3	4.8	2267	3.48	96.4	3.6
3	4.8	2275	3.63	96.7	3.3
3	4.8	2280	3.78	96.9	3.1
3	4.8	2307	3.80	98.1	1.9
3	4.8	2307	3.99	98.1	1.9
3	4.8	2282	3.73	97.0	3.0
6	4.6	2234	6.07	95.0	5.0
6	4.6	2252	6.52	95.8	4.2
6	4.6	2239	6.19	95.2	4.8
6	4.6	2222	6.57	94.5	5.5
6	4.6	2242	6.77	95.3	4.7
6	4.6	2206	6.67	93.8	6.2

Table 4b Cement and Moisture Content, Dry Density and Resultant Compressive Strength [Ferricrete]

	Ferricrete Mix Types [No Polymer]	Maximum Dry Density [kg/m^3] =	2171	Dry Density	Estimated Voids
Cement Content [%]	Moisture Content [%]	Dry Density [kg/m^3]	Compressive Strength [MPa]	as a Percentage of MDD	in the Mix
3	8.1	2163	1.71	99.6	0.4
3	8.1	2138	1.82	98.5	1.5
3	8.1	2116	1.98	97.5	2.5
3	8.1	2115	1.86	97.4	2.6
3	8.0	2129	1.62	98.1	1.9
3	8.0	2119	1.85	97.6	2.4
4	7.9	2107	2.62	97.0	3.0
4	7.8	2118	3.03	97.6	2.4
4	7.8	2135	2.52	98.3	1.7
4	7.8	2115	2.18	97.4	2.6
4	7.8	2125	2.44	97.9	2.1
4	7.9	2113	2.82	97.3	2.7
6	7.2	2093	3.77	96.4	3.6
6	7.2	2115	3.43	97.4	2.6
6	7.2	2098	3.70	96.6	3.4
6	7.2	2078	3.83	95.7	4.3
6	7.2	2107	3.93	97.1	2.9
6	7.2	2106	3.33	97.0	3.0

Figure 5a Hornfels Beam Type with a Height of 100 mm and Span-Depth Ratio of 3.0

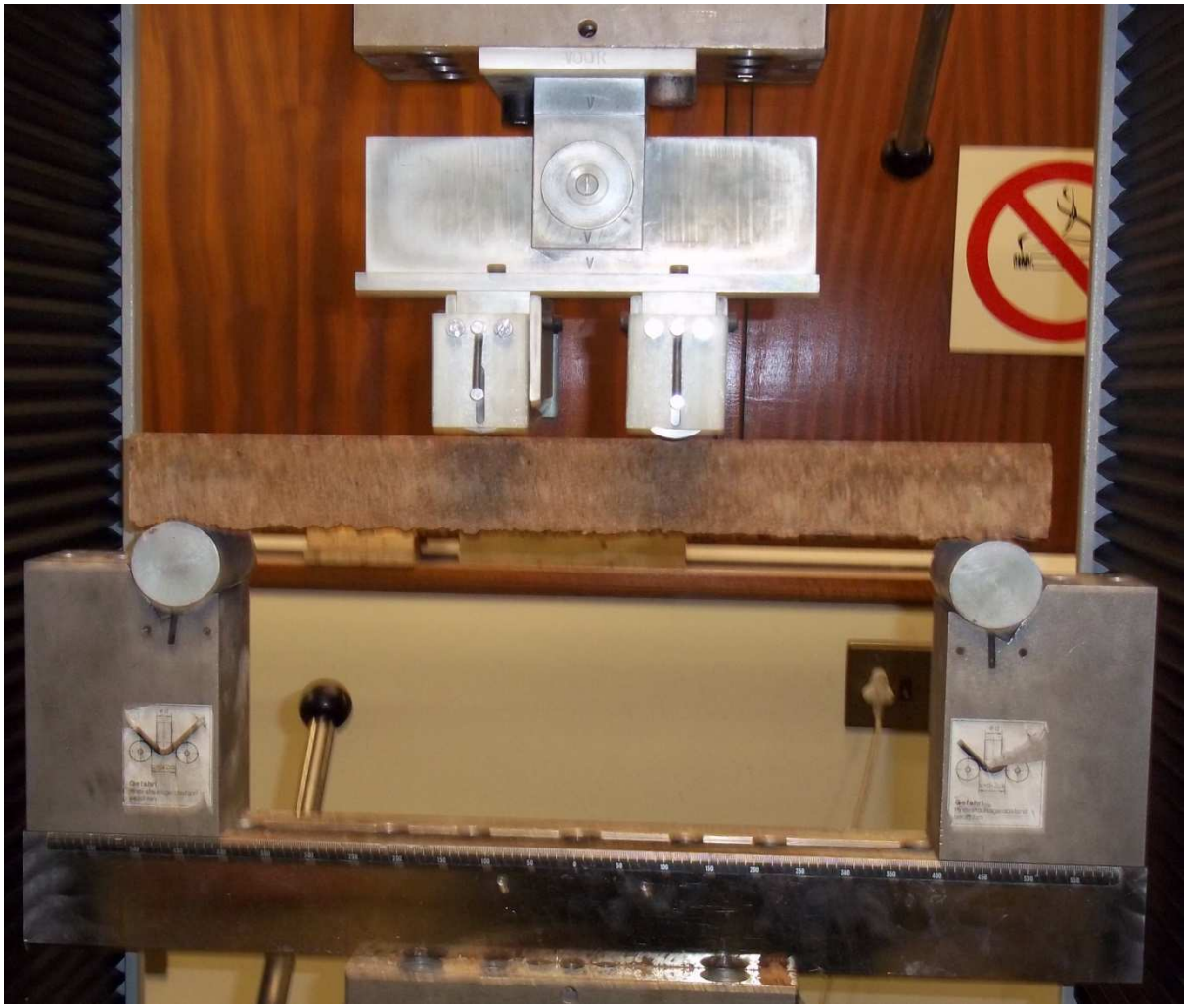

Figure 5b Ferricrete Beam Type with a Height of 50 mm and Span-Depth Ratio of 9.0

Figure 5c 3.0% Cement Contnet Hornfels Beam Type with a Height of 100 mm and Span-Depth Ratio of 3.0 [Region of Crack]

Figure 5d 2.0% Cement Hornfels Beam Type with a Height of 100 mm Tested using a Span-Depth Ratio of 3.0 [Region of Crack; 6 Beam Types per Mix Variable]

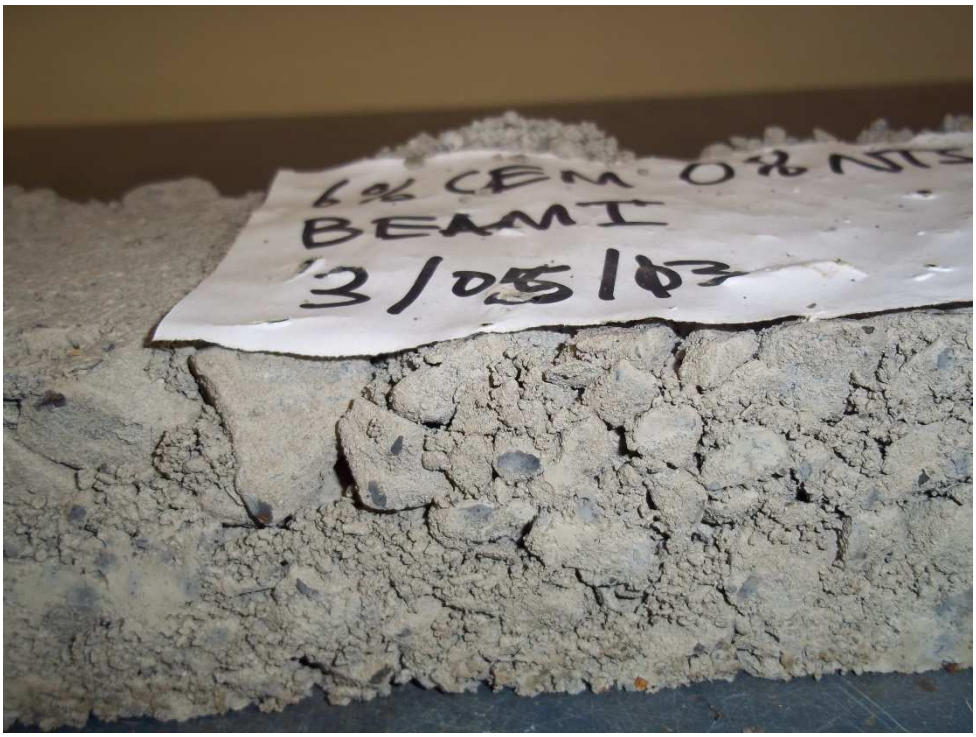

Figure 5e 6.0% Cement Hornfels Beam Type with a Height of 50 mm Tested using a Span-Depth Ratio of 9.0 [With 19.0 mm as the Maximum Aggregate Size]

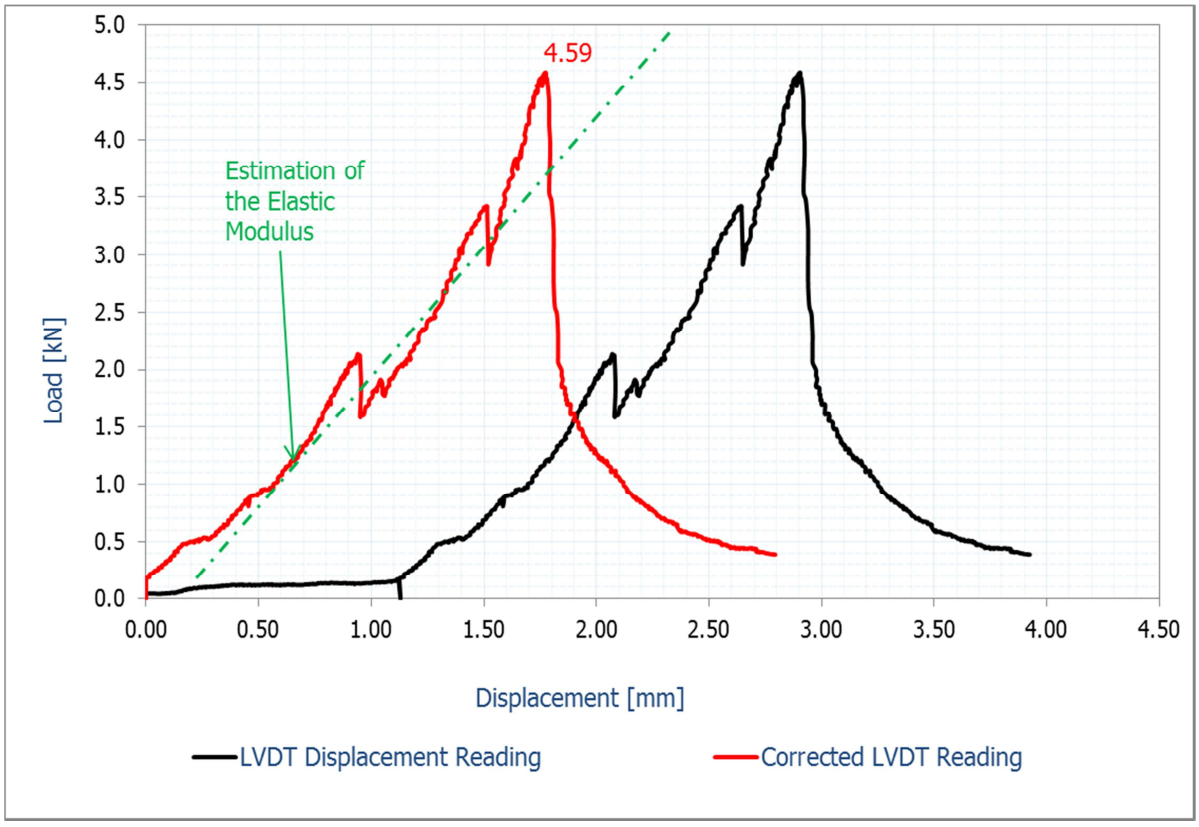

Figure 5f Typical Load Displacement Curves [LVDT Displacement Readings]

Table 5a Results for the 100 mm Beam Type [Span/Depth Ratio = 3.0]

2.0% Cement Content	Hornfels Mix Types [Pmax = 19.0 mm]				
Beam Height	Moisture Content	Density	Flexural Strength	Elastic Modulus	Shear Modulus
Beam Type [Span/Depth]	[%]	[kg/m^3]	[MPa]	[MPa]	[MPa]
100 mm [B1] 300/100	5.1	2338	0.589	2701	2078
100 mm [B2] 300/100	5.1	2315	0.594	4385	3373
100 mm [B3] 300/100	5.1	2333	0.462	1602	1233
100 mm [B4] 300/100	5.0	2311	0.362	1267	975
100 mm [B5] 300/100	5.0	2333	0.695	3193	2456
100 mm [B6] 300/100	5.0	2329	0.662	3017	2320
Mean	5.1	2326	0.560	2694	2072
Standard Deviation	0.05	10.99	0.13	1135	873
COV [%]	1.08	0.47	22.45	42.12	42.12
3.0% Cement Content	Hornfels Mix Types [Pmax = 19.0 mm]				
Beam Height	Moisture Content	Density	Flexural Strength	Elastic Modulus	Shear Modulus
Beam Type [Span/Depth]	[%]	[kg/m^3]	[MPa]	[MPa]	[MPa]
100 mm [B1] 300/100	4.9	2238	0.564	1885	1450
100 mm [B2] 300/100	4.9	2313	0.943	1218	937
100 mm [B3] 300/100	4.9	2304	0.741	3010	2315
100 mm [B4] 300/100	4.9	2236	0.417	1988	1529
100 mm [B5] 300/100	4.9	2293	0.752	1173	902
100 mm [B6] 300/100	4.9	2258	0.906	972	748
Mean	4.9	2274	0.721	1708	1313
Standard Deviation	0.00	33.98	0.20	758	583
COV [%]	0.00	1.49	27.85	44.40	44.40
6.0% Cement Content	Hornfels Mix Types [Pmax = 19.0 mm]				
Beam Height	Moisture Content	Density	Flexural Strength	Elastic Modulus	Shear Modulus
Beam Type [Span/Depth]	[%]	[kg/m^3]	[MPa]	[MPa]	[MPa]
100 mm [B1] 300/100	4.7	2246	1.463	5818	4476
100 mm [B2] 300/100	4.7	2245	1.807	7779	5984
100 mm [B3] 300/100	4.7	2230	2.050	7639	5876
100 mm [B4] 300/100	4.5	2248	1.407	15872	12209
100 mm [B5] 300/100	4.5	2227	1.379	15396	11843
100 mm [B6] 300/100	4.5	2223	1.770	9111	7008
Mean	4.6	2236	1.646	10269	7900
Standard Deviation	0.11	10.96	0.27	4288	3299
COV [%]	2.38	0.49	16.44	41.76	41.76

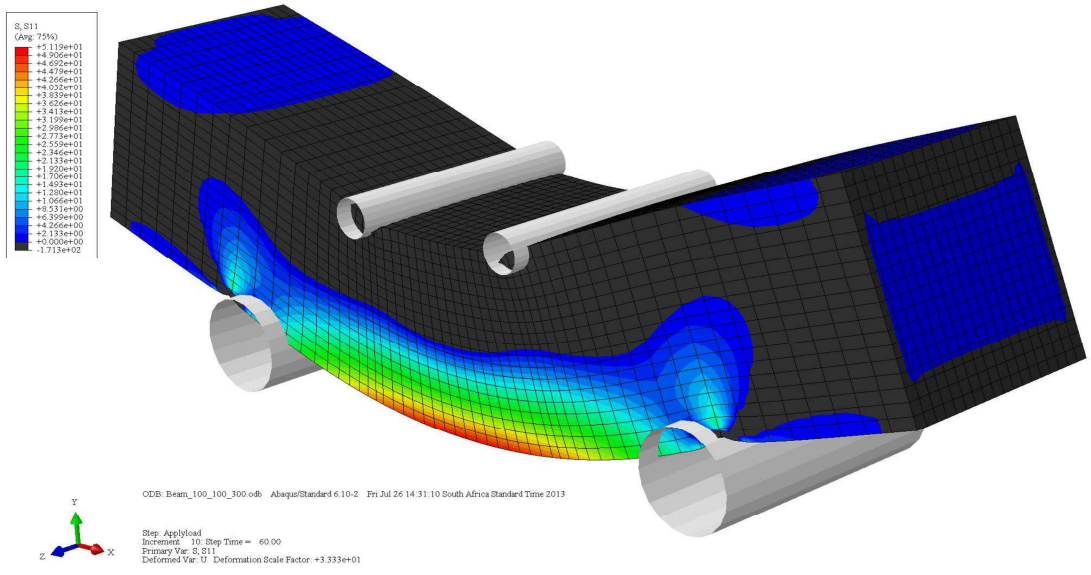

Figure 5g Model of the Beam Type with a Height of 100 mm and Span-Depth Ratio of 3.0

Table 5b Results for the 75 mm Beam Type [Span/Depth Ratio = 4.0]

2.0% Cement Content	Hornfels Mix Types [Pmax = 19.0 mm]				
Beam Height	Moisture Content	Density	Flexural Strength	Elastic Modulus	Shear Modulus
Beam Type [Span/Depth]	[%]	[kg/m^3]	[MPa]	[MPa]	[MPa]
75 mm [B1] 300/75	5.0	2338	0.439	1978	1521
75 mm [B2] 300/75	5.0	2332	0.439	938	722
75 mm [B3] 300/75	5.0	2331	0.413	1801	1385
75 mm [B4] 300/75	5.0	2328	0.259	1843	1418
75 mm [B5] 300/75	5.0	2322	0.521	1179	907
75 mm [B6] 300/75	5.0	2322	0.455	1629	1253
Mean	5.0	2329	0.421	1561	1201
Standard Deviation	0.00	6.22	0.09	412	317
COV [%]	0.00	0.27	20.70	26.41	26.41
3.0% Cement Content	Hornfels Mix Types [Pmax = 19.0 mm]				
Beam Height	Moisture Content	Density	Flexural Strength	Elastic Modulus	Shear Modulus
Beam Type [Span/Depth]	[%]	[kg/m^3]	[MPa]	[MPa]	[MPa]
75 mm [B1] 300/75	4.9	2312	0.723	3376	2597
75 mm [B2] 300/75	4.9	2313	1.424	9987	7682
75 mm [B3] 300/75	4.9	2301	1.166	8336	6412
75 mm [B4] 300/75	4.9	2326	0.675	8278	6368
75 mm [B5] 300/75	4.9	2337	0.861	8483	6525
75 mm [B6] 300/75	4.9	2325	0.912	6353	4887
Mean	4.9	2319	0.960	7469	5745
Standard Deviation	0.00	12.50	0.29	2314	1780
COV [%]	0.00	0.54	29.71	30.98	30.98
6.0% Cement Content	Hornfels Mix Types [Pmax = 19.0 mm]				
Beam Height	Moisture Content	Density	Flexural Strength	Elastic Modulus	Shear Modulus
Beam Type [Span/Depth]	[%]	[kg/m^3]	[MPa]	[MPa]	[MPa]
75 mm [B1] 300/75	4.8	2239	2.447	11293	8687
75 mm [B2] 300/75	4.8	2241	2.865	15159	11661
75 mm [B3] 300/75	4.8	2247	2.114	12445	9573
75 mm [B4] 300/75	4.6	2248	1.758	12334	9488
75 mm [B5] 300/75	4.6	2235	2.363	17637	13567
75 mm [B6] 300/75	4.6	2221	2.321	16374	12596
Mean	4.7	2238	2.311	14207	10929
Standard Deviation	0.11	9.81	0.37	2548	1960
COV [%]	2.33	0.44	15.88	17.94	17.94

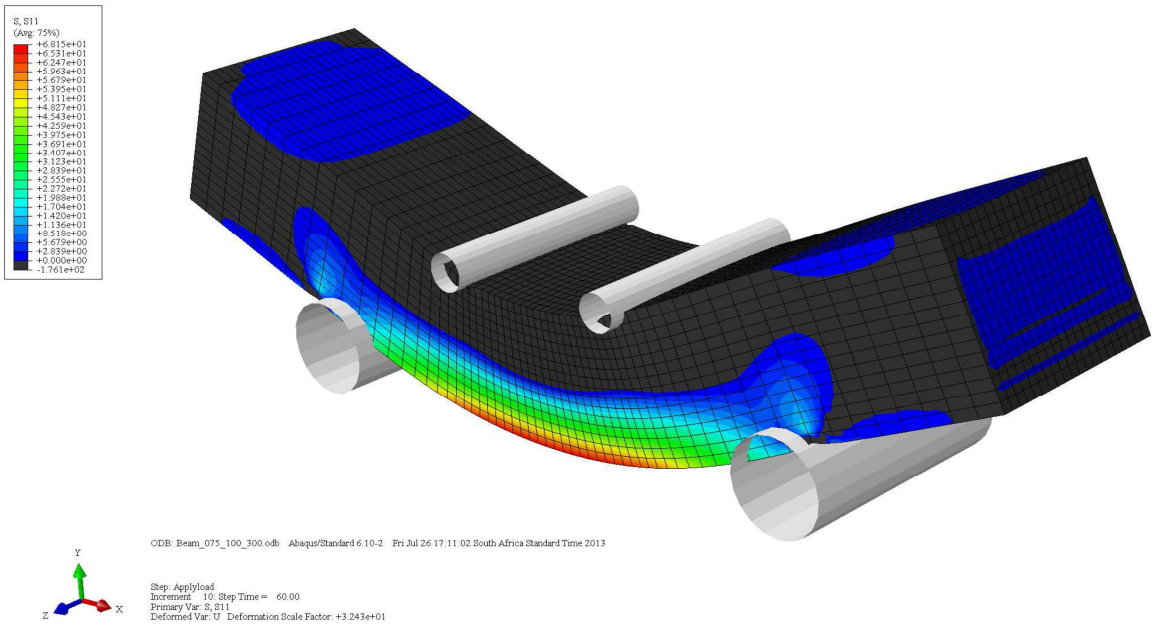

Figure 5h Model of the Beam Type with a Height of 75 mm and Span-Depth Ratio of 4.0

Table 5c Results for the 50 mm Beam Type [Span/Depth Ratio = 9.0; Pmax 19.0 mm]

2.0% Cement Content	Hornfels Mix Types [Pmax = 19.0 mm]				
Beam Height	Moisture Content	Density	Flexural Strength	Elastic Modulus	Shear Modulus
Beam Type [Span/Depth]	[%]	[kg/m^3]	[MPa]	[MPa]	[MPa]
50 mm [B1] 300/50	5.0	2329	0.295	1096	843
50 mm [B2] 300/50	5.0	2333	1.030	1093	841
50 mm [B3] 300/50	5.0	2332	1.038	1101	847
50 mm [B4] 300/50	5.0	2319	0.971	1077	828
50 mm [B5] 300/50	5.0	2323	1.059	1000	769
50 mm [B6] 300/50	5.0	2332	1.129	1448	1114
Mean	5.0	2328	0.921	1136	874
Standard Deviation	0.00	5.93	0.31	158	121
COV [%]	0.00	0.25	33.73	13.88	13.88
3.0% Cement Content	Hornfels Mix Types [Pmax = 19.0 mm]				
Beam Height	Moisture Content	Density	Flexural Strength	Elastic Modulus	Shear Modulus
Beam Type [Span/Depth]	[%]	[kg/m^3]	[MPa]	[MPa]	[MPa]
50 mm [B1] 300/50	4.8	2278	0.520	654	503
50 mm [B2] 300/50	4.8	2272	0.766	1457	1121
50 mm [B3] 300/50	4.8	2285	0.667	1713	1318
50 mm [B4] 300/50	4.7	2278	1.107	1764	1357
50 mm [B5] 300/50	4.7	2274	1.107	1622	1248
50 mm [B6] 300/50	4.7	2266	0.949	1512	1163
Mean	4.8	2275	0.853	1454	1118
Standard Deviation	0.05	6.42	0.24	409	314
COV [%]	1.15	0.28	28.31	28.11	28.11
6.0% Cement Content	Hornfels Mix Types [Pmax = 19.0 mm]				
Beam Height	Moisture Content	Density	Flexural Strength	Elastic Modulus	Shear Modulus
Beam Type [Span/Depth]	[%]	[kg/m^3]	[MPa]	[MPa]	[MPa]
50 mm [B1] 300/50	4.6	2223	1.491	1434	1103
50 mm [B2] 300/50	4.6	2225	1.684	2161	1663
50 mm [B3] 300/50	4.6	2224	1.686	2061	1585
50 mm [B4] 300/50	4.6	2222	1.684	1992	1532
50 mm [B5] 300/50	4.5	2228	1.556	2374	1826
50 mm [B6] 300/50	4.5	2229	1.513	2400	1846
Mean	4.6	2225	1.602	2070	1593
Standard Deviation	0.05	2.51	0.09	352	271
COV [%]	1.13	0.11	5.77	17.02	17.02

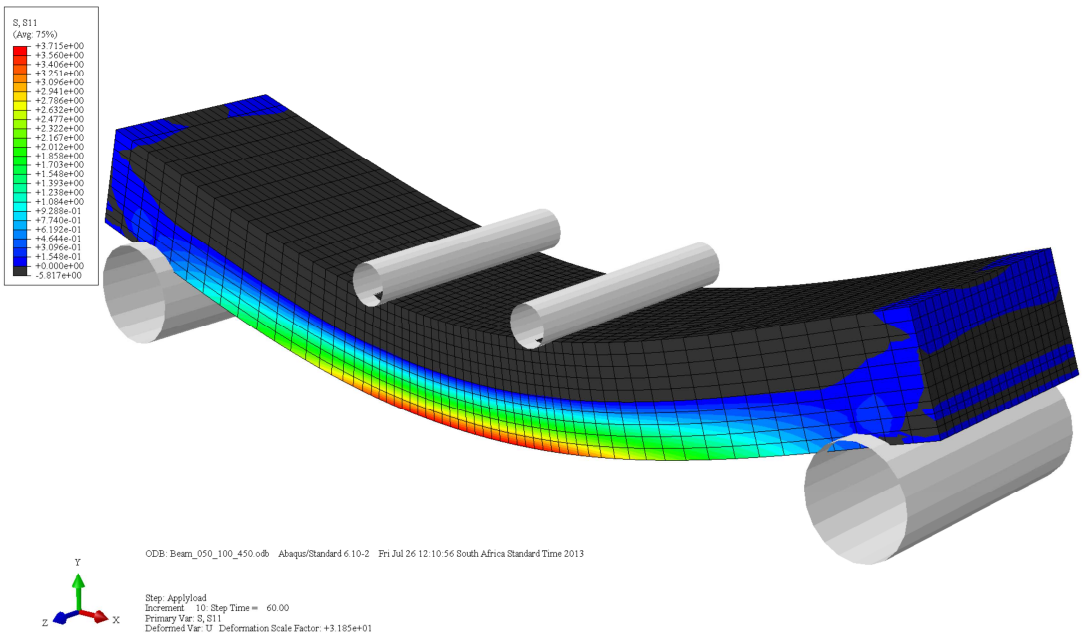

Figure 5i Model of the Beam Type with a Height of 50 mm and Span-Depth Ratio of 9.0

Table 5d Results for the 50 mm Beam Type [Span/Depth Ratio = 9.0; Pmax 13.2 mm]

2.0% Cement Content	Hornfels Mix Types [Pmax = 13.20 mm]				
Beam Height	Moisture Content	Density	Flexural Strength	Elastic Modulus	Shear Modulus
Beam Type [Span/Depth]	[%]	[kg/m^3]	[MPa]	[MPa]	[MPa]
50 mm [B1] 300/50	5.4	2286	0.975	2847	2190
50 mm [B2] 300/50	5.4	2243	0.939	2847	2190
50 mm [B3] 300/50	5.4	2246	0.936	2781	2139
50 mm [B4] 300/50	5.6	2253	0.956	2722	2094
50 mm [B5] 300/50	5.6	2270	0.972	2781	2139
50 mm [B6] 300/50	5.6	2238	0.874	2445	1881
Mean	5.5	2256	0.942	2737	2105
Standard Deviation	0.11	18.68	0.04	151	116
COV [%]	1.99	0.83	3.95	5.51	5.51
3.0% Cement Content	Hornfels Mix Types [Pmax = 13.20 mm]				
Beam Height	Moisture Content	Density	Flexural Strength	Elastic Modulus	Shear Modulus
Beam Type [Span/Depth]	[%]	[kg/m^3]	[MPa]	[MPa]	[MPa]
50 mm [B1] 300/50	5.3	2202	1.257	2978	2291
50 mm [B2] 300/50	5.3	2200	1.160	3480	2677
50 mm [B3] 300/50	5.3	2204	1.172	2955	2273
50 mm [B4] 300/50	5.3	2208	1.266	2921	2247
50 mm [B5] 300/50	5.3	2217	1.182	2915	2242
50 mm [B6] 300/50	5.3	2202	1.261	2909	2238
Mean	5.3	2205	1.216	3026	2328
Standard Deviation	0.00	6.08	0.05	224	172
COV [%]	0.00	0.28	4.12	7.39	7.39
6.0% Cement Content	Hornfels Mix Types [Pmax = 13.20 mm]				
Beam Height	Moisture Content	Density	Flexural Strength	Elastic Modulus	Shear Modulus
Beam Type [Span/Depth]	[%]	[kg/m^3]	[MPa]	[MPa]	[MPa]
50 mm [B1] 300/50	4.9	2178	2.203	5284	4065
50 mm [B2] 300/50	4.9	2140	2.400	6938	5337
50 mm [B3] 300/50	4.9	2159	2.277	11832	9102
50 mm [B4] 300/50	4.8	2198	2.391	5680	4369
50 mm [B5] 300/50	4.8	2187	2.194	5251	4040
50 mm [B6] 300/50	4.8	2151	2.390	5671	4363
Mean	4.9	2169	2.309	6776	5212
Standard Deviation	0.05	22.23	0.10	2552	1963
COV [%]	1.13	1.03	4.20	37.66	37.66

Figure 5j Ferricrete Beam Type with a Height of 50 mm and Span-Depth Ratio of 9.0

Table 5e Results for the 50 mm Beam Type [Span/Depth Ratio = 9.0; Pmax 13.2 mm]

2.0% Cement Content	Ferricrete Mix Types [Pmax = 13.20 mm]				
Beam Height	Moisture Content	Density	Flexural Strength	Elastic Modulus	Shear Modulus
Beam Type [Span/Depth]	[%]	[kg/m^3]	[MPa]	[MPa]	[MPa]
50 mm [B1] 300/50	9.2	2198	0.314	647	498
50 mm [B2] 300/50	9.2	2183	0.218	715	550
50 mm [B3] 300/50	9.2	2181	0.278	1108	852
50 mm [B4] 300/50	9.1	2177	0.219	973	748
50 mm [B5] 300/50	9.1	2179	0.299	881	678
50 mm [B6] 300/50	9.1	2184	0.197	1009	776
Mean	9.2	2184	0.254	889	684
Standard Deviation	0.05	7.47	0.05	178	137
COV [%]	0.60	0.34	19.25	20.02	20.02
3.0% Cement Content	Ferricrete Mix Types [Pmax = 13.20 mm]				
Beam Height	Moisture Content	Density	Flexural Strength	Elastic Modulus	Shear Modulus
Beam Type [Span/Depth]	[%]	[kg/m^3]	[MPa]	[MPa]	[MPa]
50 mm [B1] 300/50	9.0	2102	0.508	744	573
50 mm [B2] 300/50	9.0	2145	0.565	795	612
50 mm [B3] 300/50	9.0	2148	0.551	778	599
50 mm [B4] 300/50	9.0	2161	0.493	1562	1202
50 mm [B5] 300/50	9.0	2149	0.489	745	573
50 mm [B6] 300/50	9.0	2151	0.525	770	592
Mean	9.0	2143	0.522	899	692
Standard Deviation	0.00	20.42	0.03	325	250
COV [%]	0.00	0.95	5.96	36.20	36.20
6.0% Cement Content	Ferricrete Mix Types [Pmax = 13.20 mm]				
Beam Height	Moisture Content	Density	Flexural Strength	Elastic Modulus	Shear Modulus
Beam Type [Span/Depth]	[%]	[kg/m^3]	[MPa]	[MPa]	[MPa]
50 mm [B1] 300/50	8.6	2089	0.809	1846	1420
50 mm [B2] 300/50	8.6	2089	0.708	1567	1206
50 mm [B3] 300/50	8.6	2104	0.676	1507	1159
50 mm [B4] 300/50	8.4	2100	0.854	2918	2245
50 mm [B5] 300/50	8.4	2094	0.838	3776	2905
50 mm [B6] 300/50	8.4	2093	0.864	2896	2228
Mean	8.5	2095	0.791	2419	1860
Standard Deviation	0.11	5.82	0.08	917	705
COV [%]	1.29	0.28	10.11	37.91	37.91

Figure 5k Effect of the Pmax 19.0 mm in a Beam Type with a Height of 50 mm and Span-Depth Ratio of 9.0 [Zones of Localised Weakness]

Table 5f Beam Shear and Applied Forces for the 100 mm Beam Type

2.0% Cement Content	Hornfels Mix Types [Pmax = 19.0 mm]		Area [m^2] =	0.010
Beam Height	Force	Beam Shear Stress	Flexural Strength	Shear Modulus
Beam Type [Span/Depth]	[kN]	[MPa]	[MPa]	[MPa]
100 mm [B1] 300/100	1.940	0.194	0.589	2078
100 mm [B2] 300/100	1.884	0.188	0.594	3373
100 mm [B3] 300/100	1.478	0.148	0.462	1233
100 mm [B4] 300/100	1.184	0.118	0.362	975
100 mm [B5] 300/100	2.224	0.222	0.695	2456
100 mm [B6] 300/100	2.118	0.212	0.662	2320
Mean	1.8	0.180	0.560	2072
Standard Deviation	0.40	0.04	0.13	873
COV [%]	22.03	22.03	22.45	42.12
3.0% Cement Content	Hornfels Mix Types [Pmax = 19.0 mm]		Area [mm^2] =	0.010
Beam Height	Force	Beam Shear Stress	Flexural Strength	Shear Modulus
Beam Type [Span/Depth]	[kN]	[MPa]	[MPa]	[MPa]
100 mm [B1] 300/100	1.770	0.177	0.564	1450
100 mm [B2] 300/100	3.018	0.302	0.943	937
100 mm [B3] 300/100	2.324	0.232	0.741	2315
100 mm [B4] 300/100	1.336	0.134	0.417	1529
100 mm [B5] 300/100	2.360	0.236	0.752	902
100 mm [B6] 300/100	2.840	0.284	0.906	748
Mean	2.3	0.227	0.721	1313
Standard Deviation	0.64	0.06	0.20	583
COV [%]	27.93	27.93	27.85	44.40
6.0% Cement Content	Hornfels Mix Types [Pmax = 19.0 mm]		Area [mm^2] =	0.010
Beam Height	Force	Beam Shear Stress	Flexural Strength	Shear Modulus
Beam Type [Span/Depth]	[kN]	[MPa]	[MPa]	[MPa]
100 mm [B1] 300/100	4.588	0.459	1.463	4476
100 mm [B2] 300/100	5.784	0.578	1.807	5984
100 mm [B3] 300/100	6.429	0.643	2.050	5876
100 mm [B4] 300/100	4.505	0.451	1.407	12209
100 mm [B5] 300/100	4.505	0.451	1.379	11843
100 mm [B6] 300/100	5.784	0.578	1.770	7008
Mean	5.266	0.527	1.646	7900
Standard Deviation	0.84	0.08	0.27	3299
COV [%]	15.90	15.90	16.44	41.76

Figure 5l Beam Placement on the Flat Metal Deck [28 days of Curing at 25ºC]

Table 5g Beam Shear and Applied Forces for the 75 mm Beam Type

2.0% Cement Content	Hornfels Mix Types [Pmax = 19.0 mm]		Area [m^2] =	0.008
Beam Height	Force	Beam Shear Stress	Flexural Strength	Shear Modulus
Beam Type [Span/Depth]	[kN]	[MPa]	[MPa]	[MPa]
75 mm [B1] 300/75	0.824	0.110	0.439	1521
75 mm [B2] 300/75	0.802	0.107	0.439	722
75 mm [B3] 300/75	0.774	0.103	0.413	1385
75 mm [B4] 300/75	0.486	0.065	0.259	1418
75 mm [B5] 300/75	0.976	0.130	0.521	907
75 mm [B6] 300/75	0.876	0.117	0.455	1253
Mean	0.8	0.105	0.421	1201
Standard Deviation	0.16	0.02	0.09	317
COV [%]	20.88	20.88	20.70	26.41
3.0% Cement Content	Hornfels Mix Types [Pmax = 19.0 mm]		Area [m^2] =	0.008
Beam Height	Force	Beam Shear Stress	Flexural Strength	Shear Modulus
Beam Type [Span/Depth]	[kN]	[MPa]	[MPa]	[MPa]
75 mm [B1] 300/75	1.320	0.176	0.723	2597
75 mm [B2] 300/75	2.670	0.356	1.424	7682
75 mm [B3] 300/75	2.128	0.284	1.166	6412
75 mm [B4] 300/75	1.266	0.169	0.675	6368
75 mm [B5] 300/75	1.614	0.215	0.861	6525
75 mm [B6] 300/75	1.710	0.228	0.912	4887
Mean	1.8	0.238	0.960	5745
Standard Deviation	0.53	0.07	0.29	1780
COV [%]	29.87	29.87	29.71	30.98
6.0% Cement Content	Hornfels Mix Types [Pmax = 19.0 mm]		Area [m^2] =	0.008
Beam Height	Force	Beam Shear Stress	Flexural Strength	Shear Modulus
Beam Type [Span/Depth]	[kN]	[MPa]	[MPa]	[MPa]
75 mm [B1] 300/75	4.588	0.612	2.447	8687
75 mm [B2] 300/75	5.372	0.716	2.865	11661
75 mm [B3] 300/75	3.964	0.529	2.114	9573
75 mm [B4] 300/75	3.384	0.451	1.758	9488
75 mm [B5] 300/75	4.670	0.623	2.363	13567
75 mm [B6] 300/75	4.352	0.580	2.321	12596
Mean	4.388	0.585	2.311	10929
Standard Deviation	0.67	0.09	0.37	1960
COV [%]	15.38	15.38	15.88	17.94

Figure 5m Ferricrete Beam Type with Pmax 13.20 mm and Height of 50 mm on the Flat Metal Deck [28 days of Curing at 25ºC]

Table 5h Beam Shear and Applied Forces for the 50 mm Beam Type [P_{max} 19.0 mm]

2.0% Cement Content	Hornfels Mix Types [Pmax = 19.0 mm]		Area [m^2] =	0.005
Beam Height	Force	Beam Shear Stress	Flexural Strength	Shear Modulus
Beam Type [Span/Depth]	[kN]	[MPa]	[MPa]	[MPa]
50 mm [B1] 300/50	0.398	0.080	0.295	843
50 mm [B2] 300/50	0.333	0.067	1.030	841
50 mm [B3] 300/50	0.400	0.080	1.038	847
50 mm [B4] 300/50	0.389	0.078	0.971	828
50 mm [B5] 300/50	0.424	0.085	1.059	769
50 mm [B6] 300/50	0.418	0.084	1.129	1114
Mean	0.394	0.079	0.921	874
Standard Deviation	0.03	0.01	0.31	121
COV [%]	8.27	8.27	33.73	13.88
3.0% Cement Content	Hornfels Mix Types [Pmax = 13.2 mm]		Area [m^2] =	0.005
Beam Height	Force	Beam Shear Stress	Flexural Strength	Shear Modulus
Beam Type [Span/Depth]	[kN]	[MPa]	[MPa]	[MPa]
50 mm [B1] 300/50	0.301	0.060	0.520	503
50 mm [B2] 300/50	0.351	0.070	0.766	1121
50 mm [B3] 300/50	0.387	0.077	0.667	1318
50 mm [B4] 300/50	0.640	0.128	1.107	1357
50 mm [B5] 300/50	0.609	0.122	1.107	1248
50 mm [B6] 300/50	0.549	0.110	0.949	1163
Mean	0.473	0.095	0.853	1118
Standard Deviation	0.14	0.03	0.24	314
COV [%]	30.53	30.53	28.31	28.11
6.0% Cement Content	Hornfels Mix Types [Pmax = 13.2 mm]		Area [m^2] =	0.005
Beam Height	Force	Beam Shear Stress	Flexural Strength	Shear Modulus
Beam Type [Span/Depth]	[kN]	[MPa]	[MPa]	[MPa]
50 mm [B1] 300/50	0.862	0.172	1.491	1103
50 mm [B2] 300/50	0.973	0.195	1.684	1663
50 mm [B3] 300/50	0.988	0.198	1.686	1585
50 mm [B4] 300/50	0.921	0.184	1.684	1532
50 mm [B5] 300/50	0.899	0.180	1.556	1826
50 mm [B6] 300/50	0.909	0.182	1.513	1846
Mean	0.926	0.185	1.602	1593
Standard Deviation	0.05	0.01	0.09	271
COV [%]	5.12	5.12	5.77	17.02

Figure 5n Hornfels Beam Type with Pmax 19.0 mm and Height of 100 mm for Testig [Six Beams per Mix Variable]

Table 5i Beam Shear and Applied Forces for the 50 mm Beam Type [P_{max} 13.20 mm]

2.0% Cement Content	Hornfels Mix Types [Pmax = 13.2 mm]		Area [m^2] =	0.005
Beam Height	Force	Beam Shear Stress	Flexural Strength	Shear Modulus
Beam Type [Span/Depth]	[kN]	[MPa]	[MPa]	[MPa]
50 mm [B1] 300/50	0.502	0.100	0.975	2190
50 mm [B2] 300/50	0.546	0.109	0.939	2190
50 mm [B3] 300/50	0.501	0.100	0.936	2139
50 mm [B4] 300/50	0.512	0.102	0.956	2094
50 mm [B5] 300/50	0.576	0.115	0.972	2139
50 mm [B6] 300/50	0.468	0.094	0.874	1881
Mean	0.5	0.103	0.942	2105
Standard Deviation	0.04	0.01	0.04	116
COV [%]	7.35	7.35	3.95	5.51
3.0% Cement Content	Hornfels Mix Types [Pmax = 13.2 mm]		Area [m^2] =	0.005
Beam Height	Force	Beam Shear Stress	Flexural Strength	Shear Modulus
Beam Type [Span/Depth]	[kN]	[MPa]	[MPa]	[MPa]
50 mm [B1] 300/50	0.623	0.125	1.257	2291
50 mm [B2] 300/50	0.597	0.119	1.160	2677
50 mm [B3] 300/50	0.604	0.121	1.172	2273
50 mm [B4] 300/50	0.627	0.125	1.266	2247
50 mm [B5] 300/50	0.632	0.126	1.182	2242
50 mm [B6] 300/50	0.625	0.125	1.261	2238
Mean	0.618	0.124	1.216	2328
Standard Deviation	0.01	0.00	0.05	172
COV [%]	2.30	2.30	4.12	7.39
6.0% Cement Content	Hornfels Mix Types [Pmax = 13.2 mm]		Area [m^2] =	0.005
Beam Height	Force	Beam Shear Stress	Flexural Strength	Shear Modulus
Beam Type [Span/Depth]	[kN]	[MPa]	[MPa]	[MPa]
50 mm [B1] 300/50	1.049	0.210	2.203	4065
50 mm [B2] 300/50	1.189	0.238	2.400	5337
50 mm [B3] 300/50	1.173	0.235	2.277	9102
50 mm [B4] 300/50	1.185	0.237	2.391	4369
50 mm [B5] 300/50	1.045	0.209	2.194	4040
50 mm [B6] 300/50	1.184	0.237	2.390	4363
Mean	1.137	0.227	2.309	5212
Standard Deviation	0.07	0.01	0.10	1963
COV [%]	6.18	6.18	4.20	37.66

Figure 5o Metal Moulds Measuring 500 mm in Length, 100 mm in Height and in Width

Table 5j Beam Shear and Applied Forces for the 50 mm Beam Type [P_{max} 13.20 mm]

2.0% Cement Content	Ferricrete Mix Types [Pmax = 13.2 mm]		Area [m^2] =	0.005
Beam Height	Force	Beam Shear Stress	Flexural Strength	Shear Modulus
Beam Type [Span/Depth]	[kN]	[MPa]	[MPa]	[MPa]
50 mm [B1] 300/50	0.126	0.025	0.314	498
50 mm [B2] 300/50	0.186	0.037	0.218	550
50 mm [B3] 300/50	0.103	0.021	0.278	852
50 mm [B4] 300/50	0.090	0.018	0.219	748
50 mm [B5] 300/50	0.253	0.051	0.299	678
50 mm [B6] 300/50	0.182	0.036	0.197	776
Mean	0.2	0.031	0.254	684
Standard Deviation	0.06	0.01	0.05	137
COV [%]	39.48	39.48	19.25	20.02
3.0% Cement Content	Hornfels Mix Types [Pmax = 13.2 mm]		Area [m^2] =	0.005
Beam Height	Force	Beam Shear Stress	Flexural Strength	Shear Modulus
Beam Type [Span/Depth]	[kN]	[MPa]	[MPa]	[MPa]
50 mm [B1] 300/50	0.293	0.059	0.508	573
50 mm [B2] 300/50	0.314	0.063	0.565	612
50 mm [B3] 300/50	0.306	0.061	0.551	599
50 mm [B4] 300/50	0.285	0.057	0.493	1202
50 mm [B5] 300/50	0.294	0.059	0.489	573
50 mm [B6] 300/50	0.304	0.061	0.525	592
Mean	0.299	0.060	0.522	692
Standard Deviation	0.01	0.00	0.03	250
COV [%]	3.50	3.50	5.96	36.20
6.0% Cement Content	Hornfels Mix Types [Pmax = 13.2 mm]		Area [m^2] =	0.005
Beam Height	Force	Beam Shear Stress	Flexural Strength	Shear Modulus
Beam Type [Span/Depth]	[kN]	[MPa]	[MPa]	[MPa]
50 mm [B1] 300/50	0.505	0.101	0.809	1420
50 mm [B2] 300/50	0.426	0.085	0.708	1206
50 mm [B3] 300/50	0.406	0.081	0.676	1159
50 mm [B4] 300/50	0.513	0.103	0.854	2245
50 mm [B5] 300/50	0.503	0.101	0.838	2905
50 mm [B6] 300/50	0.499	0.100	0.864	2228
Mean	0.475	0.095	0.791	1860
Standard Deviation	0.05	0.01	0.08	705
COV [%]	9.86	9.86	10.11	37.91

Figure 5p Hornfels Beam Types After Testing and Location of Crack [100 mm Height]

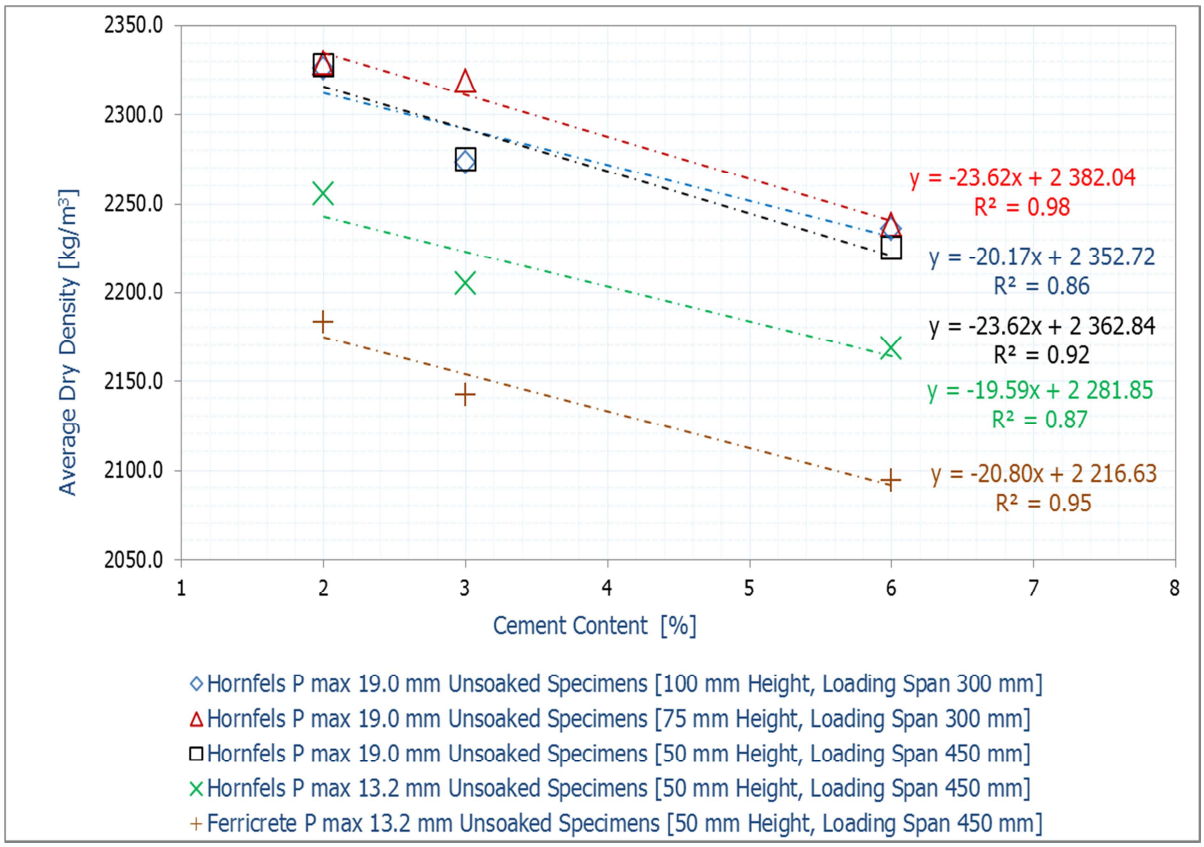

Figure 5q Average Dry Density with Different Maximum Aggregate Sizes

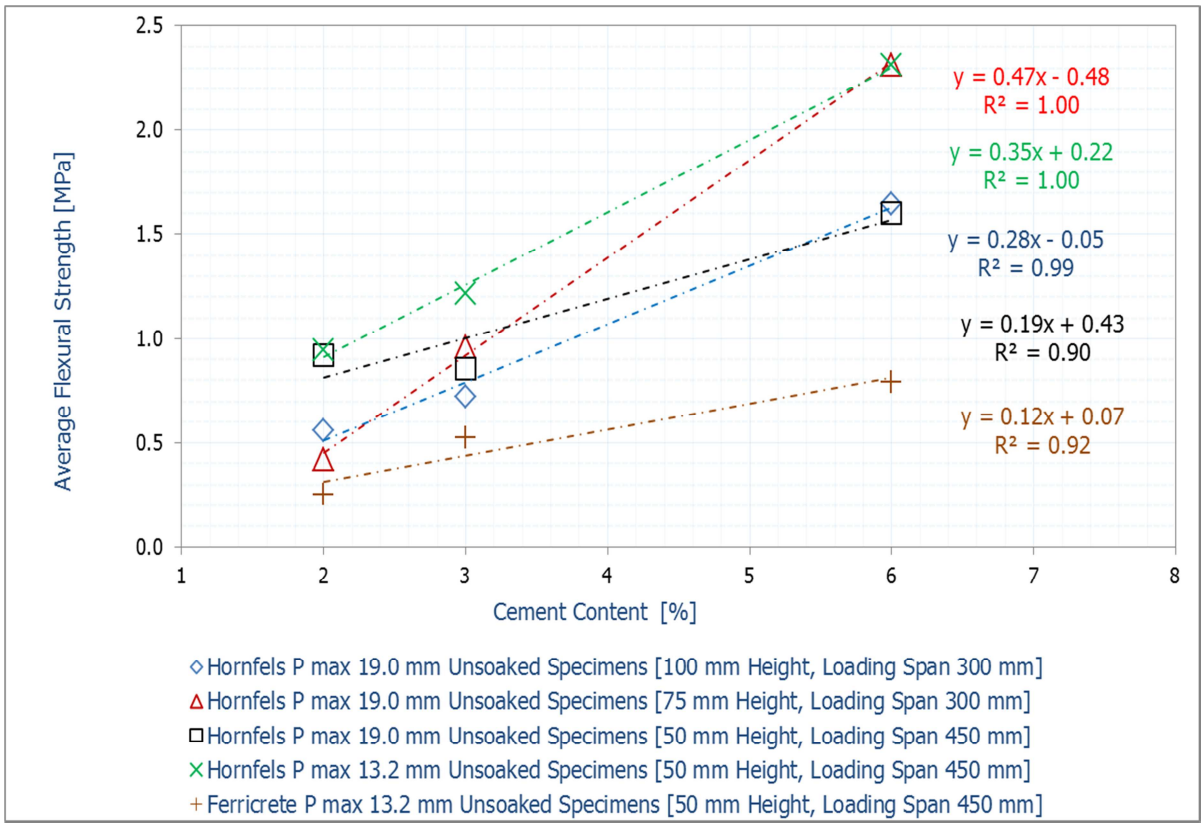

Figure 5r Average Flexural Strength with Different Span-Depth Ratios

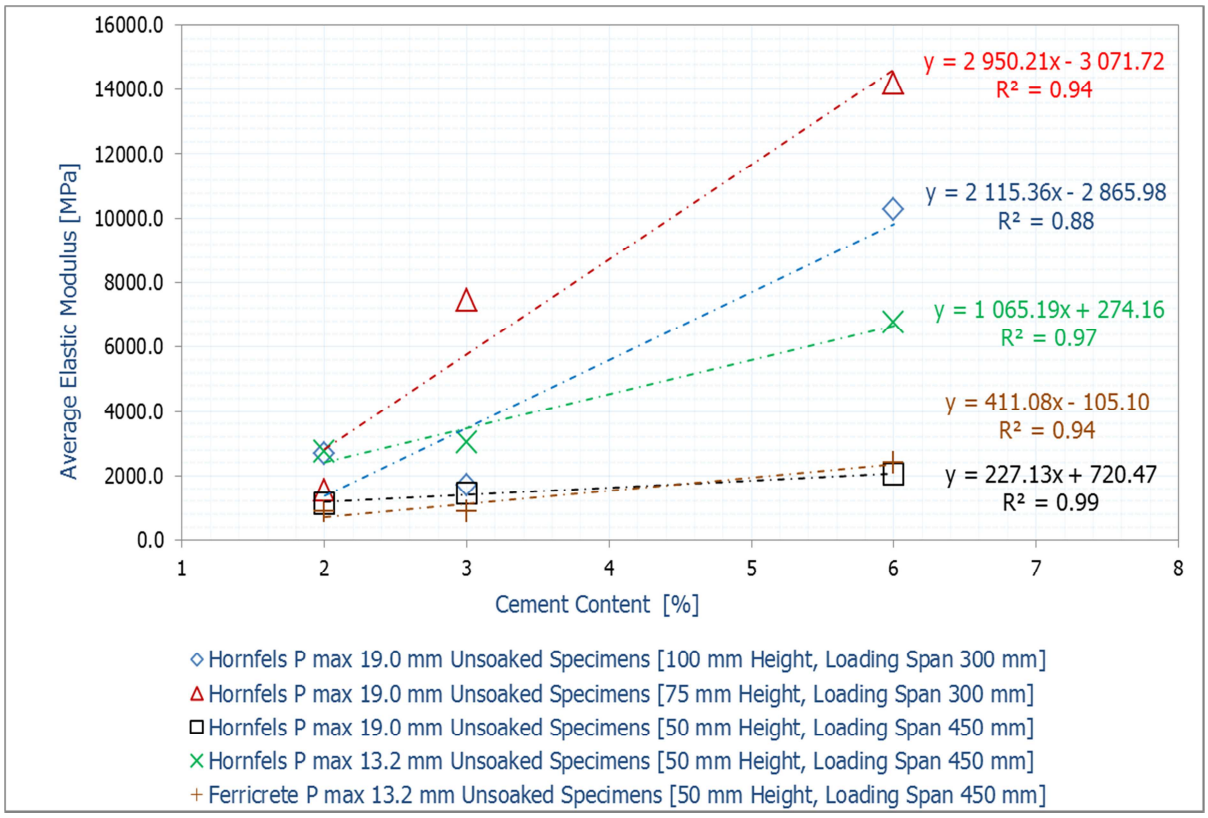

Figure 5s Average Elastic Modulus at Different Span-Depth Ratios

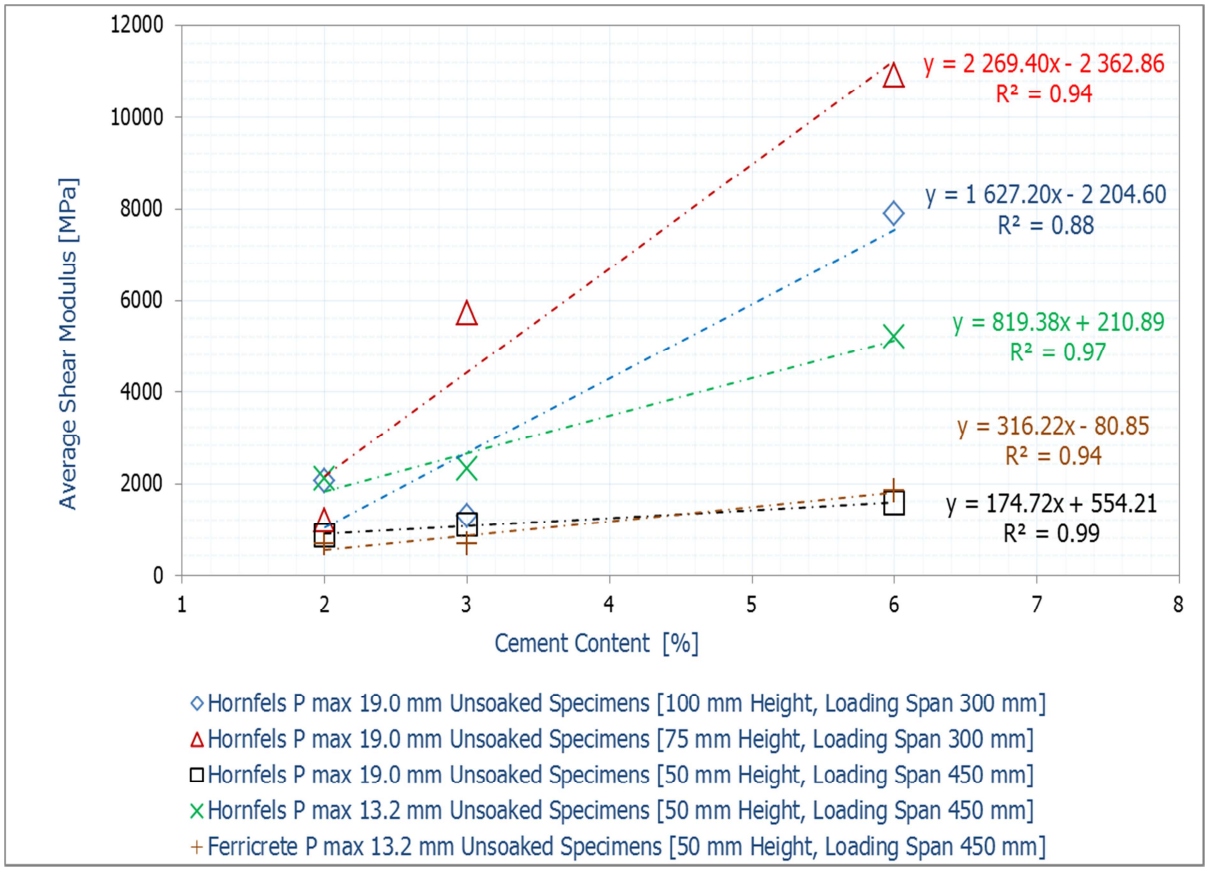

Figure 5t Average Shear Modulus at Different Span-Depth Ratios

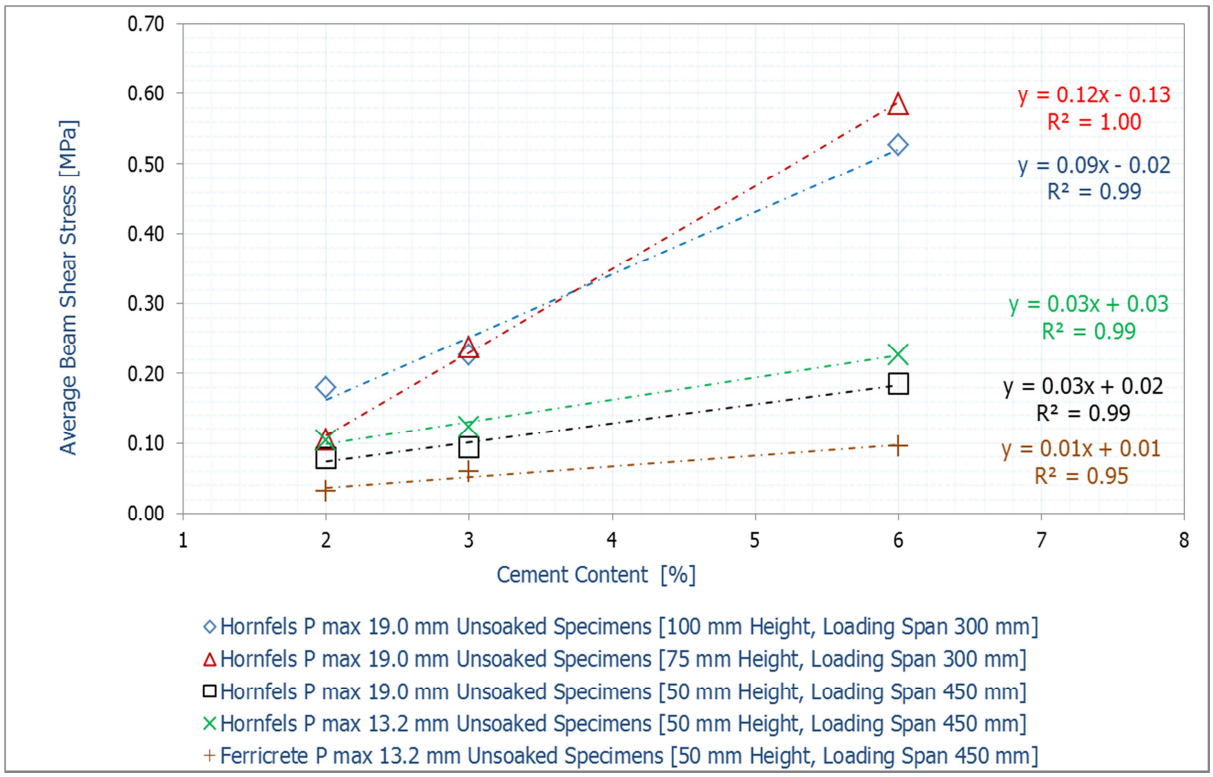

Figure 5u Average Shear Stress at Different Span-Depth Ratios

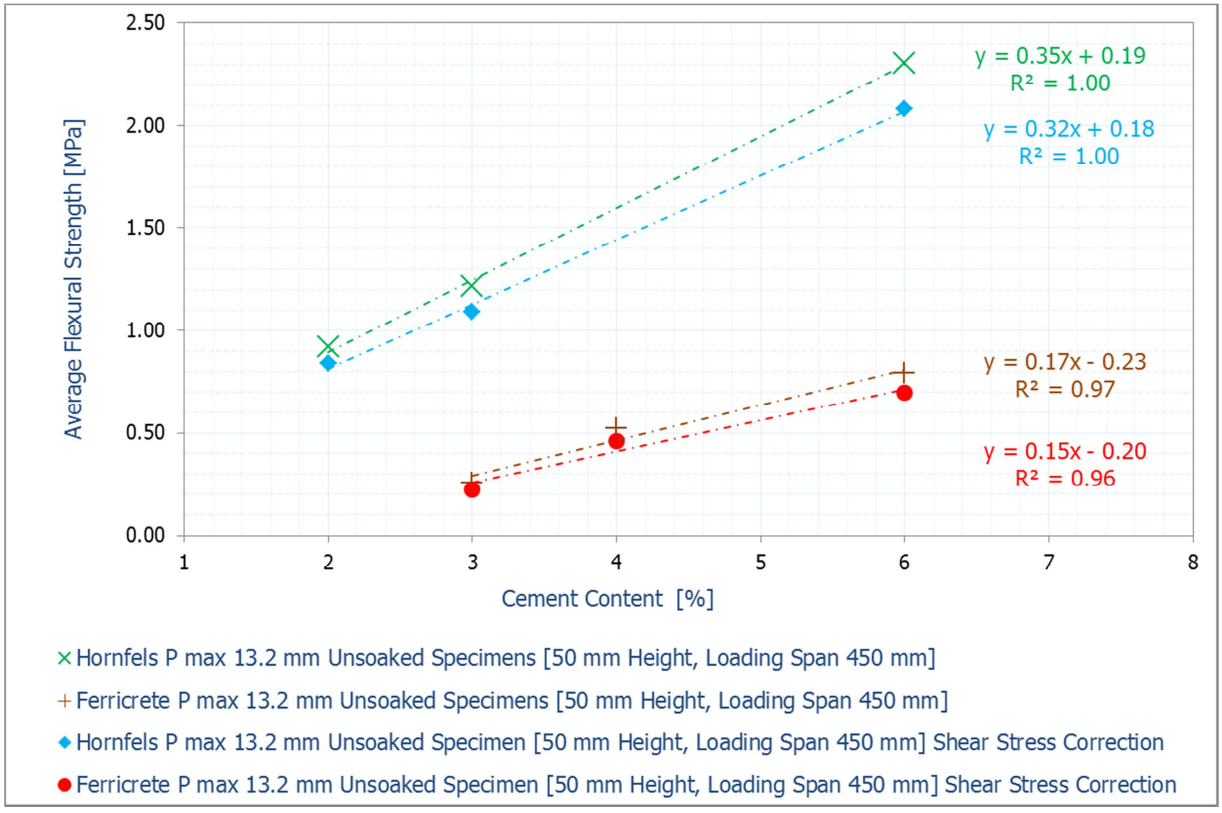

Figure 5v Effect of Shear Stress on the Flexural Strength at varying Cement Contents

FLEXURAL BEAM TEST METHOD

1.0 Scope

This test method evaluates the flexural strength of cement-stabilised materials. The test is carried out on a rectangular beam with a span-depth ratio of 9.0 supported at the ends using a four-point loading technique.

2.0 Concepts for Specifying the Beam Geometric Characteristics Relative to the Test Configurations

In order to specify the geometry of the beam an understanding of the test configurations and their influence on the measurement of the flexural strength is important. This refers to using the span-depth ratio of nine to determine the beam geometry. Equally, determination of the maximum aggregate particle size in the mix relative to the geometry of the beam ought to be appropriately correlated with a good understanding of their influence on the measurement of flexural strength. This test method considers a span-depth ratio of 9.0. This is because a span-depth of 9.0 results in negligible beam shear stresses. However, a shear stress correction factor must be applied to adjust the flexural strength value. This test method accounts for the influence of the maximum aggregate particle size in the mix on the measurement of the 'actual' flexural strength. Figure 1b shows the relationship between the beam geometric characteristics and test configurations.

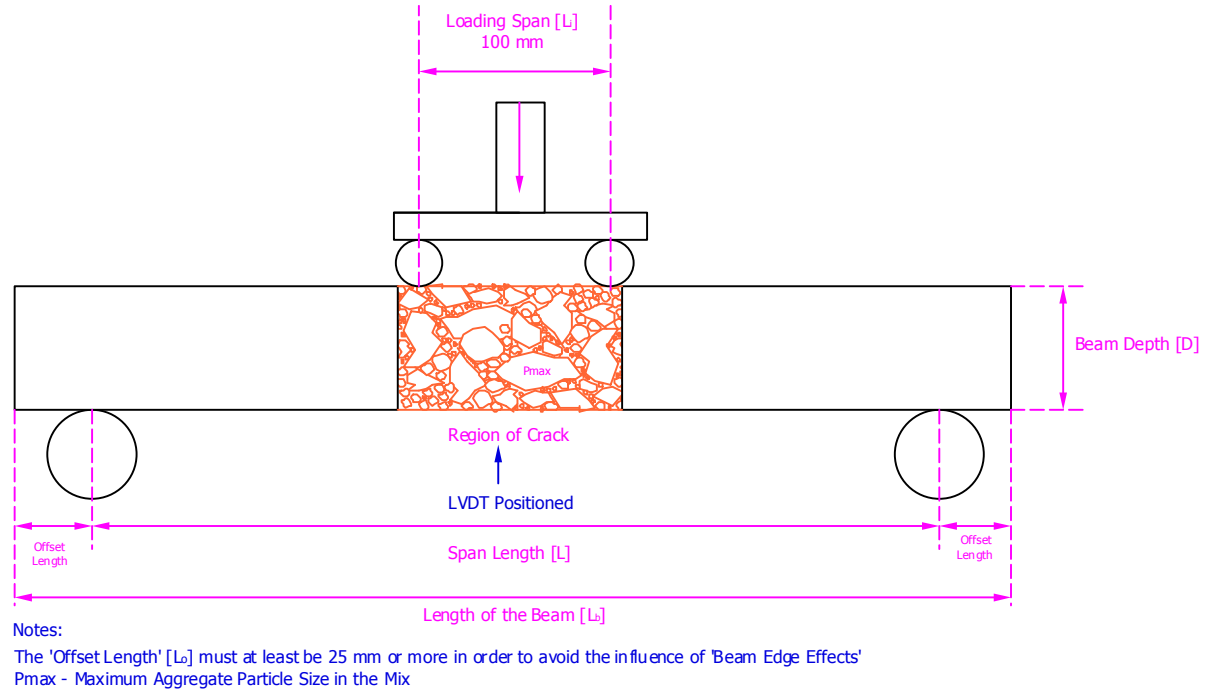

Figure 1b Beam Geometric Characteristics and Test Configurations

The loading span [L_i] is 100 mm [fixed] and an offset length at each end of the beam should be at least 25 mm or more. The beam depth [D] is dependent on the maximum aggregate particle size [P_{max}] in the mix. Equation 1 computes the beam depth [D] based on the maximum aggregate particle size in the mix; the resultant value must be adjusted to a practical value, see Example 1. Equation 2 computes the span length [L] using a span-depth ratio of 9.0. Equation 3 computes the length of the beam [L_b]. In this case, the beam width is fixed at 100 mm but appropriate correlations are required. By adopting a ratio of 5.0 i.e.

beam length to beam width, Equation 4 is developed. **Note**: The values of D, L and L_b must be multiples of five [i.e. practical values, see Example 1].

$D = 3\ (Pmax) + 10$ [mm] Equation 1

$L = 9\ (D)$ [mm] Equation 2

$L_b = L + 2\ (L_o)$ [mm] Equation 3

$L_w = (L_b)/5$ [mm] Equation 4

Laboratory Prepared Beam Example 1:

For a maximum aggregate particle size [Pmax] of 13.20 mm, the following is computed using Equations 1 to 3.

D = 3 (13.20) +10 = 49.6 mm [adjust to practical value = 50 mm]

L = 9 (50) = 450 mm [practical value - allow]

L_b = 450 + 2 (25) = 500 mm [practical value - allow]

L_w = (500)/5 = 100 mm [practical value - allow]

3.0 Apparatus and Description

a) A metal mould with internal dimensions equivalent to the beam length [L_b], width [L_w] and depth [D] is considered. However, the height of the mould should at least be 25 mm more [i.e. 25 mm + D]. This permits the footing to enter the metal mould for effective compaction without resulting in any sideways movements during compaction. This allows the rectangular metal footing to distribute the compactive effort directly to the materials without any hindrance emanating from the sides of the metal mould.

Note: Any sideways movements not only hinder the effective compaction of the materials, but could also lead to the damaging of the Bosch vibratory hammer. If the metal footing gets in contact with the metal mould sides, the Bosch hammer could be damaged.

b) The sides of the mould should be easily detachable but firmly secured during the compaction of the materials. Additionally the base plate must be of sufficient thickness to withstand the applied compactive effort
c) Mould oil to smear to the internal surfaces of the mould ensures easy removal of the beam from the metal mould [i.e. during the demoulding phase]
d) For the compaction of the beam, the Bosch vibratory hammer with a rectangular metal footing of equivalent beam length [L_b] and width [L_w] is considered. However, compaction trial runs to ascertain the suitability of the vibratory hammer relative to the length of the footing are required. The resultant dry density should be assessed relative to the modified AASHTO compaction method
e) A mixer with a bucket capacity adequate to mix a unit weight equivalent to three beams in one batch

Note: For conventional material types, at least three beams must be prepared per mix variable. For alternative material types and/or materials with admixtures, filler or additive, it is highly recommended that six beams per mix variable be prepared.

f) A balance to weigh up to 30.0 kg
g) A Linear Variable Transducer [LVDT] with a sensitivity of at least +/- 0.2 mm
h) A pair of pillars to tighten as well as loosen of the sides of the mould before compaction of the materials and/or during the demoulding of the beam
i) A stand to hold the LVDT securely into position in order to measure the beam deflection of the beam

4.0 Preparation of the Beams and Curing

The mixing of the materials with cement and water should preferably occur in one mix batch at the optimum moisture content [OMC] of the natural materials. For determining the maximum dry density [MDD] and OMC of the natural materials, Method A7 [TMH1, 1986] is considered. In order to establish the required cement content in the mix, the Unconfined Compressive Strength [UCS] i.e. Method A14 [TMH1, 1986] should be carried out.

However, before mixing the materials with cement and water, the amount of hygroscopic moisture should be determined. This involves oven drying a sample of about 600 to 700 grams in the draught oven for 24 hours at 110ºC and assessing the mass difference. The mix water is reduced by a quantity equivalent to the hygroscopic moisture content. This is to ensure that the required moisture content is added to the mix. The next step is to calculate and weigh-out the quantity of cement required to stabilise the material. Cement is added as a percentage of the dry materials.

In order to ensure that cement particles are evenly distributed, dry mixing of cement and material is carried out before adding water to the mixture. Immediately after adding water, the mixing process begins. The mixing process should result in an even distribution of moisture. After mixing is accomplished, compaction of the beam follows i.e. no delay time between the mixing and compaction phases. Compaction time is determined after a series of compaction trial runs following the determination of the MDD and OMC using the modified AASHTO compaction method. For heights less than 60 mm, compaction of the beam should proceed in one layer for a specified compaction time. For heights more than 60 mm, compaction should commence in two or more layers depending on the beam depth. Where the compaction of the beam is in two or more layers, scarification after every compaction and before the next layer should be realised. Scarification improves the integrity of the beam by ensuring continuity and/or bonding between layers.

The compacted beams are weighed in their individual moulds and placed in a controlled environment [i.e. set at 25ºC] for not more than 48 hours. After 48 hours, the beams should be demoulded by simply detaching the sides of the metal mould. By keeping the beam in the metal mould for 48 hours allows the beam to gain some substantial strength for easy handling when demoulded. The demoulding of the beam should take place within the controlled environment. After demoulding, the beam depth [D] is recorded along with its mass as well as that of the metal mould. The demoulded beams are then carefully transferred to a flat surface for the remainder of the 28 days of the curing duration. At 28 days, the flexural strength testing using the four point loading technique is carried out. Beams might be tested after 4 hours of soaking or as dry [i.e. without soaking]. Accelerated curing maybe considered to provide a good indication of the likely 28 days curing using an appropriate curing temperature.

5.0 Flexural Strength Test Configurations

The following test parameters are applied:

a) the type of loading is monotonic type and displacement controlled

b) displacement rate is 0.0025 mm/second or 1.5 mm/minute
c) inner loading span of 100 mm
d) loading span [L] see, Equation 2
e) termination of test is set at 35% of the maximum peak force value
f) seating force [if required] minimum value accepted by the test machine

6.0 Calculation of Flexural Strength

For the determination of flexural strength, the four-point loading test technique is applied and Equation 4 computes the flexural strength value. This is when the loading-span is neither half nor a third of the inner loading span [i.e. 100 mm].

$$f = (3F (L - L_i))/ (2L_w \times D^2) \quad \text{Equation 4}$$

Where:
f – Flexural strength in MPa
F – Peak force at a point of fracture in kN
L – Length of the support span in mm
L_i – Length of the inner loading span in mm
L_w – Width of the beam in mm
D – Depth [or height] of the beam in mm

7.0 Field Slabs [Proposed Alternative Beam Preparation]

In order to obtain beams from the road section for the evaluation of the flexural strength, slabs of variable dimensions maybe tactfully extracted. This requires a good consideration in keeping the slab intact. This suggests that extraction of the slab from a road section must take into consideration of the required beam dimensions for testing, the maximum aggregate particle size in the mix and the test configurations. Example 2 shows the proposed beam geometry for a span-depth ratio of 9.0 with a maximum aggregate particle size of 26.50 mm. A minimum beam length of 860 mm and depth of 90 mm is required. Testing follows similar procedures as laboratory.

Field Prepared Beam Example 2:

For a maximum aggregate particle size [Pmax] of 26.50 mm from the field road section, the following is computed using Equations 1 to 3.

D = 3 (26.5) +10 = 89.5 mm [adjust to practical value = 90 mm]

L = 9 (90) = 810 mm [practical value - allow]

L_b = 810 + 2 (25) = 860 mm [practical value - allow]

L_w = (860)/5 = 172 mm [adjust to practical value of 175 mm]

This suggests for a span-depth ratio of 9.0, a rectangular beam measuring 860 mm in length, 175 mm in width and 90 mm in depth, [i.e. height] is appropriate. The consideration to undertake accelerated curing compared to curing for 28 days may be included. Reporting must include how long the beam is cured and under what curing conditions.

SHRINKAGE TEST METHOD

1.0 Scope

This test method evaluates shrinkage of cement-stabilised materials. A cylindrical specimen with a diameter of 100 mm and height of 300 mm is considered. Shrinkage is measured in the axial direction.

2.0 Apparatus

a) A split metal mould, 100 mm in diameter, 400 mm high. The mould should be fastened using nuts and bolts at two equal distance levels, i.e. along its height as well as with hinges to allow its opening as illustrated in Figure 1a.

Figure 1a Split Mould [Nuts and Bolts with Hinges]

b) Mould oil to smear to the mould internal surfaces
c) Vibratory hammer as the compaction method with footing of about 100 mm in diameter
d) Scarifier with a diameter of about 100 mm
e) A mixer with a bucket capacity of not less than 10.0 kg
f) A balance to weigh up to 20.0 kg
g) Dial gauge with a scale of about 0.1 mm
h) 2 plexiglass pieces, i.e. circular piece with a diameter of 100 mm and a square piece measuring at least 300 mm
i) A pair of pillars to tighten as well as during the demoulding of the specimen
j) A rigid frame with a straight base plate and metal frame fastened tightly together to position the dial gauge in place, see Figure 2a
k) A standard draught oven capable of measuring up to 120ºC degree equipped with a temperature gauge

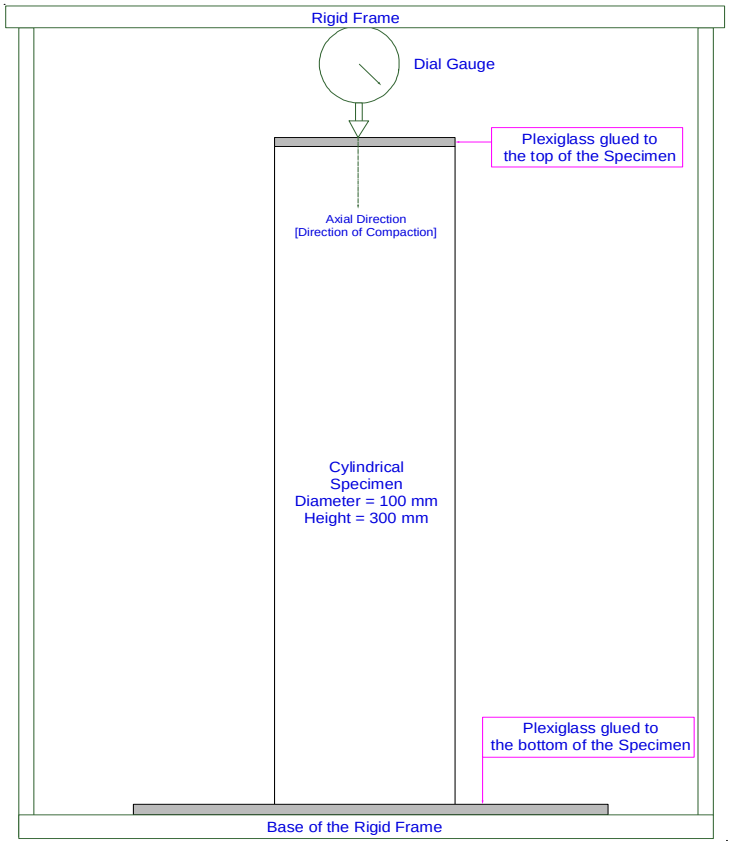

Figure 2a General Test Setup [Specimen, Dial Gauge and Rigid Frame]

The rigid frame provides a secure positioning of the dial gauge. The dial gauge is mounted onto the top plexiglass, which is glued on top of the cylinder specimen using epoxy glue.

3.0 Preparation of Specimen and Testing

At least three specimens with a maximum aggregate size of 19.0 mm should be prepared in the same mixing batch for the evaluation of shrinkage. The mixing of the material [for three specimens] should take place at the optimum moisture content [OMC] of the natural material. For determining the maximum dry density [MDD] and OMC of the natural materials, Method A7 [TMH1, 1986] is considered. In order to establish the required cement content in the mix, the Unconfined Compressive Strength [UCS] i.e. Method A14 [TMH1, 1986] is undertaken. The shrinkage testing is only considered after conforming the UCS strength and other related material characterisation tests.

Calculate and weigh out the quantity of cement required for a known mass of the material to prepare three specimens. Assess the amount of hygroscopic moisture in the material by oven drying a sample of about 600 to 700 grams in the draught oven for 24 hours at 110ºC. In order to ensure that the required moisture content added to the mix, the quantity of mix-water reduced by a value equivalent to the hygroscopic moisture content. Then calculate and weigh the amount of water required for the measured quantity of the material.

In order to ensure that cement particles are evenly distributed in the material dry mixing of cement and material is carried out before adding water to the mixture. After adding water mixing of the stabilised materials should start immediately. This should also ensure that water is evenly spread throughout the particles. After mixing is completed, compaction should immediately take place using the vibratory hammer.

Through prior compaction trial runs, the compaction time per layer is determined. Each specimen is compacted in 5 layers of 60 mm height. Scarification of the layer after each compaction is done to ensure suitable bonding. For each specimen, a specimen number is allocated corresponding to when the specimen is compacted. The time of mixing to the end of compaction must not exceed 20 minutes. Each beam is left in the metal mould covered with a plastic bag. Figure 3a illustrates the compaction and the handling of the specimens immediately after compaction

Figure 3a Compaction of the Specimens and Specimen Handling

Demoulding of the specimen requires the use of pillars to loosen the nuts from the bolts. The demoulding of the specimen must take place in a controlled environment set at 25ºC on the square plexiglass. In order to ensure that no direct handling of the specimen occurs, the square plexiglass at the bottom is used as a 'tray' to move the specimen. For each specimen, the height is recorded [using a straight edge ruler] along with its wet mass [using a measuring scale] before placing in the draught oven. The draught oven, which is beforehand is set at the test temperature [in this case 70ºC] before the preparation of the specimen, is checked for its consistency in maintaining the temperature. Figure 4a shows the demoulding, weighing and placement of the specimen in the draught oven.

Figure 4a Demoulding of the Cylinder Specimen

Figure 5a Weighing and General Test Setup.

4.0 Calculation of Specimen Moisture Content

Specimen moisture content [%] = $((a-b)/c\,)\,x\,100$ Equation 1

Where: a – mass of the specimen before the test [wet specimen]
b – mass of the top and bottom plexiglass pieces
c – mass of the specimen after the test [dried specimen]

5.0 Recording of the Dial Gauge Readings and Plotting the Test Curve

Figure 6a shows the conceptualised shrinkage test curve. It is, however, cautioned that each material type and quality will plot differently. Therefore, there is need to study the test curve in order to determine the detrimental shrinkage. Dial gauge readings are taken from the start of the test for the following durations [i.e. in minutes] of 0, 30, 60 [1 hr], 120 [2hrs], 360 [6hrs], 2880 [48 hrs] and 4320 [72hrs]. After 72 hours the test is concluded.

6.0 Calculation of Shrinkage

By using tangents, the peak of the curve [Point A] is connected to the end of the test [Point C]. The highest point of arch AC defines Point B. Point B defines the change in the shrinkage-time curve and denotes the beginning of extracting moisture from the inner core ofteh specimen. The difference between Point B and Point C is the detrimental shrinkage as shown in Equations 2 to 4. Material shrinkage is the average of the three specimens represented as absolute shrinkage in either microstrains or as a percentage.

Specimen shrinkage = (B – C) [mm] Equation 2

Where: B – Value in mm at Point B
C – Value in mm at Point C

Absolute Shrinkage = $((B - C)/ h_o) \times 10^{-6}$ [με] Equation 3

Where: h_o – original height of the specimen in mm

Absolute Shrinkage = $((B - C)/ h_o) \times 100$ [%] Equation 4

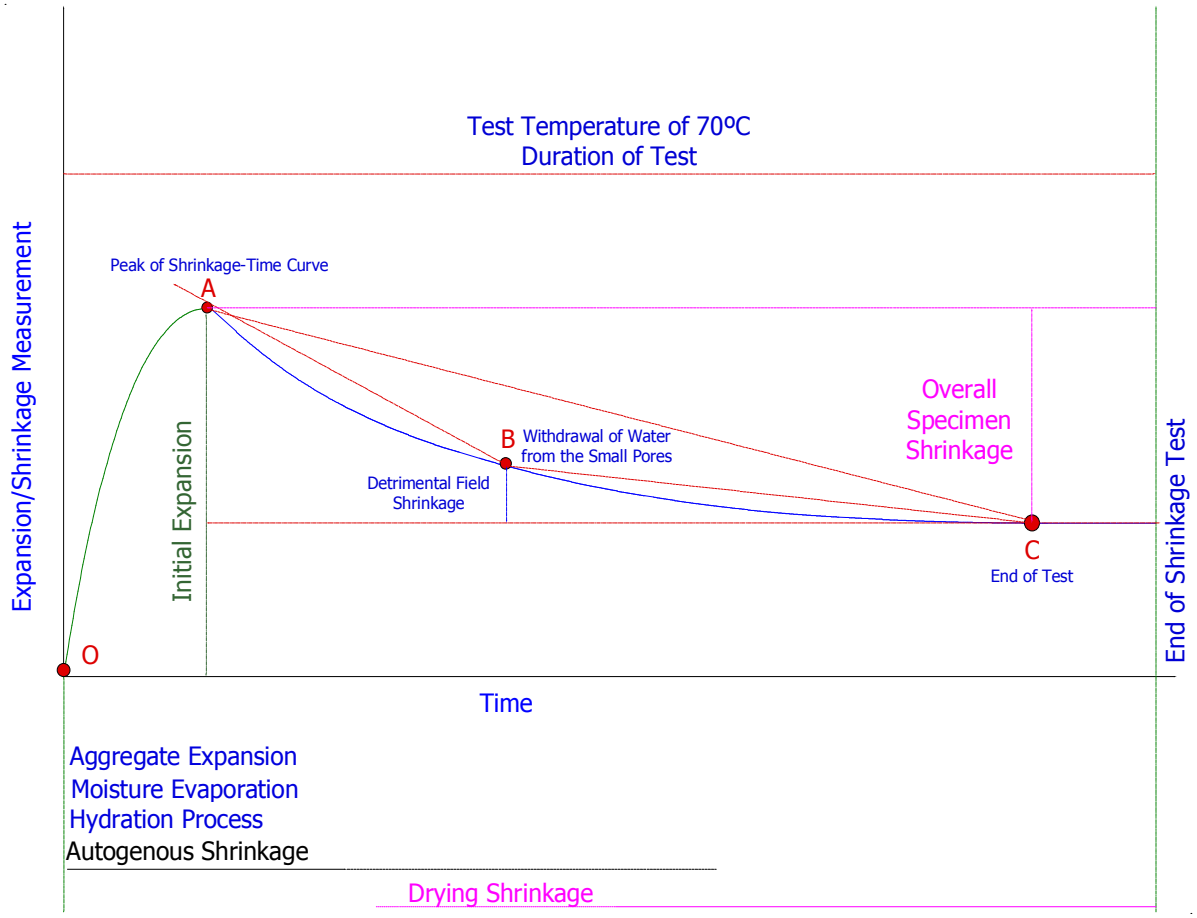

Figure 6a Typical Shrinkage Test Curve for Crushed Aggregate and Soils

7.0 Field Cores [Alternative Specimen Preparation]

Cores of 300 mm height and diameter of 100 mm can be obtained from a freshly compacted stabilised layer. However, caution should be observed when removing the cored specimen as this could lead to the damaging of the specimen. After removing the cored specimen, it must be sealed in a plastic bag. The unsealing of the specimen must be done under a controlled environment of 25ºC. In the laboratory, the wet mass and height should be recorded before placing the specimen in draught oven. The testing is done following similar test criteria as the laboratory prepared specimen. The influence of the maximum aggregate size in the field prepared core compared to the 19.0 mm for the laboratory prepared specimen must be noted.